

ORGANOMETALLICS

Volume 2, Number 3, March 1983

© Copyright 1983
American Chemical Society

Organotellurium Compounds of Biological Interest—Unique Properties of the *N*-Chlorosuccinimide Oxidation Product of 9-Telluraheptadecanoic Acid

G. Kirsch,[†] M. M. Goodman, and F. F. Knapp, Jr.*

Nuclear Medicine Group, Health and Safety Research Division, Oak Ridge National Laboratory,
Oak Ridge, Tennessee 37830

Received July 21, 1982

The product formed by *N*-chlorosuccinimide (NCS) oxidation of 9-telluraheptadecanoic acid (9-THDA) is insoluble in organic solvents and appears to have an oligomeric or polymeric structure. The product is solubilized in dilute base to the sodium salt of the monomer, the Te(IV) geminal diol of 9-THDA. While the insoluble oxidation product cannot be analyzed directly, it has been converted to products of known structure. Treatment with HBr gives the dibromide of 9-THDA, and treatment with acetic anhydride forms the Te(IV) geminal diacetate of 9-THDA. Similar NCS oxidation of the methyl ester of 9-THDA or dioctyl telluride in each case gives the Te(IV) geminal diols that exhibit normal solubility in organic solvents and the expected physical properties. In contrast, NCS oxidation of 9-selenaheptadecanoic acid (9-SHDA) gives a selenoxide (Se=O) that is readily soluble in organic solvents. The contrasting properties of the oxidation products of 9-THDA and 9-SHDA correlate directly with the heart specificity and degree of retention in the heart muscle after intravenous administration of the radiolabeled compounds 9-[^{125m}Te]THDA and 9-[⁷⁵Se]SHDA to experimental animals. The radiolabeled tellurium fatty acid shows pronounced heart uptake and prolonged retention ("trapping") and represents a new type of imaging agent for the potential clinical evaluation of heart disease. The present studies suggest that the "trapping" of tellurium fatty acids in the heart may result from the formation of an insoluble oxidation product after entry into the cells of the heart muscle.

Introduction

The field of organotellurium chemistry¹ has grown rapidly over the last few years as a result of the development of tellurium "reagents" that have unique and subtle applications in organic synthesis. One example is dianisyl telluroxide, which is a mild oxidizing agent.² In addition, a variety of new organotellurium compounds of biological interest have been synthesized and evaluated because of interest in the potential use of the ^{123m}Te-labeled agents for diagnostic applications in clinical nuclear medicine.³ The tellurium-123m radioisotope is produced by neutron irradiation of isotopically enriched tellurium-122 and has attractive radionuclidic properties for determining the tissue distribution of ^{123m}Te-labeled tissue-specific radiopharmaceuticals by external scanning or imaging techniques.

A variety of structurally modified steroids labeled in the side chain with ^{123m}Te have been prepared and evaluated,⁴

and two of these agents 24-(isopropyl[^{123m}Te]telluro)-chol-5-en-3 β -ol⁴ and 23-(isopropyl[^{123m}Te]telluro)-24-nor-5 α -cholan-3 β -ol⁵ exhibit pronounced adrenal uptake in experimental animals. These agents show promise as a means to localize unilateral adrenal disease. Model tellurium amino acids such as telluromethionine⁶ and α -amino- β -(phenyltelluro)butyric acid⁷ have also been prepared. More recently, a series of ^{123m}Te-labeled barbiturates substituted at the C-5 position have been evaluated and show significant brain uptake in experimental animals.⁸

(1) Irgolic, K. J. "The Organic Chemistry of Tellurium"; Gordon and Breach: New York, 1974.

(2) Ley, S. V.; Meerholz, C. A.; Barton, D. H. R. *Tetrahedron, Suppl.* 1981, 37, 213.

(3) Knapp, F. F., Jr. In "Selenium and Tellurium as Carbon Substitutes"; Spencer, R. D., Ed.; Grune & Stratton: New York, 1981; Chapter 16, pp 345-391.

(4) Knapp, F. F., Jr.; Ambrose, K. R.; Callahan, A. P. *J. Nucl. Med.* 1980, 21, 258.

(5) Knapp, F. F., Jr.; Ambrose, K. R.; Callahan, A. P. *J. Nucl. Med.* 1980, 21, 251.

(6) Knapp, F. F., Jr. *J. Org. Chem.* 1979, 44, 1007.

(7) Knapp, F. F., Jr.; Ambrose, K. R.; Callahan, A. P. *J. Med. Chem.* 1981, 24, 794.

[†]Laboratoire de Chimie Organique, Faculte de Science, Universite de Metz, Metz, 5700, France.

$\text{H}_3\text{C} - (\text{CH}_2)_{16} - \text{COOH}$	STEARIC ACID
$\text{H}_3\text{C} - (\text{CH}_2)_{14} - \text{COOH}$	PALMITIC ACID
$\text{H}_3\text{C} - (\text{CH}_2)_7 - \text{Te} - (\text{CH}_2)_7 - \text{COOH}$	9 - TELLURAEPTADECANOIC ACID (9 - THDA)
$\text{H}_3\text{C} - (\text{CH}_2)_7 - \text{Se} - (\text{CH}_2)_7 - \text{COOH}$	9 - SELENAEPTADECANOIC ACID

Figure 1. Structures of the naturally occurring long-chain fatty acids stearic acid and palmitic acid and the unnatural fatty acids 9-telluraheptadecanoic acid (9-THDA) and 9-selenaheptadecanoic acid (9-SHDA) where the divalent heteroatom has been introduced to replace the C-9 methylene group of heptadecanoic acid.

These agents may be useful for the evaluation of regional cerebral blood flow (perfusion).

The radiolabeled tellurium fatty acids have been more extensively studied because of their potential applications for the detection and evaluation of heart disease. We have prepared a series of long-chain fatty acids in which divalent Te(II) has been inserted between two methylene units in the alkyl chain.⁹ Some of these agents show remarkable specificity for the heart muscle (myocardium), and the uptake is dependent upon total chain length.¹⁰ A model agent, 9-[^{125m}Te]telluraheptadecanoic acid (9-THDA; Figure 1), shows myocardial uptake similar to natural fatty acids like palmitic and stearic acids which are normally concentrated by the heart from the blood.¹¹ This agent is being extensively evaluated in laboratory animals for potential clinical applications.^{11,12} The unique feature exhibited by 9-THDA is the prolonged myocardial retention. After a rapid peak uptake, the myocardial radioactivity is very slowly lost or "washed-out" from the heart tissue.

In contrast to tellurium fatty acids like 9-THDA, the selenium analogue 9-selenaheptadecanoic acid (9-SHDA; Figure 1) shows marginal heart uptake, slow blood clearance, and a rapid loss from the myocardium.^{3,13} These major differences in the biological behavior of the Te and Se fatty acid analogues were unanticipated and could not be fully rationalized by a comparison of the relative physical properties such as differences in the carbon-heteroatom bond lengths, carbon-heteroatom-carbon bond angles, or heteroatom polarizability, electronegativity, etc. Since tissue distribution studies in rats with [¹⁰⁻¹⁴C]-9-THDA appeared to indicate that the intact 9-THDA molecule was retained in the myocardium,¹⁴ we proposed that an oxidative modification of the tellurium in the 9-THDA molecule may lead to a product that could be "trapped" in the myocardium by an unknown mechanism. The facile oxidation of diorganyl tellurides in comparison to the selenium analogues is well documented.¹ The photochemical oxidation of the tellurium compounds can often be avoided by working under red lights.^{2,15}

(8) Grigsby, R. A.; Knapp, F. F., Jr.; Callahan, A. P.; Ferren, L. A.; Irgolic, K. J. *J. Nucl. Med.* 1981, 22, 12.

(9) Knapp, F. F., Jr.; Ambrose, K. R.; Callahan, A. P.; Ferren, L. A.; Grigsby, R. A.; Irgolic, K. J. *J. Nucl. Med.* 1981, 22, 988.

(10) Knapp, F. F., Jr.; Ambrose, K. R.; Callahan, A. P.; Grigsby, R. A.; Irgolic, K. J. In "Radiopharmaceuticals II"; Society of Nuclear Medicine: New York, 1979.

(11) Elmaleh, D. R.; Knapp, F. F., Jr.; Yasuda, T.; Coffey, J. L.; Kowipoda, S.; Okada, R.; Strauss, H. W. *J. Nucl. Med.* 1981, 22, 994.

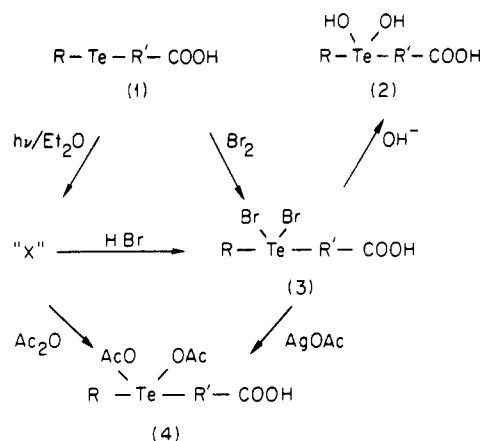
(12) Okada, R. D.; Knapp, F. F., Jr.; Elmaleh, D. R.; Pohost, G. W.; Yasuda, T.; Leppo, J.; Bocher, C. A.; Strauss, H. W. *Circulation* 1981, 65, 305.

(13) Knapp, F. F., Jr.; Butler, T. A.; Ambrose, K. R.; Callahan, A. P.; Guyer, C. E.; Roberts, J. A.; Ferren, L. A.; Grigsby, R. A.; Irgolic, K. J. In "Practical Applications of Nuclear and Radiochemistry"; Pergamon Press: New York, 1982; Chapter 23, pp 343-358.

(14) Knapp, F. F., Jr.; Vest, M.; Elmaleh, D. R.; Liss, R. H.; Strauss, H. W.; Ferren, L. A.; Callahan, A. P. *J. Nucl. Med.* 1981, 22, 75.

(15) Clive, D. L. J.; Chittattu, G. J.; Farina, V.; Kiel, W. A.; Menchen, S. M.; Russell, C. G.; Singh, A.; Wong, C. K.; Curtis, N. J. *J. Am. Chem. Soc.* 1980, 102, 4438.

Scheme I



Only recently have the properties of Te oxidation products of diorganyl tellurides been investigated in detail.¹⁶ Because the unusual properties of the tellurium fatty acids "trapped" in the heart may be very important for the development of new agents for the evaluation of heart disease, our goal in the present studies was to carefully examine the chemical oxidation products of 9-THDA.

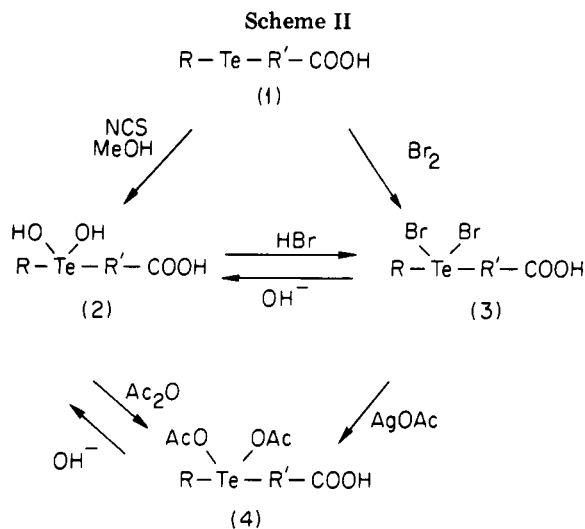
Results

In our early studies we observed that a heavy white precipitate ("X"; Scheme I) formed quickly when ether solutions of 9-telluraheptadecanoic acid (1, R = H₃C(CH₂)₇, R' = (CH₂)₇) were exposed to normal incandescent room lights. When such solutions were protected from light and stored at 4 °C, however, only minimal decomposition was observed by thin-layer chromatographic (TLC) analysis over a period of several weeks. These results suggested that 9-THDA underwent a rapid, photochemically induced oxidative decomposition in ether solution to an insoluble material of unknown composition. The white precipitate was insoluble in water and the usual organic solvents that were tested but readily dissolved in dilute alkali at room temperature. These results suggested that the carboxyl moiety was involved in the structure of the unknown material and that the framework of this material was disrupted upon conversion to the sodium salt. The existence of an oligomeric or polymeric structure involving interaction of the carboxyl group was postulated and further indicated since the oxidation products of methyl 9-telluraheptadecanoate (Me-9-THDA) and dioctyl telluride showed the expected solubility in organic solvents (vide infra).

Because of the unusual insolubility property, the autoxidation product "X" could not be analyzed directly by the usual physical methods such as proton nuclear magnetic resonance (NMR) and mass spectrometry (MS) but required conversion to compounds of known structure that could be obtained directly from the parent compound 9-THDA by well established procedures. Thus, the inherent structure of "X" required conversion to smaller components of known structure as shown in Scheme I.

Treatment of "X" with excess HBr gave a major product (3a, mp 55-57 °C) that was identical with 1-octyl-(1-carboxyheptan-7-yl)tellurium dibromide (3b, 9-THDA dibromide, mp 58-59.5 °C), formed directly by treatment of 9-THDA with Br₂ in CCl₄. In addition, Ac₂O acetylation of "X" gave the same diacetate 4 that was obtained by

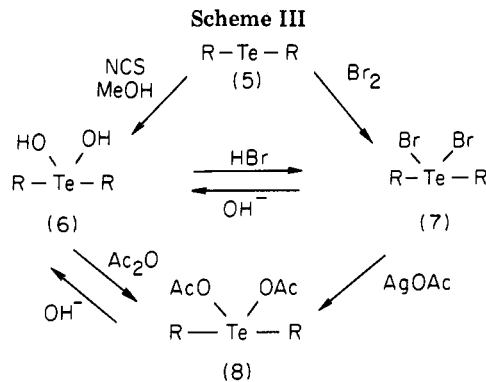
(16) Detty, M. R. *J. Org. Chem.* 1980, 45, 274.



silver(I) acetate treatment of the authentic 9-THDA dibromide **3b**. A key transformation in obtaining insight into the structure of "X" was obtained by NaOD treatment of 9-THDA dibromide **3**. The NMR spectrum of this solution was very similar to the spectrum of a NaOD solution of "X". Since treatment of **3** with NaOD was expected to convert the dibromide $R_2-Te-Br_2$ to the corresponding deuterated dihydroxy species $R_2-Te-[OD]_2$, the similarity in the spectra of the two solutions suggested that an oxidized product of 9-THDA was a major component of the material of unknown structure "X". This material probably also contains other minor components such as the tellurinic acids $R-TeOOH$ or $HOOC-R'-TeOOH$ that would be expected to be formed by cleavage of the carbon-tellurium bonds.

A study of the chemical oxidation products of 9-THDA under carefully controlled conditions was therefore initiated (Scheme II). We chose *N*-chlorosuccinimide (NCS) as the oxidizing species since a recent study has reported the oxidation of a variety of model diorganyl tellurides with this reagent.¹⁶ As expected, treatment of 9-THDA with 1 equiv of NCS gave a gummy product that was insoluble in organic solvents. The electron-impact mass spectral fragmentation of this material did not exhibit a molecular ion that corresponded to an oxygenated species which indicated that facile deoxygenation had occurred in the mass spectrometer. The elemental analyses, however, gave an empirical formula that was consistent with the structure of 1-octyl-(1-carboxyheptan-7-yl)tellurium dihydroxide (**2**, 9-THDA diol, $R = H_3C(CH_2)_7$, $R' = (CH_2)_7$; Scheme II). Further, the NMR spectrum of a NaOD solution of **2** was very similar to the NaOD spectrum of "X" (Scheme I). In addition, the diol **2** was converted to the diacetate **4** and the dibromide **3**. The latter was converted to **4** by treatment with silver(I) acetate, by the reactions described earlier. We were not able to obtain homogeneous oxidation products with *n*-butyl hypochlorite,¹⁶ and treatment of 9-THDA with this reagent gave a mixture of products.

Although the insolubility of the 9-THDA diol **2** precluded direct NMR analysis or molecular weight determination by the usual methods, an examination of the NCS oxidation products of methyl 9-telluraheptadecanoate (Me-9-THDA) and dioctyl ditelluride substantiated involvement of the carboxyl group in the unique structure of the insoluble NCS product of 9-THDA. Thus, NCS treatment of Me-9-THDA gave an oxidation product that was soluble in organic solvents and exhibited TLC mobility, elemental analysis, and NMR properties consistent with the expected dihydroxy structure.



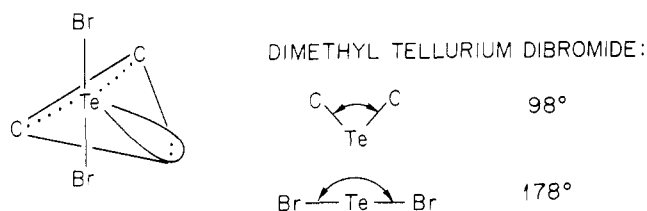
In contrast to the formation of the unexpected insoluble oxygenated product **2** formed by NCS oxidation of 9-THDA, similar NCS oxidation of the selenium analogue 9-selenaheptadecanoic acid (9-SHDA) gave the expected selenoxide 9-selenaheptadecanoic acid oxide, mp 73.5 °C. The elemental analysis, and infrared, mass spectral, and NMR spectral properties were consistent with the $H_3C-(CH_2)_7-Se(=O)(CH_2)_7COOH$ structure. Other workers have recently reported that diorganyl selenides form the expected selenoxides while tellurides give products that analyze for dihydroxy or hydrated telluroxide species.¹⁶

Dioctyl telluride was also treated with NCS and the oxidation product subjected to the transformations described earlier for the NCS product of 9-THDA. In this manner, the effect of the carboxyl group could be studied directly in a model compound. Thus, NCS oxidation of dioctyl telluride (**5**, $R = H_3C(CH_2)_7$; Scheme III) gave dioctyltellurium dihydroxide (**6**) that exhibited the expected solubility in the usual organic solvents. Treatment of the diol **6** with HBr gave the oily dibromide **7a** that was identical with dioctyltellurium dibromide (**7b**) formed by Br_2 treatment of the telluride **5**. Furthermore, the diacetate **8a** prepared by Ac_2O treatment of the diol **6** was identical with the diacetate formed by silver(I) acetate treatment of the authentic dibromide **7b**. The elemental analyses and NMR spectrum of the telluride **5**, diol **6**, dibromide **7b** and the NMR spectral properties of the diacetates **8a,b** were consistent with those of the proposed structures.

Discussion

Although the structure of the insoluble autoxidation product "X" and the NCS product **1** could not be elucidated by the usual physical methods, transformations of "X" to known derivatives of 9-THDA and the normal behavior of the NCS oxidation products of Me-9-THDA and dioctyl telluride (Scheme III) strongly suggest the structure of the insoluble 9-THDA oxidation product involves interaction between the terminal carboxyl moiety and the geminal hydroxyl groups. This unexpected finding is consistent with the prolonged myocardial retention in experimental animals that has been observed after intravenous administration of radiolabeled 9-THDA.

In contrast, we have found that the analogous selenium fatty acids such as 9-selenaheptadecanoic acid (9-SHDA; Figure 1) do not suffer facile autoxidation as observed with 9-THDA. Chemical oxidation of selenides, as described in this study and more extensively elsewhere,¹⁶ form the expected selenoxides. Evidently, the tetravalent diorganyl-selenium dihydroxide compounds are nonexistent, and the diorganyl selenoxide is the preferred bonding structure. Thus, even if selenium oxidation products could be formed by *in vivo* oxidation after the selenium fatty acids cross the myocardial cell membrane, they would not



ARE THE -OH GROUPS IN THE DIOLS
AXIAL OR DO ISOMERS EXIST ?

Figure 2. The typical trigonal-bipyramidal structure of Te(IV) compounds, illustrated for dimethyltellurium dibromide.

be expected to exhibit the unique insolubility or "trapping" properties observed for the tellurium fatty acids.

In fact, the chemical properties of the oxidized selenium fatty acids correlate directly with the biological properties that we have observed with the ^{75}Se -labeled agents such as 9- ^{75}Se selenahaptadecanoic acid. In contrast to the prolonged myocardial retention or "trapping" observed with 9- $^{123\text{m}}\text{Te}$ telluraheptadecanoic acid, even those ^{75}Se -labeled selenium fatty acids that show significant myocardial uptake such as 13-selenaheneicosonic acid show a relatively rapid release or "washout" from the heart tissue. These differences were further substantiated by a dual-labeling experiment involving injection of a mixture of 9- $^{123\text{m}}\text{Te}$ THDA and 9- ^{75}Se SHDA.³

We have also observed a dramatic difference in the properties of the radioactive contents of the heart tissue from rats after intravenous injection of 9- $^{123\text{m}}\text{Te}$ THDA and 9- ^{75}Se SHDA. The majority of the radioactivity could be extracted from the heart tissue by homogenization with CHCl_3 -MeOH (Folch medium) after injection of 9- ^{75}Se SHDA to rats. Analysis by TLC demonstrated that the radioactivity chromatographed with the expected mobility of di- and triglycerides. Since incorporation into glycerides in myocardial lipid droplets is the normal storage mode for exogenous long-chain fatty acids, these results demonstrate that this aspect of fatty acid metabolism operates for the unnatural selenium fatty acids. In contrast, we have been unable to extract radioactive lipids by these methods from heart tissue after injection of $^{123\text{m}}\text{Te}$ -labeled fatty acids such as 9-THDA. In addition to the Folch method, homogenization with dilute alkali removed only a small amount of radioactivity. We have found that the majority of the radioactivity remained associated with the tissue pulp after treatment with either organic solvent or base (unpublished studies).

The stereochemistry of the Te(IV) species described in Schemes I-III has not been established. Presumably, the two tellurium-carbon bonds lie in a trigonal plane with the tellurium lone electron pair, and the bromine (compounds 3 and 7) and oxygen (compounds 2, 4, 6, and 8) heteroatoms occupy the apices of the bipyramid. This is illustrated for the structure of dimethyltellurium dibromide in Figure 2, which has been established by X-ray diffraction.¹⁷ This configuration has been found for this example and many other cases of tetravalent Te(IV) species that have been studied by X-ray techniques. The possibility of an equilibrium between the $\text{R}_2\text{Te}(\text{OH})_2 \rightleftharpoons \text{R}_2\text{Te}=\text{O} \cdot \text{H}_2\text{O}$ species of 2 (Schemes I and II) and 6 (Scheme III) has been suggested by other workers¹⁶ and cannot be excluded in the present studies. Conversion of the diols 2 and 6 to the diacetates 4 and 8, respectively, however, suggests that the dihydroxy species probably exist and that

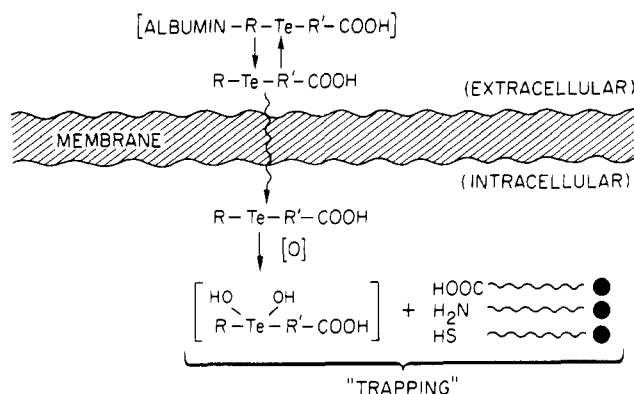


Figure 3. Potential model to account for the unique intracellular "trapping" observed with 9-telluraheptadecanoic acid (9-THDA). In this model the intracellular concentration of the "soluble" 9-THDA molecule precedes an oxidation that leads to a complex of unknown structure that is "trapped" within the myocardial cells.

the geminal oxygen species can be "frozen" by conversion to the diacetates.

Studies presently in progress are directed toward obtaining crystals of 9-THDA dibromide 3 since this derivative represents the only well-defined crystalline Te(IV) species formed in the present studies that may be amenable to X-diffraction studies. In addition, we are also attempting to determine if the new Laser Microprobe Mass Analysis (LAMMA)¹⁸ technique is sufficiently sensitive to determine the subcellular distribution of Te in myocardial cells after intravenous administration of 9-THDA to rats. This unique microprobe analytical technique involves focused laser analysis of microscopic areas of tissue slices followed by element-specific analysis by time-of-flight mass spectrometry.

Since the 9-THDA oxidation product is very insoluble except in basic solutions, oxidation of the 9-THDA prior to crossing the myocardial cell membrane after intravenous administration of the 9-THDA-albumin complex would appear unlikely. The unique "trapping" could be explained, however, by intracellular oxidation of 9-THDA after crossing the myocardial cell membrane as shown in Figure 3. We have found that the geminal hydroxyl groups of 9-THDA diol (Scheme II) are very reactive and readily form insoluble complexes of unknown structure. If the oxidation that occurs within the cell is similar to what we have observed experimentally, the geminal hydroxyl groups of the 9-THDA oxidation product could interact with carboxyl, amino, or thiol groups present in various biomolecules encountered in the cytosol or within the mitochondria. Because of the insolubility of the 9-THDA oxidation product, it appears that translocation into the cell precedes oxidation.

The studies described in this paper have provided important indirect evidence that the unique myocardial trapping observed with various tellurium long-chain fatty acids may result from the formation of insoluble oxygenated species by intracellular oxidation of the tellurium agents. This biological behavior was unanticipated and has stimulated the development of a new class of radio-labeled tellurium long-chain fatty acids that may have important diagnostic applications in the evaluation of regional myocardial blood flow (perfusion) and aberrations in fatty acid oxidation that may develop in the early stages of heart disease. In addition to $^{123\text{m}}\text{Te}$ -labeled agents such as 9-THDA, fatty acids containing stable tellurium and

(17) Gillespie, R. J. *Can. J. Chem.* 1961, 39, 318.

(18) Hirche, H. J.; Heinrichs, J.; Schaefer, H. E.; Schramm, M. *Fresenius Z. Anal. Chem.* 1981, 308, 224.

radiolabeled with iodine isotopes attached to a terminal phenyl group¹⁹ or a vinyl iodide moiety²⁰ are also being investigated.

Experimental Section

General Data. All chemicals and solvents were analytical grade and were used without further purification. The methyl 9-telluraheptadecanoate (Me-9-THDA) and 9-telluraheptadecanoic acid (9-THDA) were prepared as described earlier and exhibited the expected physical properties.¹⁰ Column chromatography was performed with acidic grade silicic acid, 60–200 mesh (Sigma Chemical Co.). The melting points were determined in open capillary tubes using a Buchi SP apparatus and are uncorrected. The thin-layer chromatographic analysis (TLC) were performed by using 250- μ m thick layers of silica gel G PF-254 coated on glass plates (Analtech, Inc.). The infrared spectra (IR) were recorded on a Beckman 18-A spectrophotometer with NaCl plates or KBr pellets. The low-resolution mass spectra (MS) were recorded by using a Kratos MS-25 low-resolution instrument under the following conditions: ionizing energy, 70 eV; accelerating potential, 8000 V; trap current, 100 μ A; probe temperature, 200–300 °C. The proton nuclear magnetic resonance spectra (NMR) were obtained at 60 MHz with a Varian 360-A instrument or at 200 MHz with a Nicolet high-resolution instrument. Samples (30–40 mg) were dissolved in the solvents indicated and resonances are reported downfield (δ) from the internal tetramethylsilane standard. Elemental analyses were determined at Galbraith Laboratories, Knoxville, TN. Unless otherwise indicated, the tellurium compounds were handled under red lights and inert atmosphere to minimize photochemical decomposition or autoxidation.

Methyl 9-Selenaheptadecanoate. Selenium metal (790 mg, 10 mmol) was stirred in absolute EtOH (50 mL) under argon at 0–5 °C. Powdered NaBH₄ (380 mg, 10 mmol) was added in small increments and the mixture stirred until the Se had dissolved and the solution became colorless (Na₂Se). The solution was warmed to room temperature, and following the addition of 230 mg (10 mmol) of Na metal in ~10 mL of absolute EtOH, a mixture of methyl 8-bromooctanoate (2.32 g, 0.97 mmol) and bromooctane (2.01 g, 1.04 mmol) was added dropwise in 20 mL of absolute EtOH. The mixture was stirred 2 h at room temperature, diluted with H₂O, and extracted three times (50 mL) with ether. The combined extracts were washed with water (3 \times) and dried over anhydrous Na₂SO₄, and the solvent was removed in vacuo. The oily product was applied in petroleum ether to a silicic acid column (200 g) and fractions 100 mL in volume eluted with petroleum ether (1–6) and C₆H₆ (7–16). Aliquots of the fractions were monitored by TLC (solvent C₆H₆), and fractions 11 and 12 were combined to give 1.16 g (33%) of methyl 9-selenaheptadecanoate as an oil: TLC, *R_f* 0.33 (C₆H₆); IR (neat) 1180 (s), 1440 (s), 1465 (s), 1750 (vs), 2860 (vs), 3300 (vs) cm⁻¹; low-resolution MS, ions at *m/z* (relative intensity) 350 (M⁺[⁸⁰Se], 85), 319 (M⁺[⁸⁰Se] – 31, 12), 205 (21), 193 ([⁸⁰Se], 22); high-resolution MS, *m/z* calcd for C₁₇H₃₄O₂Se 350.1723, found 350.1714; NMR (CDCl₃) δ 0.88 (t, *J* \approx 6 Hz, 3 H terminal CH₃), 2.33 (t, *J* \approx 8 Hz, 2 H, CH₂COOCH₃), 2.57 (t, *J* \approx 8 Hz, 4 H, CH₂SeCH₂), 3.66 (s, 3 H, COOCH₃). Anal. Calcd for C₁₇H₃₄O₂Se: C, 58.44; H, 9.81. Found: C, 58.67; H, 9.89.

Selenoxide of Methyl 9-Selenaheptadecanoate. The ester (349 mg, 1 mmol) was dissolved in 2 mL of a 1:1 mixture of CH₂Cl₂–CH₃OH at 0 °C. After the addition of *N*-chlorosuccinimide (NCS; 143 mg, 1.05 mmol), the mixture was stirred 30 min at 0–5 °C, 2 mL of CH₂Cl₂ was then added followed by 3 mL of 10% NaOH, and the mixture was stirred 5 min. The organic layer was obtained, washed with H₂O (2 \times), and dried over anhydrous Na₂SO₄, and the solvent was removed in vacuo to give 282 mg (77%) of the selenoxide as a white solid: mp 61 °C; TLC, *R_f* 0.67 (8% MeOH–CHCl₃); IR (neat) 805 (s), 1175 (s), 1200 (s), 1235 (s), 1445 (s), 1465 (s), 1745 (vs), 2860 (vs), 2920 (vs) cm⁻¹; MS, M⁺ at *m/z* 366 (⁸⁰Se) absent, ions present at *m/z* (relative intensity) 350 (M⁺[⁸⁰Se] – 16, 35; M⁺ of methyl 9-selenaheptadecanoate), 205 ([⁸⁰Se], 20), 193 ([⁸⁰Se], 28); NMR (CDCl₃) δ 0.81

(t, *J* \approx 6 Hz, 3 H, terminal CH₃), 2.23 (t, *J* \approx 10 Hz, 2 H, CH₂COOCH₃), 2.47 (t, *J* \approx 10 Hz, 4 H, CH₂Se(O)CH₂), 3.59 (s, 3 H, COOCH₃).

9-Selenaheptadecanoic Acid. The ester (175 mg, 0.5 mmol) was dissolved in absolute EtOH (50 mL) and refluxed under argon with 1 mL of 1 N NaOH for 1 h. After being cooled, the mixture was diluted with H₂O and acidified to pH 2–3 with 1 N HCl, and the cloudy solution was extracted with ether (3 \times). The combined extracts were washed with H₂O (3 \times) and dried over anhydrous Na₂SO₄, and the solvent was removed in vacuo to give a white solid. Crystallization from petroleum ether gave the acid as white plates (148 mg, 85%): mp 39 °C; TLC, *R_f* 0.50 (8% MeOH–CHCl₃); low-resolution MS, ions at *m/z* (relative intensity) 336 (M⁺[⁸⁰Se], 54), 206 (rearrangement ion, 7), 192 (20); high-resolution MS, *m/z* calcd for C₁₆H₃₂SeO₂ 336.1566, found 336.1577; NMR (CDCl₃) δ 0.82 (t, *J* \approx 6 Hz, 3 H, terminal CH₃), 2.28 (t, *J* \approx 8 Hz, 3 H, CH₂COOH), 2.43 (t, *J* \approx 8 Hz, 4 H, CH₂SeCH₂). Anal. Calcd for C₁₆H₃₂SeO₂: C, 57.28; H, 9.62. Found: C, 57.30; H, 9.71.

Selenoxide of 9-Selenaheptadecanoic Acid. The 9-selenaheptadecanoic acid (83 mg, 0.25 mmol) was treated with NCS (37 mg, 0.27 mmol) in 1 mL of a 1:1 mixture of CH₂Cl₂–MeOH at 0 °C for 30 min. After the addition of CH₂Cl₂ (2 mL) and 1 N NaOH (2 mL), the aqueous layer was washed with CH₂Cl₂, acidified with CH₃COOH, and cooled. The precipitate was washed with H₂O and dried to give 70 mg (80%) of the selenoxide: mp 73.5 °C; TLC, *R_f* 0.35 (8% MeOH–CHCl₃); IR (KBr) 750 (s), 905 (w), 1095 (w), 1340 (s), 1460 (s), 1675 (br s), 2850 (vs), 2920 (vs) cm⁻¹; MS, M⁺ at *m/z* 356 (⁸⁰Se) absent, ion present at *m/z* (relative intensity) 336 (M⁺[⁸⁰Se] – 16, 20; M⁺ of 9-selenaheptadecanoic acid); NMR (CDCl₃) δ 0.82 (t, *J* \approx 6 Hz, 3 H, terminal CH₃), 1.72 (t, *J* \approx 6 Hz, 4 H, CH₂CH₂Se(O)CH₂CH₂), 2.10 (t, *J* \approx 6 Hz, 2 H, CH₂COOH), 2.96 (m, 4 H, CH₂Se(O)CH₂).

Oxidation of 9-Telluraheptadecanoic Acid. a. NCS Oxidation of 9-THDA. In a typical preparation, the 9-THDA (287 mg, 0.74 mmol) was dissolved in 2 mL of the 1:1 mixture of CH₂Cl₂–MeOH and stirred with NCS (107 mg, 0.79 mmol) for 0 °C for 30 min. The reaction mixture was then treated with 3 mL of CH₂Cl₂ and 7 mL of 1 N NaOH and stirred for 5 min. The CH₂Cl₂ was then decanted and washed with H₂O. The H₂O layers were combined, cooled to 0–5 °C, and acidified with acetic acid to give a gummy precipitate that was insoluble in all organic solvents tested but was soluble in 1 N NaOH: IR (KBr) <600 (br s), 650 (w), 680 (s), 1220 (s), 1270 (vs), 1355 (vs), 1450 (vs), 1630 (vs), 2820 (vs), 2880 (vs) cm⁻¹; low-resolution MS, M⁺ at *m/z* 420 absent, ions present at *m/z* (relative intensity) 398 ([¹³⁰Te], <5, rearrangement ion, composition unknown), 386 ([¹³⁰Te], M⁺ of 9-THDA, M⁺ – H₂O, 5), 356 ([¹³⁰Te], <5), 256 (rearrangement ion, C₁₅M₁₄OTe, ~5); NMR (0.1 N NaOD) δ 0.88 (t, *J* \approx 6 Hz, 3 H, terminal CH₃), 2.18 (m, 4 H, CH₂CH₂Te[(OH)₂]CH₂CH₂), 2.81 (t, *J* \approx 10 Hz, 4 H, CH₂Te[(OH)₂]CH₂). Anal. Calcd for C₁₆H₃₄TeO₄: C, 46.04; H, 8.15. Found: C, 46.28; H, 8.18.

b. Autoxidation of 9-THDA. The 9-THDA (216 mg, 0.56 mmol) was dissolved in ether (20 mL) and exposed to incandescent room lights for 24 h. The resulting white solid was filtered to give 112 mg of "X" (Scheme I) as a white solid: yellow gummy mass at mp ~147 °C, orange gum at mp ~165 °C, red gum at mp ~185 °C, red mass at mp ~210 °C, black residue at mp ~265 °C; IR (KBr) 660 (vs), 1240 (s), 1275 (s), 1375 (vs), 1465 (s), 1620 (br s), 2850 (vs), 2920 (s), 3440 (br) cm⁻¹; MS, M⁺ at *m/z* 420 absent, ions present at *m/z* (relative intensity) 386 ([¹³⁰Te], 5; M⁺ of 9-THDA), 356 ([¹³⁰Te], 25), 256 ([¹³⁰Te], <5, rearrangement ion of 9-THDA), 242 (10); NMR (0.1 N NaOD) δ 0.83 (t, *J* \approx 6 Hz, 3 H, terminal CH₃), 2.13 (t, *J* \approx 10 Hz, 4 H, CH₂CH₂Te[(OH)₂]CH₂CH₂), ~2.35 (m, ~2 H, CH₂COOH), 2.76 (t, *J* \approx 10 Hz, 4 H, CH₂Te[(OH)₂]CH₂). Anal. Found: C, 42.15; H, 6.75; O, 12.98.

c. From NaOH Treatment of the Dibromide of 9-THDA. The oxygenated species 2 (Scheme I) was also prepared by NaOH treatment of the dibromides formed by Br₂ treatment of 9-THDA (3b) and HBr treatment of the NCS oxidation product of 9-THDA (3a). The oxygenated products formed from 3a and 3b exhibited the same NMR properties.

Dibromide of 9-Telluraheptadecanoic Acid (3): 1-Octyl(1-carboxyheptan-7-yl)tellurium Dibromide (9-THDA Dibromide). a. Treatment of 9-THDA with Br₂. The 9-THDA (386 mg, 1 mmol) was dissolved in 2.5 mL of CCl₄ and

(19) Goodman, M. M.; Knapp, F. F., Jr. *J. Org. Chem.* 1982, 47, 3004.

(20) Knapp, F. F., Jr.; Goodman, M. M.; Kabalka, G. W.; Sastry, K. A. R.; Callahan, A. P. *J. Nucl. Med.* 1982, 23, 10.

treated dropwise at room temperature with a solution of Br₂ (168 mg, 1.05 mmol) in 2.5 mL of CCl₄. After 5 min the solvent was evaporated under argon and the gummy product triturated with petroleum ether to give a white solid. Crystallization from petroleum ether gave 463 mg (85%) of 9-THDA dibromide: mp 58–59.5 °C; TLC, *R_f* 0.65 (8% MeOH–CHCl₃); IR (KBr) 1180, 1440, 1470, 1745 cm⁻¹; MS, M⁺ at *m/z* 548 (¹³⁰Te⁸¹Br) absent, ions present at *m/z* (relative intensity) 467 [M⁺(¹³⁰Te) – Br, <5], 386 [M⁺(¹³⁰Te) – Br₂, 40], 256 (rearrangement ion, C₁₅H₁₄O₂Te, 18); NMR (CDCl₃) δ 0.81 (t, *J* ≈ 6 Hz, terminal CH₃), 2.36 (m, 6 H, CH₂COOH and CH₂CH₂Te(Br₂)CH₂CH₂), 3.58 (t, 4 H, *J* ≈ 10 Hz, CH₂Te(Br₂)CH₂). Anal. Calcd for C₁₆H₃₂TeO₂Br₂: C, 35.35; H, 5.89; Br, 29.46. Found: C, 35.57; H, 6.00; Br, 29.68.

b. Treatment of the NCS Product of 9-THDA with HBr. The gummy NCS oxidation product of 9-THDA (2; Scheme II) was dried in vacuo to give a glossy solid (100 mg, 0.24 mmol) that was treated with concentrated HBr. A white precipitate formed immediately that was filtered and crystallized from petroleum ether to give 32 mg of 3 (Scheme II): mp 55–57 °C; TLC, *R_f* 0.65 (8% MeOH–CHCl₃); low-resolution MS and NMR identical with that described above for the dibromide 3 formed directly by Br₂ treatment of 9-THDA.

c. Treatment of the Autoxidation Product of 9-THDA with HBr. The autoxidation product of 9-THDA was dissolved in 1 N NaOD for NMR analysis as described above. Treatment with dilute HBr solution gave a precipitate that was extracted with CHCl₃. Evaporation of the solvent gave a white solid that exhibited TLC, MS, and NMR properties identical with those of authentic 9-THDA dibromide.

Diacetate of the Diol of 9-Telluraheptadecanoic Acid. a. Acetic Anhydride Treatment of the NCS Oxidation Product of 9-THDA. The NCS oxidation product (70 mg) of 9-THDA (2, Scheme II) was treated with excess acetic anhydride at 50 °C for 1 h. Evaporation of the solvent gave an oil that was homogeneous: TLC, *R_f* 0.47 (8% MeOH–CHCl₃); IR (KBr) 710, 1270, 1365, 1650 cm⁻¹; low-resolution MS, M⁺ at *m/z* 518 absent, ion present at *m/z* (relative intensity) 400 [¹³⁰Te], 5, M⁺ of 9-telluraheptadecanoic acid; NMR (CDCl₃) δ 0.91 (t, 3 H, terminal CH₃), 2.00 (s, 6 H, acetate CH₃'s), 2.95 (t, *J* = 8 Hz, 6 H, CH₂C–OOCH₃ and CH₂Te(OAc₂)CH₂).

b. Acetic Anhydride Treatment of the Autoxidation Product of 9-THDA. The white solid (32 mg) obtained by autoxidation of 9-THDA ("X"; Scheme I) was treated with excess acetic anhydride at 50 °C for 1 h. The solvent was evaporated in vacuo and the resulting oil dissolved in CDCl₃ and filtered. The TLC mobility and NMR spectrum were identical with those of authentic diacetate prepared from the AgOAc treatment of 9-THDA dibromide described below and the product prepared by Ac₂O treatment of the NCS oxidation product of 9-THDA.

c. Silver(I) Acetate Treatment of 9-THDA Dibromide. The 9-THDA dibromide (54 mg, 0.1 mmol) was treated in MeOH with silver(I) acetate (33 mg, 0.20 mmol) at room temperature for 1 h. The solution was filtered and the solvent removed under argon to give an oil (50 mg) that had the same NMR spectrum (CDCl₃) and TLC mobility as the diacetate formed in (a) above by Ac₂O treatment of the 9-THDA NCS product.

NCS Oxidation of Methyl 9-Telluraheptadecanoate. The methyl-9-THDA (300 mg, 0.75 mmol) was stirred at 0 °C in 20 mL of a 1:1 mixture of CH₂Cl₂–MeOH with 114 mg (1 mmol) of NCS for 30 min. After 20 mL of CH₂Cl₂ and 5 mL of 10% NaOH was to the mixture, it was stirred 5 min. The organic layer was washed with H₂O and dried over anhydrous MgSO₄, and the solvent was evaporated to give an oil: TLC, *R_f* 0.24 (4% MeOH–CHCl₃); IR (neat) <600 (vs), 1045 (s), 1175 (s), 1440 (s), 1465 (s), 1745 (vs), 2850 (vs), 2850 (vs), 2930 (vs); MS, ions at *m/z* (relative intensity) 400 (M⁺[¹³⁰Te] – H₂O₂, 25, M⁺ of methyl 9-telluraheptadecanoate), 356 ([¹³⁰Te], 8), 256 ([¹³⁰Te], 13, rearrangement ion); NMR (CDCl₃) δ 0.88 (t, *J* ≈ 6 Hz, 3 H, terminal CH₃), 1.73 (m, 4 H, CH₂CH₂Te[(OH)₂]CH₂CH₂), 2.31 (t, *J* ≈ 10 Hz, 2 H, CH₂COOCH₃), 2.62 (t, *J* ≈ 10 Hz, 4 H, CH₂TeCH₂), 3.67 (s, 3 H, COOCH₃).

Diocetyl Telluride (5). Tellurium metal (2.54 g, 10 mmol) was refluxed under argon in 43 mL of a 20% solution of NaOH containing 2.7 g of KBH₄. After 1.5 h the mixture turned a deep purple (Na₂Te₂) and after it was refluxed an additional 30 min, the solution turned pale yellow (Na₂Te) and no tellurium metal

remained. Bromooctane (7.72 g, 40 mmol) was added in 50 mL of MeOH and the solution refluxed 30 min and cooled. The mixture was poured into 100 mL of H₂O and extracted with ether (3×). The combined extracts were washed thoroughly with H₂O, dried over anhydrous Na₂SO₄, and filtered, and the solvent was removed in vacuo to give 6.6 g (95%) of dioctyl telluride as an oil. Distillation at 154 °C at 0.7 mmHg gave 5.5 g (78%) of the analytical sample: TLC, *R_f* 0.85 (C₆H₆); IR (neat) 1120, 1265, 1350, 1430, 2780, 2870, 2980 cm⁻¹; low-resolution MS, ions at *m/z* (relative intensity) 358 (M⁺[¹³⁰Te], 12); NMR (CDCl₃) δ 0.7, (t, 6 H, *J* ≈ 6 Hz, terminal CH₃'s), 2.52 (t, 6 H, *J* ≈ 10 Hz, CH₂TeCH₂). Anal. Calcd for C₁₆H₃₄Te: C, 54.26; H, 9.68. Found: C, 54.14; H, 9.57.

Diocetyl tellurium Dihydroxide (6). Dioctyl telluride (5; 1.76 g, 5 mmol) was treated with NCS (721 mg, 5.3 mmol) in 20 mL of a 1:1 mixture of CH₂Cl₂–MeOH. After the mixture was stirred 10 mL of CH₂Cl₂ was added followed by 20 mL of 10% NaOH. The organic layer was washed with H₂O, dried over anhydrous Na₂SO₄, and evaporated to give a gummy solid. Trituration with petroleum ether gave a white solid: mp 78 °C; TLC, *R_f* 0.20 (8% MeOH–CHCl₃); low-resolution MS, M⁺ at *m/z* 390 (¹³⁰Te) not present, ion present at *m/z* (relative intensity) 356 (M⁺[¹³⁰Te] – H₂O₂, <5, M⁺ of dioctyl telluride); NMR (CDCl₃) δ 0.89 (t, *J* ≈ 6 Hz, 6 H, terminal CH₃'s), 2.80 (t, *J* ≈ 10 Hz, 4 H, CH₂TeCH₂). Anal. Calcd for C₁₆H₃₆TeO₂: C, 49.61; H, 9.30. Found: C, 49.80; H, 9.35.

Diocetyl tellurium Dibromide (7). a. Treatment of Dioctyl Telluride with Br₂. Dioctyl telluride (1.76 g, 5 mmol) was treated in CCl₄ with Br₂ (800 mg, 10 mmol) at room temperature. The solvent was evaporated at room temperature to give the dibromide as light yellow oil (87%); TLC, *R_f* 0.75 (C₆H₆); IR (neat) 715 (w), 785 (w), 1165 (w), 1200 (w), 1380 (w), 1400 (w), 1460 (s) cm⁻¹; low-resolution MS, M⁺ at *m/z* 508 absent, ions present at *m/z* (relative intensity) 435 (M⁺[¹³⁰Te⁸²Br] – Br, 36), 356 (M⁺[¹³⁰Te] – Br₂, 90, M⁺ of dioctyl telluride); NMR (CDCl₃) δ 0.89 (t, *J* ≈ 6 Hz, 6 H, terminal CH₃'s), 2.17 (t, 4 H, *J* ≈ 6 Hz, CH₂CH₂Te(Br₂)CH₂CH₂), 3.62 (t, *J* ≈ 10 Hz, 4 H, CH₂Te(Br₂)CH₂). Anal. Calcd for C₁₆H₃₄TeBr₂: C, 37.42; H, 6.62. Found: C, 37.15; H, 6.85.

b. Treatment of the NCS Product of Dioctyl Telluride with HBr. The NCS oxidation product of dioctyl telluride 6 was treated with HBr as described for 2 (Scheme II). The product exhibited the same TLC and NMR properties as the product obtained by direct bromination of dioctyl telluride as described above.

Diocetyl tellurium Diacetate (8). a. Acetic Anhydride Treatment of the NCS Product of Dioctyl Telluride. The NCS oxidation product of dioctyl telluride 6 (100 mg, 0.26 mmol) was treated with excess Ac₂O at 50 °C. After dilution with H₂O, the reaction mixture was extracted with CH₂Cl₂, washed with H₂O, and dried over anhydrous Na₂SO₄, and the solvent was evaporated under argon to give 100 mg (83%) of the diacetate as an oil: TLC, *R_f* 0.05 (C₆H₆); IR (neat) 610 (w), 660 (vs), 940 (w), 1005 (s), 1280 (vs), 1375 (s), 1650 (vs), 285 (vs), 2920 (vs), 2960 (w) cm⁻¹; low-resolution MS, M⁺ at *m/z* 474 not present, ion present at *m/z* (relative intensity) 356 (M⁺[¹³⁰Te] – HOAc₂, 20, M⁺ of dioctyl telluride); NMR (CDCl₃) δ 0.86 (t, *J* ≈ 6 Hz, 6 H, terminal CH₃'s), 2.01 (s, 6 H, acetate CH₃'s), 2.90 (t, *J* ≈ 10 Hz, 4 H, CH₂Te(OAc₂)CH₂).

b. Silver Acetate Treatment of the Dibromide of Dioctyl Telluride (7). The dioctyl tellurium bromide (7) was treated with AgOAc and the product, obtained in the usual way, had identical TLC mobility and NMR properties as those of the authentic diacetate 8 obtained by acetylation of the NCS product of dioctyl telluride 6.

Acknowledgment. Research sponsored by the Office of Health and Environmental Research, U.S. Department of Energy, under Contract W-7405-eng-26 with the Union Carbide Corp. and supported in part by USPHS Grant HL-27209 from the National Institutes of Health. We thank L. S. Ailey for typing the manuscript.

Registry No. 1 (R = H₃C(CH₂)₇, R' = (CH₂)₇), 84057-02-3; 1 (R = H₃C(CH₂)₇, R' = (CH₂)₇) methyl ester, 84057-03-4; 2 (R = H₃C(CH₂)₇, R' = (CH₂)₇), 84057-04-5; 2 (R = H₃C(CH₂)₇, R'

= (CH₂)₇ methyl ester, 84057-05-6; 3 (R = H₃C(CH₂)₇, R' = (CH₂)₇), 84057-06-7; 4 (R = H₃C(CH₂)₇, R' = (CH₂)₇), 84057-07-8; 5 (R = (CH₂)₇CH₃), 84057-08-9; 6 (R = (CH₂)₇CH₃), 84057-09-0; 7 (R = (CH₂)₇CH₃), 84057-10-3; 8 (R = (CH₂)₇CH₃), 84057-11-4;

9-SHDA, 50514-64-2; 9-SHDA, Se oxide, 84057-12-5; Me-9-SHDA, 84057-13-6; Me-9-SHDA, Se oxide, 84057-14-7; Se, 7782-49-2; Te, 13494-80-9; methyl 8-bromooctanoate, 26825-92-3; bromooctane, 111-83-1.

Scope of Anion Addition to (η^4 -1,3-Cyclohexadiene)tricarbonyliron(0)

M. F. Semmelhack* and James W. Herndon

Department of Chemistry, Princeton University, Princeton, New Jersey 08544

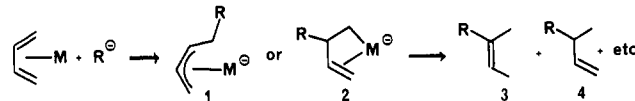
Received October 26, 1982

Reactive carbanions add to (η^4 -1,3-cyclohexadiene)tricarbonyliron(0) to produce intermediates that can be protonated to give 2- or 3-substituted cyclohexenes as the major products. Alkylolithium reagents react inefficiently, primarily by addition to a coordinated carbon monoxide to produce simple aldehydes along with ketones from addition to the diene ligand. Trapping of the intermediates with other electrophiles generally fails, with regeneration of the starting complex being the preferred pathway. However, benzoyl chloride was observed to react with the intermediate from trityl anion and (η^4 -1,3-cyclohexadiene)tricarbonyliron(0) to give a 1,4-disubstituted 2-cyclohexene. The regioselectivity of addition is not clear from the additions to the 1,3-cyclohexadiene ligand, but preliminary results concerning the addition of 2-lithio-2-methylpropionitrile to (η^4 -1,3-butadiene)tricarbonyliron(0) require that addition is preferred at C-2 of the 1,3-diene ligand.

Introduction

The ability of nucleophiles to add to carbon-carbon double bonds is enhanced by coordination with transition metals. Specific types of complexes bearing alkene,^{1,2} allyl,³ propargyl,⁴ cyclohexadienyl,⁵ and arene⁶ ligands have been developed for organic synthesis. Absent from this list are examples of addition of carbon nucleophiles to coordinated 1,3-dienes. We are aware of a single example of carbon-carbon bond formation by addition of carbon anions to a discrete (η^4 -1,3-diene)metal complex. In this case, cyanide anion was observed to add at C-1 of the diene ligand in (η^3 -allyl)(η^4 -1,3-butadiene)(η^6 -benzene)molybdenum(II).⁷ Palladium(II)-promoted addition of nucleophiles to 1,3-butadiene has been demonstrated for a variety of nucleophiles and is beginning to be developed as a synthesis method for 1,4-disubstituted alkenes.⁸ However, these reactions are more likely examples of nucleophile addition to (η^2 -alkene)palladium(II) complexes; the details of the process are not yet clear.

Coupling of carbon nucleophiles with 1,3-diene ligands offers special opportunities for organic synthesis. The 1,3-diene unit is common in open-chain systems and in rings and is known to form stable complexes with a variety of transition metals. The initial addition might give either an allylmetal complex (1) or a chelated homoallyl arrangement (2), and each of these intermediates has im-



portant potential in synthesis. The metal system in 1 and 2 might be cleaved by protonation (to give 3, 4, or other isomers), by carbonylation, by direct coupling with alkenes and organic halides, etc. While the idea of adding carbon nucleophiles to coordinated 1,3-dienes is a simple extension of recent organo-transition-metal studies, there are important questions to answer in developing the idea as synthesis methodology. In the general development of nucleophile addition to alkene, allyl, cyclohexadienyl, and arene ligands, a major question in each case has concerned the range of anions that add efficiently. In many cases, alternate pathways such as ligand displacement and electron-transfer reduction of the metal completely prevent simple addition to the ligand. Solutions to these problems can sometimes be found through choice of solvent,⁹ other ligands on the metal,¹⁰ and modification of the nucleophile itself.¹¹

In choosing the appropriate diene-metal system for development, we were attracted to the Fe(CO)₃ activating

(1) The complexes of cyclopentadienyldicarbonyliron(II) with olefins have been studied extensively. For examples, see: Rosenblum, M. *Acc. Chem. Res.* 1974, 7, 122-128.

(2) Examples of oxygen and nitrogen nucleophiles adding to (olefin)-palladium(II) complexes are numerous. General addition of carbon nucleophiles has been realized only recently. For examples, see: Hegedus, L. S.; Williams, R. E.; McGuire, M. A.; Hayashi, T. *J. Am. Chem. Soc.* 1980, 102, 4973-4979.

(3) For a recent review, see: Trost, B. M. *Acc. Chem. Res.* 1980, 13, 385-393.

(4) For examples and leading references, see: (a) Nicholas, K. M. *Tetrahedron Lett.* 1980, 1595-1599. (b) Nicholas, K. M.; Mulvaney, M.; Bayer, M. *J. Am. Chem. Soc.* 1980, 102, 2509. (c) Padmanabhan, S.; Nicholas, K. M. *Tetrahedron Lett.* 1982, 2555-2559.

(5) Cyclohexadienyldicarbonyliron(II) complexes were among the first organometallic systems to be studied in reaction with carbon nucleophiles: Birch, A. J.; Cross, P. E.; Lewis, J.; White, D. A.; Wild, S. B. *J. Chem. Soc. A* 1968, 332-340. For recent reviews, see: (a) Birch, A. J. *Ann. N.Y. Acad. Sci.* 1980, 333, 101-106. (b) Pearson, A. J. *Acc. Chem. Res.* 1980, 13, 463-469.

(6) Arenes coordinated with several different metal-ligand systems are reported to couple with carbon nucleophiles. For recent examples, see: Semmelhack, M. F.; Clark, G. R.; Garcia, J. L.; Harrison, J. J. *Thebar-anonh, Y.; Wulff, W.; Yamashita, A. Tetrahedron* 1981, 37, 3957-3966.

(7) Green, M. L. H.; Mitchard, L. C.; Silverthorn, W. E. *J. Chem. Soc., Dalton Trans.* 1973, 1952-1954.

(8) For examples and leading references, see: Aakermark, B.; Ljungqvist, A.; Panunzio, M. *Tetrahedron Lett.* 1981, 1055-1058.

(9) For one example of a dramatic solvent effect, see the addition of alkylolithium reagents with (η^5 -cyclohexadienyl)iron(II) in dichloromethane: Bandara, B. M. R.; Birch, A. J.; Khor, T.-C. *Tetrahedron Lett.* 1980, 3625-3629. With (η^2 -alkene)palladium(II) complexes, hexamethylphosphoric triamide influences both efficiency and regioselectivity.²

(10) In some cases, added phosphines³ or triethylamine² are crucial to successful addition of carbon nucleophiles.

(11) Nucleophile additions are often highly nucleophile dependent. For example, the regioselectivity and efficiency of additions to (η^3 -allyl)palladium(II) and (η^2 -alkene)palladium(II) complexes can be correlated with pK_a of the carbon anion. See references 2 and 3 and Hegedus, L. S.; Darlington, W. H.; Russell, C. E. *J. Org. Chem.* 1980, 45, 5193-5195.

= (CH₂)₇ methyl ester, 84057-05-6; 3 (R = H₃C(CH₂)₇, R' = (CH₂)₇), 84057-06-7; 4 (R = H₃C(CH₂)₇, R' = (CH₂)₇), 84057-07-8; 5 (R = (CH₂)₇CH₃), 84057-08-9; 6 (R = (CH₂)₇CH₃), 84057-09-0; 7 (R = (CH₂)₇CH₃), 84057-10-3; 8 (R = (CH₂)₇CH₃), 84057-11-4;

9-SHDA, 50514-64-2; 9-SHDA, Se oxide, 84057-12-5; Me-9-SHDA, 84057-13-6; Me-9-SHDA, Se oxide, 84057-14-7; Se, 7782-49-2; Te, 13494-80-9; methyl 8-bromooctanoate, 26825-92-3; bromooctane, 111-83-1.

Scope of Anion Addition to (η^4 -1,3-Cyclohexadiene)tricarbonyliron(0)

M. F. Semmelhack* and James W. Herndon

Department of Chemistry, Princeton University, Princeton, New Jersey 08544

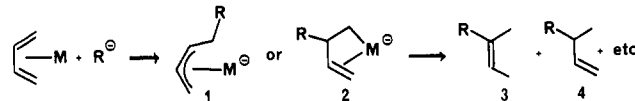
Received October 26, 1982

Reactive carbanions add to (η^4 -1,3-cyclohexadiene)tricarbonyliron(0) to produce intermediates that can be protonated to give 2- or 3-substituted cyclohexenes as the major products. Alkyl lithium reagents react inefficiently, primarily by addition to a coordinated carbon monoxide to produce simple aldehydes along with ketones from addition to the diene ligand. Trapping of the intermediates with other electrophiles generally fails, with regeneration of the starting complex being the preferred pathway. However, benzoyl chloride was observed to react with the intermediate from trityl anion and (η^4 -1,3-cyclohexadiene)tricarbonyliron(0) to give a 1,4-disubstituted 2-cyclohexene. The regioselectivity of addition is not clear from the additions to the 1,3-cyclohexadiene ligand, but preliminary results concerning the addition of 2-lithio-2-methylpropionitrile to (η^4 -1,3-butadiene)tricarbonyliron(0) require that addition is preferred at C-2 of the 1,3-diene ligand.

Introduction

The ability of nucleophiles to add to carbon-carbon double bonds is enhanced by coordination with transition metals. Specific types of complexes bearing alkene,^{1,2} allyl,³ propargyl,⁴ cyclohexadienyl,⁵ and arene⁶ ligands have been developed for organic synthesis. Absent from this list are examples of addition of carbon nucleophiles to coordinated 1,3-dienes. We are aware of a single example of carbon-carbon bond formation by addition of carbon anions to a discrete (η^4 -1,3-diene)metal complex. In this case, cyanide anion was observed to add at C-1 of the diene ligand in (η^3 -allyl)(η^4 -1,3-butadiene)(η^6 -benzene)molybdenum(II).⁷ Palladium(II)-promoted addition of nucleophiles to 1,3-butadiene has been demonstrated for a variety of nucleophiles and is beginning to be developed as a synthesis method for 1,4-disubstituted alkenes.⁸ However, these reactions are more likely examples of nucleophile addition to (η^2 -alkene)palladium(II) complexes; the details of the process are not yet clear.

Coupling of carbon nucleophiles with 1,3-diene ligands offers special opportunities for organic synthesis. The 1,3-diene unit is common in open-chain systems and in rings and is known to form stable complexes with a variety of transition metals. The initial addition might give either an allylmetal complex (1) or a chelated homoallyl arrangement (2), and each of these intermediates has im-



portant potential in synthesis. The metal system in 1 and 2 might be cleaved by protonation (to give 3, 4, or other isomers), by carbonylation, by direct coupling with alkenes and organic halides, etc. While the idea of adding carbon nucleophiles to coordinated 1,3-dienes is a simple extension of recent organo-transition-metal studies, there are important questions to answer in developing the idea as synthesis methodology. In the general development of nucleophile addition to alkene, allyl, cyclohexadienyl, and arene ligands, a major question in each case has concerned the range of anions that add efficiently. In many cases, alternate pathways such as ligand displacement and electron-transfer reduction of the metal completely prevent simple addition to the ligand. Solutions to these problems can sometimes be found through choice of solvent,⁹ other ligands on the metal,¹⁰ and modification of the nucleophile itself.¹¹

In choosing the appropriate diene-metal system for development, we were attracted to the Fe(CO)₃ activating

(1) The complexes of cyclopentadienyldicarbonyliron(II) with olefins have been studied extensively. For examples, see: Rosenblum, M. *Acc. Chem. Res.* 1974, 7, 122-128.

(2) Examples of oxygen and nitrogen nucleophiles adding to (olefin)-palladium(II) complexes are numerous. General addition of carbon nucleophiles has been realized only recently. For examples, see: Hegedus, L. S.; Williams, R. E.; McGuire, M. A.; Hayashi, T. *J. Am. Chem. Soc.* 1980, 102, 4973-4979.

(3) For a recent review, see: Trost, B. M. *Acc. Chem. Res.* 1980, 13, 385-393.

(4) For examples and leading references, see: (a) Nicholas, K. M. *Tetrahedron Lett.* 1980, 1595-1599. (b) Nicholas, K. M.; Mulvaney, M.; Bayer, M. *J. Am. Chem. Soc.* 1980, 102, 2509. (c) Padmanabhan, S.; Nicholas, K. M. *Tetrahedron Lett.* 1982, 2555-2559.

(5) Cyclohexadienyldicarbonyliron(II) complexes were among the first organometallic systems to be studied in reaction with carbon nucleophiles: Birch, A. J.; Cross, P. E.; Lewis, J.; White, D. A.; Wild, S. B. *J. Chem. Soc. A* 1968, 332-340. For recent reviews, see: (a) Birch, A. J. *Ann. N.Y. Acad. Sci.* 1980, 333, 101-106. (b) Pearson, A. J. *Acc. Chem. Res.* 1980, 13, 463-469.

(6) Arenes coordinated with several different metal-ligand systems are reported to couple with carbon nucleophiles. For recent examples, see: Semmelhack, M. F.; Clark, G. R.; Garcia, J. L.; Harrison, J. J. *Thebar-anonh, Y.; Wulff, W.; Yamashita, A. Tetrahedron* 1981, 37, 3957-3966.

(7) Green, M. L. H.; Mitchard, L. C.; Silverthorn, W. E. *J. Chem. Soc., Dalton Trans.* 1973, 1952-1954.

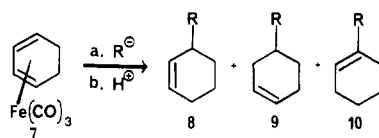
(8) For examples and leading references, see: Aakermark, B.; Ljungqvist, A.; Panunzio, M. *Tetrahedron Lett.* 1981, 1055-1058.

(9) For one example of a dramatic solvent effect, see the addition of alkyl lithium reagents with (η^5 -cyclohexadienyl)iron(II) in dichloromethane: Bandara, B. M. R.; Birch, A. J.; Khor, T.-C. *Tetrahedron Lett.* 1980, 3625-3629. With (η^2 -alkene)palladium(II) complexes, hexamethylphosphoric triamide influences both efficiency and regioselectivity.²

(10) In some cases, added phosphines³ or triethylamine² are crucial to successful addition of carbon nucleophiles.

(11) Nucleophile additions are often highly nucleophile dependent. For example, the regioselectivity and efficiency of additions to (η^3 -allyl)palladium(II) and (η^2 -alkene)palladium(II) complexes can be correlated with pK_a of the carbon anion. See references 2 and 3 and Hegedus, L. S.; Darlington, W. H.; Russell, C. E. *J. Org. Chem.* 1980, 45, 5193-5195.

Table I. Reactions of Carbanions with Complex 7

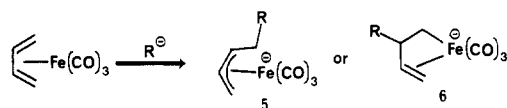


entry	carbanion	isomer distribution ^b			yield, ^a %
		8	9	10	
1	LiC(CH ₃) ₂ CN ^c (A)	87	9	4	98
2	LiCH(CH ₃)CN ^{c,f} (B)	70	17	13	57
3	LiC(CH ₃) ₂ CO ₂ Et ^d (C)	54	45	1	100
4	LiCH(CH ₃)CO ₂ - <i>t</i> -Bu (D)	<i>i</i>	<i>i</i>	<i>i</i>	59
5	LiCH ₂ COC(CH ₃) ₃ (E)	<i>i</i>	<i>i</i>	<i>i</i>	0
6	KCH ₂ COC(CH ₃) ₃ ^h (E)	<i>i</i>	<i>i</i>	<i>i</i>	25
7	LiC(<i>n</i> -Bu)(OR)CN ^{c,g} (F)	0	80	20	78
8	LiCHPh ₂ ^c (G)	34	66	0	80
9	LiCPh ₃ ^e (H)	72	28	0	72
10	2-lithio-1,3-dithiane (I)	63		37	60
11	LiCH ₂ SPh (J)		59	41	42
12	LiPh (K)	<i>i</i>	<i>i</i>	<i>i</i>	47
13	LiC(CH ₃) ₂ CO ₂ Li (L)	100	0	0	82

^a The yields are based on distilled, chromatographed mixtures of isomers. ^b The mixture of isomers yielded a single product upon hydrogenation or dehydrogenation. ^c The ratio was determined by GLPC and comparison with authentic samples. ^d The ratio was determined by GLPC with the aid of ¹H NMR. ^e The ratio was determined by integration of key peaks in the ¹H NMR of the mixture [δ 4.17 (8 H, R = CPh₃) and δ 3.70 (9 H, R = CPh₃)]. ^f The regioisomeric mixture was methylated and compared with authentic samples for entry 1. ^g R = 1-ethoxyethyl. The products are 9 and 10 with R = COC₂H₅, obtained by disassembly of the cyanohydrin acetal according to the published procedure: Stork, G.; Maldonado, L. *J. Am. Chem. Soc.* 1971, 93, 5286. ^h The solvent was a mixture of HMPA and dibenzo-18-crown-6. ⁱ The isomer distribution has not been established.

group because of the wide range of substituted dienes that are known to coordinate with this unit,¹² the oxidative and thermal stability of (η^4 -1,3-diene)Fe(CO)₃ complexes, and the high availability/low cost of the starting iron species Fe(CO)₅. It is also desirable to have high electrophilic reactivity for the complex; in this respect, the Fe(CO)₃ activating group is not favorable. No examples of nucleophile addition of the (η^4 -1,3-diene)Fe(CO)₃ complexes have been reported, and a series of papers has established the tendency of these complexes to react as *nucleophiles*, coupling with acetyl chloride under Friedel-Crafts conditions, for example.¹³ At the same time, electrophilic reactivity parallel with the isoelectronic (arene)Cr(CO)₃ complexes might be expected, where synthetically useful carbanions add readily.⁶

Of the putative intermediates 5 and 6 from addition to (η^4 -1,3-diene)Fe(CO)₃, only an example of 5 [the parent compound (η^3 -allyl)tricarbonyliron(0)] has been reported, from electrochemical reduction of (η^3 -allyl)iodotricarbonyliron(II).¹⁴ The paucity of information about



species such as 5 is surprising, since they might have been expected to arise from reaction of allylic halides with the tetracarbonyliron dianion, a well-studied reagent.¹⁵ Similarly, complexes of type 6 are likely to be stable, with predictable reactivity, and their absence from the literature might be attributed to lack of interest and/or lack of access.

(12) Koerner von Gustorf, E. A.; Grevels, F. W.; Fischler, I. "The Organic Chemistry of Iron"; Academic Press: New York, 1978; Vol. 1, pp 525-627.

(13) For examples and leading references, see: Lillya, C. P.; Graf, R. E. *J. Organomet. Chem.* 1976, 122, 377-391.

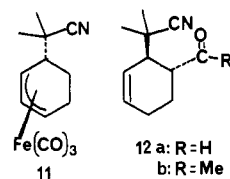
(14) Gubin, S. P.; Denisovich, L. I. *J. Organomet. Chem.* 1968, 15, 471-480.

(15) For a review, see: Collman, J. P. *Acc. Chem. Res.* 1975, 8, 342-347.

Results and Discussion

In the first phase of this project, we have determined that reactive carbon anions will add to a prototype complex, (η^4 -1,3-cyclohexadiene)Fe(CO)₃, 7, to give an intermediate that can be protonated to form monosubstituted cyclohexenes.¹⁶ This paper describes the range of anions that add successfully, the alternate pathways with certain classes of anions, and the opportunities for double-bond isomers of the product cyclohexenes.

The reaction of 2-lithio-2-methylpropionitrile (anion A, Table I) in THF at -78 °C followed by warming to 25 °C gave a solution containing four cyclohexene derivatives. Three were the isomers 8A-10A from protonation of the intermediate (perhaps 11) while the fourth component (12a) was shown to have incorporated both the anion unit and a formyl group. The structure of 12a has been as-



signed on the basis of spectral data, especially comparison of the ¹H NMR spectrum with that of 12b, which was prepared by a different sequence of reactions and for which the structure was determined by X-ray diffraction analysis.¹⁷ The general pathway for formation of 12a is presumably alkyl migration to CO followed by protonation of an acyliron intermediate.¹⁵ This process is known to be disfavored by polar, aprotic solvents such as hexamethylphosphoric triamide (HMPA),¹⁸ we find that formation of 12a is completely suppressed by working in

(16) For a preliminary account of this work, see: Semmelhack, M. F. *Pure Appl. Chem.* 1981, 53, 2379-2388.

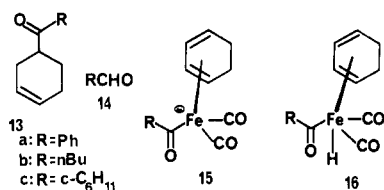
(17) Semmelhack, M. F.; Herndon, J. W.; Springer, J. P., manuscript in preparation.

(18) Collman, J. P.; Finke, R. G.; Cawse, J. N.; Brauman, J. I. *J. Am. Chem. Soc.* 1978, 100, 4766-4772.

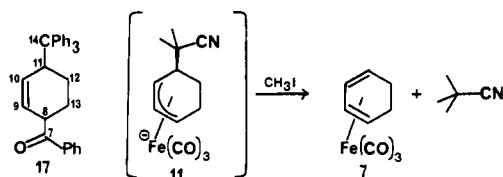
THF/HMPA mixtures. Table I displays the results of a systematic series of experiments with various carbon nucleophiles. The isomeric cyclohexenes are often difficult to separate and only in certain cases (as indicated) are the separate isomers firmly identified by alternate synthesis and by thorough spectral analysis on pure samples. In other cases, the fraction from distillation or chromatography containing only the isomers 8–10 was obtained, analyzed as a mixture, and converted to a single dihydro isomer by hydrogenation.

Ketone enolates appear to define the minimum reactivity necessary for addition to 7. The lithium enolate of pinacolone gives no adduct under the standard conditions. Increasing the reactivity of the enolate by employing a potassium counter ion and an excess of dibenzo-18-crown-6 in the medium brings the yield up to 25% (entry 6). Less reactive nucleophiles such as diethyl malonate anion, alkoxide anions, and simple amines show no evidence of interaction with 7 at temperatures up to 25 °C. Cyano-stabilized anions and ester enolate anions react with good efficiency (entries 1–4 and 7). The more reactive sulfur-stabilized anions such as 2-lithio-1,3-dithiane (I) and ((phenylthio)methyl)lithium (J) undergo rapid reaction with 7, and the simple products can be isolated in moderate yield (entries 10 and 11). The yields are affected by difficulties in isolation of the sulfur-containing products from residual iron species and can probably be improved.

Simple organolithium and organomagnesium reagents show a tendency to attack at the carbon monoxide ligand, as evidenced by the formation of ketone (13) and aldehyde (14) products. Following the standard procedure, phenyllithium gave tetrahydrobenzophenone (13a) in 26% yield and benzaldehyde (5%) as well as the products from addition to the diene (entry 12). Similar reaction with *n*-butyllithium gave the simple adduct (8, R = *n*-Bu) in only 14% yield, accompanied by ketone 13b (33%) and valeraldehyde (11%). Under the usual conditions, organomagnesium derivatives give only low conversion of 7 and no evidence for direct addition to the diene ligand. From phenylmagnesium bromide and from cyclohexylmagnesium bromide, the ketones 13a and 13c were detected in 10–15% yield as the only products. These results can be accommodated by initial addition to a coordinated CO producing 15, followed by protonation to give 16, and finally stepwise or concerted 1,2 addition of acyl and hydride across the 1,3-diene ligand. Reductive elimination from 16 would give the aldehydes 14.



Attempts to cleave the putative intermediate allyl complex 11 with other electrophiles have been less successful. The intermediate from addition of (triphenylmethyl)lithium to 7 reacts with benzoyl chloride to produce a mixture from which was isolated the 1,4-substitution product 17

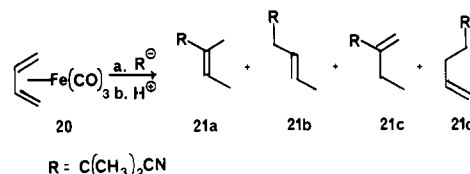


in 53% yield. However, the corresponding intermediate

from addition of anion A to complex 7 failed to couple with a variety of electrophiles. With excess methyl iodide (and with chlorotrimethylsilane), the primary process was detachment of the anion unit, allowing recovery of 7 and methylation (or silylation) of the anion.

The ratio of olefin isomers appears to vary with different anion reactants, in a way which is not yet understood. The isomer mixture was shown to be independent of time and temperature in contact with the trifluoroacetic acid. For example, the isomer distribution in entry 1 of Table I was the same when the mixture was allowed to stir for 16 h at 23 °C after addition of the trifluoroacetic acid and after only 5 min at -78 °C. Two rather similar anions (compare Table I entries 8 and 9) give different major isomers under the same reaction conditions. The dianion (L, entry 13) of isobutyric acid leads to a single isomer (>98%). The trisubstituted olefin products 10, which presumably arise by hydride elimination/readdition, generally appear in only small amounts. We view the olefin isomers as arising from protonation of the (undetected) intermediate (η^3 -allyl)Fe(CO)₃ anion (i.e., 11) and we are continuing studies aimed at controlling the site of protonation.

From the results in Table I, the regioselectivity of addition of anions to 7 is not obvious. As part of their general analysis of nucleophile addition to coordinated polyenes, Davies, Green, and Mingos have predicted that 1,3-dienes should receive nucleophiles at the terminal (C-1) position.¹⁹ The simplest mechanism for formation of products 8 and 9 is addition to the terminal position to give 11 followed by protonation at one or the other of the ends of the allyl system. However, an alternate mechanism can be envisaged, in which addition occurs at an internal (C-2) position to give 18 followed by a series of hydrogen shifts resulting in structure 11 (Scheme I). Support for the second mechanism comes from the observation of 12 as a minor product, which we suggest can form by addition at C-2 followed by migration of the alkyl ligand (C-1) to a CO ligand, to give 19 (Scheme I). Preliminary results with other 1,3-diene ligands also show the preference for addition at C-2 with anion A. For example, addition of A to (η^4 -1,3-butadiene)Fe(CO)₃ (20) leads to a mixture of four products (69% yield together) that have been tentatively identified as 21a–d, in a ratio of 89:6:4:1 for a:b:c:d. The major product has been rigorously characterized, and the minor isomers were assigned on the basis of GLPC retention time comparisons with samples from alternate synthesis. Therefore, a preference of ca. 20:1 for addition at C-2 is demonstrated for this diene ligand. Work is in progress to establish the selectivity features of this reaction, to determine the scope of additions with other 1,3-diene ligands and with other metal–ligand systems, and to fully characterize the new intermediates such as 11 and 18.

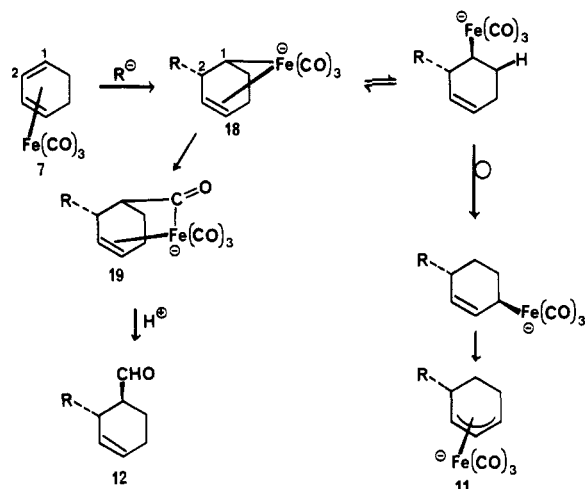


Experimental Section

General Considerations. ¹H NMR spectra were obtained at 60-MHz (Perkin-Elmer R24B), 90 MHz (JEOL FX-90Q), and 500-MHz (Yale Regional NMR Facility), as indicated. ¹³C NMR spectra were obtained with the JEOL FX-90Q spectrometer at

(19) Davies, S. G.; Green, M. L. H.; Mingos, D. M. P. *Tetrahedron* 1978, 34, 3047–3077.

Scheme I



22.5 MHz. The chemical shifts are reported in parts per million downfield from internal tetramethylsilane. IR spectra were obtained on a Perkin-Elmer 299 instrument and were calibrated against the 1601-cm⁻¹ band of polystyrene. Microanalyses were obtained from Scandinavian Microanalytical Laboratories, Herlev, Denmark. High-resolution mass spectral data were obtained on an AEI MS-9 double-focusing mass spectrometer. GC-MS data were obtained from a Hewlett-Packard 5987 GC-MS instrument. Ether solvents were dried by distillation from sodium benzophenone ketyl under argon. Hexamethylphosphoric triamide (HMPA) and diisopropylamine were purified by distillation from calcium hydride under argon and stored over 4-Å molecular sieves at ambient temperature in a desiccator. Reactions involving organolithium reagents were carried out under dry argon in oven-dried glassware. Woelm silica gel (32–64 μm) was used for all gravity flow chromatography. Melting points are uncorrected unless otherwise noted. The term "flash distillation" refers to a vacuum distillation at 25 °C with a receiver at -78 °C. The term "short-path distillation" refers to the process in which the entire distillation apparatus (a tube closed at one end, held horizontally), with the exception of the receiver, was slowly heated in an air bath from 25 to 150 °C under vacuum; the distillate was collected at -78 °C, and boiling points for fractions refer to the bath temperature range. All boiling points are uncorrected. The term "under argon" means that the system was evacuated with an oil pump and refilled with argon three times, and a positive pressure (ca. 30 mm) of argon was maintained during the experiment.

Only the parent ion in the mass spectra is generally reported, to establish molecular weight. In cases where the spectra have been analyzed, the data are expressed with the nominal fragment weight followed in parentheses by the percent intensity (taking the base peak as 100%) and a suggestion for the atoms or group lost.

Complexes 7 and 20 were prepared according to literature procedures, distilled, and characterized by comparison of ¹H NMR spectral data.^{20,21}

Column A refers to a 12 ft × 0.125 in. GLPC column packed with 5% Carbowax 20M on Chromosorb W. Column B refers to a 6 ft × 0.125 in. GLPC column packed with 3% OV-17 on Chromosorb W. Column C refers to a 12 ft × 0.125 in. GLPC column packed with 5% SE-30 on Chromosorb W. Column D refers to a 12 ft × 0.375 in. GLPC column packed with 5% OV-17 on Chromosorb W.

Procedures for Generation of Anions A–F Reported in Table I. a. **Generation of Nitrile and Ester-Stabilized Anions.** To a solution of diisopropylamine (0.413 mL, 2.95 mmol) in THF (8 mL) under argon at -78 °C was added rapidly via

syringe a solution of *n*-butyllithium in hexane (2.75 mmol). The mixture was allowed to stir at -78 °C for a period of 20 min, after which time the compound to be metalated (2.95 mmol) was added neat rapidly via syringe, followed by addition of hexamethylphosphoramide (HMPA, 2 mL). The mixture was allowed to stir at -78 °C for 20 min. This solution was used immediately in reaction with complex 7 (see below).

b. **Generation of Lithium Lithioisobutyrate (L).** To a solution of diisopropylamine (0.800 mL, 5.72 mmol) in tetrahydrofuran (8 mL) under argon at -78 °C was added rapidly via syringe a solution of *n*-butyllithium in hexane (5.30 mmol). The mixture was allowed to stir at -78 °C for a period of 20 min, after which time isobutyric acid (0.250 mL, 2.70 mmol) was added rapidly neat via syringe, followed by addition of hexamethylphosphoramide (2 mL). The mixture was allowed to stir at 25 °C for a period of 30 min. This solution was used immediately in reaction with complex 7 (see below).²²

c. **Generation of 2-Lithio-1,3-dithiane and Phenyl-Stabilized Anions G and H.** To a solution of the compound to be metalated (2.75 mmol) in tetrahydrofuran (8 mL) under argon at -78 °C was added rapidly via syringe a solution of *n*-butyllithium in hexane (2.70 mmol), followed by addition of hexamethylphosphoramide (2 mL). The mixture was allowed to stir at 0 °C for a period of 1.5 h. This solution was used immediately in the reaction with complex 7 (see below).

d. **Generation of ((Phenylthio)methyl)lithium.**²³ To a solution of thioanisole (0.26 mL, 2.3 mmol) in tetrahydrofuran (8 mL) and hexamethylphosphoramide (2 mL) at -78 °C under argon was added via syringe a solution of *n*-butyllithium in hexane (1.40 mmol), and the mixture was allowed to stir at -78 °C for a period of 20 min. This solution was used immediately in the reaction with complex 7 (see below).

General Procedure for Addition of Anions to (η⁴-1,3-Cyclohexadiene)tricarbonyliron (7) Followed by Protonation. To a solution of the anion in tetrahydrofuran/hexamethylphosphoramide (see above) at -78 °C (under argon) was added rapidly via syringe complex 7 (0.500 g, 2.3 mmol). The cooling bath was removed, and the mixture was allowed to stir at 25 °C for 1.5 h and then cooled to -78 °C. Trifluoroacetic acid (1.5 mL, 19.5 mmol) was added over a period of 30 s, and the mixture was allowed to stir for 30 min at this temperature. The mixture was poured into saturated aqueous sodium carbonate solution (water in the case of carboxylic acid dianions) in a separatory funnel, and the aqueous layer was extracted two times with 30–60 °C petroleum ether. The organic layer was washed once with saturated aqueous sodium chloride solution and dried over magnesium sulfate, and the solvent was removed on a rotary evaporator. The residue was treated as described in subsequent sections (see below).

Characterization of the Products from Anion A with Complex 7. Column chromatography of the residue from the general procedure (5 g of silica gel) gave a fraction of green solid [Fe₃(CO)₁₂] eluted with hexane followed by a fraction containing the mixture of olefins 8A–10A eluted with hexane/dichloromethane (7:3). The mixture of olefins was distilled in a short-path apparatus (80–110 °C (1.0 mm)) to give a clear, colorless liquid; 0.33 g, 98% yield. Analysis by GLPC (column A at 130 °C) showed three peaks at 13.0, 15.3, and 16.5 min in the area ratio 6.5:80:13.5. GC-MS established that the components were isomers, consistent with the formula C₁₀H₁₅N (below). ¹H NMR (CDCl₃): δ 5.4–5.9 (m, 2 H, vinyl H), 1.25 (s, 6 H, CH₃) overlapping with 1.3–2.5 (br m, 7 H). IR (neat): 3025 (m), 2940 (s), 2245 (m, CN), 1660 (w, C=C), 1460 (s), 1395 (m), 1378 (m), 1200 (w), 735 (m) cm⁻¹. GC-MS (retention time 13.0): *m/e* (relative intensity) 149 (7), 81 (100), 79 (71), 69 (69). GC-MS (retention time 16.5 min): *m/e* (relative intensity) 149 (6), 81 (100), 76 (69), 71 (29), 69 (30), 56 (10); mass spectral mol wt 149.1209, calcd 149.1204.

The minor isomer at a retention time of 13.0 min was identified by comparison of retention time with a sample of 10A prepared by alternative synthesis (see below). The minor isomer at a retention time of 16.5 min was identified by comparison of re-

(20) (η⁴-1,3-Cyclohexadiene)tricarbonyliron(0) can be prepared via a thermal procedure⁶ or photochemically by using a procedure analogous to that of Von Gustdorf.²¹ In our hands, better yields were obtained with the photochemical procedure.

(21) Von Gustorf, E. K.; Pfajfer, Z.; Grevels, F. W. *Z. Naturforsch. B: Anorg. Chem., Org. Chem., Biochem. Biophys., Biol.* 1971, 26B, 66–67.

(22) Creger, P. L. *J. Am. Chem. Soc.* 1967, 89, 2500–01.

(23) Garcia, J. L. Ph.D. Thesis, Princeton University, 1982. This is a modification of literature procedures.²⁴

(24) Corey, E. J.; Seebach, D. *J. Org. Chem.* 1966, 31, 4097–4099.

tention time with a sample of 9A prepared by alternative synthesis (see below). The major isomer (retention time 15.3 min) was assigned structure 8A by logical elimination. The mixture of isomers was converted by hydrogenation (83 mg, 50 psi of H₂, 6 mg of PtCl₂, 1:1 ethyl alcohol/acetic acid, 25 °C, 24 h) to a single isomer (retention time 11.3 min, column A at 130 °C). The hydrogenation product was characterized by spectral data. ¹H NMR (CDCl₃): δ 1.3 (s, 6 H, CH₃), 1.0–2.1 (m, other H). GC-MS: *m/e* (relative intensity) 83 (M – CH₂C(CH₃)CN, 12), 81 (3), 69 (100), 59 (3), 55 (48), 41 (31).

Characterization of the Products from Complex 7 and 2-Lithiopropionitrile (Anion B). Column chromatography of the residue from the general procedure gave a forerun of colored byproducts eluted with hexane. Elution with hexane/dichloromethane (7:3) afforded the mixture of olefin isomers 8B–10B. The mixture of olefins was distilled in a short-path apparatus (80–110 °C (1.0 mm)) to give a clear, colorless liquid; 0.18 g, 55% yield. ¹H NMR (CDCl₃): δ 5.54 (m, 2 H, vinyl H), 1.25 (d, 3 H, *J* = 6 Hz, CH₃), 1.3–2.8 (m, 8 H, all other H). IR (neat): 3040 (m), 2980 (s), 2250 (m, C≡N), 1650 (w), 1460 (s), 1440 (m), 1385 (m), 1260 (w), 1150 (w), 738 (m) cm⁻¹. GC-MS: *m/e* (relative intensity) 135 (parent, 4), 9 (2), 81 (100), 79 (31), 77 (9), 57 (15); the same pattern was recorded for all isomers; mass spectral mol wt 135.1050, calcd 135.1048.

The mixture of olefin isomers was converted via methylation (see below) to a mixture of olefins 8A–10A. GLPC analysis of the reaction mixture (column A at 130 °C) revealed three peaks at 13.0, 15.3, and 16.5 min in the area ratio 17:70:13. These isomers were assigned as 10A, 8A, and 9A, respectively, based on comparison of retention times with samples from an alternate synthesis (see below).

The mixture of olefin isomers 8B–10B was converted by hydrogenation (53 mg, 50 psi of H₂, 116 mg of 5% Pd/C, 2:1 ethyl alcohol/acetic acid 25 °C, 4 h) to a single isomer (retention time 8.2 min, column A at 130 °C). The hydrogenation product was characterized by spectral data. ¹H NMR (CDCl₃): δ 1.10 (d, 3 H, *J* = 7 Hz, CH₃), 1.0–2.3 (m, all other H). IR (neat): 2960 (s), 2245 (m, C≡N), 1460 (s), 1440 (s), 1385 (m), 1260 (w), 1140 (w) cm⁻¹. GC-MS: *m/e* (relative intensity) 84 (M – acrylonitrile, 3), 83 (46), 67 (4), 56 (6), 55 (100).

Characterization of the Products 8C–10C from Complex 7 and Ethyl 2-Lithio-2-methylpropionate (Anion C). Column chromatography of the residue from the general procedure on 5 g of silica gel gave a fraction of green solid [Fe₃(CO)₁₂] eluted with hexane followed by a fraction containing the mixture of olefins 8C–10C eluted with hexane/dichloromethane (7:3). The mixture of olefins was distilled in a short-path apparatus (90–120 °C (1.0 mm)) to give a clear, colorless liquid; 0.46 g, 99% yield. Analysis by GLPC (column A at 140 °C) showed three peaks at 15.5, 16.8, and 17.9 min in the area ratio 1:44:55. GC-MS established that the components were isomers, consistent with the formula C₁₂H₂₀O₂ (below). ¹H NMR (CDCl₃): δ 5.4–4.9 (ABq overlapping with singlet, 2 H, vinyl H, *J* = 10 Hz), 4.00 (q, 2 H, *J* = 7 Hz, OCH), 1.16 (t, 3 H, *J* = 7 Hz, OCH₂CH₃), 1.05 (s, 6 H, CH₃) 1.35–2.65 (m, 7 H). IR (neat): 3040 (m), 2950 (s), 1730 (s, C=O), 1640 (w, C=C), 1470 (s), 1390 (s), 1370 (m), 1310 (w), 1260 (s, CO), 1150 (s, CO), 1030 (m) cm⁻¹. GC-MS: *m/e* (relative intensity) 123 (M – COOEt, 14), 117 (7), 116 (100), 88 (68), 81 (30), 79 (20), 73 (16), 67 (26); the same pattern was recorded for all isomers; mass spectral mol wt 196.1457, calcd 196.1463.

The major isomer at a retention time of 17.9 min was identified by comparison of retention time with a sample of 8C prepared by alternative synthesis (see below). The minor isomer at a retention time of 16.8 min was assigned structure 9C by a process of elimination. Alternative assignment as 10C is ruled out because of the area ratio 1:1 for the signals, due to the vinyl H and OCH₂ in the ¹H NMR spectrum of the mixture.

The mixture of isomers was converted by hydrogenation (57 mg, 50 psi of H₂, 100 mg of 5% Pd/C, 1:1 ethyl alcohol/acetic acid, 25 °C, 24 h) to a single isomer (retention time 12.5 min, column A at 140 °C). ¹H NMR (CDCl₃): δ 3.98 (q, 2 H, *J* = 7 Hz, OCH₂), 1.16 (t, 3 H, *J* = 7 Hz, OCH₂CH₃), 1.10 (s, 6 H, CH₃), 1.10–2.40 (m, all other H). IR (neat): 2955 (s), 2720 (s), 2860 (s), 1725 (s), 1455 (s), 1375 (m), 1265 (s), 1140 (w), 1070 (w) cm⁻¹. GC-MS: *m/e* (relative intensity) 125 (M – COOEt, 13), 116 (100), 88 (58), 83 (13), 73 (H), 69 (34).

Characterization of the Products from Complex 7 and tert-Butyl 2-Lithiopropionate (Anion D). Column chromatography of the residue from the general procedure on 5 g of silica gel gave a fraction of green solid [Fe₃(CO)₁₂] eluted with hexane followed by a fraction containing the mixture of olefins 8D–10D eluted with hexane/dichloromethane (7:3). The mixture of olefins was distilled in a short-path apparatus (110 °C (2.0 mm)) to give a clear, colorless liquid, 0.28 g (59% yield), as a mixture of five isomers (olefin position, diastereoisomers) that could not be fully separated. ¹H NMR (CDCl₃): δ 5.5 (m, 2 H, vinyl H), 1.41 (s, 9 H, CH₃), 1.0–1.4 (m, CH₃, adjacent to carboxy), 1.4–2.5 (m, all other H). IR (neat): 3030 (w), 2980 (s), 2940 (w), 1725 (s, C=O), 1660 (m), 1460 (s), 1360 (s), 1150 (s), 850 (m) cm⁻¹. GC-MS: *m/e* (relative intensity) 154 (M – isobutylene, 9), 136 (4), 109 (25), 91 (2), 81 (30), 67 (16), the same pattern was recorded for all isomers; mass spectral mol wt 210.1605, calcd 210.1620.

The mixture of isomers was converted by hydrogenation (67 mg, 50 psi of H₂, 100 mg of 5% Pd/C, 1:1 ethyl alcohol/acetic acid, 25 °C, 4 h) to a single isomer with a retention time of 6.7 min (column A at 140 °C). The hydrogenation product was characterized by spectral data. ¹H NMR (CDCl₃): δ 1.0 (d, 3 H, *J* = 6 Hz, CH₃), 1.32 (s, 9 H, CH₃), 0.9–2.0 (m, all other H). IR (neat): 2975 (s), 2925 (s), 2855 (m), 1725 (s, C=O), 1450 (m), 1370 (s), 1255 (m), 1150 (s), 1050 (m), 850 (m) cm⁻¹. GC-MS: *m/e* (relative intensity) 157 (8), 156 (M – isobutylene, 6), 111 (2), 74 (41), 69 (15), 57 (100).

Characterization of the Products 8E–10E from Complex 7 and the Potassium Enolate of Pinacolone (Anion E). The potassium enolate of pinacolone was prepared from potassium hydride (0.182 g, 4.53 mmol) and pinacolone (0.368 mL, 2.94 mmol) according to the procedure of Brown²⁵ using hexamethylphosphoramide (8 mL) and dibenzo-18-crown-6 (1.0 g) as the solvent. Complex 7 (0.500 g, 2.3 mmol) was added neat dropwise via syringe at 25 °C over a period of 2 min, and the mixture was allowed to stir for 6 h at 25 °C. The mixture was cooled to 0 °C, and trifluoroacetic acid (1.5 mL, 19.5 mmol) was added. The mixture was treated as outlined in the general procedure. Column chromatography of the residue from the general procedure on 5 g of silica gel gave a fraction of green solid [Fe₃(CO)₁₂] eluted with hexane followed by a fraction containing the mixture of olefins 8E–10E eluted with hexane/dichloromethane (7:3). The mixture of olefins was distilled in a short-path apparatus (90–120 °C (1.0 mm)) to give a clear, colorless liquid; 0.10 g, 25% yield. ¹H NMR (CDCl₃): δ 5.48 (m, 2 H, vinyl H), 2.41 (d, 1 H, *J* = 6 Hz, COCH), 1.06 (s, 9 H, CH₃), 1.3–2.5 (m, all other H). IR (neat): 3025 (m), 2970 (s), 2930 (s), 1705 (s, C=O), 1640 (s), 1475 (m), 1365 (w), 1265 (s), 1100 (w), 1060 (m), 1005 (m), 855 (s) cm⁻¹. GC-MS: *m/e* (relative intensity) 180 (M, 6), 123 (55), 101 (18), 95 (26), 86 (11), 81 (100), 67 (17); mass spectral mol wt 180.1510, calcd 180.1514.

The mixture of isomers was converted by hydrogenation (53 mg, 50 psi of H₂, 103 mg of 5% Pd/C, 3:1 ethyl alcohol/acetic acid, 25 °C, 4 h) to a single isomer (retention time 7.4 min, column B programmed from 100 to 250 °C at 16 °C/min). ¹H NMR (CDCl₃): δ 1.10 (s, 9 H, CH₃), 2.30 (d, 2 H, *J* = 7 Hz, COCH), 1.0–2.10 (m, all other H). IR (neat): 2920 (s), 2860 (m), 1705 (s), 1475 (m), 1445 (m), 1360 (m), 1260 (m), 1100 (m), 1055 (m), 960 (m) cm⁻¹. GC-MS: *m/e* (relative intensity) 182 (M, 6), 125 (71), 97 (100), 83 (15), 69 (8), 67 (6).

Characterization of the Products from Complex 7 and 2-(1-Ethoxyethoxy)-2-lithiohexanenitrile (Anion F). The residue from the general procedure was dissolved in methanol (4 mL) and 5% aqueous sulfuric acid (1 mL) and the mixture stirred for 20 min at 25 °C. The resulting solution was poured into water in a separatory funnel and extracted with diethyl ether. The ether layer was shaken vigorously with 10% aqueous sodium hydroxide solution for a period of 15 min and dried over magnesium sulfate and the solvent was evaporated. The residue after evaporation was placed on a short column of silica gel (5 g) and eluted with hexane (50 mL). Elution with hexane/dichloromethane (7:3) afforded the mixture of olefins 9F and 10F. The mixture of olefins was distilled in a short-path apparatus (95–115 °C (1.2 mm)) to give a clear, colorless liquid; 0.29 g, 78% yield. Analysis by GLPC (Column A at 150 °C) showed two peaks at

12.2 and 16.2 min in the area ratio 80:20. GC-MS established that the components were isomers consistent with the formula $C_{11}H_{18}O$ (below). 1H NMR ($CDCl_3$): δ 6.5 (m, <0.2 H), 5.6 (m, 2 H, vinyl H), 0.9 (t, 3 H, $J = 6$ Hz, CH_3), 1.0–2.7 (m, all other H). IR (neat): 3030 (w), 2955 (s), 2935 (s), 2860 (s), 1705 (s), 1660 (s), 1470 (m), 1445 (m), 1375 (m), 1270 (m), 1195 (s) cm^{-1} . GC-MS (retention time 12.2 min): m/e (relative intensity) 166 (M, 9), 109 (4), 85 (100), 81 (26), 79 (15), 57 (86), 53 (10). GC-MS (retention time 16.2 min): m/e (relative intensity) 166 (parent, 15), 109 (100), 85 (5), 81 (87), 79 (28), 57 (11), 53 (17); mass spectral mol wt 166.1352, calcd 166.1358.

The major isomer (retention time 12.2 min) was identified by comparison of retention time with a sample of **9F** prepared by alternative synthesis (see below). The minor isomer at a retention time of 16.2 min was assigned structure **10F** due to the appearance of a band at 1660 cm^{-1} in the IR spectrum and the large loss of the *n*-butyl group in the mass spectrum. The mixture of isomers was converted by hydrogenation (67 mg, 50 psi of H_2 , 109 mg of 5% Pd/C, 3:1 ethyl alcohol/acetic acid, 25 °C, 2 h) to a single isomer (retention time 7.6 min, column B at 100–250 °C/16 °C per min). The hydrogenation product was characterized by spectral data. 1H NMR (CCl_4): δ 2.3 (t, 2 H, $J = 6$ Hz, α -keto CH_2), 0.9 (t, 3 H, $J = 7$ Hz, CH_3), 1.0–2.4 (m, all other H). IR (neat): 2960 (s), 2925 (s), 2860 (s), 1705 (s, C=O), 1470 (m), 1445 (m), 1375 (m), 1255 (s), 1190 (s), 1020 (s), 800 (s) cm^{-1} . GC-MS: m/e (relative intensity) 168 (M, 13), 126 (11), 111 (30), 85 (42), 83 (100), 67 (11).

Characterization of the Products from Complex 7 and (Diphenylmethyl)lithium (G). Column chromatography of the residue from the general procedure (15 g of silica gel impregnated with 15% $AgNO_3$) eluted with hexane separated diphenylmethane from the mixture of olefins **8G** and **9G** to give a clear, colorless liquid; 0.45 g, 80% yield. Analysis by GLPC (column A at 225 °C) showed two peaks at 41 and 70 min in the area ratio 34:66. 1H NMR ($CDCl_3$): δ 6.94 (s, 10 H, aromatic H), 5.40 (br s, 1.4 H, vinyl H), 5.35 (br s, 0.6 H, vinyl H), 3.51 (d, 0.3 H, $J = 11$ Hz, H adjacent to phenyls), 3.45 (d, 0.7 H, $J = 11$ Hz, H adjacent to phenyls), 1.0–2.6 (m, all other H). IR (neat): 3040 (s, 2940 (s), 1950 (w), 1890 (w), 1810 (w), 1600 (m), 1500 (s), 1460 (s), 1365 (m), 1230 (m), 920 (m), 750 (s), 710 (s) cm^{-1} . GC-MS: m/e (relative intensity) first component, 248 (M, 3), 168 (19), 167 (100), 152 (14), 115 (5), 91 (5), 81 (5), second component, 167 (100), Ph_2CH^+ , 168 (23), 165 (26), 152 (17), 129 (7), 115 (8), 91 (11), 79 (5).

The major isomer at a retention time of 70 min was identified by comparison of retention time with a sample of **9G** prepared by alternative synthesis (see below). The minor isomer at a retention time of 41 min was assigned structure **8G** by a process of elimination. Structure **10G** is not consistent with the NMR data; in particular, the presence of signals at δ 3.4–3.6 in the ratio 1:2 relative to the olefinic signals at δ 5.4–5.6. The mixture of isomers was converted by hydrogenation (17 mg, 50 psi of H_2 , 94 mg 5% Pd/C, 2:1 ethyl alcohol/acetic acid, 25 °C, 24 h) to a single isomer (retention time 4.4 min, column B programmed at 230–290 °C/16 °C per min). The hydrogenation product was characterized by spectral data. 1H NMR ($CDCl_3$): δ 7.1 (s, 10 H, aromatic H), 3.5 (d, 1 H, $J = 11$ Hz, Ph_2CHR), 1.0–1.9 (m, all other H). IR (neat): 3055 (w), 3020 (m), 2920 (s), 2850 (s), 1600 (w), 1490 (w), 1445 (m), 1260 (m), 1030 (br m), 800 (w), 750 (m), 705 (s) cm^{-1} . GC-MS: m/e (relative intensity) 250 (M, 8), 168 (44), 167 (100), 165 (23), 152 (15), 91 (13), 73 (33).

Characterization of the Products from Complex 7 and (Triphenylmethyl)lithium (Anion H). Column chromatography of the residue from the general procedure (15 g of silica gel impregnated with 15% $AgNO_3$) eluting with hexane separated triphenylmethane from the mixture of olefins **8H** and **9H**, as a white solid 0.52 g, 71% yield; mp 138–139 °C. 1H NMR ($CDCl_3$): δ 7.35 (m, 15 H, aromatic H) [5.85 (d, $J = 10.8$ Hz, vinyl H), 5.68 (s), 5.63 (dt, $J = 10.8, 3.2$ Hz, total of 2 H), 4.01 (m, 0.72 H, $Ph_3CCHC=$), 3.70 (br t, 0.28 H, $J = 11.5$ Hz, $Ph_3CCH(CH_2)_2$), 1.1–2.5 (m, 6 H, all other H), irradiate δ 5.72: δ 4.01 (5-line pattern), 3.70 (br t, $J = 11.5$ Hz). IR (CCl_4): 3080 (m), 3050 (s), 3015 (s), 2950 (s), 2910 (s), 2830 (m), 1600 (m), 1485 (s), 1440 (s), 1500 (w), 1170 (w), 1040 (m), 700 (s) cm^{-1} . Mass spectrum (EI): m/e (relative intensity) 324 (parent, 21), 244 (70), 243 (96), 165 (100), 115 (22), 91 (27); the same spectrum was recorded for all

isomers; mass spectral mol wt 324.1861, calcd 324.1878.

The major isomer was assigned as **8H** due to the greater chemical shift expected for the H substituted in the allylic position. The minor isomers was assigned as **9H** due to the NMR absorption at δ 3.70; assignment as **10H** would be inconsistent with the integration. The mixture of isomers was converted by dehydrogenation (12 mg, 57 mg of 10% Pd/C, *p*-cymene, 178 °C, 48 h) to a single compound, tetraphenylmethane: mp 277–280 °C; mixed mp with tetraphenylmethane 279–281 °C. 1H NMR ($CDCl_3$): δ 7.24 (s).

Characterization of the Products from Complex 7 and 2-Lithio-1,3-dithiane. The residue from the general procedure was dissolved in bis(2-methoxyethyl)ether and heated at 162 °C under argon for 30 min to decompose iron-sulfur complexes. The mixture was poured into water and extracted once with light petroleum ether. The organic layer was washed with water (4 times) and dried over potassium carbonate, and the solvent was removed by rotary evaporation. Column chromatography (15 g of silica gel) achieved purification of the olefins **8I–10I** from anion **I** as a mixture (elution with hexane/dichloromethane (24:1)). The mixture of olefins was distilled in a short-path apparatus (150 °C (0.8 mm)) to give a clear, colorless liquid; 0.27 g, 60%. 1H NMR (CCl_4): δ 5.4 (m, 1.6 H, vinyl H), 4.2 (s, 0.37 H, $R_2C=CRCH(SR)_2$), 3.90 (two d, 0.63 H, $R_2CHCH(SR)_2$), 2.60 (m, 4 H, SCH_2R), 1.1–2.4 (m, other H). IR (neat): 3020 (w), 2950 (s), 2850 (s), 1450 (m), 1375 (m), 1275 (m), 1120 (w), 910 (w) cm^{-1} . GC-MS: m/e (relative intensity) 200 (M, 6), 125 (2), 121 (10), 119 (100), 91 (12), 79 (10). The same spectrum was recorded for all isomers.

Comparison of the 1H NMR spectral data of the mixture with parallel data of pure samples of **8I–10I** from alternate synthesis (see below) indicated the presence of **10I** (37%) and either (or both) **8I** or **9I** (63%). The isomers were inseparable by GLPC (column A at 210 °C and column C at 200 °C). Attempts to hydrogenate the reaction mixture failed (catalytic hydrogenations using Pd/C and $(PPh_3)_3RhCl$, diimide generated from thermal decomposition of *p*-toluenesulfonyl hydrazide,²⁶ and diborane).

Characterization of the Products from Complex 7 and ((Phenylthio)methyl)lithium (J). The residue from the general procedure was dissolved in bis(2-methoxyethyl)ether and heated at 162 °C under argon for 30 min to decompose the iron-sulfur complexes. The mixture was poured into water and extracted with light petroleum ether. The organic layer was washed with water (4 times) and dried over potassium carbonate, and the solvent was removed by rotary evaporation. Column chromatography (15 g of silica gel) produced **8J–10J** as a mixture, eluted with hexane. The mixture of olefins was distilled in a short-path apparatus (160 °C (1.0 mm)) to give a clear, colorless liquid (0.19 g, 42%). Analysis by GLPC (column B, 170–280 °C, 16 °C/min) showed two peaks (6.7 and 6.9 min; relative areas 41:59). GC-MS established that the components were isomers, consistent with the formula $C_{13}H_{16}S$ (see below). 1H NMR ($CDCl_3$): δ 7.1 (m, 5 H, aromatic H), 5.7 (m, 1.6 H, vinyl H), 3.55 (s, 0.8 H, C=CRCH₂SR), 2.95 (d, 1.2 H, $J = 5$ Hz, CHR_2CH_2SR), 1.4–2.2 (m, all other H), irradiate δ 2.1: δ 2.95 becomes a singlet. IR (neat): 3040 (m), 2920 (s), 1600 (m), 1470 (s, m), 1440 (s), 1060 (w), 1040 (w), 960 (w), 750 (s), 700 (s) cm^{-1} . GC-MS (retention time 6.7 min): m/e (relative intensity) 205 (4), 204 (M, 27), 147(4), 123 (3), 110 (47), 95 (100), 79 (58). GC-MS (retention time 6.9 min), m/e (relative intensity) 205 (4), 204 (parent, 28), 143 (3), 124 (16), 123 (75), 110 (30), 95 (29), 94 (78), 81 (14), 79 (100).

The major isomer at a retention time of 6.9 min was assigned structure **8J** or **9J** on the basis of the mass spectral fragmentation pattern, especially the efficient α cleavage to give fragment ions at m/e 123 and 81, allylic cations or radicals. The minor isomer at a retention time of 6.7 min was assigned structure **10J** on the basis of the complementary fragmentation pattern (very small m/e 123 and nonexistent peak at m/e 81), and the appearance of a singlet at δ 3.55 in the 1H NMR spectrum of the mixture. The mixture was converted by hydrogenation (67 mg, diborane in diglyme, 25 °C; followed by propionic acid, 162 °C, 2 h) to a single isomer with spectral properties identical with those of cyclohexylmethyl phenyl sulfide.²⁷ 1H NMR ($CDCl_3$): δ 7.1 (m,

(26) Van Tamelen, E. E.; Dewey, R. S. *J. Am. Chem. Soc.* **1961**, *83*, 3729.

5 H, aromatic H), 2.8 (d, 2 H, $J = 6$ Hz, CH₂SPh), 1.0–2.1 (m, all other H). IR (neat): 3050 (w), 2920 (s), 2850 (s), 1580 (m), 1470 (m), 1440 (s), 1260 (w), 1070 (w), 1020 (w), 740 (s), 700 (s) cm⁻¹.

Characterization of the Products from Complex 7 and Phenyllithium (Anion K). To a solution of complex 7 (0.50 g, 2.3 mmol) in tetrahydrofuran (8 mL) and hexamethylphosphoramide (2 mL) under argon at -78 °C was added via syringe a solution of phenyllithium in hexane (2.5 mmol) over a period of 10 min. The mixture was stirred for 2 h at this temperature after which time trifluoroacetic acid (1.5 mL, 19.5 mmol) was added dropwise over a period of 1 min. The reaction mixture was treated as outlined in the general procedure. Column chromatography of the residue (10 g of silica gel) gave a fraction containing the mixture of olefins 8K–10K, eluted with hexane, followed by a fraction containing a mixture of cyclohexen-3-yl-phenyl ketone (13a) and benzaldehyde eluted with hexane/methylene chloride (7:3). The nonpolar fraction was distilled in a short-path apparatus (100–120 °C (1.0 mm)) to give a clear, colorless liquid; 0.15 g, 43% yield. ¹H NMR (CDCl₃): δ 7.03 (s, 5 H, aromatic H), 5.72 (m, 2 H, vinyl H), 3.05 (m, 0.4 H, CHRC=C), 1.0–2.9 (m, all other H). IR (neat): 3050 (m), 2950 (s), 1650 (w), 1605 (m), 1500 (m), 1450 (m), 1350 (m), 1143 (m), 930 (m), 770 (s), 750 (s), 700 (s) cm⁻¹. GC-MS: m/e (relative intensity) 158 (M, 37), 154 (20), 143 (21), 129 (34), 128 (18), 115 (51), 104 (100).

The mixture of isomers was converted by hydrogenation (53 mg, 50 psi of H₂, 127 mg of Pd/C, 1:1 ethyl alcohol/acetic acid) to give a single compound with spectral properties identical with those of cyclohexylbenzene.

Quantitative NMR of the polar fraction (dioxane standard) showed benzaldehyde to be present in 5% yield. Distillation in a short-path apparatus (130–150 °C (1.0 mm)) afforded a clear, colorless liquid (0.11 g 26% yield, free of aldehyde absorption in the NMR. GLPC analysis of the distillate (column A at 180 °C) revealed a single component (retention time 9.3 min). This component was assigned the structure 3-cyclohexen-1-yl phenyl ketone on the basis comparison of retention time and spectral properties with those an authentic sample from an alternative synthesis (see below).

Characterization of the Products from Complex 7 and Lithium Lithioisobutyrate (Anion L). According to the general procedure (except that after addition of trifluoroacetic acid, the mixture was poured into water rather than saturated aqueous sodium carbonate), a residue was obtained that was chromatographed on silica gel (5 g). A dark green solid [Fe₃(CO)₁₂] was eluted with hexane, followed by a fraction containing olefin 8L eluted with dichloromethane. Distillation in a short-path apparatus (125 °C (0.2 mm)), followed by crystallization gave 9L (0.33 g, 88% yield) as a white solid, mp 57–59 °C. ¹H NMR (CDCl₃): δ 11.5 (s, 1 H, COOH), 5.72 (br d, 1 H, $J = 11$ Hz, vinyl H), 5.48 (br d, 1 H, $J = 11$ Hz, vinyl H), 2.45 (m, 1 H, =CCHR₂), 1.20–2.05 (m, 6 H, all other H), 1.15 and 1.11 (2s, 5 H, 2CH₃). ¹³C NMR (H decoupled): δ 184 (COOH), 129 (C=C), 127 (C=C), 45 (RCCOOH), 43 (=CCHCR₂), 25, 24, 22, 21.8, 21.5. IR (CH₂Cl₂): 2500–3100 (br s, OH and CH), 1750 (m, C=O monomer), 1700 (s, C=O dimer), 1465 (m), 1400 (w), 1310 (w), 1270 (m), 1260 (m), 950 (m) cm⁻¹. GC-MS: m/e (relative intensity) 168 (M, 2), 123 (4), 107 (2), 88 (42), 81 (100), 79 (22), 67 (7).

Characterization of the Products from Complex 7 and *n*-Butyllithium. To a solution of complex 7 (0.50 g, 2.3 mmol) in THF and HMPA (2 mL) under argon at -78 °C was added dropwise over a period of 5 min a solution of *n*-butyllithium in hexane (1.62 M, 1.54 mL, 2.5 mmol). The mixture was stirred at -78 °C for a period of 2 h, after which time trifluoroacetic acid (1.5 mL, 19.5 mmol) was added, and the mixture was treated as outlined in the general procedure. Column chromatography of the residue (10 g of silica gel; hexane) gave a fraction containing unreacted complex 7 (0.12 g, 24% recovery) and a fraction that was concentrated and distilled in a short-path apparatus (70–110 °C (1.5 mm)) to give a clear, colorless liquid (0.048 g, 14% yield). The product (type 8, 9, or 10) was converted by hydrogenation (43 mg, 50 psi of H₂, 134 mg of 5% Pd/C, 1:1 ethanol/acetic acid)

to a single compound with a retention time of 3.1 min (column A at 100 °C). The compound was identified as *n*-butylcyclohexane on the basis of comparison of retention time and of spectral data with those of a standard sample.

Elution with hexane/dichloromethane (7:3) provided a mixture of valeraldehyde (11% yield based on quantitative NMR; dioxane as internal standard) and a second compound. Distillation in a short-path apparatus (90–110 °C (1.2 mm)) removed the valeraldehyde and afforded a clear, colorless liquid; 0.13 g, 34% yield. GLPC analysis revealed a single component of retention time 12.2 min (column A at 150 °C). This compound was assigned as 8 (R = COC₅H₁₁, 4-valerylcyclohexene) on the basis of spectral data comparison with a sample from a simple alternate synthesis (see below).

Characterization of the Products from Complex 7 and Phenylmagnesium Bromide. To a solution of 7 (0.50 g, 2.3 mmol) in THF (8 mL) and HMPA (2 mL) at -78 °C under argon was added via syringe a solution of phenylmagnesium bromide in diethyl ether (Alfa, 2.5 mmol) over a period of 10 min. The solution was allowed to warm to 25 °C, stirred for a period of 2 h, and then cooled again to -78 °C. Trifluoroacetic acid (1.5 mL, 19.5 mmol) was added neat dropwise over a period of 1 min, and the mixture was treated hereafter as outlined in the general procedure. Column chromatography of the residue from the general procedure (5 g of silica gel) allowed isolation of complex 7 (0.34 g, 78%) eluted with hexane. Elution with hexane/dichloromethane (7:3) afforded 38 mg (9% yield) of a compound consistent in spectral properties with literature values for cyclohex-3-en-1-yl phenyl ketone.²⁸ ¹H NMR (CDCl₃): δ 7.8 (dd, 2 H, $J = 2.5$, 8 Hz, aromatic H ortho to carbonyl), 7.4 (m, 3 H, other aromatic H), 5.5 (br s, 2 H, vinyl H), 3.4 (m, 1 H, COCHR₂), 1.0–2.4 (m, 6 H, other H). GC-MS: m/e (relative intensity) 186 (M, 2), 106 (7), 105 (100), 79 (7), 77 (31), 51 (11).

Reaction of 7 with Anion A Followed by Reaction with (a) Iodomethane. The general procedure was followed by substituting iodomethane (1.5 mL, 24.0 mmol) for trifluoroacetic acid and allowing the mixture to stir 2 h at 25 °C before pouring it into saturated aqueous sodium carbonate solution. Column chromatography of the residue from the general procedure (5 g of silica gel) gave complex 7 (0.32 g, 64% recovery) eluted with hexane. Elution with more polar solvents (hexane/dichloromethane (7:3) and dichloromethane) produced no olefinic material.

(b) With Chlorotrimethylsilane. The general procedure was followed by substituting chlorotrimethylsilane (1.0 mL, 8.0 mmol) for trifluoroacetic acid and allowing the mixture to stir for 2 h at 25 °C before pouring it into saturated aqueous sodium carbonate solution. Column chromatography of the residue from the general procedure (5 g of silica gel) afforded complex 7 (0.48 g, 96% recovery) eluted with hexane. Elution with dichloromethane produced a single compound identified as 2-(trimethylsilyl)-2-methylpropionitrile. ¹H NMR (CDCl₃): δ 1.2 (s, 6H, C(CH₃)₂), 0.2 (s, 9 H, Si(CH₃)₃).

Reaction of 7 with (Triphenylmethyl)lithium (H) Followed by Reaction with Benzoyl Chloride. The general procedure was followed by substituting benzoyl chloride (2.0 mL, 17.2 mmol) for trifluoroacetic acid. Column chromatography of the residue from the general procedure yielded a yellow oil (eluted with hexane/dichloromethane (4:1)). It was dissolved in hot ethanol and crystallized upon cooling. The crystals were recrystallized once from heptane to give 0.510 g (53% yield) of white crystals, mp 158–160 °C. The compound was characterized as 17 by spectral data. ¹H NMR (CDCl₃, 500 MHz): δ 7.86 (dd, 2 H, $J = 1.7$, 8.3 Hz, CPh, ortho H's), 7.3 (m, 18 H, all other aromatic H), 5.97 (ddd, 1 H, $J = 10.0$, 0.8, 1.2 Hz at C-9),²⁹ 5.63 (dq, 1 H, $J = 10.0$, 1.25 Hz, H at C-10),²⁹ 4.18 (m, 1 H, H at C-11), 3.80 (8-line pattern, 1 H, H at C-8), 2.50 (3-line pattern, 1 H, H at C-12), 2.14 (m, 1 H, H at C-13), 1.67 (m, 1 H, H at C-13), 1.89 (m, 1 H, H at C-13), irradiate δ 5.97: δ 5.63 (br s, 1 H, H at C-10),

(28) Sugita, K.; Tamura, S. *Bull. Chem. Soc. Jpn.* 1971, 44, 3388–3391.

(29) In the half-chair cyclohexene conformation with the 1,4-trans substituents occupying pseudo-equatorial sites, the dihedral angle between the methine hydrogens (pseudoaxial) and the vinyl hydrogens should approach 90°, leading to small vicinal coupling constants. For a discussion, see: Abraham, R. J.; Loftus, P. "Proton and Carbon-13 NMR Spectroscopy"; Heyden and Son, Ltd.: London, 1979.

4.18 (dt, $J = 5.8, 2.2$ Hz, H at C-11), 3.80 (8-line pattern, H at C-8), irradiate δ 5.63: δ 5.97 (br s, H at C-9), 4.18 (dt, $J = 5.8, 2.2$ Hz, H at C-11), 3.80 (8-line pattern, H at C-8), irradiate δ 4.18: δ 5.97 (dd, $J = 10.0, 1.2$ Hz, H at C-9), 5.63 (dd, $J = 10.0, 1.3$ Hz, H at C-10), 3.80 (td, $J = 4.8, 2.2$ Hz, H at C-8), irradiate δ 3.00: δ 5.97 (d, $J = 10.0$ Hz, H at C-9), 5.63 (dd, $J = 1.3, 10.0$ Hz, H at C-10), 4.18 (dt, $J = 5.8, 1.5$ Hz, H at C-11). ^{13}C NMR (CDCl_3 , H decoupled) δ 187 (C-7), 133 (C-15), 125 (C-1), 122, 121, 119, 118.3, 117, 115, 115.5, 56 (C-14), 42 (C-8), 37 (C-11), 25, 24 (C-12, 13). IR (CH_2Cl_2): 3080 (s), 3059 (s), 3035 (s), 2975 (s), 2885 (s), 1950 (w), 1890 (w), 1670 (s, C=O), 1600 (s, C=C), 1490 (s), 1445 (s), 1210 (s), 1032 (m), 950 (s), 730 (s), 750 (s), 680 (s) cm^{-1} . Mass spectrum (EI): m/e (relative intensity) 243 (Ph_3C^+ , 100), 165 (60), 105 (33); mol wt determination (cryoscopy in benzene) calcd 428.6, found 444. The observed small coupling constants between the vinyl and allylic protons are consistent with only a trans-1,4-diaxial arrangement of the allylic protons.²⁹ Anal. Calcd for $\text{C}_{26}\text{H}_{28}\text{O}$: C, 89.68; H, 6.58. Found: C, 89.90; H, 6.72.

Reaction of (η^4 -1,3-Butadiene)tricarbonyliron (20) with Anion A and Acid Quenching. The general procedure was followed substituting (1,3-butadiene)tricarbonyliron (20) for complex 7. Column chromatography of the residue from the general procedure (5 g of silica gel) gave a fraction of green solid [$\text{Fe}_3(\text{CO})_{12}$] eluted with hexane followed by a fraction containing the mixture of olefins 21a-d, eluted with hexane/dichloromethane (7:3). The mixture of olefins was distilled in a short-path apparatus (90–100 °C (60 mm)) to give a clear, colorless liquid; 0.22 g, 69% yield. Analysis by GLPC (column B at 40 °C) showed four peaks at 4.1, 4.3, 5.2, and 6.9 min in the area ratio 1:4:6:89. GC-MS established that the components were isomers, consistent with the formula $\text{C}_9\text{H}_{13}\text{N}$ (see below). The major isomer was separated via column chromatography (15 g of silica gel impregnated with 15% AgNO_3). The major isomer was assigned structure 21a on the basis of comparison of spectral properties with those of a sample from alternate synthesis. The structures of the minor isomers were assigned 21d (retention time 4.1 min), 21c (retention time 4.3 min), and 21b (retention time 5.9 min) on the basis comparison of GLPC properties with those of samples from alternate synthesis (see below).

Preparation of 2-(1-Cyclohexenyl)-2-methylpropionitrile and General Procedure for Methylation α to a Nitrile. To a flask containing diisopropylamine (0.67 mL, 4.8 mmol) and THF (10 mL) under argon at -78 °C was added rapidly via syringe a solution of *n*-butyllithium in hexane (4.7 mol). The mixture was allowed to stir at -78 °C for 20 min, after which time cyclohex-1-en-1-ylacetonitrile (0.27 g, 2.22 mmol)³⁰ was added via syringe over 1 min. The mixture was stirred 20 min at -78 °C, iodomethane (1.8 mL, 29 mmol) was added via syringe over 1 min, and the resulting mixture was stirred for 2 h at 25 °C. It was then partitioned between water and petroleum ether, and the water layer was washed with a second portion of petroleum ether. The combined organic solution was washed sequentially with saturated aqueous sodium thiosulfate solution and saturated aqueous sodium chloride solution and dried over magnesium sulfate, and the solvent was removed on a rotary evaporator. The residue was distilled in a short-path apparatus (80–110 °C (5 mm)) to give 10A as an homogeneous, colorless liquid. ^1H NMR (CDCl_3): δ 5.76 (m, 1 H, vinyl H), 1.99 (m, 4 H, allylic H), 1.40 (s, 6 H, CH_3), 1.56 (m, 4 H, all other H). ^{13}C NMR (CDCl_3 , H decoupled) δ 131 ($\text{R}_2\text{C}=\text{CHR}$), 119 (C=N), 117 ($\text{R}_2\text{C}=\text{CHR}$), 41 (R_3CCN), 30, 29, 28, 26, 27. GC-MS: m/e 149 (M, 7), 134 (2), 81 (100), 79 (22), 69 (11), 65 (5). The compound showed a single peak of retention time 13.0 min on GLPC analysis (column A at 130 °C).

Preparation of Cyclohex-3-en-1-ylacetonitrile. Cyclohex-3-en-1-ylacetonitrile was prepared according to the procedure of van Leusen and Oomkes³¹ from 3-cyclohexene-1-carboxaldehyde³² and tosylmethyl isocyanide.³³ ^1H NMR (CDCl_3): δ 5.72 (br s, 2 H, vinyl H), 1.5–2.6 (m, 9 H, other H). IR (neat): 3000 (s), 2250

(m), 1660 (w), 1440 (s), 1380 (s), 1270 (s), 1080 (m), 1050 (w), 950 (s) cm^{-1} . The yield was 64%.

Preparation of 2-(3-Cyclohexenyl)-2-methylpropionitrile (8A). The general procedure for methylation of nitriles was followed by using the following quantities of reagents: diisopropylamine (1.73 mL, 12.4 mmol), *n*-butyllithium (10.8 mmol), cyclohex-3-en-1-ylacetonitrile (0.50 g, 4.13 mmol), and iodomethane (2.32 mL, 37.3 mmol). A clear liquid (0.41 g, 67%) was obtained upon distillation in a short-path apparatus (80–120 °C (2.0 mm)). ^1H NMR (CDCl_3): δ 5.51 (br s, 2 H, vinyl H), 1.32 (s, 6 H, CH_3) overlapping with δ 1.3–2.4 (m, 7 H, all other H). ^{13}C NMR (CDCl_3): 122 (vinyl C), 120 (vinyl C), 45, 39, 31, 30, 29.2, 28.7, 28.3, the C=N was not observed. GC-MS: m/e (relative intensity) 149 (parent, 6), 134 (1), 107 (3), 81 (100), 79 (69), 71 (29), 69 (30). The product was shown to be pure by GLPC analysis (retention time 16.5 min, column A at 130 °C).

Methylation of the Mixture of Olefins 8B–10B. The general procedure for methylation of nitriles was followed by using diisopropylamine (0.097 mL, 0.69 mmol), *n*-butyllithium in hexane (0.52 mmol), olefins 8B–10B (0.050 g, 0.34 mmol), and iodomethane (0.5 mL, 8.0 mmol) in THF (5 mL). The product was distilled in a short-path apparatus (80–110 °C (1.0 mm)) to give a clear, colorless liquid, 39 mg (71% yield), of olefin mixture 8A–10A. ^1H NMR (CDCl_3): δ 5.60 (m, 2 H, vinyl H), 1.25 (br s, 6 H, CH_3), 1.3–2.5 (m, all other H). The mixture was analyzed by GLPC on column A, as before to give the ratios in entry 2, Table I.

Preparation of (*E*)-2,2,3-Trimethylpent-3-enitrile (21a) and 3-Ethyl-2,2-dimethylbut-3-enitrile (21c). To a flask containing diisopropylamine (4.1 mL, 0.029 mol) and THF (25 mL) at -78 °C under argon was added rapidly via syringe a solution of *n*-butyllithium in hexane (0.029 mmol). The mixture was allowed to stir for 20 min at -78 °C, and then 2-methyl-2-propionitrile (2.63 mL, 0.030 mol) was added rapidly via syringe. After the solution was stirred an additional 20 min at -78 °C, 2-butanone (3.0 g, 0.044 mol) was added dropwise over a period of 1 min. The resulting mixture was allowed to stir 2 h at 25 °C and then poured into water in a separatory funnel and extracted with diethyl ether (2 times). The combined organic extracts were washed with saturated aqueous sodium chloride solution and dried over potassium carbonate, and the solvent was removed by rotary evaporation. A mixture of the residual liquid with potassium hydrogen sulfate (7.7 g, 57 mmol) was heated in a simple distillation apparatus at 60–90 °C (60 mm) to give a cloudy liquid distillate that was partitioned between water and ether. The ether solution was washed sequentially with saturated aqueous sodium carbonate solution and saturated aqueous sodium chloride solution and dried over potassium carbonate, and the solvent was removed at 100 torr. Column chromatography of the residue (25 g of silica gel impregnated with 15% AgNO_3 , eluting with hexane/dichloromethane (7:3)) gave a fraction that was purified further by preparative GLPC (column D at 65 °C). The compounds at a retention time of 8 min (minor, 21a) and 12 min (major, 21b) were collected. For 21a: ^1H NMR (CDCl_3) δ 5.66 (qq, 1 H, $J = 5.4, 1.3$ Hz, vinyl H), 1.62 (br s, 3 H, $\text{CH}_3\text{C}=\text{C}$) overlapping with 1.67 (dq, 3 H, $J = 5.4, 1.3$ Hz, $\text{CH}_3\text{CH}=\text{C}$), 1.41 (s, 6 H, CH_3), irradiate at δ 5.66: δ 1.67 (q, $J = 1.3$ Hz), 1.62 (q, $J = 1.3$ Hz), irradiate δ 1.62: δ 5.66 (s, vinyl H). ^{13}C NMR (CDCl_3 , H decoupled): δ 119 ($\text{RCH}=\text{CR}_2$), 37 (R_3CCN), 25 ($\text{RC}(\text{CH}_3)\text{CN}$), 12, 11 (allylic CH_3), not observed C=N and = CR_2 ; IR (neat) 3030 (m), 2990 (s), 2920 (s), 2240 (s, C=N), 1660 (w), 1455 (s), 1440 (s), 1380 (s), 1200 (m), 1130 (m), 1035 (m), 830 (s) cm^{-1} ; GC-MS, m/e (relative intensity) 123 (M, 37), 108 (100), 96 (25), 93 (55), 91 (14), 81 (50), 69 (57). The geometry of the double bond is not established by spectral data; the configuration of 21a is assigned on the basis of the usual formation of the more stable isomer under these elimination conditions.³⁴ Isomer 21c: ^1H NMR (CDCl_3) δ 4.95 (s, 1 H, vinyl H), 4.73 (s, 1 H, vinyl H), 2.05 (q, 2 H, $J = 4.3$ Hz, $\text{CH}_2\text{C}=\text{C}$), 1.33 (s, 6 H, CH_3), 1.00 (t, 3 H, $J = 4.3$ Hz, CH_3CH_2).

(30) 1-Cyclohexenylacetonitrile was purchased from Aldrich Chemical Co.

(31) Van Leusen, A. M.; Oomkes, P. G. *Synth. Commun.* 1980, 10, 399–403.

(32) The 3-cyclohexene-1-carboxaldehyde was purchased from Aldrich Chemical Co.

(33) Tosylmethyl isocyanide was purchased from Aldrich Chemical Co. and used directly.

(34) Acid-catalyzed dehydration of alcohols proceeds via an E1 mechanism through a carbocation intermediate. Conformational analysis of the intermediate suggests that steric interactions are minimized in the conformation that leads to the *E* olefin. For a discussion, see: March, J. "Advanced Organic Chemistry", 2nd ed.; McGraw-Hill: New York, 1977.

Preparation of (*E*)-2,2-Dimethylhex-4-enitrile (21b). To a solution of 2-lithio-2-methylpropionitrile (prepared as directly above, 3.64 mmol) in THF (10 mL) at -78°C under argon was added neat via syringe over a period of 1 min (*E*)-crotyl bromide (0.37 mL, 3.6 mmol).³⁵ The solution was allowed to stir at 0°C for a period of 1 h and then poured into water. The mixture was washed with diethyl ether (2 times), and the combined organic extracts were washed sequentially with water and saturated aqueous sodium chloride solution and dried over magnesium sulfate, and the solvent was removed to give a clear liquid. ¹H NMR (CDCl₃): δ 5.5 (m, 2 H, vinyl H), 2.3 (d, 2 H, $J = 5$ Hz, CH₂CH=), 1.8 (d, 3 H, $J = 5$ Hz, allylic CH₃), 1.35 (s, 6 H, other CH₃). GC-MS: *m/e* (relative intensity) 123 (M, 17), 108 (24), 94 (10), 93 (15), 81 (33), 79 (12), 69 (79), 55 (100).

Preparation of 2,2-Dimethylhex-5-enitrile (21d). The previous procedure was followed by substituting 4-bromo-1-butene³⁶ (0.37 mL, 3.6 mmol) for (*E*)-crotyl bromide. ¹H NMR (CDCl₃): δ 5.8 (m, 1 H, CH₂=CHR), 5.0 (m, 2 H, CH₂=C), 2.2 (q, 2 H, $J = 6$ Hz, allylic CH₂) overlapping with 2.0 (t, 2 H, $J = 6$ Hz, other CH₂), 1.2 (s, 6 H, CH₃).

Preparation of Ethyl 3-Cyclohexene-1-carboxylate. Ethyl 3-cyclohexene-1-carboxylate was prepared from ethyl acrylate and butadiene according to the method of Onishchenko.³⁷ ¹H NMR (CDCl₃): δ 5.4 (br s, 2 H, vinyl H), 4.0 (q, 2 H, $J = 7$ Hz, OCH₂), 1.2–2.4 (m), 1.1 (t, 3 H, $J = 7$ Hz, CH₃). The yield was 84%.

Preparation of 3-Cyclohexene-1-carboxylic Acid. To a flask equipped with a condenser was added ethyl 3-cyclohexene-1-carboxylate (2.0 g, 0.013 mol), sodium hydroxide (0.55 g, 0.014 mol), methanol (15 mL), and water (15 mL). The mixture was heated at reflux for 30 min, cooled, and extracted two times with ether. The aqueous layer was cooled to 0°C and acidified with 10% aqueous hydrochloric acid. The mixture was extracted two times with ether, and the combined extracts were washed with saturated sodium chloride solution and dried over magnesium sulfate, and the solvent was removed on a rotary evaporator. The crude product (1.52 g, 93% yield) was used in subsequent experiments. ¹H NMR (CDCl₃): δ 10.9 (s, 1 H, COOH), 5.4 (s, 2 H, vinyl H), 1.0–2.5 (m, 7 H, CH₂ and CH).

Preparation of Cyclohex-3-en-1-ylidiphenylmethanol. To a solution of phenylmagnesium bromide (3.9 mmol) in diethyl ether (10 mL) under argon at 0°C was added via syringe a solution of ethyl 3-cyclohexenecarboxylate (0.30 g, 1.95 mmol) in diethyl ether (2 mL) over a period of 10 min. The mixture was stirred for 30 min at 0°C , then mixed with 1 N aqueous ammonium chloride solution in a separatory funnel, and extracted (2 times) with diethyl ether. The combined organic extracts were washed sequentially with water and saturated aqueous sodium chloride solution and then dried over magnesium sulfate, and the solvent was removed by rotary evaporation. The residue was used directly in the following reaction. ¹H NMR (CDCl₃): δ 7.2 (m, 10 H, aromatic H), 5.6 (br s, 2 H, vinyl H), 2.8 (br t, 1 H, $J = 9$ Hz, R₃CH), 2.2 (s, 1 H, exchangeable with D₂O, OH), 1.1–2.4 (m, 6 H, 3CH₂).

Preparation of 3-(Diphenylmethyl)cyclohex-1-ene (9G). To a solution of cyclohex-3-en-1-ylidiphenylmethanol (0.20 g, 0.76 mmol) and triethylsilane (0.088 g, 0.76 mmol) in dichloromethane under argon at 0°C was added via syringe trifluoroacetic acid (1 mL, 13 mmol) over a period of 10 min, and the mixture was allowed to stir for 20 h at 25°C .³⁸ Potassium carbonate was added, the mixture was decanted into a separate flask, washing the residue with dichloromethane, and the solvent was removed by rotary evaporation. The residue was filtered through silica gel using hexane as the eluent. The solvent was removed to give 9G as a clear, colorless, viscous oil. ¹H NMR (CDCl₃): δ 7.2 (br s, 10 H, aromatic H), 5.6 (br s, 2 H, vinyl H), 3.5 (d, 1 H, $J = 11$ Hz, Ph₂RCH), 1.0–2.6 (m, 7 H, all other H). IR (neat): 3040 (s), 2940 (s), 1950 (w), 1890 (w), 1810 (w), 1600 (m, C=C), 1500 (s), 1460 (s), 1365 (m), 1230 (m), 920 (m), 750 (s), 710 (s) cm⁻¹. GC-

MS: 248 (M, 3), 168 (19), 167 (100), 165 (22), 152 (14), 115 (5), 91 (5), 81 (5).

Preparation of Comparison Compounds 8I–10I. The adducts 9I³⁹ and 10I⁴⁰ from complex 7 with anion I were prepared as described in the literature. The adduct 8I was obtained from the reaction of 1-bromo-2-cyclohexene with 2-lithio-1,3-dithiane. To a flask containing a solution of 2-lithio-1,3-dithiane (8.3 mmol) in THF (20 mL) at -78°C under argon was added dropwise via syringe 1-bromo-2-cyclohexene (1.23 mL, 10.0 mmol)⁴¹ over a period of 5 min. The mixture was kept at -25°C for a period of 3 days and then poured into water. The mixture was extracted two times with light petroleum ether, and the combined solution was washed sequentially with saturated aqueous sodium carbonate solution, saturated aqueous sodium thiosulfate solution, and water, and then dried over potassium carbonate. The solvent was removed by rotary evaporation to leave a residue that was distilled through a short Vigreux column. The fraction of bp 90 – 95°C (0.03 mm) was collected; 0.98 g (59% yield). ¹H NMR (CDCl₃): δ 5.6 (br s, 2 H, vinyl H), 4.0 (d, 1 H, $J = 5$ Hz, CH(SR)₂), 2.80 (m, 4 H, SCH₂), 1.3–2.4 (m, all other H). ¹³C NMR (CDCl₃): δ 127 (d, vinyl C), 126 (d, vinyl C), 52 (d, CH(SR)₂), 38 (t), 28.6 (t), 24 (t), 23 (d, C=CHCHR), 20 (t). GC-MS: *m/e* (relative intensity) 200 (M, 3), 121 (10), 119 (100), 106 (4), 97 (3), 91 (8), 85 (5), 81 (3). The product was homogeneous by GLPC (retention time 6.4 min, column D at 210°C).

Preparation of 3-Pentanoylcyclohex-1-ene. To a solution of 3-cyclohexene-1-carboxylic acid (0.20 g, 1.6 mmol) and THF (10 mL) under argon at -78°C was added via syringe a solution of *n*-butyllithium in hexane (3.3 mmol) over a period of 10 min. The mixture was stirred at 0°C for a period of 1 h, after which time the mixture was taken up in a syringe and added dropwise to a rapidly stirred solution of 10% aqueous hydrochloric acid at 0°C over a period of 10 min. The mixture was extracted two times with ether, and the combined extracts were washed sequentially with 10% aqueous potassium hydroxide and saturated aqueous sodium chloride and dried over magnesium sulfate, and the solvent was removed on a rotary evaporator. The residue was distilled in a short-path apparatus (90 – 110°C (1.0 mm)) to give a clear liquid (0.21 g, 78% yield). ¹H NMR (CDCl₃): δ 5.6 (s, 2 H, vinyl H), 2.37 (t, 2 H, $J = 7$ Hz, COCH₂CH₂), 0.9 (t, 3 H, CH₃) overlapping with 1.0–2.8 (m, all other H). IR (neat): 3025 (m), 2980 (s), 1710 (s, C=O), 1660 (m, C=C), 1450 (m), 1360 (m), 1195 (w), 1130 (w), 730 (s) cm⁻¹. GC-MS: *m/e* (relative intensity) 166 (M, 10), 123 (4), (4), 109 (24), 95 (26), 85 (100), 81 (100), 81 (55). The product was shown to be pure by GLPC analysis (retention time 12.2 min, column A at 150°C).

Preparation of 4-Benzoylcyclohex-1-ene. The previous procedure was followed substituting a solution of phenyllithium in cyclohexane (3.3 mmol) for *n*-butyllithium in hexane. The product was purified by distillation in a short-path apparatus (100 – 130°C (0.5 mm)). ¹H NMR (CDCl₃): δ 7.8 (dd, 2 H, $J = 1.5, 9$ Hz, aromatic H ortho to carbonyl), 7.2 (m, 3 H, other aromatic H), 5.8 (br s, 2 H, vinyl H), 3.3 (m, 1 H, R₃CH), 1.4–2.5 (m, 6 H, CH₂). GC-MS: *m/e* (relative intensity) 186 (M, 2), 106 (7), 105 (100), 81 (4), 79 (6), 77 (34), 51 (14). The product was shown to be pure by GLPC analysis (retention time 9.3 min, column A at 180°C). The compound was previously reported.²⁸

Acknowledgment. We are pleased to acknowledge support of this work through a research grant from the National Science Foundation (No. CHE-7905561) and through a graduate traineeship from the Public Health Service to J.W.H. (1980–1981). In addition, the NMR facilities at Princeton and at Yale, provided partly by grants from the National Science Foundation, were employed in this project.

Registry No. A, 50654-53-0; B, 59263-57-9; C, 42492-52-4; D,

(39) Seebach, D.; Corey, E. J. *J. Org. Chem.* 1975, 40, 231–237.

(40) This compound was prepared from 1-cyclohexene-1-carboxaldehyde and 1,3-propanedithiol according to the above procedure. The 1-cyclohexene-1-carboxaldehyde was prepared according to a literature procedure. Cologne, J.; Perrot, A. *Bull. Soc. Chim. Fr.* 1957, 204–208, 658–662.

(41) Ziegler, K.; Späth, A.; Schaaf, E.; Schumann, W.; Winkelmann, E. *Justus Liebig's Ann. Chem.* 1942, 551, 80–119.

(35) (*E*)-crotyl bromide was obtained by careful fractional distillation of the commercial sample purchased from Aldrich Chemical Co.

(36) The 4-bromo-1-butene was purchased from Aldrich Chemical Co.

(37) Onishchenko, A. S. "Diene Synthesis"; Israel Program for Scientific Translations Ltd.: Jerusalem, 1964; p 93.

(38) Kursanov, D. N.; Parnes, Z. N.; Loim, N. M. *Synthesis* 1974, 633–651.

35717-09-0; E (Li), 69849-03-2; E (K), 55440-76-1; F, 62381-25-3; G, 881-42-5; H, 733-90-4; I, 36049-90-8; J, 13307-75-0; K, 591-51-5; L, 16423-62-4; 7, 12152-72-6; 8A, 82315-82-0; 8B, 82315-86-4; 8C, 84173-79-5; 8D, 84173-83-1; 8E, 82315-88-6; 8G, 82315-90-0; 8H, 84173-89-7; 8I, 82315-89-7; 8J, 65539-52-8; 8K, 15232-96-9; 8L, 84173-91-1; 9A, 82315-83-1; 9B, 82315-87-5; 9C, 84173-80-8; 9D, 84173-84-2; 9E, 24480-96-4; 9F, 84173-87-5; 9G, 60344-48-1; 9H, 84173-90-0; 9I, 53178-49-7; 9J, 82315-92-2; 9K, 4994-16-5; 9L, 84173-92-2; 10A, 54353-80-9; 10B, 26157-49-3; 10C, 84173-81-9; 10D, 84173-85-3; 10E, 775-10-0; 10F, 84173-88-6; 10I, 56028-77-4; 10J, 79597-48-1; 10K, 771-98-2; 13a, 831-14-1; 17, 84173-93-3; 20, 12078-32-9; 21a, 4786-15-6; 21b, 84173-94-4; 21c, 4786-27-0; 21d, 84173-95-5; Fe₃(CO)₁₂, 17685-52-8; isobutyronitrile, 78-82-0; propionitrile, 107-12-0; ethyl 2-methylpropionate, 97-62-1; *tert*-butyl propionate, 20487-40-5; 3,3-dimethyl-2-butanone, 75-97-8; 2-(1-ethoxyethoxy)hexanenitrile, 60427-76-1; diphenylmethane, 101-81-5; triphenylmethane, 519-73-3; 1,3-dithiane, 505-23-7; (methylthio)benzene, 100-68-5; benzene, 71-43-2; 2-methylpropionic acid, 109-72-8; *n*-butyllithium, 109-72-8; α,α -di-

methylcyclohexaneacetonitrile, 41781-05-9; α -methylcyclohexaneacetonitrile, 53154-02-2; ethyl α,α -dimethylcyclohexaneacetate, 84173-82-0; *tert*-butyl α -methylcyclohexaneacetate, 84173-86-4; 1-cyclohexyl-3,3-dimethyl-2-butanone, 23137-42-0; α -butyl- α -(1-ethoxyethoxy)cyclohexaneacetonitrile, 84192-50-7; cyclohexyldimethylmethane, 50585-08-5; tetraphenylmethane, 630-76-2; ((phenylthio)methyl)cyclohexane, 36293-56-8; benzaldehyde, 100-52-7; cyclohexylbenzene, 827-52-1; *n*-butylcyclohexane, 1678-93-9; valeraldehyde, 110-62-3; 4-valerylcyclohexane, 78932-51-1; phenyl bromide, 108-86-1; iodomethane, 74-88-4; chlorotrimethylsilane, 75-77-4; 2-(trimethylsilyl)-2-methylpropionitrile, 50638-76-1; benzoyl chloride, 98-88-4; cyclohex-1-en-1-ylacetonitrile, 6975-71-9; 2-butanone, 78-93-3; *E*-crotyl bromide, 29576-14-5; 4-bromo-1-butene, 5162-44-7; ethyl 3-cyclohexene-1-carboxylate, 15111-56-5; 3-cyclohexene-1-carboxylic acid, 4771-80-6; cyclohex-3-en-1-ylidiphenylmethanol, 84173-96-6; triethylsilane, 617-86-7; 1-bromo-2-cyclohexene, 1521-51-3; 3-pentanoylcyclohex-1-ene, 78932-51-1; 4-benzoylcyclohex-1-ene, 831-14-1.

Kinetics and Mechanism of the Substitution Reactions of (η^5 -Pentamethylcyclopentadienyl)dicarbonylrhodium(I) and (η^5 -Pentamethylcyclopentadienyl)dicarbonylcobalt(I)

Mark E. Rerek and Fred Basolo*

Department of Chemistry, Northwestern University, Evanston, Illinois 60201

Received October 5, 1982

The reaction of $\text{Co}(\eta^5\text{-C}_5\text{(CH}_3)_5\text{)(CO)}_2$ and $\text{Rh}(\eta^5\text{-C}_5\text{(CH}_3)_5\text{)(CO)}_2$ with phosphines, phosphites, and isocyanides proceeds readily to form monosubstituted products. For $\text{Rh}(\eta^5\text{-C}_5\text{(CH}_3)_5\text{)(CO)}_2$ a second substitution at a much slower rate is observed for phosphites and isocyanides. The reaction proceeds solely by a second-order process, first order in metal complex and first order in nucleophile. The rate is strongly dependent on the size of the entering ligand. The rate of replacement of CO by $\text{P}(n\text{-Bu)}_3$ for $\text{Rh}(\eta^5\text{-C}_5\text{(CH}_3)_5\text{)(CO)}_2$ in toluene at 40 °C is 10^2 slower than for the reaction of $\text{Rh}(\eta^5\text{-C}_5\text{H}_5\text{)(CO)}_2$. The reasons for this difference are discussed in terms of the mechanism first proposed for the substitution reactions of $\text{Rh}(\eta^5\text{-C}_5\text{H}_5\text{)(CO)}_2$.

Introduction

Several years ago we reported¹ that the rate of CO substitution in the 18-electron system $\text{Rh}(\eta^5\text{-C}_5\text{H}_5\text{)(CO)}_2$ is first order in $\text{Rh}(\eta^5\text{-C}_5\text{H}_5\text{)(CO)}_2$ and first order in nucleophile. The associative nature of the reaction was attributed to the ability of the cyclopentadienyl ligand to accept an electron pair from the metal, thus creating a vacant orbital susceptible to nucleophilic attack. This was the first proposed "slippage" of a cyclopentadienyl ring that has since attracted a great deal of interest,² although we had not discussed it in these terms.

Our renewed interest in organometallic reaction mechanisms has led us to reconsider this reaction. If the mechanism proposed by Schuster-Woldan and Basolo¹ is valid, then a complex with an electron-withdrawing group on the cyclopentadienyl ring should be better able to accept an electron pair from the metal and should react faster

than the parent complex. If electron-donating groups are placed on the cyclopentadienyl ring, then the complex should react more slowly due to the ring being less able to accept an electron pair from the metal. Cramer and Seiwel³ have shown this to be true for the rate of replacement of C_2H_4 by phosphines and phosphites in the series $\text{Rh}(\eta^5\text{-C}_5\text{H}_4\text{CN})(\text{C}_2\text{H}_4)_2 > \text{Rh}(\eta^5\text{-C}_5\text{H}_5)(\text{C}_2\text{H}_4)_2 > \text{Rh}(\eta^5\text{-C}_5\text{(CH}_3)_5)(\text{C}_2\text{H}_4)_2$.

Group 8 cyclopentadienyldicarbonyl compounds catalyze⁴ acetylene trimerizations and cyclizations to give pyridines and cyclobutadienes. Since creation of a vacant coordination site is fundamental to catalytic processes,⁵ an understanding of how coordinatively saturated organometallic compounds react by associative mechanisms is relevant to synthetic and catalytic transformations. We report here the kinetics of the reaction of $\text{M}(\eta^5\text{-C}_5\text{(CH}_3)_5\text{)(CO)}_2$ (M = Co, Rh) with various nucleophiles.

Experimental Section

Compounds and Solvents. All experimental operations were carried out under an atmosphere of N_2 . Heptanes and hexanes

(1) Schuster-Woldan, H. G.; Basolo, F. *J. Am. Chem. Soc.* **1966**, *88*, 1657-1663.

(2) See, for example: (a) Casey, C. P.; Jones, W. D. *J. Am. Chem. Soc.* **1980**, *102*, 6154-6156. (b) Schonberg, P. R.; Paine, R. T.; Compagna, C. F.; Duesler, E. N. *Organometallics* **1982**, *1*, 799-807. (c) Huttner, G.; Brintzinger, H. H.; Bell, L. G.; Friedlich, P.; Bejenke, V.; Neugebauer, D. *J. Organomet. Chem.* **1978**, *145*, 329-333.

(3) Cramer, R.; Seiwel, L. P. *J. Organomet. Chem.* **1975**, *92*, 245-252.

(4) Vollhardt, K. P. C. *Acc. Chem. Res.* **1977**, *10*, 1-9.

(5) Basolo, F. *Inorg. Chim. Acta* **1981**, *50*, 65-70.

Kinetics and mechanism of the substitution reactions of (η -5-pentamethylcyclopentadienyl)dicarbonylrhodium(I) and (η -5-pentamethylcyclopentadienyl)dicarbonylcobalt(I)

Mark E. Rerek, and Fred Basolo

Organometallics, 1983, 2 (3), 372-376 • DOI: 10.1021/om00075a003 • Publication Date (Web): 01 May 2002

Downloaded from <http://pubs.acs.org> on April 24, 2009

More About This Article

The permalink <http://dx.doi.org/10.1021/om00075a003> provides access to:

- Links to articles and content related to this article
- Copyright permission to reproduce figures and/or text from this article



ACS Publications
High quality. High impact.

35717-09-0; E (Li), 69849-03-2; E (K), 55440-76-1; F, 62381-25-3; G, 881-42-5; H, 733-90-4; I, 36049-90-8; J, 13307-75-0; K, 591-51-5; L, 16423-62-4; 7, 12152-72-6; 8A, 82315-82-0; 8B, 82315-86-4; 8C, 84173-79-5; 8D, 84173-83-1; 8E, 82315-88-6; 8G, 82315-90-0; 8H, 84173-89-7; 8I, 82315-89-7; 8J, 65539-52-8; 8K, 15232-96-9; 8L, 84173-91-1; 9A, 82315-83-1; 9B, 82315-87-5; 9C, 84173-80-8; 9D, 84173-84-2; 9E, 24480-96-4; 9F, 84173-87-5; 9G, 60344-48-1; 9H, 84173-90-0; 9I, 53178-49-7; 9J, 82315-92-2; 9K, 4994-16-5; 9L, 84173-92-2; 10A, 54353-80-9; 10B, 26157-49-3; 10C, 84173-81-9; 10D, 84173-85-3; 10E, 775-10-0; 10F, 84173-88-6; 10I, 56028-77-4; 10J, 79597-48-1; 10K, 771-98-2; 13a, 831-14-1; 17, 84173-93-3; 20, 12078-32-9; 21a, 4786-15-6; 21b, 84173-94-4; 21c, 4786-27-0; 21d, 84173-95-5; Fe₃(CO)₁₂, 17685-52-8; isobutyronitrile, 78-82-0; propionitrile, 107-12-0; ethyl 2-methylpropionate, 97-62-1; *tert*-butyl propionate, 20487-40-5; 3,3-dimethyl-2-butanone, 75-97-8; 2-(1-ethoxyethoxy)hexanenitrile, 60427-76-1; diphenylmethane, 101-81-5; triphenylmethane, 519-73-3; 1,3-dithiane, 505-23-7; (methylthio)benzene, 100-68-5; benzene, 71-43-2; 2-methylpropionic acid, 109-72-8; *n*-butyllithium, 109-72-8; α , α -di-

methylcyclohexaneacetonitrile, 41781-05-9; α -methylcyclohexaneacetonitrile, 53154-02-2; ethyl α , α -dimethylcyclohexaneacetate, 84173-82-0; *tert*-butyl α -methylcyclohexaneacetate, 84173-86-4; 1-cyclohexyl-3,3-dimethyl-2-butanone, 23137-42-0; α -butyl- α -(1-ethoxyethoxy)cyclohexaneacetonitrile, 84192-50-7; cyclohexyldimethylmethane, 50585-08-5; tetraphenylmethane, 630-76-2; ((phenylthio)methyl)cyclohexane, 36293-56-8; benzaldehyde, 100-52-7; cyclohexylbenzene, 827-52-1; *n*-butylcyclohexane, 1678-93-9; valeraldehyde, 110-62-3; 4-valerylcyclohexane, 78932-51-1; phenyl bromide, 108-86-1; iodomethane, 74-88-4; chlorotrimethylsilane, 75-77-4; 2-(trimethylsilyl)-2-methylpropionitrile, 50638-76-1; benzoyl chloride, 98-88-4; cyclohex-1-en-1-ylacetonitrile, 6975-71-9; 2-butanone, 78-93-3; *E*-crotyl bromide, 29576-14-5; 4-bromo-1-butene, 5162-44-7; ethyl 3-cyclohexene-1-carboxylate, 15111-56-5; 3-cyclohexene-1-carboxylic acid, 4771-80-6; cyclohex-3-en-1-ylidiphenylmethanol, 84173-96-6; triethylsilane, 617-86-7; 1-bromo-2-cyclohexene, 1521-51-3; 3-pentanoylcyclohex-1-ene, 78932-51-1; 4-benzoylcyclohex-1-ene, 831-14-1.

Kinetics and Mechanism of the Substitution Reactions of (η^5 -Pentamethylcyclopentadienyl)dicarbonylrhodium(I) and (η^5 -Pentamethylcyclopentadienyl)dicarbonylcobalt(I)

Mark E. Rerek and Fred Basolo*

Department of Chemistry, Northwestern University, Evanston, Illinois 60201

Received October 5, 1982

The reaction of Co(η^5 -C₅(CH₃)₅)(CO)₂ and Rh(η^5 -C₅(CH₃)₅)(CO)₂ with phosphines, phosphites, and isocyanides proceeds readily to form monosubstituted products. For Rh(η^5 -C₅(CH₃)₅)(CO)₂ a second substitution at a much slower rate is observed for phosphites and isocyanides. The reaction proceeds solely by a second-order process, first order in metal complex and first order in nucleophile. The rate is strongly dependent on the size of the entering ligand. The rate of replacement of CO by P(*n*-Bu)₃ for Rh(η^5 -C₅(CH₃)₅)(CO)₂ in toluene at 40 °C is 10² slower than for the reaction of Rh(η^5 -C₅H₅)(CO)₂. The reasons for this difference are discussed in terms of the mechanism first proposed for the substitution reactions of Rh(η^5 -C₅H₅)(CO)₂.

Introduction

Several years ago we reported¹ that the rate of CO substitution in the 18-electron system Rh(η^5 -C₅H₅)(CO)₂ is first order in Rh(η^5 -C₅H₅)(CO)₂ and first order in nucleophile. The associative nature of the reaction was attributed to the ability of the cyclopentadienyl ligand to accept an electron pair from the metal, thus creating a vacant orbital susceptible to nucleophilic attack. This was the first proposed "slippage" of a cyclopentadienyl ring that has since attracted a great deal of interest,² although we had not discussed it in these terms.

Our renewed interest in organometallic reaction mechanisms has led us to reconsider this reaction. If the mechanism proposed by Schuster-Woldan and Basolo¹ is valid, then a complex with an electron-withdrawing group on the cyclopentadienyl ring should be better able to accept an electron pair from the metal and should react faster

than the parent complex. If electron-donating groups are placed on the cyclopentadienyl ring, then the complex should react more slowly due to the ring being less able to accept an electron pair from the metal. Cramer and Seiwel³ have shown this to be true for the rate of replacement of C₂H₄ by phosphines and phosphites in the series Rh(η^5 -C₅H₄CN)(C₂H₄)₂ > Rh(η^5 -C₅H₅)(C₂H₄)₂ > Rh(η^5 -C₅(CH₃)₅)(C₂H₄)₂.

Group 8 cyclopentadienyldicarbonyl compounds catalyze⁴ acetylene trimerizations and cyclizations to give pyridines and cyclobutadienes. Since creation of a vacant coordination site is fundamental to catalytic processes,⁵ an understanding of how coordinatively saturated organometallic compounds react by associative mechanisms is relevant to synthetic and catalytic transformations. We report here the kinetics of the reaction of M(η^5 -C₅(CH₃)₅)(CO)₂ (M = Co, Rh) with various nucleophiles.

Experimental Section

Compounds and Solvents. All experimental operations were carried out under an atmosphere of N₂. Heptanes and hexanes

(1) Schuster-Woldan, H. G.; Basolo, F. *J. Am. Chem. Soc.* **1966**, *88*, 1657-1663.

(2) See, for example: (a) Casey, C. P.; Jones, W. D. *J. Am. Chem. Soc.* **1980**, *102*, 6154-6156. (b) Schonberg, P. R.; Paine, R. T.; Compana, C. F.; Duesler, E. N. *Organometallics* **1982**, *1*, 799-807. (c) Huttner, G.; Brintzinger, H. H.; Bell, L. G.; Friedlich, P.; Bejenke, V.; Neugebauer, D. *J. Organomet. Chem.* **1978**, *145*, 329-333.

(3) Cramer, R.; Seiwel, L. P. *J. Organomet. Chem.* **1975**, *92*, 245-252.

(4) Vollhardt, K. P. C. *Acc. Chem. Res.* **1977**, *10*, 1-9.

(5) Basolo, F. *Inorg. Chim. Acta* **1981**, *50*, 65-70.

were stored over H_2SO_4 and then distilled from Na/benzophenone. Toluene was distilled from Na. Heptane and toluene used for kinetics were bubbled with N_2 for 1 h after distillation. Dichloromethane was distilled from P_2O_5 and methanol from Mg.

The phosphines, phosphites, and isocyanides used in these studies were obtained from Strem or Aldrich Chemicals. All phosphines were distilled from Na under N_2 as were $P(OMe)_3$, $P(OEt)_3$, and $P(O-i-Pr)_3$. Tricyclohexyl phosphite was prepared from PCl_3 and $C_6H_{11}OH$ in pentane by using NEt_3 to neutralize the HCl produced. The melting point and elemental analyses were in good agreement with the reported and calculated values, respectively. All other chemicals were used as received. The compounds $Co(\eta^5-C_5(CH_3)_5)(CO)_2$ ⁶ and $Rh(\eta^5-C_5CCH_3)_5(CO)_2$ ⁷ were prepared by methods described in the literature and characterized by their IR and NMR spectra.

Instrumentation. A Perkin-Elmer 283 or 590 spectrophotometer was used to record IR spectra by using 0.2-mm CaF_2 or KBr solution cells. For kinetic measurements the absorbance mode was used. Compounds were stored in a Vacuum Atmospheres glovebox, and solutions were prepared by ampule transfer. Samples were thermostated by using a Polyscience Model-90 constant temperature (± 0.2 °C) bath.

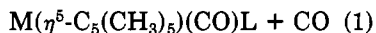
Kinetic Measurement. Prepared samples of 3.0, 5.0, or 10.0 mL were placed in a constant temperature bath. The IR cells were flushed with N_2 and sealed with rubber septa before use. Rate constants were determined by monitoring the decrease of the highest energy carbonyl absorption. Aliquots were removed at intervals to obtain 5–9 readings during 3–4 half-lives of reaction. Plots of $\log A$ vs. time were linear for more than 3 half-lives, and k_{obsd} was determined from the slope of this line by the least-squares method. The correlation of the least squares line ($R^2 > 0.996$) was very good. Approximately 8×10^{-3} M solutions of complex were used, and all kinetic experiments were carried out under pseudo-first-order conditions with at least a tenfold excess of nucleophile. The reactions all proceed to completion to give the monosubstituted product $M(\eta^5-C_5(CH_3)_5)(CO)L$.

The monosubstituted products were independently prepared by reaction with a stoichiometric amount of nucleophile and were identified by their IR and, in some cases, NMR spectra. All are very soluble in organic solvents, difficult to crystallize and appear low melting. The IR spectra of the products are consistent with a species containing one carbonyl group. Recently, Werner and Klingert⁸ reported the isolation of the compounds $Rh(\eta^5-C_5(CH_3)_5)(CO)L$ where $L = PMe_3, P(OMe)_3, P(OEt)_3, PMe_2Ph, PEt_3,$ and PH_2Ph . The reported spectra for their compounds agree with ours.

Results

The original study of $Rh(\eta^5-C_5H_5)(CO)_2$ reported¹ that phosphines would replace only one carbonyl group, but phosphites and isocyanides would replace both carbonyl groups under the experimental conditions used. This behavior is followed by $Rh(\eta^5-C_5(CH_3)_5)(CO)_2$. Under the experimental conditions used, only one carbonyl was replaced by phosphines, but both carbonyls are replaced by phosphites and isocyanides. The second replacement is much faster for isocyanides than for phosphites (vide infra). However, $Co(\eta^5-C_5(CH_3)_5)(CO)_2$ substitutes only one carbonyl whether a phosphine, phosphite, or isocyanide is added. The monosubstituted products appear inert to further substitution under our conditions.

The dependence of the rate of reaction 1 on the concentration of reagent L is given in Figure 1 for $L = P(n-Bu)_3$. The reaction is first order in complex and first order



in L. Both the Rh and Co compounds give a straight line with a zero intercept, indicating no detectable dissociative

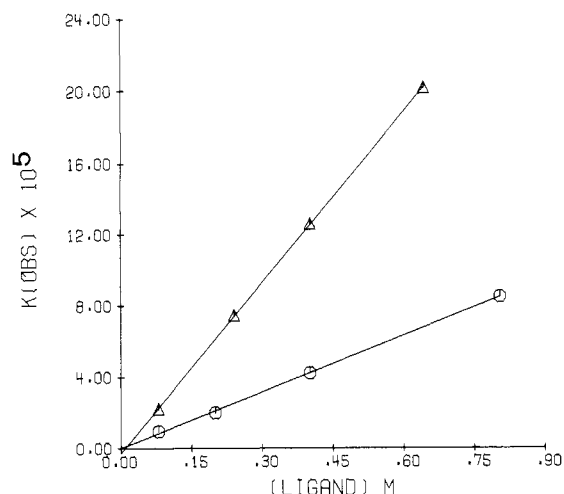


Figure 1. Plot of k_{obsd} (s^{-1}) vs. ligand concentration (M) for reaction 1 ($T = 70$ °C, $L = P(n-Bu)_3$): (O) $M = Co$, (Δ) $M = Rh$. The uncertainty of the derived rate constants are $\pm 4\%$ for $Co(\eta^5-C_5(CH_3)_5)(CO)_2$ and $\pm 3\%$ for $Rh(\eta^5-C_5(CH_3)_5)(CO)_2$.

Table I. Activation Parameters (in Toluene) for the Reaction $M(\eta^5-C_5(CH_3)_5)(CO)_2 + L \rightarrow M(\eta^5-C_5(CH_3)_5)COL + CO$

M	L	T, °C	$10^4 k, M^{-1} s^{-1}$	$\Delta H^\ddagger, kcal/mol$	$\Delta S^\ddagger, eu$
Co	$P(n-Bu)_3$	60	0.374	$+15.8 \pm 0.3$	-33.5 ± 0.8
Co	$P(n-Bu)_3$	70	0.747		
Co	$P(n-Bu)_3$	80	1.52		
Rh	$P(n-Bu)_3$	40	0.315	$+13.5 \pm 0.3$	-38.0 ± 1.0
Rh	$P(n-Bu)_3$	60	1.31		
Rh	$P(n-Bu)_3$	80	4.05		
Co	$P(OEt)_3$	60	0.303	$+18.2 \pm 0.1$	-26.7 ± 0.2
Co	$P(OEt)_3$	70	0.652		
Co	$P(OEt)_3$	80	1.50		
Rh	$P(OEt)_3$	40	0.61	$+13.6 \pm 0.1$	-36.4 ± 0.2
Rh	$P(OEt)_3$	60	2.33		
Rh	$P(OEt)_3$	80	4.16		

substitution. Table I contains the activation parameters for reaction 1 for $L = P(n-Bu)_3$ and $P(OEt)_3$ in toluene. Reaction 1 was also investigated with a variety of other ligands. Kinetic data for reaction 1 as a function of L are given in Table II. Included in the table are the ligand cone angles⁹ and relative basicities.¹⁰ Ligands with a cone angle greater than 145° such as PPh_3 , $P-c-Hx_3$, and $P(O-t-Bu)_3$ gave little or no reaction over a period of 1 week under these conditions.

Discussion

Table III lists the carbonyl stretching frequencies^{11,12} of $M(\eta^5-C_5H_5)(CO)_2$ and $M(\eta^5-C_5(CH_3)_5)(CO)_2$ ($M = Co, Rh$). The shifts to lower frequency indicates that the metals are more electron rich in the pentamethylcyclopentadienyl complexes. Thus, substitution was expected to proceed more slowly for the pentamethylcyclopentadienyl compounds than for the corresponding cyclopentadienyl compounds. This was observed experimentally; for $L = P(n-Bu)_3$, $Rh(\eta^5-C_5H_5)(CO)_2$ reacts 100 times faster than $Rh(\eta^5-C_5(CH_3)_5)(CO)_2$ in toluene at 40 °C.

(9) Tolman, C. A. *Chem. Rev.* **1977**, *77*, 313–348.

(10) (a) Streuli, C. A. *Anal. Chem.* **1959**, *31*, 1652–1654. (b) *Ibid.* **1960**, *32*, 985–987. (c) Henderson, W. A.; Streuli, C. A. *J. Am. Chem. Soc.* **1960**, *82*, 5791–5794.

(11) Fischer, E. O.; Brenner, K. S. *Z. Naturforsch., B: Anorg. Chem., Org. Chem., Biochem., Biophys., Biol.* **1962**, *17B*, 774–775.

(12) King, R. B.; Bisnette, M. B. *J. Organomet. Chem.* **1967**, *8*, 287–297.

(6) Rausch, M. D.; Gennetti, R. A. *J. Org. Chem.* **1970**, *35*, 3888–3897.

(7) Kang, J. W.; Maitlis, P. M. *J. Organomet. Chem.* **1971**, *26*, 393–399.

(8) Werner, H.; Klingert, B. *J. Organomet. Chem.* **1982**, *233*, 365–371.

Table II. Rate Constants (in Toluene) for the Reaction $M(\eta^5\text{-C}_5(\text{CH}_3)_5)(\text{CO})_2 + \text{L} \rightarrow M(\eta^5\text{-C}_5(\text{CH}_3)_5)(\text{CO})\text{L} + \text{CO}$

no.	ligand	cone angle, ^c deg	$\Delta\text{HNP},^d$ mV	$\log k, \text{M}^{-1} \text{s}^{-1}$	
				$\text{Rh}(\eta^5\text{-C}_5(\text{CH}_3)_5)(\text{CO})_2^a$	$\text{Co}(\eta^5\text{-C}_5(\text{CH}_3)_5)(\text{CO})_2^b$
1	Me_3CNC	95		-1.5	-3.19
2	PMe_3	118	114	-2.54	-2.73
3	PMe_2Ph	122	281	-3.26	-3.46
4	$\text{P}(\text{OMe})_3$	107	580	-3.50	-4.05
5	$\text{P}(\text{OEt})_3$	109	520	-3.63	-4.19
6	$\text{P}(n\text{-Bu})_3$	132	131	-3.89	-4.13
7	PMePh_2	136	424	-4.05	-4.34
8	$\text{P}(\text{O-}i\text{-Pr})_3$	130	500 ^e	-4.36	-4.46
9	$\text{P}(\text{O-c-Hx})_3$	135 ^e	480 ^e	-4.36	-4.32
10	$\text{P}(i\text{-Bu})_3$	143	167	-5.25	-5.6
11	PPh_3	145	573	<i>f</i>	<i>f</i>
12	P-c-Hx_3	170	33	<i>f</i>	<i>f</i>
13	$\text{P}(\text{O-}t\text{-Bu})_3$	170	500 ^e	<i>f</i>	<i>f</i>

^a 60 °C. ^b 70 °C. ^c Reference 9. ^d Reference 10. The relative basicities of the phosphorus ligands are given by the difference in the half-neutralization potentials, ΔHNP , from that of N,N' -diphenylguanidine taken as a standard measured in nitromethane. The smaller the ΔHNP , the greater the proton basicity. ^e Estimated value. ^f Very slow; no reaction after 3-5 days.

Table III. Carbonyl Stretching Frequencies for Group 8 Dicarbonyl Complexes in Hexane Solution

complex	$\nu_{\text{CO}}, \text{cm}^{-1}$
$\text{Co}(\eta^5\text{-C}_5\text{H}_5)(\text{CO})_2$	2037, 1965 ^a
$\text{Co}(\eta^5\text{-C}_5(\text{CH}_3)_5)(\text{CO})_2$	2011, 1949 ^b
$\text{Rh}(\eta^5\text{-C}_5\text{H}_5)(\text{CO})_2$	2051, 1987 ^a
$\text{Rh}(\eta^5\text{-C}_5(\text{CH}_3)_5)(\text{CO})_2$	2021, 1965 ^c

^a Reference 11. ^b Reference 12. ^c This work.

In addition to the electronic effect, the pentamethylcyclopentadienyl ligand exerts a greater steric demand^{13,14} than the cyclopentadienyl ligand. Steric retardation of a second-order process along with steric acceleration of a first-order process may permit a first-order process to become the favored path. However, as Figure 1 shows, this did not happen. The rate of reaction is directly proportional to the concentration of the incoming ligand. Furthermore, the zero intercept shows there is no detectable contribution from a ligand-independent (first-order) process at these experimental conditions.

The pentamethylcyclopentadienyl ligand makes the reactivities of the Co and Rh compounds more similar than are the corresponding cyclopentadienyl compounds.¹ For $\text{L} = \text{PPh}_3$ in toluene at 40 °C, $\text{Rh}(\eta^5\text{-C}_5\text{H}_5)(\text{CO})_2$ reacts ten times faster than $\text{Co}(\eta^5\text{-C}_5\text{H}_5)(\text{CO})_2$, whereas at 70 °C in toluene for $\text{L} = \text{P}(n\text{-Bu})_3$, $\text{Rh}(\eta^5\text{-C}_5(\text{CH}_3)_5)(\text{CO})_2$ reacts only three times faster than $\text{Co}(\eta^5\text{-C}_5(\text{CH}_3)_5)(\text{CO})_2$. Also the kinetic data show that the dependence of reactivity on the size of the incoming ligand is more important for the pentamethylcyclopentadienyl systems. This is best illustrated by the fact that for $\text{Rh}(\eta^5\text{-C}_5\text{H}_5)(\text{CO})_2$, $\text{P}(n\text{-Bu})_3$ reacts 9 times faster than $\text{P}(n\text{-O}i\text{Pr})_3$, whereas for $\text{Rh}(\eta^5\text{-C}_5(\text{CH}_3)_5)(\text{CO})_2$, $\text{P}(\text{OEt})_3$ reacts twice as fast as $\text{P}(n\text{-Bu})_3$. Although $\text{P}(n\text{-Bu})_3$ is a much stronger base than $\text{P}(\text{OEt})_3$ or $\text{P}(n\text{-O}i\text{Pr})_3$, the much smaller size (as measured by the cone angle) of the phosphites becomes the dominant factor for reactions of $\text{Rh}(\eta^5\text{-C}_5(\text{CH}_3)_5)(\text{CO})_2$.

The steric demands of the pentamethylcyclopentadienyl ligand do have a profound effect on the course of carbonyl substitution for these compounds. As Table II shows, when the size of the ligand becomes very large, as for P-c-Hx_3 , no reaction occurs. This is consistent with an associative process; if a ligand is too large to enter the

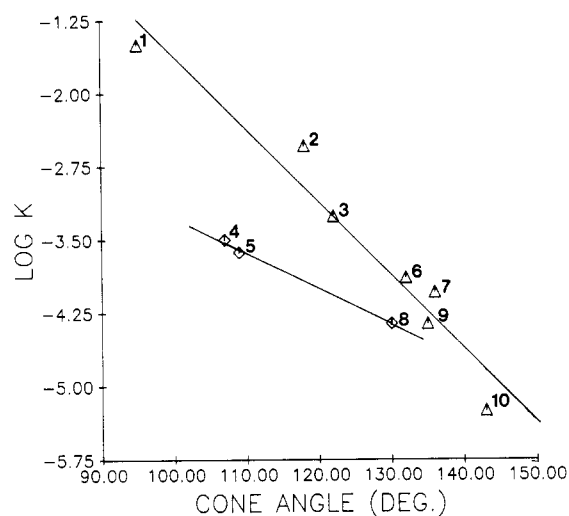


Figure 2. Plot of $\log k$ vs. cone angle (deg) for reaction 1 with $\text{M} = \text{Rh}$. The numbers correspond to those in Table II.

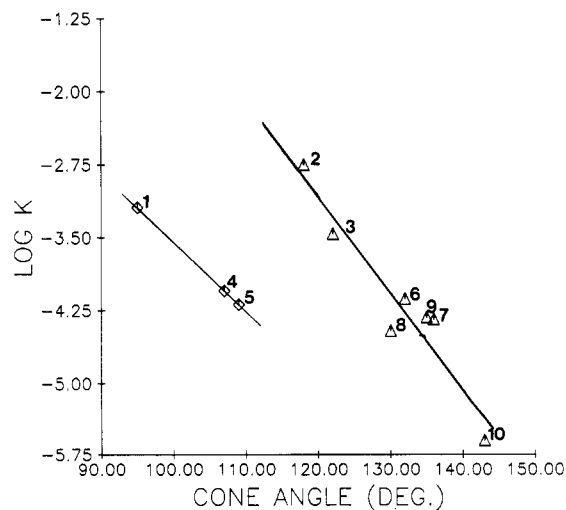


Figure 3. Plot of $\log k$ vs. cone angle (deg) for reaction 1 with $\text{M} = \text{Co}$. The numbers correspond to those in Table II.

coordination sphere of the metal no reaction occurs. A correlation between the rate of reaction and the cone angle of the incoming ligand can be drawn (Figures 2 and 3) for these compounds. The size of the ligand appears to be the dominant factor in the reactivity of a given ligand. It is well-known that steric effects play an important role in

(13) Fagan, P. J.; Manriquez, J. M.; Maata, E. A.; Seyam, A. M.; Marks, T. J. *J. Am. Chem. Soc.* 1981, 103, 6650-6667.

(14) Thompson, S. J.; White, C.; Maitlis, P. M. *J. Organomet. Chem.* 1977, 136, 87-93.

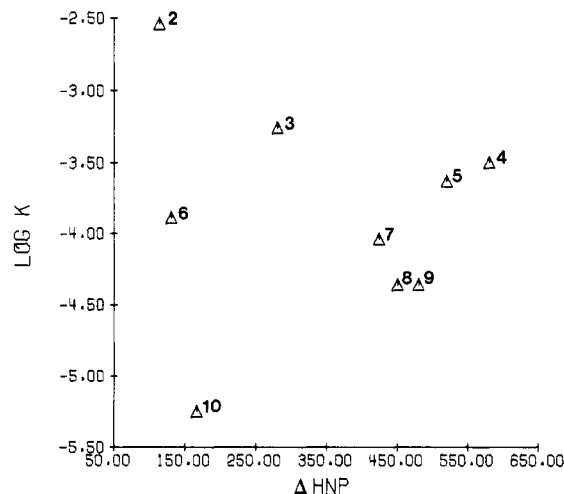


Figure 4. Plot of $\log k$ vs. ΔHNP (mV) for reaction 1: $\text{M} = \text{Rh}$. The numbers correspond to those in Table II.

associative substitution processes. To take but a few examples, the rate of replacement of CO by phosphine from the compounds $\text{Fe}_2(\text{CO})_6\text{S}_2\text{C}_6\text{H}_3\text{CH}_3$ ¹⁵ and $\text{Ru}_3(\text{CO})_{12}$ ¹⁶ decreases with increasing size of the phosphine.

Some distinction as to the nature of the ligand is necessary when this correlation is made. For $\text{Rh}(\eta^5\text{-C}_5\text{(CH}_3)_5\text{)(CO)}_2$, phosphines and Me_3CNC follow one trend, whereas phosphites follow another. With $\text{Co}(\eta^5\text{-C}_5\text{(CH}_3)_5\text{)(CO)}_2$, very small ligands such as Me_3CNC , $\text{P}(\text{OMe})_3$, and $\text{P}(\text{OEt})_3$ do not react as fast as expected on the basis of their cone angle. In both cases, the exceptions are with nucleophiles that are more weakly basic than the main group of entering ligands. Ligand basicity must be of secondary importance, but for the $\text{Rh}(\eta^5\text{-C}_5\text{(CH}_3)_5\text{)(CO)}_2$ system the correlation of rate with ligand basicity is poor (Figure 4). A similar plot is obtained for $\text{Co}(\eta^5\text{-C}_5\text{(CH}_3)_5\text{)(CO)}_2$.

This behavior contrasts that observed for reactions of the corresponding parent cyclopentadienyl systems, where the dominant factor contributing to the nucleophilic strength of the entering ligand is its basicity. This has also generally been the case for other associative displacement reactions of transition-metal organometallic compounds.¹⁷ Although the earlier plot¹ of the rates of reaction of $\text{Rh}(\eta^5\text{-C}_5\text{H}_5\text{)(CO)}_2$ vs. nucleophilic basicity showed a good linear correlation, it is of interest now to plot these rates vs. nucleophilic cone angle (Figure 5). This shows that steric factors of the entering nucleophile also contribute to its nucleophilic strength. Thus steric effects must be taken into account for most basicity correlations; P-c-Hx_3 with a ΔHNP ¹⁰ of 33 mV and a cone angle⁹ of 170° never shows the reactivity expected by virtue of being the most basic phosphine. For the $\text{Fe}(\text{N}_4\text{Me}_2)(\text{CO})_3$ system,¹⁸ a correlation between rate and basicity can only be drawn if larger, more sterically demanding ligands are ruled out. As expected, the strength of a nucleophile depends on its size and its basicity, and, depending on the substrate, one or the other of these factors may dominate. No attempt is made to delineate the contribution of basicity and steric factors in this study, although others¹⁹ have reported a

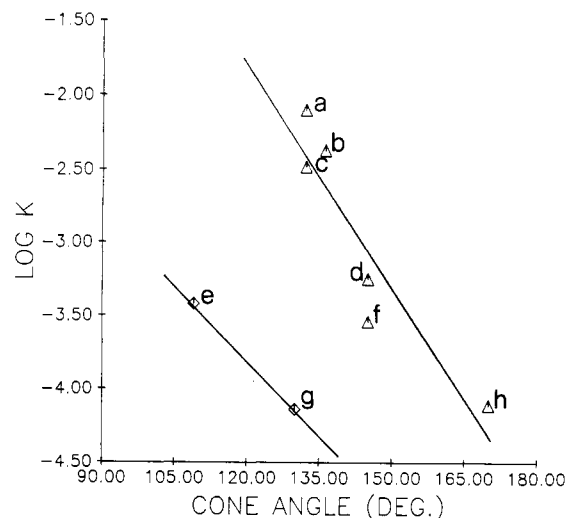
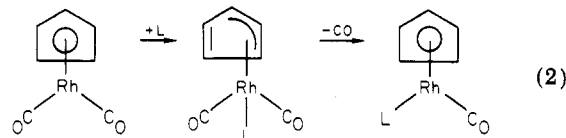


Figure 5. Plot of $\log k$ vs. cone angle (deg) for the reaction $\text{Rh}(\eta^5\text{-C}_5\text{H}_5\text{)(CO)}_2 + \text{L} \rightarrow \text{Rh}(\eta^5\text{-C}_5\text{H}_5\text{)(CO)L} + \text{CO}$: a, PEt_3 ; b, PEt_2Ph ; c, $\text{P}(n\text{-Bu})_3$; d, $\text{P}(p\text{-CH}_3\text{OC}_6\text{H}_4)_3$; e, $\text{P}(O\text{-}n\text{-Bu})_3$; f, PPh_3 ; g, $\text{P}(\text{OPh})_3$; h, P-c-Hx_3 (from ref 1).

quantitative assessment of steric and electronic factors for other systems.

All of these observations are consistent with an associative ($\text{S}_{\text{N}}2$) substitution process for the pentamethylcyclopentadienyl systems. The activation parameters for reaction 1 also support an $\text{S}_{\text{N}}2$ mechanism; ΔH^\ddagger is relatively small and ΔS^\ddagger is very negative. That ΔS^\ddagger values are more negative for reactions of $\text{Rh}(\eta^5\text{-C}_5\text{(CH}_3)_5\text{)(CO)}_2$ than for $\text{Rh}(\eta^5\text{-C}_5\text{H}_5\text{)(CO)}_2$ ¹ further supports the notion of a more crowded transition state in the pentamethylcyclopentadienyl systems.

These results are consistent with the mechanism first proposed¹ for $\text{Rh}(\eta^5\text{-C}_5\text{H}_5\text{)(CO)}_2$. In modern terms, the mechanism can be represented by (2). The essential



feature of this mechanism is the reorganization of the ring from a delocalized structure to an allyl-ene structure, where the metal is bound only to the allyl portion. Several examples are known^{2b,c} where a metal is bound to an η^3 -allyl portion of a cyclopentadienyl ring. One of particular interest here is the compound $\text{W}(\text{C}_5\text{H}_5)_2(\text{CO})_2$ that has been shown^{2c} to contain both an η^5 - and η^3 -cyclopentadienyl ring. It appears that one of the cyclopentadienyl rings has slipped to an η^3 -allyl-bonding mode to remove an electron pair from the metal so that it can maintain an 18-electron configuration. This may be what is happening for associative reactions of cyclopentadienylmetal carbonyl compounds. Such ring "slippage" creates a vacant orbital at the metal, making possible a low-energy associative reaction path. Putting more electron density on the metal by adding five methyl groups to the cyclopentadienyl ring slows down the reaction, presumably by retarding this bonding rearrangement.

Results of the initial study¹ on $\text{Rh}(\eta^5\text{-C}_5\text{H}_5\text{)(CO)}_2$ showed that cyclopentadiene is a ligand that can allow associative substitution processes in 18-electron organometallic complexes. Since then several examples have been found where such complexes react by a dissociative ($\text{S}_{\text{N}}1$)

(15) Ellgen, P. C.; Gerlach, J. N. *Inorg. Chem.* 1973, 12, 2526-2531.

(16) Pöe, A. J.; Twigg, M. V. *J. Chem. Soc., Dalton Trans.* 1974, 1860-1866.

(17) See, for example: (a) Thorsteinson, E. M.; Basolo, F. *J. Am. Chem. Soc.* 1966, 88, 3926-3936. Morris, D. E.; Basolo, F. *Ibid. Soc.* 1968, 90, 2531-2535.

(18) Chang, C. Y.; Johnson, C. E.; Richmond, T. G.; Chen, Y. T.; Troglor, W. C.; Basolo, F. *Inorg. Chem.* 1981, 20, 3167-3172.

(19) See: Schenkluhn, H.; Berger, R.; Pittel, B.; Zähres, M. *Transition Met. Chem. (Weinheim, Ger.)* 1981, 6, 277-287 and references therein.

mechanism, e.g., $V(\eta^5-C_5H_5)(CO)_4$,²⁰ $Mo(\eta^5-C_5H_5)(CO)_3Cl$,²¹ $Mn(\eta^5-C_5H_5)(CO)_3$,²² $Fe(\eta^5-C_5H_5)(CO)_2I$,²³ and $Ru(\eta^5-C_5H_5)(CO)_2Br$.²⁴ These examples serve to show the delicate balance between associative and dissociative substitution reactions in these systems. Note also that Casey and co-workers, for the mixed cyclopentadienyl-nitrosyl species $Re(\eta^5-C_5H_5)(CO)(NO)CH_3$,^{2a} $W(\eta^5-C_5H_5)(CO)_2NO$,²⁵ and $Mo(\eta^5-C_5H_5)(CO)_2NO$,²⁵ observed associative substitution reactions. Unfortunately these systems contain the NO ligand, which is known¹⁷ to permit associative reactions.

One may pose the question, why do associative reactions of cyclopentadienylmetal complexes seem to predominate "only" with the Co(triad) complexes? Some insight into this question may be provided by the mechanism proposed for the associative reactions. With the assumption that a η^3 -allyl cyclopentadienyl is essential to this reaction, then the energy needed to go from a symmetrical delocalized η^5 -cyclopentadienyl to a η^3 -allyl-ene cyclopentadienyl must be low enough to allow an associative reaction. The structure of $Co(\eta^5-C_5(CH_3)_5)(CO)_2$ was shown to contain an allyl-ene pentamethylcyclopentadienyl ring by Dahl and Byers.²⁶ This shows that in this system, for whatever the reason, the difference in energy between η^5 and η^3 bonding is small. From this it follows that the Co(triad) complexes may have a low-energy path for associative reaction. Such a path may be of higher energy for other cyclopentadienylmetal complexes, resulting in their reaction by a dissociative process. The relationship between structure and bonding on one hand and reactivity on the other deserves a serious examination for these complexes. One such examination²⁷ has appeared for $Mn(\eta^5-C_5H_5)-$

$(CO)_3$. The ring distortion in this compound is dienelike as opposed to the allyl-ene like for $Co(\eta^5-C_5(CH_3)_5)(CO)_2$, which means that an associative reaction may still require reorganization from the diene to the allyl-ene structure. Needless to say more work is required before definitive answers can be given to some of these questions.

Conclusions

This study shows that changes in (1) the nature of M(Co to Rh), (2) the nature of the cyclopentadienyl ligand (C_5H_5 to $C_5(CH_3)_5$), and (3) the nature of the incoming ligand (L) all have an effect on the substitution reactions of these complexes. Going from Co to Rh, the rate of associative substitution is expected to increase due to the larger size of Rh and also due to the weaker M-CO bond (higher ν_{CO}) and this is observed. This may also explain why the Rh complexes give further substitutions under certain conditions, whereas corresponding Co complexes do not. The $C_5(CH_3)_5$ ligand is more electron donating than the C_5H_5 ligand (lower ν_{CO}), but it is also larger creating a greater steric demand on associative substitution. Both of these factors contribute to the slower rates of substitution observed for the $C_5(CH_3)_5$ complexes. For both C_5H_5 and $C_5(CH_3)_5$ complexes, a plot of $-\log k$ vs. ligand cone angle gives a good correlation. Yet ligand basicity is also significant, since smaller but less basic ligands do not react as would otherwise be predicted. Clearly both steric and basicity effects are important in determining the rates and extent of CO substitution in these complexes.

Acknowledgment. We wish to acknowledge the donors of the Petroleum Research Foundation, administered by the American Chemical Society, and the generous loan of rhodium by the Johnson-Matthey Corp. Also, M.E.R. would like to thank Prof. Tobin J. Marks for generous use of his Perkin-Elmer 590 infrared spectrophotometer.

Registry No. $Rh(\eta^5-C_5(CH_3)_5)(CO)_2$, 32627-01-3; $Co(\eta^5-C_5(CH_3)_5)(CO)_2$, 12129-77-0; Me_3CNC , 7188-38-7; PMe_3 , 594-09-2; PMe_2Ph , 672-66-2; $P(OMe)_3$, 121-45-9; $P(OEt)_3$, 122-52-1; $P(n-Bu)_3$, 998-40-3; $PMePh_2$, 1486-28-8; $P(O-i-Pr)_3$, 116-17-6; $P(O-c-Hx)_3$, 15205-58-0; $P(i-Bu)_3$, 4125-25-1; PPh_3 , 603-35-0; $P-c-Hx_3$, 2622-14-2; $P(O-t-Bu)_3$, 15205-62-6.

(20) Faber, G. C.; Angelici, R. J. *Inorg. Chem.* **1970**, *9*, 1586-1587.

(21) White, C.; Mawby, R. J. *Inorg. Chim. Acta* **1970**, *4*, 261-266.

(22) Angelici, R. J.; Loewen, W. *Inorg. Chem.* **1966**, *6*, 682-686.

(23) Jones, D. J.; Mawby, R. J. *Inorg. Chim. Acta* **1972**, *6*, 157-160.

(24) White, C.; Tabatabaian, K. *Inorg. Chem.* **1981**, *20*, 2021-2023.

(25) Casey, C. P.; Jones, W. D.; Harsy, S. G. *J. Organomet. Chem.* **1981**, *206*, C38-C42.

(26) Byers, L. R.; Dahl, L. F. *Inorg. Chem.* **1980**, *19*, 277-284.

(27) Fitzpatrick, P. J.; LePage, Y.; Sedman, J.; Butler, I. S. *Inorg. Chem.* **1981**, *20*, 2852-2861.

Preparation of Highly Reactive Metal Powders. Preparation, Characterization, and Chemistry of Iron, Cobalt, Nickel, Palladium, and Platinum Microparticles

Arunas V. Kavaliunas, Ashley Taylor,¹ and Reuben D. Rieke*

Department of Chemistry, University of Nebraska-Lincoln, Lincoln, Nebraska 68588

Received August 30, 1982

Anhydrous metal halides of iron, cobalt, nickel, palladium, and platinum are readily reduced in glyme or THF with lithium in the presence of a small amount of naphthalene and yield finely divided, black metal powders of exceptional reactivity. Metal powders of Fe and Co react with C_6F_5X ($X = Br, I$) to yield solvated $M(C_6F_5)_2$ and MX_2 . Powders of palladium and platinum react with C_6F_5I to yield solvated $M(C_6F_5)I$ ($M = Pd, Pt$). Nickel powder reacts with C_6F_5I to yield the solvated species $Ni(C_6F_5)_2$ and NiI_2 , however, with C_6F_5Br the product is solvated $Ni(C_6F_5)Br$. In most cases the metal powders are sufficiently reactive that a stoichiometric amount of C_6F_5X to the metal powder is used. The coordinated ether of all of these organometallic compounds is exceptionally labile and is displaced with a variety of ligands: phosphines, amines, sulfides, isocyanides, diolefins, and carbon monoxide. Many of the resultant compounds are novel and most are obtained in high yields. Palladium metal powder to which has been added 2,2'-bipyridine (bpy) reacts with iodobenzene to yield $Pd(C_6H_5)I(bpy)$. Surface analyses including ESCA and BET were carried out on the highly reactive Ni, Pt, and Pd metal powders.

Introduction

In a series of papers beginning in 1972, we have described a general procedure for the preparation of highly reactive metal powders.²⁻¹⁶ The basic procedure involved the reduction of an anhydrous metal halide in an ethereal or hydrocarbon solvent. We have noted that the reactivities and in some cases products are highly dependent on the reduction conditions, i.e., anion, reducing agent, solvent, temperature, and presence of added alkali salts, Lewis acids, or Lewis bases.³⁻¹⁶

In previous communications we reported the preparation of highly reactive metal slurries of iron, cobalt, nickel, and palladium and the reactions of these metals with aryl halides.¹⁵ In this paper, we describe in detail the preparation of metal slurries of iron, cobalt, nickel, palladium, and platinum by lithium reduction of the anhydrous metal halides in ethereal solvents. These metal powders show exceptional reactivity with C_6F_5X ($X = Br, I$) and yield

solvated species of the type $M(C_6F_5)_2$ or $M(C_6F_5)X$. Since the ethers coordinated to these compounds are very labile, these compounds are valuable precursors of other, new organometallic compounds. Klabunde and co-workers have previously reported the preparation of some of these compounds by using the metal vaporization technique.^{18,24,28-32}

The reactivity of these powders has been extended to organic halides other than C_6F_5X ($X = Br, I$). For example nickel has been shown to be an effective reagent for an Ullman-type coupling reaction of an unactivated aryl halide.

Addition of iodobenzene to a palladium slurry already containing a stabilizing ligand, 2,2'-bipyridine, results in $Pd(C_6H_5)I(bpy)$ and suggests a simple and attractive method for the preparation from metal powders of compounds containing perhydrocarbon groups.

Experimental Section

Starting Materials. The preparation of metal slurries as well as the reactions of these slurries with organic halides were carried out under an atmosphere of prepurified argon, further purified by passage over BASF catalyst R 3-11 at 180 °C, P_2O_5 , and KOH.

(1) Perkin-Elmer Corp. Phys. Electronics Division, Eden Prairie, Mn 55344.

(2) Rieke, R. D.; Hudnall, P. M. *J. Am. Chem. Soc.* **1972**, *94*, 7178. Rieke, R. D.; Hudnall, P. M.; Uhm, S. *J. Chem. Soc., Chem. Commun.* **1973**, 269.

(3) Rieke, R. D.; Bales, S. E. *J. Chem. Soc., Chem. Commun.* **1973**, 789.

(4) Rieke, R. D.; Bales, S. E. *J. Am. Chem. Soc.* **1974**, *96*, 1775.

(5) Rieke, R. D.; Chao, L. *Synth. React. Inorg. Met.-Org. Chem.* **1974**, *4*, 101.

(6) Rieke, R. D.; Ofele, K.; Fischer, E. O. *J. Organomet. Chem.* **1974**, *76*, C19.

(7) Rieke, R. D. *Top. Curr. Chem.* **1975**, *59*, 1.

(8) Rieke, R. D. *Acc. Chem. Res.* **1977**, *10*, 301 and references therein.

(9) Rieke, R. D.; Wolf, W. J.; Kujundzic, N.; Kavaliunas, A. V. *J. Am. Chem. Soc.* **1977**, *99*, 4159.

(10) Uhm, S. Ph.D. Thesis, University of North Carolina-Chapel Hill, 1974.

(11) Rieke, R. D.; Kavaliunas, A. V.; Rhyne, L. D.; Frazier, D. J. J., *J. Am. Chem. Soc.* **1979**, *101*, 246.

(12) Rieke, R. D.; Kavaliunas, A. V. *J. Org. Chem.* **1979**, *44*, 3069.

(13) Rieke, R. D.; Rhyne, L. D. *J. Org. Chem.* **1979**, *44*, 3445.

(14) Rieke, R. D.; Bales, S. E.; Hudnall, P. M.; Poindexter, G. S. *Org. Synth.* **1979**, *59*, 85.

(15) Kavaliunas, A. V.; Rieke, R. D. *J. Am. Chem. Soc.* **1980**, *102*, 5944.

(16) Kavaliunas, A. V.; Rieke, R. D. *Angew. Chem., Int. Ed. Engl.* **1982**, *0000*.

(17) Shchukavev, S. A.; Tolmacheva, T. A.; Pazukhina, Y. L. *Russ. J. Inorg. Chem. (Engl. Transl.)* **1964**, *9*, 1354.

(18) Anderson, B. B.; Behrens, C. L.; Radonovich, L. I.; Klabunde, K. *J. Am. Chem. Soc.* **1976**, *98*, 5390.

(19) Goggin, P. L.; Goodfellow, R. J. *J. Chem. Soc. A* **1966**, 1462.

(20) Rosevear, D. T.; Stone, F. G. A. *J. Chem. Soc.* **1965**, 5275.

(21) Hensley, D. W.; Steward, R. P., Jr. *Inorg. Chem.* **1978**, *17*, 905.

(22) Issleib, K.; Wenschuh, E. *Z. Anorg. Allg. Chem.* **1960**, *305*, 15.

(23) Uson, R.; Fornies, J.; Navarro, R. *Synth. React. Inorg. Met.-Org. Chem.* **1977**, *7*, 235.

(24) Klabunde, K. J.; Anderson, B. B.; Neuenschwander, K. *Inorg. Chem.* **1980**, *19*, 3719.

(25) Heck, R. F. *J. Am. Chem. Soc.* **1968**, *90*, 5518, 5526, 5531, 5535, 5538.

(26) Herzog, S.; Taube, R. *Z. Chem.* **1962**, *2*, 208.

(27) Phillips, J. R.; Rosevear, D. T.; Stone, F. G. A. *J. Organomet. Chem.* **1964**, *2*, 455.

(28) Klabunde, K. J.; Low, J. Y. F. *J. Am. Chem. Soc.* **1974**, *96*, 7674.

(29) Klabunde, K. J.; Murdock, T. O. *J. Org. Chem.* **1979**, *44*, 3901.

(30) Davis, S. C.; Klabunde, K. J. *J. Am. Chem. Soc.* **1978**, *100*, 5973.

(31) Gastingier, R. G.; Anderson, B. B.; Klabunde, K. J. *J. Am. Chem. Soc.* **1980**, *102*, 4959.

(32) Klabunde, K. J.; Low, J. Y. F.; Efner, H. F. *J. Am. Chem. Soc.* **1974**, *96*, 1984.

Other manipulations of metal powders were carried out in an inert-atmosphere box containing prepurified argon. Workup of the organometallic compounds, unless otherwise specified, was done in air. 1,2-Dimethoxyethane (glyme) and tetrahydrofuran (THF) were distilled immediately prior to use from sodium-potassium alloy under argon. Anhydrous metal halides (Cerac, Inc., Ventron, and Mathey-Bishop) were used as received. PdI₂ and PtI₄ were prepared according to published procedures.¹⁷ C₆H₅I was distilled and kept protected from light. 2,2'-Bipyridine was recrystallized from hexane. The other reagents and solvents were used as received.

Physical Measurements. ¹H NMR spectra were obtained with either a Varian A-60D or EM-390 spectrometer using Me₄Si as internal standard. Infrared spectra were obtained in mineral oil mulls on a Perkin-Elmer 283 infrared spectrophotometer. Elemental analyses were performed by Galbraith Laboratories, Inc. Melting points were obtained on a Hoover Uni-Melt apparatus and are corrected. Melting points of air-sensitive compounds were obtained in sealed tubes. A Hewlett-Packard Model HP 5730A gas chromatograph was employed in gas chromatographic analyses.

Preparation of a Typical Iron Slurry. A 50-mL two-necked flask equipped with a magnetic stirrer and a condenser topped with an argon inlet was charged with 0.154 g (0.0222 mol) of freshly cut lithium, 1.221 g (0.009 63 mol) of FeCl₂ (quickly weighed in air), and 0.187 g (0.001 46 mol) of naphthalene. Glyme (18 mL) was syringed in, and vigorous stirrings were started. The initially beige mixture slowly darkened and in about 3 or 4 h became black and greasy-appearing. After some time, it reverted to a free moving black slurry. The next day, a black slurry existed in a slightly green solution with no lithium present. The slurry was washed by allowing the slurry to settle, removing the solvent above the slurry by syringe and adding fresh glyme, and stirring the slurry and again letting it settle. Usually after two such cycles, no green color is visible in solution.

Very often the piece of lithium coats with the metal powder. In such cases, the argon flow is increased and with a curved spatula the piece of lithium is rubbed against the side of the flask to expose a fresh surface of the lithium.

Preparation of a Typical Cobalt Slurry. The same apparatus as that described for the preparation of an iron slurry was charged with 1.259 g (0.009 70 mol) of CoCl₂ (quickly weighed in air), 0.159 g (0.0229 mol) of freshly cut lithium, and 0.154 g (0.001 20 mol) of naphthalene. Addition of 16 mL of glyme and stirring resulted in a blue solution as part of the CoCl₂ dissolved. In about 0.5 h, the mixture started blackening, and, after 19 h a black slurry existed in a light olive green solution. The slurry was washed in the same manner as the iron slurry to remove the small amount of lithium naphthalide.

Preparation of a Typical Nickel Slurry. The same apparatus as that described for the preparation of an iron slurry was charged with 2.285 g (0.010 48 mol) of NiBr₂ (quickly weighed in air), 0.152 g (0.0233 mol) of freshly cut lithium, and 0.156 g (0.001 21 mol) of naphthalene. Glyme (18 mL) was syringed onto this mixture and stirring started. In 1 h, the mixture was essentially black with a pink and in part black piece of lithium. After 18 h, reduction was complete; a black slurry existed in a colorless solution.

Preparation of a Typical Palladium Slurry. The usual apparatus was charged with 1.291 g (0.007 28 mol) of PdCl₂, 0.128 g (0.0184 mol) of freshly cut lithium, and 0.144 g (0.001 12 mol) of naphthalene. Glyme (18 mL) was syringed in and stirring started. After about 4 h, the flask contained a pink piece of lithium in a thick black mixture. After 26 h, a black slurry existed in a colorless solution with no lithium present.

Preparation of a Typical Platinum Slurry. The usual apparatus was charged with 1.6526 g (0.003 687 mol) of PtI₄, 0.0724 g (0.010 43 mol) of freshly cut lithium, and 0.0788 g (0.000 615 mol) of naphthalene. Glyme (16 mL) was syringed onto the mixture and the black suspension stirred. After almost 0.5 h some PtI₂ dissolved resulting in a yellow green solution containing a black-coated piece of lithium. After about 2 h the piece of lithium was pink, and after a total of 19 h a black slurry existed in a pale beige solution with no lithium present.

Preparation of a Metal Powder for Surface Analysis. The preparation of metal powders for surface analysis were identical;

the one employed for palladium is described here. Upon completion of reduction, the slurry was allowed to settle and the liquid above the black powder removed via syringe. The remainder of the solvent was removed under vacuum. The reaction vessel was then taken into an inert-atmosphere box, and the clumped metal powders were transferred to a Soxhlet extractor. The assembled apparatus was removed from the inert-atmosphere box, connected to an argon atmosphere, and freshly distilled glyme syringed into the extractor. The extraction was carried out for 26 h; the solvent in the reflux flask was removed via syringe and the remainder under vacuum. The palladium powder was then subjected to a vacuum for 18 h. The extractor was then taken into an inert-atmosphere box and the powder loaded into ampoules. The extraction thimble, containing some residual palladium powder, when exposed to air slowly, warmed up and then ignited. Surface analyses were performed by Perkin-Elmer Physical Electronics Industries, Inc., Eden Prairie, MN 53344. Samples were handled in the following manner. Glass vials were opened in a glovebox (VAC, Model DL-001-SP) containing an atmosphere of dry nitrogen. The powder was mounted on an Al backed tape and transferred into the vacuum chamber of the ESCA system (PHI, Model 550) without exposing the sample to air by means of a mechanical transfer system (PHI, Model 04-100). The spectra were obtained by using an Mg anode for X-ray excitation with a vacuum of 10⁻⁹ torr. The sputtering was effected by using a differentially pumped ion gun with an ion energy of 5 KeV and an ion current density of 5 μA cm⁻². B.E.T. surface area determinations were carried out by Quantachrome Corporation, Syosset, NY 11791.

Preparation of Fe(C₆F₅)₂(CO)₂(C₄H₁₀O₂)₂. An iron slurry was prepared in the usual manner and then allowed to settle. The solvent above the slurry was removed (most of the iron is coated about the magnetic stirring bar) and the slurry cooled to 0 °C for the slow addition of 1 equiv of C₆F₅I per iron. After the addition the flask was allowed to warm to room temperature and the brown mixture stirred for 25 h even though the reaction appeared to be complete in about 2 h. A slow stream of CO (large excess) was then bubbled through the thick brown solution for 11 h with no color change apparent. The volatiles were removed from the mixture under vacuum, and the product was dissolved in 20 mL of CH₂Cl₂ and then anaerobically filtered. Slow solvent evaporation in an inert atmosphere resulted in large yellow crystals. The crystals are often covered with a brown tarry residue that is readily removed by washing the crystals with a small amount of 2:1 hexane-CH₂Cl₂ mixture: yield 60%; mp (sealed tube) 103–114 °C; IR (Nujol) 2090 (s), 2076 (w), 2020 (vs), 1993 (m), 1976 (w) cm⁻¹; ¹H NMR (CDCl₃) δ 3.58 (s, 4 H), 3.41 (s, 6 H). Both resonances are shifted downfield from those of free glyme in CDCl₃. Anal. Calcd for C₂₂H₂₀F₁₀FeO₆: C, 42.19; H, 3.22; F, 30.34. Found: C, 42.35; H, 3.30; F, 30.54.

The analogous reaction carried out at about 55 °C between an iron slurry and 1 equiv of C₆F₅Br, followed by bubbling a large excess of CO into the mixture, resulted in the same product and in comparable yield. Because of less tarry residues and hence easier workup, we find the reaction employing C₆F₅Br more attractive.

Preparation of Ni(C₆F₅)₂[P(C₂H₅)₃]₂. A nickel metal slurry was prepared in the typical manner and then allowed to settle. About half of the liquid above the slurry was removed via syringe, and then 1 equivalent of C₆F₅I per nickel was added dropwise. A yellow color formed in the reaction mixture. The mixture was stirred at about 40 °C for 9 h and then the deep orange mixture cooled to about 0 °C. Two equivalents of P(C₂H₅)₃ per nickel were slowly syringed in; the mixture initially became greenish black and then solidified into a crystalline mass. The product was extracted with CH₂Cl₂ and the greenish brown solution filtered. Removal of solvent under reduced pressure resulted in a dark brown solid. NiI₂[P(C₂H₅)₃]₂ was removed from this mixture with several small portions of 2-propanol, leaving a light yellow crystalline powder. Recrystallization from CH₂Cl₂ by slow solvent evaporation resulted in large golden yellow crystals of Ni(C₆F₅)₂[P(C₂H₅)₃]₂ in 69% yield: mp 206–208 °C (lit.²⁷ mp 213–214 °C).

Preparation of Co(C₆F₅)₂[P(C₂H₅)₃]₂. A cobalt metal slurry was prepared in the usual manner and then allowed to settle. About half of the solvent above the slurry was removed via syringe

and the vessel cooled to 0 °C. One equivalent of C_6F_5I per cobalt was added dropwise; a greenish color forming in solution after a few drops. The mixture was then stirred at about 45 °C for 18 h after which time a deep blue solution existed. The volatiles were removed under vacuum, and the product was dissolved in 10 mL of glyme and again cooled to 0 °C. Two equivalents of $P(C_2H_5)_3$ per cobalt was added, and the deep blue color immediately changed to green. The mixture was stirred for 1 h, and then the volatiles were removed under vacuum. The product was extracted with CH_2Cl_2 and the green solution filtered. Removal of solvent under reduced pressure left a blue-green crystalline mass. $CoI_2[P(C_2H_5)_3]_2$ was washed out from this mixture with several small portions of CH_3OH , leaving a pale yellow crystalline product. Recrystallization from CH_2Cl_2 by slow solvent evaporation at room temperature resulted in greenish yellow crystals of $Co(C_6F_5)_2[P(C_2H_5)_3]_2$ in 57% yield. The compound decomposes above 140 °C to a deep blue liquid (lit.¹⁸ mp 135 °C dec). The product was identified by its mass spectrum. The same product was obtained in 29% yield from a similar reaction between cobalt powder and 1 equiv of C_6F_5Br followed by the addition of $P(C_2H_5)_3$.

Preparation of $Ni(C_6F_5)_2(C_5H_5N)_2$. A nickel slurry was prepared in the usual manner and allowed to settle. About half of the beige solution above the slurry was removed, and 1 equiv of C_6F_5I was slowly added in. The mixture became slightly yellow and was then stirred at about 50 °C for 24 h after which time it became orange-brown. The mixture was allowed to cool to room temperature, and then 1 equiv of pyridine per nickel was added to the mixture. The color became yellow-green, and the mixture was stirred for about 5 min and then allowed to stand for 1 h. Essentially the entire contents solidified into a crystalline mass. The volatiles were removed under vacuum, and the product was extracted with CH_2Cl_2 . The greenish yellow solution was filtered and the solvent removed under reduced pressure to yield a brown crystalline solid. Recrystallization from CH_2Cl_2 by slow solvent evaporation resulted in straw yellow needlelike crystals of $Ni(C_6F_5)_2(C_5H_5N)_2$ in 40% yield: mp >280 °C, discolors at about 250 °C. Anal. Calcd for $C_{22}H_{10}F_{10}N_2Ni$: C, 47.95; H, 1.83; F, 34.48; N, 5.08. Found: C, 47.81; H, 1.83; F, 34.26; N, 5.07.

In a similar reaction employing 2 equiv of pyridine per nickel essentially the same yield of $Ni(C_6F_5)_2(C_5H_5N)_2$ was obtained. The light green crystals, presumably $NiI_2(C_5H_5N)_4$, which were also obtained were readily washed out with water prior to recrystallizing $Ni(C_6F_5)_2(C_5H_5N)_2$ from CH_2Cl_2 .

Preparation of $Ni(C_6F_5)_2[(C_6H_5)_2PH]_2 \cdot C_6H_5CH_3$. A nickel slurry was prepared in the usual manner and allowed to settle. The pale beige solution above the slurry was removed, and 1 equiv of C_6F_5I was syringed in. The mixture was stirred at about 60 °C for 19 h after which time a deep orange-brown solution existed. The solution was allowed to cool, and 3 equiv of $(C_6H_5)_2PH$ was slowly syringed in. Initially the mixture became yellow and then deep green in a mildly exothermic reaction. The mixture was stirred for 0.5 h, and then all volatiles were removed under vacuum. The product was extracted with CH_2Cl_2 and the black solution filtered. Solvent evaporation under reduced pressure yielded a black tarry crystalline mass. The mixture was washed with several portions of methanol, leaving a dirty crystalline mass. This was dissolved in CH_2Cl_2 . Slow solvent evaporation from the golden yellow solution resulted in yellow crystals in 38% yield. Recrystallization from toluene affords the compound containing a toluene of crystallization: mp 161–162 °C; crystals are completely black before melting; IR (Nujol) P–H 2360 cm^{-1} ; 1H NMR ($CDCl_3$) δ 7.28 (aromatic m, 25 H), 2.32 (aliphatic s, 3 H). Anal. Calcd for $C_{43}H_{30}F_{10}NiP_2$: C, 60.24; H, 3.53; F, 22.16. Found: C, 59.74; H, 3.70; F, 21.71.

Preparation of $Pd(C_6F_5)I(C_4H_{10}O_2)$. A typical palladium slurry was prepared and then allowed to settle. The solvent above the black powder was removed, and 1 equiv of C_6F_5I was slowly syringed in and the mixture stirred at 60 °C for 40 h. The deep orange brown solution was allowed to cool, and a crop of red brown crystals formed in solution. The volatiles were removed from the flask under vacuum, and the product was dissolved in 20 mL of CH_2Cl_2 and the mixture anaerobically filtered. About 15 mL of solvent was removed under vacuum and the remainder allowed to slowly evaporate. A crop of orange red crystals formed in the brown-red solution. The crystals were washed with a small amount

of a 2:1 hexane– CH_2Cl_2 solution and dried: yield of $Pd(C_6F_5)I \cdot (C_4H_{10}O_2)$ 16% mp (sealed tube) 135 °C dec. Anal. Calcd for $C_{10}H_{10}F_5IO_2Pd$: C, 24.49; H, 2.06; F, 19.37. Found: C, 25.62; H, 2.62; F, 17.30.

Preparation of $trans-Pd(C_6F_5)I[P(C_2H_5)_3]_2$. A palladium slurry was prepared in the usual manner and then allowed to settle. About half of the pale gray solvent above the slurry was removed, and then 1 equiv of C_6F_5I per palladium was syringed in. The mixture was refluxed at 85 °C for 20 h after which time an intense red-brown solution existed. The volatiles were removed under vacuum, and the product was dissolved in 20 mL of CH_2Cl_2 . Two equivalents of $P(C_2H_5)_3$ per palladium were syringed in. The reaction was immediate and slightly exothermic and yielded a yellow solution with a small amount of black powder present. The mixture was filtered and solvent removed under reduced pressure. Recrystallization from CH_2Cl_2 resulted in pale yellow crystals covered slightly with an oily residue. Recrystallization from hot hexane yielded pale yellow crystals of $trans-Pd(C_6F_5)I[P(C_2H_5)_3]_2$ in 77% yield on the basis of the palladium chloride reduced: mp 152–154 °C (lit. mp 154–155 °C).

A small amount of orange crystals (2%) of $PdI_2[P(C_2H_5)_3]_2$ was also obtained: mp 137–139 °C (lit.¹⁹ mp 139 °C). It is believed that this compound arose from some unreduced palladium halide.

Preparation of $Pd(C_6F_5)I(bpy)$. A palladium slurry was prepared in the usual manner and allowed to settle. The solvent above the slurry was removed and the slurry cooled to 0 °C for the addition of 1 equiv of C_6F_5I . A slight yellow color was visible in solution at this temperature. The mixture was then stirred at about 70 °C for 25 h after which time a thick, deep orange-brown solution existed. The mixture was allowed to cool to room temperature, and then 1 equiv of 2,2'-bipyridine was added to the flask. The mixture became light yellow in color, and in a few minutes the entire mass solidified. Ten milliliters of fresh glyme was syringed in, the mixture was stirred for about 1 h, and then all volatiles were removed under vacuum. The product was extracted with CH_2Cl_2 and the orange solution filtered. Removal of solvent under reduced pressure resulted in an orange-brown crystalline material. The mixture was washed several times with more hexane to remove excess 2,2'-bipyridine and then dissolved in a minimum amount of acetone. The orange solution was filtered, leaving behind a small amount of the dark red-brown needles.

Slow evaporation of the acetone solution resulted in gold yellow crystals of $Pd(C_6F_5)I(C_{10}H_8N_2)$ in 59% yield: mp 285 °C. Anal. Calcd for $C_{16}H_8F_5IN_2Pd$: C, 34.53; H, 1.45; N, 5.03; F, 17.07. Found: C, 34.34; H, 1.62; N 4.83; F, 16.98.

Preparation of $[Pd(C_6F_5)IS(C_2H_5)_2]_2$. A typical palladium slurry was prepared and allowed to settle. After the solvent above the black material was removed, 1 equiv of C_6F_5I per palladium was added in. The mixture warmed up, and it was then stirred at about 70 °C for 24 h after which time a deep orange-brown solution existed. All volatiles were removed under vacuum, and the product was dissolved in 5 mL of CH_2Cl_2 . To this solution was then added 2 equiv of $S(C_2H_5)_2$, and the color immediately became yellow with some black solid present. The mixture was stirred for about 10 min and then all volatiles were removed from the flask under vacuum. The product was extracted with CH_2Cl_2 and the orange solution filtered. Removal of solvent under reduced pressure left a dark orange oil. The oil was dissolved in hexane, the mixture filtered, and slow solvent evaporation yielded poorly faceted orange-brown crystals of $[Pd(C_6F_5)IS(C_2H_5)_2]_2$ in 38% yield: mp 149–151 °C; 1H NMR ($CDCl_3$) δ 1.47 (t, 3 H) 2.70 (q, 2 H). Anal. Calcd for $C_{20}H_{20}F_{10}I_2Pd_2S_2$: C, 24.49; H, 2.06; F, 19.37. Found: C, 24.73; H, 2.13; F, 19.44. The compound is soluble in most organic solvents and yields an oil upon solvent evaporation.

Preparation of $Pd(C_6F_5)I(1,5-COD)$. A typical palladium slurry was prepared and allowed to settle. The solution above the slurry was removed and 1 equiv of C_6F_5I slowly added in. The mixture was then stirred for 46 h at about 65 °C after which time a deep orange-brown solution existed. Volatiles were removed under vacuum, and the product was dissolved in 8 mL of $CHCl_3$. To the deep brown solution was added 2 equiv of 1,5-cyclo-octadiene (1,5-COD), and the mixture was stirred at 50 °C for about 6 h, with no discernible color change occurring. The volatiles again were removed under vacuum, and the product was extracted

with CH_2Cl_2 . Solvent was removed from the filtered solution under vacuum, leaving an oily orange crystalline mass. The product was dissolved in CH_2Cl_2 and passed through a short (8-cm) alumina column. Slow solvent evaporation from the yellow solution resulted in golden yellow plates of $\text{Pd}(\text{C}_6\text{F}_5)\text{I}(1,5\text{-COD})$ in 19% yield: the crystals gradually darken and are black at about 180 °C. Anal. Calcd for $\text{C}_{14}\text{H}_{12}\text{F}_5\text{IPd}$: C, 33.07; H, 2.38; F, 18.68; Pd, 20.92. Found: C, 33.26; H, 2.38; F, 18.54; Pd, 20.81.

Preparation of $\text{Pd}(\text{C}_6\text{F}_5)\text{I}(\text{CNC}_6\text{H}_{11})_2$. A typical palladium slurry was prepared and allowed to settle and excess solvent removed via syringe. One equivalent of $\text{C}_6\text{F}_5\text{I}$ was syringed in and the mixture stirred at about 75 °C for 53 h after which time the usual deep orange brown mixture existed. Volatiles were removed under vacuum, and the product was dissolved in 4 mL of fresh glyme. Addition of 2 equiv of $\text{CNC}_6\text{H}_{11}$ to the solution resulted in a mildly exothermic reaction and an immediate color change to yellow. The mixture was stirred for 10 min, and again all volatiles were removed under vacuum. The product was extracted with C_6H_6 and the golden yellow solution filtered. Solvent removal under reduced pressure resulted in a honey-colored crystalline material. Recrystallization from CH_2Cl_2 yielded yellow crystals covered with an orange film. The orange substance was readily washed with a small amount of cyclohexane, yielding pale yellow crystals $\text{Pd}(\text{C}_6\text{F}_5)\text{I}(\text{CNC}_6\text{H}_{11})_2$ in 52% yield: mp 148.5–149 °C; IR (Nujol) ($\text{C}\equiv\text{N}$) 2230 (vs), 2248 (sh) cm^{-1} . Anal. Calcd for $\text{C}_{26}\text{H}_{22}\text{F}_5\text{IN}_2\text{Pd}$: C, 38.83; H, 3.58; F, 15.35; N, 4.53. Found: C, 38.89; H, 3.60; F, 15.49; N, 4.49.

Preparation of $\text{Pd}(\text{C}_6\text{H}_5)\text{I}(2,2'\text{-bpy})$. A typical palladium slurry was prepared and allowed to settle. After the solvent above the powder was removed, 1 equiv of 2,2'-bipyridine was added to the flask. Immediately an intense purple color formed in solution. To this mixture was added 1 equiv of iodobenzene. After several drops of $\text{C}_6\text{H}_5\text{I}$ the purple color changed to yellow. The mixture was stirred at about 70 °C for 20 h after which time a golden yellow solution existed with a black powder. The volatiles were stripped under vacuum, and the product was extracted with CH_2Cl_2 . Removal of solvent under reduced pressure left a mass of orange and gray crystals. The mixture was washed with several portions of hexane to remove the unreacted 2,2'-bipyridine and the residue recrystallized from CH_2Cl_2 . Orange crystals of $\text{Pd}(\text{C}_6\text{H}_5)\text{I}(\text{bpy})$ were obtained in 17% yield: mp 244–247 °C; crystals begin to darken at about 210 °C. Anal. Calcd for $\text{C}_{18}\text{H}_{13}\text{IN}_2\text{Pd}$: C, 41.19; H, 2.81; I, 27.20; N, 6.00. Found: C, 40.82; H, 2.86; I, 26.93; N, 5.90.

Preparation of *trans*- $\text{Pt}(\text{C}_6\text{F}_5)\text{I}[\text{P}(\text{C}_2\text{H}_5)_3]_2$. A typical platinum slurry was prepared and allowed to settle. The solvent above the black powder was removed via syringe, 2 equiv of $\text{C}_6\text{F}_5\text{I}$ per platinum were syringed in, and the mixture was heated at reflux for 55 h after which time a yellowish solution existed with a black powder. The volatiles were removed under vacuum, and the product was dissolved in a small amount of CH_2Cl_2 , and to the deep brown solution was added 1.5 equiv of $\text{P}(\text{C}_2\text{H}_5)_3$. Immediately the brown color faded. The mixture was stirred for about 1 min, and again all volatiles were removed. The product was extracted with CH_2Cl_2 and the yellow solution allowed to evaporate. The moist crystalline material was twice recrystallized from cyclohexane, each time treated with charcoal, and resulted in off-white crystals of *trans*- $\text{Pt}(\text{C}_6\text{F}_5)\text{I}[\text{P}(\text{C}_2\text{H}_5)_3]_2$ in 27% yield: mp 162–164 °C (lit.²⁰ mp 163–164 °C).

Results

Preparation of Slurries. Finely divided, extremely reactive black metal powders are readily obtained by reducing in THF or glyme an anhydrous metal halide with lithium in the presence of a small amount of naphthalene as an electron carrier. Reduction times vary depending on the metal halide but are usually complete in 20 h or less. Occasionally if coating of the piece of lithium occurs, a relatively common occurrence with iron(II) halides in glyme, reduction times may be somewhat longer.

Even though some of the metal halides are hygroscopic, we find that they can be weighed in air, if this is done quickly, and still yield satisfactory results. Glyme and THF are freshly distilled from sodium potassium alloy

Table I. Molar Ratio of Lithium to Metal Halide for Reduction in Glyme

metal halide	lithium	metal halide	lithium
Fe(II)	2.3	Pd(II)	2.6
Co(II)	2.3	Pt(II)	2.8
Ni(II)	2.3	Pt(IV)	5.1

under argon prior to use. In the rare situations where difficulties have been encountered in reductions, invariably the problem has been found to be contaminated solvents.

We have observed that during a reduction a portion of the lithium is involved in reacting with the solvent.¹⁵ To ensure complete reduction of the metal halide, we have found that a slight excess of lithium over stoichiometry is needed. The ratio of lithium to the metal halides is given in Table I. The use of the particular ratio in a given reduction may or may not result in the formation of a slight amount of lithium naphthalide. This variability is possibly caused by small amounts of contaminants introduced in a given reaction.

Reductions involving lithium are easy to judge complete since the piece of lithium is usually pink (covered with dilithium naphthalide), floats, and is thus readily visible during a reduction. If an excess of lithium has been added, the excess can easily be removed from the reaction vessel, or if it is converted to lithium naphthalide, this can be removed by allowing the slurry to settle, syringing off the olive green solution above the slurry, and adding fresh solvent. This can be repeated until a colorless solution exists with the black powder. This also results in the removal of the electron carrier naphthalene. During a reduction, the mixtures of partially reduced halides display some unusual properties. For example, a mixture may undergo changes from a very thick slurry to a very free-moving slurry during the course of a reduction. The reverse sequence of changes has also been observed. Very often in the early stages of reduction of most of these salts, a greasy material is observed that smears on the glass and appears to be insoluble in the solvent. Yet in 1 or 2 h, this substance disappears and a free-moving slurry is obtained. Reductions of iron halides yield powders that show variable attraction to the bar magnet as a function of time in a reduction. There is a time in a reduction where the product shows virtually no magnetic attraction to the stirring bar, yet this same slurry has displayed significant attraction earlier and also does at the end of the reduction.

Reactions of Slurries. The black metal powders prepared by lithium reduction of a metal halide, with the exception of iron, are not pyrophoric when exposed to air, yet they display remarkable reactivity toward organic molecules. These powders are most conveniently used as prepared, that is, they are not separated from the lithium salts, naphthalene, nor any other products formed in the reduction.

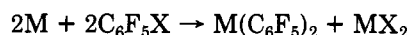
In some previous studies, Klabunde has shown that a variety of transition-metal atoms when cocondensed with $\text{C}_6\text{F}_5\text{X}$ ($\text{X} = \text{I}, \text{Br}$) undergo rapid oxidative addition to yield $\text{C}_6\text{F}_5\text{MX}$ complexes.^{18,24,28,29,31,32} Klabunde demonstrated that these complexes can be converted to a variety of new compounds depending on the metal and halogen. It was also demonstrated that $\text{C}_6\text{H}_5\text{PdX}$ can be prepared but is only stable at low temperatures.²⁸ We felt it would be of value and interest to see if transition-metal powders prepared by the simple and convenient reduction method were reactive enough to undergo oxidative addition to $\text{C}_6\text{F}_5\text{X}$ and other aryl halides.

The reaction of iron and cobalt metal powders with $\text{C}_6\text{F}_5\text{I}$ or with $\text{C}_6\text{F}_5\text{Br}$ results in disproportionation of the

Table II. Elemental Composition of Metal Powders

powder	C	H	M	I	Li	O
Ni	4.45	1.36	64.16	1.42	5.35	28.68
Pd	2.36	0.65	83.33	<0.03	2.69	10.91
Pt	1.50	0.38	85.55	0.01	2.45	8.73

presumed initially formed solvated species $M(C_6F_5)X$ ($X = Br, I$).



Nickel powder reacts with C_6F_5I to yield a disproportionated organonickel species; however, with C_6F_5Br , nickel yields the solvated $Ni(C_6F_5)Br$.¹⁵ Palladium and platinum react with C_6F_5I in glyme and yield the nondisproportionated organometallic compounds $M(C_6F_5)I(C_4H_{10}O_2)$.

Of particular significance is that these ether-coordinated transition-metal compounds are stable in the absence of air yet possess an extremely labile ether ligand. The coordinated ether is readily displaced with a variety of other ligands in most cases these displacement reactions being essentially instantaneous and resulting in organometallic compounds in yields as high as 77% on the basis of the metal halide used.

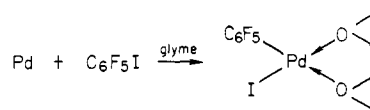
Iron. Of the metal powders described here, iron shows the greatest reactivity toward C_6F_5I . The iron slurry has to be cooled to 0 °C for the addition of C_6F_5I . The reaction of iron with C_6F_5Br is also quite exothermic, hence even for this addition the iron slurry is cooled to about 0 °C. The organoiron compound formed in the above reactions, the solvated $Fe(C_6F_5)_2$, reacts with CO at room temperature and ambient pressure to yield $Fe(C_6F_5)_2(CO)_2(C_4H_{10}O_2)_2$. It is very doubtful if this compound is eight-coordinate; most likely it is six-coordinate with one of the glymes being a molecule of crystallization. On the NMR time scale ($CDCl_3$) both molecules of glyme are equivalent and both resonances are shifted downfield from those of free glyme in $CDCl_3$. The complexity of the IR spectrum of this compound in the carbonyl region suggests a mixture of isomers. Such mixtures of isomers have been observed in bis(perfluorocarbon)iron compounds containing carbonyl and phosphine ligands.²¹

Cobalt. Cobalt metal powder readily reacts with 1 equiv of C_6F_5I or C_6F_5Br to yield the solvated species $Co(C_6F_5)_2$ and CoX_2 ($X = Br, I$). Addition of triethylphosphine to such a mixture results in an immediate reaction and formation of the air-stable $Co(C_6F_5)_2[P(C_2H_5)_3]_2$. This compound has also been obtained by phosphine displacement of the coordinated toluene from $Co(C_6F_5)_2(\pi-C_7H_8)$.¹⁸

Nickel. The reaction of nickel metal powder with C_6F_5I results in the same products as those that are obtained in the case of iron or cobalt, that is solvated $Ni(C_6F_5)_2$ and NiI_2 . The glyme coordinated to $Ni(C_6F_5)_2$ is very labile and can be displaced with other ligands. Addition of $P(C_2H_5)_3$ to a mixture of solvated $Ni(C_6F_5)_2$ and NiI_2 results in an immediate reaction and formation of the known compound $Ni(C_6F_5)_2[P(C_2H_5)_3]_2$ in 69% yield. The ether displacement is also readily affected with $(C_6H_5)_2PH$ and yields after recrystallization from toluene $Ni(C_6F_5)_2[(C_6H_5)_2PH]_2C_6H_5CH_3$. Noteworthy in this preparation is that this compound is probably not readily accessible by standard arylating methods since the reaction of a nickel halide with $(C_6H_5)_2PH$ results in $Ni[(C_6H_5)_2P]_2[(C_6H_5)_2PH]_2$.²²

Amines can also displace the coordinated glyme molecule from $Ni(C_6F_5)_2(C_4H_{10}O_2)$. Thus addition of pyridine to the orange-brown mixture of solvated $Ni(C_6F_5)_2$ and NiI_2 results in an immediate color change and the formation of $Ni(C_6F_5)_2(C_5H_5N)_2$.

Palladium. The reaction of palladium metal powder with C_6F_5I results in the formation of slightly air-sensitive orange-red crystals of $Pd(C_6F_5)I(C_4H_{10}O_2)$.¹⁶



The formation of this organopalladium compound from palladium powder and C_6F_5I differs from the related reactions involving iron, cobalt, and nickel metal powders that most likely proceed through this type of intermediate but that then disproportionate to $M(C_6F_5)_2$ and MI_2 ($M = Fe, Co, Ni$). As in the case of the other metal compounds the coordinated glyme of $Pd(C_6F_5)I(C_4H_{10}O_2)$ is exceedingly labile and can be displaced with a variety of ligands, yielding derivatives of $Pd(C_6F_5)I$ in yields ranging from 77% for the brown compound *trans*- $Pd(C_6F_5)I[P(C_2H_5)_3]_2$ to 19% for $Pd(C_6F_5)I(1,5-COD)$ where 1,5-COD is 1,5-cyclooctadiene. While some of the compounds prepared by glyme displacement from $Pd(C_6F_5)I(C_4H_{10}O_2)$ are available by standard arylating agents such as lithium or Grignard reagents, others have required more tedious procedures. For example the arylation of compounds of the type $PdCl_2(bpy)$ where *bpy* is 2,2'-bipyridine normally leads to very low yields of $Pd(C_6F_5)_2(bpy)$. The preferred method for the preparation of the organopalladium halide involves first the preparation of *trans*- $Pd(C_6F_5)Cl[As(C_6H_5)_3]_2$ and then displacement of the arsine with 2,2'-bipyridine.²³

Several similar compounds to the ones reported here have been prepared from reactions of donor ligands with the nonsolvated species $Pd(C_6F_5)Br$ that has been obtained via cocondensation of palladium vapors with a large excess of C_6F_5Br . However, it appears that there can be differences between the reactions of ligand addition to $Pd(C_6F_5)Br$ and glyme displacement from $Pd(C_6F_5)I(C_4H_{10}O_2)$. For example addition of $S(C_2H_5)_2$ to $Pd(C_6F_5)Br$ is reported to result in $Pd(C_6F_5)Br[S(C_2H_5)_2]_2$ in 4.4% yield.²⁴ The displacement of the coordinated glyme from $Pd(C_6F_5)I(C_4H_{10}O_2)$ with at least 2 equiv of $S(C_2H_5)_2$ per organopalladium compound resulted in a 38% yield of $\{Pd(C_6F_5)IS(C_2H_5)_2\}_2$.

The robust nature of the compound $Pd(C_6F_5)I(C_4H_{10}O_2)$ prompted us to examine whether an analogous compound containing a C_6H_5 group could be prepared and isolated. $Pd(C_6H_5)X$ has been proposed as an unstable intermediate in a variety of organic reactions catalyzed by palladium(II) salts.²⁵ Addition of iodobenzene to a palladium metal slurry resulted in a reaction; however, trapping of the products with $P(C_2H_5)_3$ resulted in isolation of biphenyl and *trans*- $PdI_2[P(C_2H_5)_3]_2$. These results were obtained at about 40 °C and at room temperature. The products of the above reaction suggested that $Pd(C_6H_5)I$ most likely formed but that it was unstable under the conditions of preparation. It is noteworthy and indicative of the reactivity of the metal powders described herein that a metal such as palladium reacts at room temperature with an unactivated halide such as iodobenzene.

Since iodobenzene reacted with the palladium metal powder, a practical route for preparation of derivatives of $Pd(C_6H_5)I$ appeared to be the reaction of palladium metal with iodobenzene in the presence of a stabilizing ligand. Addition of 2,2'-bipyridine to a palladium metal slurry resulted in an immediate formation of a deep purple color in solution. This purple substance is extremely air sensitive and might be a neutral 2,2'-bipyridine compound of palladium similar to the class of compounds reported by Herzog and co-workers.²⁶ Addition of 1 equiv of io-

Table III. Relative Atomic Concentrations in Percent as a Function of Sputtering Depth^a

Activated Ni						
depth	C	O	Ni	Cl	S	Li
as received	17.2	42.1	0.8	0.1	0.2	39.6
30 Å	19.4	40.4	1.3	0.3	0.0	38.7
100 Å	23.3	39.0	2.7	0.2	0.0	34.7
200 Å	25.4	35.6	4.4	0.2	0.1	34.0
Activated Pd						
	C	O	Pd	Cl	Li	
as received	22.7	44.9	1.2	0.8	30.5	
30 Å sputtered	32.8	24.8	2.1	0.9	39.3	
Activated Pt						
	C	O	Pt	Cl	Li	
as received	28.7	39.8	0.5	0.8	30.7	
30 Å sputtered	35.8	30.0	0.8	0.9	32.7	

^a The surface material was removed by Ar⁺ bombardment. The sputtering rates are determined from known thicknesses of Ta₂O₅ films. Since the sputtering rate of this material relative to Ta₂O₅ is unknown, the absolute depths are approximate. The relative atomic percents are calculated by using experimental sensitivity factors and peak areas for each of the elements shown. The relative atomic concentrations show reproducibility to ±0.2% and are correct to within ±5% of the absolute concentrations.

dobenzene and allowing the mixture to react at 70 °C resulted in a 17% yield of Pd(C₆H₅)I(bpy). After only a few drops of iodobenzene, the purple color was discharged, indicating a very small amount of the purple substance existed and that it was not the source of the product.

It is interesting to note that the attempted preparation of Ni(C₆F₅)I(bpy) by the above described procedure only led to Ni(C₆F₅)₂(bpy) in 79% yield.

Platinum. As would be expected of the metals in the nickel triad, platinum shows diminished reactivity with C₆F₅I; nevertheless it reacts under reflux in glyme and yields the solvated Pt(C₆F₅)I. Addition of P(C₂H₅)₃ results in an immediate reaction and formation of the known compound *trans*-Pt(C₆F₅)I[P(C₂H₅)₃]₂.

Surface Analysis. Surface (Table III) as well as bulk analysis (Table II) shows that the metal powders produced by this reduction technique are quite complex materials containing considerable amounts of carbon, hydrogen, and oxygen. The ESCA results are summarized in Table III. Binding energies for the Ni, Pd, and Pt powders are given in Table IV.

The binding energies for the photoelectron lines and the kinetic energies for the Auger lines are calibrated to the Au 4f_{7/2} peak taken as 83.8 eV. The binding energies and the kinetic energies are related by the following equation when referenced to the Fermi level:

$$h\nu = BE + KE$$

Since the samples were mounted on tape, some charging was observed; however, the electron energies have been referenced to the C 1s line taken at 284.6 eV. The Auger parameter (α) is equal to the sum of the binding energies of the photoelectron line plus the kinetic energies of the Auger lines and is independent of the method of charge referencing.

B.E.T. surface area measurements were carried out on the activated Ni powder and was found to have a specific surface area of 32.7 m²/g. Bulk analysis were performed on Ni, Pt, and Pd powders and the results are shown in Table II.

Table IV

Binding Energies and Kinetic Energies (eV)

Activated Ni				
For the Reactive Ni Powders Before Sputtering				
Ni 2p	Ni LMM	α		
852.2	846.8	1699.0		
O 1s	O KVV	α		
530.9	508.2	1039.1		
C 1s		Li 1s		
284.6/299.2		54.4		
For the Reactive Ni Powder After Sputtering (~30 Å)				
Ni 2p	Ni LMM	α		
852.3	846.8	1699.1		
O 1s	O KVV	α		
530.9/529.0	508.5	1039.4		
C 1s		Li 1s		
284.6/289.2				
Activated Pd				
	O 1s	C 1s	Li 1s	Pd 3d _{5/2}
as received	530.8	284.6	54.3	334.8
30 Å sputtered	531.4	284.6	54.7	334.7
Activated Pt				
	O 1s	C 1s	Li 1s	Pt 4f _{7/2}
as received	531.2	284.6	54.5	70.8
30 Å sputtered	531.4	284.6	54.7	70.8

Discussion

From the binding energies of the O 1s and the kinetic energies of the O KVV and its shape indicate that most of the Li exists as LiOH. The electron energies for the Ni lines show that the Ni is mostly Ni⁰. A small amount of oxide NiO is seen on the high-resolution spectrum of the Ni 2p line; this oxide layer is completely removed after sputtering to a depth of 30 Å. This indicates that most of the O is bound to the Li. By sputtering to a depth of 200 Å, one sees an increase of the Ni/Li ratio while the Li/O ratio remains somewhat constant. Some reduction of the LiOH to Li₂O is observed in the O 1s spectrum after sputtering. A small amount of carbonate is seen in the C 1s spectrum that is most likely bound to the Li.

The ESCA results for the activated Pd and Pt are similar to that of the activated Ni. The surfaces of the metal particles seemed to be covered with coatings of LiOH and organic carbon. The binding energies of the metals indicate that both the Pd and Pt are mainly metallic (not oxidized). The binding energy of the Li is consistent with LiOH.

The B.E.T. analysis on the activated Ni clearly shows the high surface area of these materials. The bulk analysis data indicate the very complex nature of these materials. All samples contained considerable carbon and hydrogen, particularly the nickel sample. It is not clear at this point whether this is due to trapped solvent molecules or degradation products from the solvent. Klubunde has demonstrated that codeposition of transition metals with ethereal and hydrocarbon solvents leads to cleavage of C-H as well as C-C bonds.^{29,30} These reactions result in the incorporation of carbon and hydrogen in the final metal powders. At this point, it is not clear whether these reactions are occurring in our preparation of finely divided metals. Studies are underway to clear up this point. As 2.3 to 2.6 equiv of lithium is used to reduce Ni(II), Pt(II), or Pd(II), it is highly likely that some solvent cleavage to alkoxide ions is occurring. Much of the high oxygen content is likely to originate from the reaction of the metal

powders with spurious oxygen encountered during all the manipulations. There is, of course, one primary concern with these attempts to do surface analysis on these very highly reactive metal powders. Do the results have any bearing on the freshly reduced metal powders before they are manipulated in any way? The answer is most likely that certain data will be valid. The bulk of the metal is in the zero-valent state and we do not have a simple physical mixture of M(II) salts and some reducing agent. The metal powders are very complex materials containing carbon and hydrogen. The surfaces seem to be covered with LiOH and some carbonaceous material. However, the surface composition is the one aspect that is most likely affected by the various manipulations.

The origin of the high reactivity of these metals is thus still open to much speculation. Part of this reactivity certainly comes from the high surface area and small particle size. Also, before any manipulations, this surface area must be relatively free of passivating oxide coatings. It is also possible that the adsorbed hydroxide ions, alkoxide anions, and possibly halide anions may be adsorbed on the surfaces and reduce the work function of the metal. This would enhance the metals ability to transfer an electron to the organic substrate in the initial step of these oxidative addition reactions.

Summary

Lithium reduction of transition-metal halides is not only readily effected with inexpensive apparatus and simple procedure but also yields exceptionally reactive metal powders. These powders react with C_6F_5X to yield ether-coordinated species of the type $M(C_6F_5)_2$ or $M(C_6F_5)_2X$, where $X = I$ and Br . The coordinated ether is exceptionally labile and is readily and in most cases instantly displaced by a variety of ligands to yield organometallic compounds in high yield based on two reactions, that is

a reaction of a metal powder with C_6F_5X followed by the addition of another ligand to displace the coordinated ether of the initially formed organometallic species. The displacement of the coordinated ether allows preparation of compounds with ligands which would in some cases, not survive a reaction involving a typical arylating agent.

The addition of a stabilizing ligand to a metal slurry prior to the addition of an organic halide allows preparation and isolation of organometallic compound with groups other than C_6F_5 . This route may allow the preparation of entirely new classes of organometallic compounds. Other studies utilizing these highly reactive transition-metal powders in a variety of organic syntheses will be reported in the near future.

Surface analysis indicates that these powders are finely divided and very complex materials. Carbon as well as hydrogen is found in these metals. The metal surfaces appear to be coated with LiOH and some carbonaceous material, leaving the question of origin of high reactivity still somewhat in doubt.

Acknowledgment. We gratefully acknowledge support of this work by the U.S. Army Office (supported work on iron and cobalt) and the Division of Chemical Sciences, Department of Energy (Contract No. DE-AC02-80ER10603, supported work on nickel, palladium, and platinum).

Registry No. $Fe(C_6F_5)_2(CO)_2(C_4H_{10}O_2)$, 75070-27-8; $Ni(C_6F_5)_2[P(C_2H_5)_3]_2$, 15638-54-7; $Co(C_6F_5)_2[P(C_2H_5)_3]_2$, 60528-59-8; $Ni(C_6F_5)_2(C_6H_5N)_2$, 69004-95-1; $Ni(C_6F_5)_2[(C_6H_5)_2PH]_2$, 75070-25-6; $Pd(C_6F_5)I(C_4H_{10}O_2)$, 84303-71-9; *trans*- $Pd(C_6F_5)I[P(C_2H_5)_3]_2$, 54071-55-5; $Pd(C_6F_5)I(bpy)$, 84303-72-0; $[Pd(C_6F_5)IS(C_2H_5)_2]_2$, 84303-73-1; $Pd(C_6F_5)I(1,5-COD)$, 84303-74-2; $Pd(C_6F_5)I(CNC_6H_{11})_2$, 84303-75-3; $Pd(C_6H_5)I(2,2'-bpy)$, 84303-76-4; *trans*- $Pt(C_6F_5)I[P(C_2H_5)_3]_2$, 14494-06-5; Fe , 7439-89-6; Co , 7440-48-4; Ni , 7440-02-0; Pd , 7440-05-3; Pt , 7440-06-4.

Crystal and Molecular Structures of Bent and Planar Forms of Binuclear $Co_2(\mu-PPh_2)_2(CO)_6$ (1). Comments of the Relative Energies of the Two Forms of 1 and Related Molecules

A. Dale Harley, Robert R. Whittle, and Gregory L. Geoffroy*

Department of Chemistry, The Pennsylvania State University, University Park, Pennsylvania 16802

Received September 8, 1982

The binuclear phosphido-bridged cobalt carbonyl complex $Co_2(\mu-PPh_2)_2(CO)_6$, 1, has been characterized by a complete single-crystal X-ray diffraction study. It crystallizes in the space group *Ia* (No. 9, nonstandard setting of *Cc*) with $a = 15.880$ (4) Å, $b = 8.697$ (2) Å, $c = 41.423$ (9) Å, $\beta = 94.12$ (2)°, $V = 5706$ (4) Å³, and $Z = 8$. The structure was refined by using the 3747 reflections with $I \geq 2\sigma(I)$ to give final residuals of $R = 0.042$ and $R_w = 0.046$. There are two crystallographically independent molecules of 1 in the unit cell that differ in important detail. Each Co in both molecules is coordinated by three CO's and the two $\mu-PPh_2$ bridging ligands. The Co-Co separations are 3.487 (2) and 3.573 (2) Å in molecules A and B of 1, implying no formal metal-metal bonds. The $Co_2(\mu-P)_2$ core in molecule B is essentially planar with a dihedral angle of 177.4°, whereas the $Co_2(\mu-P)_2$ core in molecule A is substantially bent, having a dihedral angle of 155.0°. Furthermore, the carbonyl ligands of planar molecule B are arranged in a staggered conformation, whereas in bent molecule A they are eclipsed. The cocrystallization of molecules of both geometries implies that there is little energy difference between these two forms of 1. This aspect is discussed in relationship to the properties and structures of other bis(phosphido)-bridged molecules.

In 1964 Hayter¹ reported the preparation of a red-orange compound that was given the binuclear formulation Co_2-

$(\mu-PPh_2)_2(CO)_6$ on the basis of its analytical and spectroscopic properties. The structure drawn below was sug-

powders with spurious oxygen encountered during all the manipulations. There is, of course, one primary concern with these attempts to do surface analysis on these very highly reactive metal powders. Do the results have any bearing on the freshly reduced metal powders before they are manipulated in any way? The answer is most likely that certain data will be valid. The bulk of the metal is in the zero-valent state and we do not have a simple physical mixture of M(II) salts and some reducing agent. The metal powders are very complex materials containing carbon and hydrogen. The surfaces seem to be covered with LiOH and some carbonaceous material. However, the surface composition is the one aspect that is most likely affected by the various manipulations.

The origin of the high reactivity of these metals is thus still open to much speculation. Part of this reactivity certainly comes from the high surface area and small particle size. Also, before any manipulations, this surface area must be relatively free of passivating oxide coatings. It is also possible that the adsorbed hydroxide ions, alkoxide anions, and possibly halide anions may be adsorbed on the surfaces and reduce the work function of the metal. This would enhance the metals ability to transfer an electron to the organic substrate in the initial step of these oxidative addition reactions.

Summary

Lithium reduction of transition-metal halides is not only readily effected with inexpensive apparatus and simple procedure but also yields exceptionally reactive metal powders. These powders react with C_6F_5X to yield ether-coordinated species of the type $M(C_6F_5)_2$ or $M(C_6F_5)_2X$, where $X = I$ and Br . The coordinated ether is exceptionally labile and is readily and in most cases instantly displaced by a variety of ligands to yield organometallic compounds in high yield based on two reactions, that is

a reaction of a metal powder with C_6F_5X followed by the addition of another ligand to displace the coordinated ether of the initially formed organometallic species. The displacement of the coordinated ether allows preparation of compounds with ligands which would in some cases, not survive a reaction involving a typical arylating agent.

The addition of a stabilizing ligand to a metal slurry prior to the addition of an organic halide allows preparation and isolation of organometallic compound with groups other than C_6F_5 . This route may allow the preparation of entirely new classes of organometallic compounds. Other studies utilizing these highly reactive transition-metal powders in a variety of organic syntheses will be reported in the near future.

Surface analysis indicates that these powders are finely divided and very complex materials. Carbon as well as hydrogen is found in these metals. The metal surfaces appear to be coated with LiOH and some carbonaceous material, leaving the question of origin of high reactivity still somewhat in doubt.

Acknowledgment. We gratefully acknowledge support of this work by the U.S. Army Office (supported work on iron and cobalt) and the Division of Chemical Sciences, Department of Energy (Contract No. DE-AC02-80ER10603, supported work on nickel, palladium, and platinum).

Registry No. $Fe(C_6F_5)_2(CO)_2(C_4H_{10}O_2)$, 75070-27-8; $Ni(C_6F_5)_2[P(C_2H_5)_3]_2$, 15638-54-7; $Co(C_6F_5)_2[P(C_2H_5)_3]_2$, 60528-59-8; $Ni(C_6F_5)_2(C_6H_5N)_2$, 69004-95-1; $Ni(C_6F_5)_2[(C_6H_5)_2PH]_2$, 75070-25-6; $Pd(C_6F_5)I(C_4H_{10}O_2)$, 84303-71-9; *trans*- $Pd(C_6F_5)I[P(C_2H_5)_3]_2$, 54071-55-5; $Pd(C_6F_5)I(bpy)$, 84303-72-0; $[Pd(C_6F_5)IS(C_2H_5)_2]_2$, 84303-73-1; $Pd(C_6F_5)I(1,5-COD)$, 84303-74-2; $Pd(C_6F_5)I(CNC_6H_{11})_2$, 84303-75-3; $Pd(C_6H_5)I(2,2'-bpy)$, 84303-76-4; *trans*- $Pt(C_6F_5)I[P(C_2H_5)_3]_2$, 14494-06-5; Fe , 7439-89-6; Co , 7440-48-4; Ni , 7440-02-0; Pd , 7440-05-3; Pt , 7440-06-4.

Crystal and Molecular Structures of Bent and Planar Forms of Binuclear $Co_2(\mu-PPh_2)_2(CO)_6$ (1). Comments of the Relative Energies of the Two Forms of 1 and Related Molecules

A. Dale Harley, Robert R. Whittle, and Gregory L. Geoffroy*

Department of Chemistry, The Pennsylvania State University, University Park, Pennsylvania 16802

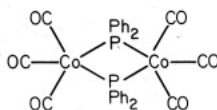
Received September 8, 1982

The binuclear phosphido-bridged cobalt carbonyl complex $Co_2(\mu-PPh_2)_2(CO)_6$, 1, has been characterized by a complete single-crystal X-ray diffraction study. It crystallizes in the space group *Ia* (No. 9, nonstandard setting of *Cc*) with $a = 15.880$ (4) Å, $b = 8.697$ (2) Å, $c = 41.423$ (9) Å, $\beta = 94.12$ (2)°, $V = 5706$ (4) Å³, and $Z = 8$. The structure was refined by using the 3747 reflections with $I \geq 2\sigma(I)$ to give final residuals of $R = 0.042$ and $R_w = 0.046$. There are two crystallographically independent molecules of 1 in the unit cell that differ in important detail. Each Co in both molecules is coordinated by three CO's and the two $\mu-PPh_2$ bridging ligands. The Co-Co separations are 3.487 (2) and 3.573 (2) Å in molecules A and B of 1, implying no formal metal-metal bonds. The $Co_2(\mu-P)_2$ core in molecule B is essentially planar with a dihedral angle of 177.4°, whereas the $Co_2(\mu-P)_2$ core in molecule A is substantially bent, having a dihedral angle of 155.0°. Furthermore, the carbonyl ligands of planar molecule B are arranged in a staggered conformation, whereas in bent molecule A they are eclipsed. The cocrystallization of molecules of both geometries implies that there is little energy difference between these two forms of 1. This aspect is discussed in relationship to the properties and structures of other bis(phosphido)-bridged molecules.

In 1964 Hayter¹ reported the preparation of a red-orange compound that was given the binuclear formulation Co_2-

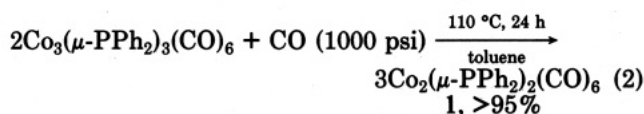
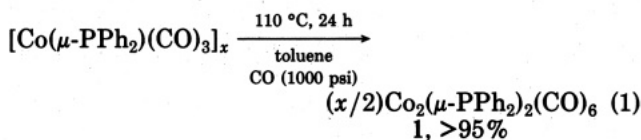
$(\mu-PPh_2)_2(CO)_6$ on the basis of its analytical and spectroscopic properties. The structure drawn below was sug-

gested.¹



Anomalously high molecular weight values (6000–8000 g/mol range) were obtained by Hayter for this material, but these were attributed to possible decomposition during the measurements. However, other workers repeatedly failed to obtain X-ray quality crystals of this species, and the conclusion was drawn that Hayter's product is probably polymeric rather than binuclear.^{2,3} This conclusion was supported by our lack of observation of any diffraction lines in the X-ray powder diffraction pattern of Hayter's compound, implying an amorphous material with the formulation $[\text{Co}(\mu\text{-PPh}_2)(\text{CO})_3]_x$.⁴

In the course of our investigations into the chemistry and interconversions of phosphido-bridged cobalt carbonyl complexes,⁴ we discovered several routes that produce authentic samples of binuclear $\text{Co}_2(\mu\text{-PPh}_2)_2(\text{CO})_6$, **1**. Of these, the most direct involves heating either oligomeric $[\text{Co}(\mu\text{-PPh}_2)(\text{CO})_3]_x$ or trinuclear $\text{Co}_3(\mu\text{-PPh}_2)_3(\text{CO})_6$ under CO pressure (eq 1 and 2). Since spectroscopic data⁴



were insufficient to fully define the nature of this complex, we undertook a complete single-crystal X-ray diffraction study, the results of which are described herein. Remarkably, the latter has shown that both bent and planar molecules of **1** cocrystallize together, implying little or no energy difference between these two forms.

Experimental Section

X-ray Structure Determination of $\text{Co}_2(\mu\text{-PPh}_2)_2(\text{CO})_6$, **1.** Orange crystals of **1**, prepared as described in ref 4, were grown by crystallization from a saturated toluene/hexane (1:10) solution of **1**. An irregularly shaped crystal of dimensions 0.25 mm \times 0.39 mm \times 0.46 mm was cut from a larger crystal and fixed into an aluminum pin and mounted onto an eucentric goniometer. Diffraction data were collected on an Enraf-Nonius four-circle CAD4 automated diffractometer controlled by a PDP8a computer coupled to a PDP 11/34 computer. The program SEARCH was used to obtain 25 accurately centered reflections that were then used in the program INDEX to obtain an orientation matrix for data collection and to provide cell dimensions.⁶ Pertinent crystal and intensity data are listed in Table I. Details of the data collection and reduction procedures have been previously described.⁷

- (1) Hayter, R. G. *J. Am. Chem. Soc.* **1964**, *82*, 823.
- (2) Ginsburg, R. E.; Rothrock, R. E.; Finke, R. G.; Collman, J. P.; Dahl, L. F. *J. Am. Chem. Soc.* **1979**, *101*, 6550.
- (3) Private communication from H. Vahrenkamp to L. F. Dahl, cited on ref 24 in ref 2.
- (4) Harley, A. D.; Guskey, G. J.; Geoffroy, G. L., submitted for publication in *Organometallics*.
- (5) Huntsman, J. R.; Ph.D. Thesis, University of Wisconsin–Madison, 1973.
- (6) Programs used in this study are either part of the Enraf-Nonius Structure Determination Package (SDP), Enraf-Nonius, Delft, Holland, 1975, or a local version X-Ray 67, Stewart, J. M., University of Maryland, Crystallographic Computer Systems.
- (7) Steinhardt, P. C.; Gladfelter, W. L.; Harley, A. D.; Fox, J. R.; Geoffroy, G. L. *Inorg. Chem.* **1980**, *19*, 332.

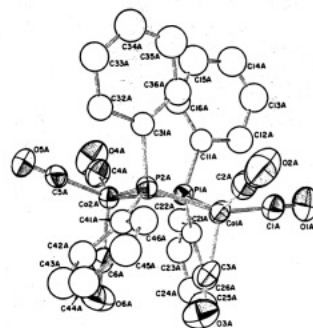


Figure 1. An ORTEP drawing of molecule A of $\text{Co}_2(\mu\text{-PPh}_2)_2(\text{CO})_6$, **1**, showing the atom numbering scheme. Thermal ellipsoids are drawn at the 25% probability level.

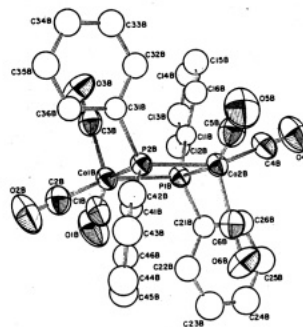


Figure 2. An ORTEP drawing of molecule B of $\text{Co}_2(\mu\text{-PPh}_2)_2(\text{CO})_6$, **1**, showing the atom numbering scheme. Thermal ellipsoids are drawn at the 25% probability level.

Although systematic absences $[hkl, h+k+l=2n+1; h0l, h=2n+1]$ initially indicated the space group $I2/a$, a zero moment test applied after data reduction suggested an acentric data set.⁸ A solution was attempted in the equivalent acentric space group Ia (nonstandard setting of Cc). A successful solution resulted which showed two crystallographically nonrelated molecules of **1** present in the asymmetric unit. The structure was solved by using normal Patterson techniques and refinement proceeded without difficulty. The hydrogen atoms of the phenyl rings were placed at their calculated positions ($\text{C-H} = 0.97 \text{ \AA}$) and assigned isotropic temperature factors of $B = 5.0 \text{ \AA}^2$. In the final cycles of least-squares refinement, 479 parameters were varied including the overall scale factor, positional parameters for all nonhydrogen atoms, anisotropic thermal parameters for the metal, phosphorus, oxygen, and carbonyl carbon atoms, and isotropic thermal parameters for the phenyl carbon atoms. Convergence was achieved with $R = 0.042$ and $R_w = 0.046$, defined as $R = \sum(|F_o| - |F_c|) / \sum|F_o|$ and $R_w = [\sum w(|F_o| - |F_c|)^2 / \sum w|F_o|^2]^{1/2}$. In the last cycle of refinement the maximum shift per error was 0.235 and the average shift per error was 0.017. A final difference map showed the largest peak to be less than 0.083 times the height of a carbon atom. The final error of an observation of unit weight was 3.733. Final positional and thermal parameters for the nonphenyl atoms of **1** are listed in Table II. Positional and isotropic thermal parameters for the phenyl carbons are given in Table III. Bond distances and angles are listed in Tables IV, and V, respectively. Table A of the supplementary material gives the derived positions of the hydrogen atoms and the structure factors are listed in Table B.

Results

$\text{Co}_2(\mu\text{-PPh}_2)_2(\text{CO})_6$ crystallizes in the monoclinic space group Ia (nonstandard setting of Cc) with two independent molecules in the asymmetric unit. ORTEP drawings of molecules A and B are shown in Figures 1 and 2, respectively. The atom numbering schemes for the two molecules are similar with A and B suffixes added to the atom labels

(8) Howells, E. R.; Phillips, D. C.; Rogers, D. *Acta Crystallogr.* **1950**, *3*, 210.

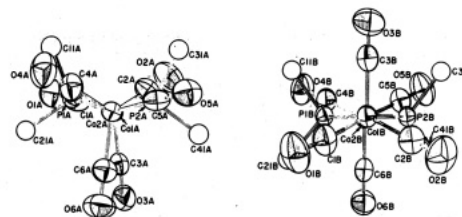
Table I. Crystal and Intensity Data for the X-ray Diffraction Study of $\text{Co}_2(\mu\text{-PPh}_2)_2(\text{CO})_6 \cdot 1$

Crystal Parameters	
crystal system: monoclinic	$V = 5706 (4) \text{ \AA}^3$
space group: Ia (No. 9)	$Z = 8$
$a = 15.880 (4) \text{ \AA}$	$\rho(\text{calcd}) = 1.528 \text{ g/cm}^3$
$b = 8.697 (2) \text{ \AA}$	$\rho(\text{measd}) = 1.53 \text{ g/cm}^3$
$c = 41.423 (9) \text{ \AA}$	abs coeff: 13.64 cm^{-1} , not corrected
$\beta = 94.12 (2)^\circ$	$T = 22 (2)^\circ \text{C}$
Measurement of Intensity Data	
diffractometer	Enraf-Nonius CAD4
radiation	$\text{Mo K}\alpha$ ($\lambda = 0.71073 \text{ \AA}$)
monochromator	graphite crystal
scan type	$\theta - 2\theta$
scan speed	variable ^a
takeoff angle	2.8°
std reflectn	3 std reflectns measd every 2.5 h used for drift correction of 0.931-1.063
data limits	$3.0 \leq 2\theta \leq 46.0$
reflections measd	$+h, \pm k, \pm l$ (where $h + k + l = 2n$)
unique data	4435
nonzero data	3747 ($I > 2\sigma(I)$)
unit weights applied	
R	0.042
R_w	0.046

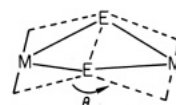
^a See ref 7.

to distinguish atoms of the two independent molecules. Comparisons of bond lengths and bond angles of molecules A and B are given in Tables IV and V.

Each Co in each molecule is ligated by three carbonyls and the two bridging $\mu\text{-PPh}_2$ ligands, but the details of the coordination geometry about Co in molecules A and B differ significantly. The most surprising difference between the molecules is in the geometry of the $\text{Co}_2(\mu\text{-P})_2$

Figure 3. ORTEP drawings of molecules A (left) and B (right) of $\text{Co}_2(\mu\text{-PPh}_2)_2(\text{CO})_6$ viewed down the Co-Co axes.

core. As can be clearly seen by comparison of Figures 1 and 2, the core of molecule B is essentially planar, having a dihedral angle θ between the P1B-Co1B-P2B and P1B-Co2B-P2B planes of 177.4° , but the $\text{Co}_2(\mu\text{-P})_2$ core in molecule A is significantly bent with a corresponding dihedral angle of 155.0° .



The P1-Co-P2 bond angles ($74.5 (2)^\circ$) in the two molecules are identical within experimental error, Table V, but the bending of molecule A does result in small differences in the $\text{Co}\cdots\text{Co}$ separations and the Co-P-Co bond angles. The latter are $102.0 (1)^\circ$ and $102.1 (1)^\circ$ in bent molecule A and $105.6 (1)^\circ$ and $105.4 (4)^\circ$ in planar molecule B. The $\text{Co}\cdots\text{Co}$ separations are $3.487 (2)$ and $3.573 (2) \text{ \AA}$ in molecules A and B, respectively. These large distances imply no direct metal-metal bonding, as expected since each metal has the requisite 18 valence electrons without the necessity of a metal-metal bond.

Another significant difference between molecules A and B is in the distribution of the terminal carbonyl ligands.

Table II. Atomic Positional and Thermal Parameters ($10^3 U(i,j)$) for $\text{Co}_2(\mu\text{-PPh}_2)_2(\text{CO})_6 \cdot 1^a$

atom	x	y	z	$U(1,1)$	$U(2,2)$	$U(3,3)$	$U(1,2)$	$U(1,3)$	$U(2,3)$
Co1A	0.0	0.1260 (2)	0.0	3.01 (7)	4.37 (7)	4.37 (7)	-0.36 (7)	0.03 (6)	0.35 (7)
Co2A	0.1690 (1)	0.3688 (2)	-0.0130 (1)	3.50 (7)	3.54 (7)	4.02 (8)	-0.34 (6)	0.30 (6)	0.16 (6)
Co1B	0.0852 (1)	0.1548 (2)	0.2469 (1)	4.88 (8)	3.23 (7)	3.70 (7)	-0.45 (7)	0.08 (6)	0.15 (6)
Co2B	-0.0554 (1)	-0.1664 (2)	0.2447 (1)	4.76 (8)	3.31 (8)	3.31 (7)	-0.38 (7)	-0.09 (6)	0.14 (6)
P1A	0.0840 (2)	0.1942 (3)	-0.0387 (1)	3.3 (1)	3.7 (1)	3.7 (1)	0.2 (1)	0.0 (1)	-0.2 (1)
P2A	0.1149 (2)	0.2303 (3)	0.0261 (1)	3.6 (1)	3.4 (1)	3.5 (1)	-0.3 (1)	0.2 (1)	0.1 (1)
P1B	0.0114 (2)	-0.0053 (3)	0.2130 (1)	4.4 (2)	3.4 (2)	3.3 (1)	0.1 (1)	0.1 (1)	0.2 (1)
P2B	0.0220 (2)	-0.0126 (3)	0.2787 (1)	4.4 (2)	3.5 (1)	3.2 (1)	-0.1 (1)	0.0 (1)	0.0 (1)
O1A	-0.0896 (6)	-0.0813 (12)	-0.0460 (3)	7.8 (7)	8.4 (7)	10.9 (8)	-3.0 (6)	-2.5 (6)	-2.4 (6)
O2A	-0.0155 (6)	-0.0913 (14)	0.0534 (3)	7.4 (6)	13.2 (9)	11.8 (9)	-2.1 (7)	-1.2 (6)	7.7 (8)
O3A	-0.1068 (6)	0.3946 (13)	0.0096 (2)	7.3 (6)	10.2 (8)	6.4 (6)	4.0 (6)	0.6 (5)	-0.2 (5)
O4A	0.2731 (6)	0.3552 (13)	-0.0676 (2)	7.4 (6)	13.1 (9)	6.0 (5)	-1.5 (6)	2.8 (5)	-0.5 (5)
O5A	0.3022 (5)	0.4621 (10)	0.0348 (2)	4.2 (5)	6.6 (6)	8.7 (6)	-1.3 (4)	-1.3 (4)	-1.9 (5)
O6A	0.0565 (7)	0.6355 (11)	-0.0215 (2)	9.5 (7)	6.2 (6)	10.2 (7)	3.9 (6)	2.0 (6)	2.1 (5)
O1B	0.0858 (9)	0.3835 (12)	0.1961 (3)	17 (1)	6.0 (6)	7.9 (7)	-3.4 (7)	-1.9 (7)	3.6 (6)
O2B	0.0994 (9)	0.3708 (13)	0.3008 (3)	15 (1)	6.7 (7)	9.1 (8)	-2.5 (7)	0.7 (7)	-5.0 (7)
O3B	0.2558 (6)	0.0242 (15)	0.246 (3)	4.8 (5)	13 (1)	9.6 (8)	1.1 (6)	-0.4 (5)	0.3 (7)
O4B	-0.0767 (8)	-0.3797 (12)	0.1905 (2)	13.3 (9)	7.0 (6)	6.6 (6)	-2.2 (7)	0.8 (6)	-2.9 (6)
O5B	-0.0602 (8)	-0.4016 (13)	0.2946 (3)	13.7 (9)	8.5 (8)	8.2 (7)	-3.6 (7)	-2.7 (7)	5.7 (7)
O6B	-0.2219 (6)	-0.0181 (13)	-0.2451 (3)	4.8 (5)	11.1 (8)	7.3 (6)	0.5 (6)	0.4 (5)	0.5 (6)
C1A	-0.0555 (7)	-0.0012 (14)	-0.0279 (3)	4.2 (6)	5.1 (7)	8.9 (4)	-1.0 (6)	0.7 (1)	1.9 (7)
C2A	-0.0074 (8)	-0.0064 (15)	0.0319 (3)	5.0 (7)	6.3 (8)	7.8 (8)	-1.1 (6)	-1.0 (6)	2.5 (7)
C3A	-0.0654 (6)	0.2890 (14)	0.0055 (2)	2.9 (6)	6.1 (7)	4.3 (6)	-1.0 (6)	-0.1 (4)	0.6 (5)
C4A	0.2327 (8)	0.3626 (15)	-0.0458 (3)	5.2 (7)	7.1 (8)	4.9 (7)	-1.1 (6)	0.4 (6)	0.1 (6)
C5A	0.2518 (7)	0.4277 (12)	0.0159 (3)	3.8 (6)	3.5 (5)	6.9 (8)	-0.4 (5)	2.0 (6)	0.2 (5)
C6A	0.0975 (7)	0.5328 (14)	-0.0176 (3)	4.2 (6)	5.2 (7)	6.2 (7)	-0.8 (6)	-0.6 (6)	-0.2 (6)
C1B	0.0829 (9)	0.2987 (16)	0.2164 (3)	9 (1)	5.0 (8)	5.2 (8)	-2.0 (7)	-0.6 (7)	-0.1 (7)
C2B	0.0934 (8)	0.2878 (15)	0.2799 (3)	6.4 (8)	5.6 (8)	6.4 (8)	-1.8 (7)	0.8 (7)	0.1 (7)
C3B	0.1903 (9)	0.0702 (15)	0.2465 (3)	6.1 (8)	5.6 (8)	4.4 (7)	-1.3 (7)	-0.1 (6)	-0.1 (6)
C4B	-0.0680 (8)	-0.2976 (14)	0.2120 (3)	7.4 (8)	4.0 (7)	4.8 (7)	-0.1 (6)	0.3 (6)	-0.0 (6)
C5B	-0.0591 (8)	-0.3084 (17)	0.2754 (3)	6.4 (8)	7.0 (9)	5.2 (7)	-1.1 (7)	-0.8 (6)	0.6 (7)
C6B	-0.1556 (8)	-0.0724 (15)	0.2452 (3)	5.8 (8)	5.9 (8)	4.0 (6)	-1.5 (6)	0.9 (6)	-0.1 (6)

^a The form of the anisotropic thermal parameter is $\exp[-2\pi^2(U(11)h^2a^{*2} + U(22)k^2b^{*2} + U(33)l^2c^{*2} + 2U(12)hka^*b^* + 2U(13)hla^*c^* + 2U(23)klb^*c^*)]$.

Table III. Atomic Positional and Isotropic Thermal Parameters for the Phenyl Carbon Atoms of $\text{Co}_2(\mu\text{-PPh}_2)_2(\text{CO})_6$, 1^a

molecule A					molecule B				
atom	x	y	z	U, Å ²	atom	x	y	z	U, Å ²
C11A	0.1379 (6)	0.028 (1)	-0.0554 (2)	4.4 (2)	C11B	0.0856 (6)	-0.091 (1)	0.1869 (2)	3.5 (2)
C12A	0.0948 (8)	-0.006 (1)	-0.0789 (3)	6.4 (3)	C12B	0.1085 (7)	-0.010 (1)	0.1592 (3)	5.3 (3)
C13A	0.1368 (9)	-0.199 (2)	-0.0886 (3)	7.5 (4)	C13B	0.1711 (7)	-0.073 (1)	0.1414 (3)	5.7 (3)
C14A	0.2116 (9)	-0.235 (1)	-0.0764 (3)	7.9 (4)	C14B	0.2107 (8)	-0.207 (1)	0.1496 (3)	5.9 (3)
C15A	0.2566 (9)	-0.146 (1)	-0.0545 (3)	7.9 (4)	C15B	0.1883 (7)	-0.284 (1)	0.1761 (3)	5.9 (3)
C16A	0.2185 (7)	-0.012 (1)	-0.0437 (3)	5.6 (3)	C16B	0.1256 (7)	-0.227 (1)	0.1994 (2)	4.8 (3)
C21A	0.0338 (5)	0.285 (1)	-0.0750 (2)	3.7 (2)	C21B	-0.0701 (6)	0.080 (1)	0.1849 (2)	4.2 (2)
C22A	0.0767 (6)	0.302 (1)	-0.1023 (2)	4.9 (3)	C22B	-0.1125 (8)	0.213 (1)	0.1939 (3)	5.7 (3)
C23A	0.0436 (8)	0.394 (1)	-0.1279 (2)	6.4 (3)	C23B	-0.1829 (9)	0.265 (2)	0.1742 (3)	7.2 (4)
C24A	-0.0308 (8)	0.464 (1)	-0.1265 (3)	6.4 (3)	C24B	-0.2090 (9)	0.187 (2)	0.1474 (3)	7.2 (4)
C25A	-0.0763 (8)	0.450 (2)	-0.1002 (3)	7.5 (4)	C25B	-0.1671 (8)	0.058 (2)	0.1375 (3)	6.7 (3)
C26A	-0.0451 (7)	0.357 (1)	-0.0739 (3)	5.8 (3)	C26B	-0.0971 (7)	0.002 (1)	0.1565 (3)	5.4 (3)
C31A	0.1908 (6)	0.089 (1)	0.0445 (2)	3.9 (2)	C31B	0.1066 (6)	-0.102 (1)	0.3044 (2)	3.7 (2)
C32A	0.2527 (6)	0.138 (1)	0.0679 (2)	4.6 (2)	C32B	0.1441 (7)	-0.236 (1)	0.2964 (2)	4.9 (3)
C33A	0.3144 (8)	0.036 (1)	0.0799 (2)	6.0 (3)	C33B	0.2153 (7)	-0.288 (1)	0.3144 (3)	5.4 (3)
C34A	0.3142 (8)	-0.108 (2)	0.0687 (3)	7.4 (4)	C34B	0.2482 (7)	-0.209 (1)	0.3406 (3)	5.4 (3)
C35A	0.2551 (9)	-0.159 (1)	0.0469 (3)	7.5 (4)	C35B	0.2122 (7)	-0.076 (1)	0.3497 (3)	5.5 (3)
C36A	0.1919 (7)	-0.059 (1)	0.0335 (3)	5.3 (3)	C36B	0.1424 (6)	-0.019 (1)	0.3317 (2)	4.3 (2)
C41A	0.0889 (6)	0.338 (1)	0.0618 (2)	4.1 (2)	C41B	-0.0490 (6)	0.068 (1)	0.3073 (2)	3.7 (2)
C42A	0.0971 (7)	0.499 (1)	0.0629 (2)	5.5 (3)	C42B	-0.0612 (7)	-0.002 (1)	0.3365 (2)	5.4 (3)
C43A	0.0756 (8)	0.578 (1)	0.0902 (3)	6.7 (3)	C43B	-0.1192 (8)	0.056 (1)	0.3565 (3)	6.0 (3)
C44A	0.0418 (8)	0.505 (1)	0.1155 (3)	6.2 (3)	C44B	-0.1663 (7)	0.181 (1)	0.3471 (3)	6.2 (3)
C45A	0.0306 (8)	0.351 (1)	0.1145 (3)	6.6 (3)	C45B	-0.1572 (8)	0.249 (1)	0.3184 (3)	6.1 (3)
C46A	0.0530 (7)	0.268 (1)	0.0874 (2)	5.4 (3)	C46B	-0.0962 (6)	0.199 (1)	0.2988 (2)	4.8 (2)

^a The form of the isotropic thermal parameter is $\exp(-U(\sin^2 \theta)/\lambda)$.

Table IV. Selected Bond Distances (Å) in $\text{Co}_2(\mu\text{-PPh}_2)_2(\text{CO})_6$, 1

	molecule A	molecule B
Co1...Co2	3.487 (2)	3.573 (2)
Co1-P1	2.237 (3)	2.246 (3)
Co1-P2	2.245 (3)	2.247 (3)
Co2-P1	2.249 (3)	2.238 (3)
Co2-P2	2.238 (3)	2.245 (3)
Co1-C1	1.79 (1)	1.78 (1)
Co1-C2	1.76 (1)	1.79 (1)
Co1-C3	1.78 (1)	1.83 (1)
Co2-C4	1.75 (1)	1.77 (1)
Co2-C5	1.79 (1)	1.78 (1)
Co2-C6	1.82 (1)	1.79 (1)
C1-O1	1.13 (2)	1.12 (2)
C2-O2	1.17 (2)	1.13 (2)
C3-O3	1.15 (2)	1.11 (2)
C4-O4	1.15 (2)	1.14 (2)
C5-O5	1.12 (1)	1.14 (2)
C6-O6	1.11 (2)	1.15 (2)

Table V. Selected Bond Angles (deg) in $\text{Co}_2(\mu\text{-PPh}_2)_2(\text{CO})_6$, 1

	molecule A	molecule B
P1-Co1-P2	74.5 (1)	74.4 (1)
P1-Co2-P2	74.4 (1)	74.6 (1)
Co1-P1-Co2	102.0 (1)	105.6 (1)
Co1-P2-Co2	102.1 (1)	105.4 (1)
P1-Co1-C1	89.6 (4)	90.5 (5)
P1-Co1-C2	141.8 (4)	152.3 (4)
P1-Co1-C3	105.2 (4)	100.4 (4)
P2-Co1-C1	155.3 (4)	152.4 (5)
P2-Co1-C2	89.9 (4)	89.0 (5)
P2-Co1-C3	94.5 (3)	101.0 (4)
P1-Co2-C4	88.4 (4)	89.3 (4)
P1-Co2-C5	154.0 (4)	153.6 (5)
P1-Co2-C6	97.4 (4)	100.4 (4)
P2-Co2-C4	144.9 (4)	153.9 (4)
P2-Co2-C5	88.4 (4)	90.6 (4)
P2-Co2-C6	103.2 (4)	99.6 (4)
C1-Co1-C2	91.4 (6)	94.8 (6)
C1-Co1-C3	108.0 (5)	104.4 (6)
C2-Co1-C3	110.7 (6)	104.5 (6)
C4-Co2-C5	95.2 (5)	95.2 (6)
C4-Co2-C6	109.3 (6)	104.6 (6)
C5-Co2-C6	105.6 (5)	103.5 (6)
Co1-C1-O1	178 (1)	174 (1)
Co1-C2-O2	177 (1)	179 (1)
Co1-C3-O3	178 (1)	177 (1)
Co2-C4-O4	178 (1)	178 (1)
Co2-C5-O5	177 (1)	178 (1)
Co2-C6-O6	176 (1)	176 (1)
Co1-P1-C11	112.4 (4)	107.2 (3)
Co1-P1-C21	117.2 (3)	117.2 (4)
Co2-P1-C11	115.3 (3)	116.6 (3)
Co2-P1-C21	108.1 (3)	106.5 (4)
Co1-P2-C31	114.4 (3)	106.1 (4)
Co1-P2-C41	112.0 (3)	116.8 (3)
Co2-P2-C31	112.6 (3)	117.4 (3)
Co2-P2-C41	115.6 (3)	107.5 (3)

This is best illustrated in Figure 3 that shows the two molecules viewed down the Co-Co axes. It can be clearly seen that the carbonyls in planar molecule B are nearly perfectly staggered with respect to the two ends of the molecule, whereas those in bent molecule A are essentially eclipsed. These views also show that the phosphorus atoms in bent molecule A eclipse two pairs of the carbonyls, whereas in planar molecule B they lie between the CO's.

There is also a slight difference in the orientation of the phenyl groups of the $\mu\text{-PPh}_2$ ligands in the two molecules. In bent molecule A, the planes defined by the phosphorus atoms and the two phenyl carbon atoms attached to each phosphorus are nearly perpendicular (88.0° and 85.3°) to the plane defined by the corresponding phosphorus and the two metal atoms (Table VI). This is of course the expected geometry for tetrahedrally coordinated phosphorus and is also anticipated in view of the eclipsing of these phosphorus atoms with the terminal CO's, Figure 3. However, in planar molecule B, the planes defined by the phosphorus atoms and the phenyl carbons attached to phosphorus are twisted away from perpendicular to the corresponding Co1-P-Co2 planes, with dihedral angles of

82.5° and 82.4° (Table VI). The twisting is also reflected in the magnitude of the Co-P-C bond angles (Table V). The enhanced twisting of the phosphorus phenyl substituents in the planar molecule B compared to bent molecule A is apparently due to increased steric interaction with the terminal carbonyls in the former molecule. An

Table VI. Selected Dihedral Angles between Planes in $\text{Co}_2(\mu\text{-PPh}_2)_2(\text{CO})_6$

plane 1	plane 2	dihedral angle, deg
Co1A-P1A-Co2A	Co1A-P2A-Co2A	148.2
Co1B-P1B-Co2B	Co1B-P2B-Co2B	176.7
P1A-Co1A-P2A	P1A-Co2A-P2A	155.0
P1B-Co1B-P2B	P1B-Co2B-P2B	177.5
Co1A-P1A-Co2A	C11A-P1A-C21A	85.3
Co1A-P2A-Co2A	C31A-P2A-C41A	88.0
Co1B-P1B-Co2B	C11B-P1B-C21B	82.5
Co1B-P2B-Co2B	C31B-P2B-C41B	82.4

analogous effect has been previously noted by Dahl and co-workers² in the structure of the isoelectronic and isostructural dianion $[\text{Fe}_2(\mu\text{-PPh}_2)_2(\text{CO})_6]^{2-}$ that is also planar with a ligand distribution similar to molecule B of 1 and that shows a comparable twisting of the bridging phosphorus substituents.

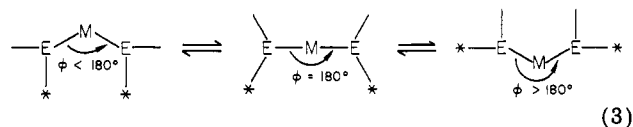
The structures of the dianion $[\text{Fe}_2(\mu\text{-PPh}_2)_2(\text{CO})_6]^{2-}$ and the planar molecule B of $\text{Co}_2(\mu\text{-PPh}_2)_2(\text{CO})_6$ are remarkably similar. The $\text{Fe}_2(\mu\text{-P})_2$ core of the dianion is strictly planar as imposed by a crystallographic inversion center in the middle of the dimer.² The P-Fe-P ($74.5(1)^\circ$) and Fe-P-Fe ($105.5(1)^\circ$) bond angles in the dianion are identical within experimental error to the corresponding angles in molecule B of $\text{Co}_2(\mu\text{-PPh}_2)_2(\text{CO})_6$, although the Fe-Fe separation ($3.630(3) \text{ \AA}$) in the former is 0.06 \AA longer than the Co-Co separation ($3.573(2) \text{ \AA}$) in the latter. Likewise, the Fe-P bond distances ($2.280\text{-}\text{\AA}$ average) are $\sim 0.04 \text{ \AA}$ longer than the Co-P bond distances ($2.244\text{-}\text{\AA}$ average), reflecting the smaller van der Waals radius of Co as compared to Fe.

Discussion

The presence of two molecules of the same composition but of significantly different geometries in the unit cell of $\text{Co}_2(\mu\text{-PPh}_2)_2(\text{CO})_6$ is surprising but quite significant since it implies that there is relatively little energy difference between these two geometrical forms of the molecule. The factors that determine whether a bis(phosphido)- or bis(sulfido)-bridged complex of composition $\text{M}_2(\mu\text{-ER}_x)_2\text{L}_6$ adopts a bent or planar geometry have been extensively discussed, particularly by Dahl and co-workers.^{2,9,10} A highly bent structure with a dihedral angle in the $85\text{-}110^\circ$ range, as in $\text{Fe}_2(\mu\text{-PPh}_2)_2(\text{CO})_6$ ($\theta = 100^\circ$), is strongly favored when metal-metal bonding is necessary to achieve an inert-gas configuration at each metal. However, steric interaction of bulky substituents on the bridging ligands should disfavor severely bent structures. Planar structures with $\theta \approx 180^\circ$ are favored when metal-metal bonding is not required since the latter minimizes steric repulsion between the bridging ligands and planarity is also favored by electronic factors.^{2,10} However, as noted by Dahl and co-workers² in their analysis of the structure of $[\text{Fe}_2(\mu\text{-PPh}_2)_2(\text{CO})_6]^{2-}$ and is also apparent from consideration of the planar form of $\text{Co}_2(\mu\text{-PPh}_2)_2(\text{CO})_6$, planarity increases steric interaction between the terminal and bridging ligands on the two metals. The particular geometry which an $\text{M}_2(\mu\text{-ER}_x)_2\text{L}_6$ complex adopts is thus dependent upon the relative magnitudes of both electronic and steric factors.

The fact that both bent and planar molecules of $\text{Co}_2(\mu\text{-PPh}_2)_2(\text{CO})_6$ cocrystallize together strongly implies that there is relatively little energy difference between the two

forms of the molecule and that the electronic factors which favor planarity are closely balanced by the steric factors which favor slight bending. These crystallographic results suggest that $\text{Co}_2(\mu\text{-PPh}_2)_2(\text{CO})_6$ is quite "floppy" in solution with interconverting molecules present having a range of dihedral angles around the values found in the solid state ($\sim 150^\circ \rightarrow 21^\circ$). This conclusion is in accord with other studies which indicate that bent $\text{M}_2(\mu\text{-ER}_x)_2(\text{CO})_6$ molecules undergo axial-equatorial exchange of the substituents on the bridging atoms by a "butterfly" type mechanism through a planar intermediate (eq 3).¹¹⁻¹³ Particularly



relevant to this study is Dessy et al.'s¹³ analysis of the ^1H NMR spectra of $\text{Fe}_2(\mu\text{-PMe}_2)_2(\text{CO})_6$ and $[\text{Fe}_2(\mu\text{-PMe}_2)_2(\text{CO})_6]^{2-}$ from which it was concluded that both molecules are bent in solution and that they undergo axial-equatorial methyl group exchange by the intramolecular process depicted in eq 3. As expected, the more rigid neutral molecule with a strong metal-metal bond undergoes this process with a much higher coalescence temperature ($+74^\circ\text{C}$) than does the formally nonmetal-metal bonded dianion (-66°C). The very low activation free energy ($\Delta G^\ddagger \approx 10 \text{ kcal/mol}$)¹³ for the "flapping" motion of the dianion implies relatively little energy difference between bent and planar forms of this species and is consistent with the crystallographic results presented here for $\text{Co}_2(\mu\text{-PPh}_2)_2(\text{CO})_6$, which is of course isoelectronic with $[\text{Fe}_2(\mu\text{-PMe}_2)_2(\text{CO})_6]^{2-}$. It would be interesting to record variable-temperature ^1H NMR spectra of $\text{Co}_2(\mu\text{-PMe}_2)_2(\text{CO})_6$ to obtain an accurate activation free energy for axial-equatorial methyl group exchange in this species to provide a direct comparison to $[\text{Fe}_2(\mu\text{-PMe}_2)_2(\text{CO})_6]^{2-}$. In view of the crystallographic results presented herein, we suspect the activation energy for this exchange process will be much lower for the dicobalt complex than for $[\text{Fe}_2(\mu\text{-PMe}_2)_2(\text{CO})_6]^{2-}$. Unfortunately, $\text{Co}_2(\mu\text{-PMe}_2)_2(\text{CO})_6$ has not been previously reported, but it should derive by a reaction analogous to eq 2 using the known trinuclear precursor $\text{Co}_3(\mu\text{-PMe}_2)_3(\text{CO})_6$.¹⁴ That study will perhaps be the subject of a future communication.

Acknowledgment. This research was supported by the National Science Foundation (Grant No. 8201160) and in part by grants from the Standard Oil Company of Ohio, Air Products and Chemicals, Union Carbide, and Celanese corporations. G.L.G. gratefully acknowledges the Camille and Henry Dreyfus Foundation for a Teacher-Scholar Award (1978-1983) and the John Simon Guggenheim Memorial Foundation for a fellowship (1982).

Registry No. 1, 15553-97-6.

Supplementary Material Available: Listings of the derived positions of the hydrogen atoms (Table A), the structure factors (Table B), and bond angles and distances (Table C) for $\text{Co}_2(\mu\text{-PPh}_2)_2(\text{CO})_6$ (30 pages). Ordering information is given on any current masthead page.

(11) (a) Adams, R. D.; Cotton, F. A. *J. Am. Chem. Soc.* **1970**, *92*, 5003. (b) Adams, R. D.; Cotton, F. A.; Cullen, W. R.; Hunter, D. L.; Mihichuk, L. *Inorg. Chem.* **1975**, *14*, 1395.

(12) Flood, T. C.; DiSanti, F. J.; Campbell, K. D. *Inorg. Chem.* **1978**, *17*, 1643.

(13) (a) Dessy, R. E.; Rheingold, A. L.; Howard, G. D. *J. Am. Chem. Soc.* **1972**, *94*, 746.

(14) Keller, E.; Vahrenkamp, H. *J. Organomet. Chem.* **1978**, *155*, C41.

(9) Coleman, J. M.; Dahl, L. F. *J. Am. Chem. Soc.* **1967**, *89*, 542.

(10) Burdett, J. K. *J. Chem. Soc., Dalton Trans.* **1977**, 423.

A facile atmospheric pressure synthesis of the hexacarbonylmetalate ions, $M(CO)_6^-$, of niobium and tantalum

Christopher G. Dewey, John E. Ellis, Kristi L. Fjare, Kathryn M. Pfahl, and Garry F. P. Warnock

Organometallics, **1983**, 2 (3), 388-391 • DOI: 10.1021/om00075a006 • Publication Date (Web): 01 May 2002

Downloaded from <http://pubs.acs.org> on April 24, 2009

More About This Article

The permalink <http://dx.doi.org/10.1021/om00075a006> provides access to:

- Links to articles and content related to this article
- Copyright permission to reproduce figures and/or text from this article



ACS Publications
High quality. High impact.

A Facile Atmospheric Pressure Synthesis of the Hexacarbonylmetalate Ions, $M(\text{CO})_6^-$, of Niobium and Tantalum

Christopher G. Dewey, John E. Ellis,* Kristi L. Fjare, Kathryn M. Pfahl, and Garry F. P. Warnock

Department of Chemistry, University of Minnesota, Minneapolis, Minnesota 55455

Received October 5, 1982

Treatment of the pentachlorides of niobium and tantalum with 6 equiv of alkali-metal naphthalenide or 1-methylnaphthalenide in DME at -60 to -80 °C provides thermally unstable red-brown intermediates that may be $M(\text{C}_{10}\text{H}_8)_2^-$ or $M(1\text{-MeC}_{10}\text{H}_7)_2^-$ ($M = \text{Nb, Ta}$). These species readily react with CO at atmospheric pressure at -60 °C to provide 30–54% yields of the corresponding $M(\text{CO})_6^-$, isolated as Et_4N^+ , $n\text{-Bu}_4\text{N}^+$, and $\text{Na}(\text{diglyme})_2^+$ salts. This two-step reductive carbonylation procedure is the first reported atmospheric pressure synthesis of the hexacarbonylmetalate(1-) ions of niobium and tantalum. The synthesis and properties of unsolvated $\text{NaTa}(\text{CO})_6^-$ are also described.

Introduction

Studies of the metal carbonyl chemistry of niobium and tantalum have been severely hampered by the lack of simple procedures for the synthesis of $\text{Nb}(\text{CO})_6^-$ and $\text{Ta}(\text{CO})_6^-$. Standard methods for the preparation of these ions have involved very high-pressure reductive carbonylations of the pentahalides of these metals, and yields are generally only 10–20%.^{1,2} For this reason it was felt that a low-pressure route to these materials using standard glassware would be extremely valuable in facilitating research on these anions. It is surprising that only 12 papers on the chemistry of these materials have been published since they were first reported in 1961.³

In this paper reasonably efficient (30–54% isolated yields) atmospheric pressure syntheses of $\text{Nb}(\text{CO})_6^-$ and $\text{Ta}(\text{CO})_6^-$ are reported. The procedure employed is the first atmospheric pressure synthesis for these useful compounds. It is anticipated that this procedure will be of general importance in the synthesis of other early transition-metal compounds of the type ML_x^{2-} , where L is a potential π -acceptor ligand.

Experimental Section

General Procedures and Materials. All operations were carried out under an atmosphere of nitrogen, argon, or carbon monoxide. Nitrogen or argon were purified by passage through columns of activated BASF catalyst, anhydrous magnesium perchlorate, and molecular sieves. Solutions were transferred via stainless-steel cannulae and syringes; otherwise reactions were performed by using standard Schlenk apparatus. Tetrahydrofuran, diethyl ether, and 1,2-dimethoxyethane (DME) were distilled at atmospheric pressure from alkali-metal benzophenone ketyls, while diglyme was distilled in vacuo from benzophenone radical anion. 1-Methylnaphthalene was refluxed for 12 h over sodium metal and then distilled in vacuo. Methanol was dried by refluxing over magnesium turnings and then distilled. Acetone, pentane, and water were purged with nitrogen for 1 h before use. Tantalum and niobium pentachlorides were freshly sublimed at

atmospheric pressure. All other reagents and solvents were obtained from commercial sources, freed of oxygen and moisture when necessary, and used without further purification.

Infrared spectra were recorded on a Perkin-Elmer 283 grating spectrometer in 0.1-mm sealed NaCl cells, equipped with Becton-Dickinson steel stopcocks to permit filling outside the drybox. Nujol and Fluorolube mulls of air-sensitive compounds were prepared in a Vacuum Atmospheres Corp. drybox under continuously recirculating nitrogen. NMR samples sealed into 5-mm Pyrex tubes were run on either a Varian T60 or FT80 spectrometer. Melting points are uncorrected and were obtained in sealed capillaries on a Thomas-Hoover unimelt apparatus. Microanalyses were carried out by Galbraith Laboratories or H. Malissa and G. Reuter Analytische Laboratorien.

Tetrabutylammonium Hexacarbonyltantalate(1-), $[\text{n-Bu}_4\text{N}][\text{Ta}(\text{CO})_6^-]$ (1). A cold solution of TaCl_5 in DME was prepared by slowly adding 20.1 g (56.1 mmol) of freshly sublimed TaCl_5 via a bent Schlenk tube or preferably via an Archimedean screw type powder addition funnel (Kontes K-629100; Normag 8055) to 300 mL of vigorously stirred DME held at -50 °C. Rapid addition of the TaCl_5 to the DME will cause strong local heating and decomposition even with efficient stirring at low temperature. A solution of lithium 1-methylnaphthalenide (MeNp) was prepared by slowly adding by syringe 12.0 mL of 30% lithium dispersion (ca. 6.5 equiv of Li) in mineral oil to an ice cold solution of 55 mL of MeNp in 425 mL of DME under an argon atmosphere. An exothermic reaction ensues. If the solution is not precooled, much brown, insoluble, and presumably polymeric material forms as the Li-MeNp reacts with DME at elevated (>40 °C) temperature. The deep green, nearly black Li-MeNp mixture was stirred for 2.5 h while the solution gradually warmed to room temperature. It was then cooled to -60 °C with continued stirring. Subsequently, the cold TaCl_5 solution at -60 °C in DME was added via a 15-gauge cannula to the cold Li-MeNp solution (a large diameter cannula is used to facilitate the addition and minimize heating of the TaCl_5 solution during transfer). Immediately after adding all of the TaCl_5 , the solution had assumed a deep red-brown color. Carbon monoxide was then bubbled vigorously (~ 10 bubbles per second through a Nujol bubbler vent) through the stirred solution with a gas dispersion tube at atmospheric pressure for 1 h at -60 °C. The rate of CO addition was then decreased substantially (~ 1 – 2 bubbles per second) while the solution was stirred for 14 h at -60 °C (30–40% yields of product have been obtained when the CO addition was continued for only 4 h at -60 °C). The very dark solution was then filtered through a plug of diatomaceous earth (Celite) into a flask containing solid $n\text{-Bu}_4\text{NBr}$ (18.2 g, 56.1 mmol) to give a dark solution (often these filtered solutions are bright orange, especially for Li-Np or Na-Np reductive carbonylations). As much DME as possible was removed from the filtrate on a rotary evaporator in vacuo at 30–50 °C (the fairly expensive DME is thereby recycled). The resulting nearly black tar was vigorously triturated and washed with pentane (5×200 mL) under a protective blanket of nitrogen until it solidified to a sticky brown yellow solid. (If the solution is bright orange initially, addition of excess pentane often gives a homogeneous yellow solid during the second tritu-

(1) (a) Werner, R. P. M.; Podall, H. E. *Chem. Ind. (London)* 1961, 144. (b) Werner, R. P. M.; Filbey, A. H.; Manastyrskij, S. S. *Inorg. Chem.* 1964, 3, 298.

(2) Ellis, J. E.; Davison, A. *Inorg. Synth.* 1976, 16, 68.

(3) (a) Davison, A.; Ellis, J. E. *J. Organomet. Chem.* 1970, 23, C1. (b) Davison, A.; Ellis, J. E. *Ibid.* 1971, 31, 239. (c) Davison, A.; Ellis, J. E. *Ibid.* 1972, 36, 113. (d) Wrighton, M. S.; Handeli, D. I.; Morse, D. L. *Inorg. Chem.* 1976, 15, 434. (e) Ellis, J. E.; Faltynek, R. A. *Ibid.* 1976, 15, 3168. (f) Rudie, A. W.; Lichtenberg, D. W.; Katcher, M. L.; Davison, A. *Ibid.* 1978, 17, 2859. (g) Rehder, D.; Bechtold, H.-C.; Kececi, A.; Schmidt, H.; Siewing, M. Z. *Naturforsch., B: Anorg. Chem., Org. Chem.* 1982, 37B, 631. (h) Bechtold, H.-C.; Rehder, D. *J. Organomet. Chem.* 1982, 233, 215. (i) Calderazzo, F.; Pampaloni, G.; Pelizzi, G. *Ibid.* 1982, 233, C41. (j) Calderazzo, F.; Pampaloni, G.; Zanazzi, P. F. *J. Chem. Soc., Chem. Commun.* 1982, 1304.

ration with 100 mL of pentane. When naphthalene is used instead of 1-methylnaphthalene, tars are not obtained). The solid was dried in vacuo and dissolved in a mixture of 100 mL of 95% ethanol and 100 mL of acetone. Then, without filtering (if the solution is clear) 300 mL of water was added that caused much solid to precipitate. The flask was then pumped on to remove as much acetone as possible to maximize the yield of product. The supernatant was carefully removed via cannula, and an additional 200 mL of water was added. The solid was swirled, filtered off on a coarse porosity fritted disk, washed with water (3 × 50 mL), and dried in vacuo. Without further purification the solid gave acceptable analyses. By this procedure 18.0 g (54% yield) of $[\text{Bu}_4\text{N}][\text{Ta}(\text{CO})_6]$ was obtained. Similar scale preparations have provided 45–50% yields of compound 1.

Anal. Calcd for $\text{C}_{22}\text{H}_{36}\text{NO}_6\text{Ta}$: C, 44.67; H, 6.13. Found: C, 45.12; H, 6.44.

Compound 1 may be handled in air for brief periods of time; however, solutions containing 1 are very oxygen sensitive. Nujol mull infrared spectra of 1 show a very broad asymmetric band with a maximum absorption at ca. 1835 cm^{-1} and a shoulder at 1863 cm^{-1} . Dilute solutions of 1 in CH_3CN and other polar solvents all show one rather sharp intense band at ca. 1860 cm^{-1} . Compound 1 melts at 117–118 °C without decomposition.

Tetraethylammonium Hexacarbonyltantalate(1-), $[\text{Et}_4\text{N}][\text{Ta}(\text{CO})_6]$ (2). Essentially the same procedure for the synthesis of 1 was initially followed. A cold solution containing 9.0 g of TaCl_5 in DME (250 mL) was added by cannula to a cold (-70 °C) Li-MeNp solution (obtained from 5.0 mL of 30% Li dispersion in mineral oil and 30 mL of 1-methylnaphthalene) in DME (400 mL). Vigorous stirring was employed while the reactants mixed. Carbon monoxide was subsequently rapidly bubbled through the red-brown solution at -70 °C for 1 h. The bubbling rate was then greatly reduced while the stirred solution slowly warmed to room temperature overnight (Occasionally sufficient decomposition material clogs the gas dispersion tube that CO addition will stop overnight unless the maximum inlet CO pressure is ca. 3–4 in. of mercury. This condition is met by placing a safety bubbler containing a 3–4-in. height of mercury between the CO tank and the reaction vessel. No clogging occurs, however, when the reaction temperature is maintained at -60 °C). Most of the DME was then removed as described previously from the resulting deep yellow-brown solution. The very crude lithium salt was washed with pentane (3 × 100 mL) to remove 1-methylnaphthalene and dried in vacuo to give a pyrophoric brown solid. This was dissolved in acetone (50 mL) and subsequently filtered into a solution of excess Et_4NBr (10.6 g) in ethanol (40 mL). Addition of 300 mL of water caused precipitation of the product, contaminated with small amounts of immiscible liquid, probably containing 1-methylnaphthalene. The somewhat sticky product was filtered, washed with water (2 × 25 mL), and dried in vacuo at 25 °C. Two recrystallizations from $\text{THF-Et}_2\text{O}$ provided 6.38 g (53% yield) of yellow crystalline 2 of satisfactory purity.

Anal. Calcd for $\text{C}_{14}\text{H}_{20}\text{NO}_6\text{Ta}$: C, 35.09; H, 4.21; N, 2.92. Found: C, 35.27; H, 4.37; N, 2.81.

Dry crystalline compound 2 is remarkably stable to air and may be left in air for several hours before it begins to change to a white non-carbonyl containing solid. However, like 1, it forms very oxygen sensitive solutions in a variety of polar organic solvents. Compound 2 darkens above 142 °C without melting. Decomposition is rapid above 190 °C. The Nujol mull spectrum of 2 in the $\nu(\text{CO})$ region exhibits a very broad asymmetric absorption with a maximum at ca. 1835 cm^{-1} . Weak shoulders are also present at ca. 1875 and 1851 cm^{-1} .

Sodium Hexacarbonyltantalate(1-), $\text{Na}[\text{Ta}(\text{CO})_6]$ (3). Unsolvated $\text{Na}[\text{Ta}(\text{CO})_6]$ was easily obtained by treating a methanolic slurry of $[\text{Et}_4\text{N}][\text{Ta}(\text{CO})_6]$ (1.50 g of 2 in 130 mL of MeOH) with a solution of NaBPh_4 (1.15 g) in 25 mL of MeOH. After the solution was stirred at 40 °C for 0.5 h and 25 °C for 1.5 h, a voluminous white precipitate of $[\text{Et}_4\text{N}][\text{BPh}_4]$ formed. This was filtered off to give an orange solution that was evaporated to dryness in vacuo at or below room temperature. The orange residue was dissolved in diethyl ether (80 mL), and filtered to give a very oxygen-sensitive, red-orange solution. Evaporation of the ether solution provided a finely divided solid that was washed with pentane and dried to provide 0.85 g (73% yield) of

pyrophoric yellow orange $\text{Na}[\text{Ta}(\text{CO})_6]$ of satisfactory purity.

Anal. Calcd for $\text{C}_6\text{NaO}_6\text{Ta}$: C, 19.37; H, 0.00; Na, 6.18. Found: C, 19.50, H, 0.08; Na, 6.25.

Nujol mull infrared spectra of 3 show no absorptions in the 4000–3200- cm^{-1} region and exhibit a characteristic two-band pattern in the $\nu(\text{CO})$ region: 1874 (m), 1835 (s, br) cm^{-1} . In polar solvents such as CH_3CN , a single intense band in the $\nu(\text{CO})$ region is present at 1860 cm^{-1} . Compound 3 darkened rapidly above 152 °C and exploded at 155 °C.

Bis(diglyme)sodium Hexacarbonyltantalate, $[\text{Na}(\text{diglyme})_2][\text{Ta}(\text{CO})_6]$ (4). Solid freshly sublimed TaCl_5 (20.0 g, 55.8 mmol) was slowly added with vigorous stirring to a cold (-70 °C) slurry of sodium naphthalenide (336 mmol), prepared by adding the appropriate amount of naphthalene and sodium dispersion in mineral oil (40% by weight in sodium) to 600 mL of DME. Carbon monoxide was bubbled through the rapidly stirred solution for 12 h that was maintained at -70 °C. The resulting brown mixture was warmed to room temperature and filtered through Celite to yield a deep yellow solution. Diglyme was added (16.0 mL, 112 mmol), and the DME was removed in vacuo. Trituration of the residue with pentane produced a bright yellow solid. The product was dissolved in THF and then filtered. After evaporation of most of the THF, pentane was added to precipitate compound 4. This was filtered, washed with pentane, and dried to produce 10.8 g (30% yield) of crystalline bright yellow 4 of satisfactory purity.

Anal. Calcd for $\text{C}_{18}\text{H}_{28}\text{NaO}_{12}\text{Ta}$: C, 33.76; H, 4.41. Found: C, 33.75; H, 4.24.

Compound 4 is an air-sensitive solid that dissolves in polar solvents to provide very air sensitive solutions. This compound has been previously prepared by a high-pressure reductive carbonylation procedure.^{1a} The Nujol mull infrared spectrum of 4 in the $\nu(\text{CO})$ region consists of a sharp weak spike at 2015 cm^{-1} and a broad intense band at 1835 cm^{-1} . Compound 4 melts with decomposition at 170–172 °C (lit.^{1a} 173–176 °C).

Tetraphenylphosphonium Hexacarbonyltantalate(1-), $[\text{PPh}_4][\text{Ta}(\text{CO})_6]$ (5). By the same procedure shown for the synthesis of compound 4, TaCl_5 (20.0 g, 55.8 mmol) was reduced by sodium naphthalenide (335 mmol) in 600 mL of DME at -80 °C. Subsequently CO was bubbled through the mixture at atmospheric pressure for 20 h at -80 °C. The solution was then filtered through Celite into a flask containing 20.9 g (55.8 mmol) of $[\text{PPh}_4]\text{Cl}$. After solvent removal, the residue was washed with pentane, dissolved in THF (200 mL), and filtered. All but ca. 15 mL of THF was removed from the bright orange solution. Addition of excess diethyl ether (200 mL) caused the product to precipitate almost completely. The product was removed by filtration, washed with ether, and dried in vacuo to give 12.6 g (33% yield) of compound 5 of satisfactory purity.

Anal. Calcd for $\text{C}_{30}\text{H}_{20}\text{O}_6\text{PTa}$: C, 52.34; H, 2.93. Found: C, 52.12; H, 3.01.

Compound 5 decomposes without melting above 170 °C and may be handled for several hours in air as a crystalline solid. The Nujol mull infrared spectrum of 5 closely resembles that of $[\text{Ph}_4\text{As}][\text{Ta}(\text{CO})_6]^{2-}$ and has in the $\nu(\text{CO})$ region a broad intense bifurcated absorption with maxima at 1859 and 1837 cm^{-1} . In polar solvents, a single intense band in the $\nu(\text{CO})$ region is observed at ca. 1860 cm^{-1} .

Tetraethylammonium Hexacarbonylniobate(1-), $[\text{Et}_4\text{N}][\text{Nb}(\text{CO})_6]$ (6). By the same procedure shown for the synthesis of compound 2, a solution of freshly sublimed NbCl_5 (9.8 g, 36 mmol) in 150 mL of DME at -60 °C was added to a cold slurry of lithium 1-methylnaphthalenide (216 mmol) in 350 mL of DME at -80 °C. Carbon monoxide was bubbled through the vigorously stirred solution for 12 h at -80 °C. Filtration of the resulting deep brown slurry through Celite into a flask containing solid Et_4NBr (14.0 g, 66.6 mmol) yielded a bright yellow solution. After the solution was stirred for 2 h at room temperature to ensure a complete metathesis, the DME was removed under vacuum. Trituration of the residue with pentane followed by recrystallization from acetone-water provided 6.7 g (47% yield) of bright yellow analytically pure 6.

Anal. Calcd for $\text{C}_{14}\text{H}_{20}\text{NNbO}_6$: C, 43.00; H, 5.15. Found: C, 43.15; H, 5.42.

Compound 6 darkens above 140° without melting. Mull spectra of 6 closely resemble those of 2 and consist in the $\nu(\text{CO})$ region

of a very broad band with an absorption maximum at about 1837 cm^{-1} .

Tetrabutylammonium Hexacarbonylniobate(1-), $[\text{n-Bu}_4\text{N}][\text{Nb}(\text{CO})_6]$ (7). Exactly the same procedure for the synthesis of compound 1 was used *except* commercial quality "resublimed" NbCl_5 (21.05 g, 77.9 mmol) was used. It was noted that the DME solution of this NbCl_5 was a turbid brown rather than the characteristic clear yellow color obtained when freshly sublimed NbCl_5 is used. After metathesis with *n*- Bu_4NBr and purification of the product as described for 1, 9.90 g (25% yield) of homogeneous yellow solid 7 of satisfactory purity was obtained.

Anal. Calcd for $\text{C}_{22}\text{H}_{36}\text{NNbO}_6$: C, 52.49; H, 7.20; N, 2.78. Found: C, 52.76; H, 7.05; N, 2.55.

Compound 7 has a Fluorolube mull spectrum showing a very broad band with an absorption maximum at about 1830 cm^{-1} . Solution spectra of 7 in polar solvents are essentially superimposable with those of 1 and show a single intense band at 1860 cm^{-1} . Compound 7 melts at 116–117 °C.

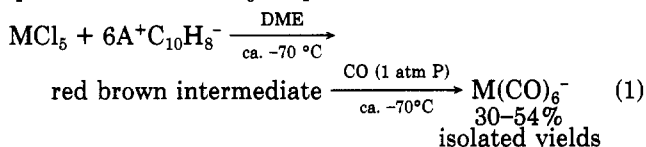
Bis(diglyme)sodium Hexacarbonylniobate, $[\text{Na}(\text{diglyme})_2][\text{Nb}(\text{CO})_6]$ (8). By the same procedure used to prepare compound 4, freshly sublimed NbCl_5 (20.0 g, 74 mmol) was reduced with sodium naphthalene (444 mmol) in DME followed by addition of CO at -80 °C. Following addition of diglyme (21.2 mL, 148 mmol), the product was purified as before to yield 12.3 g (30% yield) of 8 of satisfactory purity.

Anal. Calcd for $\text{C}_{18}\text{H}_{28}\text{NaNbO}_{12}$: C, 39.15; H, 5.11. Found: C, 38.88; H, 4.95.

Compound 8 has essentially the same properties as 4 and was prepared previously by a high-pressure procedures in 26% yield.^{1b} It decomposes from 146 to 149 °C (lit.^{1b} 145 °C dec) to form a black tar. The Nujol mull infrared spectrum of 8 is practically superimposable on that of 4, and in the $\nu(\text{CO})$ region contains a sharp weak spike at 2015 cm^{-1} and a broad intense band at ca. 1834 cm^{-1} .

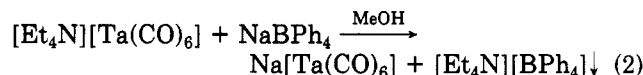
Results and Discussion

Addition of a solution of MCl_5 ($\text{M} = \text{Nb}, \text{Ta}$) in 1,2-dimethoxyethane (DME) at -50 to -60 °C to a cold solution or slurry containing 6–6.5 equiv of lithium or sodium naphthalene in DME at -60 to -80 °C quickly gives a deep red-brown solution under a nitrogen or argon atmosphere. Carbon monoxide is rapidly absorbed by this solution at low temperatures and pressures to provide useful quantities of $\text{M}(\text{CO})_6^-$ (eq 1). While the mixture was



stirred for 4–15 h at -60 °C and carbon monoxide was slowly added via a gas dispersion tube at atmospheric pressure, the color changed to a deep yellow-brown. After filtration, removal of most of the DME and addition of diglyme or a suitable complex cation, the anions were isolated in 30–54% yields as crystalline salts. These include $[\text{Et}_4\text{N}][\text{M}(\text{CO})_6]$, $[\text{n-Bu}_4\text{N}][\text{M}(\text{CO})_6]$, $[\text{PPh}_4][\text{Ta}(\text{CO})_6]$, and $[\text{Na}(\text{diglyme})_2][\text{M}(\text{CO})_6]$. The tetraethylammonium salts have been previously mentioned in the literature, but no infrared or analytical data were presented in support of their formulations.^{3b,5} These materials are probably the most easily isolated and handled of the salts containing $\text{Nb}(\text{CO})_6^-$ and $\text{Ta}(\text{CO})_6^-$. As in the case of $[\text{Et}_4\text{N}][\text{V}(\text{CO})_6]$,⁴ these crystalline Et_4N^+ salts may be exposed to air and fluorescent lamp radiation for several hours without deleterious effect. Tetrabutylammonium hexacarbonyltantalate has been described previously, but no details on its synthesis have been presented.^{3d} Tetra-

phenylphosphonium hexacarbonyltantalate(1-) and $[\text{n-Bu}_4\text{N}][\text{Nb}(\text{CO})_6]$ are new species, while $[\text{Na}(\text{diglyme})_2][\text{M}(\text{CO})_6]$ have been previously characterized.^{1a,b} Unsolvated $\text{Na}[\text{Ta}(\text{CO})_6]$, a pyrophoric solid, has been obtained in 73% yield from the cation-exchange reaction (2). Only



unsolvated $\text{Na}[\text{V}(\text{CO})_6]$ has been previously described.⁵ It should be possible to prepare $\text{Na}[\text{Nb}(\text{CO})_6]$ by the same cation-exchange method described above from $[\text{Et}_4\text{N}][\text{Nb}(\text{CO})_6]$, since unsolvated $\text{Na}[\text{V}(\text{CO})_6]$ has also been obtained in this manner.⁶ The infrared spectra in the $\nu(\text{CO})$ region and other properties of the various $\text{M}(\text{CO})_6^-$ salts are described in the Experimental Section.

Our best results, thus far, have been obtained by using lithium 1-methylnaphthalene, which is more soluble in DME at low temperatures than lithium or sodium naphthalene. By this procedure, 45–54% yields of $\text{Ta}(\text{CO})_6^-$ and $\text{Nb}(\text{CO})_6^-$ are consistently obtained, provided high quality, freshly sublimed MCl_5 is used and the temperature of the reaction mixture is kept at or below -60 °C. However, 30–35% yields of $\text{M}(\text{CO})_6^-$ ($\text{M} = \text{Nb}, \text{Ta}$) have been consistently obtained by using sodium naphthalene as the reducing agent. Although the best yields are obtained by the slow addition of a solution of cold MCl_5 in DME to a cold solution or slurry containing alkali-metal naphthalene, 25–30% yields of $\text{M}(\text{CO})_6^-$ are also obtained by the slow addition of solid MCl_5 to the cold naphthalene–DME mixtures. Whether this reduction is performed under an inert atmosphere followed by CO addition ("two-step" process) or under an atmosphere of CO ("one-step" process) appears to be unimportant. Also when carbon monoxide is added to the reduced species at 50–130 psi at low temperature in Fischer-Porter pressure bottles, there is little improvement in yield. However, when the same one- or two-step reductive carbonylations are carried out at room temperature at 14.7–130 psi pressures of CO, significantly lower yields of $\text{M}(\text{CO})_6^-$ are obtained, indicating that the red-brown intermediate is quite thermally unstable. Although the reductions can be done in diglyme with only slight decreases in the yield of $\text{M}(\text{CO})_6^-$, THF *cannot* be used successfully in the preparation of $\text{Nb}(\text{CO})_6^-$ and $\text{Ta}(\text{CO})_6^-$, since the pentachlorides of these metals react vigorously with this solvent even at low temperatures. No attempts to perform this one- or two-step reductive carbonylation procedure in other solvents have been made presently.

Further studies are underway to optimize the yield of $\text{M}(\text{CO})_6^-$ by this low-temperature method and to characterize and examine the reactions of the red-brown niobium and tantalum intermediates with other potential π -acceptor ligands. Presently, we speculate that these materials are bis(naphthalene)metalate anions of niobium and tantalum. Wreford and co-workers have established that the reduction of $(\text{dmpe})_2\text{TaCl}_4$ by $\text{Na-C}_{10}\text{H}_8$ in the absence of CO provides the unusual naphthalene complex $\text{TaCl}(\eta^4\text{-C}_{10}\text{H}_8)(\text{dmpe})_2$.⁷ In this reaction the naphthalene may play a crucial role by associating with the tantalum at some stage during the reduction of Ta(IV) to Ta(I), thereby preventing the formation of unreactive metal clusters. It

(4) Ellis, J. E.; Faltynek, R. A.; Rochfort, G. L.; Stevens, R. E.; Zank, G. A. *Inorg. Chem.* 1980, 19, 1082.

(5) (a) Hieber, W.; Peterhaus, J.; Winter, E. *Chem. Ber.* 1961, 94, 2572. (b) Calderazzo, F.; Ercoli, R. *Chim. Ind. (Milan)* 1962, 44, 990. (c) Calderazzo, F.; Pampaloni, G.; Vitali, D. *Gazz. Chim. Ital.* 1981, 111, 455.

(6) Fjare, K. L. M.S. Thesis, University of Minnesota, Minneapolis, MN, 1981.

(7) Albright, J. O.; Datta, S.; Dezube, B.; Kouba, J. K.; Marynick, D. S.; Wreford, S. S.; Foxman, B. *J. Am. Chem. Soc.* 1979, 101, 611.

seems likely that the naphthalene or 1-methylnaphthalene in our process also functions as more than a mere soluble electron carrier during the reduction process. Similar reductions of MCl_5 carried out in the absence of naphthalene in the presence of CO at atmospheric pressure give zero or exceedingly poor yields of $M(CO)_6$. It is noteworthy that neutral bis(naphthalene)vanadium has been reportedly obtained by the reduction of VCl_3 by Li-Np.⁸ Also, neutral bis(arene) complexes of Nb and Ta are known,⁹ but the only bis(arene)metalate ion presently established is apparently $V(C_6H_6)_2^-$.¹⁰ Although the reactions of bis(arene)niobium and tantalum complexes with carbon monoxide have not yet been reported, Calderazzo and Cini showed in 1965 that bis(mesitylene)vanadium(0) reacted with CO (at 35 °C (100 atm.)) to give the disproportionation product [(mesitylene)V(CO)₄][V(CO)₆].¹¹ Earlier it had been reported, apparently incorrectly, that bis(toluene)vanadium(0) gave $V(CO)_6$ under similar conditions.¹² Interestingly, tris(cyclooctatetraene)niobate(1-) provided $Nb(CO)_6^-$ in an unspecified yield when heated under high pressures of CO at 110 °C in THF.¹³ Our suggestion that the intermediates in our two-step reductive carbonylation procedure are $M(C_{10}H_8)_2^-$ is also consistent with the observation that both naphthalene groups in $Cr(C_{10}H_8)_2$ and $Mo(C_{10}H_8)_2$ are readily displaced by CO to quantitatively produce the corresponding $M(CO)_6$ at 25 °C and 1 atm of pressure.¹⁴

Alkali-metal naphthalenides have been used previously in "one-step" reductive carbonylations of early transition

metal complexes. One of the earliest reports on such a system involved the reduction of $CrCl_3$ by $Na-C_{10}H_8$ under high pressures of CO at 25 °C to ultimately give a 10% yield of $Cr(CO)_6$.¹⁵ However, undoubtedly the most important previous contribution in this area, especially in terms of its influence on the present study, was Datta and Wreford's observation that $(dmpe)_2TaCl_4$ could be reductively carbonylated at atmospheric pressures and 25 °C by $Na-C_{10}H_8$ to provide good yields of $(dmpe)_2Ta(CO)_2Cl$.¹⁶ This study provided the first indication that group 5 metal halides could undergo efficient reductive carbonylation at atmospheric pressure. Efforts are presently underway to determine whether our low-temperature reductive carbonylation procedure can be extended to group 4 metal complexes.¹⁷

Acknowledgment. We thank the donors of the Petroleum Research Fund, administered by the American Chemical Society, and the National Science Foundation (Grant CHE 82-10496) for continuing support of this work.

Registry No. 1, 57288-90-1; 2, 67292-38-0; 3, 15602-40-1; 4, 12189-44-5; 5, 84280-29-5; 6, 82581-56-4; 7, 84280-30-8; 8, 12189-43-4.

(15) Shapiro, H.; Podall, H. E. *J. Inorg. Nucl. Chem.* 1962, 24, 925.
(16) Datta, S.; Wreford, S. S. *Inorg. Chem.* 1977, 16, 1134.

(17) **Note Added in Proof:** Further experiments have shown that the "red brown intermediate" of tantalum is not as thermally unstable as originally suggested. In one preparation, a DME solution of the intermediate was warmed to 25 °C and maintained at this temperature for 12 h under a nitrogen atmosphere. Carbonylation of the resulting mixture at 1 atm P and room temperature provided approximately 30% yields of $[Et_4N][Ta(CO)_6]$. When the same procedure was attempted with niobium, no formation of $Nb(CO)_6^-$ occurred. Also, a sodium benzophenone reduction of $TaCl_5$ in DME at -70 °C followed by an atmospheric pressure carbonylation at -70 °C provided a 20% yield of $[Et_4N][Ta(CO)_6]$.

Very recently, we learned that another group has also developed an atmospheric pressure reductive carbonylation synthesis of $Nb(CO)_6^-$. Calderazzo, F.; Englert, U.; Pamploni, G.; Pelizzi, G.; Zamboni, R. *Inorg. Chem.*, in press.

- (8) Henrici-Olive, G.; Olive, S. *J. Am. Chem. Soc.* 1970, 92, 4831.
(9) Cloke, F. G. N.; Green, M. L. H. *J. Chem. Soc., Dalton Trans.* 1981, 1938.
(10) Elschenbroich, G.; Gerson, F. *J. Am. Chem. Soc.* 1975, 97, 3556.
(11) Calderazzo, F.; Cini, R. *J. Chem. Soc.* 1965, 818.
(12) Pruet, R. Y.; Whyman, J. E. *Chem. Ind. (London)* 1960, 79, 119.
(13) Guggenberger, L. J.; Schrock, R. R. *J. Am. Chem. Soc.* 1975, 97, 6693.
(14) Kundig, E. P.; Timms, P. L. *J. Chem. Soc., Chem. Commun.* 1977, 912.

An Improved Synthesis of Key Intermediates in Metallole 4B Chemistry

Georges Manuel,* Guy Bertrand, and Fatiha El Anba

Laboratoire des Organométalliques, ERA 829, Université Paul-Sabatier, 31062 Toulouse Cédex, France

Received September 23, 1982

The base-induced rearrangement with Et_2NLi of 6-oxa-3-metallabicyclo[3.1.0]hexanes is a convenient method for the synthesis of cyclic allylic alcohols of silicon and germanium—key intermediates of siloles and germeles.

The remarkably rich chemistry of π -cyclopentadienyl transition-metal complexes has prompted chemists to investigate heterocyclopentadienyl ligands.¹ For compara-

tive studies with carbon analogues, metalloles of group 4B are of special interest.² However, although C-aryl-substituted 4B metalloles are well-known,³ non-C-substituted

(1) See, for example: Green, M. L. H. "Organometallic Compounds 2", 3rd ed.; Methuen: London, 1968, p 302. Hoberg, H.; Richter, W. *J. Organomet. Chem.* 1980, 195, 347. Mathey, F.; Mitschler, A.; Weiss, R. *J. Am. Chem. Soc.* 1977, 99, 3537. Santini, C.; Fischer, J.; Mathey, F.; Mitschler, A. *Inorg. Chem.* 1981, 20, 2848. de Lauzon, G.; Deschamps, B.; Mathey, F. *Nouv. J. Chim.* 1980, 4, 683. Abel, E. W.; Nowel, I. W.; Modinos, A. G. J.; Towers, C. *J. Chem. Soc., Chem. Commun.* 1973, 258. Ashe, A. J., III; Dicphouse, T. R. *J. Organomet. Chem.* 1980, 202, C95.

(2) See, for example: Jutzi, P.; Karl, A. *J. Organomet. Chem.* 1977, 128, 57. Abel, E. W.; Blackmore, T.; Whitley, R. *J. Chem. Soc., Dalton Trans.* 1976, 2484. Muir, K. W.; Walker, R.; Abel, F. W.; Blackmore, T.; Whitley, R. *J. Chem. Soc., Chem. Commun.* 1975, 698. Sakurai, H.; Hayashi, J. *J. Organomet. Chem.* 1973, 63, C10. Jutzi, P.; Karl, A.; Burschka, C. *Ibid.* 1981, 215, 27. Herberich, G. E.; Müller, B.; Hessner, B.; Oschmann, W. *Ibid.* 1980, 195, 253.

seems likely that the naphthalene or 1-methylnaphthalene in our process also functions as more than a mere soluble electron carrier during the reduction process. Similar reductions of MCl_5 carried out in the absence of naphthalene in the presence of CO at atmospheric pressure give zero or exceedingly poor yields of $M(CO)_6^-$. It is noteworthy that neutral bis(naphthalene)vanadium has been reportedly obtained by the reduction of VCl_3 by Li-Np.⁸ Also, neutral bis(arene) complexes of Nb and Ta are known,⁹ but the only bis(arene)metalate ion presently established is apparently $V(C_6H_6)_2^-$.¹⁰ Although the reactions of bis(arene)niobium and tantalum complexes with carbon monoxide have not yet been reported, Calderazzo and Cini showed in 1965 that bis(mesitylene)vanadium(0) reacted with CO (at 35 °C (100 atm.)) to give the disproportionation product $[(mesitylene)V(CO)_4][V(CO)_6]$.¹¹ Earlier it had been reported, apparently incorrectly, that bis(toluene)vanadium(0) gave $V(CO)_6$ under similar conditions.¹² Interestingly, tris(cyclooctatetraene)niobate(1-) provided $Nb(CO)_6^-$ in an unspecified yield when heated under high pressures of CO at 110 °C in THF.¹³ Our suggestion that the intermediates in our two-step reductive carbonylation procedure are $M(C_{10}H_8)_2^-$ is also consistent with the observation that both naphthalene groups in $Cr(C_{10}H_8)_2$ and $Mo(C_{10}H_8)_2$ are readily displaced by CO to quantitatively produce the corresponding $M(CO)_6$ at 25 °C and 1 atm of pressure.¹⁴

Alkali-metal naphthalenides have been used previously in "one-step" reductive carbonylations of early transition

metal complexes. One of the earliest reports on such a system involved the reduction of $CrCl_3$ by $Na-C_{10}H_8$ under high pressures of CO at 25 °C to ultimately give a 10% yield of $Cr(CO)_6$.¹⁵ However, undoubtedly the most important previous contribution in this area, especially in terms of its influence on the present study, was Datta and Wreford's observation that $(dmpe)_2TaCl_4$ could be reductively carbonylated at atmospheric pressures and 25 °C by $Na-C_{10}H_8$ to provide good yields of $(dmpe)_2Ta(CO)_2Cl$.¹⁶ This study provided the first indication that group 5 metal halides could undergo efficient reductive carbonylation at atmospheric pressure. Efforts are presently underway to determine whether our low-temperature reductive carbonylation procedure can be extended to group 4 metal complexes.¹⁷

Acknowledgment. We thank the donors of the Petroleum Research Fund, administered by the American Chemical Society, and the National Science Foundation (Grant CHE 82-10496) for continuing support of this work.

Registry No. 1, 57288-90-1; 2, 67292-38-0; 3, 15602-40-1; 4, 12189-44-5; 5, 84280-29-5; 6, 82581-56-4; 7, 84280-30-8; 8, 12189-43-4.

(15) Shapiro, H.; Podall, H. E. *J. Inorg. Nucl. Chem.* 1962, 24, 925.

(16) Datta, S.; Wreford, S. S. *Inorg. Chem.* 1977, 16, 1134.

(17) **Note Added in Proof:** Further experiments have shown that the "red brown intermediate" of tantalum is not as thermally unstable as originally suggested. In one preparation, a DME solution of the intermediate was warmed to 25 °C and maintained at this temperature for 12 h under a nitrogen atmosphere. Carbonylation of the resulting mixture at 1 atm P and room temperature provided approximately 30% yields of $[Et_4N][Ta(CO)_6]$. When the same procedure was attempted with niobium, no formation of $Nb(CO)_6^-$ occurred. Also, a sodium benzophenone reduction of $TaCl_5$ in DME at -70 °C followed by an atmospheric pressure carbonylation at -70 °C provided a 20% yield of $[Et_4N][Ta(CO)_6]$.

Very recently, we learned that another group has also developed an atmospheric pressure reductive carbonylation synthesis of $Nb(CO)_6^-$. Calderazzo, F.; Englert, U.; Pamploni, G.; Pelizzi, G.; Zamboni, R. *Inorg. Chem.*, in press.

- (8) Henrici-Olive, G.; Olive, S. *J. Am. Chem. Soc.* 1970, 92, 4831.
 (9) Cloke, F. G. N.; Green, M. L. H. *J. Chem. Soc., Dalton Trans.* 1981, 1938.
 (10) Elschenbroich, G.; Gerson, F. *J. Am. Chem. Soc.* 1975, 97, 3556.
 (11) Calderazzo, F.; Cini, R. *J. Chem. Soc.* 1965, 818.
 (12) Pruet, R. Y.; Whyman, J. E. *Chem. Ind. (London)* 1960, 79, 119.
 (13) Guggenberger, L. J.; Schrock, R. R. *J. Am. Chem. Soc.* 1975, 97, 6693.
 (14) Kundig, E. P.; Timms, P. L. *J. Chem. Soc., Chem. Commun.* 1977, 912.

An Improved Synthesis of Key Intermediates in Metallole 4B Chemistry

Georges Manuel,* Guy Bertrand, and Fatih El Anba

Laboratoire des Organométalliques, ERA 829, Université Paul-Sabatier, 31062 Toulouse Cédex, France

Received September 23, 1982

The base-induced rearrangement with Et_2NLi of 6-oxa-3-metallabicyclo[3.1.0]hexanes is a convenient method for the synthesis of cyclic allylic alcohols of silicon and germanium—key intermediates of siloles and germales.

The remarkably rich chemistry of π -cyclopentadienyl transition-metal complexes has prompted chemists to investigate heterocyclopentadienyl ligands.¹ For compara-

tive studies with carbon isologues, metalloles of group 4B are of special interest.² However, although C-aryl-substituted 4B metalloles are well-known,³ non-C-substituted

(1) See, for example: Green, M. L. H. "Organometallic Compounds 2", 3rd ed.; Methuen: London, 1968, p 302. Hoberg, H.; Richter, W. *J. Organomet. Chem.* 1980, 195, 347. Mathey, F.; Mitschler, A.; Weiss, R. *J. Am. Chem. Soc.* 1977, 99, 3537. Santini, C.; Fischer, J.; Mathey, F.; Mitschler, A. *Inorg. Chem.* 1981, 20, 2848. de Lauzon, G.; Deschamps, B.; Mathey, F. *Nouv. J. Chim.* 1980, 4, 683. Abel, E. W.; Nowel, I. W.; Modinos, A. G. J.; Towers, C. *J. Chem. Soc., Chem. Commun.* 1973, 258. Ashe, A. J., III; Dicphouse, T. R. *J. Organomet. Chem.* 1980, 202, C95.

(2) See, for example: Jutzi, P.; Karl, A. *J. Organomet. Chem.* 1977, 128, 57. Abel, E. W.; Blackmore, T.; Whitley, R. *J. Chem. Soc., Dalton Trans.* 1976, 2484. Muir, K. W.; Walker, R.; Abel, F. W.; Blackmore, T.; Whitley, R. *J. Chem. Soc., Chem. Commun.* 1975, 698. Sakurai, H.; Hayashi, J. *J. Organomet. Chem.* 1973, 63, C10. Jutzi, P.; Karl, A.; Burschka, C. *Ibid.* 1981, 215, 27. Herberich, G. E.; Müller, B.; Hessner, B.; Oschmann, W. *Ibid.* 1980, 195, 253.

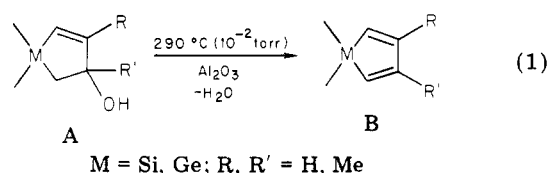
Table I. Comparative Results Observed with Methods I and II for the Synthesis of Compounds 5 and 6

R	M	yield, %	
		method I ^a	method II ^b
Me	Si (5a)	70	86
Me	Ge (5b)	70	70
Ph	Si (6a)		78
Ph	Ge (6b)		72

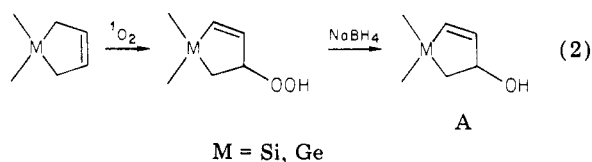
^a Photooxygenation-reduction. ^b Base-promoted rearrangement. ^c Yield in % from the corresponding metallacyclopentene.

siloles⁴⁻⁶ and germoles⁷ have been synthesized only recently.

Dehydration on alumina of 1-metallacyclopent-4-en-3-ols (A) appears to be the most convenient method for obtaining non-C-substituted^{5,7} or C-methylated⁸ siloles or germoles (B) (eq 1).

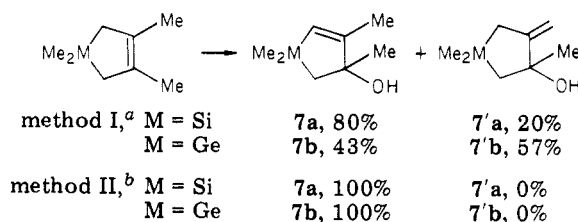


The metallacyclopentanol substrates A may be obtained by dye-sensitized photooxygenation-reduction of the corresponding metallacyclopent-3-ene^{8,9} (eq 2), but this synthesis involves the use of special equipment for generating singlet oxygen⁹ and is not always regioselective.⁸



We report here an improved synthesis of key intermediates (A) involving base-induced rearrangement of the easily available 6-oxa-3-metallabicyclo[3.1.0]hexanes 1-4.¹⁰ We will emphasize the general character and stereospecificity of this method compared with those previously reported,^{8,9} as well as the role of the heteroatom (Si, Ge) in

Scheme I. Comparative Results Observed for the Synthesis of Isomeric Compounds 7 and 7' with Methods I and II



^a Photooxygenation-reduction. ^b Base-promoted rearrangement.

Table II. Comparative Results Observed with Methods I and II for the Synthesis of Compounds 8 and 9

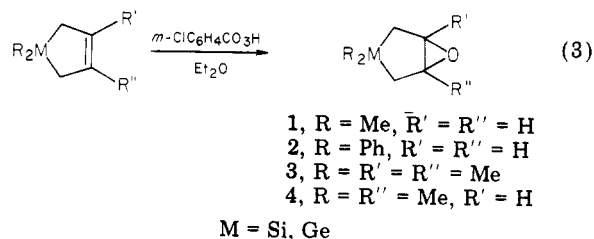
	8a/9a (Si)	8b/9b (Ge)
method I ^a	58/42	68/32
method II ^b	77/23	83/17

^a Photooxygenation-reduction. ^b Base-promoted rearrangement.

the rearrangement in comparison to analogous reactions in the carbon series.

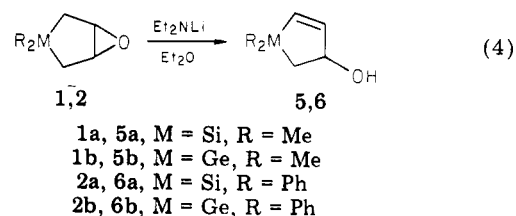
Results and Discussion

The starting epoxides 1-4 were obtained in almost quantitative yield from the corresponding metallacyclopentenes by oxidation with *m*-chloroperbenzoic acid¹⁰ (eq 3).



- 1, R = Me, R' = R'' = H
- 2, R = Ph, R' = R'' = H
- 3, R = R' = R'' = Me
- 4, R = R'' = Me, R' = H

The base-promoted rearrangements were carried out with lithium diethylamide, a poor nucleophilic but a strong basic reagent. Under these conditions, the desired allylic alcohols 5 and 6 were obtained in good yield from derivatives 1 and 2 (R' = R'' = H; eq 4; Table I).



The results observed with C-dimethylated derivatives 3 are more interesting since the base-induced rearrangement leads to only one product 7 (Si, 83%, and Ge, 76% yield). Indeed, formation of the isomeric exocyclic ethylenic derivative 7' was not observed at all (Scheme I). The stereospecificity of the base-promoted rearrangement should be of great interest to elucidate, for example, the mechanism of the dehydration in the case of the C-methylated silole and germole.⁸ Indeed, allylic alcohol 7 was never obtained in the pure isomeric form from the previously reported synthetic method.⁸

In the case of nonsymmetrical epoxides 4, two isomeric allylic alcohols 8 and 9 (Si, 85%, and Ge, 70% yield) were obtained (eq 5). In this case, although the base-induced

(3) See, for example: Braye, E. H.; Hübel, W.; Caplier, I. *J. Am. Chem. Soc.* **1964**, *86*, 4406. Gilman, H.; Cottis, S. G.; Atwell, W. H. *Ibid.* **1964**, *86*, 1596. Curtis, M. D. *Ibid.* **1969**, *91*, 6011. Atwell, W. H.; Weyenberg, D. R.; Gilman, H. *J. Org. Chem.* **1967**, *32*, 885. Brunet, J. C.; Demey, N. *Ann. Chim. (Paris)* **1973**, *8*, 123. Barton, T. J.; Gottsman, E. E. *Synth. Inorg. Met. Org. Chem.* **1973**, *3*, 210. Gilman, H.; Atwell, W. H. *J. Organomet. Chem.* **1964**, *2*, 291. Okinoshima, H.; Yamamoto, K.; Kumada, M. *J. Am. Chem. Soc.* **1972**, *94*, 9263.

(4) Barton, T. J.; Burns, G. T. *J. Organomet. Chem.* **1979**, *179*, C17.

(5) Laporterie, A.; Mazerolles, P.; Dubac, J.; Iloughmane, H. *J. Organomet. Chem.* **1981**, *206*, C25. Laporterie, A.; Dubac, J.; Mazerolles, P.; Iloughmane, H. *J. Organomet. Chem.* **1981**, *216*, 321.

(6) Burns, G. T.; Barton, T. J. *J. Organomet. Chem.* **1981**, *209*, C25.

(7) Laporterie, A.; Manuel, G.; Dubac, J.; Mazerolles, P.; Iloughmane, H. *J. Organomet. Chem.* **1981**, *210*, C33.

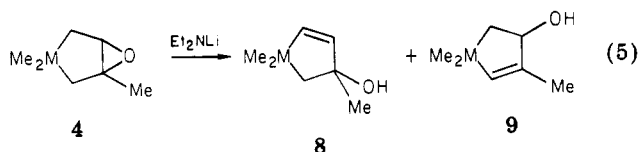
(8) Laporterie, A.; Manuel, G.; Dubac, J.; Mazerolles, P. *Nouv. J. Chim.* **1982**, *6*, 67.

(9) Laporterie, A.; Dubac, J.; Mazerolles, P. *J. Organomet. Chem.* **1980**, *202*, C89.

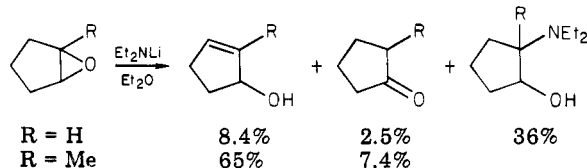
(10) Manuel, G.; Mazerolles, P.; Florence, J. C. *R. Hebd. Seances Acad. Sci. Ser. C* **1969**, *269*, 1553. Manuel, G.; Mazerolles, P.; Florence, J. C. *J. Organomet. Chem.*, **1971**, *30*, 5. Manuel, G.; Mazerolles, P.; Lesbre, M.; Pradel, J. P. *Ibid.* **1973**, *61*, 147.

(11) Mazerolles, P.; Manuel, G. *Bull. Soc. Chim. Fr.* **1966**, *1*, 327. Mazerolles, P.; Manuel, G.; Thoumas, F.; C. R. *Hebd. Seances Acad. Sci., Ser. C*, **1968**, *267*, 619. Manuel, G.; Mazerolles, P.; Cauquy, G. *Synth. React. Inorg. Met. Org. Chem.* **1974**, *4*, 133.

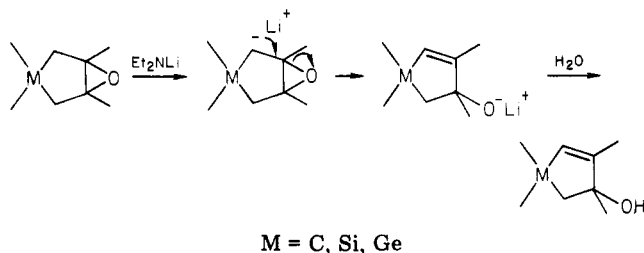
rearrangement is not stereospecific, the selectivity is better than that in the photooxygenation-reduction method⁹ (Table II).



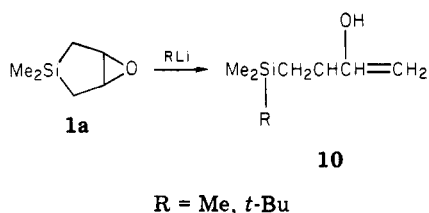
It is interesting to note that the reaction of carbon epoxides with strong bases such as lithium diethylamide may take a number of courses depending on the structure of the oxirane. With the carbon analogues of derivatives 1 and 4, Crandall et al.^{12,13} reported the formation of several products in poor yield.



These contrasting results between the carbon and the silicon or germanium series could be rationalized by a mechanism involving preliminary abstraction of a proton from the position α to M. The presence of a silicon or a germanium atom increases the lability of the hydrogen in the α -position (probably because of the stabilization of the negative charge, in the transition state, by empty 3d (Si) or 4d (Ge) orbitals¹⁴) and, in a similar way, the α -ethylenic bond in the final product could be stabilized ($p\pi$ - $d\pi$ stabilization).



The choice of deprotonating agent is critical since the more nucleophilic organolithium compounds *tert*-butyllithium and methyllithium react with 1a to give ring-opening products presumably by attack at silicon.



Conclusion

The base-induced rearrangement of 6-oxa-3-sila- or 6-oxa-3-germabicyclo[3.1.0]hexanes appears to be a very simple and stereoselective method for obtaining different precursors of 4B metalloles. These results emphasize the role of the Si or Ge heteroatom; in contrast with the carbon

series, we only observed the formation of cyclic allylic alcohols.

Experimental Section

General Data. All boiling points reported in this section are uncorrected. The infrared spectra (liquid film) were obtained on a Perkin-Elmer Model 457 spectrophotometer. The ¹H NMR spectra were obtained on a Varian Associates EM 360 A nuclear magnetic resonance spectrometer. Chemical shifts are reported in δ units, parts per million (ppm) downfield from internal tetramethylsilane. All chemicals used are of commercial origin unless otherwise indicated. 6-Oxa-3-sila- (or 6-oxa-3-germa-) bicyclo[3.1.0]hexanes (1-4) were prepared as described¹⁰ from corresponding 1-sila- (or germa-) cyclopent-3-enes.¹¹

General Procedure. A 100-mL, dry, three-necked, round-bottomed flask equipped with a serum cap, a mechanical stirrer, and a gas inlet was flushed with nitrogen and charged with 2.3 g (30 mmol) of dry diethylamine, 20 mL of dry pentane, and 10 mL (25 mmol) of *n*-butyllithium (or methyllithium) in hexane. After the mixture had been cooled to 20 °C, 10 mmol of epoxides 1-4 in 30 mL of dry diethyl ether was added. The reaction mixture was refluxed for 10 h. Then, 10 mL of a saturated aqueous solution of NaCl was slowly introduced, and the brown color disappeared. The organic phase was washed four times with water. After removal of the solvents, the residue was distilled under vacuum.

It is necessary to use an excess of amine for complete transformation of alkyllithium into lithium diethylamide because alkyllithium readily reacts with epoxides 1-4 to give linear products 10. Diethylamine did not react with epoxides 1-4 even at 100 °C in a sealed tube.

1,1-Dimethyl-1-sila- or 1,1-dimethyl-1-germacyclopent-4-en-3-ols (5a or 5b) and 1,1,3- or 1,1,4-trimethyl-1-silacyclopent-4-en-3-ols or 1,1,3- or 1,1,4-trimethyl-1-germacyclopent-4-en-3-ols (8a, 9a, 8b, or 9b) were previously reported.⁸

1,1-Diphenyl-1-silacyclopent-4-en-3-ol (6a): bp 152 °C (0.3 mm); ¹H NMR (CDCl₃) δ 1.30 (AB part of ABX system, J_{AB} = 15 Hz, J_{AX} = 8 Hz, J_{BX} = 6 Hz, 2 H, SiCH₂), 4.5 (br s, 1 H, OH), 4.8 (m, 1 H, CHOH), 6.6 (A'B' part of A'B'X system, $J_{A'B'}$ = 10 Hz, J_{AX} = J_{BX} = 2 Hz, 2 H, CH=CH), 7.1 (m, 10 H, PhSi); IR (cm⁻¹) 3450 (s), 3120 (w), 2980 (s), 2890 (m), 1560 (w), 1450 (m), 1400 (w), 1340 (w), 1280 (w), 1140 (m), 1040 (m), 910 (w), 880 (m), 760 (m), 720 (m). Anal. Calcd for C₁₆H₁₆OSi: C, 76.15; H, 6.39. Found: C, 76.03; H, 6.41.

1,1-Diphenyl-1-germacyclopent-4-en-3-ol (6b): bp 167 °C (0.3 mm); ¹H NMR (CDCl₃) δ 1.55 (AB part of ABX system, J_{AB} = 14 Hz, J_{AX} = 8 Hz, J_{BX} = 6 Hz, 2 H, GeCH₂), 4.7 (br s, 1 H, OH), 4.9 (m, 1 H, CHOH), 6.6 (A'B' part of A'B'X system, $J_{A'B'}$ = 10 Hz, J_{AX} = J_{BX} = 2 Hz, 2 H, CH=CH), 7.2 (m, 10 H, PhGe); IR (cm⁻¹) 3450 (s), 3080 (m), 3060 (m), 3000 (w), 1540 (w), 1490 (m), 1440 (s), 1140 (m), 1100 (m), 1020 (s), 870 (m), 800 (s), 750 (s), 700 (s). Anal. Calcd for C₁₆H₁₆GeO: C, 64.72; H, 5.43. Found: C, 64.83; H, 5.44.

1,1,3,4-Tetramethyl-1-silacyclopent-4-en-3-ol (7a): bp 90 °C (24 mm); ¹H NMR, ref 8; IR (cm⁻¹) 3360 (s), 2950 (s), 1585 (m), 1440 (m), 1400 (w), 1360 (m), 1250 (m), 1180 m, 1110 m, 1000 m, 930 m, 900 w, 830 m, 680 m, 640 (m). Anal. Calcd for C₈H₁₆OSi: C, 61.47; H, 10.32. Found: C, 61.57; H, 10.30.

1,1,3,4-Tetramethyl-1-germacyclopent-4-en-3-ol (7b): bp 101 °C (30 mm); ¹H NMR, ref 8; IR (cm⁻¹) 3350 (s), 2950 (s), 1595 (m), 1450 (m), 1370 (m), 1240 (m), 1180 (s), 1170 (m), 1000 (m), 940 (m), 820 (s), 740 (w), 700 (w), 660 (w), 600 (m). Anal. Calcd for C₈H₁₆GeO: C, 47.85; H, 8.03. Found: C, 47.98; H, 8.00.

4-(Trimethylsilyl)but-1-en-3-ol (10). A flask with side arm (septum closure) and condenser was charged with 10 mL (20 mmol) of 2 M solution of methyllithium in diethyl ether. To this solution was slowly added 1.3 g (10 mmol) of 6-oxa-3,3-dimethyl-3-silabicyclo[3.1.0]hexane (1a) in 10 mL of dry hexane. The reaction mixture was refluxed under nitrogen atmosphere for 5 h, hydrolyzed, and extracted with Et₂O, and the extracts were dried over anhydrous Na₂SO₄. Solvents were removed by distillation, and the residue was distilled to give 1.0 g of alcohol 10 (77%): bp 85 °C (49 mm); n_D^{20} 1.4421; n_D^{20} 0.8507°; ¹H NMR (CCl₄) δ 0.03 (s, 9 H, CH₃Si), 0.9 (dd, 2 H, SiCH₂), 2.9 (br s, 1 H, OH), 4.16 (m, 1 H, CHOH), 5.0 (m, 2 H, CH₂=C), 5.8 (m, 1 H, C=CH); IR (cm⁻¹) 3350 (s), 3080 (m), 2960 (s), 2900 (s), 1630 (m), 1400 (s), 1250 (s), 1200 (m), 1040 (s), 870 (s), 760 (m), 690 (s). Anal.

(12) Crandall, J. K.; Chang, L. H. *J. Org. Chem.* **1967**, *32*, 435.

(13) Crandall, J. K.; Lin, L. H. *J. Org. Chem.* **1968**, *33*, 2375.

(14) Attridge, C. J. *Organomet. Chem. Rev., Sect. A* **1970**, *5*, 323.

Calcd for $C_7H_{16}OSi$: C, 58.17; H, 11.19. Found: C, 58.02; H, 11.05.

Acknowledgment. The authors are grateful to Dr. P. Mazerolles and Pr. J. Dubac for helpful discussions.

Registry No. 1a, 65181-02-4; 1b, 51343-29-4; 2a, 51343-26-1;

2b, 51343-35-2; 3a, 33459-96-0; 3b, 51343-31-8; 4a, 33460-17-2; 4b, 51343-30-7; 5a, 77225-27-5; 5b, 77225-28-6; 6a, 71404-32-5; 6b, 84279-87-8; 7a, 82763-88-0; 7b, 82763-89-1; 7'a, 82763-90-4; 7'b, 82763-91-5; 8a, 82763-85-7; 8b, 82763-86-8; 9a, 82763-87-9; 9b, 82764-03-2; 10, 18269-52-8.

Asymmetric Synthesis of *trans*-2,3-Diaryloxiranes. Benzylidene Transfer from Chiral Arsonium Ylides

David G. Allen and Stanley Bruce Wild*

Research School of Chemistry, The Australian National University, Canberra, A.C.T., Australia 2600

Received August 13, 1982

Potassium diphenylarsenide reacts with (-)-menthyl chloride in boiling tetrahydrofuran to produce (+)-diphenylneomenthylarsine. Quaternization of this compound with benzyl bromide affords (+)-benzylidiphenylmenthylarsonium bromide, which upon reduction with lithium aluminium hydride gives the epimeric (-)-diphenylmenthylarsine. Equilibrium concentrations of the semistabilized benzylidene ylide derived from the menthylarsonium salt, and from a variety of other optically active arsonium salts containing asymmetric arsenic atoms, react with prochiral aromatic aldehydes to produce good to excellent yields of *trans*-2,3-diaryloxiranes having optical purities of up to 41%. The degree of asymmetric induction depends upon the nature of substituents within the ylide and on the substrate molecule and upon reaction conditions. The stereochemistry of the products has been rationalized in terms of the conformational differences between the intermediate *erythro*-betaines.

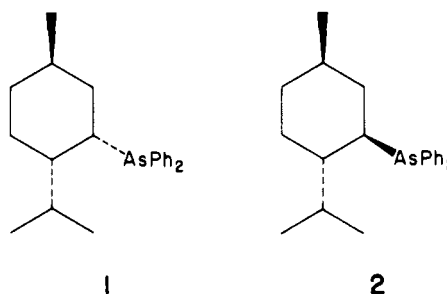
Arsonium ylides react with aromatic aldehydes to produce oxiranes,¹ olefins,² or a mixture of both,³ depending upon the nature of substituent groups of the ylide and substrate molecule and on reaction conditions. In the case of semistabilized ylides derived from benzylarsonium salts, the distribution of products is largely determined by the electronic nature of the substituents on the ylide.⁴ Moreover, the substituted oxirane or olefin invariably has the *trans* stereochemistry.^{5,6} Benzylidene transfer from an optically active arsonium ylide to an aromatic aldehyde is therefore a potentially attractive route to optically active *trans*-2,3-diaryloxiranes.

Derivatives of readily available natural products are extremely attractive reagents for asymmetric synthesis. In this article we report the preparation of two epimeric tertiary arsines derived from (-)-menthol and their application to 2,3-diaryloxirane synthesis. The results are compared with those obtained by use of chiral arsonium ylides containing asymmetric arsenic atoms, a preliminary account of which has already been published.⁵

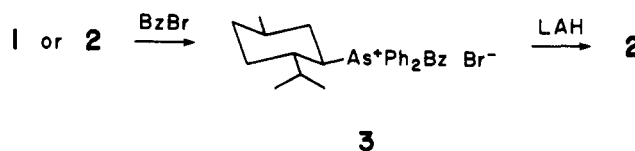
Results and Discussion

Synthesis. (+)-Diphenylneomenthylarsine (1) and (-)-Diphenylmenthylarsine (2). Nucleophilic displacement of chloride from (-)-menthyl chloride by the diphenylarsenide ion proceeds stereospecifically (with inversion of configuration) to produce (+)-diphenylneo-

menthylarsine (1): mp 146-148 °C; $[\alpha]_D +69.6^\circ$ (CH_2Cl_2). The yield of the product was dependent upon the nature of the counterion associated with the arsenide ion. Use of $[K(\text{dioxane})_2][AsPh_2]$ gave a 41% yield of the tertiary arsine, whereas the lithium and sodium salts led to 29 and 26.5% yields, respectively. Nevertheless, a reaction time of 60 h was required for the orange color of the potassium salt to be completely dissipated in boiling tetrahydrofuran. A lengthy reaction time was also found necessary for the preparation of the corresponding tertiary phosphine under similar conditions, and a marked dependence upon the counterion associated with the phosphide was noted.⁷



Quaternization of 1 with benzyl bromide in benzene at 60 °C affords the epimeric benzylarsonium salt 3, $[\alpha]_D +2.5^\circ$ (CH_2Cl_2). Reduction of this compound with lithium aluminium hydride produced (-)-diphenylmenthylarsine, 2, in almost quantitative yield, as a low melting solid (mp 52 °C), $[\alpha]_D -79.6^\circ$ (CH_2Cl_2). The latter can be reconverted into 3 by treatment with benzyl bromide in benzene.



(7) Morrison, J. D.; Masler, W. F. *J. Org. Chem.* 1974, 39, 270. Aguiar, A. M.; Bahacca, N. S.; Burnett, R. E.; Masler, W. F.; Morrison, J. D.; Morrow, C. J. *Ibid.* 1976, 41, 1545.

(1) Henry, M. C.; Wittig, G. *J. Am. Chem. Soc.* 1960, 82, 563. Allen, D. W.; Jackson, G. *J. Organomet. Chem.* 1976, 110, 315.

(2) Johnson, A. W. *J. Org. Chem.* 1960, 25, 183. Johnson, A. W.; Schubert, H. *Ibid.* 1978, 35, 2678. Lloyd, D.; Singer, M. I. C. *Tetrahedron* 1972, 353.

(3) Johnson, A. W.; Martin, J. O. *Chem. Ind. (London)* 1965, 1726. Gosney, I.; Lillie, T. J.; Lloyd, D. *Angew. Chem., Int. Ed. Engl.* 1977, 16, 487.

(4) Trippett, S.; Walker, M. A. *J. Chem. Soc. C* 1971, 1114. Kendurkar, P. S.; Tewari, R. S. *J. Organomet. Chem.* 1973, 60, 247. Kumari, N.; Kendurkar, P. S.; Tewari, R. S. *Ibid.* 1975, 96, 237. Kendurkar, P. S.; Tewari, R. S. *Ibid.* 1976, 108, 175. Tewari, R. S.; Chaturvedi, S. C. *Indian J. Chem., Sect. B* 1979, 18B, 359.

(5) Allen, D. G.; Roberts, N. K.; Wild, S. B. *J. Chem. Soc., Chem. Commun.* 1978, 346.

(6) Still, W. C.; Novack, V. J. *J. Am. Chem. Soc.* 1981, 103, 1283.

Calcd for $C_7H_{16}OSi$: C, 58.17; H, 11.19. Found: C, 58.02; H, 11.05.

Acknowledgment. The authors are grateful to Dr. P. Mazerolles and Pr. J. Dubac for helpful discussions.

Registry No. 1a, 65181-02-4; 1b, 51343-29-4; 2a, 51343-26-1;

2b, 51343-35-2; 3a, 33459-96-0; 3b, 51343-31-8; 4a, 33460-17-2; 4b, 51343-30-7; 5a, 77225-27-5; 5b, 77225-28-6; 6a, 71404-32-5; 6b, 84279-87-8; 7a, 82763-88-0; 7b, 82763-89-1; 7'a, 82763-90-4; 7'b, 82763-91-5; 8a, 82763-85-7; 8b, 82763-86-8; 9a, 82763-87-9; 9b, 82764-03-2; 10, 18269-52-8.

Asymmetric Synthesis of *trans*-2,3-Diaryloxiranes. Benzylidene Transfer from Chiral Arsonium Ylides

David G. Allen and Stanley Bruce Wild*

Research School of Chemistry, The Australian National University, Canberra, A.C.T., Australia 2600

Received August 13, 1982

Potassium diphenylarsenide reacts with (-)-menthyl chloride in boiling tetrahydrofuran to produce (+)-diphenylneomenthylarsine. Quaternization of this compound with benzyl bromide affords (+)-benzylidiphenylmenthylarsonium bromide, which upon reduction with lithium aluminium hydride gives the epimeric (-)-diphenylmenthylarsine. Equilibrium concentrations of the semistabilized benzylidene ylide derived from the menthylarsonium salt, and from a variety of other optically active arsonium salts containing asymmetric arsenic atoms, react with prochiral aromatic aldehydes to produce good to excellent yields of *trans*-2,3-diaryloxiranes having optical purities of up to 41%. The degree of asymmetric induction depends upon the nature of substituents within the ylide and on the substrate molecule and upon reaction conditions. The stereochemistry of the products has been rationalized in terms of the conformational differences between the intermediate *erythro*-betaines.

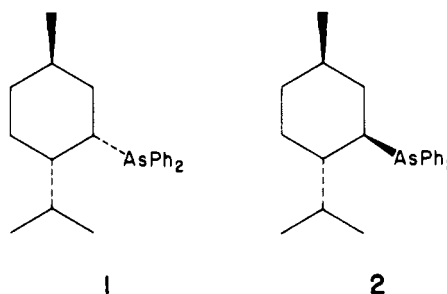
Arsonium ylides react with aromatic aldehydes to produce oxiranes,¹ olefins,² or a mixture of both,³ depending upon the nature of substituent groups of the ylide and substrate molecule and on reaction conditions. In the case of semistabilized ylides derived from benzylarsonium salts, the distribution of products is largely determined by the electronic nature of the substituents on the ylide.⁴ Moreover, the substituted oxirane or olefin invariably has the *trans* stereochemistry.^{5,6} Benzylidene transfer from an optically active arsonium ylide to an aromatic aldehyde is therefore a potentially attractive route to optically active *trans*-2,3-diaryloxiranes.

Derivatives of readily available natural products are extremely attractive reagents for asymmetric synthesis. In this article we report the preparation of two epimeric tertiary arsines derived from (-)-menthol and their application to 2,3-diaryloxirane synthesis. The results are compared with those obtained by use of chiral arsonium ylides containing asymmetric arsenic atoms, a preliminary account of which has already been published.⁵

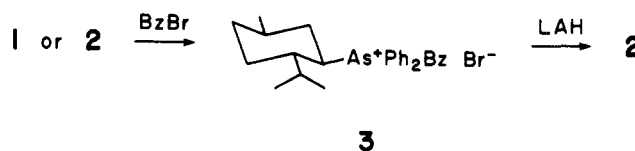
Results and Discussion

Synthesis. (+)-Diphenylneomenthylarsine (1) and (-)-Diphenylmenthylarsine (2). Nucleophilic displacement of chloride from (-)-menthyl chloride by the diphenylarsenide ion proceeds stereospecifically (with inversion of configuration) to produce (+)-diphenylneo-

menthylarsine (1): mp 146-148 °C; $[\alpha]_D +69.6^\circ$ (CH_2Cl_2). The yield of the product was dependent upon the nature of the counterion associated with the arsenide ion. Use of $[K(\text{dioxane})_2][AsPh_2]$ gave a 41% yield of the tertiary arsine, whereas the lithium and sodium salts led to 29 and 26.5% yields, respectively. Nevertheless, a reaction time of 60 h was required for the orange color of the potassium salt to be completely dissipated in boiling tetrahydrofuran. A lengthy reaction time was also found necessary for the preparation of the corresponding tertiary phosphine under similar conditions, and a marked dependence upon the counterion associated with the phosphide was noted.⁷



Quaternization of 1 with benzyl bromide in benzene at 60 °C affords the epimeric benzylarsonium salt 3, $[\alpha]_D +2.5^\circ$ (CH_2Cl_2). Reduction of this compound with lithium aluminium hydride produced (-)-diphenylmenthylarsine, 2, in almost quantitative yield, as a low melting solid (mp 52 °C), $[\alpha]_D -79.6^\circ$ (CH_2Cl_2). The latter can be reconverted into 3 by treatment with benzyl bromide in benzene.



(7) Morrison, J. D.; Masler, W. F. *J. Org. Chem.* 1974, 39, 270. Aguiar, A. M.; Bahacca, N. S.; Burnett, R. E.; Masler, W. F.; Morrison, J. D.; Morrow, C. J. *Ibid.* 1976, 41, 1545.

(1) Henry, M. C.; Wittig, G. *J. Am. Chem. Soc.* 1960, 82, 563. Allen, D. W.; Jackson, G. *J. Organomet. Chem.* 1976, 110, 315.

(2) Johnson, A. W. *J. Org. Chem.* 1960, 25, 183. Johnson, A. W.; Schubert, H. *Ibid.* 1978, 35, 2678. Lloyd, D.; Singer, M. I. C. *Tetrahedron* 1972, 353.

(3) Johnson, A. W.; Martin, J. O. *Chem. Ind. (London)* 1965, 1726. Gosney, I.; Lillie, T. J.; Lloyd, D. *Angew. Chem., Int. Ed. Engl.* 1977, 16, 487.

(4) Trippett, S.; Walker, M. A. *J. Chem. Soc. C* 1971, 1114. Kendurkar, P. S.; Tewari, R. S. *J. Organomet. Chem.* 1973, 60, 247. Kumari, N.; Kendurkar, P. S.; Tewari, R. S. *Ibid.* 1975, 96, 237. Kendurkar, P. S.; Tewari, R. S. *Ibid.* 1976, 108, 175. Tewari, R. S.; Chaturvedi, S. C. *Indian J. Chem., Sect. B* 1979, 18B, 359.

(5) Allen, D. G.; Roberts, N. K.; Wild, S. B. *J. Chem. Soc., Chem. Commun.* 1978, 346.

(6) Still, W. C.; Novack, V. J. *J. Am. Chem. Soc.* 1981, 103, 1283.

Table I. Reaction Conditions and Yields of *trans*-2,3-Diphenyloxirane

salt	base	solvent	temp, °C	yield		configuratn
				chemical	optical ^a	
3	NaOEt	EtOH	25	62	23	2 <i>R</i> ,3 <i>R</i>
3	LiOEt	EtOH	25	38	14	2 <i>R</i> ,3 <i>R</i>
(<i>R</i>)-4b	NaOEt	EtOH	25	86	8	2 <i>R</i> ,3 <i>R</i>
(<i>R</i>)-4b	LiOEt	DMF	25	62	5	2 <i>R</i> ,3 <i>R</i>
(<i>R</i>)-5	NaOEt	EtOH	25	94	8	2 <i>R</i> ,3 <i>R</i>
(<i>RS</i>)-6a	NaOEt	EtOH	25	88	19	2 <i>R</i> ,3 <i>R</i>
(<i>SR</i>)-6a	NaOEt	EtOH	0	74	17	2 <i>S</i> ,3 <i>S</i>
(<i>SR</i>)-6a	LiOEt	EtOH	25	96	23	2 <i>S</i> ,3 <i>S</i>

^a Calculated from the value of $[\alpha]_D^{20} + 291^\circ$ (*c*. 0.056, acetone) reported for optically pure material.²²

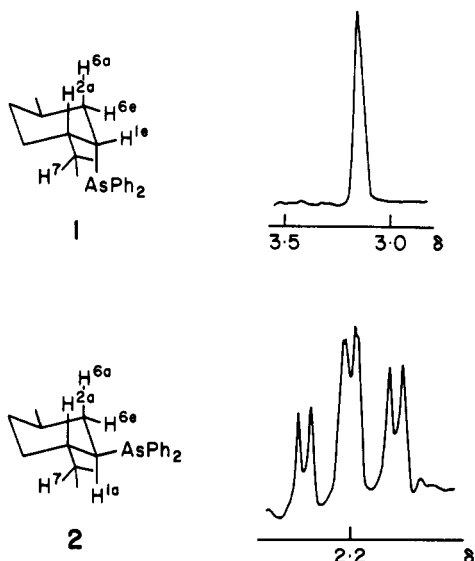


Figure 1. ¹H NMR spectra (200 MHz) of 1 and 2 in the region of H¹.

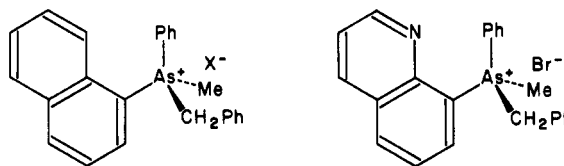
The stereochemistries of 1 and 2 were corroborated by their ¹H NMR spectra (Figure 1). In compound 1 H^{1a} appears as a broad singlet at δ 3.10 due to a small axial-equatorial coupling with H^{2a} and H^{6a}, and an additional small equatorial-equatorial coupling with H^{6e}. However, in 2 H^{1a} was observed as a distorted doublet of triplets because of relatively large axial-axial coupling to H^{2a} and H^{6a} ($J = \text{ca. } 12 \text{ Hz}$) and a smaller axial-equatorial coupling to H^{6e} ($J = \text{ca. } 3 \text{ Hz}$). The ¹H NMR spectra of the phosphorus analogues of 1 and 2 have been interpreted similarly.⁸ In salt 3 H^{1a} was observed as a doublet of triplets centered at δ 5.0. The signals are flanked by the AB pattern of resonances due to the diastereotopic pair of benzylic methylene protons, which are also adjacent to the arsonium center.

Quaternization of 1 and 2. As previously indicated, quaternization of 1 or 2 with benzyl bromide in benzene produced the same salt 3. It can be reduced by LiAlH₄ to 2. Alternatively, treatment of 3 with sodium ethoxide in the presence of a carbonyl compound (*vide infra*) also produces pure 2 in high yield. Proton NMR evidence suggested that the reaction of 1 with benzyl bromide first formed the expected neomenthylarsonium salt, and that this subsequently rearranged to 3. Further work on the mechanism of the epimerization is in progress.

The salts (+)-(*R*)-4a,b were obtained by resolution of the racemic cation with hydrogen (-)-(*RR*)-dibenzoyl-tartrate, followed by metathesis of the less soluble salt with the appropriate anion. The absolute configuration of the arsenic atom in the cation has been determined by X-ray

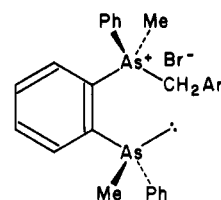
crystal structure analysis.⁹ The chelating tertiary arsines were resolved by fractional crystallization of internally diastereoisomeric palladium(II) complexes containing the bidentates and an optically active ortho-metalated amine: dimethyl(α -methylbenzyl)amine in the case of (*RR*,*SS*)-*o*-phenylenebis(methylphenylarsine)¹⁰ and dimethyl(1-ethyl- α -naphthyl)amine for (*R,S*)-methylphenyl(8-quinolyl)arsine.¹¹ The absolute configurations of both tertiary arsines are known from X-ray studies.^{11,12}

Asymmetric Arsonium Salts. The optically active arsonium salts (-)-(*R*)-5 and (-)-(*RS*)- and (+)-(*SR*)-6a-d were obtained by quaternization of the respective optically active tertiary arsine with the appropriate benzyl halide. The reaction is stereospecific and proceeds with retention of configuration of the asymmetric arsonium center.¹³



(*R*) - 4a, X = Br
- 4b, X = PF₆

(*R*) - 5



(*RS*) - 6a, Ar = C₆H₅
- 6b, Ar = *p*-MeC₆H₄
- 6c, Ar = *o*-MeOC₆H₄
- 6d, Ar = *o*-ClC₆H₄
- 6e, Ar = α -Np

Oxiranes. The oxirane syntheses were usually performed in ethanol solution. A small equilibrium concentration of the ylide was generated from the optically active arsonium salt by use of lithium or sodium ethoxide and a slight excess of the aromatic aldehyde added. The reaction mixture was then stirred for ca. 18 h at 25 °C. After removal of solvent the products were separated by column chromatography under an argon atmosphere by use of petroleum ether-chloroform mixture as eluent. The optically pure tertiary arsines were recovered in high yield

(9) Allen, D. G.; Henrick, K.; Raston, C. L.; Roberts, N. K.; White, A. H.; Wild, S. B. unpublished work.

(10) Roberts, N. K.; Wild, S. B. *J. Chem. Soc., Dalton Trans.* 1979, 2015.

(11) Allen, D. G.; McLaughlin, G. M.; Robertson, G. B.; Steffen, W. L.; Salem, G.; Wild, S. B. *Inorg. Chem.* 1982, 21, 1007.

(12) Skelton, B. W.; White, A. H. *J. Chem. Soc., Dalton Trans.* 1979, 1556.

(13) The apparent inversion of configuration which takes place upon quaternization or elimination of the tertiary arsine is consistent with the rules of Cahn et al. for the assignment of absolute configurations.¹⁴

(14) Cahn, R. S.; Ingold, C. K.; Prelog, V. *Angew. Chem., Int. Ed. Engl.* 1966, 5, 385.

from the respective reaction mixtures. The results of a series of experiments leading to *trans*-2,3-diphenyloxirane are summarized in Table I.

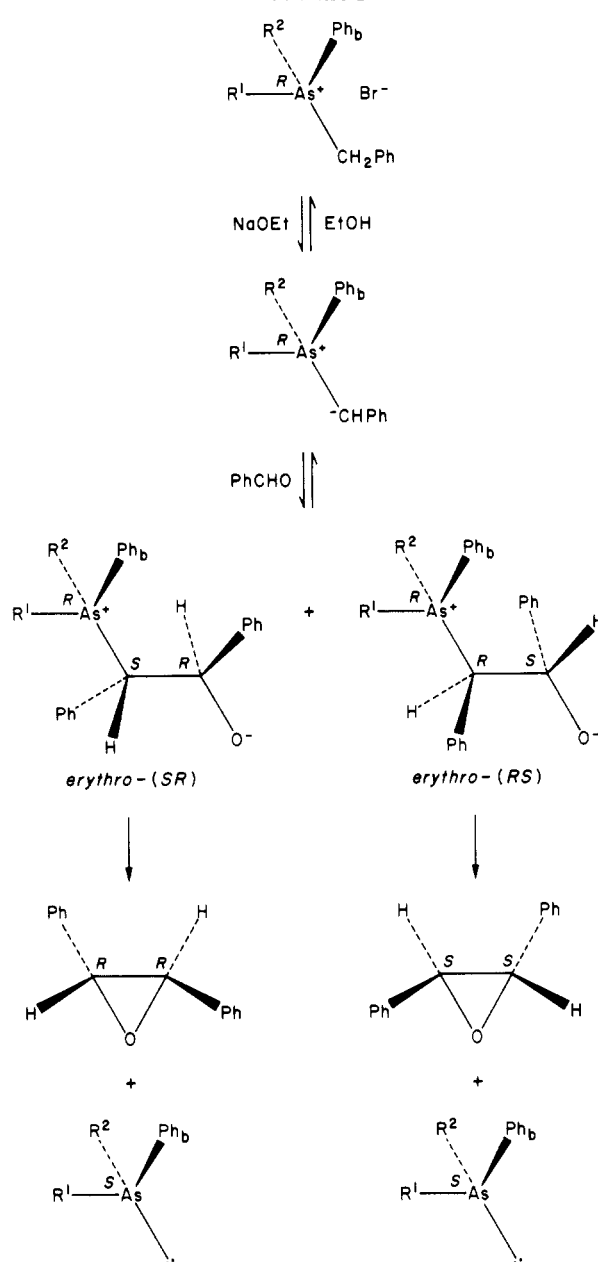
In the case of unsubstituted benzylidene transfer, the highest optical yield (23%) was obtained from **3** in the presence of sodium ethoxide, and from (*RS*)-**6a** when lithium ethoxide was used as base. However, use of lithium ethoxide in conjunction with **3** led to a reduction in chemical and optical yield of product. Furthermore, reducing the temperature of the reaction to 0 °C did not improve the stereoselectivity of reactions involving (*RS*)-**6a**. The structurally similar arsonium ions (+)-(*R*)-**4a,b** and (-)-(*R*)-**5** gave similar, but reduced, levels of asymmetric induction. For reactions involving salts containing an asymmetric arsenic atom, the product invariably had the absolute configuration of the arsonium ion from which it was prepared.

Substitution Effects. Substituents on the aromatic ring of the benzylidene group, as well as on the substrate molecule influenced the chemical and optical yields of the *trans*-oxirane. In general, the highest optical yields were obtained with the ylide derived from **3**. Significantly, the rate of the reaction increased dramatically as the para group became more electronegative. Benzylidene transfer from deprotonated (-)-(*RS*)-**6a** to *p*-chlorobenzaldehyde proceeded at 3 times the rate as that to *p*-tolualdehyde (as determined by polarimetry at 20 °C). The increased rate of the nucleophilic addition was accompanied by a decrease in the stereoselectivity of the reaction. A corresponding decrease in the stereoselectivity of the reaction was found with increasing nucleophilicity of the benzylidene carbon atom. Whereas (+)-(*RR*)-*trans*-2,3-diphenyloxirane was produced from (-)-(*RS*)-**6a** in 19% optical yield, (+)-(*2R*)-phenyl-(*3R*)-*p*-tolylloxirane formed to the extent of 15% from (-)-(*RS*)-**6b** and benzaldehyde under the same conditions.

The highest optical yields were obtained when an *o*-anisyl group was attached to the benzylidene carbon atom. Dissymmetric (+)-*trans*-2,3-bis(*o*-anisyl)oxirane was produced in 38% optical yield from a reaction involving (-)-(*RS*)-**6c** and *o*-anisaldehyde under the usual conditions. Use of lithium ethoxide as base led to a further improvement in the optical yield (to 41%). However, the major influence was associated with the *o*-anisyl group of the ylide. Thus, the ylide derived from (-)-(*RS*)-**6c** gave a 29% optical yield of (+)-*trans*-2-(*o*-anisyl)-3-phenyloxirane upon treatment with benzaldehyde, whereas (-)-(*RS*)-**6a** and *o*-anisaldehyde under the same conditions gave an 18% optical yield.

Stereochemical Considerations. The mechanism of the reaction must account for the exclusive formation of *trans*-2,3-diaryloxiranes with a preponderance of the enantiomer having the absolute configuration of the arsonium ion from which the ylide was generated. Furthermore, in both systems the byproduct of the reaction was optically pure tertiary arsine. The alternative pathways leading to *trans*-2,3-diphenyloxirane are shown in Scheme I. The addition of the ylide to one or other of the prochiral faces of the aldehyde produces intermediate betaines containing two new asymmetric centers. Thus, there are four betaines possible. However, since *trans*-2,3-diaryloxiranes are the only geometric isomers formed, the erythro (*RS,SR*) pair presumably offer the lower energy pathway to product. The absence of *cis*-2,3-diaryloxiranes among the products accordingly implies stereospecific formation of the erythro-betaines or perhaps, as suggested by Johnson et al.¹⁵ (in

Scheme I

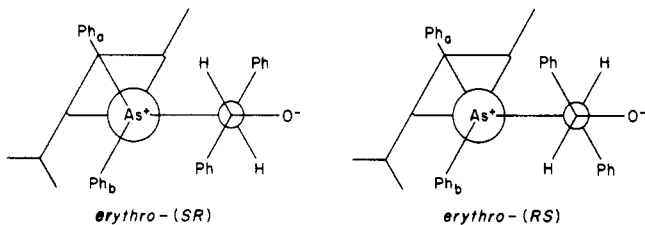


^a **3**, R¹ = menthyl, R² = Ph_a; (*R*)-**4a**, R¹ = α -naphthyl, R² = Me, Ph_b = *p*-MeC₆H₄; (*R*)-**5**, R¹ = 8-quinolyl, R² = Me; (*RS*)-**6a**, R¹ = (*S*)-2-(MePhAs)C₆H₄, R² = Me.

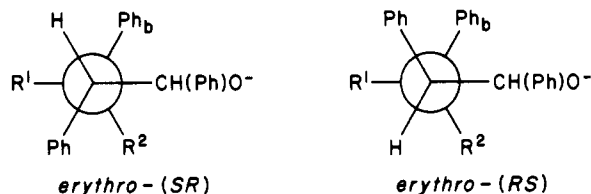
accounting for the stereospecificity of alkylidene transfer from sulfonium and oxosulfonium ylides), reversion of the less favored *threo*-betaines to starting materials.

In Scheme I the arsonium centers have been designated the *R* absolute configuration, the group of highest priority being indicated by R¹. This corresponds to the α -naphthyl group in (*R*)-**4a,b**, the 8-quinolyl group in (*S*)-**5**, and the (*S*)-2-(methylphenylarsino)phenyl group in (*RS*)-**6a-e** (the second aromatic group in (*R*)-**4a,b** is *p*-tolyl). For the salts **4-6**, R² is a methyl group. However, in the case of **3**, R² is phenyl and the pair of phenyl groups Ph_a/Ph_b is diastereotopic in the parent salts and in the intermediate betaines. Molecular models of the betaines indicate that Ph_b experiences a larger steric interaction with the menthyl ring compared to Ph_a.

A mechanism for the transmission of chirality from the menthyl group to the new asymmetric centers in the betaines now becomes evident. An alternative view of the erythro-betaines (along the benzylic carbon-arsenic bond)

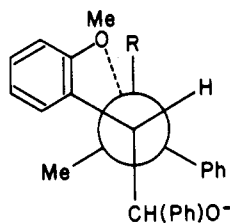


is shown below, where $R^1 =$ menthyl and $R^2 = Ph_a$.



In the *erythro*-(*SR*)-betaine the phenyl substituent on the benzylic carbon atom is anti to Ph_b , whereas the less favorable gauche arrangement of these two groups exists in the *erythro*-(*RS*) diastereoisomer. Internal nucleophilic displacement of **3** from the former betaine by the oxygen atom produces *trans*-2,3-diaryloxiranes having the *RR* absolute configuration in agreement with the experimental results. In the case of the betaines derived from the ylides containing formally asymmetric arsonium centers the situation is similar, the group R^1 being the bulkiest group present, that is, 1-naphthyl, 8-quinolyl, or 2-(methylphenylarsino)phenyl for betaines derived from (*R*)-**4a,b**, (*R*)-**5**, or (*RS*)-**6a-e**, respectively, and $R^2 = Me$ in all cases (the arsenic center had the *R* absolute configuration). The anti disposition of the bulky groups in the *erythro*-(*SR*) diastereoisomer may be anticipated to provide the lower energy transition state to betaine decomposition, thereby producing *trans*-2,3-diaryloxiranes of *RR* absolute configuration.

Use of the (*o*-methoxybenzyl)arsonium salt (*-*)-(*RS*)-**6c** as ylide precursor led to the highest level of optical induction in the product. In this case, a chelating interaction involving the *o*-methoxy group and the arsonium center may restrict rotation about the arsenic-benzyl bond of the betaines, thereby increasing the effective chirality of the system.



Anchimeric assistance involving overlap of a pair of 2p electrons on a methoxyl oxygen atom with a vacant 3d (or 4d) orbital of phosphorus (or arsenic) has been invoked by McEwen and his colleagues¹⁶ to account for the increased rates observed for the quaternization of tertiary phosphines (and arsines) containing *o*-methoxyphenyl groups, as well as the reduced rate of alkaline hydrolysis of similarly substituted benzyltriarylphosphonium salts. From the present work it is apparent that through space interactions of this type involving five-membered rings may also be significant in certain reactions of tertiary phosphines and arsines and their quaternary derivatives.

(16) McEwen, W. E.; Lau, K. W. *J. Org. Chem.* **1982**, *47*, 3595 and references contained therein.

We have also made a preliminary investigation of asymmetric cyclopropane synthesis. Both reactive⁴ and stabilized¹⁷ arsonium ylides are known to react with α,β -unsaturated esters to produce substituted cyclopropanes. The salt (*-*)-(*RS*)-**6a** reacts rapidly with potassium hydride in tetrahydrofuran to give a red solution of the semistabilized ylide. Upon treatment with methyl acrylate and subsequent hydrolysis of the ester produced, (+)-(*1S,2S*)-*trans*-2-phenylcyclopropanecarboxylic acid was isolated in 68% yield with an optical purity of 25%¹⁸ in the case of the ylide derived from (*RS*)-**6a** and 90% yield and 5% optical purity for the ylide of (*-*)-menthylarsonium salt **3**. The corresponding reaction with an oxosulfonium salt has not been performed because of the difficulty in preparing the appropriate precursor.²⁰ However, optical yields of 7–43% have been reported for the synthesis of certain substituted cyclopropanes from oxosulfonium alkylides.²¹

Experimental Section

Reactions involving air-sensitive compounds were performed under an argon atmosphere by use of the Schlenk technique. Solvents were dried and distilled in a stream of argon before use. The petroleum ether used had a boiling point of 48–65 °C. Proton NMR spectra were recorded at 34 °C by use of JEOL MH-100 (100 MHz), Bruker HX-90 (90 MHz), CXP-200 (200 MHz), and Hitachi-Perkin-Elmer R-24B (60 MHz) spectrometers. Chemical shifts are quoted relative to Me_4Si in $CDCl_3$ solution. Optical rotations were measured in a 1-dm cell thermostated to 20 °C by use of a Perkin-Elmer Model 241 polarimeter. (*-*)-Menthyl chloride, $[\alpha]_D -45.5^\circ$ (*c* 2.2, heptane), was prepared from (*-*)-menthol according to the method of Smith and Wright.²⁶ The compound $[K(dioxane)_2][AsPh_2]$ was prepared and isolated as described by Lange and Tzschach.²⁶ Microanalyses were performed by staff within the School. All new compounds analyzed satisfactorily.

(+)-Diphenylneomenthylarsine (**1**). A solution of $[K(dioxane)_2][AsPh_2]$ (25.1 g, 0.056 mol) in tetrahydrofuran (150 mL) was treated with (*-*)-menthyl chloride (10.1 g, 0.058 mol) and the mixture heated under reflux. Potassium chloride precipitated from the reaction mixture as the orange-red color of the arsenide ion began to fade. After 60 h the color due to the anion had disappeared, whereupon the solvent was removed (40 °C, 20 mmHg) and the residue suspended in diethyl ether (200 mL) and water (200 mL) added. The organic layer was separated and dried ($MgSO_4$), and the solvent was removed to leave a crystalline residue, which crystallized from warm methanol (200 mL) as white needles: mp 146–148 °C (12.7 g, 41.6%); $[\alpha]_D +69.6^\circ$ (*c* 0.4, CH_2Cl_2); ¹H NMR (200 MHz in C_6D_6) δ 0.54 (d, *J* = 6.0 Hz, 3 H, $CHMeMe$), 0.60 (d, *J* = 6.2 Hz, 3 H, $CHMe$), 0.80 (d, *J* = 6.4 Hz, 3 H, $CHMeMe$), 0.84–1.84 (br m, 9 H), 3.10 (br s, 1 H, H^{1e}), 7.22–7.72 (br m, 10 H, aromatics). Anal. Calcd for $C_{22}H_{29}As$: C, 71.7; H, 7.9. Found: C, 71.9, H, 7.8.

(+)-Benzylidiphenylmenthylarsonium Bromide (**3**). A solution of **1** or **2** (5.3 g) in dry benzene (15 mL) was maintained at 60 °C for 48 h in the presence of benzyl bromide (2.9 g). During this period the product separated as a white solid. The precipitation was completed by gradual dilution of the mixture with petroleum ether. Recrystallization of the crude product from ethanol-diethyl ether afforded the pure compound as white

(17) Nesmeyanov, N. A.; Mikulshina, V. V. *Zh. Org. Khim.* **1971**, *7*, 696.

(18) The optical purity was determined by comparison with the value $[\alpha]_D -368^\circ$ (*c* 0.931) reported for (*-*)-(*2R,3R*)-2-phenylcyclopropane-3-carboxylic acid.¹⁹

(19) Walborsky, H. M.; Plonsker, L. *J. Am. Chem. Soc.* **1961**, *83*, 2138.

(20) Johnson, C. R.; Schroeck, C. W. *J. Am. Chem. Soc.* **1971**, *93*, 5303.

(21) Johnson, C. R.; Schroeck, C. W. *J. Am. Chem. Soc.* **1973**, *95*, 7418.

(22) Read, J.; Campbell, I. G. M. *J. Chem. Soc.* **1930**, 2377.

(23) MacDonald, H. H. J.; Crawford, R. J. *Can. J. Chem.* **1972**, *50*, 428.

(24) Imuta, M.; Ziffer, H. J. *Org. Chem.* **1979**, *44*, 2505.

(25) Smith, J. G.; Wright, G. F. *J. Org. Chem.* **1952**, *17*, 1116.

(26) Lange, W.; Tzschach, A. *Chem. Ber.* **1962**, *95*, 1360.

prisms: mp 188–190 °C (4.09 g, 53%); $[\alpha]_D +2.5^\circ$ (*c* 2.0, CH₂Cl₂); ¹H NMR (200 MHz in CDCl₃) δ 0.65 (d, *J* = 6.7 Hz, 3 H, CHMe₂), 0.91 (d, *J* = 6.7 Hz, 3 H, CHMe), 0.94 (d, *J* = 6.7 Hz, 3 H, CHMe₂), 4.71, 5.18 (ABq, *J*_{AB} = 13.2 Hz, 2 H, CH₂Ph), 5.0 (d of t, *J*_{H^{1a}-H^{2a}, H^{6a}} = ca. 12 Hz, *J*_{H^{1a}-H^{6a}} = ca. 3 Hz, 1 H, H^{1a}), 1.0–2.7 (br m, 9 H), 6.8–7.8 (br, 10 H, aromatics). Anal. Calcd for C₂₉H₃₆AsBr: C, 64.6; H, 6.7; Br, 14.8. Found: C, 64.4; H, 6.6; Br, 14.8.

(-)-Diphenylmethylarsine (2). A suspension of 3 (1.4 g) in THF (100 mL) was treated with LiAlH₄ (0.5 g) and the reaction mixture heated under reflux for 20 min. The solvent was removed and diethyl ether (50 mL) added, followed by water (0.5 mL), aqueous sodium hydroxide solution (15%, 0.5 mL), water (1.5 mL), and an excess of anhydrous MgSO₄. The mixture was filtered, and the filtrate was evaporated to dryness. The crude product remained as a viscous oil that slowly crystallized. Distillation of this material (bp 152–158 °C (0.01 mm)) gave the pure product: mp 52–53 °C (0.81 g, 86%); $[\alpha]_D -79.6^\circ$ (*c* 1.47, CH₂Cl₂); ¹H NMR (200 MHz in C₆D₆) δ 0.68 (d, *J* = 6.4 Hz, 3 H, CHMe₂), 0.77 (d, *J* = 6.8 Hz, 3 H, CHMe), 0.91 (d, *J* = 7 Hz, 3 H, CHMe₂), 2.25 (d of t, *J*_{H^{1a}-H^{2a}, H^{6a}} = ca. 12 Hz, *J*_{H^{1a}-H^{6a}} = ca. 3 Hz, 1 H, H^{1a}), 2.60 (d of septets, *J*_{H⁷-Me^{2,3}} = ca. 7 Hz, *J*_{H⁷-H^{2a}} = ca. 3 Hz, 1 H, H⁷), 0.95–1.86 (br m, 9 H), 6.94–7.85 (br m, 10 H, aromatics). Anal. Calcd for C₂₂H₂₉As: C, 71.7; H, 7.9. Found: C, 71.9, H, 7.9.

(*RR*,*SS*)-, (+)-(*RR*)-, and (-)-(*SS*)-*o*-Phenylenebis(methylphenylarsine). The bis(tertiary arsine) was prepared, separated into diastereoisomers, and resolved as previously described.¹⁰

(+)-(*R*)-Benzylmethyl- α -naphthyl-*p*-tolylarsonium Bromide ((+)-(*R*)-4a) and Hexafluorophosphate ((+)-(*R*)-4b). The racemic cation was resolved by use of hydrogen (-)-(*RR*)-dibenzoyltartrate. Metathesis of the less soluble diastereoisomeric salt with the appropriate anion gave the optically active arsonium bromide and hexafluorophosphate, whose absolute configurations were determined by X-ray crystal structure analysis.⁹

(-)-(*R*)- and (+)-(*S*)-Methylphenyl-8-quinolyarsine ((-)-(*R*)-5 and (+)-(*S*)-5). The synthesis and resolution of this compound was carried out as described in ref 11. The absolute configurations were determined by X-ray crystal structure analysis.

(-)-(*R*)-*threo*-Benzylmethyl[(*S*)-2-(methylphenylarsino)phenyl]phenylarsonium Bromide Hemihydrate ((-)-(*RS*)-6a). This salt was prepared by quaternization of (-)-(*SS*)-1 with benzyl bromide as previously reported.¹⁰

(-)-(*R*)-*threo*-Methyl(*p*-methylbenzyl)[(*S*)-2-(methylphenylarsino)phenyl]phenylarsonium Bromide Hemihydrate ((-)-(*RS*)-6b). A solution of (-)-(*SS*)-*o*-phenylenebis(methylphenylarsine) (1.5 g) in propan-2-ol (5 mL) was treated with *p*-methylbenzyl bromide (1.0 g), and the reaction mixture was allowed to stand 4 days at 25 °C. A viscous gum separated that was separated from the mother liquor and then triturated in the presence of petroleum ether until solid. The product could not be crystallized: yield 2.2 g (99%); $[\alpha]_D -81.3^\circ$ (*c* 0.8, CH₂Cl₂); ¹H NMR (60 MHz in CDCl₃) δ 1.26 (s, 3 H, MeAs), 2.23 (s, 3 H, *p*-MeC₆H₄), 2.44 (br s, 1 H, 0.5 H₂O), 2.68 (s, 3 H, MeAs⁺), 4.93, 5.21 (ABq, *J* = 21 Hz, 2 H, *p*-MeC₆H₄CH₂As⁺), 6.8–7.9 (br m, 18 H, aromatics).

(-)-(*R*)-(*o*-Methoxybenzyl)methyl[(*S*)-2-(methylphenylarsino)phenyl]phenylarsonium Bromide ((-)-(*RS*)-6c). A solution of (-)-(*SS*)-*o*-phenylenebis(methylphenylarsine) (1.5 g) and *o*-methoxybenzyl bromide (0.8 g) in benzene (3 mL) was heated for 16 h at 70 °C. The product separated as white crystals, which were filtered off, washed with diethyl ether, and recrystallized from ethanol by the addition of diethyl ether. The pure product formed white needles: mp 166–166.5 °C (2.09 g, 94%); $[\alpha]_D -52.3^\circ$ (*c* 0.72, CH₂Cl₂); ¹H NMR (100 MHz in CDCl₃) δ 1.17 (s, 3 H, MeAs), 2.66 (s, 3 H, MeAs⁺), 3.37 (s, 3 H, OMe), 4.7, 4.95 (ABq, *J* = 12 Hz, 2 H, *o*-MeOC₆H₄CH₂As⁺), 6.6–7.9 (br m, 18 H, aromatics).

The enantiomer (+)-(*SR*)-6c was prepared similarly from (+)-(*RR*)-*o*-C₆H₄(AsMePh)₂, $[\alpha]_D +95^\circ$ (*c* 0.70, CH₂Cl₂).

(-)-(*R*)-*threo*-(*o*-Chlorobenzyl)methyl[(*S*)-2-(methylphenylarsino)phenyl]phenylarsonium Bromide Hemihydrate ((-)-(*RS*)-4d). Reaction of (-)-(*SS*)-*o*-phenylenebis(methylphenylarsine) (2.0 g) with *o*-chlorobenzyl bromide (1.0 g) in propan-2-ol for 4 days at 25 °C, followed by workup as described for 4b, gave the pure product as an amorphous white solid (3.0

g, 98%); $[\alpha]_D -96.4^\circ$ (*c* 1.0, CH₂Cl₂); ¹H NMR (60 MHz in CDCl₃) δ 1.26 (s, 3 H, MeAs), 2.02 (br s, 1 H, 0.5 H₂O), 2.77 (s, 3 H, MeAs⁺), 5.10, 5.33 (ABq, *J* = 21 Hz, 2 H, *o*-ClC₆H₄CH₂As⁺), 6.9–8.1 (br m, 18 H, aromatics).

(-)-(*R*)-*threo*-Methyl[(*S*)-2-(methylphenylarsino)phenyl](α -naphthylmethyl)phenylarsonium Bromide Hemihydrate ((-)-(*RS*)-4e). A solution of (-)-(*SS*)-*o*-phenylenebis(methylphenylarsine) (0.82 g) and 1-(bromomethyl)naphthalene (0.45 g) in propan-2-ol (2 mL) was stood for 3 days at 25 °C. The gradual addition of diethyl ether (ca. 50 mL) caused the crude product to precipitate as a white solid, which after recrystallization from ethanol–diethyl ether mixture formed white prisms: mp 134–136 °C (1.11 g, 93%); $[\alpha]_D -78.2^\circ$ (*c* 0.966, CH₂Cl₂); ¹H NMR (100 MHz in CDCl₃) δ 1.25 (s, 3 H, MeAs), 2.43 (br s, 1 H, 0.5 H₂O), 2.64 (s, 3 H, MeAs⁺), 5.33, 5.70 (ABq, *J* = 17 Hz, 2 H, α -C₁₀H₇CH₂As⁺), 6.9–8.1 (br m, 21 H, aromatics).

(-)-(*R*)-Benzylmethylphenyl(8-quinolyarsonium Bromide ((-)-(*R*)-5). A solution of (+)-(*S*)-methylphenyl-8-quinolyarsine (1.25 g) and benzyl bromide (1.5 mL) in propan-2-ol was set aside for 2 h and then diluted with benzene (20 mL). The solid which precipitated was filtered off, washed with diethyl ether, and recrystallized from ethanol–diethyl ether mixture. The pure bromide formed colorless needles: mp 186–187 °C (1.97 g, 99%); $[\alpha]_D -3.2^\circ$ (*c* 0.696, EtOH); ¹H NMR (100 MHz in CDCl₃) δ 2.68 (s, 3 H, MeAs⁺), 5.04, 5.15 (ABq, *J* = 13 Hz, 2 H, CH₂Ph), 7.05–9.10 (br m, 16 H, aromatics).

Synthesis of Oxiranes. In general, an equilibrium concentration of the appropriate ylide in ethanol was generated from the respective arsonium salt (by use of lithium or sodium ethoxide) in the presence of the aromatic aldehyde. The reaction was allowed to proceed for 18 h at 25 °C. At this stage, the solvent was removed and the products extracted into dichloromethane. The organic layer was washed with water, dried (MgSO₄), concentrated, and transferred to a column of basic alumina (Activity 3). Petroleum ether eluted the optically pure tertiary arsine and petroleum ether–chloroform (ca. 10:1) the oxirane. The preparation of *trans*-2,3-diphenyloxirane from the arsonium salts containing asymmetric arsenic atoms is given in detail below to illustrate the reaction procedure. The results are summarized in Table I. The preparation and isolation of the substituted *trans*-2,3-diaryloxiranes listed in Table II were conducted similarly. The products were identified by comparison of their physical and spectroscopic properties with authentic material.

(+)-(*RR*)-*trans*-2,3-Diphenyloxirane. From (-)-(*RS*)-6a and Benzaldehyde. To a solution of sodium ethoxide (from 0.055 g of Na (2.4 mmol)) in ethanol (20 mL) was added (-)-(*RS*)-6a-0.5H₂O (1.12 g, 1.9 mmol). Benzaldehyde (0.21 g, 1.98 mmol) was then added to the pale yellow solution of the ylide and the reaction mixture stirred for 18 h at 25 °C. The solvent was then removed by distillation (20 mmHg, 40 °C) and the residual oil dissolved in dichloromethane. After being washed with water and subsequent drying, the organic layer was taken to dryness. ¹H NMR spectroscopy of the residue indicated *trans*-2,3-diphenyloxirane and the bis(tertiary arsine) 1 as the only products. Column chromatography of the mixture on the basic alumina (Activity 3) gave first, by elution with petroleum ether (-)-(*SS*)-1 (0.72 g, 92%), $[\alpha]_D -94.4^\circ$ (*c* 0.21, CH₂Cl₂), and second, with petroleum ether–chloroform (10:1), the *trans*-oxirane (0.327 g, 88%), $[\alpha]_D +54.9^\circ$ (*c* 0.61, Me₂CO).

From (+)-(*R*)-4a and Benzaldehyde. Solid (+)-(*R*)-4a (0.70 g, 1.48 mmol) was added to a solution of sodium ethoxide (from 0.04 g of Na (1.74 mmol)) and benzaldehyde (0.16 g, 1.51 mmol) in ethanol (20 mL). The pale orange solution was then stirred for 18 h at 25 °C and worked up as described above. Petroleum ether eluted (-)-(*S*)-methyl- α -naphthyl-*p*-tolylarsine (0.40 g, 88%), $[\alpha]_D -115.9^\circ$ (*c* 0.593, CHCl₃), and light petroleum–chloroform, the *trans*-oxirane (0.25 g, 86%), $[\alpha]_D +24.2^\circ$ (*c* 0.67, Me₂CO).

From (-)-(*R*)-5 and Benzaldehyde. Use of (-)-(*R*)-5 (1.0 g, 2.14 mmol) as the ylide precursor and benzaldehyde (0.312 g, 2.94 mmol) as the substrate in the presence of sodium ethoxide (from 0.065 g Na (2.82 mmol)) under the usual conditions gave (+)-(*RR*)-*trans*-2,3-diphenyloxirane (0.395 g, 94%), $[\alpha]_D +22.6^\circ$ (*c* 0.60, Me₂CO), and (+)-(*S*)-methylphenyl-8-quinolyarsine (0.59 g, 93%), $[\alpha]_D +110^\circ$ (*c* 1.4, diethyl ether).

Table II. Effect of Substitution on Yields of *trans*-Ar¹CH-CHOAr²

salt	substrate	base	product		specific rotation, ^a deg	yield		
			Ar ¹	Ar ²		chemical ^a	optical	configuratr ⁿ
3	<i>p</i> -MeC ₆ H ₄ CHO	NaOEt	Ph	<i>p</i> -MeC ₆ H ₄	+86.3	58	23 ^d	2 <i>R</i> ,3 <i>R</i>
(<i>RS</i>)-6a	<i>p</i> -MeC ₆ H ₄ CHO	NaOEt	Ph	<i>p</i> -MeC ₆ H ₄	+71.0	84	19 ^d	2 <i>R</i> ,3 <i>R</i>
(<i>RS</i>)-6b	C ₆ H ₅ CHO	NaOEt	Ph	<i>p</i> -MeC ₆ H ₄	+57.0	71	15 ^d	2 <i>R</i> ,3 <i>R</i>
3	<i>p</i> -ClC ₆ H ₄ CHO	NaOEt	Ph	<i>p</i> -ClC ₆ H ₄	+76.2	56	21 ^d	2 <i>R</i> ,3 <i>R</i>
(<i>RS</i>)-6a	<i>p</i> -ClC ₆ H ₄ CHO	NaOEt	Ph	<i>p</i> -ClC ₆ H ₄	+56.4	79	16 ^d	2 <i>R</i> ,3 <i>R</i>
3	<i>p</i> -O ₂ NC ₆ H ₄ CHO	NaOEt	Ph	<i>p</i> -O ₂ NC ₆ H ₄	+45.0	68	16 ^d	2 <i>R</i> ,3 <i>R</i>
(<i>RS</i>)-6a	<i>p</i> -O ₂ NC ₆ H ₄ CHO	NaOEt	Ph	<i>p</i> -O ₂ NC ₆ H ₄	+18.1	75	7 ^d	2 <i>R</i> ,3 <i>R</i>
3	<i>o</i> -O ₂ NC ₆ H ₄ CHO	NaOEt	Ph	<i>o</i> -O ₂ NC ₆ H ₄	+91.4	57	<i>f</i>	<i>g</i>
(<i>RS</i>)-6a	<i>o</i> -O ₂ NC ₆ H ₄ CHO	NaOEt	Ph	<i>o</i> -O ₂ NC ₆ H ₄	+45.3	80	<i>f</i>	<i>g</i>
3	<i>o</i> -MeOC ₆ H ₄ CHO	NaOEt	Ph	<i>o</i> -MeOC ₆ H ₄	+39.3	88	22 ^e	<i>g</i>
(<i>RS</i>)-6a	<i>o</i> -MeOC ₆ H ₄ CHO	NaOEt	Ph	<i>o</i> -MeOC ₆ H ₄	+30.8	80	18 ^e	<i>g</i>
(<i>RS</i>)-6a	<i>o</i> -MeOC ₆ H ₄ CHO	LiOEt	Ph	<i>o</i> -MeOC ₆ H ₄	+33.3	73	19 ^e	<i>g</i>
(<i>RS</i>)-6c	C ₆ H ₅ CHO	NaOEt	Ph	<i>o</i> -MeOC ₆ H ₄	+50.7	76	29 ^e	<i>g</i>
(<i>RS</i>)-6c	<i>o</i> -MeOC ₆ H ₄ CHO	NaOEt	<i>o</i> -MeOC ₆ H ₄	<i>o</i> -MeOC ₆ H ₄	+8.8	78	38 ^e	<i>g</i>
(<i>RS</i>)-6c	<i>o</i> -MeOC ₆ H ₄ CHO	LiOEt	<i>o</i> -MeOC ₆ H ₄	<i>o</i> -MeOC ₆ H ₄	+9.5	67	41 ^e	<i>g</i>
(<i>RS</i>)-6d	<i>o</i> -ClC ₆ H ₄ CHO	NaOEt	<i>o</i> -ClC ₆ H ₄	<i>o</i> -ClC ₆ H ₄	+0.5	50	<i>f</i>	<i>g</i>
(<i>RS</i>)-6e	α -C ₁₀ H ₇ CHO	NaOEt	α -Np	α -Np	-22.9	56	<i>f</i>	<i>g</i>

^a Values of $[\alpha]_D^{20}$ (*c* 1.0, EtOH) except for reference compounds,^d where reported concentrations were used for comparison. ^b Reactions performed in ethanol at 25 °C. ^c Yields of isolated products after column chromatography on basic alumina. ^d Calculated on the basis of the following specific rotations reported for optically pure compounds: (2*S*,3*S*)-2-(*p*-tolyl)-3-phenyloxirane, $[\alpha]_D^{-380}$ (*c* 0.16, EtOH);²³ (2*R*,3*R*)-2-(*p*-chlorophenyl)-3-phenyloxirane, $[\alpha]_D + 362$ (*c* 1.36, EtOH);²⁴ (2*R*,3*R*)-2-(*p*-nitrophenyl)-3-phenyloxirane, $[\alpha]_D + 278$ (*c* 1.01, EtOH);²⁴ ^e Determined from ¹H NMR spectra in CDCl₃ in the presence of tris[trifluoroacetyl-(+)-camphorato]europium(III). ^f Method *e* unsatisfactory due to insufficient resolution of methine protons. ^g Assumed to be 2*R*,3*R*.

Reaction of the Benzyldiene Ylides with Substituted Aromatic Aldehydes. The substituted *trans*-2,3-diaryloxiranes were prepared by use of equivalent quantities of the optically active arsonium salts and the appropriate aromatic aldehyde in the presence of lithium or sodium ethoxide in ethanol solution under similar conditions to those described above. The identity of known products was confirmed by comparison of the melting points and ¹H NMR spectra with those reported in the literature. However, the following are new compounds. (***RR,SS***)-*trans*-2-(*o*-Methoxyphenyl)-3-phenyloxirane: colorless oil; bp 126–128 °C (0.05 mmHg); ¹H NMR (100 MHz in CDCl₃) δ 3.79 (br s, 4 H, OMe and oxirane CH), 4.26 (d, *J* = 2 Hz, 1 H, oxirane CH), 6.8–7.4 (br m, 9 H, aromatics). (***RR,SS***)-*trans*-2,3-Bis-(*o*-methoxyphenyl)oxirane: colorless needles; mp 158–159 °C; ¹H NMR (90 MHz in CDCl₃) δ 3.78 (s, 6 H, OMe), 4.18 (s, 2 H, oxirane CH), 6.7–7.4 (br m, 8 H, aromatics). The enantiomeric excesses of *trans*-2-(*o*-methoxyphenyl)-3-phenyloxirane and *trans*-2,3-bis(*o*-methoxyphenyl)oxirane were determined by use of the optically active shift reagent tris[trifluoroacetyl-(+)-camphorato]europium(III). The NMR shifts observed were small, and the method was not suitable for the determination of the enantiomeric excesses of *trans*-2-(*o*-nitrophenyl)-3-phenyloxirane, *trans*-2,3-bis(*o*-chlorophenyl)oxirane, or *trans*-2,3-bis(α -naphthyl)oxirane.

***trans*-2-Phenylcyclopropanecarboxylic Acid.** A suspension of the salt 3 (1.55 g, 2.78 mmol) and potassium hydride (0.23 g, 5.7 mmol) in tetrahydrofuran (35 mL) was stirred for 10 min at 25 °C. Methyl acrylate (0.25 g, 3.32 mmol) was then added to the orange solution of the ylide and the reaction mixture stirred for 18 h. Methanol was then added to destroy the excess of hydride, and the solvents were removed by distillation under reduced pressure. The residue was thoroughly extracted into dichloromethane and the extract washed with water, dried (MgSO₄), and evaporated to dryness. At this stage the residue was heated under reflux for 4 h in a mixture of sodium hydroxide (0.6 g), water (1 mL), and ethanol (12 mL) to hydrolyze the ester. Evaporation of the mixture, followed by extraction of the residue with dichloromethane, drying (MgSO₄), and reevaporation pro-

duced a residue of which was then transferred to a column of basic alumina (Activity 3) for purification by elution with petroleum ether. Acidification of the aqueous layer, followed by extraction with diethyl ether, gave the cyclopropanecarboxylic acid as an oil (0.42 g, 90%), $[\alpha]_D + 17.8$ ° (*c* 0.98, CHCl₃) (lit.¹⁹ $[\alpha]_D - 368$ °). Use of (-)-(*RS*)-6a as the ylide precursor gave the compound in 68% yield, $[\alpha]_D - 93$ ° (*c* 0.90, CHCl₃).

Acknowledgment. The assistance of Mr. P. Gugger in certain aspects of this work is gratefully acknowledged.

Registry No. (+)-1, 83845-71-0; (-)-2, 83845-72-1; 3 (isomer 1), 83845-73-2; 3 (isomer 2), 83845-74-3; (+)-(*R*)-4a, 83845-75-4; (+)-(*R*)-4b, 83915-69-9; (-)-(*R*)-5, 83845-77-6; (+)-(*S*)-5, 83845-78-7; (*RS*)-6a, 83845-79-8; (*SR*)-6a, 67842-82-4; (*RS*)-6b, 83845-80-1; (*RS*)-6c, 83845-81-2; (*SR*)-6c, 67746-52-5; (*RS*)-6d, 83845-82-3; (*RS*)-6e, 83845-83-4; *p*-CH₃C₆H₄CH₂Br, 104-81-4; *o*-CH₃OC₆H₄CH₂Br, 52289-93-7; *o*-ClC₆H₄CH₂Br, 611-17-6; *p*-CH₃C₆H₄CHO, 104-87-0; *o*-CH₃OC₆H₄CHO, 123-11-5; α -C₁₀H₇CHO, 66-77-3; C₆H₅CH₂Br, 100-39-0; α -C₁₀H₇CH₂Br, 3163-27-7; *p*-ClC₆H₄CHO, 104-88-1; *p*-O₂NC₆H₄CHO, 555-16-8; *o*-O₂NC₆H₄CHO, 552-89-6; *o*-ClC₆H₄CHO, 89-98-5; PhCHO, 100-52-7; (-)-(*SS*)-*o*-phenylenebis(methylphenylarsine), 57341-01-2; (+)-(*S*)-methylphenyl-8-quinolylarsine, 80183-99-9; (2*S*,3*S*)-2,3-diphenyloxirane, 40102-60-1; (2*R*,3*R*)-2-(*p*-tolyl)-3-phenyloxirane, 70332-46-6; (2*R*,3*R*)-2-(*p*-chlorophenyl)-3-phenyloxirane, 62137-66-0; (2*R*,3*R*)-2-(*p*-nitrophenyl)-3-phenyloxirane, 70332-48-8; (2*R*,3*R*)-2-(*o*-nitrophenyl)-3-phenyloxirane, 83915-70-2; (2*R*,3*R*)-2-(*o*-methoxyphenyl)-3-phenyloxirane, 83845-84-5; (2*R*,3*R*)-2,3-bis(*o*-methoxyphenyl)oxirane, 83915-71-3; (2*R*,3*R*)-2,3-bis(*o*-chlorophenyl)oxirane, 83915-72-4; (2*R*,3*R*)-2,3-bis(α -naphthyl)oxirane, 83915-73-5; (-)-(*S*)-methyl- α -naphthyl-*p*-tolylarsine, 83845-85-6; (+)-(*S*)-methylphenyl-8-quinolylarsine, 80183-99-9; potassium diphenylarsenide, 21498-51-1; (-)-menthyl chloride, 16052-42-9; lithium diphenylarsenide, 19061-48-4; sodium diphenylarsenide, 41006-64-8; (2*R*,3*R*)-2,3-diphenyloxirane, 25144-18-7; (-)-*trans*-2-phenylcyclopropanecarboxylic acid, 3471-10-1; methyl acrylate, 96-33-3.

Stereoselective Syntheses of Some Cyclohexene Derivatives Using Complexes of Molybdenum

J. W. Faller,* H. H. Murray, D. L. White, and K. H. Chao

Department of Chemistry, Yale University, New Haven, Connecticut 06511

Received July 6, 1982

Substituted cyclohexene derivatives have been obtained by sequential nucleophilic addition and hydride abstraction reactions on the (η^4 -cyclohexa-1,3-diene)molybdenum cation $[\text{CpMo}(\text{CO})_2(\eta^4\text{-C}_6\text{H}_8)]^+$. An unusual η^3 -bicyclo[4.3.0]allyl complex has been obtained from an intramolecular nucleophilic ring closure reaction. Methods of removing substituted olefins and allyls from the metal center without isomerization of the double bond are also presented. The structure of $\text{CpMo}(\text{CO})_2(\eta^3\text{-C}_6\text{H}_8)$ has been studied by ^1H NMR and X-ray crystallographic analysis. Crystal data: space group $P2_1/n$; $a = 8.586$ (3) Å, $b = 9.063$ (1) Å, $c = 15.353$ (2) Å; $\beta = 97.38$ (1)°; $V = 1184.8$ (7) Å³; M_r , 298.20; $Z = 4$; ρ (calcd) = 1.672 g cm⁻³. For 1809 reflections ($F^2 \geq 3.0\sigma(F^2)$), $R_1 = 0.024$ and $R_2 = 0.025$.

Introduction

The ability to alkylate allylic sites of olefins while controlling the stereochemistry of the product has been a subject of continuing interest to synthetic chemists. Many approaches^{1,2} (allylic halogenation followed by coupling with an organometallic reagent or lithiation followed by the addition of alkylating agents or appropriately functionalized groups) give allylic carbon-carbon bond formation but often lack an ability to control the stereochemistry of the product.

A very effective approach that allows substantial opportunity for control of stereochemistry utilizes the activation of olefin attending conversion to an organometallic allyl complex. The electrophilicity of the allyl functionality can be further enhanced by making the complex cationic.^{3,4} In the final step a nucleophile is added to the allyl complex forming an olefin complex. Due to steric constraints or electronic polarizations⁵ in the complexed allyl cation, high stereoselectivity can often be obtained in these reactions.

In view of the moderate cost of molybdenum precursors compared with the noble metals and owing to the versatility of cyclopentadienylmolybdenum complexes in accommodating allyl, olefin, and diene moieties, we have investigated their use in the stereoselective syntheses of some model cyclohexene derivatives. The binding of the cyclohexene moiety (as an allyl or diene) to molybdenum metal centers activates otherwise unreactive carbon centers and allows the formation of carbon-carbon bonds with a high degree of stereoselectivity.

Using these methods, we have effected several stereoselective syntheses of substituted cyclohexene complexes. These studies have provided detailed information on the stereochemistry of the reactions and have also shown that the ligated olefin can be removed from the metal center without isomerization of the olefinic bond.

Experimental Section

All reactions were carried out in oven-dried (140 °C) glassware under dry nitrogen gas using standard inert atmosphere techniques. All solvents were dried before use. THF was distilled from sodium and benzophenone, and acetonitrile and dichloromethane were distilled from calcium hydride before use as reaction solvents. All NMR spectra were obtained on a Bruker HX-270

(270 MHz ^1H , 41.44 MHz ^2H) spectrometer. IR spectra were usually obtained on a Perkin-Elmer 237B grating spectrophotometer reference to the 1601-cm⁻¹ band of polystyrene. In certain cases IR spectra were obtained on a Nicolet 7199 FT-IR instrument, in which cases the frequencies are reported to the nearest 0.1 cm⁻¹. HPLC separations were carried out with Altex pumps and UV detection at 300 nm.

Syntheses. $\text{CpMo}(\text{CO})_2(\eta^3\text{-C}_6\text{H}_8)$. The $\text{CpMo}(\text{CO})_2(\eta^3\text{-C}_6\text{H}_8)$ complex was synthesized following Hayter's procedure for an analogous allyl.⁶ The allyl bromide needed for this synthesis was conveniently obtained by treatment of cyclohexene with *N*-bromosuccinimide.⁷

A 200-mL, three-neck, round-bottom flask equipped with a magnetic stirrer, reflux condenser, thermometer, and nitrogen inlet was charged with 10.0 g (37.9 mmol) of $\text{Mo}(\text{CO})_6$ (sublimed) and 40 mL of CH_3CN , and the resulting suspension was heated to reflux. After 5 h at reflux, the reaction mixture (a yellow solution) was treated with a solution of 6.1 g (37.9 mmol) of 3-bromo-1-cyclohexene in 10 mL of THF. A bright orange solid immediately precipitated. The reaction mixture was cooled to 0 °C, and the supernatant was decanted. The crystals were washed under nitrogen with two 10-mL portions of CH_3CN . The residual solvent was removed in vacuo at 25 °C to yield a 13.9 g (92.7%) of $[(\text{CH}_3\text{CN})_2\text{MoBr}(\eta^3\text{-C}_6\text{H}_9)(\text{CO})_2]$ as bright yellow crystals.

In the final step of the synthesis, lithium cyclopentadienide was added to the $[(\text{CH}_3\text{CN})_2\text{MoBr}(\eta^3\text{-C}_6\text{H}_9)(\text{CO})_2]$ giving the desired allyl product in 79.4% yield. Lithium cyclopentadienide was prepared from a solution of 0.69 g (10.4 mmol) of freshly distilled cyclopentadiene in 10 mL of THF by the addition of 6.9 mL of 1.6 *M* *n*-BuLi in hexane. The resulting suspension was added via syringe to a suspension of $[(\text{CH}_3\text{CN})_2\text{MoBr}(\eta^3\text{-C}_6\text{H}_9)(\text{CO})_2]$ in 25 mL of THF contained in a 100-mL, round-bottom flask equipped with a magnetic stirrer and a no-air stopper. The yellow starting material dissolved over about 15 min to form an orange solution. After the solution was stirred for 2 h at 25 °C, removal of the solvent on a rotary flash evaporator left an orange-red crystalline residue.

The crude orange-red product was dissolved in CH_2Cl_2 and chromatographed over a 2.5 × 12 cm column of alumina (Fisher Adsorption Grade). Removal of solvent from the yellow eluant gave 2.36 g (79.4%) of a yellow crystalline product. Recrystallization from pentane yielded a product: mp 95-95.5 °C; ^1H NMR (CDCl_3 , 25 °C) δ 5.29 (s, Cp), 3.68 (m, H(1) and H(3)), 4.16 (t, $J = 7.1$ Hz, H(2)), 1.91 (dddd, $J = 14.5, 11.5, 6.0, 1.8$ Hz, H(4 β) and H(6 β)), 1.67 (dddd, $J = 14.5, 6.8, 1.9, 0.2$ Hz, H(4 α) and H(6)), 0.96 (dddd, $J = 14.5, 6.0, 0.2$ Hz, H(5 β)), 0.33 (ddd, $J = 14.5, 11.5, 6.8$ Hz, H(5 α)). Carbonyl bands were observed in cyclohexane solution in the IR spectrum at 1947 and 1875 cm⁻¹. Anal. Calcd for $\text{C}_{13}\text{H}_{14}\text{MoO}_2$: C, 52.36; H, 4.72. Found: C, 52.21; H, 4.75. The

(1) B. M. Trost, P. E. Strege, L. Weber, T. J. Fullerton, and T. J. Dietsche. *J. Am. Chem. Soc.*, **100**, 3407 (1978).

(2) B. M. Trost. *Acc. Chem. Res.*, **13**, 385 (1980).

(3) D. A. White. *Organomet. Chem. Rev. Sect. A*, **3**, 497 (1968).

(4) J. W. Faller and A. M. Rosan. *J. Am. Chem. Soc.*, **98**, 3388 (1976).

(5) J. W. Faller. "Fundamental Research in Homogenous Catalysis", Vol. 2, Yoshio Ishii and Minoru Tsutsui, Eds., Plenum Press, New York, 1978, pp 117-24.

(6) R. G. Hayter. *J. Organomet. Chem.*, **13**, 1 (1968).

(7) H. J. Dauben, Jr., and L. L. McCoy, *J. Am. Chem. Soc.*, **81**, 4863-4873 (1959).

(8) The metal side of the ring is labeled alpha (α) and the non-metal side is labeled beta (β).

structure was confirmed by single-crystal X-ray diffraction analysis.

[CpMo(CO)₂(η⁴-C₆H₈)]⁺[PF₆]⁻. A 100-mL, three-neck, round-bottom flask equipped with a magnetic stirrer, nitrogen inlet, and addition funnel was charged with 2.85 g (9.56 mmol) of [CpMo(CO)₂(η³-C₆H₉)] and 20 mL of CH₂Cl₂. To this solution at 0 °C was added 3.62 g (9.32 mmol) of [Ph₃C]⁺[PF₆]⁻. The resulting brown-yellow suspension was stirred for 1 h at 0 °C. The solvent was reduced to about one-third of its previous volume in vacuo; the cation was precipitated by adding the solution to 200 mL of diethyl ether being agitated with gaseous nitrogen. The yellow precipitate was removed from the ether by centrifugation followed by decanting of the ether. The cation complex was washed with dry ether, giving 4.03 g (9.11 mmol) of [CpMo(CO)₂(η⁴-C₆H₈)]PF₆ in 97.5% yield as a yellow powder melting with decomposition above 300 °C: ¹H NMR (C₃D₈O, 25 °C) δ 6.15 (m, 2 H, H(1), H(4)), 6.05 (s, 5 H, Cp), 5.05 (m, 2 H, H(2), H(3)), 2.31 (d, 2 H, J = 13.2 Hz), 1.44 (d, 2 H, J = 13.3 Hz, H(5), H(6)). Carbonyl bands were observed in CH₂Cl₂ solution in the IR spectrum at 2017 and 1962 cm⁻¹. Anal. Calcd for C₁₃F₆H₁₃MoO₂P: C, 35.31; H, 2.96. Found: C, 35.16; H, 2.99.

CpMo(CO)₂(η³-C₆H₈-4-D). A 25 mL, three-neck flask equipped with a magnetic stirrer and nitrogen inlet was charged with 0.5 g (1.13 mmol) of [CpMo(CO)₂(η⁴-C₆H₈)]PF₆ and 10 mL of dry THF. The solution was cooled to 0 °C, and 0.074 g (1.13 mmol) of NaN₂CBD₃ was added. The reaction mixture was stirred for 30 min, and the solvent was then removed in vacuo.

The crude product was dissolved in CH₂Cl₂ and chromatographed on a column of alumina. Removal of the CH₂Cl₂ from the yellow eluant gave 0.28 g (0.97 mmol, 83%) of the yellow crystalline product: ²H NMR (CHCl₃, 25 °C) δ 1.90 (s, H(4), H(6)). The ¹H NMR spectrum and the solution IR spectrum of the monodeuterio complex compared well with the perprotio parent complex. The loss of vicinal J_{HH} coupling (11.5, 6.0 Hz) at the 5α and 5β resonances, loss of geminal J_{HH} coupling (14.5 Hz) at the 4α resonance, and decreased intensity of the 4β resonance were the major differences between the ¹H NMR spectra of the parent perprotio and the monodeuterio derivative.

CpMo(CO)₂(η³-C₆H₈-4-CH₃). A 25-mL, three-neck flask equipped with a magnetic stirrer and nitrogen inlet was charged with 0.86 g (1.94 mmol) of [CpMo(CO)₂(η⁴-C₆H₈)]PF₆ and 10 mL of freshly distilled THF. The suspension was cooled to 0 °C, and then 6.9 mL of 2.8 M CH₃MgBr (19.5 mmol) was added over a 5-min period. The reaction was stirred for 15 min at 0 °C, and the excess CH₃MgBr was then slowly quenched by dropwise addition of water. The solvent was then removed in vacuo, leaving a pale yellow solid. The neutral methylated complex was purified by extraction with CH₂Cl₂ and chromatography on silica. Removal of the CH₂Cl₂ from the yellow eluant gave 0.37 g (1.2 mmol, 61%) of CpMo(CO)₂(η³-C₆H₈-4-(CH₃)) as a bright yellow solid melting at 102–104 °C: ¹H NMR (CDCl₃, 25 °C) δ 5.28 (s, Cp), 4.14 (dd, 6.3, J = 5.8 Hz, H(2)), 3.71 (br d, J = 6.3 Hz, H(1)), 3.60 (br d, J = 5.8 Hz, H(3)), 2.03 (dddd, J = 15.0, 11.5, 6.1, 2.6 Hz, H(6β)), 1.91 (q, ddd, J = 7.1, 6.7, 2.9, 1.4 Hz, H(4α)), 1.58 (dddd, J = 15.0, 6.3, 3.4, 1.4 Hz, H(6α)), 1.15 (d, J = 7.1 Hz, methyl), 0.72 (dddd, J = 13.7, 6.1, 1.4, 1.4 Hz, H(5β)), 0.52 (dddd, J = 13.7, 11.5, 6.7, 6.3 Hz, H(5α)). The assignment of the H(6), H(4α), and H(5) protons were made on the basis of spin-decoupling experiments upon the ¹H NMR spectrum of the monodeuterio analogue. Carbonyl bands were observed in cyclohexane solution in the IR spectrum at 1951 and 1877 cm⁻¹. Anal. Calcd for C₁₄H₁₆MoO₂: C, 54.03; H, 5.17. Found: C, 53.98; H, 5.19.

[CpMo(CO)₂(η⁴-C₆H₇(CH₃))]PF₆. A 25-mL, three-neck, round bottom flask equipped with a magnetic stirrer and a nitrogen inlet was charged with 0.37 g (1.2 mmol) of CpMo(CO)₂(η³-C₆H₈(CH₃)) and 10 mL of freshly distilled CH₂Cl₂. The resulting solution was cooled to 0 °C and then treated with 0.46 g (1.2 mmol) of (C₆H₅)₃CPF₆. The reaction was stirred at 0 °C for 75 min, and about half of the CH₂Cl₂ solvent was removed in vacuo. The concentrated reaction mixture was then added dropwise to dry ether being agitated with gaseous nitrogen. The yellow precipitate was centrifuged and the ether decanted. The cation was washed once with dry ether, yielding 0.47 g (1.0 mmol, 86%) of the cation, a yellow solid melting with decomposition above 300 °C: ¹H NMR (C₃D₈O, 25 °C) δ 6.22 and 6.09 (both m, H(1) and H(4)), 6.04 (s, Cp), 4.87 and 4.82 (both m, H(2) and H(3)),

3.38 (q, H(5α)), 2.09 and 1.94 (both d, H(6α) and H(6β)), 1.11 (d, methyl). Carbonyl bands were observed in CH₂Cl₂ at 2018 and 1963 cm⁻¹.

CpMo(CO)₂(η³-C₆H₇(CH₃)). A 25-mL, three-neck flask equipped with a magnetic stirrer and a nitrogen inlet was charged with 10 mL of freshly distilled THF and 470 mg (1.0 mmol) of [CpMo(CO)₂(η³-C₆H₇(CH₃))]PF₆. The temperature of the reaction flask was lowered to 0 °C, and 3.6 mL of 2.8 M (10 mmol) of CH₃MgBr was added over a 5-min period. The reaction was stirred for 15 min at 0 °C, 6 drops of distilled water were slowly added to quench the excess of Grignard, and then the solvent was removed in vacuo. The neutral yellow product was extracted with dry CH₂Cl₂ and chromatographed on silica with CH₂Cl₂. Removal of the solvent gave 122 mg (0.37 mmol, 27% yield) of the disubstituted allyl complex as a yellow solid melting at 112–113 °C: ¹H NMR (CDCl₃, 25 °C) δ 5.28 (s, Cp), 4.16 (t, J = 7.1 Hz, H(2)), 3.70 (d, J = 7.1 Hz, H(1) and H(3)), 1.92 (dddd, J = 7.1, 6.9, 3.0, 2.5 Hz, H(4β) and H(6β)), 1.23 (d, J = 6.9 Hz, Me), 0.85 (dt, J = 14.3, 7.1 Hz, H(5α)), 0.59 (dt, J = 14.3, 3.0 Hz, H(5β)). Carbonyl bands were observed in CH₂Cl₂ at 1958 and 1884 cm⁻¹. Anal. Calcd for C₁₅H₁₆MoO₂: C, 55.22; H, 5.55. Found: C, 54.12; H, 5.82.

CpMo(CO)₂(η³-C₆H₈(C(CH₃)₂CHO)). A 15-mL, pear-shaped flask equipped with a magnetic stirrer and nitrogen inlet was charged with 960 mg (2.5 mmol) of [(η⁵-CpMo(CO)₂(η⁴-C₆H₈)]⁺[BF₄]⁻ and 5 mL of CH₃CN. This suspension was treated with 0.40 mL (370 mg, 3.0 mmol) of (2-methyl-1-propenyl)-1-pyrrolidine at 0 °C. After being stirred for 30 min at 0 °C, the reaction mixture was hydrolyzed with 10 mL of water. The resulting tan precipitate was isolated by filtration and dissolved in CH₂Cl₂, and the solution was dried over anhydrous Na₂SO₄. The product was purified by chromatography on a 4.5 × 10 cm column of silica gel with CH₂Cl₂. The major yellow band was isolated, the solvent was removed, and the yellow solute was recrystallized from 15 mL of pentane to yield 610 mg (66%) of product, melting at 131–132 °C: ¹H NMR (CDCl₃, 25 °C) δ 0.44 (m, 1 H, H(5)), 0.84 (d², J = 6.0, 14.0 Hz, 1 H, H(5)), 1.13 (d, J = 7.0 Hz, 6 H), 1.57 (m, 1 H), 1.87 (m, 1 H), 1.98 (approximately d, J = 7.5 Hz, 1 H); 3.36 (approximately d, J = 7.3 Hz, 1 H, allyl-1- or -3-H), 3.69 (m, 1 H, allyl-3- or -1-H), 4.34 (t, J = 7.2 Hz, 1 H, allyl-2-H), 5.31 (s, 5 H, Cp), 9.53 (s, 1 H, CHO); IR (cyclohexane) 1949.3, 1876.9, 1733.0 cm⁻¹ (aldehyde). Anal. Calcd for C₁₇H₂₀MoO₃: C, 55.44; H, 5.47. Found: C, 55.47; H, 5.51.

[CpMo(CO)₂(η³-C₆H₈-4-C(CH₃)₂CH₂OH)]. A 35-mL, pear-shaped flask equipped with a magnetic stirrer and nitrogen inlet was charged with 0.368 g (1.00 mmol) of [CpMo(CO)₂(η³-C₆H₈-4-C(CH₃)₂CHO)] and 15 mL of THF. This solution was treated with 150 mg (approximately 6 mmol at 89% purity) of LiBH₄ and then stirred for 1 h at 25 °C. TLC on silica gel with CH₂Cl₂ indicated that no starting material (R_f = 0.54) remained, and only product (R_f = 0.20) was present. The reaction mixture was hydrolyzed with 5 mL of water, the layers were separated, and the aqueous layer was extracted with CH₂Cl₂. The combined organic phases were dried over anhydrous Na₂SO₄, and the solvent was removed on a rotary flash evaporator. The resulting yellow solid was recrystallized from 20 mL of 50/50 CH₂Cl₂-pentane to yield 0.33 g (89%) of crystalline product: mp 172 °C dec; ¹H NMR (CDCl₃, 25 °C) δ 0.42 (m, 1 H, H(4)), 0.98 (s, 6 H, CH₃), 1.05 (t, J = 7.0 Hz, 1 H), 1.56 (s, 1 H), 1.59 (m, 1 H), 1.77 (d³, J = 1.1, 1.5, 7.7 Hz, 1 H), 1.99 (m, 1 H), "δ" 3.49 (AB, Δν = 0.19 ppm, J = 1.1 Hz, 2 H, OCH₂), 3.68 (approximately d, J = 7.3 Hz, 1 H, allyl-1-H or -3-H), 3.74 (approximately d, J = 7.3 Hz, 1 H, allyl-3-H or -1-H), 4.36 (t, J = 7.35 Hz, allyl-2-H), 5.31 (s, 5 H, Cp); IR (cyclohexane) 1873.8, 1948.2 cm⁻¹. Anal. Calcd for C₁₇H₂₂MoO₃: C, 55.14; H, 5.99. Found: C, 55.10; H, 6.02.

[CpMo(CO)₂(η³-9,9-dimethyl-7-oxabicyclo[4.3.0]nonenyl)]. A solution of 118 mg (0.357 mmol) of Ph₃C⁺(BF₄)⁻ in 3 mL of CH₃CN was prepared under a nitrogen atmosphere and added to a solution of 132 mg (0.357 mmol) of [CpMo(CO)₂(η³-C₆H₈-4-C(CH₃)₂CH₂OH)] in 1 mL of CH₃CN. The yellow solution immediately turned orange. It was stirred at room temperature for 1.5 h. (A small quantity of white crystals were observed in the reaction mixture after about 15 min.) Then 55 mL (40 mg, 0.39 mmol) of Et₃N was added to the reaction mixture, and it was stirred for an additional hour at 25 °C. The white solid was then isolated by filtration and dried in vacuo at 25 °C to yield 12 mg

of apparently polymeric material, insoluble in either acetone or water, derived from Ph_3CH (IR absorptions at 3100–3000, 1592 (m), and 1482 (s) cm^{-1}).

Solvent was removed from the filtrate on a rotary flash evaporator, and the residue was dissolved in CH_2Cl_2 , and chromatography on a 9×230 mm column of type 60/E alumina (E. Merck) with CHCl_3 (containing 0.75% EtOH as preservative) eluted a minor red, air-unstable byproduct ($k' = 0$) of unknown composition, a yellow band ($k' = 0.5$) containing the desired product plus other components, and a broad yellow band ($k' = 1.4$ – 1.6) containing unreacted starting material and other components.

The first yellow band described above was rechromatographed on 9×230 mm of Silica Gel H (E. Merck) using 75/25 (v/v) CHCl_3 -hexane. The initial band ($k' = 0.1$) was collected and purified by chromatography on a like column using hexane. The material eluting at $k' = 4.6$ was homogeneous by TLC on both alumina and silica gel. A total of 5 mg (2.5%) was obtained, identified as the trityl ether of the starting material $\text{CpMo}(\text{CO})_2[\eta^3\text{-C}_6\text{H}_8\text{-4-C}(\text{CH}_3)_2\text{CH}_2\text{OC}(\text{C}_6\text{H}_5)_3]$, on the basis of its NMR data: (CDCl_3 , 270 MHz, 25 °C) δ 0.28 (m, 1 H, H(5)), 0.94 (s, 3 H, CH_3), 1.08 (s, 3 H, CH_3), 0.94 (m, 1 H, H(5)), 1.55 (m, 1 H, H(6)), 1.78 (m, 1 H, H(6)), 2.07 (d^2 , $J = 2.5, 8.0$ Hz, 1 H, H(4)), "d" 2.90 (AB quartet, $\Delta\nu = 0.11$ ppm, $J = 9$ Hz, 2 H, OCH_2), 3.31 (approximately d, $J = 7.3$ Hz, 1 H, H(3)), 3.63 (approximately d^2 , $J = 2$ Hz, 7 Hz, 1 H, H(1)), 4.07 (t, $J = 7.3$ Hz, 1 H, H(2)), 5.23 (s, 5 H, Cp), 7.28 (m, 9 H, Ar), 7.46 (m, 6 H, Ar).

A second yellow product ($k' = 4.8$) was obtained from the Silica Gel H/75/25 CHCl_3 -hexane system. A total of 22 mg (18% yield, 10% conversion) was obtained, which was homogeneous by TLC on both silica gel and alumina. Recrystallization from cyclohexane gave analytically pure material: mp 180 °C dec; NMR (CDCl_3 , 270 MHz, 25 °C) δ 0.74 (d^3 , $J_{5\alpha-4\alpha} = 4.85$, $J_{5\alpha-6\alpha} = 7.8$, $J_{5\alpha-6\beta} = 9.8$ Hz, 1 H, H(5 α)), 0.85 (s, 3 H, CH_3), 1.00 (s, 3 H, CH_3), 1.79 (approximately d^3 , $J_{2-6\alpha} = 1.4$, $J_{1-6\alpha} = 3.2$, $J_{6\alpha-6\beta} = 14.5$, $J_{6\alpha-5\alpha} = 7.8$ Hz, 1 H, H(6 α)), 1.91 (approximately d^3 , $J_{2-6\beta} = 1.4$, $J_{1-6\beta} = 2.5$, $J_{6\alpha-6\beta} = 14.5$, $J_{5\alpha-6\beta} = 9.8$ Hz, 1 H, H(6 β)), "d" 3.57 (ABq, $\Delta\nu = 0.15$ ppm, $J = 7.5$ Hz, 2 H, OCH_2), 3.69 (d^3 , $J_{3-2} = 6.1$, $J_{3-4\alpha} = 3.4$, $J_{3-1} = 1.9$ Hz, 1 H, H(3)), 3.89 (approximately d (q), $J_{1-2} = 6.1$, $J_{1-6\alpha} = 3.2$, $J_{1-6\beta} = 2.5$ Hz, 1 H, H(1)); δ 4.31 (approximately t, $J_{2-3} = 6.9$, $J_{2-1} = 6.1$, $J_{2-6\alpha} = 1.4$, $J_{2-6\beta} = 1.4$ Hz, 1 H, H(2)); 4.44 (approximately t, $J_{3-4\alpha} = 3.4$, $J_{5\alpha-4\alpha} = 4.85$ Hz, 1 H, H(4 α)), 5.31 (s, 5 H, Cp); IR (cyclohexane) 1948, 1874 cm^{-1} ; mass spectrum, m/e (relative intensity) (370 M^+ , 6.4), 3.42 ($\text{M}^+ - \text{CO}$, 13.0), 3.14 ($\text{M}^+ - 2\text{CO}$ s, 37.3). Anal. Calcd for $\text{C}_{17}\text{H}_{20}\text{MoO}_3$: C, 55.44; H, 5.47. Found: C, 55.18; H, 5.38. The structure was confirmed by single-crystal X-ray diffraction analysis.

The last yellow band ($k' = 1.4$ – 1.6) from the original alumina/ CHCl_3 chromatography was rechromatographed on Silica Gel H with CHCl_3 to give 12 mg (9.1% recovery) of unreacted starting material ($k' = 1.2$), identified by its NMR spectrum. This material had a camphor like odor, and additional resonances in the alkyl region of its NMR that were indicative of the presence of free ligand (see below).

In a second preparation of the title compound, the CH_3CN was removed from the reaction mixture on a rotary flash evaporator. The residue then was extracted with pentane, and the extract was examined by GC-MS [6 ft \times $\frac{1}{8}$ in. UC-W98 column; 5 min at 150 °C, 150–200 °C at 30°/min]. A component with retention time 3.7 min was identified as 9,9-dimethyl-7-oxabicyclo[4.3.0]-nonene: mass spectrum, m/e (relative intensity) 153.2 (5.5), 152.2 (49.5, M^+), 151.2 (11.5), 138.1 (1.0), 137.1 (11.1, ($\text{M} - \text{CH}_3$), 129.2 (2.0), 124.1 (24.5), 123.2 (3.2, $\text{M}^+ - \text{CH}_4$), 111.2 (2.4), 110.2 (7.8), 109.1 (100), 107.2 (10.9, $\text{M} - \text{C}_3\text{H}_6$). Calcd for $\text{C}_{10}\text{H}_{16}\text{O}$: ($\text{M} + 1$)/ M , 11.08%. Found: 11.11%.

A second component with a 5.6-min retention time was identified as 3- or 4-(1,1-dimethyl-2-hydroxyethyl)-1-cyclohexene: mass spectrum, m/e (relative intensity) 155.2 (0.5), 154.2 (4.2, M^+), 137.2 (2.9), 136.1 (26.7, $\text{M}^+ - \text{H}_2\text{O}$), 124.2 (3.1), 123.2 (27.0), 122.2 (2.7), 121.2 (13.0), 119.2 (0.9, $\text{M} - \text{CH}_3\text{O}^+$), 109.1 (1.7), 108.2 (10.4), 107.2 (73.0), 105.1 (4.1, $\text{M} - \text{C}_2\text{H}_5\text{ON}^+$), 4.1 (7.2), 95.2 (6.9), 93.1 (13.0), 92.1 (2.3), 9.1 (12.0, $\text{M} - \text{C}_2\text{H}_5\text{ON}^+$).

[$\text{CpMo}(\text{CO})(\text{NO})(\eta^3\text{-C}_6\text{H}_9)]^+[\text{PF}_6]^-$. A 25-mL flask equipped with a magnetic stirrer and nitrogen inlet was charged with 370 mg (1.24 mmol) of $(\eta^5\text{-C}_5\text{H}_5)\text{Mo}(\text{CO})_2(\eta^3\text{-C}_6\text{H}_9)$ and 5 mL of CH_3CN . The resulting solution was cooled to 0 °C and treated

Table I. TLC Data (R_f)

	$\text{Al}_2\text{O}_3/\text{CHCl}_3$ -hexane ^a	silica gel/ CHCl_3
$\text{CpMo}(\text{CO})_2(\text{C}_6\text{H}_8\text{-C}(\text{CH}_3)_2\text{CH}_2\text{OH})$	0.38	0.0
$\text{CpMo}(\text{CO})_2(\text{C}_6\text{H}_8\text{-C}(\text{CH}_3)_2\text{CH}_2\text{OCPh}_3)$	0.76	0.76
$\text{CpMo}(\text{CO})_2(\text{C}_6\text{H}_8\text{-C}(\text{CH}_3)_2\text{CH}_2\text{-O})$	0.11	0.12
Ph_3CH	0.11	0.37

^a CHCl_3 -hexane ratio is 50/50.

with 217 mg (1.24 mmol) of NOPF_6 . Foaming occurred, and the solution turned dark brown. The reaction mixture was added via syringe to 40 mL of anhydrous ether under nitrogen. A dark brown tarry mass separated and solidified upon cooling in an ice bath. The supernatant was removed via syringe, and the precipitate was washed with two 10-mL portions of ether. Drying in vacuo yielded 0.43 g (75%) of crude product, a red-brown powder.

The ^1H NMR spectrum ($(\text{C}_6\text{D}_6\text{O})$, 25 °C) of this product indicated that it was a mixture of endo and exo isomers. Two cyclopentadienyl resonances were observed at 6.34 and 6.04 ppm (5:2), as well as a major central allyl triplet at 5.59 ppm ($J = 7.0$ Hz), two major terminal allyl multiplets at 5.01 and 6.69 ppm, and two minor ones at 5.90 and 6.13 ppm. The minor allyl triplet is apparently obscured by other resonances. One carbonyl and one nitrosyl band were seen in CH_3CN in the IR at 2062 and 1712 cm^{-1} , respectively. Owing to the width of the bands in acetonitrile only one set of IR bands was observed even though the ^1H NMR indicated the presence of two isomers.

$\text{CpMo}(\text{CO})(\text{NO})(\eta^2\text{-C}_6\text{H}_7(\text{CH}_3)_2\text{D})$. A 25-mL, three-neck flask equipped with a nitrogen inlet and a magnetic stirrer was charged with 30 mg (0.92 mmol) of $\text{CpMo}(\text{CO})_2(\eta^3\text{-C}_6\text{H}_7(\text{CH}_3)_2)$ and about 5 mL of freshly distilled CH_3CN . The solution was cooled to 0 °C and stirred for 5 min. To the yellow acetonitrile solution was added 16.2 mg (0.091 mmol) of NOPF_6 . An immediate reaction occurred with the evolution of CO. The reaction was allowed to stir for 1 min, and the acetonitrile solution was slowly added dropwise into ether being agitated with nitrogen gas. The cation was precipitated and centrifuged, the ether decanted, and the cation dried with a stream of dry nitrogen at room temperature for 30 min.

All of the cation from the previous reaction was taken up in dry THF and then cooled to 0 °C. With the assumption of a quantitative reaction, 6 mg (0.09 mmol) of NaNcBD_3 was added to the THF solution. The reaction was allowed to proceed for 30 min at 0 °C. Then the solvent was removed under vacuum and the olefin complex extracted with 3×15 mL portions of petroleum ether. Upon removal of the petroleum ether, $\text{CpMo}(\text{CO})(\text{NO})(\eta^2\text{-C}_6\text{H}_7(\text{CH}_3)_2\text{D})$ was obtained as a yellow oil: ^1H NMR (CDCl_3 , 25 °C, two isomeric olefin complexes) δ 5.51 (s, Cp, major), 5.49 (s, Cp minor), 3.03 (d), 3.11 (d, olefin (major isomer)), 3.52 (d), 3.03 (d, olefin (minor isomer)), 1.24 (d), 1.14 (d), 0.88 (d), 0.86 (d, methyl resonances), 2.74 and 2.62 (both m, allyl protons), 1.52 (m), 1.28 (m), 0.64 (m, alkyl protons). The IR spectrum of the neutral olefin complex in pentane exhibited two broad bands, one at 1960 and one at 1635 cm^{-1} for CO and NO, respectively. The breadth is due to the superposition of bands from two isomers obtained by the addition of D^+ to exo and endo cation with the nucleophile adding to the same side of the allyl moiety in each case.

cis,cis-3,5-Dimethyl-6-deuteriocyclohexene. The carbonyl nitrosyl olefin complex (after NMR analysis) was allowed to remain in an NMR tube in CDCl_3 . Periodically O_2 was bubbled through the solution. After 7 days of standing at room temperature, the insoluble molybdenum oxides were filtered off, leaving only the $\text{C}_6\text{H}_7(\text{CH}_3)_2\text{D}$ as a free organic ligand in CDCl_3 ready for ^1H NMR spectroscopic analysis. Presumably, the ligand could have been isolated at the stage by careful distillation or by gas chromatographic separation: ^1H NMR (CDCl_3 , 25 °C) δ 5.60 (ddd, H(1)), 5.50 (ddd, H(2)), 2.23 (br, s, H(3)), 2.01 (br, s, H(6)), 1.70 (br m, H(5)), 1.28 (br m, H(4) the methylenes), 0.96 (d, methyl (3)), 0.94 (d, methyl (5)). These assignments were made on the

basis of spin-decoupling experiments and careful analysis of long-range allylic coupling and vicinal coupling observed at the olefinic protons along with deuterium decoupling of the proton spectra. The olefinic protons exhibited very distinctive couplings at δ 5.60 (ddd, $J = 9.9, 5.0, 2.2$ Hz) and 5.50 (ddd, $J = 9.9, 2.0, 1.0$ Hz) that were consistent with the disubstituted olefin in a pseudochair configuration with both methyls in equatorial positions. Other isomers of this olefin obtained by isomerization of the double bond would generate a compound with only one olefinic proton.

Mass Spectrum. The 3,5-dimethylcyclohexene monodeuterio olefin was subjected to mass spectroscopic analysis. Isolation of the free ligand for the mass spectroscopic analysis was as follows. The neutral carbonyl nitrosyl olefin complexes were taken up in THF, and then less than 1 equiv of potassium *tert*-butoxide was added. After 1 day of standing at room temperature, the solution was filtered. The filtrate containing the olefin was then ready for GC-MS analysis. The results⁹ from the electron-impact mass spectroscopy were as follows: 70-eV ionizing potential; parent ion m/e 111.3; loss of terminal CH_3 m/e 96.2; retro Diels-Alder of parent m/e 68.1; loss of CH_2 yielding diene fragment m/e 82.2.

3-Deuteriocyclohexene. The $\text{C}_6\text{H}_9\text{D}$ olefin was isolated for NMR analysis following the procedure for the 3,5-dimethyl olefin (O_2 , CDCl_3 solvent, and time): ^1H NMR (CDCl_3 , 25 °C) δ 5.68 (s, 2 H, olefin), 2.00 (m, 3 H, allylic H), 1.62 (m, 4 H, alkyl-H).

Mass Spectrum. For mass spectroscopic analysis the perdeuterio and monodeuterio olefin complexes were treated with base as before. The results⁹ from the electron-impact mass spectrum were as follows. C_6H_{10} : 70-eV ionizing potential, parent m/e 82.1; loss of CH_3 m/e 67.0; retro Diels-Alder m/e 54.2. This data is in good agreement with published results.⁹ $\text{C}_6\text{H}_9\text{D}$: 70-eV ionizing potential, parent m/e 83.1; loss of CH_3 m/e 68.0; loss of CH_2D m/e 67.1; retro Diels-Alder retaining D m/e 55.1; retro Diels-Alder with loss of D m/e 54.1; 95% $\text{C}_6\text{H}_9\text{D}$, 5% C_6H_{10} via mass spectra analysis.

The $\text{C}_6\text{H}_9\text{D}$ olefin, 3-deuteriocyclohexene, was also obtained by decomposition of the neutral dicarbonyl complex $\text{CpMo}(\text{CO})_2(\eta^3\text{-C}_6\text{H}_9)$. The complex was dissolved in pentane, chloroform, or dichloromethane and treated with a twofold excess of trifluoroacetic acid. The reaction mixtures were stirred in air for 1–2 h and worked up by passage through a short alumina column to remove precipitates, trifluoroacetic acid, and some byproduct metal carbonyl complexes. When pentane was used as solvent, the yield was somewhat lower, however, this solvent had the advantage of not eluting metal complexes from the alumina along with the olefin. Decomposition of $\text{CpMo}(\text{CO})_2(\eta^3\text{-C}_6\text{H}_9)$ with $\text{CF}_3\text{CO}_2\text{D}$ gave 3-deuteriocyclohexene: ^2H NMR (CHCl_3 , 25 °C) δ 2.00 (s, allylic D and no indication of other deuterated products).

The acid decomposition of the allyl complexes gave yields of $60 \pm 4\%$ in pentane and $78 \pm 9\%$ in chloroform, as determined by GC analysis.

Crystallographic Analyses. Crystals of $(\eta^5\text{-C}_5\text{H}_5)\text{Mo}(\text{CO})_2(\eta^3\text{-C}_6\text{H}_9)$ were grown from hexane solution by cooling. All diffraction measurements were performed on an Enraf-Nonius CAD-4 fully automated four-circle diffractometer using graphite-monochromatized Mo $K\alpha$ radiation. Unit cells were determined from 25 randomly selected reflections by using the CAD-4 automatic search, center, index, and least-squares routines. The space group $P2_1/n$ was determined from the systematic absences $h0l$, $l + h = 2n + 1$, and $0k0$, $k = 2n + 1$, observed during data collection.

All calculations were performed on a Digital PDP 11/45 computer using the Enraf-Nonius SDP program library. The structure was solved by the heavy-atom method. Anomalous dispersion corrections^{10a} were added to the neutral-atom scattering factors^{10b} used for all non-hydrogen atoms. Full-matrix least-squares refinements minimized the function $\sum w(F_o - F_c)^2$ where the weighting factor $w = 1/\sigma(F)^2$, $\sigma(F) = (F_o)^2/2F_o$, and $(F_o)^2 = [(I_{\text{raw}})^2 + (pF_o^2)^2]^{1/2}/Lp$. Crystallographic data for the structure is listed in Table II.

(9) H. Budzikiewicz, C. Djerassi, and D. H. Williams. "Mass Spectroscopy of Organic Compound", Holden-Day, Amsterdam, 1967.

(10) "International Tables for X-ray Crystallography", Vol. IV, Kynoch Press, Birmingham, England, 1975: (a) Table 2.3.1, pp 149–50; (b) Table 2.2B, pp 99–101.

Table II. Experimental Data for X-ray Diffraction Study of $(\eta^5\text{-C}_5\text{H}_5)\text{Mo}(\text{CO})_2(\eta^3\text{-C}_6\text{H}_9)$

(A) Crystal Parameters at 24 (2) °C			
space group	$P2_1/n$, No. 14	V , Å ³	1184.8 (7)
a , Å	8.586 (3)	Z	4
b , Å	9.063 (1)	M_r	298.20
c , Å	15.353 (2)	ρ_{calcd} , g/cm ³	1.672
β , deg	97.38 (1)		
(B) Measurement of Intensity Data			
radiation	Mo $K\alpha$, $\lambda = 0.71073$ Å		
monochromator	graphite		
detector aperture	horizontal, $A + B \tan \theta$ ($A = 3.0$ mm, $B = 1.0$ mm); vertical, 4.0 mm		
reflectns measd	+ $h, +k, \pm l$		
max 2θ , deg	54		
scan type	moving crystal-stationary counter		
ω scan rate, deg/min	max, 10; min, 1.67		
ω scan width, deg	1.0		
bkgd	$1/4$ additional scan at each end of scan		
std reflectns	three measured after each 90 min, showing only random fluctuations of $\pm 2\%$		
reflectns measd	2885 including absences		
data used ($F^2 > 3\sigma(F^2)$)	1809		
(C) Treatment of Data			
abs coeff μ , cm ⁻¹	10.619		
p factor	0.01		
final residuals R_1 and R_2	0.024 and 0.025		
esd of unit weight	1.59		

A crystal of approximate dimensions 0.34 mm \times 0.17 mm \times 0.12 mm was selected and mounted in a thin-walled glass capillary. ω -Scan peak widths at half-peak height were in the range 0.1–0.2°. From a total of 2885 reflections, 1809 with $F^2 > 3.0\sigma(F^2)$ were used in the structure solution and refinement. Standard reflections monitored periodically to check alignment, and possible decomposition showed no significant variation during data collection. Full-matrix least-squares refinement using anisotropic thermal parameters for the non-hydrogen atoms and isotropic thermal parameters fixed at 4.0 for hydrogen atoms converged to the final residuals $R_1 = 0.024$ and $R_2 = 0.025$. No attempt was made to refine the hydrogen thermal parameters. The largest peak in the final difference Fourier synthesis was 0.25 e/Å³ and was in the vicinity of the metal atom. The largest value of the shift/error parameter on the final cycle of refinement was 0.02. The error in an observation of unit weight was 1.59. Final atomic coordinates are listed in Table III. Bond distances and angles with errors from the inverse matrix obtained on the final cycle of least-squares refinement are listed in Tables IV and V. Thermal parameters and structure factor amplitudes are included in the supplementary material.

Results

$\text{CpMo}(\text{CO})_2(\eta^3\text{-C}_6\text{H}_9)$. In order to provide detailed stereochemical information on this complex, as well as provide a basis for evaluating proton-proton coupling constants, an X-ray diffraction study of the parent cyclohexenyl complex was undertaken. The structure is shown in Figure 1 and pertinent data given in Tables II–V. The features of the $\text{CpMo}(\text{CO})_2(\text{allyl})$ fragment, as expected, are similar to those of the analogous $\text{CpMo}(\text{CO})_2(\text{C}_3\text{H}_5)$.¹¹ The angle between the carbonyls is the same within experimental error (82.5 (2) vs. 82.7 (1)°); however, the C(1)–C(2)–C(3) angle within the allyl portion of the six-membered ring is constrained and decreases to 116.7 (3)° from the 121.4 (4)° found in the C_3H_5 complex. The central allyl carbon C(2) is closer to the metal than

(11) J. W. Faller, D. F. Chodosh, and D. Katahira. *J. Organomet. Chem.*, 187, 227 (1980).

Table III. Table of Positional Parameters for $\text{CpMo}(\text{CO})_2(\text{C}_6\text{H}_9)$

atom	x/a	y/b	z/c
Mo	0.14335 (3)	0.26920 (3)	0.10273 (2)
O(1)	0.0008 (3)	0.5588 (2)	0.1661 (2)
O(2)	-0.1824 (3)	0.2433 (3)	-0.0115 (2)
Cp(1)	0.2739 (4)	0.2351 (4)	-0.0217 (2)
Cp(2)	0.2970 (4)	0.3776 (4)	0.0063 (3)
Cp(3)	0.3887 (4)	0.3743 (4)	0.0900 (3)
Cp(4)	0.4177 (4)	0.2268 (5)	0.1100 (3)
Cp(5)	0.3464 (4)	0.1429 (4)	0.0410 (3)
C(1)	0.1291 (4)	0.2370 (3)	0.2547 (2)
C(2)	0.1397 (4)	0.1043 (3)	0.2076 (2)
C(3)	0.0060 (4)	0.0622 (3)	0.1504 (2)
C(4)	-0.1547 (4)	0.0858 (4)	0.1796 (2)
C(5)	-0.1695 (4)	0.2304 (4)	0.2285 (2)
C(6)	-0.0228 (4)	0.2733 (4)	0.2906 (2)
C(7)	0.0521 (4)	0.4504 (3)	0.1426 (2)
C(8)	-0.0610 (4)	0.2527 (3)	0.0313 (2)
Hp(1)	0.210 (4)	0.207 (3)	-0.077 (2)
Hp(2)	0.263 (3)	0.451 (3)	-0.026 (2)
Hp(3)	0.402 (3)	0.448 (3)	0.116 (2)
Hp(4)	0.463 (3)	0.184 (3)	0.156 (2)
Hp(5)	0.352 (3)	0.049 (3)	0.035 (2)
H(1)	0.219 (4)	0.267 (3)	0.292 (2)
H(2)	0.235 (3)	0.055 (3)	0.206 (2)
H(3)	0.011 (4)	-0.021 (3)	0.113 (2)
H(4 α)	-0.234 (3)	0.080 (3)	0.130 (2)
H(4 β)	-0.170 (3)	0.007 (3)	0.220 (2)
H(5 α)	-0.193 (3)	0.304 (3)	0.186 (2)
H(5 β)	-0.256 (4)	0.221 (3)	0.264 (2)
H(6 α)	-0.023 (3)	0.380 (3)	0.301 (2)
H(6 β)	-0.011 (4)	0.224 (3)	0.338 (2)

Table IV. Bond Distances (Å) for $\text{CpMo}(\text{CO})_2(\text{C}_6\text{H}_9)$

Mo-Cp(1)	2.355 (3)	C(1)-C(2)	1.412 (4)
Mo-Cp(2)	2.324 (3)	C(1)-C(6)	1.515 (4)
Mo-Cp(3)	2.343 (3)	C(1)-H(1)	0.94 (3)
Mo-Cp(4)	2.375 (3)		
Mo-Cp(5)	2.382 (3)	C(2)-C(3)	1.406 (4)
Mo-C(1)	2.371 (3)	C(2)-H(2)	0.93 (3)
Mo-C(2)	2.200 (3)		
Mo-C(3)	2.381 (3)	C(3)-C(4)	1.520 (4)
Mo-C(7)	1.952 (3)	C(3)-H(3)	0.95 (3)
Mo-C(8)	1.951 (2)		
		C(4)-C(5)	1.523 (4)
Cp(1)-Cp(2)	1.367 (5)	C(4)-H(4 α)	0.96 (3)
Cp(1)-Cp(5)	1.363 (5)	C(4)-H(4 β)	0.96 (3)
Cp(1)-Hp(1)	0.99 (3)		
		C(5)-C(6)	1.529 (4)
Cp(2)-Cp(3)	1.418 (5)	C(5)-H(5 α)	0.94 (3)
Cp(2)-Hp(2)	0.86 (3)	C(5)-H(5 β)	0.98 (3)
Cp(3)-Cp(4)	1.387 (5)	C(6)-H(6 α)	0.98 (3)
Cp(3)-Hp(3)	0.78 (3)	C(6)-H(6 β)	0.85 (3)
Cp(4)-Cp(5)	1.382 (5)		
Cp(4)-Hp(4)	0.86 (3)	C(7)-O(1)	1.154 (3)
Cp(5)-Hp(5)	0.86 (3)	C(8)-O(2)	1.162 (3)

the terminal carbons [Mo-C(2) = 2.200 (3) Å compared to Mo-C(1) = 2.371 (3) Å] in the cyclohexenyl complex, as is found also in the allyl complex [Mo-C(2) = 2.236 (4) and Mo-C(1) = 2.359 (3) Å]. The allyl hydrogen atoms are also nearly in the plane of allyl carbons C(1), C(2), C(3), but deviate slightly toward the metal atom [distance (Å) from the C(1)-C(2)-C(3) plane: H(1), 0.03 (3); H(2), 0.14 (3); H(3), 0.09 (3)]. The six-membered ring is effectively in a chair conformation.

Although carbon-hydrogen distances are underestimated by X-ray techniques, fairly accurate angles involving hydrogen can be anticipated.¹² In order to test the accuracy of predicting the H positions from the skeletal

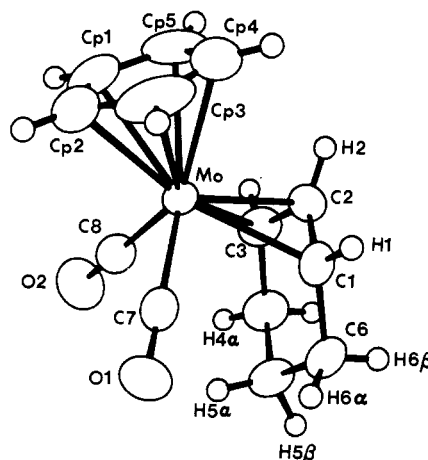


Figure 1. A perspective ORTEP diagram of $(\text{C}_6\text{H}_9)\text{Mo}(\text{CO})_2(\eta^3\text{-C}_6\text{H}_9)$ showing 50% probability ellipsoids for the non-hydrogen atoms. The hydrogen atoms were refined with B fixed at 4.0, but the thermal parameters were reduced to $B = 1.0$ in the drawing.

carbon structure and to locate any unusual features, the expected hydrogen positions were also calculated by using the C-C-C angles and assuming a 109.5° H-C-H angle. The calculated positions only differed by an average of 0.07 Å from the refined positions. In turn, the angles between these hydrogen positions provided the data to estimate coupling constants and assign the resonances in the NMR spectrum. The coupling constants were estimated on the basis of the Karplus relationships,¹³⁻¹⁵ eq 1, in which ϕ is the dihedral angle (see Table VI).

$$J_{\text{HH}} = 7 - \cos \phi + 5 \cos^2 \phi \quad (1)$$

A combined analysis of the X-ray crystallographic data of $\text{CpMo}(\text{CO})_2(\eta^3\text{-C}_6\text{H}_9)$ and the 270-MHz ^1H and 41.44-MHz ^2H NMR data of $\text{CpMo}(\text{CO})_2(\eta^3\text{-C}_6\text{H}_9)$ and $\text{CpMo}(\text{CO})_2(\eta^3\text{-C}_6\text{H}_8\text{D})$ unequivocally established that the addition of D^- to $[\text{CpMo}(\text{CO})_2(\eta^4\text{-C}_6\text{H}_8)]\text{PF}_6$ resulted in deuterium incorporation solely at the 4 β position.³ This observation of exo H^- addition to the conjugated diene cation was consistent with a similar observation by Brookhart and Lamanna.¹⁶ The addition of H^- to $[(\eta^6\text{-C}_6\text{D}_6)\text{Mn}(\text{CO})_3]^+$ gave (6-exo- ^1H -hexadeuteriocyclohexadienyl)manganese tricarbonyl. The hydride addition was observed to occur strictly from the face opposite the metal. The positions of the deuterium remaining in the product of the abstraction of hydride from $\text{CpMo}(\text{CO})_2(\eta^3\text{-4-deuterio-cyclohexene})$ with triphenylcarbenium hexafluorophosphate followed by the addition of hydride provides evidence for the mechanism of the hydride abstraction in this reaction.

$\text{CpMo}(\text{CO})_2(\eta^3\text{-C}_6\text{H}_8(\text{CH}_3))$. The addition of the CH_3MgBr to $[\text{CpMo}(\text{CO})_2(\eta^4\text{-C}_6\text{H}_9)]\text{PF}_6$ resulted in alkylation at the 4 β -position of the ring, an axial position. The reaction of this methylated cyclohexenyl complex with triphenylcarbenium hexafluorophosphate followed by the addition of hydride resulted in the regeneration of the starting material, the (4 β -methylcyclohexenyl)dicarbonylcyclopentadienylmolybdenum. This showed the large directing effect of the methyl substituent. When the above reaction was carried out with D^- rather than H^- , the

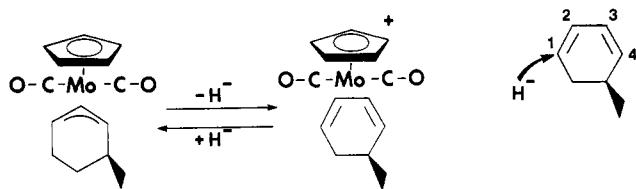
(13) M. Karplus, *J. Chem. Phys.*, **30**, 11 (1959) ($J_{\text{HH}} = 10 \cos^2 \phi$ for ϕ between 0° and 90°, $J_{\text{HH}} = 16 \cos^2 \phi$ for ϕ between 90° and 180°).

(14) M. Karplus, *J. Am. Chem. Soc.*, **85**, 2870 (1963).

(15) A. B. Bothner-By, *Adv. Magn. Reson.*, **1**, 195 (1965).

(16) M. Brookhart and W. Lamanna, *J. Am. Chem. Soc.*, **102**, 3490 (1980).

(12) M. R. Churchill, *Inorg. Chem.*, **12**, 1213-4 (1973); R. G. Teller and R. Bau, *Struct. Bonding (Berlin)*, **44**, 1 (1981).



assignment of the 6α and 6β protons in the ^1H NMR spectrum of $\text{CpMo}(\text{CO})_2(\eta^3\text{-C}_6\text{H}_8(\text{CH}_3))$ was unequivocal.

$\text{CpMo}(\text{CO})_2(\eta^3\text{-C}_6\text{H}_7(\text{CH}_3)_2)$. The reaction of the 4β -methyl neutral dicarbonyl complex with triphenylcarbenium hexafluorophosphate followed by the addition of the CH_3MgBr resulted in the stereoselective (98%) synthesis of ($4\beta,6\beta$ -dimethylcyclohexenyl)dicarbonylcyclopentadienylmolybdenum complex. Again the directing effect of the substituted methyl group is demonstrated.

$\text{C}_6\text{H}_7\text{D}(\text{CH}_3)_2$. The addition of NOPF_6 followed by NaNCBD_3 to the $4\beta,6\beta$ -dimethylated cyclohexenyl complex resulted in the neutral olefin complex. Decomposition of the neutral olefin complex resulted in the isolation of the *cis,cis*-3,5-dimethyl-6-deuteriocyclohexene. With the isolation of this compound we provide an example of the potential uses of the cyclopentadienyldicarbonylmolybdenum moiety in the stereoselective synthesis of substituted cyclic olefin complexes.

$\text{CpMo}(\text{CO})_2[\eta^3\text{-C}_6\text{H}_8(\text{C}(\text{CH}_3)_2\text{CH}_2\text{OH})]$. The addition of the pyrrolidine enamine of isobutyraldehyde to the cationic complex $[\text{CpMo}(\text{CO})_2(\eta^4\text{-C}_6\text{H}_8)][\text{PF}_6]$ followed by hydrolysis gave the neutral 4β -substituted aldehyde complex $\text{CpMo}(\text{CO})_2(\eta^3\text{-C}_6\text{H}_8(\text{C}(\text{CH}_3)_2\text{CHO}))$. The aldehyde moiety was reduced with LiBH_4 in THF to the corresponding alcohol.

$\text{CpMo}(\text{CO})_2(\eta^3\text{-9,9-dimethyl-7-oxabicyclo[4.3.0]nonenyl})$. The neutral dicarbonyl alcohol complex $\text{CpMo}(\text{CO})_2(\eta^3\text{-C}_6\text{H}_8(\text{C}(\text{CH}_3)_2\text{CH}_2\text{OH}))$ underwent intramolecular nucleophilic addition to yield the bicyclo[4.3.0] organometallic complex upon reaction with one equivalent of triphenylcarbonium ion. The mass spectrum and elemental analysis of the product was consistent with a dicarbonylbicyclic complex. The structural assignment of the bicyclo[4.3.0] complex was based on an analysis of ^1H NMR data (geminal and vicinal coupling constants) and X-ray crystal structure data. *N.B.* To simplify comparisons of coupling constants, the numbering scheme used for this complex retains that used for the other compounds in this paper and avoids indicating the position of allylic attachment in names. Proper nomenclature would number the bridgeheads of the bicyclic compound as 1 and 6, which yields a [4.3.0]non-4-en-3-yl.

$\text{C}_6\text{H}_9\text{D}$. The reaction of NOPF_6 followed by D^- addition to $\text{CpMo}(\text{CO})_2(\eta^3\text{-C}_6\text{H}_9)$ resulted in the neutral monodeuterated olefin complex. Decomposition of the olefin complex gave 3-deuteriocyclohexene. The same olefin was obtained in the facile decomposition of $\text{CpMo}(\text{CO})_2(\eta^3\text{-C}_6\text{H}_9)$ with CF_3COOD in a variety of solvents. These reaction sequences demonstrated the olefin ligand can be taken from the metal center and isolated *without isomerization of the olefinic bond*, hence, demonstrating the use of molybdenum complexes for the synthesis of regioselectively substituted cyclic olefins.

Discussion

The Assignment of the ^1H NMR Spectrum and the Structure of $\text{CpMo}(\text{CO})_2(\eta^3\text{-C}_6\text{H}_9)$. The X-ray crystallographic analysis of $\text{CpMo}(\text{CO})_2(\eta^3\text{-C}_6\text{H}_9)$ showed the cyclohexenyl ring to be in a chair conformation with the axial substituent at carbons 4 and 6 directed away from

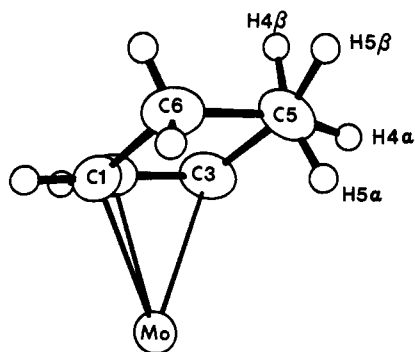
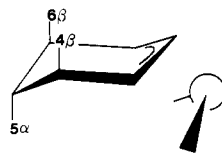


Figure 2. A view down the $\text{C5}\rightarrow\text{C4}$ axis of the C_6H_9 ring.

the metal (i.e., on the non-metal side of the ring or the β side). The axial substituent at carbon 5 is directed in



toward the metal (i.e., it is on the metal side of the ring or the α side). It is the angular relationship (dihedral angle) and its effect on the coupling of the protons at carbons 5 and 4 or 6 of which provides the basis for the assignment of the ^1H NMR spectra given in the Experimental Section. These assignments are critical, as they allow a distinction of substitution on the metal vs. the non-metal side of the ring. This allows ^1H NMR spectroscopy to be used as a reliable method of determining the selectivity of hydride abstractions and additions. In a similar manner the positions of substituents and conformations of the rings in other substituted cyclohexenyl complexes can be obtained.

Owing to the strain induced in the ring by the shorter bond lengths in the (η^3 -allyl)Mo fragment, the dihedral angles in the cyclohexenyl complex are not 60° and 180° as expected for cyclohexane itself. The large deviations from a perfect staggered configuration can be seen in the view down the $\text{C}(5)\text{-C}(4)$ bond shown in Figure 2. Since X-ray results do not provide a high degree of accuracy for the location of hydrogen atoms (i.e., estimated standard deviations in angles of $\pm 2^\circ$), several values for the angles are shown in Table VI. The angles between methylene 5 and 4 are crystallographically independent of those between 5 and 6; hence there is an internal check on the magnitude of the angles. Calculated positions based on the C_6 ring are also included. All of these results provide consistent and unambiguous assignments in the NMR spectrum.

An important feature is the observation of a large difference between equatorial-equatorial and axial-equatorial coupling in the η^3 -cyclohexenyl, whereas analogous couplings in a cyclohexane system would be nearly equal.

From the dihedral angles obtained from the crystal structure, one very large (>11 Hz) vicinal coupling between the 5α proton and the 4β proton (an axial-axial relationship) and one very small (<2 Hz) vicinal coupling from the 5β proton to the 4α proton (an equatorial-equatorial relationship) is expected from the Karplus¹³⁻¹⁵ relationship. These couplings provide the key to assigning the well-separated 5-methylene protons at δ 0.33 and 0.96 to the 5β and 5α protons, respectively. This in turn leads to a distinction in the metal side (δ 1.67) and the non-metal side (δ 1.91) protons at carbon 4 in the cyclohexenyl ring on the basis of vicinal couplings.

Table V. Selected Bond Angles (deg) for $\text{CpMo}(\text{CO})_2(\eta^3\text{-C}_6\text{H}_5)$

Cp(1)-Mo-Cp(2)	34.0 (1)	Cp(2)-Cp(3)-Cp(4)	106.5 (3)	C(1)-C(2)-C(3)	116.7 (3)
Cp(2)-Mo-Cp(3)	35.4 (1)	Cp(2)-Cp(3)-Hp(3)	118 (2)	C(1)-C(2)-H(2)	122 (2)
Cp(3)-Mo-Cp(4)	34.2 (1)	Cp(4)-Cp(3)-Hp(3)	135 (2)	C(3)-C(2)-H(2)	120 (2)
Cp(4)-Mo-Cp(5)	33.8 (1)	Mo-Cp(3)-Hp(3)	113 (2)	Mo-C(2)-H(2)	102 (2)
Cp(5)-Mo-Cp(1)	33.4 (1)	Cp(3)-Cp(4)-Cp(5)	108.1 (4)	C(2)-C(3)-C(4)	118.5 (3)
C(1)-Mo-C(2)	35.7 (1)	Cp(3)-Cp(4)-Hp(4)	132 (2)	C(2)-C(3)-H(3)	119 (2)
C(2)-Mo-C(3)	35.5 (1)	Cp(5)-Cp(4)-Hp(4)	120 (2)	C(4)-C(3)-H(3)	113 (2)
C(1)-Mo-C(3)	60.7 (1)	Mo-Cp(4)-Hp(4)	117 (2)	Mo-C(3)-H(3)	112 (2)
C(7)-Mo-C(8)	82.7 (1)	Cp(1)-Cp(5)-Cp(4)	108.7 (3)	C(3)-C(4)-C(5)	113.8 (2)
Cp(2)-Cp(1)-Cp(5)	108.9 (3)	Cp(1)-Cp(5)-Hp(5)	124 (2)	H(4 α)-C(4)-H(4 β)	109 (2)
Cp(2)-Cp(1)-Hp(1)	124 (2)	Cp(4)-Cp(5)-Hp(5)	127 (2)	C(4)-C(5)-C(6)	114.3 (3)
Cp(5)-Cp(1)-Hp(1)	127 (2)	Mo-Cp(5)-Hp(5)	125 (2)	H(5 α)-C(5)-H(5 β)	110 (2)
Mo-Cp(1)-Hp(1)	118 (2)	C(2)-C(1)-C(6)	119.1 (3)	C(1)-C(6)-C(5)	113.4 (2)
Cp(1)-Cp(2)-Cp(3)	107.8 (3)	C(2)-C(1)-H(1)	117 (2)	H(6 α)-C(6)-H(6 β)	113 (2)
Cp(1)-Cp(2)-Hp(2)	121 (2)	C(6)-C(1)-H(1)	113 (2)	Mo-C(7)-O(1)	178.7 (3)
Cp(3)-Cp(2)-Hp(2)	131 (2)	Mo-C(1)-H(1)	115 (2)	Mo-C(8)-O(2)	179.7 (2)
Mo-Cp(2)-Hp(2)	121 (2)				

Table VI. Calculated and Observed Vicinal Couplings in $\text{CpMo}(\text{CO})_2(\eta^3\text{-C}_6\text{H}_5)$

angle ^a	ϕ , deg	J (calcd), Hz	J (obsd), Hz
a-a			11.4
4 β -5 α , x	159.2	11.7	
4 β -5 α , c	157.1	11.4	
6 β -5 α , x	164.5	12.2	
6 β -5 α , c	156.7	11.4	
e-e			0.2
4 α -5 β , x	78.5	2.2 ^b	
4 α -5 β , c	80.2	2.1 ^b	
6 α -5 β , x	82.6	2.0 ^b	
6 α -5 β , c	80.8	2.1 ^b	
β a- β e			6.0
4 β -5 β , x	40.4	7.0	
4 β -5 β , c	38.6	7.3	
6 β -5 β , x	44.8	6.3	
6 β -5 β , c	38.1	7.4	
α a- α e			6.8
5 α -4 α , x	40.4	7.0	
5 α -4 α , c	38.4	7.4	
5 α -6 α , x	37.0	7.6	
5 α -6 α , c	37.8	7.5	

^a x = X-ray data; c = calculated, assuming 109.5° H-C-H angle. ^b The original equation,¹¹ $J = 10 \cos^2 \phi$, gives $J \approx 0.3$ Hz.

Selectivity of Deuteride Addition. With the ¹H NMR assignment of the 4 α - and 4 β -positions clearly established (δ 1.67 and 1.91, respectively) the stereoselectivity of deuteride addition to $[\text{CpMo}(\text{CO})_2(\eta^3\text{-C}_6\text{H}_5)]^+$ can be examined. The ²H NMR of the product from the addition of NaNCBD₃ to the diene cation exhibited one resonance at δ 1.91, which corresponds to the 4 β -position. This demonstrated that the deuteride added to the cyclohexadiene ring from the non-metal side with high stereoselectivity (>99%); see Figure 3.

Stereoselectivity of Hydride Abstraction. Having established that hydride addition to $[\text{CpMo}(\text{CO})_2(\eta^3\text{-C}_6\text{H}_5)]^+$ occurs trans to the molybdenum center, the degree of stereoselectivity of hydride abstraction from the neutral cyclohexenyl complex with trityl ion could be evaluated. This was carried out by observing the deuterium incorporation in the product from the following reaction sequence.

The (4 β -deuteriocyclohexenyl)dicarbonylcyclopentadienylmolybdenum complex was converted to a cyclic 1,3-diene cation by trityl ion abstraction as before. This was followed by hydride addition.

In this reaction sequence if hydride abstraction occurred stereoselectively from the non-metal side, the 4 β - or 6 β -positions, deuterium incorporation in the hydride addition

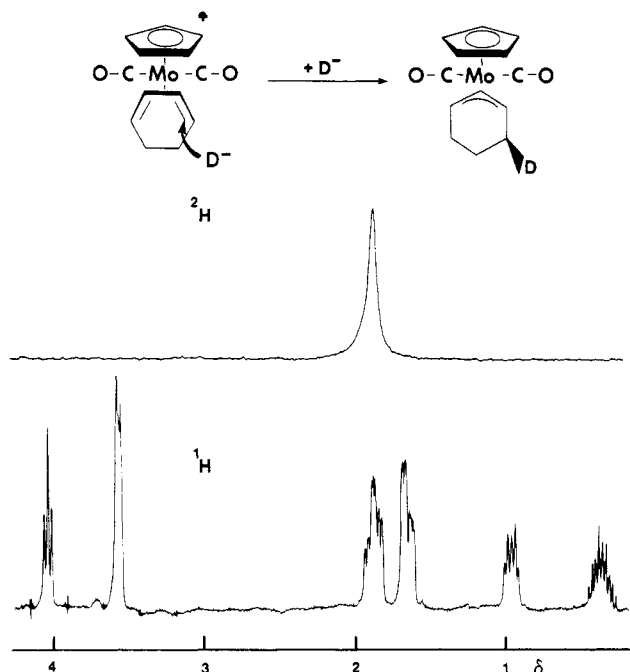


Figure 3. The 41-MHz ²H NMR spectrum of $\text{CpMo}(\text{CO})_2(\eta^3\text{-C}_6\text{H}_5\text{D})$ in CHCl_3 . A 270-MHz proton spectrum of $\text{CpMo}(\text{CO})_2(\eta^3\text{-C}_6\text{H}_5)$ is shown below for reference.

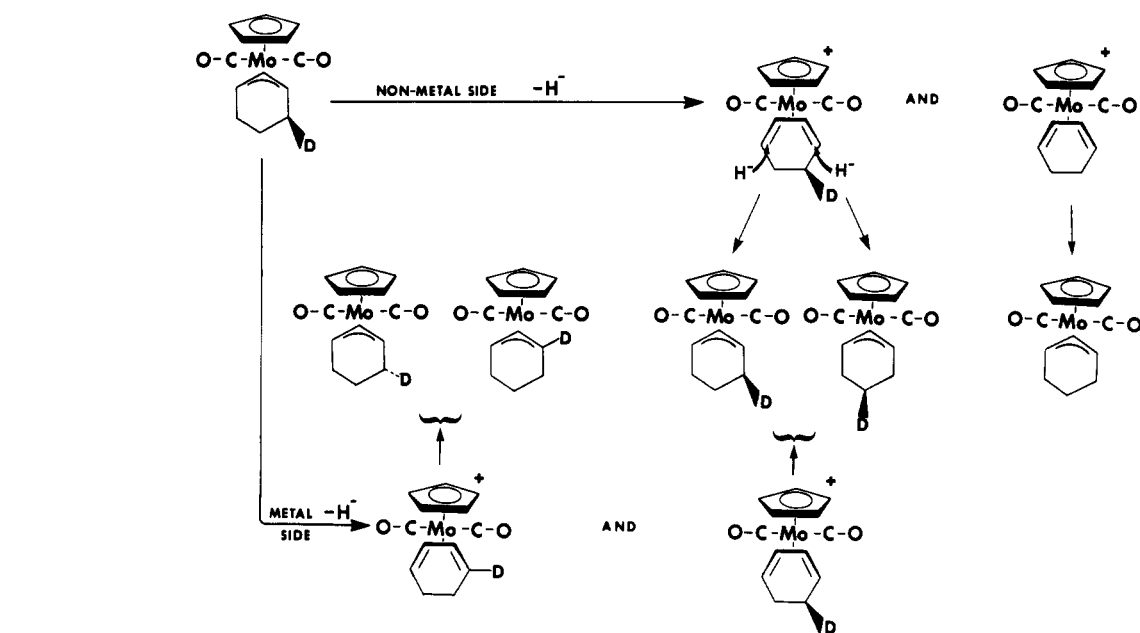
product would be found solely and equally (neglecting a small secondary isotope effect) at the 4 β - and 5 β -positions on the ring (see complexes 8 and 9 in Scheme I).

If any hydride abstraction at all occurred from the metal side of the ring, i.e., from the 4 α -position, then the $[\text{CpMo}(\text{CO})_2(\eta^3\text{-4-D-C}_6\text{H}_7)]^+$ cation 4 would be obtained. Hydride addition to this cation would give complexes 6 and 7 in equal concentrations (not considering a small secondary isotope effect). Complexes 6 and 7 have deuterium incorporated at positions 3 α and 4 α ; therefore, the ratio of deuterium at the 3 α and 4 α to the deuterium at 4 β and 5 β will be a direct measure of the stereoselectivity of metal vs. non-metal side hydride abstraction by trityl ion.

As can be seen from the ²H NMR spectrum (Figure 4) of the product from the trityl ion abstraction-hydride addition reaction sequence carried out on (4 β -deuteriocyclohexenyl)dicarbonylcyclopentadienylmolybdenum, there was no deuterium incorporation observed at the 3- and 4 α -positions, only at the 4 β and 5 β . Therefore, hydride abstraction occurred with high stereoselectivity (>99%) from the side of the ring opposite the metal.

Methyl Addition. The addition of CH_3MgBr to $[\text{CpMo}(\text{CO})_2(\eta^3\text{-C}_6\text{H}_5)]\text{PF}_6$ was seen to go in high yield

Scheme I

Table VII. Expected and Observed Vicinal Couplings in $\text{CpMo}(\text{CO})_2(\eta^3\text{-C}_6\text{H}_5(\text{CH}_3))$ at the 5α - and 5β -Positions

	chair	boat
Expected		
5α	(a-a), (a-e), (a-e)	(a-e), (a-e), (e-e)
5β	(a-e), (e-e), (e-e)	(a-a), (a-a), (a-e)
Observed		
δ 0.73 (equatorial)		δ 0.52 (axial)
(a-e, $J = 6.1$ Hz),		(a-a, $J = 11.5$ Hz),
(e-e, $J = 1.4$ Hz),		(a-e, $J = 6.7$ Hz),
(e-e, $J = 1.4$ Hz)		(a-e, $J = 6.3$ Hz)

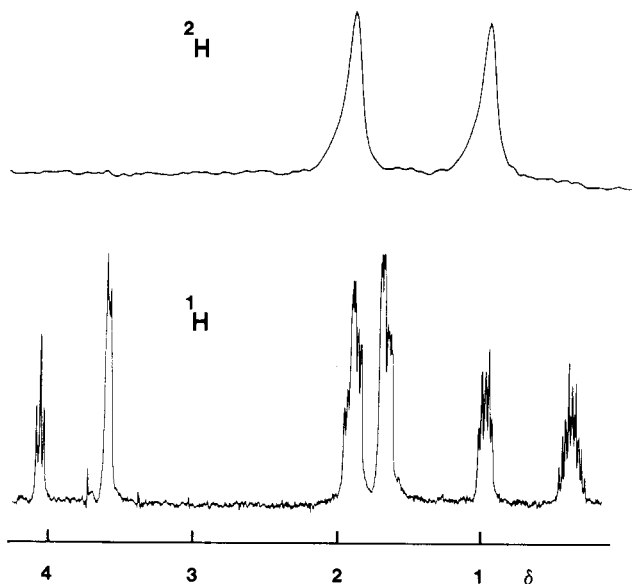


Figure 4. The 41-MHz ^2H NMR spectrum of $\text{CpMo}(\text{CO})_2(\eta^3\text{-C}_6\text{H}_6\text{D})$ in CHCl_3 after the hydride abstraction and addition sequence of Scheme I. A 270-MHz proton spectrum of $\text{CpMo}(\text{CO})_2(\eta^3\text{-C}_6\text{H}_5)$ is shown below for reference.

(61%) and with high (>99%) stereoselectivity to the methylated complex $\text{CpMo}(\text{CO})_2(\eta^3\text{-C}_6\text{H}_5(\text{CH}_3))$. By analyzing the splitting of the 5α and 5β protons which arises from the vicinal coupling of the 4 and 6 protons and assuming a non-metal side addition, we determined that the methyl substituent was in an axial position on the η^3 -allyl ring.

Conformation of the η^3 -Allyl Ring in $\text{CpMo}(\text{CO})_2(\eta^3\text{-C}_6\text{H}_5(\text{CH}_3))$. The high stereoselectivity observed in the addition of CH_3^- to $[\text{CpMo}(\text{CO})_2(\eta^3\text{-C}_6\text{H}_5)]\text{PF}_6$ required that the nucleophile added solely from the metal side or solely from the non-metal side to the diene ring. Having previously demonstrated that the nucleophile D^- added to this same cation from the non-metal side of the diene ring with >99% stereoselectivity and having no reason to assume a complete reversal (i.e., 100% non-metal side attack) in the side attacked by the nucleophile based only on the nature of the nucleophile, we assume that the methyl group added to the diene ring from the non-metal

side. In other systems Faller et al.,¹⁷ Brookhart et al.,¹⁶ and Trost² have shown addition of nucleophiles to cation complexes occurring from the non-metal side. The X-ray structures of a derivative of enamine addition also shows β attack, see below.

Methyl addition to the diene ring from the non-metal side results in the ring taking one of two idealized conformations, i.e., "chair" or "boat".



In the chair conformation the methyl substituent occupies an axial position, hence one axial-axial vicinal coupling (to the 5α proton in this case) will be eliminated. Therefore, the 5α proton will have the following vicinal couplings: one (a-a) and two (a-e). The 5β proton will have one (a-e) and two (e-e) vicinal couplings. In the boat conformation, in which the methyl occupies an equatorial position, the 5α proton will have two (a-e) and one (e-e) couplings, the 5β -proton will have two (a-a) and one (a-e) vicinal couplings.

Examining the boat and chair models and the vicinal coupling to the protons at the 5-carbon position, it is possible to distinguish the two conformations. The protons

at the 5-carbon in the monomethylated cyclohexene complex had chemical shifts of δ 0.73 and 0.52 and had a geminal coupling of 13.7 Hz. Table VII lists the expected vicinal couplings at the 5α - and the 5β -positions for the chair and boat conformations.

Considering the observed vicinal couplings of the protons at the 5-carbon for the monomethylated complex, the following has been established: the equatorial proton at the 5-position (δ 0.73 resonance) in $\text{CpMo}(\text{CO})_2(\eta^3\text{-C}_6\text{H}_8\text{(CH}_3))$ has two (e-e) and one (a-e) vicinal couplings. In Table VII only one proton is expected to have this vicinal coupling pattern; the 5β proton with the cyclic allyl in the chair conformation. The axial proton at the 5α -position (δ 0.52) has one (a-a) and two (a-e) vicinal couplings. From Table VII, only one proton is expected to have these couplings i.e., the 5α proton with the ring in the chair conformation. Thus, the methyl-substituted cyclohexenyl ring of $\text{CpMo}(\text{CO})_2(\eta^3\text{-C}_6\text{H}_8\text{(CH}_3))$ is in a chair conformation with the methyl group occupying an axial position.

In summary, having assumed (from analogous systems) the direction of nucleophilic attack to the 1,3-diene cation and having analyzed the vicinal coupling of the five axial and five equatorial protons, we have been able to determine the conformation of the ring and make chemical shift assignments for the 5α - and 5β -protons.

The Directing Effect of a Methyl Substituent. With the $\text{CpMo}(\text{CO})_2(\eta^3\text{-4}\beta\text{-methylcyclohexenyl})$ complex in hand and the stereoselectivity of hydride abstraction well-characterized, the directing effect of the methyl substituent was investigated. The abstraction of hydride from $\text{CpMo}(\text{CO})_2(\eta^3\text{-4}\beta\text{-methylcyclohexenyl})$ with trityl ion to yield the cyclic 1,3-diene cation was followed by hydride addition. This reaction sequence regenerated only the starting material. The absence of formation of the 5β -methylcyclohexenyl complex clearly demonstrated the large directing effect of the methyl substituent in the cationic cyclic 1,3-diene complex. The steric constraints imposed by the β -methyl group vicinal to the 4-position in the cyclic 1,3-diene cation resulted in >99% stereoselectivity of non-metal side of H^- addition to the 1-position of the cation.

Assignment of the 6α and 6β Resonances of $\text{CpMo}(\text{CO})_2(\eta^3\text{-C}_6\text{H}_8\text{(CH}_3))$. Having previously demonstrated the high stereoselectivity of the hydride addition to the 5β -methylcyclohexadiene cation, the assignment of the 6α and 6β protons in $\text{CpMo}(\text{CO})_2(\eta^3\text{-4-methylcyclohexenyl})$ was possible.

When the above reaction sequence was carried out with D^- rather than H^- , the chemical shift of the six protons in $\text{CpMo}(\text{CO})_2(\eta^3\text{-4}\beta\text{-methylcyclohexenyl})$ was unequivocally established. A comparison of the ^1H NMR spectra of the perprotio- and monodeuterio-4-methylcyclohexenyl complexes reveals two striking features that assist in assigning the 6α and 6β protons. Specifically, the absence of the δ 2.03 resonance in the ^1H NMR spectrum of the monodeuterio complex and the 5.3-Hz upfield shift of the δ 1.58 resonance with the loss of J_{HH} geminal coupling in the δ 1.58 resonance were observed.

From this information, the resonances at δ 2.03 and 1.53 were assigned to the 6β and 6α protons, respectively. This is consistent with addition of D^- to the 1,3-diene cation from the non-metal side at the 1-position of the cation.

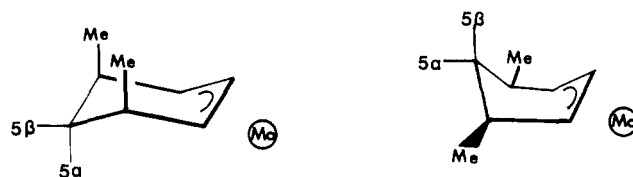
$\text{CpMo}(\text{CO})_2(\eta^3\text{-C}_6\text{H}_7\text{(CH}_3)_2)$. To further explore the directing effect of the methyl substituent in $[\text{CpMo}(\text{CO})_2(\eta^4\text{-C}_6\text{H}_7\text{(CH}_3))]^+$ to nucleophilic addition, CH_3MgBr was added to the methyl-substituted 1,3-diene cation. The reaction proceeded in 27% yield with 98% stereoselectivity. The ^1H NMR spectrum of the product had only

Table VIII. Expected and Observed Vicinal Couplings in $\text{CpMo}(\text{CO})_2(\eta^3\text{-C}_6\text{H}_7\text{(CH}_3)_2)$ at the 5α and 5β Protons

chair		boat	
Expected			
5α (a-e), (a-e)		(a-e), (a-e)	
5β (e-e), (e-e)		(a-a), (a-a)	
Observed			
δ 0.59		δ 0.83	
(e-e, $J = 3.0$ Hz),		(a-e, $J = 7.1$ Hz),	
(e-e, $J = 3.0$ Hz)		(a-e, $J = 7.1$ Hz)	

one syn proton resonance at δ 3.70 and one methyl resonance at δ 1.23, indicating the cyclic allyl product had high symmetry. The methyl substituent was assumed to have added via the β side of the ring, as did and for the same reasons as the first methyl. Therefore, the dimethyl product was the $4\beta,6\beta$ -dimethyl-substituted cyclohexenyl complex.

Conformational Analysis of the $4\beta,6\beta$ -Dimethylcyclohexenyl Ring. In determining which ideal conformation (chair or boat) best describes the $4\beta,6\beta$ -dimethylcyclohexenyl product, we compared expected vicinal coupling patterns of the 5α and 5β protons for the chair and boat conformation with observed data. With the $4\beta,6\beta$ -dimethylcyclohexenyl ring in a boat conformation, the methyls would be in equatorial positions, the 5β proton would have two (a-a) vicinal couplings, and the 5α proton would have two (a-a) couplings. In the chair conformation the 5β proton would have two (e-e) couplings and the 5α proton would have two (a-e) couplings.



Following the previously established trends for the (a-a) and (e-e) vicinal couplings, the chair and boat configurations should be easily distinguishable. The (a-a) vicinal relationship splittings of ~ 11 Hz, and (e-e) vicinal relationship gives splittings of ~ 1 Hz.

Double-resonance experiments in conjunction with calculated NMR spectra allowed an analysis of the splitting pattern observed for the 5α and 5β protons of the dimethyl-substituted cyclohexenyl complex.

The resonance at δ 0.83 was observed to have two vicinal couplings of 7.1 Hz each, and the δ 0.59 resonance had two vicinal couplings of 3.0 Hz.

Table VIII lists the observed vicinal interactions of the 5α and 5β protons for $\text{CpMo}(\text{CO})_2(\eta^3\text{-C}_6\text{H}_7\text{(CH}_3)_2)$ and the idealized interactions of these protons when the cyclohexenyl ring is in a chair and boat conformation.

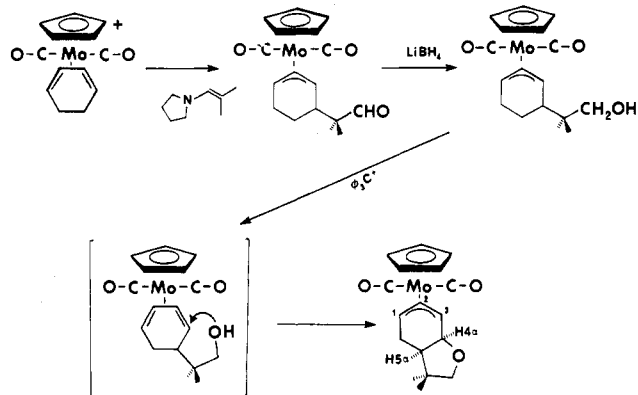
The lack of any vicinal couplings >7.1 Hz suggests that (a-a) interactions are not present, and a chair conformation is present. The resonance at δ 0.83 has two (e-e) vicinal interactions as seen by the 7.1-Hz splitting and is assigned the 5α proton. The smaller (e-e) couplings distinguish the δ 0.59 resonance as the 5β proton.

Comparing the expected and observed vicinal interactions again indicate the η^3 -cyclohexenyl ring to be best described by the chair conformation. Hence, the methyl substituents are in axial positions (4β and 6β) on the ring.

The great effective bulk of the molybdenum center bonded to the allyl functionality is the factor that overpowers the steric interaction of the two axial methyl groups. By way of analogy, the transition-metal center acts in the same manner as a *tert*-butyl substituent on a

cyclohexane ring. The tendency of the bulkier substituent to occupy an equatorial position overrides the other steric interactions, and thus, in this case, the two methyl substituents occupy in axial positions.

Functionalization of the η^3 -Cyclohexenyl Ring. The use of (2-methyl-1-propenyl)-1-pyrrolidine, an enamine of isobutyraldehyde, as a nucleophile to cationic organometallic complexes has been previously demonstrated.¹⁷ The following reaction sequence demonstrates its usefulness in functionalizing and eventually undergoing an intramolecular nucleophilic attack resulting in an unusual η^3 -cyclohexenyl bicyclo[4.3.0] complex.



The hydrolysis of the product from the reaction of $[\text{CpMo}(\text{CO})_2(\eta^4\text{-C}_6\text{H}_8)]^+$ and the enamine of isobutyraldehyde gave the 4 β -substituted 2,2-dimethylpropanol complex in good (66%) yield. As in other substituted η^3 -cyclohexenyl complexes the substituent was observed to add stereoselectively (>99%) from the non-metal side of the ring.

The aldehyde functionality was readily reduced to the primary alcohol with LiBH_4 , giving $\text{CpMo}(\text{CO})_2[\eta^3\text{-C}_6\text{H}_8\text{-}4\beta\text{-C}(\text{CH}_3)_2\text{CH}_2\text{OH}]$ in good (89%) yield. The ability to reduce the aldehyde to an alcohol without affecting the organometallic complex is an important property of the complex and demonstrates its stability in potential applications as a synthetic reagent.

Treatment of the alcohol with trityl cation apparently proceeds by abstraction of the 6 β -hydrogen to form the $\text{CpMo}(\text{CO})_2[\eta^4\text{-C}_6\text{H}_7\text{-}5\beta\text{-C}(\text{CH}_3)_2\text{CH}_2\text{OH}]$ cation. This cation cyclizes and loses the acidic OH proton to yield the [4.3.0] complex. The intramolecular reaction proceeds via attack adjacent to the substituent. This proximity effect overrides the steric interaction that yielded the 4,6-sub-

stitution pattern in the dimethylcyclohexenyl complex; hence the [3.3.1] system is not formed.

Conclusions

The neutral $\text{CpMo}(\text{CO})_2(\eta^3\text{-allyl})$ systems impart sufficient hydridic character to methylenes adjacent to the allyl fragment to allow hydride abstraction. The resulting stabilized cationic diene systems can be attacked, not only by soft nucleophiles such as enamines but also by hard nucleophiles such as Grignard reagents. This contrasts with many systems that undergo reductive decomposition with nucleophiles formed from very weakly acidic reagents.

We anticipate that these systems will prove to be of significant value in the syntheses of natural products or their synthetic precursors. For example, they may provide alternative or complementary methodologies to those using (diene) $\text{Fe}(\text{CO})_3$ developed by Pearson for a wide range of intermediates in natural product syntheses.¹⁸

Acknowledgment. We wish to thank the National Science Foundation for support of the NSF Northeast Regional NMR Facility (Grant CHE-79-16210). This work was supported by the National Science Foundation (Grant CHE-11201).

Registry No. $\text{CpMo}(\text{CO})_2(\eta^3\text{-C}_6\text{H}_9)$, 84117-08-8; $\text{Mo}(\text{CO})_6$, 13939-06-5; $(\text{CH}_3\text{CN})_2\text{MoBr}(\eta^3\text{-C}_6\text{H}_9)(\text{CO})_2$, 33154-64-2; $[\text{CpMo}(\text{CO})_2(\eta^4\text{-C}_6\text{H}_8)]^+[\text{PF}_6]^-$, 84117-10-2; $\text{CpMo}(\text{CO})_2(\eta^3\text{-C}_6\text{H}_8\text{-}4\text{-D})$, 84117-11-3; NaNcBD_3 , 25895-62-9; $\text{CpMo}(\text{CO})_2(\eta^3\text{-C}_6\text{H}_8\text{-}4\text{-CH}_3)$, 84117-12-4; CH_3Br , 74-83-9; $(\text{C}_6\text{H}_5)_3\text{CPF}_6$, 437-17-2; $\text{CpMo}(\text{CO})_2(\eta^3\text{-C}_6\text{H}_7(\text{CH}_3)_2)$, 84117-13-5; $\text{CpMo}(\text{CO})_2(\eta^3\text{-C}_6\text{H}_8(\text{C}(\text{CH}_3)_2\text{CHO}))$, 84117-14-6; $\text{CpMo}(\text{CO})_2(\eta^3\text{-C}_6\text{H}_8\text{-}4\text{-C}(\text{CH}_3)_2\text{CH}_2\text{OH})$, 84117-15-7; $\text{CpMo}(\text{CO})_2(\eta^3\text{-}9,9\text{-dimethyl-7-oxabicyclo[3.3.0]nonenyl})$, 84117-16-8; $\text{CpMo}(\text{CO})_2[\eta^3\text{-C}_6\text{H}_8\text{-}4\text{-C}(\text{CH}_3)_2\text{CH}_2\text{OC}(\text{C}_6\text{H}_5)_3]$, 84117-17-9; *exo*- $[\text{CpMo}(\text{CO})(\text{NO})(\eta^3\text{-C}_6\text{H}_9)]^+[\text{PF}_6]^-$, 84117-19-1; *endo*- $[\text{CpMo}(\text{CO})(\text{NO})(\eta^3\text{-C}_6\text{H}_9)]^+[\text{PF}_6]^-$, 84171-24-4; NOPF_6 , 16921-91-8; $\text{CpMo}(\text{CO})(\text{NO})(\eta^2\text{-C}_6\text{H}_7(\text{CH}_3)_2\text{D})$ (isomer 1), 84117-20-4; $\text{CpMo}(\text{CO})(\text{NO})(\eta^2\text{-C}_6\text{H}_7(\text{CH}_3)_2\text{D})$ (isomer 2), 84171-25-5; $[(\text{CpMo}(\text{CO})_2(\eta^4\text{-C}_6\text{H}_7(\text{CH}_3)))]^+[\text{PF}_6]^-$, 84117-22-6; lithium cyclopentadienide, 16733-97-4; (2-methyl-1-propenyl)-1-pyrrolidine, 2403-57-8; 9,9-dimethyl-7-oxabicyclo[4.3.0]nonene, 84108-27-0; 3-(1,1-dimethyl-2-hydroxyethyl)-1-cyclohexene, 84108-28-1; 4-(1,1-dimethyl-2-hydroxyethyl)-1-cyclohexene, 84108-29-2; *cis,cis*-3,5-dimethyl-6-deuteriocyclohexene, 84108-30-5; 3-deuteriocyclohexene, 84108-31-6; 3-bromo-1-cyclohexene, 1521-51-3.

Supplementary Material Available: Tables of anisotropic temperature factors and structure factors for (S)-2 (9 pages). Ordering information is given on any current masthead page.

(18) A. J. Pearson, *Acc. Chem. Res.*, **13**, 463 (1980).

Isomers of $(\text{PhMeSi})_6$ and $(\text{PhMeSi})_5$

San-Mei Chen, Lawrence D. David, Kenneth J. Haller, Cynthia L. Wadsworth, and Robert West*

Department of Chemistry, University of Wisconsin, Madison, Wisconsin 53706

Received September 20, 1982

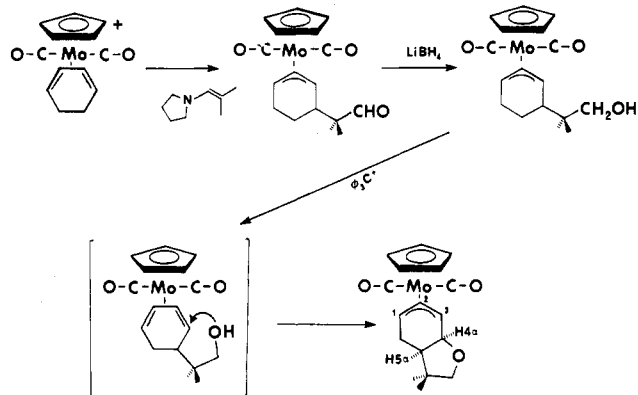
The reaction of PhMeSiCl_2 with Li in THF in the presence of $\text{Ph}_3\text{SiSiMe}_3$ produces a mixture containing 62% of five different isomers of $(\text{PhMeSi})_6$ and 25% of three isomers of $(\text{PhMeSi})_5$. The isomers were separated by a combination of fractional crystallization and HPLC, and structures are assigned on the basis of ^1H NMR data. The structure of the all-trans isomer of $(\text{PhMeSi})_6$ (**2a**) was determined by X-ray crystallography. The crystals are triclinic of space group $P\bar{1}$ with $a = 1127.6$ pm, $b = 2250.7$ pm, $c = 830.7$ pm, $\alpha = 98.24^\circ$, $\beta = 100.01^\circ$, and $\gamma = 92.12^\circ$ and two molecules per unit cell. The ring is in the chair form with phenyl groups equatorial and is somewhat distorted from idealized cyclohexane geometry.

Most of the extensive recent work on cyclosilanes¹ has dealt with symmetrically disubstituted compounds $(\text{R}_2\text{Si})_n$.

When two different substituents are present on the silicon atoms, geometric isomers are of course possible, and a few

cyclohexane ring. The tendency of the bulkier substituent to occupy an equatorial position overrides the other steric interactions, and thus, in this case, the two methyl substituents occupy in axial positions.

Functionalization of the η^3 -Cyclohexenyl Ring. The use of (2-methyl-1-propenyl)-1-pyrrolidine, an enamine of isobutyraldehyde, as a nucleophile to cationic organometallic complexes has been previously demonstrated.¹⁷ The following reaction sequence demonstrates its usefulness in functionalizing and eventually undergoing an intramolecular nucleophilic attack resulting in an unusual η^3 -cyclohexenyl bicyclo[4.3.0] complex.



The hydrolysis of the product from the reaction of $[\text{CpMo}(\text{CO})_2(\eta^4\text{-C}_6\text{H}_8)]^+$ and the enamine of isobutyraldehyde gave the 4 β -substituted 2,2-dimethylpropanol complex in good (66%) yield. As in other substituted η^3 -cyclohexenyl complexes the substituent was observed to add stereoselectively (>99%) from the non-metal side of the ring.

The aldehyde functionality was readily reduced to the primary alcohol with LiBH_4 , giving $\text{CpMo}(\text{CO})_2[\eta^3\text{-C}_6\text{H}_8\text{-}4\beta\text{-C}(\text{CH}_3)_2\text{CH}_2\text{OH}]$ in good (89%) yield. The ability to reduce the aldehyde to an alcohol without affecting the organometallic complex is an important property of the complex and demonstrates its stability in potential applications as a synthetic reagent.

Treatment of the alcohol with trityl cation apparently proceeds by abstraction of the 6 β -hydrogen to form the $\text{CpMo}(\text{CO})_2[\eta^4\text{-C}_6\text{H}_7\text{-}5\beta\text{-C}(\text{CH}_3)_2\text{CH}_2\text{OH}]$ cation. This cation cyclizes and loses the acidic OH proton to yield the [4.3.0] complex. The intramolecular reaction proceeds via attack adjacent to the substituent. This proximity effect overrides the steric interaction that yielded the 4,6-sub-

stitution pattern in the dimethylcyclohexenyl complex; hence the [3.3.1] system is not formed.

Conclusions

The neutral $\text{CpMo}(\text{CO})_2(\eta^3\text{-allyl})$ systems impart sufficient hydridic character to methylenes adjacent to the allyl fragment to allow hydride abstraction. The resulting stabilized cationic diene systems can be attacked, not only by soft nucleophiles such as enamines but also by hard nucleophiles such as Grignard reagents. This contrasts with many systems that undergo reductive decomposition with nucleophiles formed from very weakly acidic reagents.

We anticipate that these systems will prove to be of significant value in the syntheses of natural products or their synthetic precursors. For example, they may provide alternative or complementary methodologies to those using (diene) $\text{Fe}(\text{CO})_3$ developed by Pearson for a wide range of intermediates in natural product syntheses.¹⁸

Acknowledgment. We wish to thank the National Science Foundation for support of the NSF Northeast Regional NMR Facility (Grant CHE-79-16210). This work was supported by the National Science Foundation (Grant CHE-11201).

Registry No. $\text{CpMo}(\text{CO})_2(\eta^3\text{-C}_6\text{H}_9)$, 84117-08-8; $\text{Mo}(\text{CO})_6$, 13939-06-5; $(\text{CH}_3\text{CN})_2\text{MoBr}(\eta^3\text{-C}_6\text{H}_9)(\text{CO})_2$, 33154-64-2; $[\text{CpMo}(\text{CO})_2(\eta^4\text{-C}_6\text{H}_8)]^+[\text{PF}_6]^-$, 84117-10-2; $\text{CpMo}(\text{CO})_2(\eta^3\text{-C}_6\text{H}_8\text{-}4\text{-D})$, 84117-11-3; NaNcBD_3 , 25895-62-9; $\text{CpMo}(\text{CO})_2(\eta^3\text{-C}_6\text{H}_8\text{-}4\text{-CH}_3)$, 84117-12-4; CH_3Br , 74-83-9; $(\text{C}_6\text{H}_5)_3\text{CPF}_6$, 437-17-2; $\text{CpMo}(\text{CO})_2(\eta^3\text{-C}_6\text{H}_7(\text{CH}_3)_2)$, 84117-13-5; $\text{CpMo}(\text{CO})_2(\eta^3\text{-C}_6\text{H}_8(\text{C}(\text{CH}_3)_2\text{CHO}))$, 84117-14-6; $\text{CpMo}(\text{CO})_2(\eta^3\text{-C}_6\text{H}_8\text{-}4\text{-C}(\text{CH}_3)_2\text{CH}_2\text{OH})$, 84117-15-7; $\text{CpMo}(\text{CO})_2(\eta^3\text{-}9,9\text{-dimethyl-7-oxabicyclo[3.3.0]nonenyl})$, 84117-16-8; $\text{CpMo}(\text{CO})_2[\eta^3\text{-C}_6\text{H}_8\text{-}4\text{-C}(\text{CH}_3)_2\text{CH}_2\text{OC}(\text{C}_6\text{H}_5)_3]$, 84117-17-9; *exo*- $[\text{CpMo}(\text{CO})(\text{NO})(\eta^3\text{-C}_6\text{H}_9)]^+[\text{PF}_6]^-$, 84117-19-1; *endo*- $[\text{CpMo}(\text{CO})(\text{NO})(\eta^3\text{-C}_6\text{H}_9)]^+[\text{PF}_6]^-$, 84171-24-4; NOPF_6 , 16921-91-8; $\text{CpMo}(\text{CO})(\text{NO})(\eta^2\text{-C}_6\text{H}_7(\text{CH}_3)_2\text{D})$ (isomer 1), 84117-20-4; $\text{CpMo}(\text{CO})(\text{NO})(\eta^2\text{-C}_6\text{H}_7(\text{CH}_3)_2\text{D})$ (isomer 2), 84171-25-5; $[(\text{CpMo}(\text{CO})_2(\eta^4\text{-C}_6\text{H}_7(\text{CH}_3)))]^+[\text{PF}_6]^-$, 84117-22-6; lithium cyclopentadienide, 16733-97-4; (2-methyl-1-propenyl)-1-pyrrolidine, 2403-57-8; 9,9-dimethyl-7-oxabicyclo[4.3.0]nonene, 84108-27-0; 3-(1,1-dimethyl-2-hydroxyethyl)-1-cyclohexene, 84108-28-1; 4-(1,1-dimethyl-2-hydroxyethyl)-1-cyclohexene, 84108-29-2; *cis,cis*-3,5-dimethyl-6-deuteriocyclohexene, 84108-30-5; 3-deuteriocyclohexene, 84108-31-6; 3-bromo-1-cyclohexene, 1521-51-3.

Supplementary Material Available: Tables of anisotropic temperature factors and structure factors for (S)-2 (9 pages). Ordering information is given on any current masthead page.

(18) A. J. Pearson, *Acc. Chem. Res.*, **13**, 463 (1980).

Isomers of $(\text{PhMeSi})_6$ and $(\text{PhMeSi})_5$

San-Mei Chen, Lawrence D. David, Kenneth J. Haller, Cynthia L. Wadsworth, and Robert West*

Department of Chemistry, University of Wisconsin, Madison, Wisconsin 53706

Received September 20, 1982

The reaction of PhMeSiCl_2 with Li in THF in the presence of $\text{Ph}_3\text{SiSiMe}_3$ produces a mixture containing 62% of five different isomers of $(\text{PhMeSi})_6$ and 25% of three isomers of $(\text{PhMeSi})_5$. The isomers were separated by a combination of fractional crystallization and HPLC, and structures are assigned on the basis of ^1H NMR data. The structure of the all-trans isomer of $(\text{PhMeSi})_6$ (**2a**) was determined by X-ray crystallography. The crystals are triclinic of space group $P\bar{1}$ with $a = 1127.6$ pm, $b = 2250.7$ pm, $c = 830.7$ pm, $\alpha = 98.24^\circ$, $\beta = 100.01^\circ$, and $\gamma = 92.12^\circ$ and two molecules per unit cell. The ring is in the chair form with phenyl groups equatorial and is somewhat distorted from idealized cyclohexane geometry.

Most of the extensive recent work on cyclosilanes¹ has dealt with symmetrically disubstituted compounds $(\text{R}_2\text{Si})_n$.

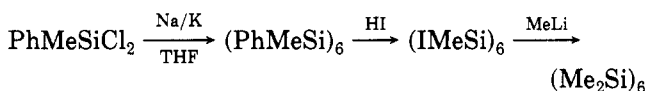
When two different substituents are present on the silicon atoms, geometric isomers are of course possible, and a few

Table I. Yields and Spectral Properties of (PhMeSi)_n Isomers

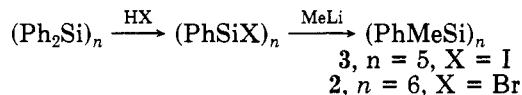
isomer	yield, %	mp, °C	¹ H NMR, ppm		¹³ C NMR, ppm		λ _{max}					
			CH ₃	C ₆ H ₅	CH ₃	C ₆ H ₅	nm	ε				
2a	16	320	0.808 (s)	7.20 (s)	-4.1 (s)	127.7	320	300				
							128.2	64 000				
							134.9	71 000				
							136.4					
2b	15	174	0.787 (2)	7.24 (1)	-3.79 (3)	127.5	326	360				
							0.751 (1)	7.22 (2)	-3.98 (2)	128.0	261	58 000
							0.634 (2)	7.16 (2)	-6.84 (1)	134.9	222	98 000
							0.610 (1)			135.2		
										135.9		
2c	5	180	0.676 (s)	7.30 (s)			332					
							258					
							220					
2d	18	56	0.765 (1)	7.38 (1)	-3.72 (1)	127.6	261	42 000				
							0.588 (2)	7.36 (2)	-3.76 (2)	128.2	222	52 000
								7.25 (1)		134.9	214	sh
										135.2		
										135.9		
2e	8	65	0.738 (1)	7.26 (2)	-4.32 (2)	127.5	278	sh				
							0.705 (2)	7.24 (1)	-4.56 (1)	128.2	258	37 000
							0.586 (2)	7.26 (1)	-5.52 (2)	135.0	222	85 000
							0.495 (1)	7.16 (2)	-6.84 (1)	135.2	217	sh
3a	17	55	0.633 (2)	7.3	-4.20 (1)	127.5	298	4 000				
							0.609 (1)	7.4	-4.56 (4)	128.0	258	36 000
							0.529 (2)			134.9	223	100 000
										135.5		
3b			0.585 (2)	7.30			320	2 500				
			0.575 (2)									
3c	8	40	0.345 (1)	7.36			256	31 000				
			0.708 (1)	7.40			222	78 000				
			0.605 (2)									
			0.505 (2)									

such structures have been identified, for example the (*t*-BuMeSi)₄ isomers.^{2,3}

In 1972 Hengge and Lunzer⁴ reported that reaction of phenylmethylchlorosilane (1) with sodium-potassium alloy in tetrahydrofuran (THF) gave 10% of (PhSiMe)₆ (2) showing only two singlets in the ¹H NMR spectrum. These workers therefore deduced that the product was a single isomer, the all-trans form. General structural proof was provided by the reaction of 2 with HI and then MeLi to produce the well-known compound (Me₂Si)₆. Mixtures



of isomers of both 2 and (PhMeSi)₅ (3) have also been prepared by partial halodephenylation of the perphenyl cyclic compounds (Ph₂Si)₅ and (Ph₂Si)₆, followed by methylation.⁵



We have now investigated the (PhMeSi)_n series more fully, making use of the reaction of 1 with lithium metal at 0 °C.

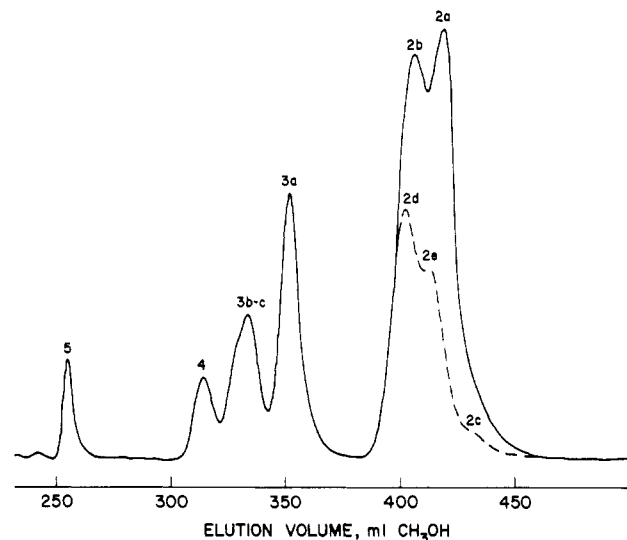


Figure 1. High-pressure liquid chromatograph of reaction mixture before (solid line) and after (dashed line) removal of isomers 2a and 2b by crystallization.

Results and Discussion

Synthesis, Isomer Separation, and Structural Assignment. Reaction of 1 with lithium in THF at 0 °C in the presence of 1,1,1-trimethyltriphenyldisilane⁶ as an equilibrating catalyst produced a mixture containing about 62% of isomers of 2 and 25% of isomers of 3. A small amount of polymeric material was also formed, and minor quantities of byproducts including 3% of H(PhMeSi)₄H (4) and 2% of its oxidation product, H(PhMeSiO)₃PhMeSiH (5).⁷

(1) For reviews see: West, R. *Pure Appl. Chem.* 1982, 54, 1041. West, R. In "Comprehensive Organometallic Chemistry"; Abel, E., Ed.; Pergamon Press: Oxford, England, 1981; Chapter 9.4. Hengge, E. *J. Organomet. Chem., Libr.* 1971, 4, 261. West, R.; Carberry, E. C. *Science (Washington, D.C.)* 1975, 189, 179.

(2) Biernbaum, M.; West, R. *J. Organomet. Chem.* 1977, 131, 179.

(3) Helmer, B. J.; West, R. *J. Organomet. Chem.*, in press.

(4) Hengge, E.; Lunzer, F. *Synth. Inorg. Met.-Org. Chem.* 1972, 2, 93.

Our attempts to replicate the synthesis of 2 following the published directions have been unsuccessful.

(5) Hengge, E.; Marketz, H. *Monatsh. Chem.* 1970, 101, 528. Hengge, E.; Lunzer, F. 1976, 107, 371.

(6) Brook, A. G.; Gilman, H. *J. Am. Chem. Soc.* 1954, 76, 278.

Table II. Atomic Coordinates of Non-Hydrogen Atoms

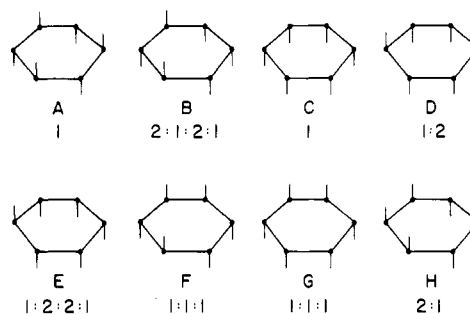
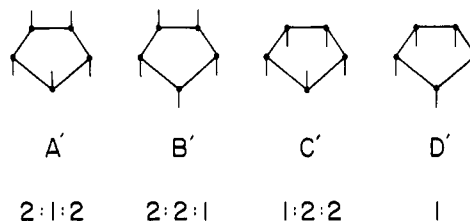
atom	x	y	z
Si(1)	0.95477 (6)	0.34882 (3)	0.07413 (9)
C(1)	0.89781 (22)	0.41479 (11)	0.2006 (3)
C(2)	0.8836 (3)	0.41291 (15)	0.3630 (4)
C(3)	0.8340 (3)	0.45878 (17)	0.4537 (4)
C(4)	0.7954 (3)	0.50780 (15)	0.3813 (5)
C(5)	0.8084 (3)	0.51115 (15)	0.2241 (5)
C(6)	0.8597 (3)	0.46558 (14)	0.1348 (5)
C(7)	0.9751 (4)	0.36891 (16)	-0.1321 (4)
Si(2)	0.80032 (6)	0.27149 (3)	0.02435 (8)
C(8)	0.66224 (22)	0.30238 (11)	-0.0906 (3)
C(9)	0.60926 (27)	0.35118 (15)	-0.0168 (4)
C(10)	0.51114 (29)	0.37633 (16)	-0.1009 (5)
C(11)	0.4637 (3)	0.35320 (15)	-0.2593 (5)
C(12)	0.5085 (4)	0.30299 (17)	-0.3341 (5)
C(13)	0.6081 (3)	0.27843 (15)	-0.2502 (4)
C(14)	0.7679 (3)	0.25453 (16)	0.2282 (4)
Si(3)	0.85734 (6)	0.18619 (3)	-0.13858 (8)
C(15)	0.73485 (21)	0.12297 (10)	-0.17949 (29)
C(16)	0.62636 (24)	0.12861 (12)	-0.1230 (4)
C(17)	0.53777 (27)	0.08179 (14)	-0.1560 (4)
C(18)	0.55642 (27)	0.02815 (13)	-0.2460 (4)
C(19)	0.66266 (27)	0.02116 (13)	-0.3029 (4)
C(20)	0.75144 (26)	0.06787 (12)	-0.2694 (4)
C(21)	0.8828 (3)	0.20581 (16)	-0.3442 (4)
Si(4)	1.03388 (6)	0.15325 (3)	0.01033 (9)
C(22)	1.10175 (22)	0.09107 (11)	-0.1154 (3)
C(23)	1.1726 (3)	0.05042 (14)	-0.0378 (4)
C(24)	1.2279 (3)	0.00627 (14)	-0.1266 (5)
C(25)	1.21459 (28)	0.00105 (14)	-0.2930 (4)
C(26)	1.1460 (3)	0.04063 (17)	-0.3746 (4)
C(27)	1.0917 (3)	0.08497 (16)	-0.2858 (4)
C(28)	0.9938 (3)	0.12469 (17)	0.1972 (4)
Si(5)	1.19211 (6)	0.22889 (3)	0.08800 (8)
C(29)	1.31217 (22)	0.19526 (11)	0.2309 (3)
C(30)	1.42179 (26)	0.18019 (14)	0.1859 (4)
C(31)	1.50626 (28)	0.15164 (15)	0.2862 (5)
C(32)	1.48357 (28)	0.13802 (14)	0.4330 (4)
C(33)	1.3763 (3)	0.15235 (14)	0.4827 (4)
C(34)	1.29211 (27)	0.18013 (14)	0.3816 (4)
C(35)	1.2514 (3)	0.24361 (17)	-0.1009 (4)
Si(6)	1.13634 (6)	0.32036 (3)	0.22277 (8)
C(36)	1.26236 (22)	0.37995 (11)	0.2375 (3)
C(37)	1.24289 (27)	0.43681 (13)	0.1980 (4)
C(38)	1.3367 (3)	0.48096 (14)	0.2217 (5)
C(39)	1.4517 (3)	0.46838 (15)	0.2869 (4)
C(40)	1.47388 (28)	0.41239 (16)	0.3258 (4)
C(41)	1.38011 (25)	0.36823 (14)	0.2991 (4)
C(42)	1.1220 (3)	0.31213 (15)	0.4415 (4)

From this product mixture isomers **2a** and **2b** were separated by fractional crystallization, and the remaining mixture was separated by reverse-phase HPLC (see Figure 1 and Experimental Section). Five of the eight possible isomers of **2**, and three of the four possible isomers of **3**, were identified in the products. Yields of these isomers, designated **2a-e** and **3a-c**, are shown along with some of their properties in Table I.

A combination of X-ray crystallography and ¹H NMR spectroscopy was used to assign structures to **2a-e**. The eight possible isomers of **2** are shown diagrammatically in Chart I, together with their expected ¹H NMR patterns in the methyl region. Only two isomers A and C are predicted to show a singlet in the methyl region of the proton NMR spectrum. Both of these isomers were found in the reaction products, as **2a** and **2c**. The X-ray crystal structure of **2a** shows that it is the all-trans isomer A, and therefore **2c** is the all-cis isomer C.

Isomer **2a** has the largest downfield shift, 0.808 ppm, of the methyl protons of any of the compounds in the series.

(7) Compound **4** may possibly arise from ring opening of the cyclic compound (PhMeSi)₄. It is surprisingly labile to oxygen; when **4** was left standing exposed to air, it is quantitatively converted to **5**.

Chart I. Possible Isomers of (PhMeSi)₆ and Predicted Methyl Region ¹H NMR PatternsChart II. Possible Isomers of (PhMeSi)₅ and Predicted Methyl Region ¹H NMR Patterns

The reason for this deshielding is not clear, but we propose that in any event a methyl group in a structure **2** which is cis to two phenyl groups, as in **2a**, will have a downfield shift relative to other methyls that do not have this environment. On this basis it is possible to make tentative assignments of structures for the other isomers.⁸

The two isomers of **2** with lowest symmetry B and E would both be expected to show 2:2:1:1 patterns in the methyl proton region. Two isomers having this pattern were found, **2b** and **2e**. Isomer **2b** has three methyl groups with relatively large downfield shifts, consistent with structure B which has three methyls each cis to two phenyl groups. Isomer **2e** has only one methyl with a relatively large downfield shift, consistent with structure E.

The last isomer of **2** in the mixture is **2d**, with a 1:2 methyl proton pattern. From symmetry **2d** must be either D or H. Because two of the six methyl groups in **2d** show a relatively large downfield shift of 0.765 ppm, we favor structure D, which has two methyls flanked by *cis*-phenyl groups. Structure H has no methyl groups with this type of environment.

It is difficult to rationalize the observed isomeric distribution of products **2a-e**. On steric grounds one might expect the all-trans isomer **2a** to be favored, and the all-cis isomer **2c** to be strongly disfavored. Perhaps the six-membered rings of **2a-e** may be distorted from the expected chair arrangement in ways which relieve steric compression, so that there are several isomers of **2** with nearly equal energy. Nonbonded attractive forces between substituent groups may also play a part in stabilizing some structures. The ¹H NMR signals in the phenyl region cannot be separated for all of the compounds, but where they can they are consistent with the methyl NMR data (Table I). Carbon-13 NMR spectra (Table I) were likewise consistent with the assigned structures.

On a similar NMR basis a somewhat more speculative assignment can be made for the isomers **3a-c** of (PhMeSi)₅. Because all three isomers show 2:2:1 patterns in the methyl region of the proton NMR, the all-cis structure D'

(8) Because environmental factors will also play a part in determining ¹H chemical shifts, some variations in ¹H δ between methyl groups in similar environments but in different compounds are expected.

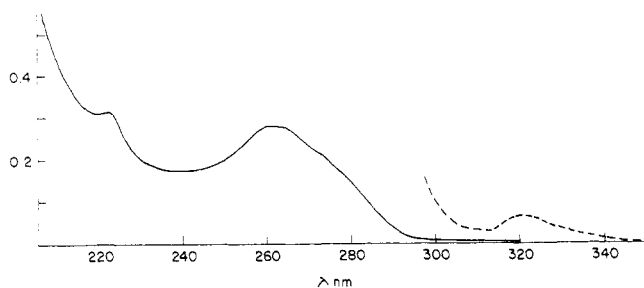


Figure 2. Ultraviolet spectrum of **2a**. Absorbance units on the vertical axis apply to the solid curve and should be multiplied by 5 for the dashed line curve.

that should show only a singlet can be eliminated (Chart II). Of the remaining structures, only B' has no methyl groups *cis* to phenyls on each side. We therefore assign this structure to **3b**, which has no downfield methyl resonances. Structure C' has a single methyl group flanked by two *cis*-phenyls, and tentatively we assign this structure to **3c**, which has one methyl group shifted much downfield from the others. Isomer **3a** has three methyl groups with about the same downfield shift, consistent with structure A'. Inspection of models shows that A' should be the least hindered five-membered ring structure, and **3a** is in fact the isomer formed in largest amount (Table I).

Isomers **2a** and **2b** were separately treated with preformed triphenylsilyllithium in THF, in an attempt to bring about equilibration of the various isomers. Within 1 h substantial amounts of the five-membered rings **3a-c** were formed, in the same relative proportions as in the catalyzed reaction mixture. However conversion to other isomers of **2** was very slow, being only slight after 48 h after which decomposition of the mixture supervened.

Electronic Spectra. The ultraviolet absorption bands for **2a-e** and **3a-c** are shown in Table I. Some, but not all, of the isomers of **2** show a weak absorption near 320 nm. This is similar in position but much weaker than the long wavelength absorption of $(\text{PhMeSi})_n$ high polymers.⁹ The **2** isomers all show strong bands near 260 and 220 nm, assignable to mixed transitions involving interaction between benzene ring and polysilane orbitals.¹⁰ These strong bands appear to contain several different transitions observable as shoulders; the spectrum of **2a** is shown in Figure 2 as an example. Compound **3a** also shows strong bands near 260 and 220 nm and in addition a moderately intense absorption at 298 nm, which may be a cyclosilane excitation.¹¹ The electronic spectrum of the **3b-c** mixture is similar.

Anion Radicals and Electron Spin Resonance Spectra. Cyclosilanes are known to undergo reduction to electron-delocalized anion radicals. Both permethyl¹¹ and perphenyl¹² four- and five-membered rings form anion radicals that are stable at low temperature; six-membered cyclosilane anion radicals are much less stable. For the anion radical of the monophenyl-substituted five-membered ring $\text{PhSi}_5\text{Me}_9^-$, the electron spin resonance spectrum shows that the unpaired electron is associated with the polysilane ring.¹³ In the corresponding six-membered ring anion radical $\text{PhSi}_6\text{Me}_{11}^-$, the electron is located on the benzene ring, and decomposition to the cyclopenta-

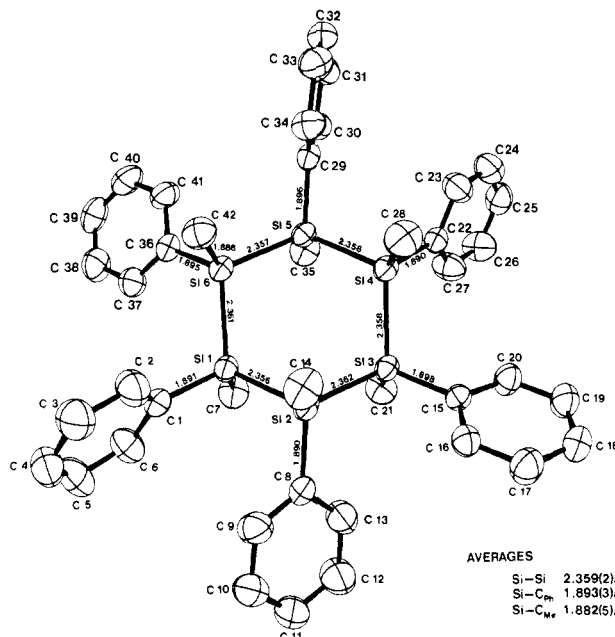


Figure 3. Structure of **2a** in plane view showing some important bond lengths. Hydrogen atoms are omitted for clarity.

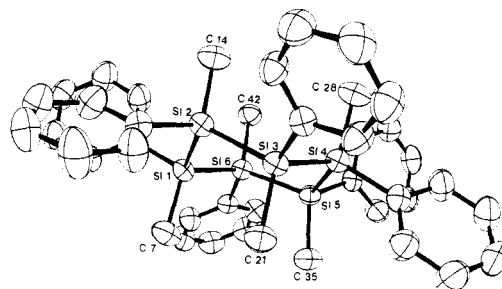


Figure 4. Structure of **2a** showing chair cyclohexane conformation. Hydrogen atoms are omitted.

silane anion $(\text{Me}_2\text{Si})_5^-$ takes place even at -90°C .

The isomers of **2** also fail to give stable anion radicals. Each of the isomers was separately reduced at -100°C , and in every case the only ESR spectrum observed was that of benzene anion radical. However, the isomers **3a**, and a mixture of **3b** and **3c**, were reduced electrolytically to species that showed ESR spectra assignable to the cyclopolysilane anion radicals. In each case the spectrum consisted of a single broad line containing unresolved hydrogen hyperfine coupling and doublet of sidebands attributable to coupling by ^{13}C . The observed *g* values near 2.0040 are intermediate between those for $(\text{Me}_2\text{Si})_5^-$ ($g = 2.0032$)¹¹ and $(\text{Ph}_2\text{Si})_5^-$ ($g = 2.0046$).¹²

Crystal Structure of 2a. Molecules of **2a** exist in the chair form, as shown in Figures 3 and 4, similar to the conformation established for $(\text{Me}_2\text{Si})_6$ (**6**)¹⁴ and proposed for $(\text{Ph}_2\text{Si})_6$.¹⁵ In this all-trans isomer the methyl groups occupy the axial and the phenyl groups the equatorial positions. The unit cell of **2a** does not impose any symmetry on the molecule: the variable rotation of the phenyl rings relative to the Si_6 ring is presumably determined by crystal packing forces.

The torsion angles in the Si_6 ring in **2a** vary considerably, from 47.9 to 61.8° (Table III, average 55.2°), in contrast

(9) Djurovich, P. I.; West, R., unpublished results.

(10) Pitt, C. G.; Bock, H. *J. Chem. Soc., Chem. Commun.* **1972**, 28.

(11) Carberry, E.; West, R.; Glass, G. E. *J. Am. Chem. Soc.* **1969**, *91*, 5446.

(12) Kira, M.; Bock, H. *J. Organomet. Chem.* **1979**, *164*, 277.

(13) West, R.; Kean, E. S. *J. Organomet. Chem.* **1975**, *96*, 323. Buchanan, A. C.; West, R. *Ibid.* **1979**, *172* 273.

(14) Carrell, H. L.; Donohue, *Acta Crystallogr., Sect. B*, **1972**, *B28*, 1566.

(15) Hönig, H.; Hassler, K. *Monatsh. Chem.* **1982**, *113*, 285.

(16) Bolton, J. R. *Mol. Phys.* **1963**, *6*, 219.

Table III. Selected Interatomic Distances (Å) and Angles (deg) for 2a

Distances					
Si(1)-Si(2)	2.356 (1)	Si(1)-C(1)	1.891 (3)	Si(1)-C(7)	1.882 (3)
Si(2)-Si(3)	2.362 (1)	Si(2)-C(8)	1.890 (3)	Si(2)-C(14)	1.881 (3)
Si(3)-Si(4)	2.358 (1)	Si(3)-C(15)	1.898 (2)	Si(3)-C(21)	1.890 (3)
Si(4)-Si(5)	2.358 (1)	Si(4)-C(22)	1.890 (3)	Si(4)-C(28)	1.880 (3)
Si(5)-Si(6)	2.357 (1)	Si(5)-C(29)	1.896 (3)	Si(5)-C(35)	1.875 (3)
Si(6)-Si(1)	2.361 (1)	Si(6)-C(36)	1.895 (2)	Si(6)-C(42)	1.886 (3)
Si-Si(av)	2.359 (2)	Si-C _{Ph} (av)	1.893 (3)	Si-C _{Me} (av)	1.882 (5)
Bond Angles					
Si(1)-Si(2)-Si(3)	109.79 (4)	Si(3)-Si(4)-Si(5)	112.99 (4)	Si(5)-Si(6)-Si(1)	110.19 (4)
Si(2)-Si(3)-Si(4)	107.93 (4)	Si(4)-Si(5)-Si(6)	114.06 (4)	Si(6)-Si(1)-Si(2)	111.91 (4)
Torsion Angles					
Si Ring					
Si(1)-Si(2)-Si(3)-Si(4)	61.09 (5)	Si(4)-Si(5)-Si(6)-Si(1)	47.92 (5)		
Si(2)-Si(3)-Si(4)-Si(5)	56.07 (5)	Si(5)-Si(6)-Si(1)-Si(2)	53.52 (5)		
Si(3)-Si(4)-Si(5)-Si(6)	50.97 (5)	Si(6)-Si(1)-Si(2)-Si(3)	61.77 (5)		
C _{Ph} -Si-Si-C _{Ph}					
C(1)-Si(1)-Si(2)-C(8)	59.38 (13)	C(22)-Si(4)-Si(5)-C(29)	66.11 (12)		
C(8)-Si(2)-Si(3)-C(15)	63.57 (12)	C(29)-Si(5)-Si(6)-C(36)	73.94 (12)		
C(15)-Si(3)-Si(4)-C(22)	67.27 (12)	C(36)-Si(6)-Si(1)-C(1)	69.49 (12)		
C _{Me} -Si-Si-C _{Me}					
C(7)-Si(1)-Si(2)-C(14)	175.25 (18)	C(28)-Si(4)-Si(5)-C(35)	167.58 (18)		
C(14)-Si(2)-Si(3)-C(21)	177.93 (17)	C(35)-Si(5)-Si(6)-C(42)	162.86 (16)		
C(21)-Si(3)-Si(4)-C(28)	172.14 (17)	C(42)-Si(6)-Si(1)-C(7)	170.99 (17)		
C _{Ph} -Si-Si-C _{Me}					
C(1)-Si(1)-Si(2)-C(14)	57.74 (6)	C(7)-Si(1)-Si(2)-C(8)	58.14 (16)		
C(8)-Si(2)-Si(3)-C(21)	56.13 (15)	C(14)-Si(2)-Si(3)-C(15)	58.22 (15)		
C(15)-Si(3)-Si(4)-C(28)	53.04 (16)	C(21)-Si(3)-Si(4)-C(22)	51.84 (15)		
C(22)-Si(4)-Si(5)-C(29)	51.18 (16)	C(28)-Si(4)-Si(5)-C(29)	50.29 (16)		
C(29)-Si(5)-Si(6)-C(42)	42.22 (14)	C(35)-Si(5)-Si(6)-C(36)	46.70 (15)		
C(36)-Si(6)-Si(1)-C(7)	52.62 (15)	C(42)-Si(6)-Si(1)-C(1)	48.88 (15)		

to those of **6** which all lie between 53.2 and 53.7°. The C_{Ph}-Si-Si-C_{Ph} and C_{Me}-Si-Si-C_{Me} angles in **2a** also vary over a range of more than 15° (Table III): the trans C-Si-Si-C torsional angles in **6** vary only from 168 to 170.9°. Finally, the Si-Si-Si bond angles in **2a** vary from 107.9 to 114.1°, compared to **6** where the variation is only from 111.6 to 112.4°. Thus the ring structure in **2a** is quite distorted from the ideal cyclohexane geometry and from the nearly symmetrical structure of **6**.

The Si-Si bond lengths in **2a** (Table II), 235.6-236.2 pm are in the normal range for Si-Si single bonds but are slightly longer than for **6**, 233.8 pm. The Si-C_{Me} lengths of 188.2 (5) pm are significantly shorter than for **6**, wherein they range from 191.3 to 194.3 pm. Part of the shortening may be associated with the axial orientation of these bonds; in **6**, the axial Si-C bonds average 2.2 pm shorter than the equatorial bonds. The Si-Ph bond lengths, 189.3 (3) pm, in **2a** are normal, as are the C-C bond lengths in the aromatic rings.

Experimental Section

All reactions were carried out under an atmosphere of dry nitrogen. The THF was dried over sodium and distilled. Compound **1** was obtained from Petrarch Systems, Inc. All NMR spectra were run by using CDCl₃ as solvent and Me₄Si as an internal standard. ¹H NMR spectra were recorded on a WP 200SY NMR spectrometer. ¹³C NMR spectra were obtained by using a JEOL FX-200 NMR spectrometer. Infrared spectra were taken on a Perkin-Elmer Model 657 infrared spectrophotometer. Mass spectra were recorded on a Varian AEI MS 902 at 70 eV. Ultraviolet spectra were run in spectrograde THF and were recorded by using a Varian Cary Model 18 spectrometer. ESR spectra were obtained on a Varian E-15 spectrometer with a Varian V-4343 variable-temperature controller.

Preparation and Isolation of (PhMeSi)_n Isomers. The reaction was carried out in a 1-L three-necked flask equipped with a mechanical stirrer, dropping funnel, and nitrogen inlet. Freshly

distilled THF (600 mL), cut lithium wire (2.92 g, 0.42 mol), and 0.1 g of 1,1,1-trimethyltriphenyldisilane were added and the mixture was cooled to 0 °C in ice. A solution of 38.2 g (0.2 mol) of PhMeSiCl₂ in 200 mL of THF was added with stirring during 1 h, and the mixture was stirred for an additional 24 h, maintaining the temperature at 0 °C. At this time the mixture was reddish brown, and nearly all the lithium had been consumed.

The mixture was filtered through glass wool to remove excess lithium, and 20 mL of water was added to dissolve lithium salts. The THF layer was separated, dried over MgSO₄, and filtered. Evaporation of the THF in a rotary evaporator yielded 24 g of an oil containing some solid, which was diluted with 50 mL of hexane and stirred overnight. The hexane-insoluble solid was filtered off and recrystallized from toluene to give 3.0 g of pure **2a**. An additional 0.7 g of **2a** was obtained by evaporating toluene from the mother liquor.

Most of the solvent was evaporated from the hexane solution, leaving a viscous oily mixture, which was allowed to stand for 2 days to precipitate 3.0 g of white solid. An addition 0.6 g of solid was obtained after another day. The combined solids were recrystallized from 15:1 hexane/toluene to give pure **2b**. Next, 10 mL of methanol was added to the oil, and the mixture was stirred to precipitate a small amount of isomer **2d** and mixed with a trace of **2b**. The remaining oil was separated by reversed-phase HPLC on Partisil ODS-2 using Whatman M9 or M20 columns with 100% methanol as the mobile phase to separate isomers **2c-e**, **3a-c** (Table I), **4**, and **5**.

Molecular weight by mass spectra (*m/e*): calculated for **2a-e** 720.2372; found for **2a** 720.2365 (deviation -0.7 ppm), **2b**, 720.2340 (deviation -3.2 ppm), **2c**, 720.2375 (deviation 0.3 ppm), **2d**, 720.2375 (deviation 0.3 ppm), **2e**, 720.2375 (deviation 0.3 ppm). Molecular weight by mass spectra: calculated for **3**, 600.1977; found for **3a**, 600.1974 (deviation -0.3 ppm), **3b**, **3c**, 600.1956 (deviation -2.1 ppm). Anal. Calcd for C₄₂H₄₈Si₆: C, 70.00; H, 6.67. Found: for **2a**, C, 69.81; H, 6.80; for **2b**, C, 69.77; H, 6.97.

Isomers **2a-e**, and **3a-c**, produced very similar mass spectra within each family. Large parent and P + 1 peaks are found, as well significant Si₄ fragments. A typical mass spectrum, with assignments and intensities relative to the base peak, is that for

2c (*m/e* (relative intensity)): 721 (P + 1, 55.7), 720 (P, 82.1), 450 (Ph₄Me₂Si₄, 1.5), 388 (Ph₃Me₃Si₄, 3.6), 197 (Ph₂MeSi, 100), 135 (PhMe₂Si, 82.7), 105 (PhSi, 20.9), 78 (PhH, 22.7), 43 (MeSi, 17.1). Mass spectrum for **3a** (*m/e* (relative intensity)): 601 (P + 1, 54), 600 (P, 96), 480 (Ph₄Me₄Si₄, 1.3), 450 (Ph₄Me₂Si₄, 2.4), 388 (Ph₃Me₃Si₄, 8.9), 283 (Ph₂Me₃Si₃, 2.7), 240 (Ph₂Me₂Si₂, 6.1), 197 (Ph₂MeSi, 100), 135 (PhMe₂Si, 83), 105 (PhSi, 30), 78 (PhH, 11), 43 (MeSi, 23).

Compound **4** was identified as a silane by its strong Si-H absorption in the infrared at 2100 cm⁻¹. The ¹H NMR showed a pattern attributable to Si-H at 4.32 (1), 4.35 (3), 4.38 (3), and 4.40 (1) ppm (*J*_{CH₃-H} = 5.45 Hz) as well as lines at 0.40 (s, CH₃SiPh) and 0.35 (d, CH₃SiH) ppm and phenyl resonances clustered at 7.30 ppm; the relative intensities were correct for the assigned structure. Mass spectrum (*m/e* (relative intensities)): 483 (P + 1, 11.0), 482 (P, 26.2), 362 (Ph₃Me₃Si₃H₂, 22.5), 361 (Ph₂Me₃Si₃H, 70.8), 360 (Ph₃Me₃Si₃, 9.2), 285 (Ph₂Me₃Si₃H₂, 23.7), 284 (Ph₂Me₃Si₃H, 100.0), 241 (Ph₂Me₂Si₂H, 52.9), 240 (Ph₂Me₂Si₂, 69.3), 197 (Ph₂MeSi 99.6), 105 (PhSi, 90.3). Compound **5** also showed an SiH infrared band at 2100 cm⁻¹ and ¹H NMR at 4.35 (1), 4.37 (3), 4.38 (3), 4.40 (1) (SiH, *J*_{CH₃-H} = 3.40 Hz), 0.386 (d, CH₃SiH), 0.33 (s, CH₃SiPh), 7.3 (C₆H₅) ppm. Anal. Calcd for C₂₈H₃₄Si₄O₃: C, 63.40; H, 6.41. Found: C, 63.08; H, 6.42. Mass spectrum (*m/e* (relative intensity)): 531 (P + 1, 2.7), 530 (P, 12.8), 529 (Ph₄Me₄Si₄O₃H, 21.3), 451 (Ph₃Me₄Si₄O₃, 8.7), 257 (Ph₂Me₂Si₂OH, 1.2), 197 (Ph₂MeSi, 32.2), 135 (PhMe₂Si, 18.6), 121 (PhSiMeH, 11.4), 44 (MeSiH, 100).

Anion Radicals. Anion radicals were generated by electrolytic reduction of solutions approximately 0.01 M in cyclosilane and 0.2 M in tetra-*n*-butylammonium perchlorate. Purified THF was used as solvent for the five-membered rings that were electrolyzed initially at -90 °C. For the six-membered rings, which required lower temperatures, a 3:1 mixture of 2-methyltetrahydrofuran/1,2-dimethoxyethane was used as solvent, and electrolysis was carried out at -110 °C. The *g* values were determined relative to a pitch sample by using a Hewlett-Packard 5254L electronic frequency counter and were reproducible to ±0.0001.

Each of the isomers **2a-e**, upon reduction, produced solutions that showed seven-line ESR spectra identical with that for the anion radical of benzene.¹⁶ Isomer **3a** reduced to a green solution that gave a single broad ESR line at *g* = 2.0040, with peak width Δ*H*_{pp} = 2.5 G, and two pairs of weak doublet sidebands with couplings 16.4 and 23 G. The spectrum faded above -65 °C. The mixture of **3b, c** gave a brick-red solution upon reduction, with a similar broad central ESR line (Δ*H*_{pp} = 2.06 G) at *g* = 2.0039 and a doublet sideband with hyperfine splitting constant of 14.1 G. This radical was exceptionally stable; the ESR signal began to disappear only above -20 °C.

Crystal Structure of 2a. Crystals of **2a** suitable for X-ray diffraction studies were obtained by slow evaporation of a xylene solution. A single crystal of approximate dimensions 0.4 × 0.4 × 0.6 mm was mounted in a thin-walled glass capillary for the X-ray study. Preliminary examination of the crystal on a Syntex P1 diffractometer showed the crystal to be triclinic. The assumed space group P1 (No. 2) was verified by subsequent successful solution and refinement of the structure. The unit cell parameters (at 19 ± 1 °C, γ(Mo Kα) = 0.71073 Å) are *a* = 11.276 (2) Å, *b* = 22.507 (3) Å, *c* = 8.307 (2) Å, α = 98.24 (1)°, β = 100.01 (2)°, and γ = 92.12 (2)°. These parameters were determined from a least-squares refinement utilizing the setting angles of 30 accurately centered reflections (25° < 2θ < 36°), each collected at ±2θ. The unit cell volume of 2051 Å³ led to a calculated density of 1.17 g/cm³ for two formula units of Si₆C₄₂H₄₈ per unit cell. The

experimental density measured by flotation was 1.18 g/cm³.

X-ray intensity data were collected by using a Syntex P1 diffractometer equipped with a graphite-monochromated Mo Kα radiation source. A total of 9421 unique reflections with (sin θ)/λ ≤ 0.649 Å⁻¹ were collected by using a θ-2θ step-scan technique with a scan range of 0.78° below 2θ(Mo Kα₁) to 0.65° above 2θ(Mo Kα₂) and a variable scan rate (2.0-24.0°/min). Throughout data collection four standard reflections from diverse regions of reciprocal space were monitored every 50 reflections. The intensities of the standard reflections showed no systematic variations during the time required to collect the data. The intensity data were reduced and standard deviations calculated by using methods similar to those described previously.¹⁷ Since the linear absorption coefficient is only 0.255 mm⁻¹ for Mo K_α radiation and the crystal was of nearly equant habit, an absorption correction was not deemed necessary.

The structure was solved by direct methods using the MULTAN¹⁸ package and the 410 reflections with the highest values of |*E*|. An *E* map based upon these reflections revealed two silicon and seven carbon atoms. Difference electron density maps revealed the rest of the 48 non-hydrogen atoms. The model was refined by a blocked full-matrix technique using the 5756 reflections with *F*_o > 3σ(*F*_o); atomic form factors were taken from Cromer and Waber¹⁹ and that for hydrogen from Stewart, Davidson, and Simpson.²⁰ Anisotropic refinement on the non-hydrogen atoms converged with *R*₁ = ∑||*F*_o - |*F*_c||/∑|*F*_o| = 0.069 and *R*₂ = [∑ω(|*F*_o - |*F*_c||)²/∑ω(*F*_o)²]^{1/2} = 0.109. All 48 hydrogen atoms were assumed to vibrate isotropically and their position, and thermal parameters were included with the parameters being refined. This final model converged with *R*₁ = 0.044 and *R*₂ = 0.056. The final difference electron density map was featureless. The estimated error in an observation of unit weight was 1.30, and the final data/parameter ratio was 9.2. Atomic coordinates and the associated thermal parameters are listed in Tables II and IV. Selected interatomic distances and angles are given in Table III. A listing of the observed and calculated structure factors (×10) is available as supplementary material.

Acknowledgment. This work was supported by the U. S. Air Force Office of Scientific Research, Air Force System Command, UASF, under Grants AFOSR 78-3570 and 82-0067. The United States Government is authorized to reproduce and distribute reprints for governmental purposes notwithstanding any copyright notation thereon.

Registry No. 1, 149-74-6; **2a**, 84129-73-7; **2b**, 84129-74-8; **2c**, 84129-75-9; **2d**, 84129-76-0; **2e**, 84129-77-1; **3a**, 84129-78-2; **3b**, 84129-79-3; **3c**, 84129-80-6; **4**, 84098-82-8; **5**, 84098-83-9.

Supplementary Material Available: Tables of interatomic bond angles and bond distances for **2a**, atomic coordinates and *B*_{iso} values of hydrogen atoms, thermal parameters for non-hydrogen atoms, and structure factor amplitudes (31 pages). Ordering information is given on any current masthead page.

(17) Whitesides, T. H.; Slaven, R. W.; Calabrese, J. C. *Inorg. Chem.* 1974, 13, 1895.

(18) Germain, G.; Main, P.; Wolfson, M. M. *Acta Crystallogr., Sect. A* 1971, A27, 368.

(19) Cromer, D. T.; Waber, J. T. "International Tables for X-ray Crystallography"; Kynoch Press: Birmingham, England, 1974; Vol. 4, p 99, Table 2.2B.

(20) Stewart, R. F.; Davidson, E. R.; Simpson, W. T. *J. Chem. Phys.* 1965, 42, 3175.

Reactions of Solvated Metal Atoms with Organometallic Complexes in Solution. A Metal Atom Microsolution Spectroscopic and Synthetic Study of the Reaction Pathways Available to Singly Metal-Metal Bonded Organometallic Complexes and Their Organometallic Anions

Geoffrey A. Ozin,* Kraig M. Coleson, and Helmut X. Huber

Lash Miller Chemical Laboratories, University of Toronto, Toronto, Ontario M5S 1A1, Canada

Received June 24, 1982

Metal vapor microsolution infrared and ultraviolet-visible spectroscopic and synthetic methods have been employed to elucidate the reaction pathways available to a selection of solvated metal atoms and organometallic complexes in cryogenic solutions. In this first study, we have focused attention on binuclear complexes containing single metal-metal bonds and have found that electron transfer from the deposited metal atom to the organometallic complex is the only solution-phase reaction competitive with metal agglomeration in the temperature range 140-180 K. The dimeric complexes are reduced to their respective monomeric anions via an electron transfer metal-metal bond cleavage reaction with concomitant production of a solvated cation. In one case, we have observed further reduction of a monomeric monoanion to the corresponding super-reduced trianion with accompanying loss of one ligand. At the preparative level, attention has been directed to the representative reaction of solvated iron atoms with dimanganese decacarbonyl. In solution at 140 K, dimanganese decacarbonyl is reduced by solvated iron atoms to pentacarbonyl manganate(I-). The electron transfer reaction and subsequent processes observed during warmup and desolvation are found to be strongly solvent dependent. The secondary reactions for tetrahydrofuran solvated iron cations are shown to involve back electron transfer upon desolvation. For toluene solvated iron atoms, nucleophilic attack of pentacarbonyl manganate(I-) on solvated iron(0) leads to the production of multimetallic cluster anions such as $\text{FeMn}(\text{CO})_9^-$ and $\text{Fe}_2\text{Mn}(\text{CO})_{12}^-$. These observations, together with the results of control experiments, allow one to devise a reaction scheme for the solution-phase reactions of iron atoms and dimanganese decacarbonyl. This study has demonstrated the feasibility of reacting solvated metal atoms with organometallic complexes in solution and should open up some interesting new avenues for future synthetic research.

Introduction

The recent demonstration by Stone¹ and Lewis² that organometallic complexes containing highly labile ligands are a useful source of coordinately unsaturated fragments, which are able to add to a wide variety of organometallic complexes, suggests that solvated metal atoms,³ produced by depositing metal vapors into a lightly stabilizing or weakly coordinating solvent, might react with organometallic complexes to provide a new route to multimetallic clusters.

We have recently demonstrated the utility of an in situ metal atom microsolution UV-visible spectroscopic technique for investigating the fate of a metal atom deposited into solutions of various ligands,⁴ as well as ligands attached to various liquid oligomers or polymers.⁵ Presently, metal atom diffusion, solvation, complexation, and agglomeration processes have all been observed.⁴⁻⁶ In one system, the direct addition of a deposited diffusing metal atom M to the metal center of $(\text{arene})_2\text{M}'$ to produce $(\text{arene})_2\text{MM}'$ clusters was clearly established.⁷

In this study, we present our results for another reaction pathway accessible to solvated metal atoms, namely, electron transfer to organometallic complexes in solution, and discuss the factors which influence the course of this reaction. To probe this reaction in the range 140-180 K, we have extended our original metal atom microsolution UV-visible spectroscopic studies⁴⁻⁷ to include the infrared region. These spectroscopic studies in combination with the corresponding metal atom synthetic experiments have also allowed us to probe the subsequent reactions that follow on warming the samples to ambient temperatures and removal of solvent.

Experimental Section

The metal atom microsolution reactor and metal atom preparative rotary reactor have both been described previously.⁴⁻⁷ Monatomic metal vapors for the microsolution studies were generated by direct resistive heating of filaments of the respective metal. Vanadium (99.99%), iron (99.999%), nickel (99.99%), tungsten (99.95%), and tantalum (99.95%) were purchased from A. D. MacKay, New York as 0.01 in. sheets and cut to size for the filaments. Chromium (99.999%) was also obtained from A. D. MacKay but as a powder and vaporized from a resistively heated tantalum Kundsen cell, wall thickness 0.015 in. and orifice diameter 0.02 in. Metal deposition rates were monitored on a calibrated quartz crystal microbalance.⁶ Monatomic iron vapor for the preparative scale studies was generated by direct resistive heating of lumps of iron (Alfa, 99.98% purity, lot no. 040181) in an integral crucible (Sylvania Emmisive Products, no. CS-1009)

(1) F. G. A. Stone, *Acc. Chem. Res.*, **14**, 318 (1981); *Inorg. Chim. Acta*, **50**, 33 (1981) and references cited therein.

(2) J. Lewis, R. B. A. Parry, and P. R. Raithby, *J. Chem. Soc., Dalton Trans.*, 1509 (1982) and references cited therein.

(3) K. J. Klabunde, H. F. Efner, T. O. Murdock, and R. Ropple, *J. Am. Chem. Soc.*, **98**, 1021 (1976); K. J. Klabunde and S. C. Davis, *Ibid.*, **100**, 5973 (1978); K. J. Klabunde, S. C. Davis, H. Hattori, and Y. Tanaka, *J. Catal.*, **54**, 254 (1978); K. J. Klabunde, D. Ralston, R. Zoellner, H. Hattori, and Y. Tanaka, *Ibid.*, **55**, 213 (1978).

(4) G. A. Ozin, C. G. Francis, H. X. Huber, M. P. Andrews, and L. Nazar, *J. Am. Chem. Soc.*, **103**, 2453 (1981).

(5) G. A. Ozin and C. G. Francis, *J. Mol. Struct.*, **59**, 55 (1980); *J. Macromol. Sci., Chem.* **A16** (1), 167 (1981) and references cited therein.

(6) G. A. Ozin, C. G. Francis, H. X. Huber, and L. Nazar, *Inorg. Chem.*, **20**, 3635 (1981).

(7) G. A. Ozin and M. P. Andrews, *Angew. Chem.*, **21**, 212 (1982); M. P. Andrews, C. G. Francis, and G. A. Ozin, *Inorg. Synth.*, in press; M. P. Andrews and G. A. Ozin, *Angew. Chem., Int. Ed. Engl.* **21**, 550 (1982).

(8) (a) Unpublished observations for $[(\text{mesitylene})_2\text{Fe}](\text{PF}_6)_2$ in acetone: 245 (vs), 305 (vs), 425 (s), 500 (vw, sh) nm. (b) For this to be true, the band around 290 nm must be assigned to the intense MLCT excitation of $(\text{tol})_2\text{Fe}^{2+}$ with a contribution from $\text{Mn}(\text{CO})_5^-$. The absence of purple $(\text{tol})_2\text{Fe}^+$ is implied by the nonobservation of absorptions in the 580-nm region (E. O. Fischer and F. Rohrscheid, *Z. Naturforsch., B: Anorg. Chem., Org. Chem., Biochem., Biophys., Biol.* **17B**, 483 (1962).

composed of a tungsten wire coated with alumina, which was insulated with Kaowool. 2-Methyltetrahydrofuran (2-MTHF) was purchased from Aldrich and freed of BHT inhibitor by refluxing over LiAlH_4 followed by distillation under nitrogen. Spectral grade methylcyclohexane (MCH) was purchased from Fischer and used without purification. Reagent grade hexanes and tetrahydrofuran were distilled from LiAlH_4 under nitrogen. Reagent grade toluene was distilled from sodium-potassium alloy under nitrogen. $\text{Mo}(\text{CO})_6$, $[(\eta^5\text{-C}_5\text{H}_5)\text{Mo}(\text{CO})_3]_2$, $\text{Mn}_2(\text{CO})_{10}$, and $\text{Re}_2(\text{CO})_{10}$ were purchased from Alfa and $[(\text{mesitylene})_2\text{Fe}](\text{PF}_6)_2$ was obtained from L. F. Nazar of this laboratory. $\text{Mn}_2(\text{CO})_{10}$ was sublimed prior to use. All other organometallic complexes were used without purification. 2,2'-Bipyridyl was purchased from Aldrich, used without purification and sublimed before use. $\text{KMn}(\text{CO})_5$ was prepared by reduction of $\text{Mn}_2(\text{CO})_{10}$ under nitrogen with sodium-potassium alloy in tetrahydrofuran. $\text{NaMn}(\text{CO})_5$ was similarly prepared from sodium amalgam in 2MTHF. Carbon monoxide (C.P. grade, 99.5% purity, Matheson) was used without purification.

In the metal atom microsolution spectroscopic studies⁶ all organometallic solutions were anaerobically syringed onto a CsCl, NaCl, or Suprasil optical window (held in a horizontal configuration at 140–150 K under dynamic vacuum conditions, maintaining a pressure of about 10^{-3} torr) through a silicon rubber septum held in a 0.25-in. Cajon fitting using a Precision sampling 100 μL Pressure Lok syringe purchased from Chromatographic Specialties. The sample window was maintained at the desired temperature with an Air Products Displex closed cycle helium refrigeration system and a proportional temperature controller. UV-visible spectra were recorded on a Varian Techtron 635 spectrometer and infrared spectra on a Perkin-Elmer 180 spectrometer.

Spectroscopic Procedure. The basic metal atom microsolution technique has been described in detail previously.^{4–7} UV-visible spectra were recorded on solution samples prepared and held in a horizontal configuration.⁶ The corresponding infrared spectra were recorded by cooling the solution to an immobile glass (77 K) and rotating the spectroscopic window by 90° into the sample beam. After the spectrum was recorded the window was again rotated into the horizontal mode and warmed to a predetermined temperature (usually 140–180 K) at which the sample was fluid and ready for further reaction with metal atoms. This procedure did not appear to produce any noticeable sample inhomogeneities even after numerous such cycles over a period of several hours.

In a typical metal atom microsolution experiment about 150 μL of a dilute solution of the organometallic complex were syringed onto the spectroscopic window and the spectrum of the original solution recorded. Up to 10^{-4} g of metal atoms were then titrated into the solution at a rate of about 10^{-6} g/min. (The choice of deposition conditions depended upon the concentration of the solution at the chosen reaction temperature; too high a metal atom deposition rate leads to extensive metal agglomeration.) The spectrum was again recorded, and the procedure was repeated until the organometallic complex was almost or completely consumed. The sample was subsequently warmed in a stepwise manner to room temperature and spectroscopically monitored for further reactions induced by thermal methods or by desolvation.

Metal Atom Preparative Studies. The preparative reactions were performed by using standard metal atom solution-phase techniques.⁹ The reactions in THF were performed by direct deposition of the metal vapor into a solution of the organometallic complex. The reaction product was cannulated from the reaction vessel and handled by standard Schlenk methods. For the reactions of $\text{Fe}(\text{toluene})_2$, the iron complex was preformed in the metal atom reactor under solution-phase conditions and subsequently cannulated out of the reactor and filtered through Celite at 195 K to remove any colloidal metal. The filtrate was combined with the organometallic reagent in Schlenk flasks and handled by standard low-temperature techniques.

Reaction of Iron Atoms with Dimanganese Decacarbonyl in Tetrahydrofuran. One gram of iron was deposited over a

2-h period into a THF solution of 3.0 g of $\text{Mn}_2(\text{CO})_{10}$ at 150 K and the resultant solution filtered to remove colloidal metal. The solution was warmed slowly to ambient and the solvent removed under vacuum. Excess $\text{Mn}_2(\text{CO})_{10}$ was removed by hexane extraction, leaving a brown insoluble solid as the sole reaction product. This solid was identified as colloidal metal with chemisorbed CO^{10} by a broad IR band extending from 2050 to 1700 cm^{-1} with a maximum around 1950–1900 cm^{-1} .

Reaction of Iron Atoms in Toluene with Potassium Pentacarbonylmanganate(I-) in Tetrahydrofuran under CO. A filtered toluene solution of 1 g of iron in 100 mL of toluene was combined with 1 g of $\text{KMn}(\text{CO})_5$ in 50 mL of THF and stirred at 195 K for 3 days under 1 atm of CO. The solution was slowly warmed to ambient under a CO atmosphere. A tan insoluble solid (0.12 g) was isolated and characterized by IR spectroscopy as chemisorbed CO on colloidal metal. A purple THF-soluble material (1.02 g) was also isolated and shown by IR to contain $\text{Mn}(\text{CO})_5^-$, $\text{FeMn}(\text{CO})_9^-$, and $\text{Fe}_2\text{Mn}(\text{CO})_{12}^-$ (Figure 7A). The anions could be partially separated by reacting the mixture with CH_3I in THF at ambient, followed by evacuation of the volatiles at 10^{-3} torr and extraction with hexanes. This effectively removed $\text{Mn}(\text{CO})_5^-$ and $\text{FeMn}(\text{CO})_9^-$. A dark blue solid (0.134 g, 6% yield based on $\text{Mn}(\text{CO})_5^-$, 3% yield based on evaporated Fe) remained and was identified as spectroscopically pure $\text{Fe}_2\text{Mn}(\text{CO})_{12}^-$ by its characteristic IR and UV-visible spectra¹¹ (Figure 7B).

Results and Discussion

A. Metal Atom Microsolution Spectroscopic Studies. 1. Photochemical Control Experiments.

Radiation emitted from the metal evaporation source during deposition was investigated as a possible source of interference for all of the organometallic complexes studied. In particular, $\text{Mn}_2(\text{CO})_{10}$ in THF but not in 2MTHF has been reported¹⁴ to photolyze to Mn^{2+} and $\text{Mn}(\text{CO})_5^-$. Since $\text{Mn}(\text{CO})_5^-$ is one of our reaction products (vide infra), we examined our system for photochemistry induced by radiation from the metal vapor source. For example, irradiation of a dilute solution of $\text{Mn}_2(\text{CO})_{10}$ in 2MTHF at 140–150 K and 10^{-6} torr using a tungsten filament at approximately 2800 °C (in place of the metal vapour source), just below its vaporization temperature, gave no IR detectable quantities of $\text{Mn}(\text{CO})_5^-$ and no observable consumption of $\text{Mn}_2(\text{CO})_{10}$. Similarly, $[(\eta^5\text{-C}_5\text{H}_5)\text{Mo}(\text{CO})_3]_2$ in 2MTHF was irradiated by a tantalum filament at about 2500 °C, and again no reaction was observed by IR spectroscopy. Thus photolysis from the metal vapor source was not an important reaction under the conditions chosen for our microsolution experiments.

2. Reactions in 2-Methyltetrahydrofuran. $\text{Mn}_2(\text{CO})_{10}$ in 2MTHF was reduced by V, Cr, and Fe atoms at 140–180 K. The consumption of $\text{Mn}_2(\text{CO})_{10}$ and produc-

(10) G. Blyholder, *J. Phys. Chem.*, **68**, 2772 (1964) and references cited therein.

(11) (a) U. Anders and W. A. G. Graham, *J. Chem. Soc., Chem. Commun.*, 291 (1966); (b) J. K. Ruff, *Inorg. Chem.*, **7**, 1818 (1968).

(12) We prepared $\text{Na}^+ \text{bpy}^-$ and $\text{Fe}(\text{bpy})_3$ from Na atom and Fe atom bpy reactions in 2MTHF and find (in agreement with traditional literature preparations) that although these species as well as $\text{Fe}(\text{bpy})_3^{2+}$ absorb in the 500–600-nm region (C. Mahon and W. L. Reynolds, *Inorg. Chem.*, **6**, 1927 (1967)), the former is purple in color, whereas $\text{Fe}(\text{bpy})_3^{2+}$ is bright red. Also $\text{bpy}/\text{Mn}_2(\text{CO})_{10}/\text{THF}$ solutions do not show any visible absorptions around 500 nm. (G. A. Ozin, K. Coleson, and R. Wright, unpublished observations).

(13) J. E. Ellis and E. A. Flom, *J. Organomet. Chem.*, **99**, 263 (1975).

(14) J. E. Ellis and R. A. Faltynek, *J. Chem. Soc., Chem. Commun.*, 966 (1975).

(15) (a) L. K. Beard, Jr., M. P. Silvon, and P. S. Skell, *J. Organomet. Chem.*, **209**, 245 (1981); (b) L. J. Radonovich, M. W. Eyring, T. J. Groshens, and K. J. Klabunde, *J. Am. Chem. Soc.*, **104**, 2816 (1982) and references cited therein.

(16) R. E. Dessy, R. L. Pohl, and R. B. King, *J. Am. Chem. Soc.*, **88**, 5121 (1966); R. Pearson and P. E. Figdore, *Ibid.*, **102**, 1541 (1980).

(17) R. E. Dessy, P. M. Weissman, and R. L. Pohl, *J. Am. Chem. Soc.*, **88**, 5117 (1966) and references cited therein.

(9) R. E. Mackenzie and P. L. Timms, *J. Chem. Soc., Chem. Commun.*, 650 (1974).

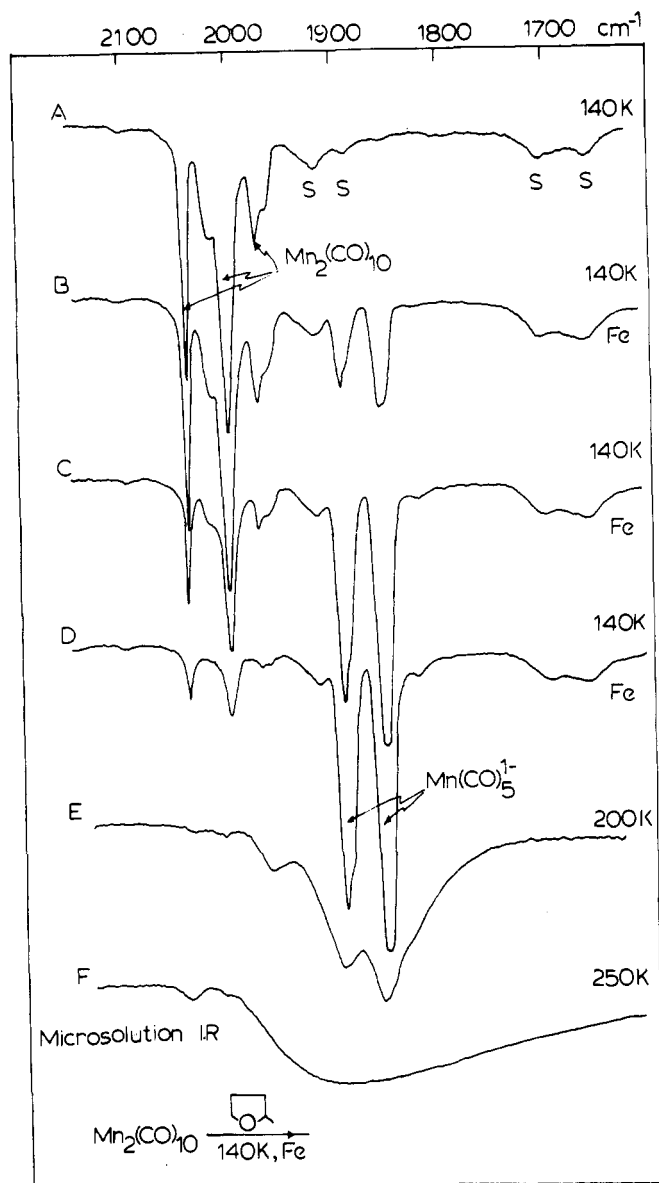


Figure 1. Microsolution infrared study of the reactions of Fe atoms with $\text{Mn}_2(\text{CO})_{10}/2\text{MTHF}$ at 140 K: (A) solution film; (B–D) gradually increasing concentrations of Fe; (E and F) warming at 200 and 250 K (S denotes solvent absorptions; note that all microsolution IR spectra were recorded at 77 K).

tion of $\text{Mn}(\text{CO})_5^-$ was conveniently monitored by IR spectroscopy (see, for example, Figure 1). Some differences were however observed between these metals. At 140 K, Cr atoms did not react with $\text{Mn}_2(\text{CO})_{10}$ and instead appeared to form solvated Cr atoms. Upon warming to 160 K, smooth reduction to $\text{Mn}(\text{CO})_5^-$ was observed. Fe atoms reduced $\text{Mn}_2(\text{CO})_{10}$ to $\text{Mn}(\text{CO})_5^-$ at 140 K in 2MTHF, but V atoms produced another species simultaneously with $\text{Mn}(\text{CO})_5^-$ having IR carbonyl bands at 1928 (s) and 1770 (m) cm^{-1} (Figure 2). Similar absorptions were also observed (1920, 1790 cm^{-1}) by direct reaction of $\text{Mn}(\text{CO})_5^-$ with V atoms in 2MTHF. Characterization of this species was not pursued. All of the reduction products were indefinitely stable in 2MTHF at 140–180 K; however, warming the samples slowly to room temperature under vacuum resulted in solvent evaporation, loss of the infrared absorptions of the reduced products, and the concurrent growth of a broad absorption around 1900 cm^{-1} that seems to appear upon desolvation of the metal cations (see, for example, Figure 1). The metal carbonyl anions may coordinate or back electron transfer to the metal cations to

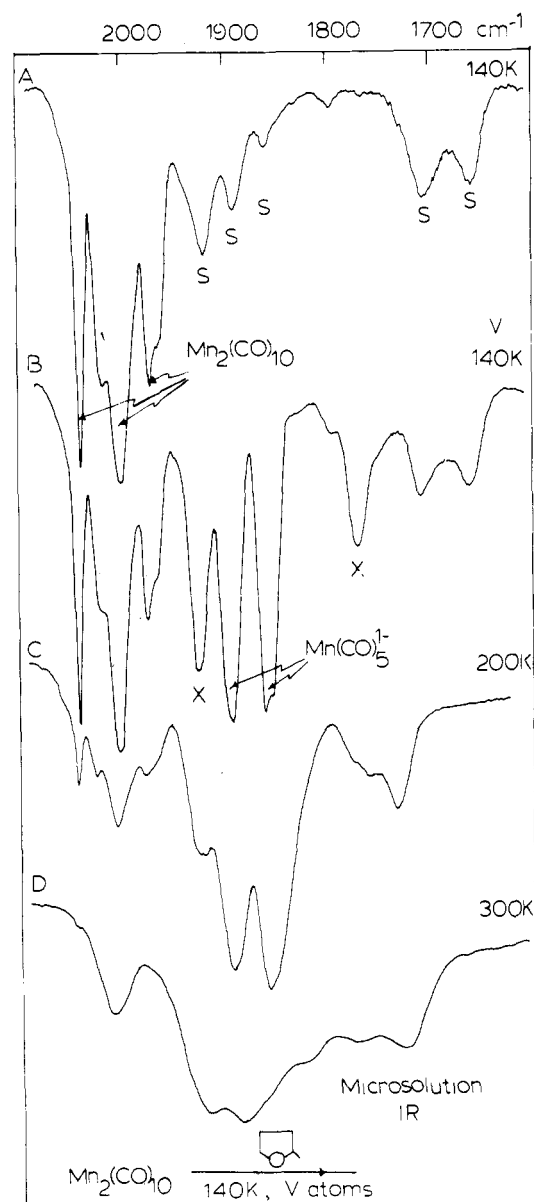


Figure 2. Microsolution infrared study of the reaction of V atoms with $\text{Mn}_2(\text{CO})_{10}/2\text{MTHF}$ at 140 K: (A) solution film; (B) following deposition of V; (C and D) warming to 200 and 300 K. (The species marked X is a new carbonyl product whose identity was not determined—see text.)

give neutral metal carbonyls and colloidal metal with chemisorbed CO. In preparative experiments (vide infra) we observe (IR) some formation of colloidal metal with chemisorbed CO as a product of these reactions.

In the case of iron it was possible to determine the initial fate of the iron atoms by addition of 2,2'-bipyridyl in 2MTHF to the product of the iron atom reduction of $\text{Mn}_2(\text{CO})_{10}$ in 2MTHF at 140 K. Upon warming to room temperature, the characteristic red color and UV-visible spectrum¹² of $\text{Fe}(\text{bpy})_3^{2+}$ as well as the UV absorption¹³ of $\text{Mn}(\text{CO})_5^-$ at 290 nm were both clearly apparent.

$\text{Mn}_2(\text{CO})_{10}$ in 2MTHF was unreactive toward Ni atoms at 150 K or upon subsequent warming to 180 K. On the other hand $[(\eta^5\text{-C}_5\text{H}_5)\text{Mo}(\text{CO})_3]_2$ in 2MTHF was cleanly reduced to $(\eta^5\text{-C}_5\text{H}_5)\text{Mo}(\text{CO})_3^-$ by Ni atoms at 140 K. Significantly, $\text{Na}[\text{Mn}(\text{CO})_5]$ in 2MTHF was reduced by Ni atoms at 140 K to form $\text{Mn}(\text{CO})_4^{3-}$ to a limited extent (Figure 3), the presence of the super-reduced carbonyl anion being indicated by IR absorptions at 1824 (m) and 1672 (vs) cm^{-1} that are sufficiently close to those of $\text{Mn}(\text{CO})_4^{3-}$ in HMPA at room temperature (1805 (w), 1670 (vs)

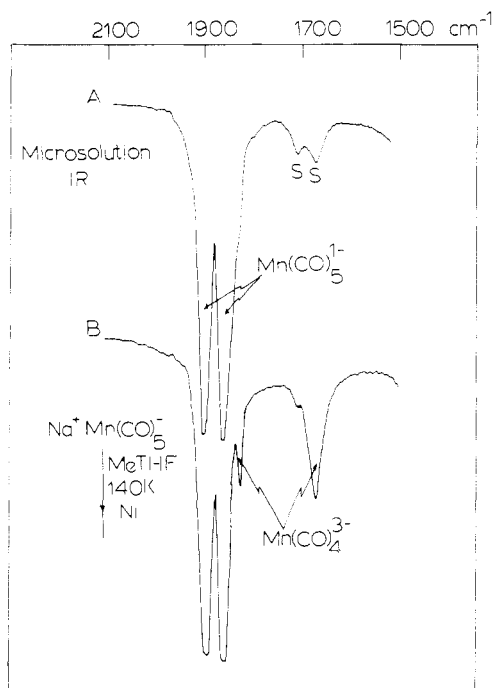


Figure 3. Microsolution infrared study of the reaction of Ni atoms with $\text{Na}[\text{Mn}(\text{CO})_5]/2\text{MTHF}$ at 140 K: (A) solution film; (B) following deposition of Ni atoms.

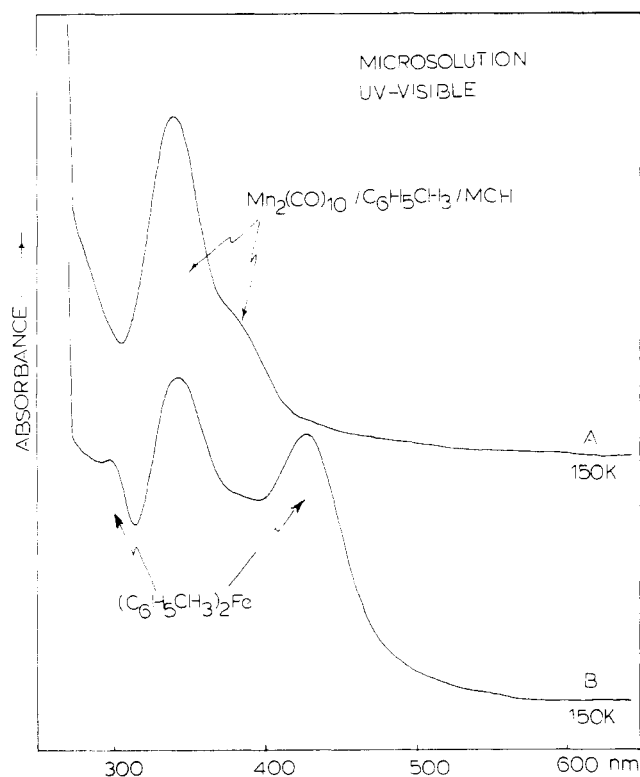


Figure 4. Microsolution UV-visible study demonstrating the lack of observable reaction between (A) a solution of $\text{Mn}_2(\text{CO})_{10}/\text{C}_6\text{H}_5\text{CH}_3/\text{MCH}$ at 150–180 K and (B) $(\text{C}_6\text{H}_5\text{CH}_3)_2\text{Fe}$ formed by Fe atom deposition into solution A.

cm^{-1}) for the minor differences to be attributed to counterion, solvent, and temperature effects. No reaction was observed for $\text{Re}_2(\text{CO})_{10}$ or $\text{Mo}(\text{CO})_6$ in 2MTHF with V atoms at 150 K or upon subsequent warming.

3. Reactions in Mixed Solvent Systems. The reaction between $\text{Mn}_2(\text{CO})_{10}$ and Fe atoms in a 1:10 toluene/MCH solvent mixture was monitored by in situ UV-visible and IR spectroscopy. In this *nonpolar* medium,

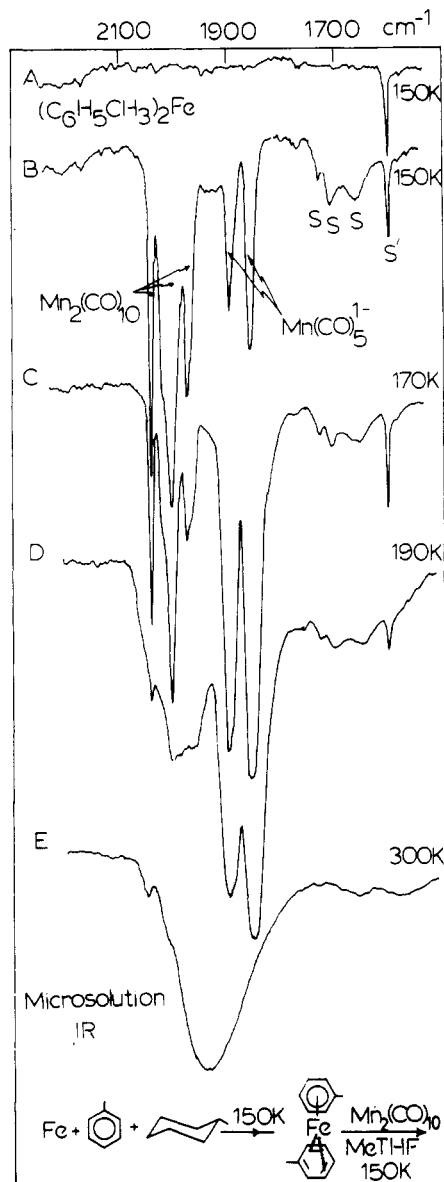


Figure 5. Microsolution infrared study of the reaction of (A) preformed $(\text{C}_6\text{H}_5\text{CH}_3)_2\text{Fe}$ in a $\text{C}_6\text{H}_5\text{CH}_3/\text{MCH}$ (1/10) mixed solvent at 150 K followed by (B) injection of $\text{Mn}_2(\text{CO})_{10}/2\text{MTHF}$ at 150 K followed by (C–E) warming to 170, 190, and 300 K.

formation of $(\text{toluene})_2\text{Fe}$ was clearly observed by UV-visible spectroscopy,⁴ but no reduction of $\text{Mn}_2(\text{CO})_{10}$ to $\text{Mn}(\text{CO})_5^-$ was observed in the range 150–180 K (Figure 4).

In contrast, when $(\text{toluene})_2\text{Fe}$ was preformed from Fe atoms in 1:10 toluene/MCH followed by syringe addition of $\text{Mn}_2(\text{CO})_{10}$ in the *polar* solvent 2MTHF, slow reduction was observed spectroscopically over a period of several hours at 150 K (Figures 5 and 6). Consumption of $\text{Mn}_2(\text{CO})_{10}$ and formation of $\text{Mn}(\text{CO})_5^-$ was conveniently monitored by IR spectroscopy (Figure 5), whereas simultaneous consumption of $\text{Mn}_2(\text{CO})_{10}$ and $(\text{toluene})_2\text{Fe}$ was best observed in the UV-visible (Figure 6), where one observes concomitant growth of the UV absorption of $\text{Mn}(\text{CO})_5^-$ at 290 nm. A weak band in the visible near 400 nm is thought to be associated with the orange cation $[(\text{toluene})_2\text{Fe}^{2+}]$ by comparison with the optical data of $[(\text{mesitylene})_2\text{Fe}^{2+}]$.^{8a,b} When $[(\eta^5\text{-C}_5\text{H}_5)\text{Mo}(\text{CO})_3]^-$ in 2MTHF was added to preformed $(\text{toluene})_2\text{Fe}$ in 1:10 toluene/MCH at 150K, reduction to $(\eta^5\text{-C}_5\text{H}_5)\text{Mo}(\text{CO})_3^-$ was complete within minutes as indicated by the IR spectrum.

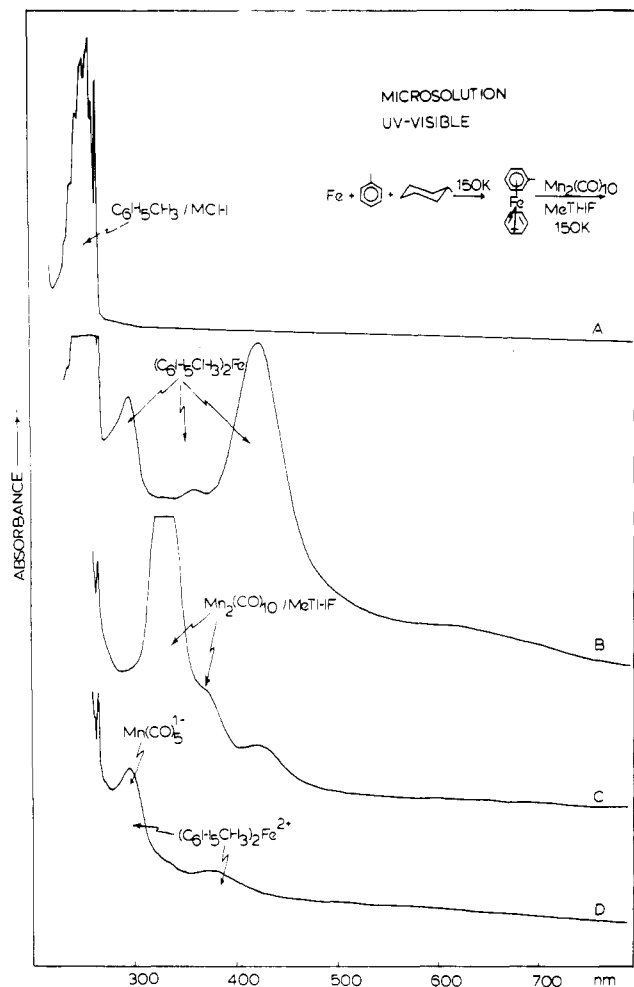


Figure 6. Microsolution UV-visible study of the reaction of (A and B) preformed $(\text{C}_6\text{H}_5\text{CH}_3)_2\text{Fe}$ in a $\text{C}_6\text{H}_5\text{CH}_3/\text{MCH}$ (1/10) mixed solvent at 150 K followed by (C) injection of $\text{Mn}_2(\text{CO})_{10}/2\text{MTHF}$ at 150 K and (D) standing for 60 min at 150 K.

B. Preparative Studies. The combined results of the microsolution and preparative studies on the reactions of solvated Fe atoms and $\text{Mn}_2(\text{CO})_{10}$ in solution are summarized in Scheme I. In pure THF (step 1) electron transfer occurs to produce $\text{Fe}(\text{THF})_x^{2+}$ (subsequently trapped as $\text{Fe}(\text{bpy})_3^{2+}$, step 2¹²) and $\text{Mn}(\text{CO})_5^-$, which back electron transfers upon desolvation (step 3) to yield colloidal metal with chemisorbed CO as the sole product of the reaction. In pure toluene, $\text{Fe}(\text{toluene})_2$ is formed (step 4), but no reaction with $\text{Mn}_2(\text{CO})_{10}$ occurs below the decomposition temperature of $\text{Fe}(\text{toluene})_2$ and again colloidal metal with chemisorbed CO is the primary product when the system is warmed above 243 K (step 5).

In contrast, when preformed $\text{Fe}(\text{toluene})_2$ is reacted with $\text{Mn}_2(\text{CO})_{10}$ in THF or 2MTHF at 150 K, the electron transfer metal-metal bond cleavage reaction occurs slowly (microsolution observations) to form $\text{Mn}(\text{CO})_5^-$ (step 6), which subsequently reacts with $\text{Fe}(\text{toluene})_2$ ¹⁸ to form multimetallic clusters (steps 7 and 9). Under 1 atm of CO this reaction can be trapped in its early stages (steps 8 and

(18) In independent control experiments we have been able to demonstrate that multimetallic carbonyl anions do not result from the reaction of $[(\text{mesitylene})_2\text{Fe}][\text{PF}_6]_2$ with $\text{K}[\text{Mn}(\text{CO})_5]$. In this system we found that back electron transfer occurred in THF at room temperature to produce $\text{Mn}_2(\text{CO})_{10}$. The fate of the iron was not determined. The product of the $(\text{toluene})_2\text{Fe}$ reaction with $\text{Mn}_2(\text{CO})_{10}$ can therefore be safely proposed to arise from the reaction of $\text{Mn}(\text{CO})_5^-$ with $(\text{toluene})_2\text{Fe}$ and not $(\text{toluene})_2\text{Fe}^{2+}$. We note in passing that nucleophilic attack on $(\text{toluene})_2\text{Fe}$ is not unprecedented¹⁵ and that $\text{Mn}(\text{CO})_5^-$ is a moderate strength nucleophile.¹⁶

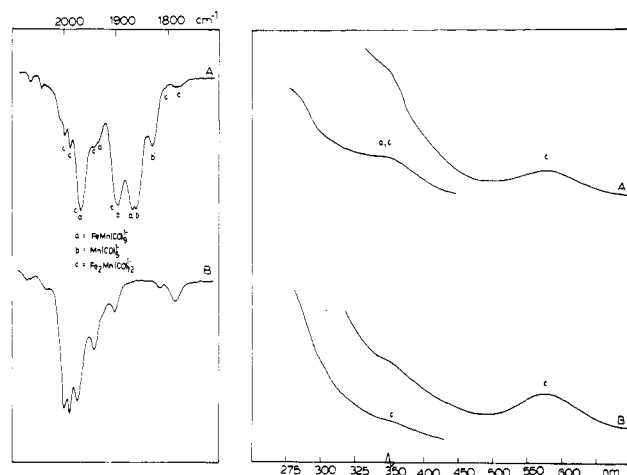
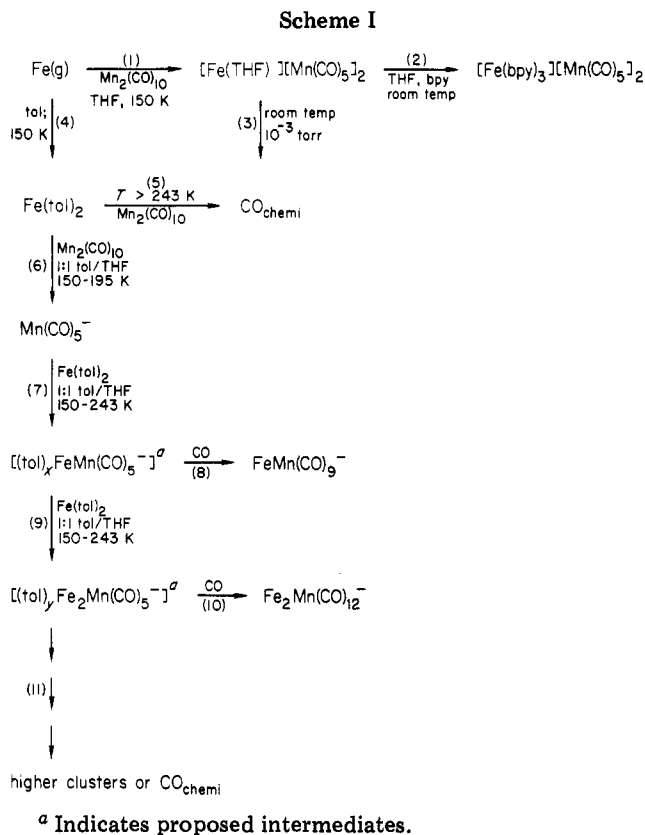


Figure 7. Infrared and UV-visible spectra of (A) the crude macro synthetic THF-soluble reaction products, formed from the reaction of preformed $(\text{C}_6\text{H}_5\text{CH}_3)_2\text{Fe}$ in $\text{C}_6\text{H}_5\text{CH}_3$ solvent at 150 K with $\text{K}[\text{Mn}(\text{CO})_5]$ under a CO atmosphere in THF at 150 K and (B) the THF-soluble product following methylation, vacuum drying, and hexane extraction of the mixture shown in (A)—see text for details (b' is an impurity band found in some of our samples of $\text{Mn}(\text{CO})_5^-$).

10) and known clusters $\text{FeMn}(\text{CO})_9^-$ and $\text{Fe}_2\text{Mn}(\text{CO})_{12}^-$ isolated and spectroscopically characterized (Figure 7). When the $\text{Mn}(\text{CO})_5^-$ is produced in situ by the reduction of $\text{Mn}_2(\text{CO})_{10}$ in THF with $\text{Fe}(\text{toluene})_2$ in toluene, the $\text{Mn}_2(\text{CO})_{10}$ can act as a source of CO and $\text{Fe}_2\text{Mn}(\text{CO})_{12}^-$ is isolated along with significant amounts of unidentified metal carbonyl cluster anions. In the absence of any source of additional CO, $\text{Fe}(\text{toluene})_2$ reacts with $\text{Mn}(\text{CO})_5^-$ (e.g., under N_2) to produce low yields of unidentified metal carbonyl cluster anions (step 11).

Conclusion

Microsolution infrared and UV-visible spectroscopic studies have shown that electron transfer from metal atoms

to singly metal-metal bonded organometallic complexes is the only reaction competitive with metal agglomeration in a *polar* organic solvent. The observation that $\text{Mn}_2(\text{CO})_{10}$ in 2MTHF at 150 K is reduced by V, Cr, and Fe atoms but not by Ni atoms, while $[(\eta^5\text{-C}_5\text{H}_5)\text{Mo}(\text{CO})_3]_2$ is reduced by Ni atoms, but $\text{Re}_2(\text{CO})_{10}$ is not reduced by V atoms, is consistent with the reduction potentials reported for these metal-metal bonded systems.¹⁷

The solution-phase preparative studies indicate that multimetallic clusters can be synthesized by nucleophilic attack of toluene solvated metal atoms by organometallic anions, either generated in situ by the electron-transfer reaction described above or added directly as the organometallic reagent. The reaction of solvated iron atoms with $\text{Mn}_2(\text{CO})_{10}$ or $\text{Mn}(\text{CO})_5^-$ is, however, complicated by solvent effects and the availability of several competing

reaction pathways of the type indicated in Scheme I.

With the experiences gained from this initial study, we have now turned our attention to the reactions of solvated metal atoms with multiple metal-metal and metal-carbon bonds, where the electron-transfer reaction may be minimized and other pathways are expected to predominate.

Acknowledgment. The financial assistance of the National Research Council of Canada's operating grant program is gratefully acknowledged.

Registry No. Fe, 7439-89-6; V, 7440-62-2; Cr, 7440-47-3; Ni, 7440-02-0; $\text{Mn}_2(\text{CO})_{10}$, 10170-69-1; $[(\eta^5\text{-C}_5\text{H}_5)\text{Mo}(\text{CO})_3]_2$, 12091-64-4; $\text{Na}[\text{Mn}(\text{CO})_5]$, 13859-41-1; $\text{KMn}(\text{CO})_5$, 15693-51-3; $\text{Re}_2(\text{CO})_{10}$, 14285-68-8; $\text{Mo}(\text{CO})_6$, 13939-06-5; $\text{Fe}(\text{toluene})_2$, 69006-35-5; $\text{FeMn}(\text{CO})_9^-$, 84143-94-2; $\text{Fe}_2\text{Mn}(\text{CO})_{12}^-$, 12560-40-6; $\text{Mn}(\text{CO})_5^-$, 14971-26-7; $\text{Mn}(\text{CO})_4^{3-}$, 61769-24-2.

Crystal and Molecular Structure of Benzylidiphenylferrocenylphosphonium Chloride: Through-Space Overlap Effects in the Wittig Reaction

William E. McEwen,* Charles E. Sullivan, and Roberta O. Day

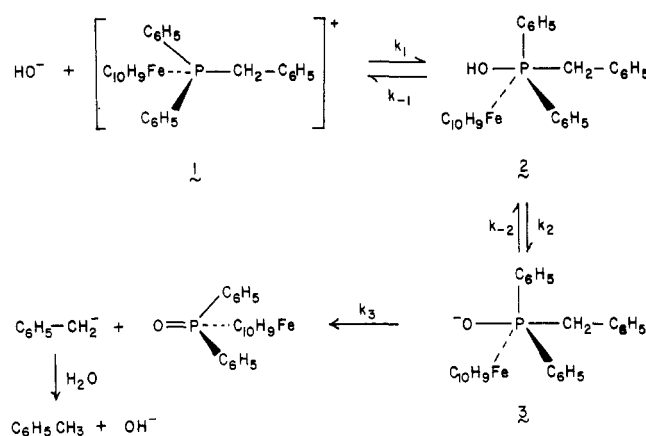
Department of Chemistry, University of Massachusetts, Amherst, Massachusetts 01003

Received July 20, 1982

Of the possible types of interactions that can occur between the phosphorus and the iron atoms of benzylidiphenylferrocenylphosphonium chloride, the one which seems to be the strongest on the basis of X-ray crystallographic data is that which involves overlap of the filled h_a molecular orbital of the ferrocenyl group with an empty 3d orbital of phosphorus. The implications of this result with respect to the rates and stereochemistry of the Wittig reactions of (carbomethoxymethylene)diphenylferrocenylphosphorane and of (carbomethoxymethylene)diferrocenylphenylphosphorane, respectively, with benzaldehyde are considered.

The mechanism of the alkaline cleavage of ordinary acyclic quaternary phosphonium salts having benzyl as a leaving group is well established. As applied to the benzylidiphenylferrocenylphosphonium ion 1, it consists of the following steps:¹⁻³ (1) rapid, reversible attack by a hydroxide ion at a face of the phosphonium tetrahedron to give a hydroxyphosphorane, 2, in which the hydroxyl group now occupies an apical position in the resulting trigonal bipyramid; (2) rapid, reversible removal of a proton from the hydroxyphosphorane 2 to generate its conjugate base, 3, which also has trigonal-bipyramidal geometry; (3) irreversible, rate-determining expulsion of a benzyl carbanion (which is probably protonated as it is being formed⁴) from an apical position in the trigonal bipyramid to generate a phosphine oxide.

On the basis of this mechanism, it is anticipated that the presence of an electron-donating group bonded to phosphorus will cause retardation of the rate of reaction by decreasing the magnitude of K_1 and K_2 , the equilibrium constants of the first two steps of the reaction. Previous workers, notably Hoffman,⁵ McEwen and his colleagues,¹⁻³ and Allen and his co-workers,⁶⁻¹¹ have documented these



statements for a number of different systems. Allen's work is especially notable in that, in certain cases, he was able to determine the relative importance of K_1K_2 , on the one hand, and of k_3 , on the other.

(6) Allen, D. W. *J. Chem. Soc. B* 1970, 1490.

(7) Allen, D. W.; Hutley, B. G.; Mellor, M. T. *J. Chem. Soc., Perkin Trans. 2* 1972, 63.

(8) Allen, D. W.; Hutley, B. G. *J. Chem. Soc., Perkin Trans. 2* 1972, 67.

(9) Allen, D. W.; Grayson, S. J.; Harness, I.; Hutley, B. G.; Mowat, I. W. *J. Chem. Soc., Perkin Trans. 2* 1973, 1912.

(10) Allen, D. W.; Hutley, B. G.; Mellor, M. T. *J. Chem. Soc., Perkin Trans. 2* 1974, 1690.

(11) Allen, D. W.; Nowell, I. W.; Oades, A. C.; Walker, P. E. *J. Chem. Soc., Perkin Trans. 1* 1978, 98.

(1) Zanger, M.; Vander Werf, C. A.; McEwen, W. E. *J. Am. Chem. Soc.* 1959, 81, 3806.

(2) McEwen, W. E.; Kumli, K. F.; Blade-Font, A.; Zanger, M.; Vander Werf, C. A. *J. Am. Chem. Soc.* 1964, 86, 2378.

(3) McEwen, W. E.; Axelrad, G.; Zanger, M.; Vander Werf, C. A. *J. Am. Chem. Soc.* 1965, 87, 3948.

(4) Corfield, J. R.; Trippett, S. *Chem. Commun.* 1970, 1287.

(5) Hoffman, H. *Justus Liebigs Ann. Chem.* 1960, 634, 1.

to singly metal-metal bonded organometallic complexes is the only reaction competitive with metal agglomeration in a *polar* organic solvent. The observation that $\text{Mn}_2(\text{CO})_{10}$ in 2MTHF at 150 K is reduced by V, Cr, and Fe atoms but not by Ni atoms, while $[(\eta^5\text{-C}_5\text{H}_5)\text{Mo}(\text{CO})_3]_2$ is reduced by Ni atoms, but $\text{Re}_2(\text{CO})_{10}$ is not reduced by V atoms, is consistent with the reduction potentials reported for these metal-metal bonded systems.¹⁷

The solution-phase preparative studies indicate that multimetallic clusters can be synthesized by nucleophilic attack of toluene solvated metal atoms by organometallic anions, either generated in situ by the electron-transfer reaction described above or added directly as the organometallic reagent. The reaction of solvated iron atoms with $\text{Mn}_2(\text{CO})_{10}$ or $\text{Mn}(\text{CO})_5^-$ is, however, complicated by solvent effects and the availability of several competing

reaction pathways of the type indicated in Scheme I.

With the experiences gained from this initial study, we have now turned our attention to the reactions of solvated metal atoms with multiple metal-metal and metal-carbon bonds, where the electron-transfer reaction may be minimized and other pathways are expected to predominate.

Acknowledgment. The financial assistance of the National Research Council of Canada's operating grant program is gratefully acknowledged.

Registry No. Fe, 7439-89-6; V, 7440-62-2; Cr, 7440-47-3; Ni, 7440-02-0; $\text{Mn}_2(\text{CO})_{10}$, 10170-69-1; $[(\eta^5\text{-C}_5\text{H}_5)\text{Mo}(\text{CO})_3]_2$, 12091-64-4; $\text{Na}[\text{Mn}(\text{CO})_5]$, 13859-41-1; $\text{KMn}(\text{CO})_5$, 15693-51-3; $\text{Re}_2(\text{CO})_{10}$, 14285-68-8; $\text{Mo}(\text{CO})_6$, 13939-06-5; $\text{Fe}(\text{toluene})_2$, 69006-35-5; $\text{FeMn}(\text{CO})_9^-$, 84143-94-2; $\text{Fe}_2\text{Mn}(\text{CO})_{12}^-$, 12560-40-6; $\text{Mn}(\text{CO})_5^-$, 14971-26-7; $\text{Mn}(\text{CO})_4^{3-}$, 61769-24-2.

Crystal and Molecular Structure of Benzylidiphenylferrocenylphosphonium Chloride: Through-Space Overlap Effects in the Wittig Reaction

William E. McEwen,* Charles E. Sullivan, and Roberta O. Day

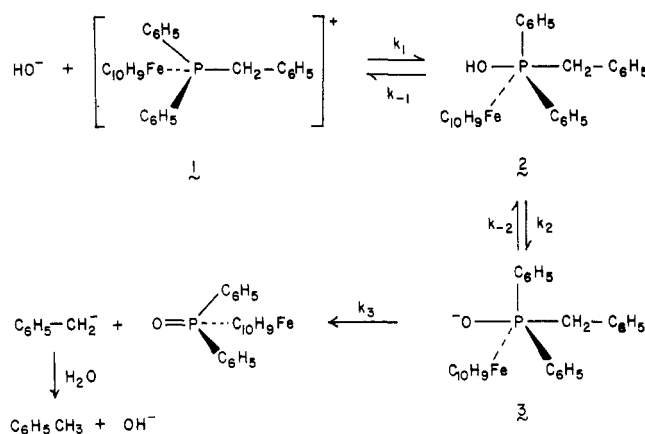
Department of Chemistry, University of Massachusetts, Amherst, Massachusetts 01003

Received July 20, 1982

Of the possible types of interactions that can occur between the phosphorus and the iron atoms of benzylidiphenylferrocenylphosphonium chloride, the one which seems to be the strongest on the basis of X-ray crystallographic data is that which involves overlap of the filled h_a molecular orbital of the ferrocenyl group with an empty 3d orbital of phosphorus. The implications of this result with respect to the rates and stereochemistry of the Wittig reactions of (carbomethoxymethylene)diphenylferrocenylphosphorane and of (carbomethoxymethylene)diferrocenylphenylphosphorane, respectively, with benzaldehyde are considered.

The mechanism of the alkaline cleavage of ordinary acyclic quaternary phosphonium salts having benzyl as a leaving group is well established. As applied to the benzylidiphenylferrocenylphosphonium ion 1, it consists of the following steps:¹⁻³ (1) rapid, reversible attack by a hydroxide ion at a face of the phosphonium tetrahedron to give a hydroxyphosphorane, 2, in which the hydroxyl group now occupies an apical position in the resulting trigonal bipyramid; (2) rapid, reversible removal of a proton from the hydroxyphosphorane 2 to generate its conjugate base, 3, which also has trigonal-bipyramidal geometry; (3) irreversible, rate-determining expulsion of a benzyl carbanion (which is probably protonated as it is being formed⁴) from an apical position in the trigonal bipyramid to generate a phosphine oxide.

On the basis of this mechanism, it is anticipated that the presence of an electron-donating group bonded to phosphorus will cause retardation of the rate of reaction by decreasing the magnitude of K_1 and K_2 , the equilibrium constants of the first two steps of the reaction. Previous workers, notably Hoffman,⁵ McEwen and his colleagues,¹⁻³ and Allen and his co-workers,⁶⁻¹¹ have documented these



statements for a number of different systems. Allen's work is especially notable in that, in certain cases, he was able to determine the relative importance of K_1K_2 , on the one hand, and of k_3 , on the other.

(6) Allen, D. W. *J. Chem. Soc. B* 1970, 1490.

(7) Allen, D. W.; Hutley, B. G.; Mellor, M. T. *J. Chem. Soc., Perkin Trans. 2* 1972, 63.

(8) Allen, D. W.; Hutley, B. G. *J. Chem. Soc., Perkin Trans. 2* 1972, 67.

(9) Allen, D. W.; Grayson, S. J.; Harness, I.; Hutley, B. G.; Mowat, I. W. *J. Chem. Soc., Perkin Trans. 2* 1973, 1912.

(10) Allen, D. W.; Hutley, B. G.; Mellor, M. T. *J. Chem. Soc., Perkin Trans. 2* 1974, 1690.

(11) Allen, D. W.; Nowell, I. W.; Oades, A. C.; Walker, P. E. *J. Chem. Soc., Perkin Trans. 1* 1978, 98.

(1) Zanger, M.; Vander Werf, C. A.; McEwen, W. E. *J. Am. Chem. Soc.* 1959, 81, 3806.

(2) McEwen, W. E.; Kumli, K. F.; Blade-Font, A.; Zanger, M.; Vander Werf, C. A. *J. Am. Chem. Soc.* 1964, 86, 2378.

(3) McEwen, W. E.; Axelrad, G.; Zanger, M.; Vander Werf, C. A. *J. Am. Chem. Soc.* 1965, 87, 3948.

(4) Corfield, J. R.; Trippett, S. *Chem. Commun.* 1970, 1287.

(5) Hoffman, H. *Justus Liebigs Ann. Chem.* 1960, 634, 1.

We have reported previously that benzylidiphenylferrocenylphosphonium iodide undergoes the alkaline cleavage reaction about 2 orders of magnitude more slowly than benzyltriphenylphosphonium iodide.¹² Thus, since steric effects play no major role in determining the rates of decomposition of quaternary phosphonium hydroxides,¹³⁻¹⁵ it is clear that the ferrocenyl group is functioning as a moderately strong electron-donating group toward the phosphorus. This is of particular interest in view of the report⁶ that benzyltri-2-thienylphosphonium hydroxide undergoes decomposition 2.5×10^5 times more rapidly than does benzyltriphenylphosphonium hydroxide. Since the thienyl group is a well-known " π -excessive" system, it is clear that, in this or related compounds, $p\pi$ - $d\pi$ overlap plays no major role in the stabilization of the phosphonium cation. Thus, the decreased reactivity of the ferrocenylphosphonium hydroxide as against that of the phenyl analogue must be attributable either to a direct, through-space overlap of an electron pair of the ferrocenyl group with an empty 3d (or hybrid) orbital of phosphorus or else to the operation of an inductive effect. Similar effects have been reported¹⁶ for quaternary (*o*-methoxyphenyl)phosphonium salts.

In analogy with the known stabilizing effect of a ferrocenyl group on an α -carbocationic center,¹⁷ several models may be considered to explain the stabilization of the phosphonium cation 1. Dannenberg, Levenberg, and Richards¹⁸ have considered a model for ferrocenyl-carbonium ions which contains a planar-substituted ring, conjugated as in fulvene, with the iron atom shifted toward the cationic center. The unsubstituted ring remains in the normal position relative to the iron. Cais¹⁹ has proposed a structure in which the substituted ring is bent to allow better overlap between iron and ligand orbitals. Gleiter and Seeger²⁰ have proposed a structure in which both rings are tilted and the cationic center is bent toward the iron atom. Traylor and his co-workers²¹ have considered a model that is a resonance hybrid of structures in which both the original cationic center and the carbon atoms of the substituted ring share the positive charge. For ferrocenylphosphonium cations, McEwen, Smalley, and Sullivan¹² have considered a model that involves overlap of the filled h_a molecular orbital of the ferrocenyl group with an empty 3d orbital of the phosphorus atom.

In order to determine which, if any, of the models best fits a ferrocenylphosphonium ion, the crystal and molecular structure of benzylidiphenylferrocenylphosphonium chloride has been determined by single-crystal X-ray diffraction analysis.

(12) McEwen, W. E.; Smalley, A. W.; Sullivan, C. E. *Phosphorus* 1972, 259.

(13) Aksnes, G.; Songstad, J. *Acta Chem. Scand.* 1962, 16, 1426.

(14) Aksnes, G.; Brudvik, L. *Acta Chem. Scand.* 1963, 17, 1611.

(15) Pagilagan, R.; McEwen, W. E. *Chem. Commun.* 1966, 652.

(16) Keldsen, G. L.; McEwen, W. E. *J. Am. Chem. Soc.* 1978, 100, 7312, and references cited therein.

(17) Larsen, J. W.; Ashkenazi, P. *J. Am. Chem. Soc.* 1975, 97, 2140.

(18) Dannenberg, J. J.; Levenberg, M. K.; Richards, J. H. *Tetrahedron* 1973, 29, 1575.

(19) Cais, M. *Organomet. Chem. Rev.* 1966, 1, 435.

(20) Gleiter, R.; Seeger, R. *Helv. Chim. Acta* 1971, 54, 1217.

(21) Traylor, T. G.; Hanstein, W.; Berwin, H. J.; Clinton, N. A.; Brown, R. S. *J. Am. Chem. Soc.* 1971, 93, 5715.

(22) McEwen, W. E.; Lau, K. W. "Abstracts of Papers", 183rd National Meeting of the American Chemical Society, Las Vegas, Nev., Mar 28-Apr 2, 1982; American Chemical Society, Washington, D.C., 1982; Paper No. 114. Rate data on S_N2 reactions of methoxy substituted 5-phenyl dibenzophospholes with benzyl chloride suggest that the through space 2p-3d overlap effect involves an incipient 3d_z orbital of the phosphorus.

(23) Moffitt, W. *J. Am. Chem. Soc.* 1954, 76, 3386.

(24) "International Tables for X-Ray Crystallography"; The Kynoch Press: Birmingham, England, 1969; Vol. 1, p 99. Equipoints: $\pm(x, y, z)$; $\pm(1/2 + x, 1/2 - y, 1/2 + z)$.

Table I. Atomic Coordinates in Crystalline Benzylidiphenylferrocenylphosphonium Chloride

atom type ^a	fractional coordinates ^b		
	10 ⁴ x	10 ⁴ y	10 ⁴ z
Fe	6923.8 (4)	6121.8 (3)	2463.8 (3)
P	3978.8 (7)	5038.5 (4)	2229.8 (5)
Cl	3832 (1)	6377 (1)	5583 (1)
CF1	5707 (3)	5273 (2)	1967 (2)
CF2	6926 (3)	4959 (2)	2422 (2)
CF3	8075 (3)	5245 (2)	1918 (3)
CF4	7618 (4)	5727 (2)	1189 (2)
CF5	6149 (3)	5748 (2)	1205 (2)
CF6	6006 (5)	6730 (2)	3528 (3)
CF7	7254 (6)	6433 (3)	3828 (3)
CF8	8283 (5)	6714 (3)	3256 (4)
CF9	7707 (5)	7192 (3)	2596 (4)
CF10	6267 (5)	7202 (2)	2752 (3)
CA1	2867 (3)	5749 (2)	1717 (2)
CA2	2387 (3)	6364 (2)	2253 (2)
CA3	1547 (4)	6906 (2)	1834 (3)
CA4	1185 (4)	6856 (2)	893 (3)
CA5	1674 (4)	6260 (2)	353 (3)
CA6	2509 (4)	5702 (2)	765 (3)
CB1	3594 (3)	4153 (2)	1643 (2)
CB2	2218 (3)	3920 (2)	1518 (2)
CB3	1938 (4)	3238 (2)	1063 (3)
CB4	2992 (5)	2794 (2)	720 (3)
CB5	4344 (5)	3014 (2)	843 (2)
CB6	4650 (4)	3693 (2)	1308 (2)
CM	3711 (3)	4940 (2)	3495 (2)
CC1	2373 (3)	4538 (2)	3710 (2)
CC2	1138 (3)	4936 (2)	3806 (2)
CC3	-87 (4)	4542 (2)	3955 (3)
CC4	-93 (4)	764 (2)	4006 (3)
CC5	1118 (4)	3362 (2)	3935 (2)
CC6	2347 (3)	3750 (2)	3779 (2)

^a Atoms are labeled to agree with Figure 1. ^b Numbers in parentheses are estimated standard deviations.

Table II. Selected Bond Lengths (Å), Bond Angles (deg), and Nonbonded Distances (Å)

Bond Lengths			
P-CF1	1.768 (3)	Fe-CF9	2.039 (4)
P-CA1	1.803 (3)	Fe-CF10	2.047 (4)
P-CB1	1.804 (3)	CF1-CF2	1.453 (4)
P-CM	1.819 (3)	CF2-CF3	1.418 (5)
CM-CC1	1.510 (4)	CF3-CF4	1.406 (5)
Fe-CF1	2.028 (3)	CF4-CF5	1.425 (5)
Fe-CF2	2.047 (3)	CF5-CF1	1.432 (4)
Fe-CF3	2.057 (4)	CF6-CF7	1.384 (6)
Fe-CF4	2.050 (4)	CF7-CF8	1.380 (7)
Fe-CF5	2.041 (3)	CF8-CF9	1.375 (7)
Fe-CF6	2.054 (4)	CF9-CF10	1.415 (6)
Fe-CF7	2.032 (4)	CF10-CF6	1.402 (6)
Fe-CF8	2.017 (4)		
Bond Angles			
CF1-P-CM	111.6 (1)	CF1-CF2-CF3	106.4 (3)
CF1-P-CA1	108.7 (1)	CF2-CF3-CF4	109.7 (3)
CA1-P-CM	112.1 (1)	CF3-CF4-CF5	108.5 (3)
CB1-P-CA1	106.9 (1)	CF4-CF5-CF6	107.4 (3)
CB1-P-CM	109.9 (1)	CF10-CF6-CF7	107.7 (4)
CF1-P-CF1	107.4 (1)	CF6-CF7-CF8	108.6 (4)
P-CM-CC1	111.7 (2)	CF7-CF8-CF9	109.0 (4)
P-CF1-CF2	126.1 (2)	CF8-CF9-CF10	107.4 (4)
P-CF1-CF5	125.6 (2)	CF9-CF10-CF6	107.3 (4)
CF5-CF1-CF2	108.1 (3)		
Nonbond Distances			
CB1-CC1	3.233 (4)	CF3-CF8	3.210 (6)
CF1-CF6	3.396 (5)	CF4-CF9	3.260 (6)
CF2-CF10	3.284 (5)	CF5-CF10	3.371 (5)
P-Fe	3.449 (1)		

Crystals of benzylidiphenylferrocenylphosphonium chloride are monoclinic of space group $P2_1/n$ (alternate

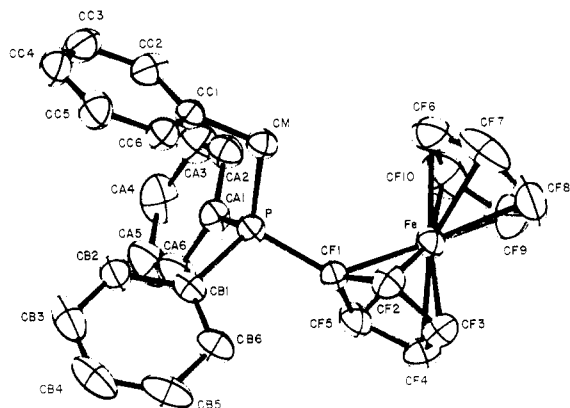


Figure 1. ORTEP plot of benzyldiphenylferrocenylphosphonium chloride with thermal ellipsoids shown at the 50% probability level. Hydrogen atoms are omitted for purposes of clarity.

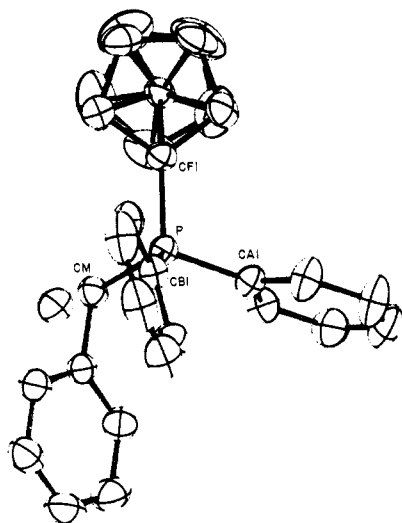


Figure 2. ORTEP plot of benzyldiphenylferrocenylphosphonium chloride viewed normal to the plane defined by CF1, CF2, and CF5. Thermal ellipsoids are at the 50% probability level.

setting of $P2_1/c-C_2^5$ ²⁴ with $a = 9.700$ (3) Å, $b = 17.593$ (6) Å, $c = 14.159$ (4) Å, $\beta = 90.23$ (2)°, and $Z = 4$. A total of 5531 independent reflections ($+h,+k,\pm l$) was examined, out to a maximum of $2\theta_{\text{MoK}\alpha} = 55^\circ$ using an Enraf-Nonius CAD4 diffractometer, the θ - 2θ scan mode, and graphite-monochromated Mo $K\alpha$ radiation. Initial coordinates for all atoms were obtained by a combination of direct methods (MULTAN) and standard Fourier difference techniques. Full-matrix least-squares refinement²⁵ (32 non-hydrogen atoms anisotropic, 26 hydrogen atoms isotropic) led to a conventional residual $R = \sum ||F_o| - |F_c|| / \sum |F_o|$ of 0.041 and a weighted residual $R_w = \{ \sum w(|F_o| - |F_c|)^2 / \sum w|F_o|^2 \}^{1/2}$ of 0.046 for the 3522 reflections having $I \geq 2\sigma_I$.

Atomic coordinates are given in Table I, while important bond lengths, bond angles, and nonbonded contacts are given in Table II. Anisotropic thermal parameters for non-hydrogen atoms, refined parameters for hydrogen atoms, and a list of observed and calculated structure factor amplitudes are available upon request. The atom labeling scheme is given in the ORTEP plot of Figure 1. As can be seen in the ORTEP plot of Figure 2, the ferrocene moiety is nearly eclipsed.

(25) The function minimized was $\sum w(|F_o| - |F_c|)^2$, where $w^{1/2} = 2F_o L p / \sigma_f$. Mean atomic scattering factors were taken from ref 24, 1974; Vol. IV, pp 72-98. Real and imaginary dispersion corrections for Cl, Fe, and P were taken from the same source, pp 149-50.

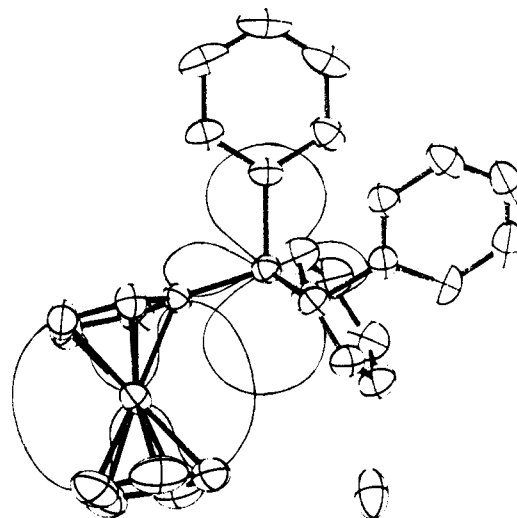


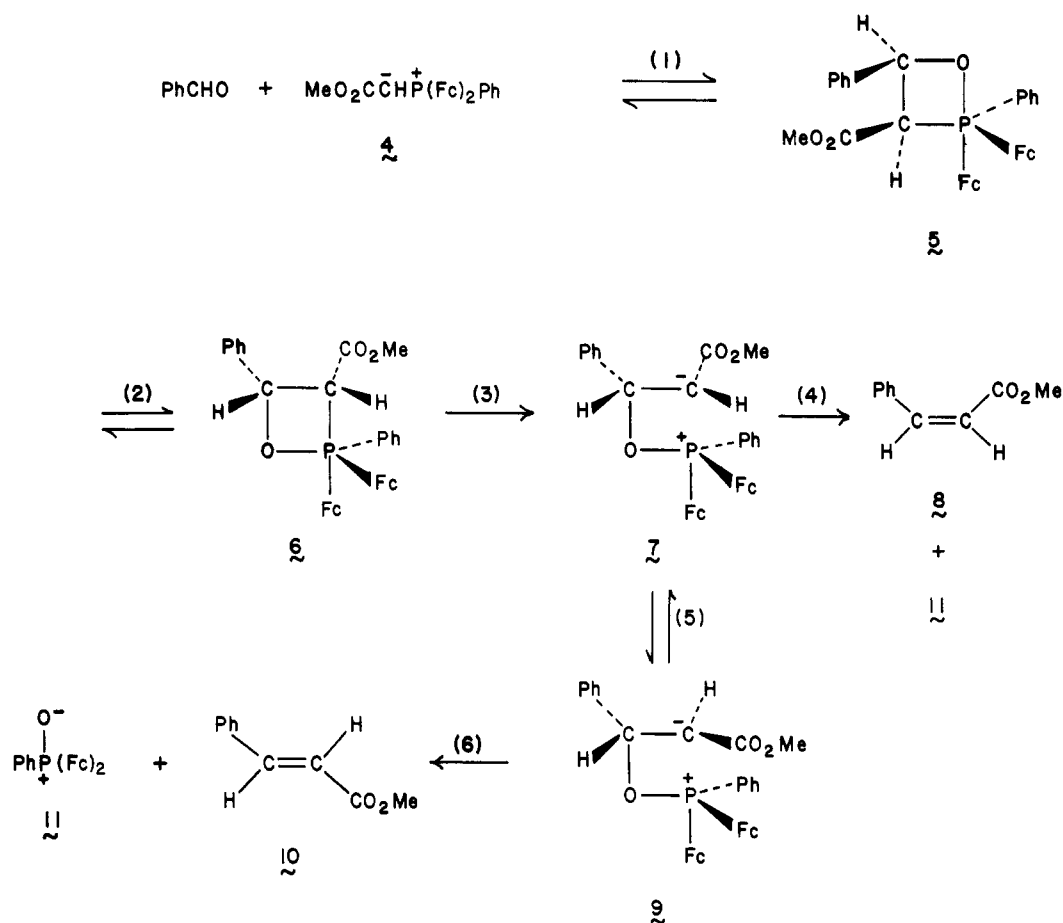
Figure 3. ORTEP plot of benzyldiphenylferrocenylphosphonium chloride showing the overlap of the h_a molecular orbital of the ferrocenyl group with the $3d_{z^2}$ orbital of phosphorus, where the z axis has been taken arbitrarily to be coincident with the P-CB1 bond.

Of the various models considered above for the benzyldiphenylferrocenylphosphonium ion, the one which seems most plausible in view of the X-ray crystallographic data is that which involves overlap of the filled h_a molecular orbital of the ferrocenyl group with an empty $3d$ orbital of phosphorus.¹² As shown in Figure 3, the superimposition of the h_a orbital of the ferrocenyl group, drawn to scale on the basis of Moffitt's²³ calculations, and what is essentially one lobe of an incipient $3d_{z^2}$ orbital of phosphorus²² on the ORTEP plot of the benzyldiphenylferrocenylphosphonium cation viewed normal to the plane defined by CF1, P, CB1, shows a distinct overlap. However, one of the features of one of the models considered for α -ferrocenyl carbocations²¹ is also apparent in the benzyldiphenylferrocenylphosphonium cation; i.e., the P-CF1 bond length (1.768 (3) Å) is significantly shorter than the two other P aromatic C bond lengths (1.803 (3) and 1.804 (3) Å), which suggests a delocalization of positive charge into the ferrocene system.

The molecular geometry goes against any model that suggests bending the P atom out of the plane of the substituted ring toward the Fe atom. The atoms CF1, CF2, CF3, CF4, and CF5 are coplanar to within ± 0.006 Å, with the P atom displaced 0.151 Å out of this plane in a direction away from the Fe atom. The atoms CF6, CF7, CF8, CF9, and CF10 are also coplanar to within ± 0.005 Å. The dihedral angle between the planes of the two cyclopentadienyl rings is 4.7° . The distances of the atoms of the unsubstituted ring from the least-squares plane of the substituted ring shows that the tilting of the rings results in an increased separation of CF1 from CF6 and CF5 from CF10 relative to the distances between the other eclipsed atoms of the two rings.

As implied in the discussion of the overlap of the filled h_a molecular orbital of the ferrocenyl group with what might be an incipient, empty $3d_{z^2}$ orbital of phosphorus, an examination of the bond angles about the P atom suggests a small distortion in the direction of a trigonal bipyramid, where CB1, CM, and CF1 occupy quasiequatorial positions and CA1 and a vacant orbital occupy axial ones. With reference to this "trigonal bipyramid"; the equatorial-P-equatorial bond angles tend to be larger than the axial-P-equatorial ones. The exception to this trend (CB1-P-CM = 109.9°) can be explained by crowding between the "B" and "C" phenyl rings. Further evidence of

Scheme I



this crowding is found in the P-CM-CC1 bond angle that is opened up to 111.7° as opposed to the tetrahedral value of 109°28'.

With a reasonable suggestion for the nature of the stabilization of a phosphonium cation by an attached ferrocenyl group available, it became of interest to investigate the effect of such a possible structural arrangement on the course of a Wittig reaction.

Although several mechanisms for the Wittig reaction have been proposed,²⁶⁻³⁰ that of Bestmann and his co-workers³¹⁻³⁵ seems to accommodate more of the experimental facts than any other. As applied to the reaction of (carbomethoxymethylene)diferrocenylphenylphosphorane (4) with benzaldehyde, cycloaddition would be expected to give the oxaphosphetane 5 that has the Z configuration, and, in accord with the selection rules³⁶ for

Table III. Physical Properties of Stable Ylides

phosphorane	mp, °C	pK _A ^a
12, carbomethoxy-methylenetriphenyl	168-169 ⁴⁵	9.1
13, carbomethoxy-methylenediphenyl-(p-methoxyphenyl)	136.5-137.5 ¹²	9.3
14, carbomethoxymethylene-diphenylferrocenyl	204-206 ¹²	9.7
4, carbomethoxymethylene-diferrocenylphenyl	171-175 ¹²	10.0

^a Of the parent phosphonium iodide, taken in absolute methanol at 25 °C.¹²

the entry and exit of nucleophiles in the interconversion of tetra- and pentacoordinated phosphorus, the oxygen occupies an apical position. Before 5 can decompose to form an alkene and diferrocenylphenylphosphine oxide (11), it must undergo a pseudorotation to 6, which brings the incipient departing carbanionic center into the apical position. Bond rupture, which occurs following formation of 6, gives the dipolar intermediate 7. Since the carbanionic center of 7 has the stabilizing feature of being bonded to a carbomethoxy group and since the phosphonio group can be stabilized by through space overlap with an h_g molecular orbital of the ferrocenyl group if the geometry accommodates such an interaction, its half-life is sufficient to permit rotation in 7, which allows 7 to equilibrate with the thermodynamically more stable conformer 9. The latter, on decomposition, gives (E)-methyl cinnamate (10) and the phosphine oxide 11 (Scheme I). In fact, we have found that the ratio of E:Z methyl cinnamate in this reaction is 96:4. In the absence of a stabilizing group on the carbanionic center (or on the phosphonio group³⁷), a

(26) Schlosser, M. *Top. Stereochem.* 1970, 5, 1.

(27) Schlosser, M.; Tuong, H. B. *Angew. Chem., Int. Ed. Engl.* 1979, 18, 633.

(28) Bergelson, L. D.; Vauer, V. A.; Barsukov, L. I.; Shemyakin, M. M. *Dokl. Akad. Nauk SSSR* 1962, 143, 111.

(29) Vedejs, E.; Meier, G. P.; Snoble, K. A. *J. Am. Chem. Soc.* 1981, 103, 2823.

(30) Krishnamurthy, V. V.; Olah, G. A. "Abstracts of Papers", 183rd National Meeting of the American Chemical Society, Las Vegas, Nev., Mar 28-Apr 2, 1982; American Chemical Society: Washington, D.C., 1982; Paper No. 144.

(31) Bestmann, H. J. *Pure Appl. Chem.* 1979, 51, 515.

(32) Bestmann, H. J. *Pure Appl. Chem.* 1980, 52, 711.

(33) Bestmann, H. J.; Roth, E. W.; Böhme, R.; Burzlaff, H. *Angew. Chem., Int. Ed. Engl.* 1979, 18, 876.

(34) Bestmann, H. J. *Bull. Soc. Chim. Belg.* 1981, 90, 519.

(35) Bestmann, H. J.; Chandrasekhar, J.; Downey, W. G.; Schleyer, P. V. R. *J. Chem. Soc., Chem. Commun.* 1980, 978.

(36) Marquarding, D.; Ramirez, F.; Ugi, I.; Gillespie, P. *Angew. Chem., Int. Ed. Engl.* 1973, 12, 91, and references cited therein.

Table IV. Reactions of Stable Ylides with Benzaldehyde

ylide	methyl cinnamate		
	yield, %	ratio of <i>E</i> : <i>Z</i>	$10^4 k_2$, L mol ⁻¹ s ⁻¹
12	80	85:15	18.5 ± 0.1
13	82	84:16	18.5 ± 0.1
11	75	96:4	19.2 ± 0.5
4	78	96:4	3.80 ± 0.15

(*Z*)-alkene is ordinarily the favored product in a Wittig reaction.

A principal drawback of the Bestmann mechanism is its inability to account in a completely satisfactory manner for the high stereoselectivity in the initial cycloaddition to form 5. The mechanism does not take into account a possible, initial betaine-oxaphosphetane equilibrium,³³ nor does it account for the results of certain crossover experiments.^{27,38,39} In addition, the effects of solvent polarity and the addition of lithium salts can be difficult to justify by the Bestmann (or any other) mechanism. It is not even certain which step in the Bestmann mechanism is rate limiting, and, in this connection, we thought that kinetics investigations of the reactions of various ylides, including those containing ferrocenyl groups, might provide useful information.

The preparations of four stable ylides and the determinations of the pK_A values of their conjugate acids in absolute methanol at 25 °C have been reported previously.¹² The physical constants of these ylides are summarized in Table III.

Each of the ylides 4 and 12–14 has been caused to react with benzaldehyde at 35.0°, and the rate data are presented in Table IV. Also, preparative scale reactions were carried out in refluxing benzene, and the ratio of *E*:*Z* methyl cinnamates formed were determined by vapor-phase chromatography. These results are also given in Table IV.

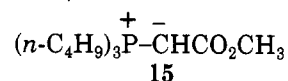
What is striking about the kinetics data is that the presence of one or two ferrocenyl groups in place of phenyl in the ylide does not bring about a significant difference in the rate of reaction but does have an effect on the *E*:*Z* ratio of methyl cinnamates formed. Of course, the latter effect is necessarily small in the reactions under consideration because the *E* isomer predominates in all of the reactions summarized in Table IV. Fortunately, Allen⁴⁰ has provided a much more convincing example of this effect. He found that reaction of the semistabilized ylide derived from benzyltriphenylphosphonium bromide (by the action of sodium ethoxide in ethanol solution) with benzaldehyde gives a 52:48 ratio of *cis*:*trans* stilbene, whereas reaction of the ylide derived from benzylferrocenyldiphenylphosphonium bromide with benzaldehyde under the same conditions gives a 33:67 ratio of *cis*:*trans* stilbene. Provided that the Bestmann mechanism is operative, these and additional facts lead to the tentative conclusion that step 3 is rate limiting. It is clear that step 1 cannot be rate limiting because ³¹P NMR spectral experiments conducted at -50 °C demonstrate that oxaphosphetanes are formed exceptionally rapidly.²⁹ Theoretical studies indicate that the pseudorotation process, step 2, also occurs relatively rapidly.³⁵ If step 4 (or step 6) were rate limiting, a large decrease in rate for the re-

actions of the ferrocenyl ylides would be anticipated, and this is not observed (Table IV). Furthermore, steps 4 and 6 should be distinctly exothermic, and this ordinarily coincides with a relatively rapid rate of reaction. By a process of elimination, then, step 3 is probably the rate-limiting step, and this is consistent with the fact that such a step would be highly endothermic.³²

Our evidence indicates that there is significant stabilization of a ferrocenylphosphonium cation by through space overlap of a filled h_a orbital of the ferrocene with an empty 3d orbital of the phosphorus. Why, then, does this not lead to an acceleration of step 3 of the Wittig reactions of 4 and 14 with benzaldehyde? The answer is that, in the transition state of step 3, the phosphonio group of the developing betaine does not have the correct geometry to permit the type of overlap depicted in Figure 3. Bond reorganization must occur before the overlap can become of importance. Thus, acceleration of step 3 (and of the entire reaction) is not observed, but partial control of the geometry of alkene formation, which occurs subsequent to bond reorganization, is observed.

The fact that the rate of reaction of 4 with benzaldehyde is about 5 times slower than that of 14 with benzaldehyde is probably attributable to varying position of the equilibria of steps 1 and 2. On the basis of the concept of through space overlap of a filled h_a orbital of a ferrocenyl group with an empty 3d orbital of phosphorus, the concentrations of the oxaphosphetanes would be less for the 4 system than for the 14 system at equilibrium, and this would be sufficient to explain the difference in rates in the reactions of 4 and 14, respectively, with benzaldehyde.

One point of interest with respect to synthetic organic chemistry should be mentioned. The ylides 4 and 14 are crystalline and insensitive to oxygen and moisture in the air. Thus, these reagents are much more convenient to use than the unstable ylide (carbomethoxymethylene)tri-*n*-butylphosphorane 15, that also has been reported to give



methyl cinnamate in an *E*:*Z* ratio of 96:4 by reaction with benzaldehyde.⁴² Also of possible importance is the fact that chiral ferrocenylphosphine ligands are particularly helpful in generating large enantiomeric excesses of products in a variety of transition-metal-catalyzed asymmetric syntheses.⁴³ It is conceivable that the high stereospecificity of these reactions is aided by the through-space overlap effect.

Experimental Section

Melting points and boiling points are uncorrected. Melting points were taken on a "Mel-Temp". Infrared spectra were taken in chloroform solution on a Beckman IR-5 or IR-10 recording spectrophotometer. Nuclear magnetic resonance spectra were taken in deuteriochloroform on a Varian Associates A-60 instrument using tetramethylsilane as an internal standard. Gas chromatography was carried out on an Aerograph Autoprep A-700 using a 20 ft × 3/8 in., 30% silicone rubber on Chromosorb W column, hereinafter referred to as column "A".

Benzylidiphenylferrocenylphosphonium Chloride. This compound was prepared and purified as described previously.⁴⁴ **(Carbomethoxymethylene)triphenylphosphorane (12).** This stable ylide, mp 168–169 °C, was prepared by the method of Denney and Ross.⁴⁵

(37) Meyers, A. I.; Lawson, J. P.; Carver, D. R. *J. Org. Chem.* **1981**, *46*, 3119.

(38) Speziale, A. J.; Bissing, D. E. *J. Am. Chem. Soc.* **1963**, *85*, 3878.

(39) Bissing, D. E.; Speziale, A. J. *J. Am. Chem. Soc.* **1965**, *87*, 2683.

(40) Allen, D. W. *Z. Naturforsch.; B: Anorg. Chem., Org. Chem.* **1980**, *35B*, 981.

(41) Olsen, D. K.; Torian, B. E.; Morgan, C. D.; Braun, L. L. *J. Org. Chem.* **1980**, *45*, 4049.

(42) Bissing, D. E. *J. Org. Chem.* **1965**, *30*, 1296.

(43) Hayashi, T.; Konishi, M.; Fukushima, M.; Mise, T.; Kagstani, M.; Tajika, M.; Kumada, M. *J. Am. Chem. Soc.* **1982**, *104*, 180 (and references cited therein).

(44) McEwen, W. E.; Fountaine, J. E.; Schulz, D. N.; Shiao, W. I. *J. Org. Chem.* **1976**, *41*, 1684.

Other Stable Ylides. (Carbomethoxymethylene)diphenyl- (*p*-methoxyphenyl)phosphorane (13), (carbomethoxymethylene)diphenylferrocenylphosphorane (14), and (carbomethoxymethylene)diferrocenylphenylphosphorane (4) were prepared as described previously.¹²

***cis*-Methyl Cinnamate (8).** Methyl phenylpropiolate (8.00 g, 0.05 mol) was dissolved in 200 mL of 95% ethanol to which had been added 0.5 g of Lindlar catalyst and three drops of synthetic quinoline. The mixture was then hydrogenated twice (fresh catalyst the second time) in a Parr apparatus at a starting pressure of 20 psi. The pressure dropped to 18 psi each time in about 45 min. The solution was then removed from the hydrogenator, the catalyst removed by filtration, and the ethanol removed on the steam bath. The crude product was then taken up in ether and extracted with 100 mL of 2% hydrochloric acid, followed by 100 mL of water. The ether solution was dried over MgSO₄ and the ether removed on the steam bath. The residue was subjected to preparative gas chromatography on column "A" to remove any remaining unreduced methyl phenylpropiolate. Pure *cis*-methyl cinnamate (8) was obtained as a colorless liquid: NMR δ 3.62 (s, COOCH₃), 5.86 (d, *cis* vinyl proton, $J = 12$ Hz), 6.83 (d, *cis* vinyl proton, $J = 12$ Hz), 7.08-7.63 (m, aromatic protons).

Reactions of Ylides 4 and 12-14 with Benzaldehyde. Each ylide (0.025 mol) was dissolved in 150 mL of anhydrous benzene. Benzaldehyde (0.025 mol) was then added, and the solution was refluxed for 15 h. The benzene solution, after having been washed with 10% hydrochloric acid and water, was steam distilled.

The benzene-ester solution from the steam distillate was dried over MgSO₄ and the solvent removed on the steam bath. Gas chromatography of the residual oil (column "A", 175 °C, He flow rate of 300 cm³/min) showed two components in the ratio indicated in Table IV. The residual oil was then vacuum distilled (bp 80-81 °C (0.25 mm)) to give about 3 g of a fragment, colorless oil that crystallized on brief standing. Gas chromatographic analysis of the distilled material gave the same component ratio as did the crude material. Increases in peak height upon addition of authentic samples of *cis*- and *trans*-methyl cinnamate, respectively, showed that the major component was *trans*-methyl cinnamate and the minor component *cis*-methyl cinnamate. The expected phosphine oxide was isolated from the residue of each steam distillation.⁴⁶

(45) Denney, D. B.; Ross, S. T. *J. Org. Chem.* 1962, 27, 998.

(46) Diphenylferrocenylphosphine oxide, mp 167-168.5 °C, was isolated from the nonsteam volatile fraction of 4 with benzaldehyde. A mixture melting point test with authentic⁴⁷ compound showed no depression, and NMR and IR spectra of the two samples were identical. Diferrocenylphenylphosphine oxide, mp 245-247 °C dec, was obtained from the nonsteam volatile fraction of the reaction of 14 with benzaldehyde. A mixture melting point test with authentic material⁴⁷ showed no depression, and the NMR and IR spectra of the two samples were identical.

Kinetics Procedure. Benzene and methanol were Fisher "Certified" reagent grade chemicals and were dried and stored over Linde 4-Å molecular sieves.

Benzaldehyde was also Fisher "Certified" reagent grade material and was purified by washing with sodium carbonate solution followed by vacuum distillation just prior to use. Fresh benzaldehyde solutions were prepared for each run.

All ylides used for kinetic runs had been chromatographed on alumina shortly before use.

Standard HCl solutions was obtained from Fisher Scientific Co. and had a normality of 0.1000. The normality of several lots was checked against primary standard THAM (tris(hydroxymethyl)aminomethane) either by potentiometric methods or by use of bromocresol purple as a visual indicator. Such checks showed deviations of less than one part in a thousand from the indicated normalities. Pipets used were of type I, class A, and met the standards set forth in NBS (National Bureau of Standards) circular 602. Burets used were of 5- and 10-mL capacity, precision bore, and also met the standards for class A set forth in NBS circular 602.

Sufficient ylide to make a 0.02 M solution in benzene after final dilution was dissolved in 50 mL of anhydrous benzene, and this solution was equilibrated at 35.0 ± 0.03 °C overnight. Reaction was initiated by pipetting 50 mL of benzaldehyde solution into the solution of the ylide. The initial concentration of both reactants was thus 0.02 M. The reaction was followed by withdrawing 10-mL aliquots periodically, quenching in 100 mL of cold (5 °C) methanol and titrating, in the cases of the triphenyl and diphenyl-*p*-anisyl ylides, to a pH of 6.0, 0.1000 N HCl being used as the titrant. For the diphenylferrocenyl and diferrocenylphenyl ylides, titration was carried out to a pH of 5.8. A Corning Model 12 pH meter was used for these titrations.

Rate constants were calculated in the usual manner, and they are given in Table IV.

Acknowledgment is made to the donors of the Petroleum Research Fund, administered by the American Chemical Society, for the support of this research.

Registry No. 4, 37299-25-5; 8, 19713-73-6; 12, 2605-67-6; 13, 38208-26-3; 14, 12100-52-6; diphenylferrocenylphosphine oxide, 54060-24-1; diferrocenylphenylphosphine, 12278-69-2; methyl phenyl propiolate, 4891-38-7; benzyldiphenylferrocenylphosphonium chloride, 58384-30-8.

Supplementary Material Available: Refined parameters for hydrogen atoms, anisotropic thermal parameters, and observed and calculated structure factor amplitudes for benzyldiphenylferrocenylphosphonium chloride (16 pages). Ordering information is given on any current masthead page.

(47) Sollott, G. P.; Mertwoy, H. E.; Portnoy, S.; Snead, J. L. *J. Org. Chem.* 1963, 28, 1090.

Steric Effects on Reactivity in Silicon Chemistry

Frank K. Cartledge

Department of Chemistry, Louisiana State University, Baton Rouge, Louisiana 70803

Received August 24, 1982

Reactivity data for a number of reactions taking place at Si atoms in silanes containing a variety of alkyl groups have been examined for statistical correlations with steric parameters. E_s , ν , and E_s° , derived from carbonyl reactions, are moderately successful in describing steric effects at Si. A set of $E_s(\text{Si})$ parameters for eight alkyl groups and for H has been defined from rates of acid-catalyzed hydrolysis of SiH compounds. Correlations with the $E_s(\text{Si})$ parameters are described and analyzed. Additivity of steric effects in R¹R²R³SiX compounds is often observed. The $E_s(\text{Si})$ parameters are most closely related to ν' parameters, which describe steric effects in nucleophilic substitution reactions at saturated carbon.

Introduction

Attempting to correlate structural changes with reactivity differences is as important a goal in silicon chem-

istry as it is in the much better developed chemistry of carbon compounds. Organic chemists have tried to separate substituent effects into steric and several kinds of

Other Stable Ylides. (Carbomethoxymethylene)diphenyl- (*p*-methoxyphenyl)phosphorane (13), (carbomethoxymethylene)diphenylferrocenylphosphorane (14), and (carbomethoxymethylene)diferrocenylphenylphosphorane (4) were prepared as described previously.¹²

***cis*-Methyl Cinnamate (8).** Methyl phenylpropiolate (8.00 g, 0.05 mol) was dissolved in 200 mL of 95% ethanol to which had been added 0.5 g of Lindlar catalyst and three drops of synthetic quinoline. The mixture was then hydrogenated twice (fresh catalyst the second time) in a Parr apparatus at a starting pressure of 20 psi. The pressure dropped to 18 psi each time in about 45 min. The solution was then removed from the hydrogenator, the catalyst removed by filtration, and the ethanol removed on the steam bath. The crude product was then taken up in ether and extracted with 100 mL of 2% hydrochloric acid, followed by 100 mL of water. The ether solution was dried over MgSO₄ and the ether removed on the steam bath. The residue was subjected to preparative gas chromatography on column "A" to remove any remaining unreduced methyl phenylpropiolate. Pure *cis*-methyl cinnamate (8) was obtained as a colorless liquid: NMR δ 3.62 (s, COOCH₃), 5.86 (d, *cis* vinyl proton, $J = 12$ Hz), 6.83 (d, *cis* vinyl proton, $J = 12$ Hz), 7.08-7.63 (m, aromatic protons).

Reactions of Ylides 4 and 12-14 with Benzaldehyde. Each ylide (0.025 mol) was dissolved in 150 mL of anhydrous benzene. Benzaldehyde (0.025 mol) was then added, and the solution was refluxed for 15 h. The benzene solution, after having been washed with 10% hydrochloric acid and water, was steam distilled.

The benzene-ester solution from the steam distillate was dried over MgSO₄ and the solvent removed on the steam bath. Gas chromatography of the residual oil (column "A", 175 °C, He flow rate of 300 cm³/min) showed two components in the ratio indicated in Table IV. The residual oil was then vacuum distilled (bp 80-81 °C (0.25 mm)) to give about 3 g of a fragment, colorless oil that crystallized on brief standing. Gas chromatographic analysis of the distilled material gave the same component ratio as did the crude material. Increases in peak height upon addition of authentic samples of *cis*- and *trans*-methyl cinnamate, respectively, showed that the major component was *trans*-methyl cinnamate and the minor component *cis*-methyl cinnamate. The expected phosphine oxide was isolated from the residue of each steam distillation.⁴⁶

(45) Denney, D. B.; Ross, S. T. *J. Org. Chem.* 1962, 27, 998.

(46) Diphenylferrocenylphosphine oxide, mp 167-168.5 °C, was isolated from the nonsteam volatile fraction of 4 with benzaldehyde. A mixture melting point test with authentic⁴⁷ compound showed no depression, and NMR and IR spectra of the two samples were identical. Diferrocenylphenylphosphine oxide, mp 245-247 °C dec, was obtained from the nonsteam volatile fraction of the reaction of 14 with benzaldehyde. A mixture melting point test with authentic material⁴⁷ showed no depression, and the NMR and IR spectra of the two samples were identical.

Kinetics Procedure. Benzene and methanol were Fisher "Certified" reagent grade chemicals and were dried and stored over Linde 4-Å molecular sieves.

Benzaldehyde was also Fisher "Certified" reagent grade material and was purified by washing with sodium carbonate solution followed by vacuum distillation just prior to use. Fresh benzaldehyde solutions were prepared for each run.

All ylides used for kinetic runs had been chromatographed on alumina shortly before use.

Standard HCl solutions was obtained from Fisher Scientific Co. and had a normality of 0.1000. The normality of several lots was checked against primary standard THAM (tris(hydroxymethyl)aminomethane) either by potentiometric methods or by use of bromocresol purple as a visual indicator. Such checks showed deviations of less than one part in a thousand from the indicated normalities. Pipets used were of type I, class A, and met the standards set forth in NBS (National Bureau of Standards) circular 602. Burets used were of 5- and 10-mL capacity, precision bore, and also met the standards for class A set forth in NBS circular 602.

Sufficient ylide to make a 0.02 M solution in benzene after final dilution was dissolved in 50 mL of anhydrous benzene, and this solution was equilibrated at 35.0 ± 0.03 °C overnight. Reaction was initiated by pipetting 50 mL of benzaldehyde solution into the solution of the ylide. The initial concentration of both reactants was thus 0.02 M. The reaction was followed by withdrawing 10-mL aliquots periodically, quenching in 100 mL of cold (5 °C) methanol and titrating, in the cases of the triphenyl and diphenyl-*p*-anisyl ylides, to a pH of 6.0, 0.1000 N HCl being used as the titrant. For the diphenylferrocenyl and diferrocenylphenyl ylides, titration was carried out to a pH of 5.8. A Corning Model 12 pH meter was used for these titrations.

Rate constants were calculated in the usual manner, and they are given in Table IV.

Acknowledgment is made to the donors of the Petroleum Research Fund, administered by the American Chemical Society, for the support of this research.

Registry No. 4, 37299-25-5; 8, 19713-73-6; 12, 2605-67-6; 13, 38208-26-3; 14, 12100-52-6; diphenylferrocenylphosphine oxide, 54060-24-1; diferrocenylphenylphosphine, 12278-69-2; methyl phenyl propiolate, 4891-38-7; benzyldiphenylferrocenylphosphonium chloride, 58384-30-8.

Supplementary Material Available: Refined parameters for hydrogen atoms, anisotropic thermal parameters, and observed and calculated structure factor amplitudes for benzyldiphenylferrocenylphosphonium chloride (16 pages). Ordering information is given on any current masthead page.

(47) Sollott, G. P.; Mertwoy, H. E.; Portnoy, S.; Snead, J. L. *J. Org. Chem.* 1963, 28, 1090.

Steric Effects on Reactivity in Silicon Chemistry

Frank K. Cartledge

Department of Chemistry, Louisiana State University, Baton Rouge, Louisiana 70803

Received August 24, 1982

Reactivity data for a number of reactions taking place at Si atoms in silanes containing a variety of alkyl groups have been examined for statistical correlations with steric parameters. E_s , ν , and E_s° , derived from carbonyl reactions, are moderately successful in describing steric effects at Si. A set of $E_s(\text{Si})$ parameters for eight alkyl groups and for H has been defined from rates of acid-catalyzed hydrolysis of SiH compounds. Correlations with the $E_s(\text{Si})$ parameters are described and analyzed. Additivity of steric effects in R¹R²R³SiX compounds is often observed. The $E_s(\text{Si})$ parameters are most closely related to ν' parameters, which describe steric effects in nucleophilic substitution reactions at saturated carbon.

Introduction

Attempting to correlate structural changes with reactivity differences is as important a goal in silicon chem-

istry as it is in the much better developed chemistry of carbon compounds. Organic chemists have tried to separate substituent effects into steric and several kinds of

electronic effects. Such a separation would aid in the interpretation of organosilicon reaction mechanisms in much the same way as it does in organic reactions. Silicon chemists in general use correlations in which the substituent constants have been defined in organic reactions, and the correlations meet with varying degrees of success. This paper attempts to isolate steric effects in some organosilicon reactions as a first step in a complete separation of substituent effects.

Our attention was first drawn to this problem because we have been aware that most structure reactivity correlations in organosilicon reaction chemistry use the Taft σ^* constants.¹ It is usually assumed in the interpretation of these correlations that σ^* represents a polar substituent effect. However, several workers have contended recently that σ^* constants are basically steric substituent constants, with perhaps a minor polar component.² If the latter interpretation is correct, substantial amounts of reactivity data in organosilicon chemistry would need to be reexamined and possibly reinterpreted.

Organosilicon chemists have long been aware of the significance of steric effects on reactivity.³ Since Si is a larger element than C, attack at a Si atom might be expected to be less hindered than attack at C. That would presumably be true for comparable systems, but, in fact, the Si systems of common interest are R_3SiX derivatives, having three organic groups and no small hydrogen atoms attached to Si. Indeed, the importance of steric effects on the susceptibility of a Si atom to nucleophilic attack is well-known to synthetic organic chemists. The use of $t\text{-BuMe}_2\text{Si}$ protecting groups,⁴ which are orders of magnitude less reactive than Me_3Si counterparts, is an important example. While an attempt to understand reactivity trends in Si chemistry is of considerable importance in itself, a study of broader significance seems possible with Si compounds. Silicon systems potentially allow for a rational and very complete test of the additivities, or lack thereof, of steric effects on reactivity. Many reactions taking place at Si can use silanes having one, two, or three R groups attached to Si along with Me groups, or even sometimes, as in acid-catalyzed Si-H hydrolysis, along with H atoms.

Correlations with Carbonyl-Derived Steric Parameters

Our initial interest lay in determining the degree to which steric reactivity parameters, all of which have been defined with respect to carbon systems, are successful in correlating steric effects in Si reactions. For that purpose we have picked from the literature a number of reactions for which significant amounts of reactivity data exist. The series selected all involve reaction taking place at a Si atom. They represent cases in which the largest number of different alkyl-substituted silanes has been studied. Thirdly, they include series in which alkyl groups on Si vary substantially in size, thus giving the possibility of observing steric effects. Because we want to isolate steric effects in this initial correlation, we have concentrated on alkyl groups without polar substituents. There seems to be general agreement that hydrocarbon alkyl groups have

small polar effects and even much smaller differential polar effects when compared with one another.^{2b,5}

The eight reaction series listed below have been examined. The reactions span a wide range of types, including examples using both nucleophilic and electrophilic reagents. There is even one example in which apparent steric acceleration of rate is observed.

Series 1: $R_3SiH + HCl$ in 95 vol % EtOH/ H_2O at 34.8 °C^{6,7} [k_{rel} = 1.0 (Et₃), 1.7 (PrMe₂), 1.25 (Pr₂Me), 0.63 (Pr₃), 0.06 (*i*-Pr₃), 0.59 (Bu₃), 0.17 (*i*-Bu₃), 1.8 (ClCH₂Me₂), 22 (Pr₂H), and 120 ((*c*-C₆H₁₁)H₂)].

Series 2: $R_3SiH + KOH$ in 95 vol % EtOH/ H_2O at 34.5 °C⁸ [k_2 (M⁻¹ min⁻¹) = 0.423 (EtMe₂), 0.364 (PrMe₂), 0.0806 (*i*-PrMe₂), 0.0012 (*t*-BuMe₂), 0.168 (Et₂Me), 0.106 (Pr₂Me), 0.00695 (*i*-Pr₂Me), 0.093 (Et₃), 0.0409 (Pr₃), and 0.00083 (*i*-Pr₃)].

Series 3: $R_3SiH + Br_2$ in DMF at 25 °C⁹ [k_2 (M⁻¹ min⁻¹) = 691.6 (EtMe₂), 851.5 (Et₂Me), 1055 (Et₃), 711.6 (PrMe₂), 937.6 (Pr₂Me), 1187 (Pr₃), 150.7 (*i*-Pr₃), and 459.3 (*i*-Bu₃)].

Series 4: $R_3SiH + O_3$ in CCl₄ at 0 °C¹⁰ or 20 °C¹¹ [k_{rel} = 236 ((*c*-C₆H₁₁)₃), 226 (*t*-Bu(*c*-C₆H₁₁)₂), 100 (Bu₃), 84 (Et₃), 28.5 (*i*-Pr₂H), 21.7 (Bu₂H), 94.5 (Pr₃), 60 (Bu₂Me), 56 (Pr₂Me), and 50.5 (Et₂Me)].

Series 5: $R_3SiOPh + OH^-$ in 51.4 wt % EtOH/ H_2O at 25 °C¹² [k_2 (M⁻¹ s⁻¹) = 330 (Me₃), 2.1 (Et₃), 0.66 (Pr₃), 0.41 (Bu₃), 1.72 (*t*-BuMe₂)].

Series 6: $R_3SiOPh + H^+$ in 51.4 wt % EtOH/ H_2O at 25 °C¹² [k_2 (M⁻¹ s⁻¹) = 10.4 (Me₃), 0.22 (Et₃), 0.12 (Pr₃), 0.081 (Bu₃), and 5.91 (*t*-BuMe₂)].

Series 7: R_3SiF in 66.7% aqueous acetone¹³ [k_2 (M⁻¹ min⁻¹) = 10 (Et₂Me), 2.5 (Et₃), 1.5 (*i*-PrBuMe), 1.0 (Bu₃), and 0.017 (*i*-Pr₃)].

Series 8: $R_3SiH + 1\text{-hexyne}$ in THF at 20 °C with 0.1 M H_2PtCl_6 ¹⁴ [k_{rel} = 1.94 (EtMe₂), 1.52 (Et₂Me), 0.82 (Et₃), 0.67 (Pr₂Me), 0.60 (Pr₃), and 0.39 (*i*-Pr₂Me)].

The original steric parameter of Taft, E_s ,¹⁵ has received considerable attention recently. Although the assumption that acid-catalyzed ester hydrolysis shows little rate dependence on polar substituent effects is generally accepted, the usual E_s values have been criticized for being based on too few different reaction series^{2b} or too many.¹⁶ Dubois and co-workers have determined an extensive set of so-called E_s' parameters, defined by using a single reaction, acid-catalyzed esterification of carboxylic acids in MeOH at 40 °C.¹⁶ In most cases, E_s' does not vary significantly from the E_s values of Taft. We have chosen to examine silane reactivity correlations with E_s' and with two other common measures of steric effects ν ¹⁷ and E_s° .¹⁸ These

(5) (a) Levitt, L. S.; Widing, H. F. *Prog. Phys. Org. Chem.* **1976**, *12*, 119. (b) Taft, R. W.; Levitt, L. S. *J. Org. Chem.* **1977**, *42*, 916-8.

(6) Baines, J. E.; Eaborn, C. *J. Chem. Soc.* **1956**, 1436.

(7) Steward, O. W.; Pierce, O. R. *J. Am. Chem. Soc.* **1961**, *83*, 4932-6.

(8) Barie, W. P., Jr.; Ph.D. Thesis, Pennsylvania State University, 1954.

(9) Hetflejš, J.; Mares, F.; Chvalovsky, V. *Collect. Czech. Chem. Commun.* **1972**, *37*, 1713-20.

(10) Spialter, L.; Pazdernik, L.; Bernstein, S.; Swansiger, W. A.; Buell, G. R.; Freeburger, M. E. *J. Am. Chem. Soc.* **1971**, *93*, 5682-6.

(11) Aleksandrov, Yu. A.; Tarunin, B. I. *Dokl. Akad. Nauk SSSR, Ser. Khim.* **1973**, *212*, 869-71.

(12) Akerman, E. *Acta Chem. Scand.* **1956**, *10*, 298; **1957**, *11*, 373.

(13) Sommer, L. H.; Musolf, M. C., unpublished studies cited in ref 3b, p 142.

(14) Voronkov, M. G.; Pukhnarevich, V. B.; Kopylova, L. I.; Nestunovich, V. A.; Tsetlina, E. O.; Trofimov, B. A.; Pola, I.; Khalval'skii, V. *Dokl. Akad. Nauk SSSR, Ser. Khim.* **1976**, *227*, 91-3.

(15) Taft, R. W. Jr.; In "Steric Effects in Organic Chemistry"; Newman, M., Ed.; Wiley: New York, 1956.

(16) MacPhee, J. A.; Panaye, A.; Dubois, J.-E. *Tetrahedron* **1978**, *34*, 3553-62.

(17) (a) Charton, M. *J. Am. Chem. Soc.* **1975**, *97*, 1552. (b) Charton, M. *J. Org. Chem.* **1976**, *41*, 2217-20.

(1) Mileshekevich, V. P.; Novikova, N. F. *Usp. Khim.* **1981**, *50*, 85-110.

(2) (a) Charton, M. *J. Org. Chem.* **1979**, *44*, 903-6. (b) DeTar, D. F. *Ibid.* **1980**, *45*, 5166-74. (c) DeTar, D. F. *J. Am. Chem. Soc.* **1980**, *102*, 7988-90.

(3) (a) Eaborn, C. "Organosilicon Compounds"; Butterworths: London, 1960. (b) Sommer, L. H. "Stereochemistry, Mechanism, Silicon"; McGraw-Hill: New York, 1965. (c) Boe, B. *J. Organomet. Chem.* **1976**, *107*, 139. (d) Corriu, R. J. P.; Guerin, C. *Ibid.* **1980**, *198*, 231.

(4) Corey, E. J.; Snider, B. B. *J. Am. Chem. Soc.* **1972**, *94*, 2549.

Table I. Steric Parameter Correlations with the Equation $\log k = \delta \Sigma E_s$ (or ν) + b

	n^a	δ	b	S^b	F^c	r^d	α^e
Series 1							
E_s'	10	0.746	0.560	0.442	34	0.899	0.0005
ν	10	-1.54	3.00	0.460	31	0.891	0.001
$E_s'^o$	10	0.680	0.887	0.376	50	0.928	0.0005
Series 2							
E_s'	10	1.83	-0.207	0.325	72	0.949	0.0001
ν	10	-3.62	5.43	0.343	64	0.943	0.0001
$E_s'^o$	10	1.24	0.069	0.259	118	0.968	0.0001
E_s (Si)	10	1.82	-0.152	0.086	1144	0.996	0.0001
Series 3							
E_s'	8	0.158	2.94	0.266	2	0.507	0.199
$E_s'^o$	8	0.160	3.03	0.241	4	0.623	0.099
E_s (Si)	8	0.437	3.09	0.177	12	0.819	0.013
Series 4							
E_s'	10	-0.314	1.62	0.126	56	0.935	0.001
$E_s'^o$	10	-0.233	1.52	0.147	39	0.911	0.001
E_s (Si)	10	-0.228	1.67	0.133	50	0.928	0.001
Series 5							
E_s'	5	2.65	1.78	0.735	17	0.924	0.025
$E_s'^o$	5	2.07	2.36	0.382	73	0.980	0.003
E_s (Si)	5	2.80	1.71	0.867	12	0.892	0.042
Series 6							
E_s'	5	2.39	0.712	0.715	15	0.913	0.030
$E_s'^o$	5	1.78	1.13	0.674	17	0.923	0.026
E_s (Si)	5	2.85	0.865	0.178	287	0.995	0.001
Series 7							
E_s'	5	1.81	1.25	0.470	16	0.920	0.027
$E_s'^o$	5	1.27	1.73	0.247	68	0.978	0.004
E_s (Si)	5	1.91	1.44	0.207	98	0.985	0.002
Series 8							
E_s'	6	0.604	0.231	0.122	19	0.909	0.012
$E_s'^o$	6	0.442	0.372	0.084	44	0.958	0.003
E_s (Si)	6	0.705	0.292	0.123	19	0.907	0.012

^a Number of compounds in the correlation. ^b Standard deviation of regression. ^c F value. ^d Correlation coefficient. ^e Significance level.

correlations are shown in Table I.

The organosilicon reaction that has been most thoroughly studied with respect to structure-reactivity relations is Si-H hydrolysis. The reaction occurs under both acid and base catalysis and has been compared, in terms of structure-reactivity effects, with carboxylic acid ester hydrolysis.¹⁹ Measurements of rates of hydrolysis of 18 R_3SiH compounds under the same acid-catalyzed conditions show a range of 130 in relative rates.^{6,7} When data for five of these compounds, $i\text{-Pr}_3SiH$, $i\text{-Bu}_3SiH$, $(ClCH_2)_2Me_2SiH$, $PhMe_2SiH$, and Ph_3SiH , are removed, the span in rates is only a factor of 13. This restricted series gives a moderately good ($r = 0.961$) correlation with σ^* and a ρ^* value of 0.77.⁷ Clearly, however, the reaction is very susceptible to steric effects. If one includes all the compounds for which values of E_s' and σ_1 exist, including one compound each of types $RSiH_3$ and R_2SiH_2 , one obtains a correlation with E_s' alone that has a correlation coefficient of 0.899 ($F = 34$). The compounds showing the greatest deviations from the correlation are $i\text{-Bu}_3SiH$ and $i\text{-Pr}_3SiH$. Indeed, when the single point for $i\text{-Bu}_3SiH$ is omitted from the correlation, the correlation coefficient

increases to 0.974 ($F = 128$). One parameter correlations with σ_1 and σ^* have correlation coefficients of 0.681 ($F = 8.6$) and 0.797 ($F = 17$), respectively. Although there are no indications from these correlations that polar effects are having a significant influence on rates in the acid-catalyzed hydrolysis, the only even moderately polar group included in the correlations is $ClCH_2$. The original work of Steward⁷ includes several fluoroalkyl and cyanoalkyl substituents, and the data for hydrolysis of such compounds have not been included because either E_s' or σ_1 is not known. The rate data indicate, however, that polar effects are present.

In the further correlations noted in Table I, we have restricted the series to those compounds containing only hydrocarbon alkyl groups in order to avoid ambiguities with polar effects. In most of the series in Table I it is obvious that steric effects are important. Correlation coefficients are given for each correlation, and the standard assumption in statistical practice is that r^2 gives the fraction of the variation in rate that can be accounted for by the steric parameter. Only in series 3 is r^2 less than 0.8. This does not necessarily imply that the reactions are all subject to steric effects to the exclusion of electronic effects, since only alkyl groups without electronegative atoms are included in the correlations. It does, however, imply something about the ability to correlate steric effects in a wide variety of reactions at Si in compounds with one, two, and three R groups attached. Series 2 is particularly interesting in that regard since it contains the following

(18) (a) Pal'm, V. A. "Fundamentals of the Quantitative Theory of Organic Reactions"; Khimiya: Leningrad, 1967; Chapter 10 (in Russian). (b) Pal'm, V. A. "Introduction to Theoretical Organic Chemistry"; Vysshaya Shkola: Moscow, 1974 (in Russian). (c) Shorter, J. In "Advances in Linear Free Energy Relationships"; Chapman, N. B., Shorter, J., Eds.; Plenum Press: London, 1972; p 95.

(19) Reference 3b, pp 127-130.

Table II. Steric Substituent Constants

R ₃ in R ₃ SiH	log <i>k</i> _{rel}	<i>E</i> _s (Si) ^a (substituent)	<i>E</i> _s ' ^c	<i>E</i> _s ^{°d}
Et ₃	0	-0.149 (Et)	-0.08	-0.28
Pr ₃	-0.201	-0.216 (Pr)	-0.31	-0.51
PrMe ₂	0.230	0 (Me)	0	0
Pr ₂ H	1.34	+1.33 (H)	+1.12	+1.12
<i>i</i> -Pr ₃	-1.22	-0.556 (<i>i</i> -Pr)	-0.48	-0.88
Bu ₃	-0.229	-0.225 (Bu)	-0.31	-0.51
<i>i</i> -Bu ₃	-0.770	-0.405 (<i>i</i> -Bu)	-0.93	-1.13
(<i>c</i> -C ₆ H ₁₁) ₂ H	2.08	-1.02 (<i>c</i> -C ₆ H ₁₁)	-0.69	-1.09
<i>t</i> -BuMe ₂		-1.46 ^b (<i>t</i> -Bu)	-1.43	-2.03

^a *E*_s(Si) was defined from the relationship $\log k_{\text{rel}} = \Sigma (E_s(\text{Si}) + 0.149)$. In cases in which R₃SiH contains two different R groups, *E*_s(Si) for one of the groups was obtained by using *E*_s(Si) already defined for a group higher in the table. ^b For Me, Et, Pr, and *i*-Pr groups, substituent effects in base-catalyzed SiH hydrolysis are very close to twice those in acid-catalyzed hydrolysis. *E*_s(Si) for the *t*-Bu group was defined as $0.5(\log k_{t\text{-BuMe}_2\text{SiH}}/\log k_{\text{Me}_3\text{SiH}})$. ^c From ref 16. ^d Calculated by using the equation referred to in the text, but using *E*_s' values as the 'base rather than *E*_s.

compounds: EtMe₂, Et₂Me, Et₃; PrMe₂, Pr₂Me, Pr₃; *i*-PrMe₂, *i*-Pr₂Me, *i*-Pr₃. It is also clear, however, that the correlation coefficients and *F* values are not as large as one would like to see in a statistical correlation of reactivity data. One is used to seeing correlation coefficients of 0.98 or better for rate and equilibrium data in substituted benzenes being correlated with σ constants. In general such a high degree of correlation is probably not to be expected when dealing with steric effects.

The ν values of Charton¹⁷ have been derived in part from van der Waals radii and in part from successful correlations using the primary ν values obtained from radii of single atom or AX₃ groups. There is an excellent correlation between ν and *E*_s' for the groups under consideration and hence corresponding correlation of the silane reactivity data. Therefore, we have not included ν in all the reaction series.

It is very common, particularly in the Russian literature, to see correlations with a "hyperconjugation-free" steric parameter, *E*_s[°], defined by Pal'm¹⁸ with the following equation: $E_s^\circ = E_s' - 0.33(n_H - 3) - 0.13n_C$, in which *n*_H is the number of α hydrogens and *n*_C is the number of α C-C bonds in the substituent group. The *E*_s[°] parameters used here have been derived with the equation above, but from *E*_s' values, not *E*_s. Correlations in Table I are sometimes significantly better with *E*_s[°] than with *E*_s' or ν . The importance of this observation is not clear at present, particularly since the two series (5 and 8) in which *E*_s[°] gives significantly better correlation than *E*_s' have only 5 and 6 points, respectively, in the data set. The significance of hyperconjugation-free steric parameters has been severely questioned.^{2b,16,20}

Steric Parameters for Si Reactions

The quite varied results obtained in the correlations in Table I might be due to a lack of additivity in substituent effects, since much of the data include R₃SiX compounds with varying combinations of the same or different R groups. On the other hand, it may simply be that different reaction mechanisms call forth different steric effects from the same substituent group, making it inappropriate to use the steric parameters derived from carbonyl addition reactions for reactions taking place at Si. Steric effects depend on distance of the group from the reaction center, and C-Si bonds, being longer than C-C bonds, push the groups further away from the reaction site.

We have taken a simple approach to defining a set of steric substituent constants to be applicable to Si reactions.

We have used rate data for acid-catalyzed Si-H hydrolysis^{6,7} and assumed that the reaction is subject only to steric effects, at least for the hydrocarbon alkyl groups. The parameters, designated *E*_s(Si), are defined with the relationship $\log k_{\text{rel}} = \Sigma (E_s(\text{Si}) + 0.491)$. In most cases the *E*_s(Si) value is being defined as a third of the effect in an R₃SiH compound. In cases in which the silane contains two different R groups, *E*_s(Si) for one of the groups was obtained by using *E*_s(Si) already defined for a group higher in Table II. Thus, the present definition assumes that steric effects will be additive. That assumption can be tested to some extent with the silane hydrolysis data. The *E*_s(Si) value for the propyl group can be defined from PrMe₂SiH, Pr₂MeSiH, or Pr₃SiH, and the respective values are -0.216, -0.175, and -0.216. For the time being we have not included the ClCH₂, NCCH₂CH₂, or Ph groups that were included in the SiH hydrolysis studies, in order to be sure that we are dealing only with steric effects. In the case of the Ph group, it would be possible to derive an *E*_s(Si) value from either PhMe₂SiH or Ph₃SiH. In that case additivity is not so clearly present. The two derived values are -0.192 and -0.323, respectively. It is worth noting that series 2, which has the widest range of compounds of type R_nMe_{3-n}SiX, shows an excellent correlation with *E*_s(Si). We are aware, however, that there may be problems with additivity relationships, particularly in comparisons among different reaction series. For instance, in a short series of compounds, hydrolysis rates of silyl ethers, R₃SiOR' (R₃ = *t*-BuMe₂, *t*-BuPh₂, *i*-Pr₃; R' = Bu, *c*-C₆H₁₁) have been determined under both acid- and base-catalyzed conditions.²¹ The *i*-Pr₃Si group is hydrolyzed most slowly under basic conditions, but at an intermediate rate under acidic conditions. This may be due to an inversion in the relative magnitudes of steric effects for *i*-Pr and Ph groups in the two reactions. However, alternatively, it may be due to an acceleration of hydrolysis by the Ph group that operates under basic but not acidic conditions. There are other indications that the latter may be the case, which is one of our reasons for not including the Ph group in the present correlations.

The most striking difference between the *E*_s(Si) values and *E*_s' is that branching at the α position has a larger effect on *E*_s(Si), as for instance with Et and *i*-Pr (but not so much for *t*-Bu). On the other hand, β branching has a smaller effect on *E*_s(Si), e.g., *i*-Bu. A reasonable reason for these two effects lies in the greater length of C-Si (ca. 1.87 Å) as compared to C-C (ca. 1.53 Å) bonds.

Several of the reaction series in Table I show excellent correlations with *E*_s(Si) (*r* > 0.98). The poorest correlation with all of the substituent constants is in series 3. With

(20) (a) Charton, M. *J. Org. Chem.* 1978, 43, 3995. (b) Charton, M.; Charton, B. I. *Ibid.* 1982, 47, 8-13.

(21) Unico, R. F.; Bedell, L. *J. Org. Chem.* 1980, 45, 4797.

Table III. Multiple Correlations of Steric and Inductive Parameters with the Equation $\log k = \rho \Sigma \sigma_I + \delta \Sigma E_s + b$

	n^a	ρ	δ	b	S^b	F^c	r^d	α^e
Series 3								
$E_s(\text{Si})$	8	-4.32	0.800	2.32	0.074	49	0.976	0.001
E_s'	8	-0.253	0.169	2.92	0.292	0.9	0.509	0.473
$E_s'^{\circ}$	8	-2.44	0.260	2.83	0.245	2	0.689	0.2
Series 4								
$E_s(\text{Si})$	10	-2.16	-0.261	1.33	0.118	33	0.951	0.001
E_s'	10	-0.287	-0.318	1.58	0.134	25	0.936	0.001
$E_s'^{\circ}$	10	-1.21	-0.251	1.32	0.150	19	0.919	0.002
Series 5								
$E_s(\text{Si})$	5	36.1	2.23	7.45	0.539	18	0.973	0.053
E_s'	5	25.0	2.16	5.66	0.694	10	0.955	0.087
$E_s'^{\circ}$	5	3.51	2.01	2.88	0.463	25	0.980	0.039
Series 6								
$E_s(\text{Si})$	6	10.0	0.435	1.83	0.098	16	0.956	0.025
E_s'	6	8.66	0.379	1.57	0.121	10	0.932	0.047
$E_s'^{\circ}$	6	1.94	0.405	0.66	0.096	17	0.958	0.023

^a Number of compounds in the correlation. ^b Standard deviation of regression. ^c F value. ^d Correlation coefficient. ^e Significance level.

Table IV. Correlations of $E_s(\text{Si})$ with Other Steric Parameters^a Using the Equation $Q = m(E_s(\text{Si})) + b$

steric parameter, Q	m	b	S^b	F^c	r^d	α^e
E_s'	0.950	-0.097	0.228	24.8	0.912	0.004
E_s' (Taft)	1.011	-0.102	0.229	27.7	0.920	0.003
$E_s'^{\circ}$	1.316	-0.197	0.211	55.5	0.958	0.001
ν	-0.477	0.569	0.112	26.0	0.916	0.004
ν'	-0.628	0.297	0.030	646	0.996	0.0001

^a Substituents included are Me, Et, Pr, Bu, *i*-Pr, *i*-Bu, and *t*-Bu. ^b Standard deviation of regression. ^c F value. ^d Correlation coefficient. ^e Significance level.

that data and with several other series, multiple correlations with the steric parameters and σ_I^b parameters were carried out and are shown in Table III. Most of the correlation coefficients go up, but the correlations are not necessarily significantly better. A notable exception is that the multiple correlation with $E_s(\text{Si})$ and σ_I in series 3 is now a good one, and the same multiple correlation in series 5 shows a greater F value. In general, particularly taking into account the multiple correlations, $E_s(\text{Si})$ does a substantially better job of correlating the rate data than do E_s , ν , or $E_s'^{\circ}$. After having made those observations, we are nevertheless reluctant to promote extensive use of a new set of steric parameters. In the first place the parameters are defined in a relatively crude manner, as described above. Several of the substituents for which $E_s(\text{Si})$ is defined in Table II (H, *i*-Bu, *c*-C₆H₁₁) are represented in only two of the series in Table I. It will be necessary to have much more experimental data before a good evaluation of the individual constants can be made. Secondly, science aims in the direction of simplification, and a proliferation of steric parameters for different types of compounds or reactions is not necessarily desirable. However, as with other reactivity parameters, such as the many σ scales, it may be possible to find the underlying common features only after several scales are available.

It is already clear that some relationships exist among the steric parameters. For the seven substituents that are common to several scales, it is clear from Table IV that the scale best correlated with the $E_s(\text{Si})$ scale is ν' . The ν' values were derived by Charton²² to correlate reactivity in cases involving expansion of coordination from four to five, in contrast to the expansion from three to four in the carbonyl-derived scales. It is also interesting to note that

the ν' scale is successful in correlating reactivity in hydrolysis of alkyl-substituted phosphorus esters and chlorides.²³ It remains to be seen in an extensive series of substituents whether expansion of coordination from four to five is subject to steric effects in a consistently different way from expansion from three to four. At the moment the range of alkyl groups studied is small. The observation of the correlation in Table IV is highly suggestive, however, since the defining series for $E_s(\text{Si})$, as well as the other series showing excellent correlation with $E_s(\text{Si})$ all clearly involve nucleophilic attack at Si.

Conclusions

The steric parameters derived for the purpose of describing steric effects on reactions of organic carbonyl compounds are moderately successful in describing steric effects in reactions taking place at Si atoms. A set of $E_s(\text{Si})$ parameters defined for alkyl groups from rates of acid-catalyzed hydrolysis of SiH compounds is quite useful for predicting steric effects in a wide range of reactions taking place at Si, with correlation often being excellent. The reactions considered show a wide range of sensitivities to steric effects, and the sensitivity is a potentially very useful criterion for the definition of a reaction mechanism.

The major difference in the parameters derived from Si compounds and those derived from carbonyl compounds is a greater effect of branching α to the reaction center and a smaller effect of branching β to the reaction center. The steric effects on rate appear to be usually additive. The set of steric parameters most closely related to those defined for Si is the set of ν' parameters²² derived for correlation of nucleophilic substitution at four-coordinate carbon. The good correlation of these two sets of steric

(22) Charton, M. *J. Am. Chem. Soc.* 1975, 97, 3694-7.

(23) Charton, M.; Charton, B. *J. Org. Chem.* 1978, 43, 2383-6.

parameters suggests that Charton is correct in his assessment that steric effects are more sensitive to reaction type than to the identity of the atom under attack and that a reaction involving expansion of coordination from four to five will show a different sensitivity to α and β branching than a reaction involving change of coordination from three

to four.

Acknowledgment. The statistical analyses were performed on PROPHEET, a biomedical computer system sponsored by the National Institute of Health, Division of Research Resources.

UV-PES, ^{13}C NMR, and Theoretical Studies on the Alkyne-Cluster Interaction in $\text{Fe}_3(\text{CO})_9(\mu_3\text{-}\eta^2\text{-EtC}_2\text{Et})$

Gaetano Granozzi,*^{1a} Eugenio Tondello,^{1a} Maurizio Casarin,^{1b} Silvio Aime,^{1c} and Domenico Osella^{1c}

Istituto di Chimica Generale ed Inorganica, University of Padova, 35100 Padova, Italy, Istituto di Chimica e Tecnologia dei Radioelementi del CNR, 35100 Padova, Italy, and Istituto di Chimica Generale ed Inorganica, University of Torino, Torino, Italy

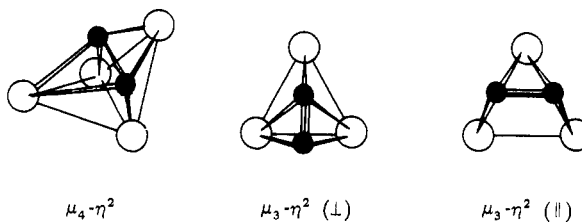
Received June 29, 1982

^{13}C NMR, UV-PES, and CNDO theoretical results of $\text{Fe}_3(\text{CO})_9(\mu_3\text{-}\eta^2\text{-EtC}_2\text{Et})$ are reported. ^{13}C alkyne resonances have very different chemical shifts according to the different coordination environments of the two acetylenic carbon atoms. Variable-temperature NMR experiments indicate localized exchange processes of the carbonyls at each $\text{Fe}(\text{CO})_3$ unit. The gas-phase UV-PE spectrum is assigned by comparison arguments with data on simpler related systems. The CNDO results contribute to the discussion of the PE data and provide interesting insights into the alkyne-cluster bonding mechanism. The relevant role of the cluster \rightarrow alkyne back-donation is stressed by both the experimental and theoretical data. The qualitative picture of the electronic structure proposed by Blount et al. receives strong support by the present theoretical data.

Introduction

The Dewar-Chart-Duncanson model,² originally developed to describe the bonding interaction in transition-metal olefin complexes, has been successfully extended to include the description of the σ - π bond in mononuclear alkyne complexes.³ This bonding scheme, however, is unable to account for the interaction of alkynes chemisorbed on transition-metal surfaces; actually the strong alkyne-surface binding rises from multicentered interactions, which imply significant rehybridization of the acetylenic carbons and formation of strong σ -carbon-metal bonds.⁴

The very rich chemistry of alkyne-cluster compounds⁵ provides a variety of structural arrangements, which can be envisaged as reasonable models for chemisorbed species on metallic surfaces.⁶ According to Muetterties et al.,^{6b} three basic bonding modes (namely, $\mu_4\text{-}\eta^2$, $\mu_3\text{-}\eta^2$ (\perp), and $\mu_3\text{-}\eta^2$ (\parallel) types) can account for the interaction between the



alkyne and a metallic cluster. It is generally accepted that in this class of molecules the interaction with three or four metal centers leads to an enhanced activation of the coordinated alkyne when compared with mono- and binuclear complexes. The bond order reduction can be compared with sufficient confidence to that occurring in chemisorption experiments on metallic surfaces. This cluster-surface analogy,⁶ then provides a novel methodological route to the study of surface phenomena by means of molecular spectroscopic techniques.

In an attempt to get a more detailed picture of the multicentered ligand-metal cluster interactions, we have already investigated⁷ compounds of type I, which, on the basis of the above considerations, represent good models for the dissociative chemisorption of monosubstituted alkynes (and acetylene itself) on metal surfaces by cleavage of the C-H bond.

We report here the results of a ^{13}C NMR, UV-PES, and theoretical (CNDO) study of the strictly related system $\text{Fe}_3(\text{CO})_9(\mu_3\text{-}\eta^2\text{-RC}_2\text{R})$ (II, R = C_2H_5), which can be envi-

(1) (a) University of Padova. (b) CNR of Padova. (c) University of Torino.

(2) (a) Dewar, M. J. S. *Bull. Soc. Chem. Fr.* 1951, 18, C71. (b) Chatt, J.; Duncanson, L. A. *J. Chem. Soc.* 1953, 2939.

(3) For a recent detailed discussion see: Tatsumi, K.; Hoffmann, R.; Templeton, J. L. *Inorg. Chem.* 1982, 21, 466.

(4) For a general survey on this topic see: (a) Muetterties, E. L. *Angew. Chem., Int. Ed. Engl.* 1978, 17, 545. (b) Ozin, G. A.; McIntosh, D. F.; Power, W. J.; Messmer, R. P. *Inorg. Chem.* 1981, 20, 1782. (c) Geurts, P.; Van Der Avoird, A. *Surf. Sci.* 1981, 103, 431 and references cited therein.

(5) Johnson, B. F. G.; Lewis, J. *Adv. Inorg. Chem. Radiochem.* 1981, 24, 225.

(6) (a) Ugo, R. *Catal. Rev.* 1975, 11, 225. (b) Muetterties, E. L.; Rhodin, T. N.; Band, E.; Brucker, C. F.; Pretzer, W. R. *Chem. Rev.* 1979, 79, 91.

(7) (a) Granozzi, G.; Tondello, E.; Aime, S.; Osella, D. "EuChem Conference the Challenge of Polynuclear Inorganic Compounds", Venice, 28-30 September 1981, Commun. C9. (b) Granozzi, G.; Tondello, E.; Bertonecello, R.; Aime, S.; Osella, D. *Inorg. Chem.*, in press.

parameters suggests that Charton is correct in his assessment that steric effects are more sensitive to reaction type than to the identity of the atom under attack and that a reaction involving expansion of coordination from four to five will show a different sensitivity to α and β branching than a reaction involving change of coordination from three

to four.

Acknowledgment. The statistical analyses were performed on PROPHEET, a biomedical computer system sponsored by the National Institute of Health, Division of Research Resources.

UV-PES, ^{13}C NMR, and Theoretical Studies on the Alkyne-Cluster Interaction in $\text{Fe}_3(\text{CO})_9(\mu_3\text{-}\eta^2\text{-EtC}_2\text{Et})$

Gaetano Granozzi,*^{1a} Eugenio Tondello,^{1a} Maurizio Casarin,^{1b} Silvio Aime,^{1c} and Domenico Osella^{1c}

Istituto di Chimica Generale ed Inorganica, University of Padova, 35100 Padova, Italy, Istituto di Chimica e Tecnologia dei Radioelementi del CNR, 35100 Padova, Italy, and Istituto di Chimica Generale ed Inorganica, University of Torino, Torino, Italy

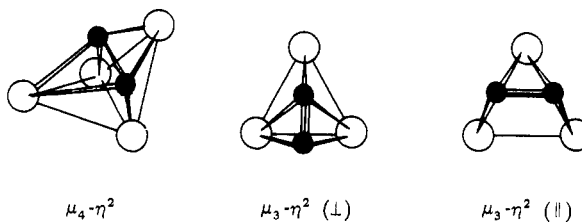
Received June 29, 1982

^{13}C NMR, UV-PES, and CNDO theoretical results of $\text{Fe}_3(\text{CO})_9(\mu_3\text{-}\eta^2\text{-EtC}_2\text{Et})$ are reported. ^{13}C alkyne resonances have very different chemical shifts according to the different coordination environments of the two acetylenic carbon atoms. Variable-temperature NMR experiments indicate localized exchange processes of the carbonyls at each $\text{Fe}(\text{CO})_3$ unit. The gas-phase UV-PE spectrum is assigned by comparison arguments with data on simpler related systems. The CNDO results contribute to the discussion of the PE data and provide interesting insights into the alkyne-cluster bonding mechanism. The relevant role of the cluster \rightarrow alkyne back-donation is stressed by both the experimental and theoretical data. The qualitative picture of the electronic structure proposed by Blount et al. receives strong support by the present theoretical data.

Introduction

The Dewar-Chart-Duncanson model,² originally developed to describe the bonding interaction in transition-metal olefin complexes, has been successfully extended to include the description of the σ - π bond in mononuclear alkyne complexes.³ This bonding scheme, however, is unable to account for the interaction of alkynes chemisorbed on transition-metal surfaces; actually the strong alkyne-surface binding rises from multicentered interactions, which imply significant rehybridization of the acetylenic carbons and formation of strong σ -carbon-metal bonds.⁴

The very rich chemistry of alkyne-cluster compounds⁵ provides a variety of structural arrangements, which can be envisaged as reasonable models for chemisorbed species on metallic surfaces.⁶ According to Muetterties et al.,^{6b} three basic bonding modes (namely, $\mu_4\text{-}\eta^2$, $\mu_3\text{-}\eta^2$ (\perp), and $\mu_3\text{-}\eta^2$ (\parallel) types) can account for the interaction between the



alkyne and a metallic cluster. It is generally accepted that in this class of molecules the interaction with three or four metal centers leads to an enhanced activation of the coordinated alkyne when compared with mono- and binuclear complexes. The bond order reduction can be compared with sufficient confidence to that occurring in chemisorption experiments on metallic surfaces. This cluster-surface analogy,⁶ then provides a novel methodological route to the study of surface phenomena by means of molecular spectroscopic techniques.

In an attempt to get a more detailed picture of the multicentered ligand-metal cluster interactions, we have already investigated⁷ compounds of type I, which, on the basis of the above considerations, represent good models for the dissociative chemisorption of monosubstituted alkynes (and acetylene itself) on metal surfaces by cleavage of the C-H bond.

We report here the results of a ^{13}C NMR, UV-PES, and theoretical (CNDO) study of the strictly related system $\text{Fe}_3(\text{CO})_9(\mu_3\text{-}\eta^2\text{-RC}_2\text{R})$ (II, R = C_2H_5), which can be envi-

(1) (a) University of Padova. (b) CNR of Padova. (c) University of Torino.

(2) (a) Dewar, M. J. S. *Bull. Soc. Chem. Fr.* 1951, 18, C71. (b) Chatt, J.; Duncanson, L. A. *J. Chem. Soc.* 1953, 2939.

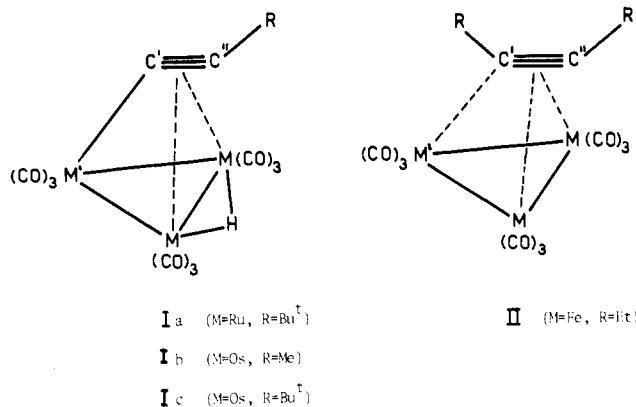
(3) For a recent detailed discussion see: Tatsumi, K.; Hoffmann, R.; Templeton, J. L. *Inorg. Chem.* 1982, 21, 466.

(4) For a general survey on this topic see: (a) Muetterties, E. L. *Angew. Chem., Int. Ed. Engl.* 1978, 17, 545. (b) Ozin, G. A.; McIntosh, D. F.; Power, W. J.; Messmer, R. P. *Inorg. Chem.* 1981, 20, 1782. (c) Geurts, P.; Van Der Avoird, A. *Surf. Sci.* 1981, 103, 431 and references cited therein.

(5) Johnson, B. F. G.; Lewis, J. *Adv. Inorg. Chem. Radiochem.* 1981, 24, 225.

(6) (a) Ugo, R. *Catal. Rev.* 1975, 11, 225. (b) Muetterties, E. L.; Rhodin, T. N.; Band, E.; Brucker, C. F.; Pretzer, W. R. *Chem. Rev.* 1979, 79, 91.

(7) (a) Granozzi, G.; Tondello, E.; Aime, S.; Osella, D. "EuChem Conference the Challenge of Polynuclear Inorganic Compounds", Venice, 28-30 September 1981, Commun. C9. (b) Granozzi, G.; Tondello, E.; Bertonecello, R.; Aime, S.; Osella, D. *Inorg. Chem.*, in press.



saged as a model for the chemisorption of a nonterminal alkyne involving partial C≡C bond activation. Compounds of type II are known for several disubstituted acetylenes,⁵ and an early X-ray structure determination has been reported by Blount et al.⁸ in 1966.

Experimental Section

Preparation. The title complex was obtained in 25% yield (with respect to the starting carbonyl) by refluxing in petroleum ether (bp 40–60 °C) $Fe_3(CO)_{12}$ with 3-hexyne in 1:1 mol. ratio for 4 h under a dry nitrogen atmosphere. The separation of the reaction mixture was carried out on TLC plates (Kieselgel P.F., eluent *n*-hexane). From the fast-moving dark brown band, II was recovered and crystallized from *n*-hexane at 0 °C. Spectral data: IR (*n*-hexane, $\nu(CO)$, cm^{-1}) 2078 (m), 2031 (vs), 2006 (s), 1994 (w), 1991 (w); ¹H NMR (CDCl₃) δ 3.60 (q, 2), 1.72 (t, 3), 1.63 (q, 2), 0.48 (t, 3); MS (at 70 eV), m/e 502 [M⁺], followed by stepwise loss of nine COs. Anal. Calcd for C₁₅H₁₀O₉Fe₃: C, 35.90; H, 2.01. Found: C, 35.41; H, 2.08. The preparation of a ¹³CO-enriched sample of II was performed by similar procedure using as starting material $Fe_3(CO)_{12}$ ~20% enriched in ¹³CO.

Spectroscopy. ¹³C NMR spectra were recorded on JEOL PS-100 spectrometer operating at 25.15 MHz in a FT mode. For the low-temperature spectra, a mixture of Freon 11 and CD₂Cl₂ was used as solvent with the addition of 0.05 M Cr(acac)₃ as an inert relaxation agent. The chemical shifts are reported downfield with respect to internal Me₄Si. He I excited PE spectra were measured on a Perkin-Elmer PS18 spectrometer using an heated inlet probe system in the 60–70 °C temperature range. The spectrometer was connected on-line with a Minc-23 computer (Digital Equip.) whose interface was built in our laboratory. Data acquisition was carried out by several sweeps (from 3 to 10) over 500 distinct channels. Typical sweep time amounts to 5–10 min. A least-squares approach⁹ was adopted in order to present the smoothed expanded portion of the spectrum. The ionization energy (IE) scale was calibrated by reference to peaks due to admixed inert gases (Xe, Ar) and to the 1s⁻¹ He ionization. The IEs reported in Figure 2 are the mean values over several distinct runs.

Calculations. Quantum mechanical calculations were performed by a version of the CNDO method¹⁰ suitable for transition-metal complexes. Fe semiempirical parameters were obtained¹⁰ from atomic spectroscopical data, whereas the C, O, and H parameters are Pople's standard ones.¹¹ The geometrical data used in the calculations refer to the X-ray structural determination⁸ of II, when R = C₆H₅, assuming a mirror plane through Fe', C', and C'' atoms (see figure above for atom labeling). The computed eigenvalues were related to the measured IEs assuming the validity of the Koopmans' theorem.¹² Gross atomic charges and overlap populations were obtained by Mulliken's population analysis¹³ of the deorthogonalized¹⁴ eigenvectors.

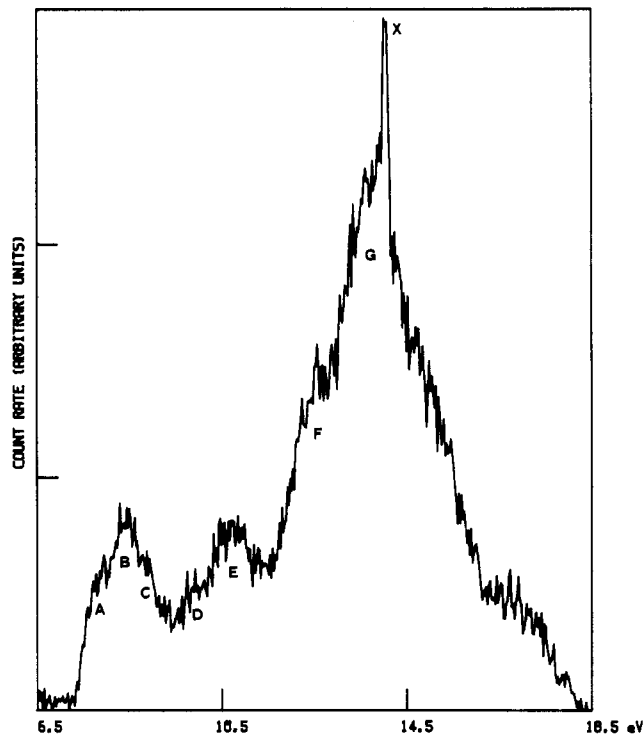


Figure 1. Full He I excited PE spectrum of the title molecule. Band due to small amount of free CO is labeled as X.

Results and Discussion

¹³C NMR Data. The ¹³C{¹H} NMR spectrum at 21 °C shows eight absorptions centered at 221.9, 212.2, 207.9, 106.8, 39.5, 21.8, 16.5, and 15.4 ppm. The four signals at higher field are easily assigned to two nonequivalent ethyl groups since, in the proton-coupled spectrum, they are split in two triplets and two quartets from low to high field, respectively. The resonances at 221.9 and 106.8 ppm are then assigned to the acetylenic carbons by comparison with the ¹³C NMR spectrum of the ¹³CO-enriched sample. The spread of the chemical shifts of the alkyne moiety indicates a marked difference in the coordination of the two acetylenic carbons. This behavior resembles that found in the $\mu_3-\eta^2(\perp)$ hydridoalkynyl derivatives I, with a further downfield shift of the resonance assigned to the C' atom. Experimental evidence in related systems¹⁵ suggests that such down field shift has to be related to the interaction with three metal atoms: it is likely that a major contribution to the observed shift is provided via a paramagnetic deshielding effect of the nonbonding electrons of the metal atoms.

At 21 °C, two CO resonances are observed at 212.2 and 207.9 ppm in the relative intensity ratio of 2:1. Two alternative exchange processes can account for the observed pattern in the carbonyl region: (a) localized exchange at the different Fe(CO)₃ units, (b) delocalized exchange of the radial COs in the plane of the Fe₃ triangle (a "merry-go-round" type process) with a static arrangement of the axial carbonyls. In order to get the equivalence of the axial carbonyls a coupled motion of the alkyne (pivoted on C') would be necessary. On going down to -100 °C the smaller peak starts to broaden, and, at -125 °C, it is split in two signals at 209.9 and 207.5 ppm. It follows that, at this temperature, the spectrum in the CO region consists of three absorptions in the relative intensity ratio of 6:1:2.

(8) Blount, J. F.; Dahl, L. F.; Hoogzand, C.; Hübel, W. *J. Am. Chem. Soc.* **1966**, *88*, 292.

(9) Proctor, A.; Sherwood, P. M. A. *Anal. Chem.* **1980**, *52*, 2315.

(10) Tondello, E. *Inorg. Chim. Acta* **1974**, *11*, L5.

(11) Pople, J. A.; Segal, G. A. *J. Chem. Phys.* **1966**, *44*, 3289.

(12) Koopmans, T. C. *Physica (Amsterdam)* **1933**, *1*, 104.

(13) Mulliken, R. S. *J. Chem. Phys.* **1955**, *23*, 1833.

(14) Löwdin, P. O. *J. Chem. Phys.* **1950**, *18*, 365.

(15) Aime, S.; Milone, L.; Valle, M. *Inorg. Chim. Acta* **1976**, *18*, 9.

Table I. CNDO Results for $\text{Fe}_3(\text{CO})_9(\mu_3\text{-}\eta^2\text{-HC}\equiv\text{C}'\text{H})^a$

MO	eigenvalue, eV	pop., %				2 H	9 CO	dominant character
		Fe		C'	C''			
		2 Fe	Fe'	C'	C''			
36a' HOMO	-5.35	66	5	2	2	23	} metal-metal bonding MOs with some mixture with π^* alkyne MOs	
26a''	-6.09	18	58	3	0	21		
35a'	-6.64	48	3	6	20	10		
34a'	-8.63	24	50	4	1	2		
25a''	-8.73	7	75	1	4	0	} 3d metallic based MOs mainly maintaining atomlike character (nonbonding)	
33a'	-8.91	52	28	2	1	1		
32a'	-9.03	5	81	0	1	0		
24a''	-9.16	85	2	0	0	0		
23a''	-9.33	86	1	0	0	0		
22a''	-9.44	78	1	0	5	0		
31a'	-9.65	72	5	6	1	3		
30a'	-10.45	61	11	8	4	4	} Fe_3 and Fe_3 -alkyne bonding MO (see text)	
29a'	-11.01	21	5	28	23	2		
21a''	-11.32	20	7	26	27	0	} π C \equiv C alkyne MOs donating charge to the cluster	
						20		

^a Reported up to 12 eV.

This result cannot discriminate between the localized exchange mechanism and the delocalized mechanism of radial COs involving a frozen pivot of the alkyne. However, we prefer the former hypothesis where the localized exchange has been frozen out only for the unique $\text{Fe}'(\text{CO})_3$ moiety. This observed exchange pathway shows some analogies with that found in the alkynyl complexes of type I,¹⁶ a closer similarity is actually found in the isostructural anion $[\text{Ru}_3(\text{CO})_9(\text{C}_2\text{-}t\text{-Bu})]^-$.¹⁷

UV-PES and Theoretical Data. The full (6.5–18.5 eV) He I excited PE spectrum of the title molecule is reported in Figure 1. The expanded scale spectrum of the lower IE region (6.8–11.3 eV) after a smoothing treatment is shown in Figure 2 together with the pertinent IEs. This latter spectral window is the most interesting one for discussing the bonding of the alkyne over the metallic triangle. It contains the ionizations from those valence MOs having predominant contributions from 3d metallic AOs and from alkyne outer orbitals. On the contrary, the higher IE region includes ionizations from levels primarily localized on the carbonyl groups (1π , 5σ , 4σ MOs) and from the σ framework of the organic portion of the cluster. In particular, band F (at 12.6 eV) probably is related to σ ionizations of the two C_2H_5 substituent groups. Since a further analysis of this region is neither easy nor productive, we shall confine ourselves to the discussion of the lower IE region.

A rational strategy for the analysis of the present results is to resort to literature data of simpler related systems; however, pertinent references are limited to the spectra of $\text{Fe}_3(\text{CO})_{12}$,¹⁸ $\text{Co}_2(\text{CO})_6(\text{RC}_2\text{R})$,¹⁹ and $\text{HM}_3(\text{CO})_9(\text{C}_2\text{R})$ ($M = \text{Ru}, \text{Os}$).⁷ On the basis of a direct comparison between the PE spectra of the isoelectronic $(\mu\text{-H})_3\text{Mn}_3(\text{CO})_{12}$ and $\text{Fe}_3(\text{CO})_{12}$ molecules, Wong et al.¹⁸ proposed a value of 7.8 eV for the IE of Fe–Fe bonds in the latter molecule. They also related the broad band spanning over ca. 2 eV (centered at about 9 eV) to the iron 3d lone pairs. Thus, we can qualitatively relate band A in our spectrum (7.95 eV)

(16) Aime, S.; Gambino, O.; Milone, L.; Sappa, E.; Rosenberg, E. *Inorg. Chim. Acta* **1975**, *15*, 53.

(17) Barner-Thorsen, C.; Hardcastle, K. I.; Rosenberg, E.; Siegel, J.; Manotti-Lanfredi, A. M.; Tiripicchio, A. *Inorg. Chem.* **1981**, *20*, 4306.

(18) Wong, K. S.; Dutta, T. K.; Fehlner, T. P. *J. Organomet. Chem.* **1981**, *215*, C48.

(19) (a) Van Dam, H.; Stufkens, D. J.; Oskam, A.; Doran, M.; Hillier, I. H. *J. Electron Spectrosc. Relat. Phenom.* **1980**, *21*, 47. (b) DeKock, R. L.; Lubben, T. V.; Hwang, J.; Fehlner, T. P. *Inorg. Chem.* **1981**, *20*, 1627.

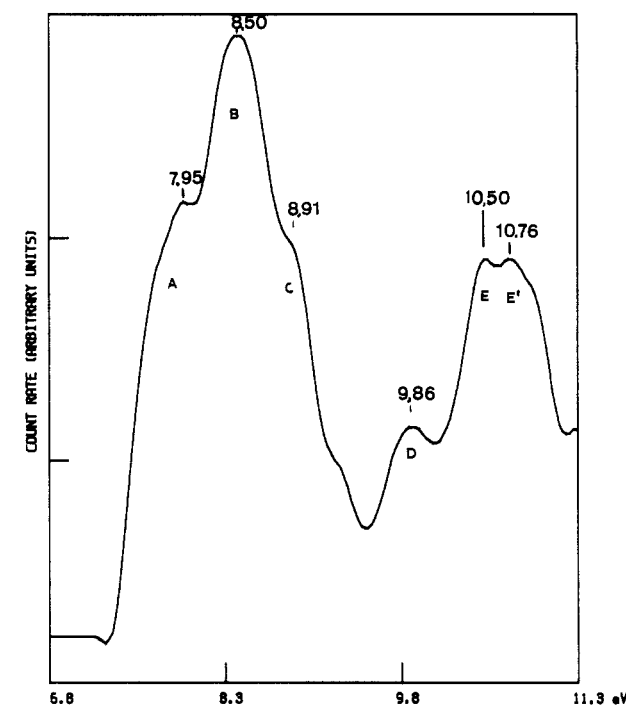


Figure 2. Expansion of the lower IE region of the PE spectrum of the title molecule. The spectral data were smoothed by using a total of 300 points.

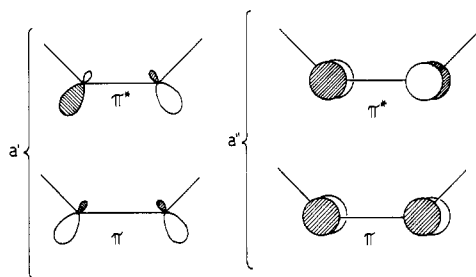
to MOs having Fe–Fe bonding character and bands B and C to lone-pair 3d MOs (Figure 2). On the other hand, reference to binuclear complexes containing alkynes^{19,20} limits the range of the ionizations related to the alkyne-based π MOs to the 10.3–11.3 eV interval, where we find the two bands labeled E and E' (Figure 2). The actual IE values of these two bands (10.50, 10.76 eV) are to be compared with that of the free 3-hexyne (9.70 eV);¹⁹ the shift toward higher IEs is the balance of various opposite contributions similar to those already discussed in a very detailed manner for the coordination of ethylene.²¹ This very subtle balance prevents any conclusion about the charge transfer within the cluster on the basis of the simple comparison between the IEs of the free and complexed

(20) Preliminary results on $(\mu\text{-RC}_2\text{R})[(\eta^5\text{-C}_5\text{H}_5)\text{Ni}]_2$ complexes indicate that alkyne π ionizations occur in the 10.7–11.3 eV range.

(21) Calabro, D. C.; Lichtenberger, D. L. *J. Am. Chem. Soc.* **1981**, *103*, 6846.

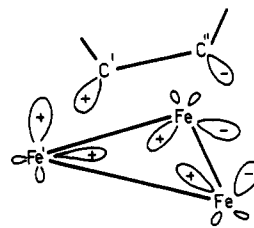
alkyne. Moreover, this qualitative analysis of the spectrum does not furnish any hypothesis on the nature of band D.

A more detailed discussion of the above spectral data and of the bonding mechanism can be obtained only on the basis of quantum mechanical considerations. EHT calculations on the title molecule have been recently reported;²² however, these results of invaluable importance for a pictorial view of the bonding scheme usually are not capable of a reasonable agreement with the PE data. Therefore, we prefer the approach based on the CNDO method, which recently revealed rather accurate in discussing the PE data of various cluster compounds.^{7,23} The EHT results²² will be used in order to extract simple considerations from the CNDO eigenvectors. The eigenvalues and the population analysis of the 14 outmost occupied MOs of $Fe_3(CO)_9(HC\equiv CH)$ are reported in Table I. The orbitals are labeled according to the irreducible representations (a' , a'') of the C_s point group; this low molecular symmetry, however, can discriminate between the involvement in each MO of the two alkyne valence sets depicted. On the basis of their energies and compositions,

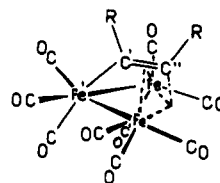


the 14 MOs can be grouped in three sets: three high-lying MOs ($36a'$, $26a''$, $35a'$), a nest of nine MOs (from $34a'$ to $30a'$), and two inner MOs close in energy ($29a'$, $21a''$). The three outmost MOs mainly represent the interaction between the frontier MOs of the $Fe_3(CO)_9$ fragment ($1e$, $1a_1$, $2a_1$, and $2e$ of ref 22) with π^* alkyne MOs. The $36a'$ HOMO and the subsequent $26a''$ MO are mainly to be related with the $1e$ Fe-Fe bonding MO of the $Fe_3(CO)_9$ fragment, so maintaining their metal-metal bonding character. The $35a'$ MO, on the contrary, has a very high contribution from C' and C'' alkyne atoms and mainly represents the bonding interaction between the a' π^* alkyne orbital (see figure above) and the out-of-plane a' components of the frontier MOs of the trimetallic fragment. An accurate inspection reveals also that the a' component of the $2e$ virtual MO of $Fe_3(CO)_9$ is involved in this MO. This bonding scheme is partially in contrast with the results of the EHT calculations,²² which predict involvement of both π^* and π alkyne MOs in the outer MOs, but in accordance with the structural evidence since it implies a significant back-bonding transfer to the a' π^* alkyne MO resulting in rehybridization and lengthening of the $C'-C''$ bond. These three high-lying MOs are probably to be related with the lowest IE band A of Figure 2. The subsequent nine MOs present high contributions from 3d metallic AOs; among them, however, the $30a'$ one is well distinct in energy and has important involvement of alkyne orbitals. We can tentatively relate bands B and C of Figure 2 to ionizations from the eight MOs from $34a'$ to $31a'$ (essentially 3d lone pairs) and the low intensity

band D to this $30a'$ MO. The schematic picture of this MO reported



reveals a very interesting feature: it shows a total metal-metal and metal-alkyne bonding character. The three iron atoms have lobes pointing in phase toward the center of the metallic triangle, in a fashion very reminiscent of the total symmetrical Walsh-like bonding mode already found in other metallic triangles.^{22,23a,b} Simultaneously, this MO is bonding with respect to the cluster-alkyne interaction through the a' π^* alkyne orbital: in particular, the C'' lobe points toward the Fe-Fe outer bonding area. This $30a'$ MO then provides an attractive picture of the bonding of the whole cluster (metal-metal bonding and cluster-alkyne back-bonding) and throws light to the approximate description suggested by Blount et al.⁸ on the basis of purely qualitative considerations on the experimental molecular parameters. Actually, they regarded



the alkyne as an olefinic coordinating group with two electrons on a sp^2 hybrid of C' pointing toward Fe' and the two remaining olefinic π electrons as interacting with the two Fe atoms via a μ -three-center bond. They also proposed that the sp^2 empty hybrid of C'' was used as part of a further three-center bond, similar to what found in the $30a'$ MO. The detection of a separate band D to be assigned to the ionization from this $30a'$ MO seems to us experimental evidence that stresses the importance of the back-bonding contribution to the alkyne-cluster bonding.

The two inner $29a'$ and $21a''$ MOs, which are to be related to E-E' bands, are mainly localized on the alkyne and are both $C'-C''$ bonding in character; they represent then the two a' - and a'' -type π $C\equiv C$ MOs mainly interacting with the two bridged iron atoms and assist the major portion of the alkyne-cluster charge transfer. The $29a'$ MO also contributes to a σ $Fe'-C'$ direct interaction.

The electronic density distribution and the interaction strengths can be conveniently discussed by means of the gross atomic charges and overlap populations reported in Figure 3; in the same figure the analogous parameters of the two separate $Fe_3(CO)_9$ and $HC\equiv CH$ fragments, each kept frozen as in the parent molecule, are also reported. In our opinion, this simple procedure can offer an aid to a better evaluation of the mutual bonding perturbations occurring in the formation of the alkyne-cluster bonding system. For instance, this procedure shows that the alkyne contribution is determinant to the equilibration of the atomic charges of the two different types of iron atoms by selective bonding-back-bonding interactions; in particular, it is clearly shown that the overall negative charge localized on the alkyne group mainly arises through back-donation from the two equivalent $Fe(CO)_3$ groups. These results are also consistent with the conclusions obtained by the analysis of the $35a'$ and $30a'$ MOs that outlined the rele-

(22) Schilling, B. E. R.; Hoffmann, R. *J. Am. Chem. Soc.* **1979**, *101*, 3456.

(23) (a) Ajò, D.; Granozzi, G.; Tondello, E.; Fragalà, I. *Inorg. Chim. Acta* **1979**, *37*, 191. (b) Granozzi, G.; Tondello, E.; Casarin, M.; Ajò, D. *Ibid.* **1981**, *48*, 73. (c) Granozzi, G.; Tondello, E.; Ajò, D.; Faraone, F. *J. Organomet. Chem.* **1982**, *240*, 191.

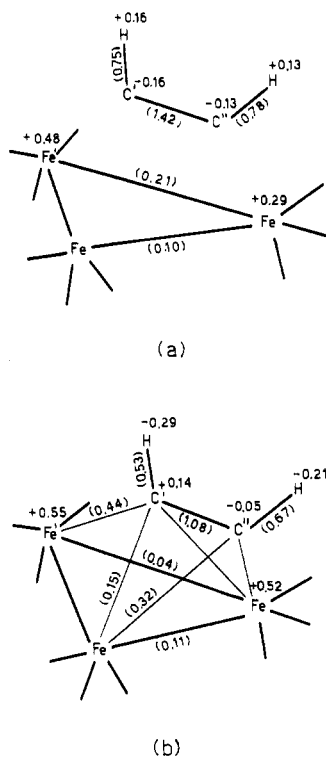


Figure 3. CNDO gross atomic charges and bond overlap populations of (a) $\text{HC}\equiv\text{CH} + \text{Fe}_3(\text{CO})_9$ and (b) the entire molecule.

Table II. Alkyne-Cluster Overlap Populations Divided in the Two a' and a'' Sets (in Electrons)

couple of atoms	contribution		total
	a'	a''	
Fe-C'	0.07	0.08	0.15
Fe'-C'	0.39	0.05	0.44
Fe-C''	0.19	0.13	0.32
Fe'-C''	-0.06	0.00	-0.06

vance of the back-bonding contributions to the overall bonding scheme. Note also the positively charged C' atom that reflects strong charge donation to Fe' ; this is also clearly seen from the overlap population analysis: despite the very similar $\text{Fe}'\text{-C}'$ and $\text{Fe-C}'$ bond distances,⁸ there are marked differences in their population values that indicate preferential $\text{Fe}'\text{-C}'$ bonding. It is also quite instructive to divide the alkyne-cluster total overlap populations in two portions related to a' - and a'' -type MOs, respectively (see Table II): almost only the a' set contributes to the $\text{Fe}'\text{-C}'$ interaction. On the contrary, both a' and a'' sets contribute in a similar extent to the remaining interactions. These data are in complete agreement with the already mentioned bonding picture of Blount et al.⁸ and points to a very similar description of the alkyne-cluster interaction in the present molecule and in structures of type I.⁷

Final considerations concern the metal-metal overlap populations: from Figure 3 it is clearly seen that the two $\text{Fe}'\text{-Fe}$ bonds decrease their overlap populations on going

from $\text{Fe}_3(\text{CO})_9$ to the organometallic cluster. This is certainly in relation with the aforementioned involvement of the symmetric part of the 2e metal-metal antibonding MO^{24} in the 35a' MO. As a result, the Fe-Fe bond carries a larger overlap population; however, the three-centered Fe-Fe bond assisted by the empty C'' sp^2 hybrid proposed by Blount et al.⁸ could be responsible for this higher overlap population.²⁵ This result gives a description of the Fe-Fe bond that conforms to the existence of some degree of unsaturation on it, in accordance with the application of the empirical EAN rule that gives a 46-electron formulation for this molecule.

Concluding Remarks

Summarizing the above results, the following conclusions can be drawn.

(i) The qualitative bonding picture derived by Blount et al.⁸ is confirmed in this study. In addition, similarities have been found between the electronic structures of I and II.

(ii) The relevant role of the back-donation in the alkyne-cluster interaction is stressed by both the experimental and the theoretical data, in good agreement with the studies on other alkyne complexes recently reported.^{26,27}

(iii) In view of the theoretical results implying the involvement of metal-metal antibonding MOs in the alkyne-cluster bonding, the observed shortening of the $\text{Fe}'\text{-Fe}$ bond distances on going from $\text{Fe}_3(\text{CO})_{12}$ (2.67 Å) to II (2.49 Å) is unexpected; we think that a possible rationalization of this feature can be based on the contraction of the metallic triangle in order to accommodate the small alkyne group. This fact could be of general importance in metal cluster chemistry, and it has to be related to the flat energy minima associated with metal-metal potential curves.

(iiii) On the basis of the EAN formalism, II has been described as a 46-electron, coordinatively unsaturated molecule: we suggest that this unsaturation could be associated to the larger population found in the unique Fe-Fe bond. Further chemical evidence is clearly needed to assess this proposal.

Acknowledgment. We thank the Consiglio Nazionale delle Ricerche (C.N.R. Rome) for generous financial support to this study.

Registry No. $\text{Fe}_3(\text{CO})_9(\mu_3\text{-}\eta^2\text{-HC}\equiv\text{C}'\text{H})$, 83802-15-7.

(24) It is worthwhile to remind that the a' component of the 2e virtual orbital of $\text{Fe}_3(\text{CO})_9$ has $\text{Fe}'\text{-Fe}$ antibonding and Fe-Fe bonding character.²²

(25) The trend of the metal-metal overlap populations is even more surprising when compared to the metal-metal distances ($\text{Fe}'\text{-Fe} = 2.48$ Å; $\text{Fe-Fe} = 2.59$ Å). These facts would confirm the suggestion that is appearing in the literature which states that there is not a strict relationship between bond distances and bond orders in metal-metal bonds. In this respect see discussion on ref 5.

(26) (a) DeKock, R. L.; Fehlner, T. P.; Housecroft, C. E.; Lubben, T. V.; Wade, K. *Inorg. Chem.* **1982**, *21*, 25. (b) Deshmukh, P.; Dutta, T. K.; Hwang, J. L.-S.; Housecroft, C. E.; Fehlner, T. P. *J. Am. Chem. Soc.* **1982**, *104*, 1740.

(27) Granozzi, G.; Bertocello, R.; Ajò, D.; Osella, D.; Aime, S. *J. Organomet. Chem.*, in press.

Polyhedral Skeletal Electron Pair Theory—Its Extension to Nonconical Fragments

David G. Evans and D. Michael P. Mingos*

Inorganic Chemistry Laboratory, University of Oxford, Oxford OX1 3QR, Great Britain

Received August 25, 1982

Molecular orbital calculations supplemented by symmetry and perturbation theory arguments have been utilized to evaluate the effect of introducing C_{2v} , $M(CO)_4$ fragments into metal polyhedral cluster compounds derived from conical $M(CO)_3$ fragments. Electron-counting rules for predicting the geometries of these lower symmetry species are provided, and site preferences and conformational consequences of the bonding model are developed.

Although we remain a long way from understanding the electronic structures of transition-metal cluster compounds in sufficient detail to be able to reliably predict their occurrence and electronic and chemical properties, the last 10 years has seen the development of simplified bonding schemes derived primarily from symmetry arguments and semiempirical molecular orbital calculations, which have provided a conceptual framework for rationalizing (and indeed at times even predicting) the gross geometrical features of such compounds.¹ The complex of ideas, which has been collectively described as the *polyhedral skeletal electron pair theory*,² has proved to be particularly effective for rationalizing the structures of a wide range of cluster compounds involving transition-metal carbonyl and cyclopentadienyl components, metallocarboranes, and metallohydrocarbons, and is particularly successful when applied to structures in which conical fragments such as $M(CO)_3$ or $M(\eta-C_5H_5)$ occupy the vertices of the polyhedron.³

This success can be attributed to the *isolobal* connection^{4,5} between such fragments and main-group fragments such as B-H and C-H. However, at its most fundamental level the success of the *polyhedral skeletal electron pair approach* can be traced to the fact that the total electron count in a cluster, be it derived from main-group or metal carbonyl fragments, is decided primarily by the number of antibonding skeletal molecular orbitals derived from the s and p orbitals of the vertex atoms. These antibonding molecular orbitals are unavailable for either metal-ligand or skeletal bonding by virtue of their high-lying nature and

their inward hybridization and therefore set an upper limit on the total electron count for a particular polyhedral arrangement.⁶ For example, if a particular geometric arrangement of vertex atoms leads to the formation of $2n$ such orbitals, where n is the number of vertex atoms, then the total electron count in a main-group cluster will be $2(4n - 2n) = 4n$ electrons and will be $2(9n - 2n) = 14n$ electrons for a transition-metal carbonyl cluster compound. The difference in electron count merely reflects the presence of the additional five d orbitals in the latter case. Table I summarizes the consequences of this simple principle for several important classes of metal and main-group polyhedral molecules, e.g., closo-triangulated polyhedra, electron precise polyhedra, and, for completeness sake, some inorganic ring and nonbonded aggregates.⁷ Some illustrative examples are also given in this table, but a more extensive discussion of the applications of this methodology are to be found in ref 1.

Although this generalized principle works surprisingly well for polyhedral molecules which have the *isolobal* fragments $M(CO)_3$, $M(\eta-C_5H_5)$, B-H, or C-H at the vertices, it is less successfully applied to cluster compounds derived from C_{2v} , $M(CO)_4$ and $M(CO)_2$ fragments (or related fragments such as $Pt(PR)_3$). The problems which are encountered with such fragments may be illustrated by the following examples from osmium and platinum cluster chemistry. In the first example $Os_5(CO)_{15}C^8$ (1) the total electron count is 74 and the observed square-pyramidal structure is consistent with the $(14n + 4)$ electron count predicted by the *polyhedral skeletal electron pair approach* for a nido octahedron (see Table I). The second example **2**⁹ has the same total electron count but the introduction of an $Os(CO)_4$ fragment has resulted in the observed edge-bridged tetrahedral structure. The platinum compound **3** derived from PtL_2 fragments has the same skeletal geometry as **2** but a total of only 70 valence electrons.¹⁰

These differences can be interpreted in terms of the frontier molecular orbitals of the $Os(CO)_3$, $Os(CO)_4$, and $Os(CO)_2$ fragments illustrated in Figure 1. The derivation of these frontier molecular orbitals and their usefulness in interpreting the stereochemical and chemical properties

(1) For recent reviews see: K. Wade, "Transition Metal Clusters", B. F. G. Johnson, Ed., Wiley-Interscience, Chichester, 1980. R. E. Benfield and B. F. G. Johnson, *Top. Stereochem.* **12**, 253 (1981); W. C. Troglor and M. C. Manning, *Coord. Chem. Rev.*, **38**, 89 (1981). D.M.P. Mingos In "Comprehensive Organometallic Chemistry", F. G. A. Stone and G. Wilkinson, Eds.; Pergamon Press, Oxford, 1982.

(2) The term *polyhedral skeletal electron pair theory* was first introduced in R. Mason, K. M. Thomas, and D. M. P. Mingos, *J. Am. Chem. Soc.*, **95**, 3802 (1973), but the basic concepts were developed in R. E. Williams, *Inorg. Chem.*, **10**, 210 (1971); K. Wade, *J. Chem. Soc., Chem. Commun.*, 792 (1971); *Inorg. Nucl. Chem. Lett.* **8**, 559, 563 (1972); D. M. P. Mingos, *Nature (London), Phys. Sci.*, **236**, 99 (1972); R. Mason and D. M. P. Mingos, *MTP Int. Rev. Sci.: Phys. Chem., Ser. Two*, **11**, 121 (1975).

(3) A recent breakdown of this approach for MCP fragments has been discussed in D. N. Cox, D. M. P. Mingos, and R. Hoffmann, *J. Chem. Soc., Dalton Trans.*, 1788 (1981); and K. Wade and M. O'Neill, *Inorg. Chem.*, **21**, 461 (1982).

(4) The term *isolobal* was first introduced by M. Elian, M. M. L. Chen, D. M. P. Mingos, and R. Hoffmann, *Inorg. Chem.*, **15**, 1148 (1976), but some of its origins can be traced to J. Halpern, *Discuss. Faraday Soc.*, **46**, 7 (1968); J. E. Ellis, *J. Chem. Educ.*, **53**, 2 (1976) and references given under 2.

(5) Recent papers dealing with the *isolobal* principle include R. Hoffmann, Nobel Lecture, 1981; *Science (Washington, DC)*, **211**, 995 (1981); F. G. A. Stone, *Acc. Chem. Res.*, **14**, 318 (1981); D. M. P. Mingos, *Trans. Amer. Crystallogr. Assoc.*, **16**, 17 (1980); T. A. Albright, *ibid.*, **16**, 35 (1980).

(6) D. M. P. Mingos, *J. Chem. Soc., Dalton Trans.*, 133 (1974); J. W. Lauher, *J. Am. Chem. Soc.*, **100**, 5305 (1978); A. J. Stone, *Inorg. Chem.*, **20**, 563 (1981); G. Ciani and A. Sironi, *J. Organomet. Chem.*, **197**, 223 (1980).

(7) See, for example: P. R. Raithby in "Transition Metal Clusters", B. F. G. Johnson, Ed., Wiley-Interscience, Chichester, 1980, for a recent review of the structures of transition-metal clusters.

(8) C. R. Eady, B. F. G. Johnson, J. Lewis, and T. Matheson, *J. Organomet. Chem.*, **57**, C82 (1973).

(9) C. R. Eady, B. F. G. Johnson, and J. Lewis, *J. Organomet. Chem.*, **57**, C84 (1973).

(10) J.-P. Barbier, R. Bender, P. Braunstein, J. Fischer, and L. Ricard, *J. Chem. Res., Synop.*, 230 (1978).

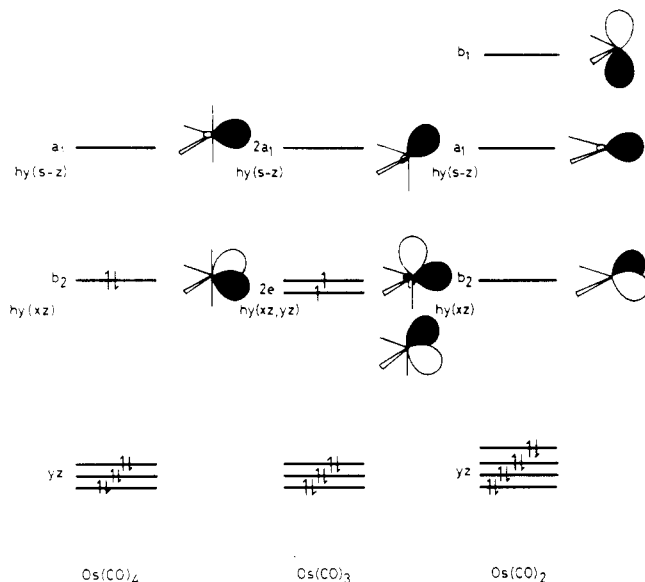
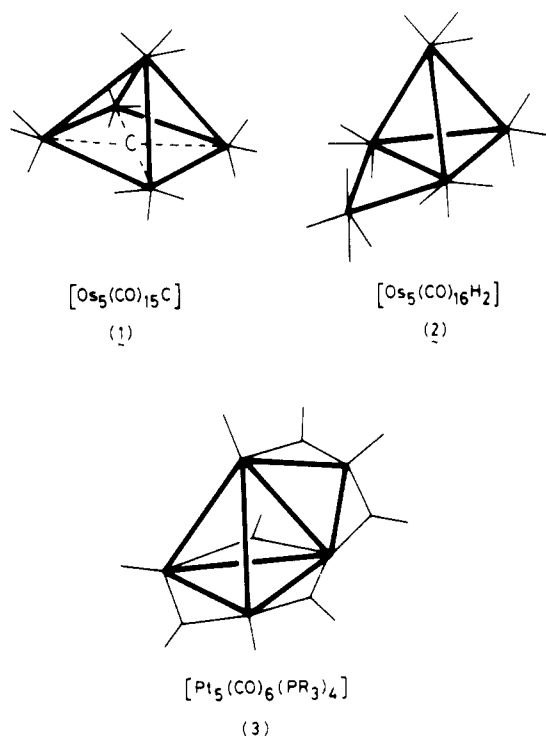
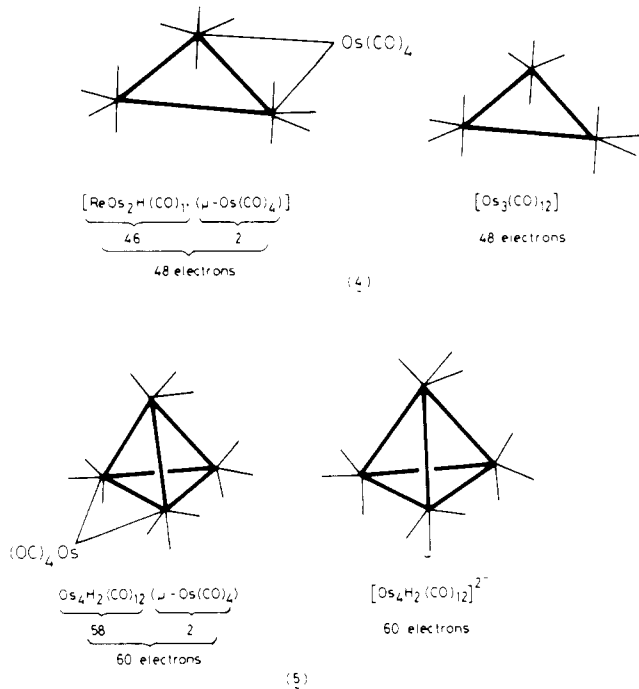


Figure 1. A comparison of the frontier molecular orbitals of $\text{Os}(\text{CO})_4$, $\text{Os}(\text{CO})_3$, and $\text{Os}(\text{CO})_2$ fragments.

ligand. The following examples illustrate the usefulness of this relationship.^{7,12} This approach is less readily ap-

of these fragments have been discussed in considerable detail elsewhere, particularly by Hoffmann and his co-workers and ourselves¹¹ and therefore only those features which are germane to the current analysis will be discussed in the following section. The *isolobal* connection between $\text{M}(\text{CO})_3$ and B-H fragments has its origins in the $2e(\text{hy}(xz, yz))$ and $2a_1(\text{hy}(s-z))$ out-pointing hybrid orbitals of the conical fragment, which bear a resemblance to the frontier orbitals of either B-H or C-H (see Figure 1).¹¹ The addition or removal of a carbonyl ligand from $\text{M}(\text{CO})_3$ leads to a loss in the correspondence between these fragments and B-H, since the lower symmetry fragments have only a single $\text{hy}(xz)$ orbital in addition to the higher lying $a_1(\text{hy}(s-z))$ orbital. The lost $\text{hy}(yz)$ component can be traced in each case (see Figure 1) to the lower set of orbitals which are generally considered to be nonbonding as far as cluster bonding is concerned.^{6,11} Since the $\text{hy}(xz)$ and $\text{hy}(s-z)$ orbitals resemble the a_1 and b_2 orbitals of the methylene singlet state, the $\text{Os}(\text{CO})_4$ and $\text{Pt}(\text{CO})_2$ fragments have been described as *isolobal* with CH_2 . The wide ramifications of this analogy⁴ have been explored in Hoffmann's Nobel prize lecture.⁵

Since this paper is in large measure concerned with the total electron count in cluster compounds derived from such fragments, it is necessary to note that for $\text{Os}(\text{CO})_4$, $\text{Os}(\text{CO})_3$, and $\text{Os}(\text{CO})_2$ fragments the total electron count is 16, 14, and 12, respectively. Therefore although $\text{Os}(\text{CO})_4$ is *isolobal* and *pseudoisoelectronic* with CH_2 , the corresponding $\text{M}(\text{CO})_2$ fragment is $\text{Os}(\text{CO})_2^{2-}$ or $\text{Pt}(\text{CO})_2$ with two electrons fewer. Consequently replacement of $\text{Os}(\text{CO})_4$ by $\text{Pt}(\text{CO})_2$ leads to a decrease in total electron count of 2. The *isolobal* connection can provide a useful way of resolving some of the bonding problems associated with the introduction of $\text{Os}(\text{CO})_4$ fragments into the cluster since this moiety can be partitioned from the cluster and treated by analogy with CH_2 as a two-electron-bridging



plied to polyhedral cluster compounds which have $\text{M}(\text{CO})_4$ fragments at a vertex, e.g., $\text{Os}_5(\text{CO})_{16}$ or $\text{Ru}_4\text{H}_2(\text{CO})_{13}$ (6).^{13,14} Therefore this paper attempts to interpret the geometric features of cluster compounds containing $\text{M}(\text{CO})_4$ fragments by considering in more detail the frontier molecular orbitals of such fragments.

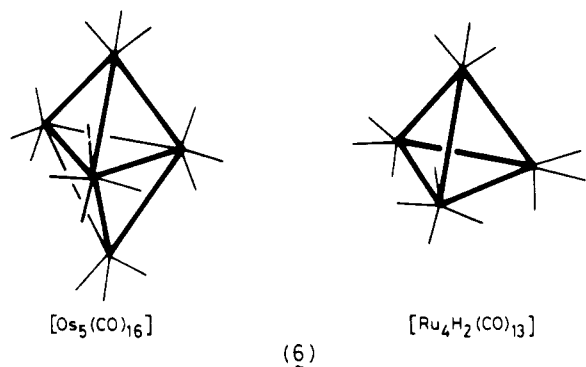
Bonding Capabilities of the $\text{M}(\text{CO})_4$ Fragment. Although the $\text{M}(\text{CO})_4$ and $\text{M}(\text{CO})_2$ fragments may be classified as being *isolobal* with CH_2 , a more careful examination of the frontier molecular orbitals of these fragments which are illustrated in Figure 2 suggests that

(11) T. A. Albright, R. Hoffmann, J. C. Thibault, and D. L. Thorn, *J. Am. Chem. Soc.*, **101**, 3801 (1979); D. M. P. Mingos, *J. Chem. Soc., Dalton Trans.*, 610 (1977); M. I. Forsyth, D. M. P. Mingos and A. J. Welch, *ibid.*, 1674 (1980); D. M. P. Mingos and C. R. Nurse, *J. Organomet. Chem.*, **184**, 281 (1980); R. Pinhas, T. A. Albright, P. Hofmann, and R. Hoffmann, *Helv. Chim. Acta*, **63**, 29 (1980).

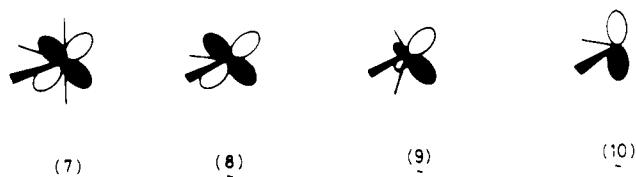
(12) J. Lewis and B. F. G. Johnson, *Adv. Inorg. Chem. Radiochem.*, **24**, 255 (1981) and references therein.

(13) P. F. Jackson, B. F. G. Johnson, J. Lewis, M. McPartlin, and W. J. Nelson, *J. Chem. Soc., Chem. Commun.*, 920 (1978); D. B. W. Yawney and R. J. Doedens, *Inorg. Chem.*, **11**, 838 (1972).

(14) C. R. Eady, B. F. G. Johnson, J. Lewis, B. E. Reichert, and G. M. Sheldrick, *J. Chem. Soc., Chem. Commun.*, 271 (1976).

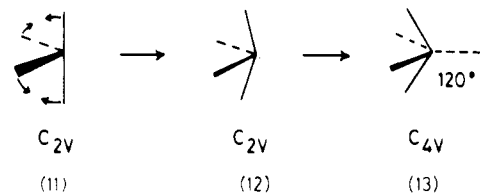


this analogy must be used with caution since both fragments have within their d manifold the yz orbitals 7 and 8. These orbitals correlate with the hybrid $hy(yz)$ orbital

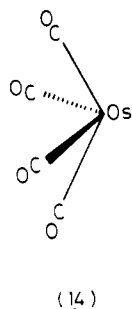


of the $M(CO)_3$ fragment (9). The orbitals 7 and 8 do not contribute as effectively as 9 to metal-metal bonding because of their lower energies and unhybridized character, but their presence cannot be totally ignored as the simple application of the *isolobal* analogy would suggest. The problem is compounded for the $M(CO)_2$ fragment by the occurrence of the p_y orbital 10 which has the same symmetry characteristics as 9 and can, if the metal d-p promotion energy is small, make a significant contribution to skeletal bonding. A more complete comparison of the bonding capabilities of $M(CO)_4$ and $M(CO)_2$ fragments is given in a subsequent paper.¹⁵

The ambiguity in classifying the $Os(CO)_4$ fragment becomes more pronounced when the distortional mode illustrated in 11-13 is considered. If the equatorial OC-



Os-CO angle is opened out from its initial value of 105° as the axial OC-Os-CO angle is reduced, then the axially symmetric $Os(CO)_4$ fragment illustrated in 14 is generated.¹⁶ The distortional mode represented in 11 has the



effect of stabilizing $hy(xz)$ and destabilizing yz (see Figure 2). In the C_{4v} limit, these orbitals represent degenerate components of the d-p hybrid orbitals $e(hy(xz,yz))$. A C_{4v}

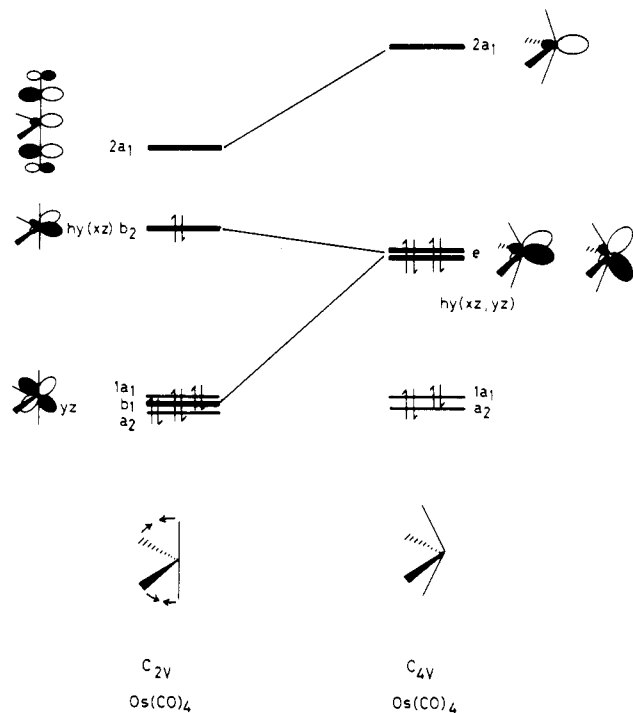
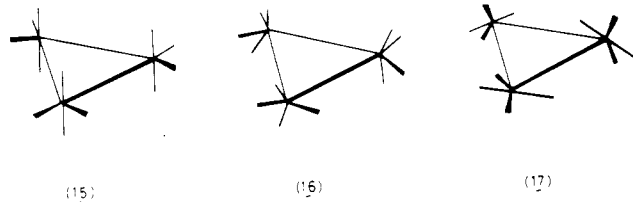


Figure 2. Schematic illustration of the effect on the frontier molecular orbitals of the $C_{2v} \rightarrow C_{4v}$ distortion of an $Os(CO)_4$ fragment. In the C_{2v} geometry the equatorial C-Os-C angle is 105° and in the C_{4v} geometry the ligands make an angle of 120° with respect to the C_4 axis. Particularly noteworthy is the large destabilization of the b_1 component, derived from yz .

fragment with the frontier orbitals illustrated in Figure 2 is more correctly described as being *isolobal* with either CH^- or BH^{2-} . Therefore, the precise designation of the *isolobal* nature of the $M(CO)_4$ fragment is sensitive to the gradient of the potential energy surface connecting 11 and 14 and the magnitude in the difference in the bonding abilities of the $hy(xz)$ and yz orbitals in 11. The latter will depend on the orbital characteristics of the cluster moiety to which $Os(CO)_4$ is bonded. The extended Hückel calculations, which are described in the Appendix, suggest an energy difference separating 11 and 14 of 2.6 eV. The greater stability of the C_{2v} fragment can be related to the fact that the destabilization of yz (see Figure 2) far outweighs the stabilization associated with $hy(xz)$.

From the analysis provided above it is clear that the bonding capabilities of the $Os(CO)_4$ fragment will be influenced primarily by the $hy(xz)$ and $hy(s-z)$ orbitals in Figure 1. These interactions are likely to be maximized for coplanar arrangements of osmium atoms, and therefore it is such molecules that will be considered initially.

Two-Dimensional Cluster Compounds. The simplest two-dimensional cluster species is the triangle, and therefore this analysis begins with a consideration of the alternative $Os_3(CO)_{12}$ geometries illustrated in 15, 16, and 17. Both 15 and 17 are based on C_{2v} fragments (although in the latter cluster this results in substantial steric crowding). Furthermore, they may both be derived from 16, which is based on conical $Os(CO)_4$ fragments, by appropriate distortions of the OC-Os-CO bond angles. With



(15) D. G. Evans and D. M. P. Mingos, to be submitted for publication.
 (16) M. Eliañ and R. Hoffmann, *Inorg. Chem.*, **14**, 1058 (1975); J. K. Burdett, *J. Chem. Soc., Faraday Trans. 2*, **70**, 1599 (1974).

Table I. Summary of the Total Number of Valence Electrons for Polyhedral Molecules and Ring Compounds^a

	main-group hydrides	examples	transition-metal carbonyls	examples
isolated atoms held together by bridging groups	$8n$		$18n$	$\text{Cu}_4\text{X}_4(\text{AsR}_3)_4$
ring compds	$6n$ ($n \geq 3$)	P_4Ph_4 , S_8	$16n$ ($n \geq 3$)	$\text{Os}_3(\text{CO})_{12}$
electron precise polyhedra ^b	$5n$ (n even ≥ 4)	cubane, P_4	$15n$ (n even ≥ 4)	$\text{Ir}_4(\text{CO})_{12}$
arachno polyhedra (deltahedra) ^c	$4n + 6$ ($n \geq 4$)	B_nH_{n+6}	$14n + 6$	
nido polyhedra (deltahedra)	$4n + 4$ ($n \geq 4$)	B_nH_{n+4}	$14n + 4$	$\text{Os}_6\text{C}(\text{CO})_{15}$
closo polyhedra (deltahedra)	$4n + 2$ ($n \geq 5$)	$\text{B}_n\text{H}_n^{2-}$	$14n + 2$	$\text{Os}_5(\text{CO})_{15}^{2-}$
capped polyhedra (deltahedra) with m capping groups	$4n + 2 + 2m$ ($n \geq 5$)	no examples	$14n + 2 + 2m$	$\text{Os}_6(\text{CO})_{18}$

^a The total number of valence electrons is expressed in terms of the number of polyhedral atoms n . ^b Electron precise polyhedra have three edges radiating from each vertex. ^c Deltahedra have triangular faces exclusively.

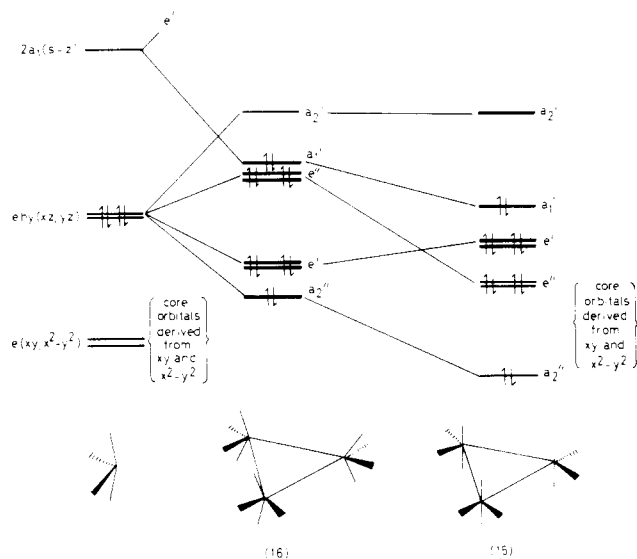
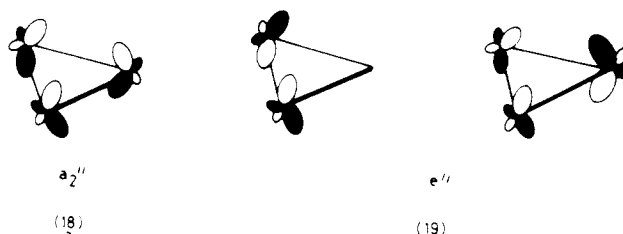


Figure 3. Comparison of the bonding molecular orbitals for $\text{Os}_3(\text{CO})_{12}$ derived from C_{4v} fragments (16) and C_{2v} $\text{Os}(\text{CO})_4$ fragments (15).

use of Stone's notation⁶ and mode of analysis the skeletal bonding molecular orbitals derived from the $2a_1$ and e -($hy(xz,yz)$) frontier orbitals of the conical $\text{M}(\text{CO})_4$ fragment illustrated in Figure 2 may be represented as radial and π -surface molecular orbitals. For 16 the radial bonding molecular orbitals derived from the a_1 orbitals are represented by a bonding a_1' and a pair of antibonding e' orbitals. The π -surface molecular orbitals derived from e -($hy(xz,yz)$) give rise to the bonding e' and a_2'' molecular orbitals and the antibonding e'' and a_2' orbitals as shown in Figure 3. For a 48-electron cluster such as $\text{Os}_3(\text{CO})_{12}$ the orbital populations are $(a_2'')^2(e')^4(e'')^4(a_1')^2$ corresponding to a net Os-Os bond order of 1 since the out of plane π interactions are cancelled out by the simultaneous electron occupation of a_2'' and e'' .

Within the framework of first-order perturbation theory the conversion of a C_{4v} $\text{M}(\text{CO})_4$ fragment into one of C_{2v} symmetry may be represented by a substantial decrease in the Coulomb integral for the yz component of the e set (i.e., it becomes more negative) and a decrease in the resonance integrals between yz orbitals on adjacent osmium atoms.¹⁷ These effects can readily be assimilated into the interaction diagram shown in Figure 3. For the conformation shown in 15 the $hy(yz)$ components of the e sets of the individual $\text{Os}(\text{CO})_4$ fragments lie perpendicular to the Os_3 plane, and therefore it is the a_2'' and e''

molecular orbitals illustrated in 18 and 19 which experience the first-order perturbation theory stabilization described above. In the final C_{2v} local geometry of $\text{Os}(\text{CO})_4$ the a_2''



and e'' orbitals approximate to being nonbonding. The cluster metal-metal bonding is therefore dominated by the e' and a_1' levels shown in Figure 3. Previously we have reported photoelectron spectral results¹⁸ which have demonstrated that the bonding picture illustrated in Figure 3 is essentially valid. Since the stabilization energy associated with e'' and a_2'' when taken with that associated with a_1' ($hy(s-z)$) greatly exceeds the destabilization of e' , derived from $hy(xz)$ (see Figure 3), the structure 15 based on C_{2v} fragments is considerably more stable (the extended Hückel calculations suggest an energy different of 9.3 eV separating 15 and 16). The magnitude of this energy separation makes it most unlikely that on the NMR time scale the carbonyls in $\text{Os}_3(\text{CO})_{12}$ could become equivalent on the basis of pseudorotation processes involving C_{4v} fragments at the vertices of the triangle. Recent NMR evidence appears to support this point of view.²⁰

For the alternative conformer 17 it is the e' and a_2' levels which are stabilized by the first-order perturbation theory effects which accompany the C_{4v} to C_{2v} transformation, and the resultant skeletal molecular orbitals correspond to a_2'' and a_1' ($hy(s-z)$), which are bonding, and e'' , which is antibonding (compare with Figure 3). It follows that for this alternative geometry the preferred electron count is 46, corresponding to the cationic species $\text{Os}_3(\text{CO})_{12}^{2+}$. The formal bond order in such a complex is 0.67, and the exclusive π nature of the interactions involved in a_2'' leads to smaller interatomic overlaps than those in the e' bonding orbitals of 15, which have a σ and π component. The calculations which we have completed suggest that the steric and electronic effects associated with 17 are most

(18) J. C. Green, E. A. Seddon, and D. M. P. Mingos, *J. Chem. Soc., Chem. Commun.*, 941 (1979); *Inorg. Chem.*, **20**, 2595 (1981).

(19) M. Elian and R. Hoffmann, *J. Am. Chem. Soc.*, **101**, 3456; (1979); D. V. Korolkov and H. Meissner, *Z. Phys. Chem. (Leipzig)*, **253**, 25 (1973); D. Ajo, G. Granozzi, E. Tondello, and I. Fragala, *Inorg. Chim. Acta*, **37**, 191 (1979); D. R. Tyler, R. A. Levenson, and H. B. Gray, *J. Am. Chem. Soc.*, **100**, 7888 (1978); M. C. Manning and W. C. Troglor, *Coord. Chem. Rev.*, **38**, 89 (1981).

(20) A. A. Koridze, O. A. Kizas, N. M. Astakhova, P. V. Petrovskii, and Y. Grishin, *J. Chem. Soc., Chem. Commun.*, 853 (1981).

(17) E. Heilbronner and H. Bock, "Das HMO Modell und seine Anwendung", Verlag Chemie, Weinheim, 1968.

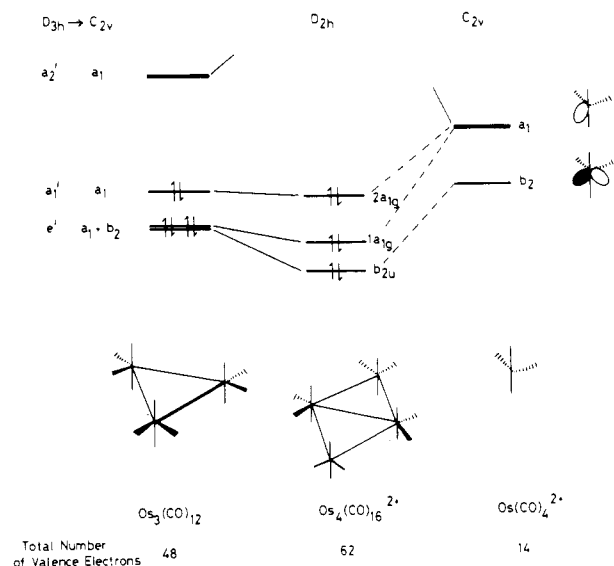
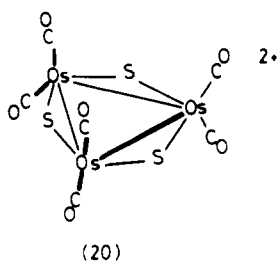
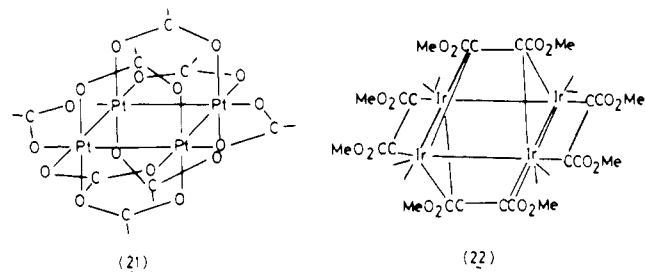


Figure 4. Schematic illustration of the effect of edge bridging an $\text{Os}_3(\text{CO})_{12}$ triangle with an $\text{Os}(\text{CO})_4^{2+}$ fragment. The number of metal-metal bonding molecular orbitals is unchanged by this process.

unfavorable and could only be avoided in a complex such as **20** where the axial ligands function as bridging groups.

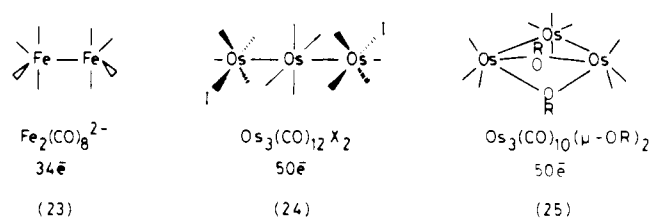


From the arguments developed above it is clear that the C_{2v} fragment has the correct bonding characteristics for forming planar ring systems, which utilize its $hy(xz)$ and $hy(s-z)$ orbitals to maximum advantage. This conclusion can readily be generalized to other ring compounds of the general type $[\text{M}(\text{CO})_4]_n$ analogous to the cycloalkanes $(\text{CH}_2)_n$. Such molecules have by analogy with $\text{Os}_3(\text{CO})_{12}$ a total of $16n$ valence electrons. Examples of 64-electron planar four metal atom ring compounds based on ML_4 fragments are provided by the compounds illustrated in **21** and **22**.^{21,22} To date no examples of larger ring cluster compounds have been reported. It also follows from this

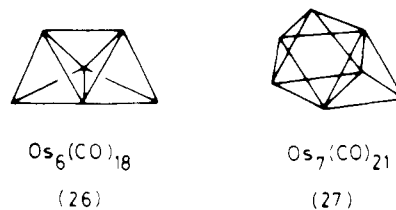


simple analysis that chain cluster compounds will be characterized by a total of $16n + 2$ valence electrons, since the presence of an additional electron pair in such com-

pounds leads to the rupture of one metal-metal bond. Some examples of such complexes are illustrated in **23-25**.

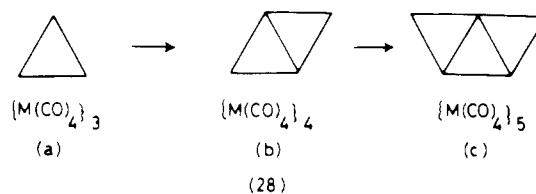


Some years ago we proposed a *capping principle* within the context of the *polyhedral skeletal electron pair theory*,²³ which has had a substantial impact on rationalizing the geometries of capped clusters of the transition metals such as **26** and **27**. This principle states that when one



or more faces of a polyhedral molecule are capped by an $\text{M}(\text{CO})_3$ (or *isolobal* fragment), if all the frontier orbitals of the capping fragment match those of the bonding skeletal molecular orbitals of the parent polyhedron, then the total number of bonding skeletal molecular orbitals remains constant. For example, $\text{Os}_4(\text{CO})_{12}^{4+}$ (tetrahedron), $\text{Os}_5(\text{CO})_{15}^{2-}$ (capped tetrahedron = trigonal bipyramid), and $\text{Os}_6(\text{CO})_{18}$ (bicapped tetrahedron) all have a total of six bonding skeletal molecular orbitals. It can be readily shown that such n vertex polyhedra are characterized by a total of $14n + 2 + 12m$ electrons (where m is the number of capping atoms on a closo deltahedron) or $15n + 12m$ electrons (for capped electron precise polyhedra).

A similar principle operates for two-dimensional cluster compounds derived by edge bridging a triangular cluster in the fashion illustrated in **28**. A schematic illustration



of the orbital interactions which result when an $\text{Os}(\text{CO})_4^{2+}$ fragment bridges one edge of a triangular $\text{Os}(\text{CO})_{12}$ cluster is given in Figure 4. The a_1 ($hy(s-z)$) and b_2 ($hy(xz)$) frontier orbitals of the $\text{Os}(\text{CO})_4^{2+}$ fragment interact with and stabilize all three bonding skeletal molecular orbitals of the $\text{Os}_3(\text{CO})_{12}$ triangle, and experience a reciprocal destabilization. In this way $\text{M}_3(\text{CO})_{12}$ and $\text{M}_4(\text{CO})_{16}$ clusters share the same total number of skeletal bonding molecular orbitals (three). The latter cluster thus has a total electron count of 62 resulting from the occupation of the b_{2u} , $1a_{1g}$, and $2a_{1g}$ molecular orbitals illustrated in Figure 4. Two

(23) The capping principle was first recognized for the capped octahedral structure observed in $\text{Rh}_7(\text{CO})_{16}^{3-}$ (D. M. P. Mingos, *Nature (London), Phys. Sci.*, **236**, 99 (1972)) and used to predict the structure of $\text{Os}_6(\text{CO})_{18}$ (K. M. Thomas, R. Mason, and D. M. P. Mingos, *J. Am. Chem. Soc.*, **95**, 3802 (1973)). The quantum mechanical basis has been described in M. I. Forsyth and D. M. P. Mingos, *J. Chem. Soc., Dalton Trans.*, 610 (1977). The principle has been widely used by C. R. Eady, B. F. G. Johnson, and J. Lewis *J. Chem. Soc., Dalton Trans.*, 2606 (1975) and R. N. Grimes, *Acc. Chem. Res.*, **11**, 420 (1978).

(21) M. A. A. F. de C. T. Carrondo and A. C. Skapski, *Acta Crystallogr., Sect. B*, **B34**, 1857 (1978).

(22) P. F. Heveltdt, B. F. G. Johnson, J. Lewis, P. R. Raithby, and G. M. Sheldrick, *J. Chem. Soc., Chem. Commun.*, 340 (1978).

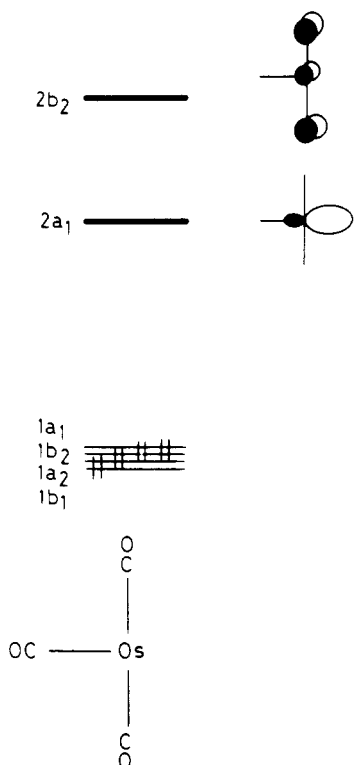
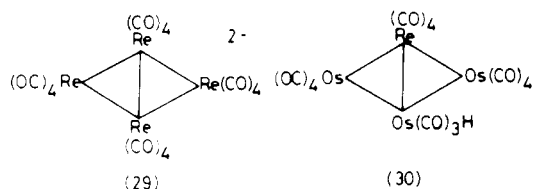


Figure 5. The frontier molecular orbitals of a T-shaped $\text{Os}(\text{CO})_3$ fragment, *isolobal* with a C_{2v} $\text{Os}(\text{CO})_4^{2+}$ fragment.

examples of clusters which have this skeletal geometry and a total of 62 valence electrons are illustrated in **29** and **30**.

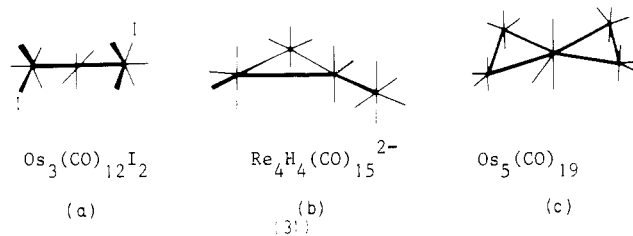


Hoffmann has noted that the hypothetical nonclassical carbonium ion $(\text{CH}_2)_4^{2+}$ and the recently synthesized di-bridged carbene complex $\text{Re}_2(\text{CO})_8(\text{CR}_2)_2^{24-26}$ may be related to these complexes by the *isolobal* analogy between $\text{M}(\text{CO})_4$ and CH_2 .

The $\text{M}_4(\text{CO})_{16}$ structure may also be edge bridged by an $\text{M}(\text{CO})_4$ fragment leading to a 76-electron pentanuclear species (**28c**). Therefore by analogy with the capped cluster compounds the total electron count in these two-dimensional condensed cluster species is equal to $48 + 14m$, where m is equal to the number of edge-bridging metal atoms.

A similar series of compounds can be derived from edge bridging of an open triangle, where the total electron count will equal $50 + 14m$. The resultant electron counts are illustrated with specific examples in **31**.²⁷

The introduction of more than one bridging $\text{M}(\text{CO})_4$ fragment into a planar cluster gives rise to unfavorable steric effects, and it is noteworthy that the doubly edge



bridged open triangular cluster $\text{Os}_5(\text{CO})_{19}$ (**31c**) may be derived from the hypothetical $\text{Os}_5(\text{CO})_{20}^{2+}$ by replacing one $\text{Os}(\text{CO})_4^{2+}$ fragment by a less sterically demanding T-shaped $\text{Os}(\text{CO})_3$ fragment. The orbitals of the latter fragment have been described elsewhere²⁸ and are reproduced in Figure 5. Above the four low-lying orbitals of mainly d character are an out-pointing $hy(s-z)$ orbital ($2a_1$) and a higher lying $2b_2$ orbital. This latter orbital is extremely localized on the carbonyl ligands (our calculations show only 17% metal character). Therefore although to a first approximation $\text{Os}(\text{CO})_4^{2+}$ and $\text{Os}(\text{CO})_3$ are *isolobal* and pseudoisoelectronic, the latter is likely to be less effective in cluster bonding since the $2b_2$ orbital has a much lower amount of metal character than the corresponding b_2 orbital in $\text{Os}(\text{CO})_4$ for which our calculations suggest 53% metal character. This is reflected in the observed crystal structure of the "bow tie" cluster $\text{Os}_5(\text{CO})_{19}$.^{27b} The four bond lengths involving the $\text{Os}(\text{CO})_3$ fragment are significantly longer than the other two, and furthermore the two triangles are skewed with dihedral angle of 21° . This distortion from a planar geometry is presumably a consequence of the more effective bonding capability of the $\text{Os}(\text{CO})_3$ $2a_1$ orbital (of σ symmetry) compared with that of the $2b_2$ orbital (of π symmetry). For $\text{Os}(\text{CO})_4$ the b_2 orbital provides the main contribution to skeletal bonding and so favors a planar geometry about the osmium atom more strongly. The "bow tie" geometry shown in **31c** has also been observed in $\text{Fe}_4\text{M}(\text{CO})_{16}^{2-}$ (where $\text{M} = \text{Pd}$ or Pt) and is illustrated in **32**.²⁹ In this cluster the central palladium or platinum atom does not use its z^2 and p_z orbitals for coordinating additional axial ligands. This phenomenon is quite general in platinum and palladium chemistry, and its implications for cluster bonding are discussed in some detail in a subsequent paper.¹⁵ The important implication in the context of the present discussion is that the presence of each palladium or platinum atom introduces an extra p_z orbital which is not utilized for metal ligand bonding and thereby reduces the total electron count by 2. Thus for example the compounds illustrated in **32** have a total of 76 electrons rather than the 78 found in **31c**. It is interesting that four of the carbonyl ligands in **32** interact with the central atom through the empty p_z orbital to form semibridging carbonyls. For completeness sake two olefin complexes which are *isolobal* with **31c** and **32** are illustrated in **33** and **34**.⁵

For the triply bridged cluster **35** the symmetry of the final six-atom cluster is identical with that of the parent triangular cluster (D_{3h}) and it is therefore a simple matter to construct an interaction diagram for the edge bridging process. This is shown in Figure 6. In this highly edge-bridged species the symmetries of the frontier orbitals of the bridging groups do not match completely the bonding skeletal MO's of the parent triangle. In particular there is an a_2' combination which is only matched by an antibonding combination in the triangle. Consequently there is an additional a_2' low-lying molecular orbital above the

(24) M. Saunders and H.-U. Siehl, *J. Am. Chem. Soc.*, **102**, 6868 (1980).

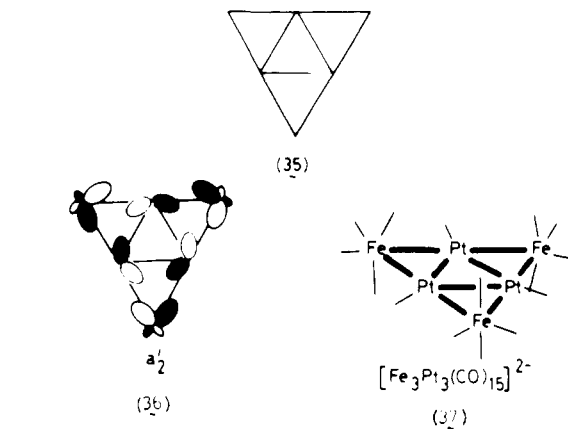
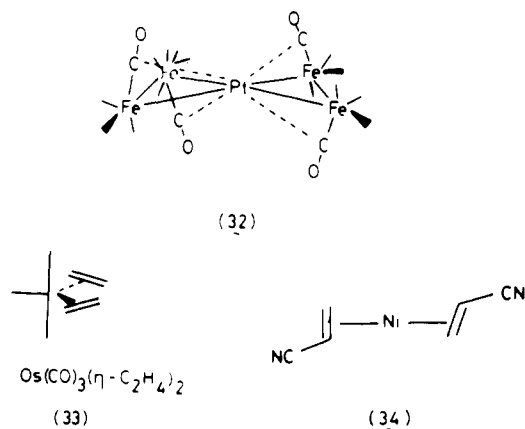
(25) E. O. Fischer, T. L. Lindner, H. Fischer, G. Huttner, P. Friedrich, and F. R. Kreissl, *Z. Naturforsch., B: Anorg. Chem., Org. Chem.*, **32B**, 648 (1977).

(26) R. Bau, B. Fontal, H. D. Kaesz, and M. R. Churchill, *J. Am. Chem. Soc.*, **89**, 6374 (1967).

(27) (a) V. G. Albano, G. Ciani, M. Freni, and P. Romitti, *J. Organomet. Chem.*, **96**, 259 (1975); (b) B. H. Farrar, B. F. G. Johnson, J. Lewis, J. N. Nicholls, P. R. Raithby, and M. J. Rosales, *J. Chem. Soc., Chem. Commun.*, 273 (1981).

(28) A. Stockis and R. Hoffmann, *J. Am. Chem. Soc.*, **102**, 2952 (1980).

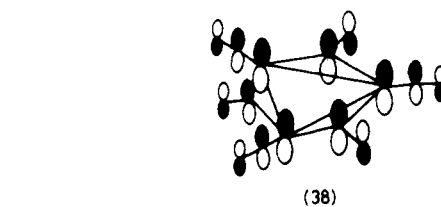
(29) G. Longoni, M. Manasserro, and M. Sansoni, *J. Am. Chem. Soc.*, **102**, 3242 (1980).



expected three skeletal molecular orbitals as illustrated in Figure 6. This situation is entirely analogous to that described in some detail by us previously,²³ where it was noted that when a trigonal prism is capped on all three of its square faces, the total number of skeletal bonding molecular orbitals increases from nine to ten as a result of an a_2' combination with similar nodal characteristics.

$\text{CO}_3(\text{CO})_3^{2-}$ where the homo is an out-of-plane bonding molecular orbital localized extensively on the carbonyl ligands (see 38).³²

It follows from the arguments developed above and in Figure 6 that for a cluster of the type illustrated in 35 the total electron count is either 90 ($48 + 14m$) or 92 ($48 + 14m + 2$) depending on whether the a_2' orbital is occupied or not. Although a species such as $\text{Os}_6(\text{CO})_{24}^{n+}$ ($n = 6$ or 4) is most unlikely by virtue of its charge and on steric grounds, *isolobal* replacement of three $\text{Os}(\text{CO})_4^{2+}$ groups by $\text{Os}(\text{CO})_3$ groups suggests the existence of $\text{Os}_6(\text{CO})_{21}$ or $\text{Os}_6(\text{CO})_{21}^{2-}$. While this work was in progress, a derivative of the former cluster $\text{Os}_6(\text{CO})_{17}(\text{P}(\text{OMe})_3)_4$ was reported and shown to have the expected structure.³⁰ The low-lying a_2' orbital in this 90-electron cluster is unoccupied, and hence it is likely that the cluster can be easily reduced to the dianion. The additional molecular orbital of a_2' symmetry is illustrated in 36. This molecular orbital is antibonding between the atoms of the central $\text{Os}_3(\text{CO})_9$ triangle and bonding between this triangle and the bridging groups. Thus occupation of this orbital can be expected to lead to an increase in bond length within the central triangle and a decrease in bond length to the bridging groups.

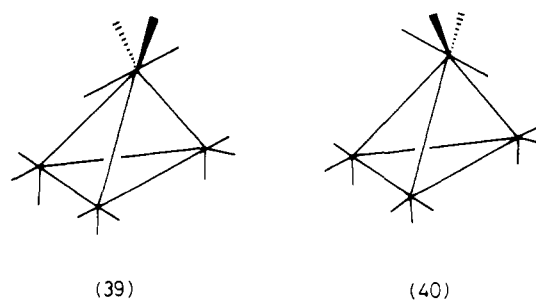


Closo Three-Dimensional Polyhedra. When the $\text{M}(\text{CO})_4$ fragment is incorporated into a three-dimensional cluster, it is necessary to take into account all three of its frontier orbitals— $hy(s-z)$, $hy(xz)$, and yz in Figure 1—since the overlap between yz and the fragment orbitals, although small, is not equal to zero.

For a tetrahedral cluster the *polyhedral skeletal electron pair theory* predicts a total of six skeletal electron pairs, accounting for the 60 valence electrons in for example $\text{Ir}_4(\text{CO})_{12}$ (see Table I). The bonding capabilities of the C_{3v} $\text{M}(\text{CO})_3$ and C_{2v} $\text{M}(\text{CO})_4$ fragments may be compared by capping an $\text{M}_3(\text{CO})_9$ cluster with the two respective fragments. The frontier orbitals and bonding capabilities of the trinuclear fragment have been analysed in detail by Schilling and Hoffmann³³ and need only be summarized here. As illustrated in the center of Figure 7, above the corelike band of nine d orbitals in $\text{Os}_3(\text{CO})_9^{2-}$ there are three orbitals which are primarily bonding within the triangle ($1e$ and $1a_1$) and three higher lying orbitals ($2a_1$ and $2e$) which can interact effectively with the frontier orbitals of the capping $\text{Os}(\text{CO})_3^{2-}$ fragment, giving rise to a total of six skeletal electron pairs in $\text{Os}_4(\text{CO})_{12}^{4-}$.

When the $\text{M}_3(\text{CO})_9^{2-}$ cluster is capped by a nonaxially symmetric $\text{M}(\text{CO})_4$ fragment, then it is necessary to consider the two conformers 39 and 40. As illustrated on the

A related platinum-iron complex has been reported (see 37), which has a total of 86 electrons.³¹ Recognizing that the absence of axial ligands coordinated to the three Pt(CO) fragments is going to introduce three additional orbitals which are not used for metal ligand bonding (by analogy with the argument developed above for 32) the bonding in 37 can easily be accounted for. In 37 the carbonyl ligands tilt toward the platinum atoms in the manner discussed above for 32 suggesting some involvement of the Pt p_z orbitals. In the 86-electron cluster $\text{Pt}_3\text{Fe}_3(\text{CO})_{15}^{2-}$ the additional molecular orbital of a_2' symmetry which results from the introduction of three edge bridging groups, illustrated in 36 is occupied. This cluster may be readily oxidized to the monoanion and X-ray crystallographic studies on 37, and the resulting 85-electron complex³¹ have demonstrated a shortening of the platinum-platinum bond lengths on removing one electron which is consistent with the nodal characteristics of the a_2' molecular orbital illustrated in 36. It is interesting to contrast the homo in 37 with that in $\text{Pt}_3(\mu-$



(30) R. J. Goudsmit, B. F. G. Johnson, J. Lewis, P. R. Raithby, and K. H. Whitmire, *J. Chem. Soc., Chem. Commun.*, 640 (1982).

(31) G. Longoni, M. Manasserro, and M. Sansoni, *J. Am. Chem. Soc.*, 102, 7973 (1980).

(32) G. Longoni and P. Chini, *J. Am. Chem. Soc.*, 98, 7225 (1976); J. W. Lauher, *ibid.*, 100, 5305 (1978).

(33) B. E. R. Schilling and R. Hoffmann, *J. Am. Chem. Soc.*, 102, 3456 (1979).

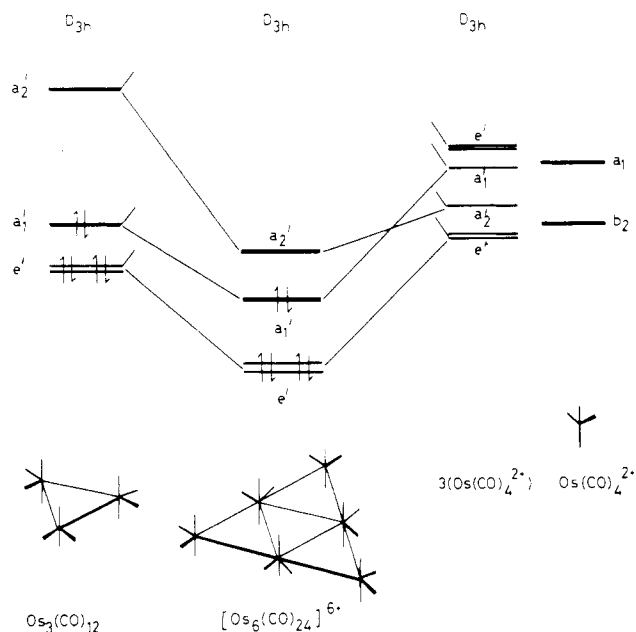


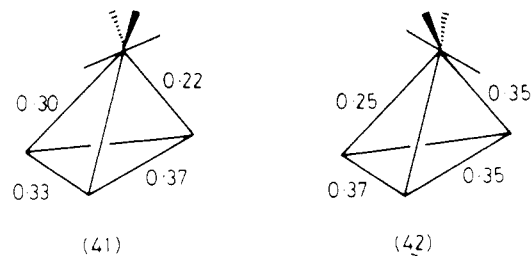
Figure 6. Construction of the molecular orbitals for the "raft" cluster $[\text{Os}_6(\text{CO})_{24}]^{6+}$ from $\text{Os}_3(\text{CO})_{12}$ and three $\text{Os}(\text{CO})_4^{2+}$ fragments. The introduction of the low-lying a_2' orbital is noteworthy and suggests the occurrence of 90- and 92-electron "raft" clusters.

right of Figure 7 for **39** the $\text{Os}(\text{CO})_4$ $hy(s-z)$ and $hy(xz)$ orbitals interact strongly with $2a_1$ and one component of $2e$, respectively, whereas yz , by virtue of its low-lying nature, interacts much more weakly with the other component of the $2e$ set in $\text{Os}_3(\text{CO})_9^{2-}$. In the alternative conformer **40** the bonding picture is very similar except that the $hy(xz)$ and yz orbitals interact with opposite components of the $2e$ set. The computed barrier to rotation of the $\text{M}(\text{CO})_4$ fragment is small with **40** being 0.3 eV more stable than **39**.

The calculations show therefore that replacing one $\text{M}(\text{CO})_3$ fragment with an $\text{M}(\text{CO})_4$ fragment in a tetranuclear cluster has not led to a change in the total electron

count. The incorporation of an $\text{M}(\text{CO})_4$ fragment does however effect the relative strengths of the metal-metal bonds.

The computed overlap populations reproduced in **41** and **42** demonstrate the magnitudes of these asymmetric bonding effects and their dependence on conformation.



Although a distortion of the $\text{M}(\text{CO})_4$ fragment from C_{2v} to C_{4v} symmetry would enhance the metal-metal bonding to the $\text{M}(\text{CO})_4$ fragment, there are two factors which militate against the equilibration of the $\text{OC}-\text{Os}-\text{CO}$ bond angles. The first, as we discussed above, is that the energy required to distort the isolated fragment is very appreciable (2.6 eV), and the second is the character of the higher lying $2a_1$ orbital ($hy(s-z)$) of the C_{2v} $\text{M}(\text{CO})_4$ fragment illustrated in Figure 2. This orbital is only 28% localized on the metal and has a high proportion of carbonyl π^* character mixed into it. The loss of overlap between π^* (CO) and the metal hybrid orbital accounts for the destabilization of $2a_1$ on pyramidalization (see Figure 2), but more importantly the localization of $2a_1$ on the carbonyl ligands leads to considerable secondary bonding interactions with orbitals on adjacent metal atoms and the resultant semibridging carbonyls provide an alternative way of alleviating the bonding deficiency of the yz orbital.

The computed metal-carbon overlap populations for conformers **39** and **40** with colinear $\text{OC}-\text{Os}-\text{CO}$ units are shown in **43** and **44**, respectively, and emphasize the importance of these supplementary bonding interactions.

Since there is little difference between conformers **39** and **40** on electronic grounds the preferred conformer is

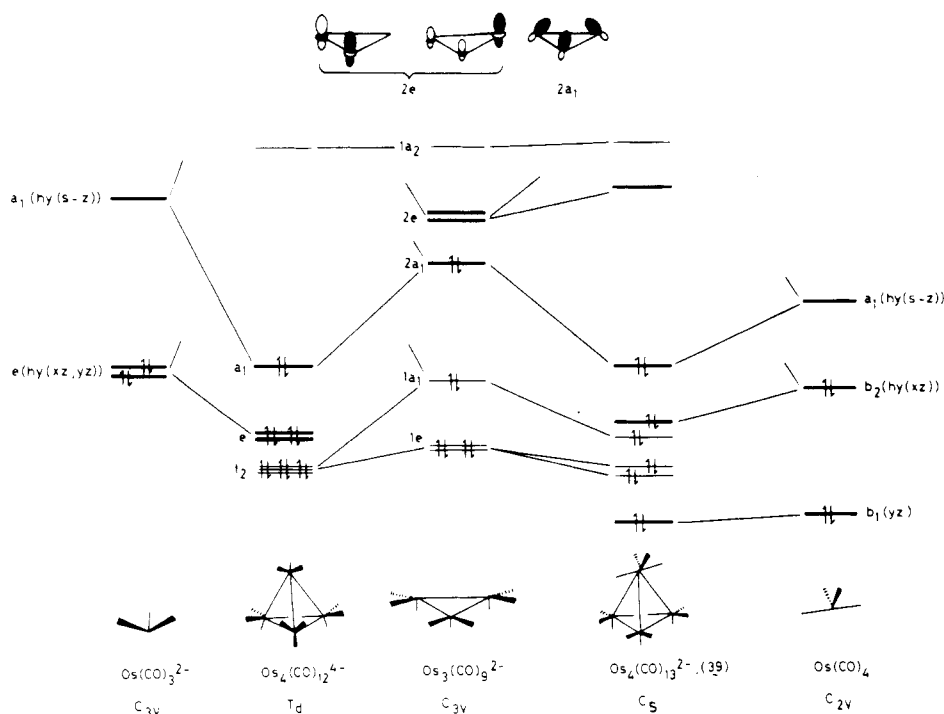
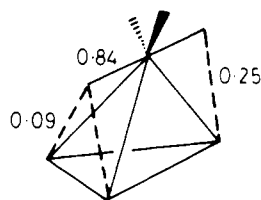
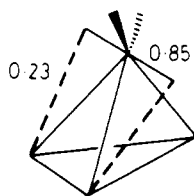


Figure 7. A comparison of the effects of capping a triangular $\text{Os}_3(\text{CO})_9^{2-}$ cluster with isoelectronic $\text{Os}(\text{CO})_3^{2-}$ and $\text{Os}(\text{CO})_4$ fragments. The two resulting tetrahedral clusters have the same electron count.



(43)

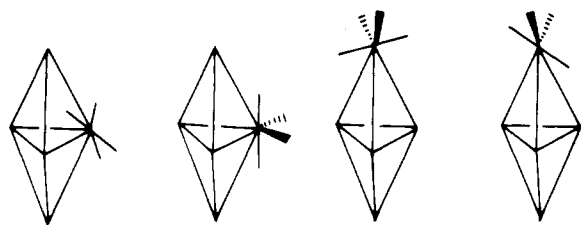


(44)

likely to be determined by steric effects. Both $\text{H}_2\text{Ru}_4(\text{C}-\text{O})_{13}$ ¹⁴ and $\text{H}_2\text{FeRu}_3(\text{CO})_{13}$ ³⁴ are known and have geometries similar to that of **40** with the expected semibridging carbonyl ligands. The $\text{M}(\text{CO})_4$ fragments in both $\text{H}_2\text{Ru}_4(\text{C}-\text{O})_{13}$ and $\text{H}_2\text{FeRu}_3(\text{CO})_{13}$ are only slightly distorted toward C_{4v} symmetry with the axial OC-M-CO angles being 174° and 172° and the equatorial OC-M-CO angles 97° and 100° , respectively. It is worth commenting that other clusters with similar stoichiometries such as $\text{Fe}_4(\text{CO})_{13}$ ²⁻³⁵ and $\text{Fe}_4\text{H}(\text{CO})_{13}$ ³⁶ have very different structures without an $\text{M}(\text{CO})_4$ group. This suggests that although one $\text{M}(\text{CO})_4$ group can be incorporated into a closo-tetrahedral cluster, without change in electron count, this does not always give the most stable structure. This is presumably a steric effect associated with the greater steric requirements of the $\text{M}(\text{CO})_4$ fragment compared with that of the $\text{M}(\text{CO})_3$ fragment.³⁷

It is apparent that the conclusion that one $\text{M}(\text{CO})_4$ fragment may be incorporated into a tetrahedral cluster without changing either the geometry or electron count may be generalized to other deltahedra and electron precise polyhedra and thereby conclude that for polyhedra of this type containing a single $\text{M}(\text{CO})_4$ fragment the results derived from the *polyhedral skeletal electron pair theory* are valid. In view of the less effective cluster bonding capability of the $\text{M}(\text{CO})_4$ fragment however three-dimensional clusters containing more than one $\text{M}(\text{CO})_4$ fragment at a vertex are unlikely to be stable.

Thus as expected $\text{Os}_5(\text{CO})_{16}$, with one $\text{Os}(\text{CO})_4$ group, has the same electron count (72) and geometry (trigonal bipyramid) as the parent deltahedron $\text{Os}_5(\text{CO})_{15}^{2-}$. Four of the site and conformational alternatives available to the $\text{Os}(\text{CO})_4$ fragment in $\text{Os}_5(\text{CO})_{16}$ are illustrated in **45-48**.



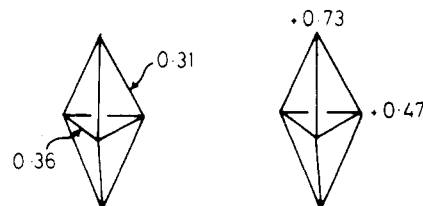
(45)

(46)

(47)

(48)

The most favorable geometric arrangement may be rationalized by reference to the six skeletal bonding molecular orbitals of $\text{Os}_5(\text{CO})_{15}^{2-}$ illustrated in Figure 8. The orbitals of the equatorial fragments make a significant contribution to all six MO's whereas those of the axial fragments make a negligible contribution to the $1e'$ set. This is reflected in the computed overlap populations and atomic charges shown in **49**.

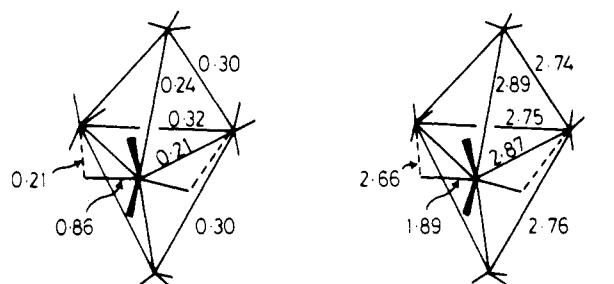


(49)

The overlap populations and charge distributions for the parent $\text{Os}_5(\text{CO})_{15}^{2-}$ ion suggest that the $\text{Os}(\text{CO})_4$ fragment can be most favorably accommodated in an equatorial site, in view of its less effective bonding capability and greater electron-withdrawing nature. The calculations show that **45**, the observed structure,¹³ lies in a deep potential well and is the most stable. Steric as well as electronic effects govern this conformational preference.

From Figure 8 it can be seen that the $1e'$ pair of skeletal MO's in $\text{Os}_5(\text{CO})_{15}^{2-}$ gives rise to the $1a_1$ and lower lying $1b_1$ levels in $\text{Os}_5(\text{CO})_{16}$. This latter is approximately nonbonding and has a major contribution from the $\text{Os}(\text{C}-\text{O})_4 yz$ orbital. The $1a_1$ level is bonding between the two equatorial $\text{Os}(\text{CO})_3$ fragments and in addition has a significant contribution from the $a_1(\text{hy}(s-z))$ orbital of $\text{Os}(\text{CO})_4$ as shown in Figure 8. The other four skeletal molecular orbitals of $\text{Os}_5(\text{CO})_{16}$ closely resemble those of $\text{Os}_5(\text{CO})_{15}^{2-}$.

The computed overlap populations for $\text{Os}_5(\text{CO})_{16}$ reproduced in **50** reflect the weaker metal-metal bonding to the $\text{Os}(\text{CO})_4$ fragment and the compensating effects of semi-bridging carbonyls. These are consistent with the observed bond lengths¹³ given in **51**.



Overlap populations

(50)

Bond lengths (Å)

(51)

The observed degree of pyramidalization of the $\text{Os}(\text{CO})_4$ fragment is again small, with the axial OC-Os-CO bond angle being 73° larger than the equatorial angle.

Open Polyhedra. In the previous section it was demonstrated that the $\text{Os}(\text{CO})_4$ fragment may occupy a vertex in a three-dimensional polyhedron if the total electron count conforms to that predicted by the *polyhedral skeletal electron pair approach*. This section considers the effect on the polyhedral geometry when this electron count is exceeded. For polyhedra based on conical $\text{M}(\text{CO})_3$ fragments the presence of an additional electron pair results in the transformation from a closo to a nido structure if the total electron count in the parent is $14n + 2$ and bond rupture if the total electron count for the parent is $15n$. These transformations arise from the population of antibonding skeletal molecular orbitals in the parent polyhedra. When the parent polyhedron contains an $\text{M}(\text{CO})_4$ fragment, an alternative distortional mode becomes available which enables the additional electron pair to reside in an effectively nonbonding molecular orbital localized on the $\text{M}(\text{CO})_4$ fragment. This process may be

(34) C. J. Gilmore and P. Woodward, *J. Chem. Soc. A*, 3453 (1971).(35) R. J. Doedens and L. F. Dahl, *J. Am. Chem. Soc.*, **88**, 4384 (1966).(36) M. Manassero, M. Sansoni, and G. Longoni, *J. Chem. Soc., Chem. Commun.*, 919 (1976).(37) D. M. P. Mingos, *Inorg. Chem.*, **21**, 464 (1982).

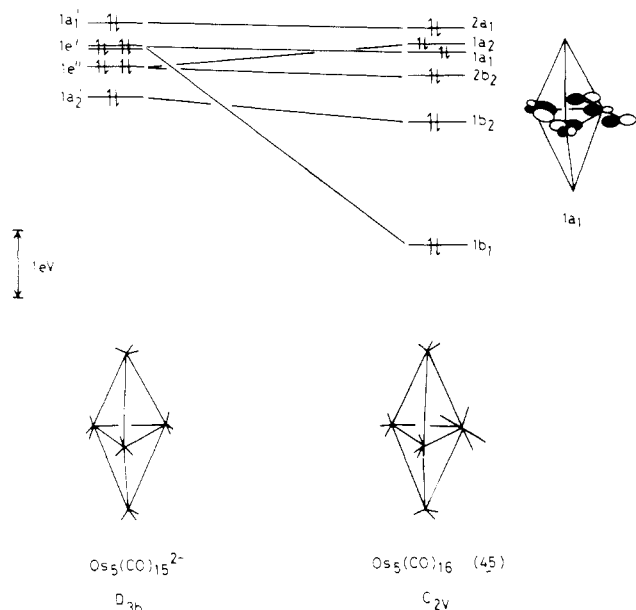
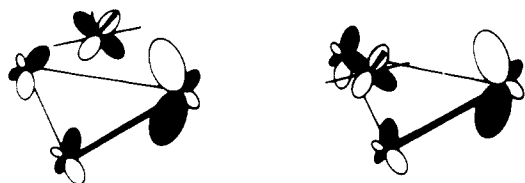


Figure 8. A comparison of the frontier molecular orbitals of $\text{Os}_5(\text{CO})_{15}^{2-}$ and $\text{Os}_5(\text{CO})_{16}$. The large stabilization associated with the $1b_1$ component of $1e'$ can be associated with the localization of this orbital on the $\text{Os}(\text{CO})_4$ fragment.

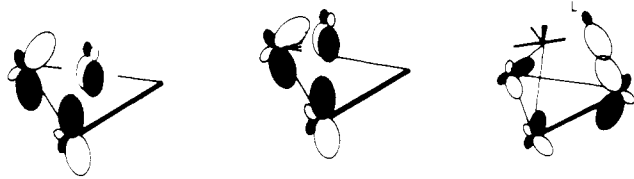
demonstrated by reference to the molecular orbital diagram for the capping process in $\text{Os}_4(\text{CO})_{13}^{2-}$ and illustrated in Figure 9.

The interaction diagram illustrated in Figure 9 for the capping process is appropriate for 60 valence electrons. When the total electron count is 62, then the additional electron pair has by necessity to occupy an orbital which is antibonding between yz of the $\text{Os}(\text{CO})_4$ fragment and one component of the e set of $\text{Os}_3(\text{CO})_9$, $(2e-yz)^*$, in Figure 9. This repulsive four-electron destabilizing interaction may be reduced by a *slip distortion*^{38,39} which places the $\text{Os}(\text{CO})_4$ fragment above one edge of the triangle, in a position where the nodal plane of the yz orbital coincides with the osmium-osmium bond as shown in **52**. This



(52)

distortion does not diminish the bonding interaction between $hy(xz)$ and the other component of the e set of out-pointing orbitals of the metal triangle, because the $hy(xz)-e(\text{Os}_3(\text{CO})_9)$ overlap integral remains almost constant as the metal atom is displaced (see **53**).



(53)

(54)

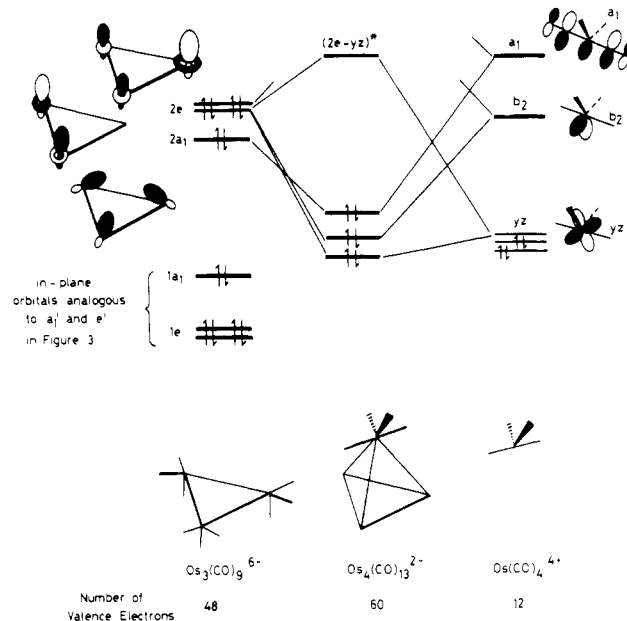
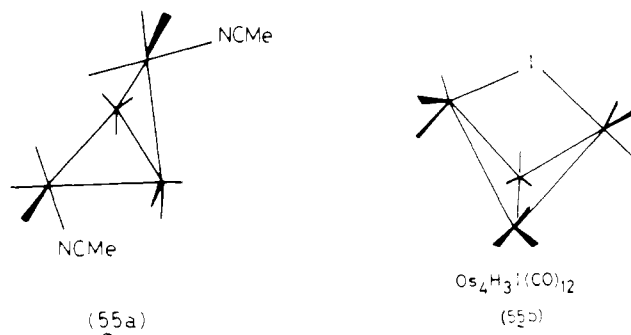


Figure 9. A more detailed illustration of the capping process involving $\text{Os}(\text{CO})_4^{4+}$ and $\text{Os}_3(\text{CO})_9^{6-}$. The introduction of an additional electron pair requires the population of $(2e-yz)^*$, which favors a slip distortion of the $\text{Os}(\text{CO})_4$ fragment to give a butterfly cluster.

This *slip distortion* can be encouraged by the incorporation of a second $\text{Os}(\text{CO})_4$ group into the cluster. This requires the addition of a ligand which not only provides the electron pair required to populate the $(2e-yz)^*$ antibonding orbital but also can stabilize this orbital by overlap with the out-pointing lobe on the metal atom farthest from the capping $\text{Os}(\text{CO})_4$ group. This stabilizing interaction, illustrated in schematic fashion in **54** gives rise to a bonding molecular orbital containing a large contribution from yz on the new $\text{Os}(\text{CO})_4$ fragment.

The recently reported 62-electron "butterfly" cluster $[\text{Os}_4(\mu\text{-H})_3(\text{CO})_{12}(\text{NCMe})_2]^+$ (**55a**) with $\text{Os}(\text{CO})_3(\text{NCMe})$ groups at the wing-tip positions provides an example of such a structure. In such complexes the occurrence of unfavorable steric interactions between the two $\text{Os}(\text{CO})_4$ or $\text{Os}(\text{CO})_3\text{L}$ groups may be reduced by the presence of a common bridging ligand which spans the two wing-tip positions. In $\text{Os}_4(\text{CO})_{12}\text{H}_3\text{I}$ (**55b**)⁴⁰ the iodine atom functions in this manner as a three-electron-bridging group replacing two axial carbonyls.



(55a)

(55b)

Similar principles apply to other closo polyhedra containing one $\text{M}(\text{CO})_4$ fragment. Consider one possible conformation of $\text{Os}_5(\text{CO})_{16}$, illustrated in **47**, in which the

(38) M. I. Forsyth, D. M. P. Mingos, and A. Welch, *J. Chem. Soc., Dalton Trans.*, 7363 (1978); M. J. Calhorda, D. M. P. Mingos, and A. J. Welch, *J. Organomet. Chem.*, **22**, 309 (1982).

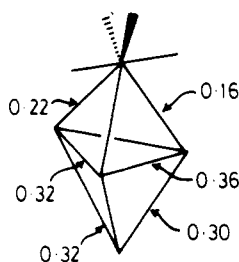
(39) C. Mealli, S. Midollini, S. Moetti, L. Sacconi, J. Silvestre, and T. A. Albright, *J. Am. Chem. Soc.*, **104**, 95 (1982).

(40) B. F. G. Johnson, J. Lewis, W. J. H. Nelson, J. Puga, P. R. Raithby, M. Schroder, and K. H. Whitmire, *J. Chem. Soc., Chem. Commun.*, 610 (1982); R. G. Bryan, B. F. G. Johnson, and J. Lewis, *ibid.*, 329 (1977).

Table II. Summary of Total Electron Counts for Polyhedra Containing $M(\text{CO})_4$ Fragments

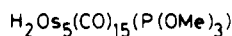
	total electron count	examples
ring compds	$16n$ ($n \geq 3$)	$\text{Os}_3(\text{CO})_{12}$ (48 e) $\text{Pt}_4(\text{OCOR})_8$ (64 e)
chain compds	$16n + 2$	$\text{Fe}_2(\text{CO})_8^{2-}$ (34 e) $\text{Os}_2(\text{CO})_{12}\text{I}_2$ (50 e) $\text{Os}_2(\text{CO})_{10}(\mu\text{-SR})_2$ (50 e)
edge-bridged ring compds with $mM(\text{CO})_4$ bridging groups	$16n + 14m$ ($m = 1, 2, \text{ or } 3$) or $16n + 14m + 2$ ($m = 3$)	$\text{Re}_4(\text{CO})_{16}^{2-}$ (62 e) $\text{Os}_6(\text{CO})_{21}$ (90 e)
edge-bridged chain compds	$16n + 14m + 2$	$\text{Re}_2\text{H}_4(\text{CO})_{15}^{2-}$ (64 e)
electron precise polyhedra (containing one $M(\text{CO})_4$ group)	$15n$	$\text{Ru}_4\text{H}_2(\text{CO})_{13}$ (60 e)
closo polyhedra (deltahedra) (containing one $M(\text{CO})_4$ group)	$14n + 2$	$\text{Os}_5(\text{CO})_{16}$
edge-bridged electron precise polyhedra with m edge-bridging $M(\text{CO})_4$ groups	$15n + 14m$	$\text{H}_2\text{Os}_5(\text{CO})_{16}$ (74 e) ($n = 4, m = 1$)
closo polyhedra (deltahedra) with m edge bridging $M(\text{CO})_4$ groups	$14n + 2 + 14m$	

$\text{Os}(\text{CO})_4$ fragment occupies an axial site. We calculate that this structure is 5.0 eV less stable than the observed structure 45. The computed overlap populations reproduced in 56 illustrates the propensity of the $\text{Os}(\text{CO})_4$ group toward slipping across a face.

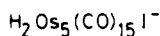


(56)

The lUMO in this conformation of $\text{Os}_5(\text{CO})_{16}$ is very similar to that discussed above for $\text{Os}_4(\text{CO})_{13}^{2-}$, and therefore addition of an electron pair to 47 can be expected to enhance the "slip" distortion of the $\text{Os}(\text{CO})_4$ fragment and give rise to an edge-bridged tetrahedral structure. This is observed for the 74-electron cluster $\text{Os}_5\text{H}_2(\text{CO})_{16}^{41}$ and the two derivatives illustrated in 57 and 58.⁴²



(57)



(58)

In such molecules the "slipped" $\text{Os}(\text{CO})_4$ fragment functions as a two-electron edge-bridging group in much the same manner as that described above for the edge-bridged triangular clusters, where the electron count for a cluster with m edge bridging $M(\text{CO})_4$ groups was found to be $48 + 14m$.

The analysis presented above suggests that the edge-bridged triangles are merely the simplest member of a more general class of edge-bridged polyhedral molecules $\{M(\text{CO})_3\}_n\{M(\text{CO})_4\}_m$, whose total electron count is $(N + 14m)$ where N is the number of electrons characteristic of

(41) J. J. Guy and G. M. Sheldrick, *Acta Crystallogr., Sect. B*, **B34**, 1725 (1978).

(42) G. R. John, B. F. G. Johnson, and J. Lewis, *J. Organomet. Chem.*, **169**, C9 (1979); G. R. John, B. F. G. Johnson, J. Lewis, W. J. H. Nelson, and M. McPartlin, *ibid.*, **17**, C14. (1979).

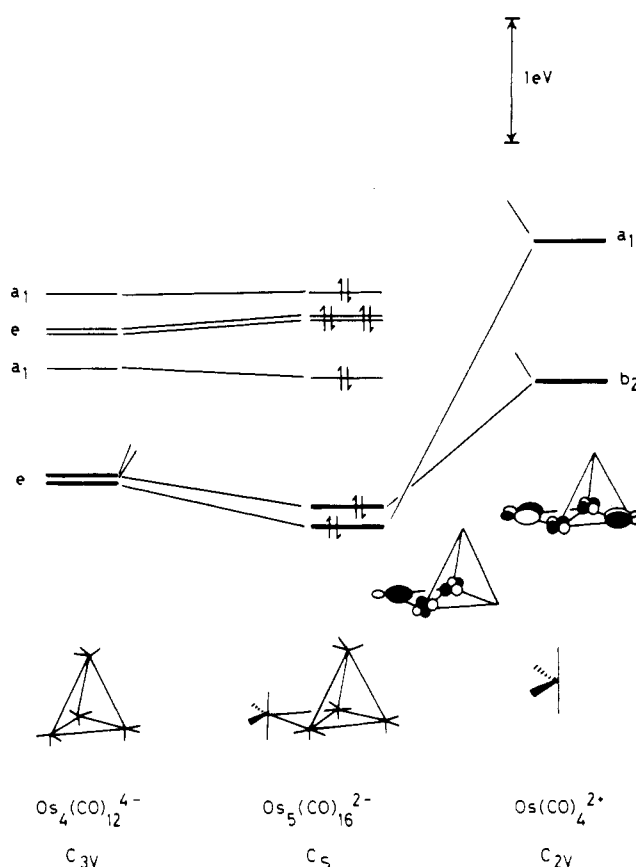


Figure 10. The frontier molecular orbitals for an edge-bridged tetrahedron constructed from $\text{Os}_4(\text{CO})_{12}^{4-}$ and $\text{Os}(\text{CO})_4^{2+}$ fragments. The number of bonding skeletal molecular orbitals remains unchanged by the bridging process.

the polyhedra $\{M(\text{CO})_3\}_n$. This is illustrated by the molecular orbital interaction diagram for an edge-bridged tetrahedral cluster shown in Figure 10. The $a_1(\text{hy}(s-z))$ and $b_2(\text{hy}(xz))$ orbitals of $\text{Os}(\text{CO})_4$ interact with and stabilize two of the six skeletal molecular orbitals of the tetrahedron whilst the $\text{Os}(\text{CO})_4$ yz orbital remains non-bonding. The total electron count is therefore $60 + 14 = 74$ electrons. For a cluster derived solely from $M(\text{CO})_3$ fragments a total electron count of 74 implies the presence of seven skeletal electron pairs and the adoption of a nido octahedral (square-pyramidal) structure as illustrated by $\text{Fe}_5(\text{CO})_{15}\text{C}$ (1).

Figure 11 illustrates some structures and the predicted electron counts which arise from this approach. In addition to those structures discussed previously in this paper, the 76-electron cluster $\text{Os}_5\text{C}(\text{CO})_{15}\text{I}^-$ (59) has been

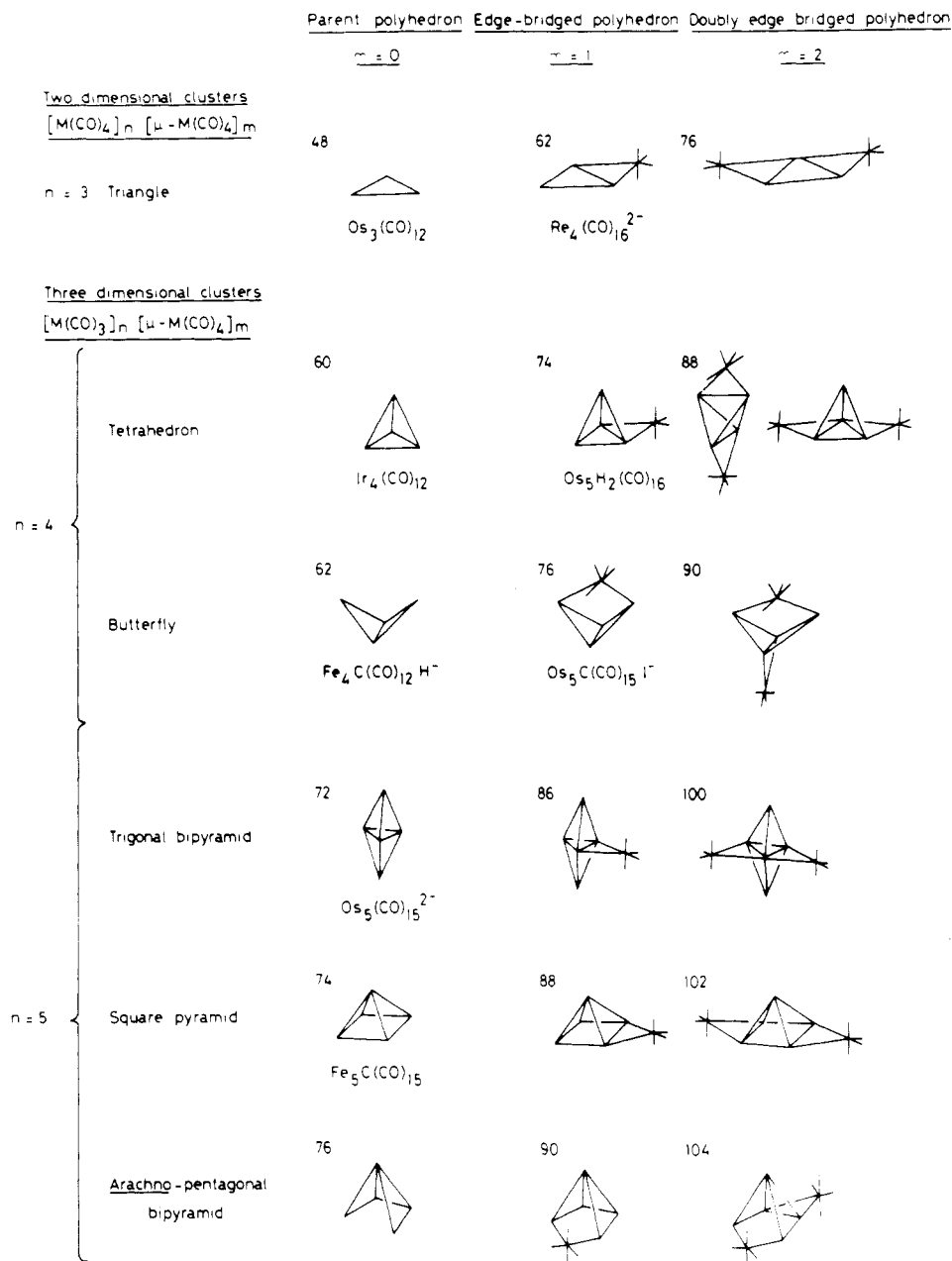
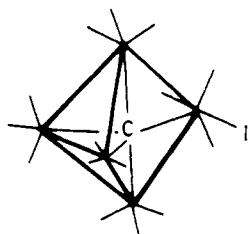


Figure 11. Summary of some observed and predicted structures and electron counts in clusters containing edge-bridging $Os(CO)_4$ fragments.

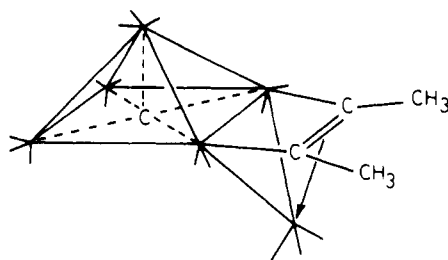
reported⁴³ and shown to have the wingtip bridged butterfly structure illustrated in Figure 11.



(59)

Although none of the other structures in Figure 11 has yet been synthesized, it is possible to regard the 88-electron

cluster $Os_6(CO)_{16}C(MeC\equiv CMe)$,⁴⁴ illustrated in 60, as being related to the edge-bridged square-pyramidal structure expected for a cluster such as $Os_6H_2(CO)_{19}$. We suggest that further examples of structures given in Figure 11 will be synthesized in due course.



(60)

(43) P. F. Jackson, B. F. G. Johnson, J. Lewis, J. N. Nicholls, M. McPartlin, and W. J. H. Nelson, *J. Chem. Soc., Chem. Commun.*, 564 (1980).

(44) C. R. Eady, J. M. Fernandez, B. F. G. Johnson, J. Lewis, P. R. Raithby, and G. M. Sheldrick, *J. Chem. Soc. Chem. Commun.*, 421 (1978).

Table III

orbital	H_{ii} , eV	Slater exponent
C 2s	-21.4	1.625
2p	-11.4	1.625
O 2s	-32.3	2.275
2p	-14.8	2.275
Os 6s	-8.0	2.14
6p	-4.5	2.10

Os d wave function ^a					
orbital	H_{ii} , eV	ξ_1	C_1	ξ_2	C_2
Os 5d	-12.5	4.29	0.59	1.97	0.58

^a Taken as contracted linear combinations of two Slater type wavefunctions.

Summary

While the *polyhedral skeletal electron pair theory* may be used to rationalize the geometries of closo structures containing one $M(\text{CO})_4$ fragment, such clusters possessing additional electron pairs do not adopt the expected nido or arachno structures. The common characteristic of the observed cluster structures is the adoption of two connectivity sites by the $M(\text{CO})_4$ fragments which maximizes the two-electron stabilizing interactions between $hy(xz)$ and the frontier orbitals of the metal polyhedron and minimizes the four-electron destabilizing interactions between yz and the complementary e component of the polyhedron, by making the former effectively nonbonding. Such edge-bridged polyhedral clusters have a total electron

count of $(N + 14m)$ where N is the number of electrons characteristic of the polyhedron and m the number of bridging $M(\text{CO})_4$ groups it possesses. The electron counts for clusters containing $M(\text{CO})_4$ groups are summarized in Table II.

Acknowledgment. We thank Mrs. Christine Palmer for her assistance with the figures and the S.E.R.C. for financial support.

Appendix

The molecular orbital calculations described in this paper were of the extended Hückel type^{45,46} using a weighted H_{ij} formula.⁴⁷ The relevant orbital parameters are summarized in Table III and conform with those which have been shown to give reliable conclusions for organo-transition-metal compounds.⁵

The following bond lengths were used for the calculations: Os-Os = 2.80 Å, Os-C = 1.89 Å, and C-O = 1.16 Å. The calculations were performed on the ICI 2980 Computer at this university using the programs ICON 8 and FMO developed by Hoffmann and co-workers.⁴⁸

(45) R. Hoffmann, *J. Chem. Phys.*, **39**, 1397 (1963).

(46) R. Hoffmann and W. N. Lipscomb, *J. Chem. Phys.*, **36**, 2179 (1962); **37**, 2872 (1962).

(47) J. H. Ammeter, H.-B. Burgi, J. C. Thibeault, and R. Hoffmann, *J. Am. Chem. Soc.*, **100**, 3668 (1978).

(48) J. Howell, A. Rossi, D. Wallace, K. Haraki, and R. Hoffmann, *QCPE*, **10**, 344 (1977).

Triangular Iron-Silver Clusters via the Addition of Silver Electrophiles to Electron-Rich Iron-Iron Bonds

Graham N. Mott, Nicholas J. Taylor, and Arthur J. Carty*

Guelph-Waterloo Centre for Graduate Work in Chemistry, University of Waterloo, Waterloo, Ontario N2L 3G1, Canada

Received October 4, 1982

The synthesis of triangular iron-silver clusters $[\text{Fe}_2\text{Ag}(\text{CO})_6\{\text{CHC}(\text{C}_6\text{H}_5)(\text{NRR}^1)\}\text{P}(\text{C}_6\text{H}_5)_2]\text{X}$, **2** ($\text{R} = \text{H}$, $\text{R}^1 = \text{CH}_3$, C_2H_5 , $\text{CH}(\text{CH}_3)_2$, $c\text{-C}_6\text{H}_{11}$; $\text{R} = \text{R}^1 = \text{C}_2\text{H}_5$; $\text{X} = \text{ClO}_4$ or PF_6), via the addition of silver ion Ag^+ to the electron-rich metal-metal bond in the μ -alkylidene complexes $[\text{Fe}_2(\text{CO})_6\{\text{CHC}(\text{C}_6\text{H}_5)(\text{NRR}^1)\}\text{P}(\text{C}_6\text{H}_5)_2]$ (**1**) is described. These compounds are rare examples of closed triangular M_2Ag clusters. Crystals of a typical derivative, **2** ($\text{R} = \text{H}$, $\text{R}^1 = \text{CH}_3$, $\text{X} = \text{ClO}_4$), are triclinic of space group $\text{P}\bar{1}$ with $a = 14.101$ (3) Å, $b = 10.654$ (4) Å, $c = 15.777$ (4) Å, $\alpha = 93.68$ (4)°, $\beta = 114.27$ (2)°, $\gamma = 95.03$ (3)°, and $Z = 2$. The structure was solved and refined to R and R_w values of 0.046 and 0.055 by using 4617 GE-XRD-6 measured reflections. In the triangular Fe_2Ag framework there are two Ag-Fe bonds (Ag-Fe(1) = 2.685 (1) Å, Ag-Fe(2) = 2.703 (1) Å) and an Fe-Fe bond (Fe(1)-Fe(2) = 2.682 (1) Å). The Fe-Fe vector is also bridged by a $\text{P}(\text{C}_6\text{H}_5)_2$ group and a μ - η^1 -alkylidene ligand. The nature of the Ag-Fe and Fe-Fe interactions is discussed. Spectroscopic (^1H and ^{31}P NMR; IR; Mössbauer) data for the new clusters are presented. The addition of silver salts to electron-rich bi- or polynuclear fragments may have potential as a general route to mixed-metal clusters.

A potentially attractive method of metal cluster synthesis is the addition of a metal-based electrophile to an electron-rich metal-metal bond.¹ The reverse process, addition of a nucleophilic fragment to an electrophilic cluster, has been successfully utilized in the generation of a substantial number of mixed-metal clusters.^{2,3} Methods

of increasing metal-metal bond nucleophilicity include anion formation⁴ and phosphine ligand substitution.⁵ We have recently described the synthesis of zwitterionic bi- and trinuclear carbonyl complexes via amination of μ - η^2 -

(1) For a recent review of mixed-metal clusters see: Roberts, D. A.; Geoffroy, G. L. In "Comprehensive Inorganic Chemistry"; Wilkinson, G., Stone, F. G. A., Abel, E. W., Eds.; Pergamon Press: Oxford, 1982; Chapter 40.

(2) Farrugia, L. J.; Howard, J. A. K.; Mitrprachachon, P.; Spencer, J. L.; Stone, F. G. A.; Woodward, P. *J. Chem. Soc., Chem. Commun.* **1978**, 260.

(3) Lanfranchi, M.; Tiripicchio, A.; Sappa, E.; MacLaughlin, S. A.; Carty, A. *J. J. Chem. Soc., Chem. Commun.* **1982**, 538, and references therein.

(4) Relatively few cluster syntheses have been carried out by using polynuclear anions. See ref 1 and (a) Schmid, G.; Bartl, K.; Boese, R. *Z. Naturforsch., B: Anorg. Chem., Org. Chem.* **1977**, **32B**, 1277. (b) Ruff, J. K.; White, R. P., Jr.; Dahl, L. F. *J. Am. Chem. Soc.* **1971**, **93**, 2159.

(5) Arabi, M. S.; Mathieu, R.; Poilblanc, R. *Inorg. Chim. Acta* **1979**, **34**, L207 and references therein.

Table III

orbital	H_{ii} , eV	Slater exponent
C 2s	-21.4	1.625
2p	-11.4	1.625
O 2s	-32.3	2.275
2p	-14.8	2.275
Os 6s	-8.0	2.14
6p	-4.5	2.10

Os d wave function ^a					
orbital	H_{ii} , eV	ξ_1	C_1	ξ_2	C_2
Os 5d	-12.5	4.29	0.59	1.97	0.58

^a Taken as contracted linear combinations of two Slater type wavefunctions.

Summary

While the *polyhedral skeletal electron pair theory* may be used to rationalize the geometries of closo structures containing one $M(\text{CO})_4$ fragment, such clusters possessing additional electron pairs do not adopt the expected nido or arachno structures. The common characteristic of the observed cluster structures is the adoption of two connectivity sites by the $M(\text{CO})_4$ fragments which maximizes the two-electron stabilizing interactions between $hy(xz)$ and the frontier orbitals of the metal polyhedron and minimizes the four-electron destabilizing interactions between yz and the complementary e component of the polyhedron, by making the former effectively nonbonding. Such edge-bridged polyhedral clusters have a total electron

count of $(N + 14m)$ where N is the number of electrons characteristic of the polyhedron and m the number of bridging $M(\text{CO})_4$ groups it possesses. The electron counts for clusters containing $M(\text{CO})_4$ groups are summarized in Table II.

Acknowledgment. We thank Mrs. Christine Palmer for her assistance with the figures and the S.E.R.C. for financial support.

Appendix

The molecular orbital calculations described in this paper were of the extended Hückel type^{45,46} using a weighted H_{ij} formula.⁴⁷ The relevant orbital parameters are summarized in Table III and conform with those which have been shown to give reliable conclusions for organo-transition-metal compounds.⁵

The following bond lengths were used for the calculations: Os-Os = 2.80 Å, Os-C = 1.89 Å, and C-O = 1.16 Å. The calculations were performed on the ICI 2980 Computer at this university using the programs ICON 8 and FMO developed by Hoffmann and co-workers.⁴⁸

(45) R. Hoffmann, *J. Chem. Phys.*, **39**, 1397 (1963).

(46) R. Hoffmann and W. N. Lipscomb, *J. Chem. Phys.*, **36**, 2179 (1962); **37**, 2872 (1962).

(47) J. H. Ammeter, H.-B. Burgi, J. C. Thibeault, and R. Hoffmann, *J. Am. Chem. Soc.*, **100**, 3668 (1978).

(48) J. Howell, A. Rossi, D. Wallace, K. Haraki, and R. Hoffmann, *QCPE*, **10**, 344 (1977).

Triangular Iron-Silver Clusters via the Addition of Silver Electrophiles to Electron-Rich Iron-Iron Bonds

Graham N. Mott, Nicholas J. Taylor, and Arthur J. Carty*

Guelph-Waterloo Centre for Graduate Work in Chemistry, University of Waterloo, Waterloo, Ontario N2L 3G1, Canada

Received October 4, 1982

The synthesis of triangular iron-silver clusters $[\text{Fe}_2\text{Ag}(\text{CO})_6\{\text{CHC}(\text{C}_6\text{H}_5)(\text{NRR}^1)\}\text{P}(\text{C}_6\text{H}_5)_2]\text{X}$, **2** ($\text{R} = \text{H}$, $\text{R}^1 = \text{CH}_3$, C_2H_5 , $\text{CH}(\text{CH}_3)_2$, $c\text{-C}_6\text{H}_{11}$; $\text{R} = \text{R}^1 = \text{C}_2\text{H}_5$; $\text{X} = \text{ClO}_4$ or PF_6), via the addition of silver ion Ag^+ to the electron-rich metal-metal bond in the μ -alkylidene complexes $[\text{Fe}_2(\text{CO})_6\{\text{CHC}(\text{C}_6\text{H}_5)(\text{NRR}^1)\}\text{P}(\text{C}_6\text{H}_5)_2]$ (**1**) is described. These compounds are rare examples of closed triangular M_2Ag clusters. Crystals of a typical derivative, **2** ($\text{R} = \text{H}$, $\text{R}^1 = \text{CH}_3$, $\text{X} = \text{ClO}_4$), are triclinic of space group $\text{P}\bar{1}$ with $a = 14.101$ (3) Å, $b = 10.654$ (4) Å, $c = 15.777$ (4) Å, $\alpha = 93.68$ (4)°, $\beta = 114.27$ (2)°, $\gamma = 95.03$ (3)°, and $Z = 2$. The structure was solved and refined to R and R_w values of 0.046 and 0.055 by using 4617 GE-XRD-6 measured reflections. In the triangular Fe_2Ag framework there are two Ag-Fe bonds (Ag-Fe(1) = 2.685 (1) Å, Ag-Fe(2) = 2.703 (1) Å) and an Fe-Fe bond (Fe(1)-Fe(2) = 2.682 (1) Å). The Fe-Fe vector is also bridged by a $\text{P}(\text{C}_6\text{H}_5)_2$ group and a μ - η^1 -alkylidene ligand. The nature of the Ag-Fe and Fe-Fe interactions is discussed. Spectroscopic (^1H and ^{31}P NMR; IR; Mössbauer) data for the new clusters are presented. The addition of silver salts to electron-rich bi- or polynuclear fragments may have potential as a general route to mixed-metal clusters.

A potentially attractive method of metal cluster synthesis is the addition of a metal-based electrophile to an electron-rich metal-metal bond.¹ The reverse process, addition of a nucleophilic fragment to an electrophilic cluster, has been successfully utilized in the generation of a substantial number of mixed-metal clusters.^{2,3} Methods

of increasing metal-metal bond nucleophilicity include anion formation⁴ and phosphine ligand substitution.⁵ We have recently described the synthesis of zwitterionic bi- and trinuclear carbonyl complexes via amination of μ - η^2 -

(1) For a recent review of mixed-metal clusters see: Roberts, D. A.; Geoffroy, G. L. In "Comprehensive Inorganic Chemistry"; Wilkinson, G., Stone, F. G. A., Abel, E. W., Eds.; Pergamon Press: Oxford, 1982; Chapter 40.

(2) Farrugia, L. J.; Howard, J. A. K.; Mitrprachachon, P.; Spencer, J. L.; Stone, F. G. A.; Woodward, P. *J. Chem. Soc., Chem. Commun.* **1978**, 260.

(3) Lanfranchi, M.; Tiripicchio, A.; Sappa, E.; MacLaughlin, S. A.; Carty, A. J. *J. Chem. Soc., Chem. Commun.* **1982**, 538, and references therein.

(4) Relatively few cluster syntheses have been carried out by using polynuclear anions. See ref 1 and (a) Schmid, G.; Bartl, K.; Boese, R. *Z. Naturforsch., B: Anorg. Chem., Org. Chem.* **1977**, **32B**, 1277. (b) Ruff, J. K.; White, R. P., Jr.; Dahl, L. F. *J. Am. Chem. Soc.* **1971**, **93**, 2159.

(5) Arabi, M. S.; Mathieu, R.; Poilblanc, R. *Inorg. Chim. Acta* **1979**, **34**, L207 and references therein.

and $\mu_3\text{-}\eta^2\text{-acetylides}$.^{6,7} Both IR and ¹³C NMR⁸ data suggest that the M–M bonds in these molecules are exceptionally electron rich. We have discovered that the addition of silver salts AgX (X = ClO₄⁻, PF₆⁻) to the iron–iron bonds of [Fe₂(CO)₆{CHC(C₆H₅)(NHR¹)}P(C₆H₅)₂] (1) affords simple adducts, the mixed trinuclear clusters [Fe₂Ag(CO)₆{CHC(C₆H₅)(NHR¹)}P(C₆H₅)₂]X. Although the third element of group 1B, gold, has a propensity to form stable clusters,⁹ mixed-metal compounds involving silver are still relatively rare. Most of the known compounds are of the types L_nM–Ag–ML_n or L_nM–AgL'_m where L_nM represents a typical carbonyl or cyclopentadienyl metal group and L' is a group 5 or 6 donor ligand. Typical examples are {($\eta^5\text{-C}_5\text{H}_5$)W(CO)₃}₂Ag,⁹ Fe(CO)₄{(*o*-triars)Ag}₂,¹⁰ and [($\eta^5\text{-C}_5\text{H}_5$)Rh(CO)]P(C₆H₅)₃]₂Ag]PF₆.¹¹ Our preliminary description¹² of the complex [Fe₂Ag(CO)₆{CHC(C₆H₅)(NHR¹)}P(C₆H₅)₂]ClO₄ represented the first account of the synthesis of a closed trinuclear cluster via simple addition of the electrophile Ag⁺ to a binuclear metal–metal bonded complex. These reactions, now described in full, bear a resemblance to the protonation of M–M bonds, the electrophile Ag⁺ being electronically and stereochemically equivalent to the proton. We note also that recently the use of [AuPPh₃] as a fragment possessing electronic and structural similarities to the hydride ligand has attracted considerable attention.¹³

Experimental Section

Materials and Procedures. Tetrahydrofuran and benzene were dried over sodium benzophenone ketyl and distilled before use. Diiron enneacarbonyl was prepared from iron pentacarbonyl (Pressure Chemical Co.) by photolysis in glacial acetic acid.¹⁴ Other chemicals were of reagent grade purity and were used as received. All manipulations were carried out under a blanket of nitrogen, with nitrogen-saturated solvents using standard Schlenk tube procedures.

Reaction of [Fe₂(CO)₆{CHC(NRR¹)(C₆H₅)}P(C₆H₅)₂] (1, R = H, R¹ = CH₃, C₂H₅, CH(CH₃)₂, *c*-C₆H₁₁; R = R¹ = C₂H₅) with AgPF₆ and AgClO₄. Typically, 0.3 g (ca. 0.5 mmol) of 1 was dissolved in benzene (30 mL). An equimolar amount of silver perchlorate dissolved in a minimum of benzene (ca. 10 mL) was added to the above vigorously stirred solution at room temperature. For silver hexafluorophosphate, tetrahydrofuran was used as a solvent, and this solution was added to a benzene solution of the iron carbonyl. Within a few seconds a red precipitate was formed. Stirring was continued for 5 min to ensure complete reaction, and the precipitate was allowed to settle. Mother liquor was removed by syringe or pumped to low volume (for THF), and the products were washed with benzene (4 × 10 mL) and dried in vacuo. Yields of adducts [Fe₂Ag(CO)₆{CHC(NRR¹)(C₆H₅)}P(C₆H₅)₂]X, 2 (X = ClO₄⁻, PF₆⁻), were ca. 90% in all cases. When R = H, these complexes are indefinitely stable in dry air in the solid state, although the perchlorate salts explode violently on heating. They are insoluble in heptane, sparingly soluble in benzene and toluene, and very soluble in chloroform and acetone. Decomposition occurs rapidly in THF. The compound 2 (R =

Table I. Crystallographic Data for [Fe₂Ag{CHC(NHCH₃)(C₆H₅)}P(C₆H₅)₂]ClO₄·C₆H₆·C₆H₅CH₃

fw	974.71
space group	P $\bar{1}$
unit cell	
<i>a</i> , Å	14.101 (3)
<i>b</i> , Å	10.654 (4)
<i>c</i> , Å	15.777 (4)
α , deg	93.68 (4)
β , deg	114.27 (2)
γ , deg	95.03 (3)
vol, Å ³	2139
<i>Z</i>	2
ρ_{calcd} , g cm ⁻³	1.511
ρ_{measd} (C ₆ H ₁₂ /CCl ₄), g cm ⁻³	1.51
<i>F</i> (000)	912
cryst size, mm	0.3 × 0.3 × 0.3
2 θ range, deg	2.0 ≤ 2 θ ≤ 45°
scan width	$\Delta\theta \pm 0.9 + 0.43 \tan \theta$
reflectns measd	6722
reflectns obsd	4617
<i>R</i>	0.046
<i>R</i> _w	0.055

R¹ = C₂H₅) is stable as a solid but decomposes in solution: IR spectra show the presence of the precursor 1. Yields, melting points, and analytical data are as follows.

2 (R = H, R¹ = CH₃, X = ClO₄): 92%; mp 130 °C dec. Anal. Calcd for Fe₂AgClPO₁₀NC₂₇H₂₀·C₆H₆: C, 44.9; H, 3.0; P, 3.5. Found: C, 44.6; H, 3.0; P, 3.3.

2 (R = H, R¹ = C₂H₅, X = ClO₄): 92%; mp 131 °C dec. Anal. Calcd for Fe₂AgClPO₁₀NC₂₈H₂₂·C₆H₆: C, 45.5; H, 3.1; P, 3.5. Found: C, 45.7; H, 3.2; P, 3.3.

2 (R = H, R¹ = CH(CH₃)₂, X = ClO₄): 90%; mp 124 °C dec. Anal. Calcd for Fe₂AgClPO₁₀NC₂₉H₂₄: C, 41.9; H, 2.9; P, 3.7. Found: C, 42.1; H, 3.1; P, 3.5.

2 (R = H, R¹ = *c*-C₆H₁₁, X = ClO₄): 92%; mp 154 °C dec. Anal. Calcd for Fe₂AgClPO₁₀NC₃₂H₂₈·C₆H₆: C, 48.0; H, 3.6; P, 3.3. Found: C, 48.5; H, 3.7; P, 3.5.

2 (R = R¹ = C₂H₅, X = ClO₄): 85%; mp 137 °C dec. Anal. Calcd for Fe₂AgClPO₁₀NC₃₀H₂₆: C, 41.5; H, 3.2; P, 3.6. Found: C, 40.6; H, 2.8; P, 3.4.

2 (R = H, R¹ = CH₃, X = PF₆): 90%; mp 135 °C dec. Anal. Calcd for Fe₂AgP₂O₆NF₆C₂₇H₂₀·C₆H₆: C, 42.7; H, 2.8. Found: C, 42.8, H, 2.9.

Reaction of [Fe₂(CO)₆{C(NHR)CH(C₆H₅)}P(C₆H₅)₂] (3, R = H, R¹ = CH₃, C₂H₅, CH(CH₃)₂) with Silver Salts. Addition of solutions of silver salts to equimolar benzene solutions of 3 resulted in rapid decomposition of the iron complexes and deposition of a silver mirror. In each case ca. 50% of the starting material remained unreacted and was recovered. Complete decomposition of starting complex 3 was achieved with two molar equivalents of silver salt. Decomposition products were not identified.

Physical Measurements. Infrared spectra as Nujol mulls on CsI plates or as solutions in CHCl₃ using matched 0.5-mm path length sodium chloride cells were recorded on a Perkin-Elmer 180 infrared spectrometer. ¹H and ³¹P NMR spectra were recorded on Bruker WP-60 (60-MHz ¹H, 24.29-MHz ³¹P) or WH-90 (36.43-MHz ³¹P) instruments using deuterated solvents for lock. Mössbauer spectra were recorded at 77 ± 5 K by using an Austin Science Associates Inc. drive equipped with a Kickstart pulse-height analyser. Details of the Mössbauer source and the fitting of lines to Lorentzian line shapes have been presented elsewhere.¹⁵

X-ray Structure Determination. A dark red prism of [Fe₂Ag(CO)₆{CHC(NHCH₃)(C₆H₅)}P(C₆H₅)₂]ClO₄·C₆H₆·C₆H₅CH₃ grown from a hot saturated toluene solution was mounted on a glass fiber and attached to a goniometer head for diffraction measurements. Preliminary Weissenberg and precession photography revealed no systematic absences, showing that the crystal belonged to the triclinic system. Space group P $\bar{1}$ was assumed and confirmed by the successful refinement of the structure. The unit-cell dimensions were obtained by refinement of the 2 θ values for 25 reflections measured on a General Electric XRD-6 Datex

(6) Carty, A. J.; Mott, G. N.; Taylor, N. J.; Yule, J. E. *J. Am. Chem. Soc.* **1978**, *100*, 3051.

(7) Carty, A. J. *Adv. Chem. Ser.* **1982**, No. 196, 163.

(8) Carty, A. J.; Mott, G. N. submitted for publication in *Inorg. Chem.*

(9) Hackett, P.; Manning, A. R. *J. Chem. Soc., Dalton Trans.* **1975**, 1606.

(10) Kasenally, A. S.; Nyholm, R. S.; Stiddard, M. H. B. *J. Chem. Soc.* **1965**, 5543.

(11) Connelly, N. G.; Lucy, A. R.; Galas, A. M. R. *J. Chem. Soc., Chem. Commun.* **1981**, 43.

(12) Carty, A. J.; Mott, G. N.; Taylor, N. J. *J. Am. Chem. Soc.* **1979**, *101*, 3131.

(13) See, for example: (a) Lauher, J. W.; Wald, K. *J. Am. Chem. Soc.* **1981**, *103*, 7648. (b) Johnson, B. F. G.; Kaner, D. A.; Lewis, J.; Raithby, P. R.; Taylor, M. J. *J. Chem. Soc., Chem. Commun.* **1982**, 314.

(14) King, R. B. In "Organometallic Syntheses"; Eisch, J. J., King, R. B., Eds.; Academic Press: New York, 1965; Vol. 1.

(15) Carty, A. J.; Paik, H. N.; Palenik, G. J. *Inorg. Chem.* **1977**, *16*, 300.

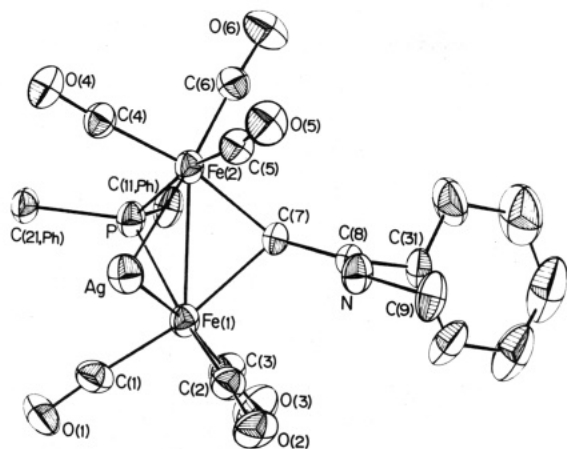


Figure 1. An ORTEP plot of the structure of the cation $[\text{Fe}_2\text{Ag}(\text{CO})_6][\text{CHC}(\text{NHCH}_3)(\text{C}_6\text{H}_5)_2]^+$ showing the atomic numbering. The silver atom also weakly interacts with a toluene molecule of crystallization. For the sake of clarity neither the anion ClO_4^- nor the molecules of solvation are shown.

automated diffractometer. Crystallographic data are summarized in Table I. Intensity data were collected at 298 ± 1 K with zirconium-filtered Mo K_α radiation using the θ - 2θ scan technique with a scan rate of 2° min^{-1} . Stationary counter-stationary crystal background counts of 10 s were taken before and after each scan. Crystal and machine stability were monitored via intensity measurements on three standard reflections after collection of each set of 100 data. No significant decline in intensity was apparent. With $\mu(\text{Mo } K_\alpha) = 12.81 \text{ cm}^{-1}$ no absorption correction was necessary. Lorentz and polarization corrections were applied to the derivation of structure factor amplitudes.

Solution and Refinement of the Structure. A Patterson function revealed the positions of all three metal atoms arranged in a triangular array. Standard Fourier and difference Fourier methods were used to identify the remaining atoms including molecules of benzene and toluene of crystallization. The latter interacts weakly with the silver atom (vide infra). Refinement of positional parameters for all 56 atoms gave an R value ($R = \sum |F_o| - |F_c| / \sum |F_o|$) of 0.18. With all atoms having isotropic thermal parameters, full-matrix least-squares refinement gave $R = 0.12$. Conversion of thermal parameters for Fe, Ag, P, and Cl to anisotropic coefficients followed by a cycle of refinement yielded $R = 0.088$. With all non-hydrogen atoms having anisotropic thermal parameters R was 0.068. At this stage a difference Fourier synthesis showed a rotational disorder of the perchlorate group; this disorder was resolved for oxygen atom O(10), and in subsequent calculations an occupancy factor of 50% was used for these two sites. Refinement to convergence afforded R and R_w ($R_w = [\sum w(|F_o| - |F_c|)^2 / \sum w|F_o|^2]^{1/2}$) values of 0.046 and 0.055, respectively. Only reflections for which $F_o^2 \geq 3\sigma(F_o^2)$ were used in the refinement. The function minimized was $\sum w(|F_o| - |F_c|)^2$, and the weights used in final cycles were given by $w^{-1} = 2.0 - 0.05|F_o| + 0.0015|F_o|^2$. A final difference map had maximum peak heights of $0.065 \text{ e } \text{Å}^{-3}$. Scattering factors, including corrections for the effects of anomalous dispersion for Fe and Ag, were taken from ref 16. Calculations using computer programs described in detail elsewhere⁶ were carried out on an IBM-360-75 system in the University of Waterloo Computing Centre. Table II contains atomic positions for all atoms and Table III a selection of bond lengths and angles. Thermal parameters have been deposited as supplementary Table S1 and remaining bond lengths and angles as Table S2. A complete listing of structure factor amplitudes is also available.

Results and Discussion

Description and Discussion of the Structure. The reaction of silver perchlorate with the iron dimers 1 results in the simple addition of a silver(1+) ion to the dinuclear

Table II. Atomic Positions (Fractional $\times 10^4$) for $[\text{Fe}_2\text{Ag}(\text{CO})_6][\text{CHC}(\text{NHCH}_3)(\text{C}_6\text{H}_5)_2]^+ \text{P}(\text{C}_6\text{H}_5)_2]^- \text{ClO}_4 \cdot \text{C}_6\text{H}_6 \cdot \text{C}_6\text{H}_5\text{CH}_3$

atom	x	y	z
Ag	-840.1 (4)	1000.3 (5)	2499.9 (4)
Fe(1)	1229.6 (6)	1296.1 (7)	3585.8 (5)
Fe(2)	535.3 (6)	1868.3 (6)	1817.3 (5)
P	1613 (1)	456 (1)	2449 (1)
O(1)	722 (5)	-1171 (4)	4115 (4)
O(2)	329 (4)	2579 (5)	4739 (3)
O(3)	3310 (4)	1725 (5)	5128 (4)
O(4)	-955 (4)	16 (4)	284 (3)
O(5)	-977 (4)	3714 (4)	1232 (3)
O(6)	1566 (4)	3096 (5)	768 (4)
N	687 (4)	4494 (4)	3417 (4)
C(1)	880 (5)	-239 (6)	3878 (4)
C(2)	627 (5)	2102 (5)	4240 (4)
C(3)	2509 (5)	1544 (6)	4511 (5)
C(4)	-378 (5)	707 (5)	901 (4)
C(5)	-410 (5)	2993 (5)	1521 (4)
C(6)	1165 (5)	2577 (5)	1170 (4)
C(7)	1620 (4)	2877 (4)	3029 (4)
C(8)	1555 (4)	4122 (4)	3431 (4)
C(9)	579 (6)	5745 (6)	3823 (6)
C(11)	3009 (4)	691 (5)	2706 (4)
C(12)	3676 (5)	70 (7)	3438 (5)
C(13)	4757 (6)	187 (9)	3668 (6)
C(14)	5174 (6)	939 (8)	3221 (8)
C(15)	4541 (6)	1577 (8)	2500 (7)
C(16)	3431 (5)	1454 (7)	2233 (6)
C(21)	1228 (5)	-1214 (5)	1952 (4)
C(22)	1879 (5)	-1811 (6)	1617 (5)
C(23)	1515 (7)	-3095 (6)	1188 (5)
C(24)	629 (6)	-3710 (6)	1144 (5)
C(25)	-24 (6)	-3130 (6)	1480 (5)
C(26)	301 (5)	-1859 (5)	1886 (5)
C(31)	2562 (5)	4988 (5)	3907 (4)
C(32)	3041 (7)	5491 (7)	3390 (7)
C(33)	4015 (9)	6372 (11)	3907 (10)
C(34)	4428 (9)	6574 (11)	4849 (10)
C(35)	3955 (7)	6023 (10)	5340 (8)
C(36)	2995 (6)	5231 (8)	4874 (6)
C(41)	2819 (9)	1035 (18)	-1373 (8)
C(42)	2723 (7)	-91 (9)	-1959 (9)
C(43)	2301 (7)	-134 (10)	-2889 (8)
C(44)	1904 (9)	879 (12)	-3334 (9)
C(45)	1994 (8)	1954 (11)	-2830 (11)
C(46)	2421 (9)	2139 (12)	-1897 (12)
C(47)	3211 (16)	1282 (29)	-392 (14)
C(51)	6101 (19)	3971 (26)	-416 (20)
C(52)	5498 (21)	4623 (30)	-1234 (24)
C(53)	4743 (19)	3860 (27)	-2127 (22)
C(54)	4958 (14)	2590 (30)	-1971 (16)
C(55)	5548 (17)	1899 (19)	-1259 (22)
C(56)	6186 (16)	2569 (27)	-353 (19)
Cl	-2243 (2)	3798 (2)	2955 (2)
O(7)	-1429 (4)	3211 (5)	2897 (5)
O(8)	-1930 (9)	4881 (9)	3581 (9)
O(9)	-3178 (6)	3203 (8)	2576 (8)
O(10A)*	-2326 (13)	4786 (12)	2179 (11)
O(10B)*	-2294 (15)	2910 (15)	3792 (12)

framework with formation of discrete $[\text{Fe}_2\text{Ag}(\text{CO})_6][\text{CHC}(\text{NRR}^1)(\text{C}_6\text{H}_5)_2]\text{P}(\text{C}_6\text{H}_5)_2]^+$ cations and ClO_4^- anions. An ORTEP II plot of the molecular structure of **2** ($R = \text{H}$, $R^1 = \text{CH}_3$, $X = \text{ClO}_4$) is displayed in Figure 1. Selected bond lengths and angles are listed in Table III. Discrete organometallic cations $[\text{Fe}_2\text{Ag}(\text{CO})_6][\text{CHC}(\text{C}_6\text{H}_5)(\text{NHCH}_3)]\text{P}(\text{C}_6\text{H}_5)_2]^+$ and anions ClO_4^- are packed together in the crystal lattice. The silver atom interacts weakly with one double bond of the toluene molecule ($\text{Ag}-\text{C}(42) = 2.51$ (1) Å, $\text{Ag}-\text{C}(43) = 2.50$ (1) Å) and has an even weaker contact to a perchlorate oxygen atom ($\text{Ag}-\text{O}(7) = 2.686$ (6) Å) but is otherwise coordinated only to the two iron atoms.

The basic trinuclear skeleton of **2** consists of an almost equilateral triangle of two iron atoms and a silver atom

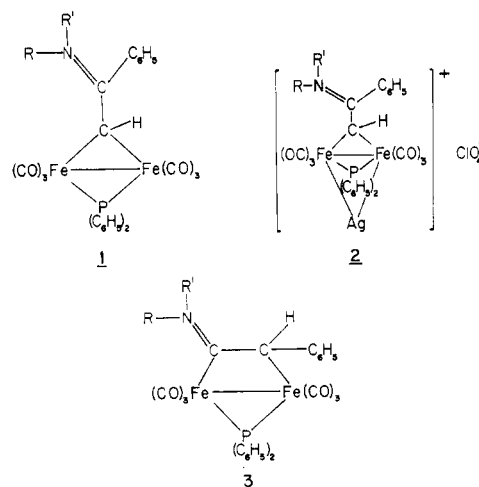
(16) "International Tables for X-ray Crystallography"; Kynoch Press: Birmingham, England, 1974; Vol. IV.

Table III. A Selection of Bond Lengths (Å) and Angles (deg) for $[\text{Fe}_2\text{Ag}(\text{CO})_6\{\text{CHC}(\text{NHCH}_3)(\text{C}_6\text{H}_5)\}_2\text{P}(\text{C}_6\text{H}_5)_2]\text{ClO}_4 \cdot \text{C}_6\text{H}_6 \cdot \text{C}_6\text{H}_5\text{CH}_3$

A. Bond Lengths					
Ag-Fe(1)	2.685 (1)	Fe(2)-C(5)	1.808 (7)	C(5)-O(5)	1.137 (8)
Ag-Fe(2)	2.703 (1)	Fe(2)-C(6)	1.762 (7)	C(6)-O(6)	1.151 (9)
Fe(1)-Fe(2)	2.682 (1)	Fe(2)-C(7)	2.048 (6)	C(7)-C(8)	1.459 (7)
Fe(1)-P	2.234 (2)	P-C(11)	1.829 (7)	C(8)-N	1.311 (9)
Fe(1)-C(3)	1.773 (7)	P-C(21)	1.838 (6)	C(8)-C(31)	1.496 (9)
Fe(1)-C(1)	1.811 (7)	C(1)-O(1)	1.118 (8)	N-C(9)	1.490 (9)
Fe(1)-C(2)	1.806 (7)	C(2)-O(2)	1.146 (9)	Ag-O(7)	2.686 (6)
Fe(1)-C(7)	2.083 (5)	C(3)-O(3)	1.142 (9)	Ag-C(42)	2.506 (11)
Fe(2)-P	2.217 (2)	C(4)-O(4)	1.139 (8)	Ag-C(43)	2.503 (12)
Fe(2)-C(4)	1.801 (6)				
B. Bond Angles					
Fe(1)-Ag-Fe(2)	59.7 (0)	C(3)-Fe(1)-C(7)	89.2 (2)	C(6)-Fe(2)-C(7)	90.7 (2)
Ag-Fe(1)-Fe(2)	60.5 (0)	Ag-Fe(2)-Fe(1)	59.8 (0)	Fe(1)-P-Fe(2)	74.1 (0)
Ag-Fe(1)-P	93.3 (0)	Ag-Fe(2)-P	93.2 (0)	Fe(1)-P-C(11)	114.0 (2)
Ag-Fe(1)-C(1)	80.9 (2)	Ag-Fe(2)-C(4)	75.9 (2)	Fe(1)-P-C(21)	123.6 (1)
Ag-Fe(1)-C(2)	73.3 (2)	Ag-Fe(2)-C(5)	76.0 (2)	Fe(2)-P-C(11)	123.1 (2)
Ag-Fe(1)-C(3)	167.1 (2)	Ag-Fe(2)-C(6)	166.0 (2)	Fe(2)-P-C(21)	119.2 (1)
Ag-Fe(1)-C(7)	97.0 (1)	Ag-Fe(2)-C(7)	97.3 (1)	C(11)-P-C(21)	102.5 (2)
Fe(2)-Fe(1)-P	52.7 (0)	Fe(1)-Fe(2)-P	53.2 (0)	Fe(1)-C(1)-O(1)	175.2 (3)
Fe(2)-Fe(1)-C(1)	122.5 (2)	Fe(1)-Fe(2)-C(4)	118.2 (2)	Fe(1)-C(2)-O(2)	172.7 (2)
Fe(2)-Fe(1)-C(2)	112.5 (2)	Fe(1)-Fe(2)-C(5)	114.8 (2)	Fe(1)-C(3)-O(3)	176.9 (2)
Fe(2)-Fe(1)-C(3)	130.7 (2)	Fe(1)-Fe(2)-C(6)	133.1 (2)	Fe(2)-C(4)-O(4)	176.2 (2)
Fe(2)-Fe(1)-C(7)	49.0 (1)	Fe(1)-Fe(2)-C(7)	50.1 (1)	Fe(2)-C(5)-O(5)	170.8 (2)
P-Fe(1)-C(1)	93.1 (2)	P-Fe(2)-C(4)	92.4 (2)	Fe(2)-C(6)-O(6)	176.4 (2)
P-Fe(1)-C(2)	164.5 (2)	P-Fe(2)-C(5)	167.5 (2)	Fe(1)-C(7)-Fe(2)	81.0 (0)
P-Fe(1)-C(3)	99.2 (2)	P-Fe(2)-C(6)	99.7 (2)	Fe(1)-C(7)-C(8)	117.6 (2)
P-Fe(1)-C(7)	76.7 (1)	P-Fe(2)-C(7)	77.7 (1)	Fe(2)-C(7)-C(8)	126.9 (2)
C(1)-Fe(1)-C(2)	92.4 (3)	C(4)-Fe(2)-C(5)	91.1 (2)	C(7)-C(8)-N	124.1 (3)
C(1)-Fe(1)-C(3)	95.0 (3)	C(4)-Fe(2)-C(6)	98.0 (3)	C(7)-C(8)-C(31)	116.3 (3)
C(1)-Fe(1)-C(7)	169.5 (2)	C(4)-Fe(2)-C(7)	167.9 (2)	N-C(8)-C(31)	119.6 (3)
C(2)-Fe(1)-C(3)	94.8 (3)	C(5)-Fe(2)-C(6)	91.7 (3)	C(8)-N-C(9)	126.3 (4)
C(2)-Fe(1)-C(7)	96.8 (2)	C(5)-Fe(2)-C(7)	97.1 (2)		

with the Fe-Fe bond bridged by a diphenylphosphido group and a single carbon atom of a dipolar $\mu\text{-}\eta^1\text{-alkylidene}$ ligand $\text{CH}_3(\text{H})^+\text{N}=\text{C}(\text{C}_6\text{H}_5)^-\text{CH}$. The iminium character of the bridging hydrocarbyl ligand is evident from the planarity at C(8) (the angles C(7)-C(8)-N, C(7)-C(8)-C(31), and N-C(8)-C(31) are 124.1 (3), 116.3 (3), and 119.6 (3)°, respectively) and the short $>\text{N}=\text{C}<$ bond length (C(8)-N = 1.311 (9) Å). The stereochemistry at the bridging alkylidene carbon atom C(7) is distorted tetrahedral with the very acute Fe(1)-C(7)-Fe(2) bond angle (81.0 (0)°) being typical for alkylidenes bridging strongly interacting metals.¹⁷ The structural features of the bridging alkylidene and phosphido groups remain essentially the same as in the precursors 1 (R = H, R¹ = $\text{c-C}_6\text{H}_{11}$ ⁶ and R = R¹ = C_2H_5 ¹⁸), the only significant differences being an increase in the angles subtended at the bridging atoms C(7) and P by the two iron atoms. Thus the angle at the alkylidene carbon atom in 1 (R = H, R¹ = $\text{c-C}_6\text{H}_{11}$, and R = R¹ = C_2H_5) averages 76.8 (0)°^{6,18} (cf. 81.0 (0)° in 2) and the Fe(1)-P-Fe(2) angle in 2 (R = H, R¹ = CH_3 , X = ClO_4) is 74.1 (0)° compared to an average of 70.3 (0)° in the two precursor type species 1. These angular increases appear to be a direct consequence of a lengthening of the Fe-Fe bond by ~ 0.12 Å on formation of the silver adduct since the average Fe-Fe distance in the two compounds of type 1^{6,18} (2.563 Å) is significantly shorter than in 2 (Fe(1)-Fe(2) = 2.682 (1) Å). Protonation of the metal-metal bond in the dimer $\text{Fe}_2(\mu\text{-SCH}_3)_2(\text{CO})_4[\text{P}(\text{CH}_3)_2\text{C}_6\text{H}_5]_2$ produces an Fe-Fe bond lengthening of the same order of magnitude.¹⁹ Somewhat surprisingly the two Ag-Fe distances (Ag-Fe(1)

= 2.685 (1); Ag-Fe(2) = 2.703 (1) Å are comparable to the Fe(1)-Fe(2) bond length despite the difference in covalent radii between iron (1.26 Å) and silver (1.44 Å).²⁰ To our knowledge these Ag-Fe distances are the first values reported for bonds between these two metals. Few other metal-silver bond lengths are available for comparison, but it is interesting that in $[(\eta^5\text{-C}_5\text{H}_5)\text{Rh}(\text{CO})\text{P}(\text{C}_6\text{H}_5)_3]_2\text{Ag}[\text{PF}_6]$ ¹¹ where the silver atom is also two-coordinate, the Rh-Ag distances (2.651 (1), 2.636 (1) Å) are slightly shorter than the Fe-Ag bond lengths in 2.



(17) Herrmann, W. A. *Adv. Organomet. Chem.* 1982, 20, 159 and references therein.

(18) Carty, A. J.; Taylor, N. J.; Smith, W. F.; Paik, H. N.; Yule, J. E. *J. Chem. Soc., Chem. Commun.* 1976, 41.

(19) Savariault, J. M.; Bonnet, J. J.; Mathieu, R.; Galy, J. C. *C.R. Hebd. Seances Acad. Sci.* 1977, 284, 663.

(20) An approximate value for the covalent radius of Fe(0) pertinent to the present situation is half of the average Fe-Fe distance in the triply bridged compounds $\text{Fe}_2(\text{CO})_9$ (2.523 (1) Å²¹ and $\text{Na}[\text{H Fe}_2(\text{CO})_9]$ (2.521 (1) Å.²² This value is the same as that estimated by Pauling²³ for the metallic (12) radius. For silver the Pauling metallic (12) value is 1.44 Å.

Table IV. IR Stretching Frequencies and Mössbauer Parameters for the Complexes $[\text{Fe}_2\text{Ag}(\text{CO})_6\{\text{CHC}(\text{NR}^1)(\text{C}_6\text{H}_5)\}_2\text{P}(\text{C}_6\text{H}_5)_2]_2^+\text{X}^-$

R	R ¹	X	$\nu(\text{CO}), \text{cm}^{-1}$	$\nu(\text{N-H}),^a \text{cm}^{-1}$	$\nu(\text{C=N}),^a \text{cm}^{-1}$	$\nu(\text{anion}),^a \text{cm}^{-1}$	$\delta, \text{mm s}^{-1}$	$\Delta, \text{mm s}^{-1}$	$\Gamma, \text{mm s}^{-1}$
H	CH ₃	ClO ₄	2050 (vw), 2025 (s), ^b 1980 (s, br)	3290 (w, br)	1575 (s), 1565 (s)	1050-1150 (s, br)	0.21	0.38	0.30
H	C ₂ H ₅	ClO ₄	2050 (vw), 2025 (s), ^b 1980 (s, br)	3295 (w, br)	1580 (s), 1567 (s)	1050-1150 (s, br)	0.21	0.39	0.29
H	CH(CH ₃) ₂	ClO ₄	2047 (vw), 2024 (s), ^b 1949 (s, br)	3285 (w)	1550 (s)	1050-1150 (s, br)	0.21	0.34	0.28
H	c-C ₆ H ₁₁	ClO ₄	2049 (vw), 2024 (s), ^b 1979 (s, br)	3275 (w)	1540 (s)	1050-1150 (s, br)	0.25	0.33	0.28
C ₂ H ₅	C ₂ H ₅	ClO ₄	2047 (m), 2020 (s), ^a 1970 (s, br)		1530 (s)	1050-1150 (s, br)	0.20	0.43	0.36
H	CH ₃	PF ₆	2050 (vw), 2025 (s), ^b 1980 (s, br)	3290 (w, br)	1585 (s), 1570 (s)	840 (s, br)	0.22	0.35	0.28

^a Nujol mull. ^b CHCl₃ solvent.

Table V. ¹H and ³¹P NMR Data for the Complexes $[\text{Fe}_2\text{Ag}(\text{CO})_6\{\text{CHC}(\text{NR}^1)(\text{C}_6\text{H}_5)\}_2\text{P}(\text{C}_6\text{H}_5)_2]_2^+\text{X}^-$

R	R ¹	X	$\delta(^1\text{H})$	$\delta(^{31}\text{P})^a$
H	CH ₃	ClO ₄ ^d	2.33 (dd, CH, ³ J _{P-H} = 23 Hz, ² J _{107-109Ag-H} = 2 Hz), 3.04 (d, CH ₃ , ³ J _{H-H} = 5 Hz), 6.97 (m), 7.94 (m, C ₆ H ₅) ^b	173.4 (dd, P(C ₆ H ₅) ₂ , ² J _{107Ag-P} = 28.22 Hz, ² J _{109Ag-P} = 32.40 Hz) ^c 173.4 (d, P(C ₆ H ₅) ₂ , ² J _{107-109Ag-P} = 30 Hz)
H	C ₂ H ₅	ClO ₄	1.19 (t, CH ₃ , ³ J _{H-H} = 7 Hz), 2.38 (d, CH, ³ J _{P-H} = 22 Hz), 3.42 (m, CH ₂), 7.00 (m), 7.87 (m, C ₆ H ₅) ^b	173.4 (d, P(C ₆ H ₅) ₂ , ² J _{107-109Ag-P} = 30 Hz)
H	CH(CH ₃) ₂	ClO ₄	1.31 (d, CH ₃ , ³ J _{H-H} = 6 Hz), 2.33 (d, CH, ³ J _{P-H} = 22 Hz) ^b	174.5 (d, P(C ₆ H ₅) ₂ , ² J _{107-109Ag-P} = 24 Hz)
H	c-C ₆ H ₁₁	ClO ₄	1.04-2.07 (m, c-C ₆ H ₁₁), 2.38 (d, CH, ³ J _{P-H} = 22 Hz), 7.16 (m), 8.00 (m, C ₆ H ₅) ^b	176.6 (d, P(C ₆ H ₅) ₂ , ² J _{107-109Ag-P} = 32 Hz)
H	CH ₃	PF ₆	2.47 (d, CH, ³ J _{P-H} = 25 Hz), 3.07 (d, CH ₃ , ³ J _{H-H} = 5 Hz), 7.01 (m), 8.04 (m, C ₆ H ₅) ^a	174.1 (d, P(C ₆ H ₅) ₂ , ² J _{107-109Ag-P} = 30 Hz), -142.3 (spt, PF ₆ , ¹ J _{F-P} = 706 Hz)

^a (CD₃)₂CO solvent. ^b CDCl₃ solvent. ^c -90 °C, spectrometer frequency 36.42 MHz. ^d ¹H NMR of the precursor complex $[\text{Fe}_2(\text{CO})_6\{\text{CHC}(\text{NHCH}_3)(\text{C}_6\text{H}_5)\}_2\text{P}(\text{C}_6\text{H}_5)_2]$ in CDCl₃ has $\delta(\text{CH})$ at 1.74 (d, ³J_{P-H} = 35 Hz) and $\delta(\text{CH}_3)$ at 3.00 (d, ³J_{H-H} = 5 Hz).

An alternative stereochemical description of the molecule emphasises the structural relationship to $\text{Fe}_2(\text{CO})_6\text{X}_3$ species, where X is a bridging ligand and the three X groups contribute a total of six electrons to the system and support a metal-metal interaction. In 2 (R = H, R¹ = CH₃, X = ClO₄) there are three bridges (Ag⁺, P(C₆H₅)₂, and ⁻CHC(NHCH₃)⁺C₆H₅, and all of the Fe-X-Fe angles are acute (Fe(1)-Ag-Fe(2) = 59.7 (0)°; Fe(1)-P-Fe(2) = 74.1 (0)°; Fe(1)-C(7)-Fe(2) = 81.0 (0)°; cf. Fe(1)-C-Fe(2) of 77.6 (0)° in $\text{Fe}_2(\text{CO})_9$; ²¹ Fe(1)-Ge-Fe(2) of 70.0 (2)° in $\text{Fe}_2(\text{CO})_6[\text{Ge}(\text{CH}_3)_2]$.²⁴ In electronic terms the phosphido and alkylidene ligands in 1 and 2 provide a total of six electrons to the dimers; in $\text{Fe}_2(\text{CO})_9$ and $\text{Fe}_2(\text{CO})_6[\text{Ge}(\text{C}-\text{H}_3)_2]_3$ the same number of electrons are contributed by three CO or Ge(CH₃)₂ ligands. It follows that while each iron atom in 1 has a full complement of 18 electrons, there is a coordination site available in a bridging position. Seen in this light, the insertion of Ag⁺, an electrophile and like H⁺ a formal zero electron donor, into the bridging site is not unexpected. Such reactions can of course be considered as simple protonation or metalation of a bent metal-metal bond. Since Ag⁺ provides no electrons for cluster bonding, the metal-metal interactions within the Fe₂Ag triangle are formally electron deficient. As such a two-

electron, three-center bonding scheme, encompassing silver ion and both iron atoms might be appropriate. It is, however, pertinent to note that the Fe-Fe bond distance (2.682 (1) Å) is well short of the value found in $[\eta^5\text{-C}_5\text{H}_5\text{Fe}(\text{CO})(\mu\text{-SMe})_2]^+$ (2.925 (4) Å) considered as containing a one-electron iron-iron bond.²⁵ Whether Fe-Fe bonding occurs along the Fe...Fe vector in 2 or simply through the bridging ligand atoms is a question of some interest that we are currently pursuing. An examination of bond distances within the "inner cores" of the two molecules 1 (R = H, R¹ = C₆H₁₁) and 2 (R = H, R¹ = CH₃, X = ClO₄) does not reveal any significant changes in Fe-C(alkylidene)(average 2.061 Å in 1 vs. 2.065 Å in 2) or Fe-P distances (average 2.233 Å in 1 vs. 2.225 Å in 2) despite the elongation of the Fe-Fe bond on adduct formation. The carbonyl IR frequencies (vide infra) are however indicative of somewhat reduced back donation to the CO groups in 2, and there is noticeable lengthening of the Fe-C(CO *trans* to C(7) bond lengths (Fe(1)-C(1) = 1.776 (3) and Fe(2)-C(4) = 1.775 (3) Å in 1 vs. Fe(1)-C(1) = 1.811 (7) and Fe(2)-C(4) = 1.801 (6) Å in 2) on addition of Ag⁺. The relatively minor modifications to the binuclear framework of 1 on addition of Ag⁺ can however be contrasted with the dramatic changes in geometry that accompany two-electron reduction of $\text{Fe}_2(\text{CO})_6(\mu\text{-PPh}_2)_2$ ²⁶ or addition of SCH₃⁺ to $\text{Fe}_2(\text{CO})_6[\mu\text{-SCH}_3]_2$.²⁷ In the former

(21) Cotton, F. A.; Troup, J. M. *J. Chem. Soc., Dalton Trans.* 1974, 800.

(22) Chin, H. B. PhD Thesis, University of California, Los Angeles, 1975.

(23) Pauling, L. "The Nature of the Chemical Bond", 3rd ed.; Cornell University Press: Ithaca, NY, 1960.

(24) (a) Brooks, E. H.; Elder, M.; Graham, W. A. G.; Hall, D. *J. Am. Chem. Soc.* 1968, 90, 3587; (b) Elder, M.; Hall, D. *Inorg. Chem.* 1969, 8, 1424.

(25) Connelly, N. G.; Dahl, L. F. *J. Am. Chem. Soc.* 1970, 92, 7472.

(26) Ginsburg, R. E.; Rothrock, R. K.; Finke, R. G.; Collman, J. P.; Dahl, L. F. *J. Am. Chem. Soc.* 1979, 101, 6550.

(27) Schultz, A. J.; Eisenberg, R. *Inorg. Chem.* 1973, 12, 518.

the two electrons enter a molecular orbital that is metal-metal antibonding.

Spectroscopic Data. The $\nu(\text{CO})$ infrared spectra of 2 in CHCl_3 (Table IV) consist of three bands, displaced ca. 15 cm^{-1} to higher frequencies than those of the precursors 1. Slightly larger displacements of terminal $\nu(\text{CO})$ frequencies occur for $\text{Fe}_2(\text{CO})_6\{\text{CHC}(\text{NHR}^1)\text{C}_6\text{H}_5\}\{\text{P}(\text{C}_6\text{H}_5)_2\}_2\text{HgCl}_2$ ($\sim 35\text{ cm}^{-1}$),²⁸ $\text{Fe}_2(\text{CO})_6[\mu\text{-P}(\text{CH}_3)_2]_2\text{HgCl}_2$ ($\sim 35\text{ cm}^{-1}$),²⁹ and $\text{Fe}(\text{CO})_6(\mu\text{-SCH}_3)_2\text{P}(\text{CH}_3)_3\text{SO}_2$ ($\sim 40\text{ cm}^{-1}$)³⁰ and still greater shifts to higher frequency for mononuclear complexes of group 6A³¹ and iron.³² Although for the binuclear compounds these shifts may provide some indication of the extent of removal of electron density from the M-M bond on addition of a Lewis acid, the spectroscopic data can be misleading. For example in the SO_2 adduct $\text{Fe}_2(\text{CO})_6(\mu\text{-SCH}_3)_2\text{P}(\text{CH}_3)_3\text{SO}_2$ the Fe...Fe distance is considered nonbonding.³⁰

In the ^1H NMR spectrum of 2 ($\text{R} = \text{H}$, $\text{R}^1 = \text{CH}_3$, $\text{X} = \text{ClO}_4$) (Table V) the resonance of the unique hydrogen on the bridging alkylidene carbon atom appears as a doublet of doublets due to coupling to both ^{31}P ($^3J_{\text{P-H}} = 23\text{ Hz}$) and $^{107,109}\text{Ag}$ ($^3J_{\text{Ag-H}} = 2\text{ Hz}$) nuclei. This resonance appears 0.36 ppm downfield of the shift in 1 ($\text{R} = \text{H}$, $\text{R}^1 = \text{CH}_3$) and presumably reflects a drift of electron density from C(7) to the diiron center as compensation for formation of the diiron-silver donor-acceptor interaction. At 183 K the ^{31}P (PPh_2) resonances of the complex 2 ($\text{R} = \text{H}$, $\text{R}^1 = \text{CH}_3$, $\text{X} = \text{ClO}_4$) consist of a well-resolved doublet of doublets due to coupling of phosphorus to both magnetic isotopes of silver. The ratio of $^2J_{\text{Ag-P}}/^2J_{\text{Ag-P}}$ (1.148) agrees well with the expected ratio of the magnetic moments (1.149)³³ for the two isotopes of silver. The room-temperature ^{31}P NMR spectra of 2 appear as a broad doublet; solvent-exchange processes involving the silver atom are most likely responsible for spectral broadening. The ^{31}P (PPh_2) chemical shifts of 2 are 15–20 ppm downfield of the corresponding resonances in 1, qualitatively consistent with a longer Fe-Fe bond and larger Fe-P-Fe angle.⁷

Mössbauer spectra of complexes 2 consist of two well-resolved lines indicative of essential electronic and structural equivalence of the two iron sites. We noted above the structural analogy between 2 and $\text{Fe}_2(\text{CO})_9$. This is further emphasized by the similarity of Δ values for these compounds ($\Delta = 0.37\text{ mm s}^{-1}$ ($\text{Fe}_2(\text{CO})_9$); $\Delta = 0.42\text{ mm s}^{-1}$ (2, $\text{R} = \text{H}$, $\text{R}^1 = \text{CH}_3$, $\text{X} = \text{ClO}_4$)) that are at the extreme low end of the range for distorted seven-coordinate geometry at iron.³⁴

Comments on the Reactions of Silver Salts³⁶ with $\mu\text{-}\eta^1\text{-}$ and $\mu\text{-}\eta^2\text{-}$ Alkylidene Complexes. In earlier papers we showed that $\nu(\text{CO})$ frequencies are lower for $\mu\text{-}\eta^1\text{-}$ alkylidenes of type 1 than for $\mu\text{-}\eta^2$ complexes of type 3.^{6,18} These differences indicate greater delocalization of electron density into the $\text{Fe}_2(\text{CO})_6(\text{P})$ core in 1 than 3. It is interesting therefore that addition of Ag^+ to complexes 3 leads not to isolable adducts but to a two-electron oxidation of the metal-metal bond and deposition of a silver mirror. This rather surprising result suggests that the isolation of discrete silver adducts may be initially dependent on the oxidation-reduction potential of the metal-metal bonded complex used as a reactant. Support for this conclusion derives from the fact that while silver(1+) has frequently been used as a selective one-electron oxidant in inorganic and organometallic chemistry^{35,36} relatively few instances of adduct formation resulting in metal-silver bond synthesis have been reported. Hackett and Manning⁹ have described a variety of carbonyl complexes containing transition-metal-silver bonds (e.g., $\text{Me}_4\text{N}\{(\eta^5\text{-C}_5\text{H}_5)\text{M}(\text{CO})_3\}_2\text{Ag}$ ($\text{M} = \text{Cr}, \text{Mo}, \text{W}$), but these were generally synthesized by metathetical reactions. Chini and co-workers³⁷ have reported the formation of $\text{Et}_4\text{N}[\text{Ag}(\text{Co}(\text{CO})_4)_2]$ by direct addition of silver(1+) iodide to 2-propanol solutions of $\text{Na}[\text{Co}(\text{CO})_4]$, and recently some remarkable polynuclear rhodium-silver clusters have been synthesized.³⁸ This latter report, together with the isolation¹¹ of the adduct $[\{(\eta^5\text{-C}_5\text{H}_5)\text{Rh}(\text{CO})\text{P}(\text{C}_6\text{H}_5)_3\}_2\text{Ag}]\text{PF}_6$, a source of the radical cation $[(\eta^5\text{-C}_5\text{H}_5)\text{Rh}(\text{CO})\text{P}(\text{C}_6\text{H}_5)_3]^+$, and the present work suggests that silver-transition-metal chemistry may have a number of unique features worthy of exploration.

Acknowledgment. We are grateful to the Natural Sciences and Engineering Research Council of Canada for financial support of the work.

Registry No. 1 ($\text{R} = \text{CH}_3$, $\text{R}^1 = \text{H}$), 70657-55-5; 1 ($\text{R} = \text{C}_2\text{H}_5$, $\text{R}^1 = \text{H}$), 70657-57-7; 1 ($\text{R} = \text{CH}(\text{CH}_3)_2$, $\text{R}^1 = \text{H}$), 82647-69-6; 1 ($\text{R} = \text{c-C}_6\text{H}_{11}$, $\text{R}^1 = \text{H}$), 67168-85-8; 1 ($\text{r} = \text{R}^1 = \text{C}_2\text{H}_5$), 59584-64-4; 2 ($\text{R} = \text{H}$, $\text{R}^1 = \text{CH}_3$, $\text{X} = \text{ClO}_4$), 84280-70-6; 2 ($\text{R} = \text{H}$, $\text{R}^1 = \text{C}_2\text{H}_5$, $\text{X} = \text{ClO}_4$), 84280-72-8; 2 ($\text{R} = \text{H}$, $\text{R}^1 = \text{CH}(\text{CH}_3)_2$, $\text{X} = \text{ClO}_4$), 84280-74-0; 2 ($\text{R} = \text{H}$, $\text{R}^1 = \text{c-C}_6\text{H}_{11}$, $\text{X} = \text{ClO}_4$), 84280-76-2; 2 ($\text{R} = \text{R}^1 = \text{C}_2\text{H}_5$, $\text{X} = \text{ClO}_4$), 84280-78-4; 2 ($\text{R} = \text{H}$, $\text{R}^1 = \text{CH}_3$, $\text{X} = \text{PF}_6$), 84280-79-5; 3 ($\text{R} = \text{CH}_3$, $\text{R}^1 = \text{H}$), 73970-08-8; 3 ($\text{R} = \text{C}_2\text{H}_5$, $\text{R}^1 = \text{H}$), 73979-53-0; 3 ($\text{R} = \text{CH}(\text{CH}_3)_2$, $\text{R}^1 = \text{H}$), 82647-71-0.

Supplementary Material Available: Table S1, anisotropic thermal parameters, Table S2, remaining bond lengths and angles, and a listing of observed and calculated structure factors for $[\text{Fe}_2\text{Ag}(\text{CO})_6\{\text{CHC}(\text{C}_6\text{H}_5)\text{NH}(\text{CH}_3)\}\text{P}(\text{C}_6\text{H}_5)_2]\text{ClO}_4\cdot\text{C}_6\text{H}_5\text{CH}_3\cdot\text{C}_6\text{H}_6$ (28 pages). Ordering information is given on any current masthead page.

(36) For a classification of the reactions of silver ion with transition-metal organometallic compounds see: Baker, P. K.; Broadley, K.; Connelly, N. G.; Kelly, B. A.; Kitchen, M. D.; Woodward, P. *J. Chem. Soc., Dalton Trans.* 1980, 1710.

(37) Chini, P.; Martinengo, S.; Longoni, G. *Gazz. Chim. Ital.* 1975, 105, 203.

(38) Heaton, B. T., paper presented at the DIC Biennial Symposium "Chemistry Towards the 21st Century", Indiana University, May 1982.

(28) Mott, G. N. PhD Thesis, University of Waterloo, 1980.

(29) Arabi, M. S. Thèse, docteur D'Etat, Université Paul Sabatier de Toulouse, 1978.

(30) Taylor, N. J.; Arabi, M. S.; Mathieu, R. *Inorg. Chem.* 1980, 19, 1740.

(31) Edgar, K.; Johnson, B. F. G.; Lewis, J.; Wild, S. B. *J. Chem. Soc. A* 1968, 2851.

(32) Demerseman, B.; Bouquet, G.; Bigorgne, M. *J. Organomet. Chem.* 1972, 35, 341.

(33) Emsley, J. W.; Feeney, J.; Sutcliffe, L. H. "High Resolution Nuclear Magnetic Resonance Spectroscopy"; Pergamon Press: Elmsford, NY, 1966; Vol. 2, Appendix A.

(34) Greenwood, N. N.; Gibb, T. C. "Mössbauer Spectroscopy"; Chapman and Hall: London, 1971; p 221.

(35) Haines, R. J.; DuPreez, A. L. *Inorg. Chem.* 1972, 11, 330.

Communications

Organosilicon Rotanes: Synthesis and an Unexpected Rearrangement

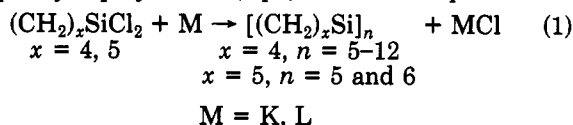
Corey W. Carlson, Xing-Hua Zhang, and Robert West*

Department of Chemistry, University of Wisconsin
Madison, Wisconsin 53706

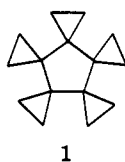
Received October 4, 1982

Summary: Reaction of 2.0 equiv of Li with $(\text{CH}_2)_4\text{SiCl}_2$ yields $[(\text{CH}_2)_4\text{Si}]_n$, $n = 5-12$; similarly, reaction of $(\text{C}-\text{H}_2)_5\text{SiCl}_2$ with 2.2 equiv of potassium gives $[(\text{CH}_2)_5\text{Si}]_n$, $n = 5$ and 6. If an excess of Li or potassium is used in the condensation of $(\text{CH}_2)_4\text{SiCl}_2$, $[(\text{CH}_2)_4\text{Si}]_6$ and a novel rearrangement product, **4**, are formed.

Recent reports have shown that cyclic polysilanes with a variety of alkyl substituents can be synthesized by alkali-metal condensation of the corresponding dialkyldichlorosilanes.¹ We have extended this approach to tetramethylenedichlorosilane $[(\text{CH}_2)_4\text{SiCl}_2]$ and pentamethylenedichlorosilane $[(\text{CH}_2)_5\text{SiCl}_2]$ and now describe the synthesis and initial characterization of several novel polyspirocyclopolysilanes (eq 1). These compounds are



silicon analogues to the carbocyclic rotanes² such as **1** and provide the first examples of rotane structures based on a central ring of silicon atoms.



To prepare the tetramethylenesilicon rotanes, $(\text{CH}_2)_4\text{SiCl}_2$ in dry THF was added dropwise to 2.0 equiv of lithium in dry THF at 0 °C.⁴ After 16 h, lithium chloride was removed by several cycles of concentration of the solution, addition of hexane, and filtration under argon. Evaporation of the solvent then left a waxy solid mixture that was separated by HPLC,⁵ yielding the rotanes

(1) (a) (*i*-Pr₂Si)₄; Watanabe, H.; Muraoka, T.; Kageyama, M.; Nagai, Y. *J. Organomet. Chem.* 1981, 216, C45-57. (b) (Me₂Si)₆; West, R.; Brough, L. F.; Wojnowski, W. *Inorg. Synth.* 1979, 19, 265-268. (c) (Me₂Si)_n; Brough, L. F.; West, R. *J. Am. Chem. Soc.* 1981, 103, 3049-3056. (d) (Et₂Si)_n; Carlson, C. W.; Matsumura, K.; West, R. *J. Organomet. Chem.* 1980, 194, C5-6. (e) (EtMeSi)_n; Katti, A.; Carlson, C. W.; West, R. unpublished studies. (f) (R₂Si)₆; Watanabe, H.; Muraoka, T.; Kohara, Y.; Nagai, Y. *Chem. Lett.* 1980, 735-736.

(2) Prange, T.; Pascod, C.; de Meijere, A.; Behrens, U.; Barnier, J.; Conia, J. *Nouv. J. Chim.* 1980, 5, 321-327. Fitjer, L. *Angew. Chem., Int. Ed. Engl.* 1976, 15, 763-4; Proksch, E.; de Meijere, A. *Tetrahedron Lett.* 1976, 52, 4851-4854. Ripoll, J. L.; Limasset, J. C.; Conia, J. M. *Tetrahedron* 1971, 27, 2431-2452.

(3) West, R. *J. Am. Chem. Soc.* 1954, 76, 6012-6014.

(4) This reaction requires degassed, peroxide-free THF and the exclusion of air since one of the products, $[(\text{CH}_2)_4\text{Si}]_6$, is moderately oxygen sensitive.

(5) MeOH/THF on a Whatman M-9 column containing Partisil-10 ODS was used.

Table I. Yields and NMR Data for Tetramethylenesilicon Rotanes

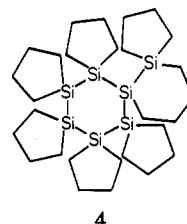
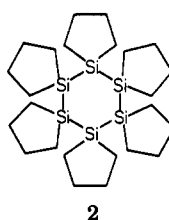
$[(\text{CH}_2)_4\text{Si}]_n$, $n =$	yield, % wt	¹³ C, ^{c,d} ppm	²⁹ Si, ^c ppm
5	20 ^a	9.50, 29.70	-29.85
6	39 ^a	10.43, 29.81	-29.37
7	14 ^a	11.17, 29.86	-29.85
8	7.3 ^b	11.93, 29.91	-28.68
9	5.5 ^b	12.52, 29.84	-26.50
10	2.6 ^b	12.70, 29.84	-23.91
11	2.9 ^b	12.70, 29.86	-24.58
12	1.4 ^b	12.77, 29.91	-24.80

^a GLC analysis. ^b HPLC analysis. ^c In benzene-*d*₆.
^d Intensity ratio for each pair is 1:1.

$[(\text{CH}_2)_4\text{Si}]_n$, where $n = 5-12$ (Table I).⁶ The HPLC results suggest that smaller amounts of additional rotanes, up to at least $n = 25$, are also present. This result closely resembles those from the analogous condensations of Me₂SiCl₂^{1c} and EtMeSiCl₂,^{1e} where reaction with exactly 2 equiv of lithium produces mixtures containing large-ring compounds.

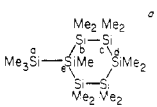
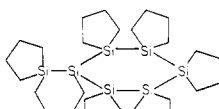
Condensation of $(\text{CH}_2)_5\text{SiCl}_2$ ³ was best effected by using 2.2 equiv of potassium in refluxing THF. The reaction mixture contained only two volatile products, $[(\text{CH}_2)_5\text{Si}]_5$ and $[(\text{CH}_2)_5\text{Si}]_6$ (in 40% and 11% yields, respectively, by GLC analysis). After 18 h, workup was carried out by the usual procedure,^{1b} and the crystalline rotanes were separated by successive recrystallization from ethanol-THF. In contrast to the facile reaction of lithium with other dialkyldichlorosilanes, the reaction of $(\text{CH}_2)_5\text{SiCl}_2$ with lithium proceeded slowly and gave mostly insoluble polymeric products.

The condensation of dialkyldichlorosilanes using excess lithium or potassium typically results in equilibration among the different rings and leads to high yields of the thermodynamically favored cyclosilane. Thus, the reaction of Me₂SiCl₂ with excess Na/K gives mainly (Me₂Si)₆, and the reaction of Et₂SiCl₂ with excess potassium gives predominantly (Et₂Si)₅. For $(\text{CH}_2)_4\text{SiCl}_2$, the products are quite different. When $(\text{CH}_2)_4\text{SiCl}_2$ was condensed with 2.2 equiv of lithium in THF at 0 °C and stirred for 12 h, the only products isolated were $[(\text{CH}_2)_4\text{Si}]_6$ (**2**, 28%) and a mixture consisting of $[(\text{CH}_2)_4\text{Si}]_7$ (**3**, 1%) and an isomer of $[(\text{CH}_2)_4\text{Si}]_7$ (12%), to which we assign structure **4**. Analogous results were obtained by using 2.2 equiv of potassium in refluxing THF. A mixture of **2** (45%), **3** (3%), and **4** (40%) was also obtained when **2** was stirred in THF solution with (triphenylsilyl)lithium for 48-72 h.



(6) All of the rotanes gave molecular weights by high-resolution mass spectrometry in agreement with the formulas assigned.

Table II

	chem shifts, ppm				
	Si _a	Si _b	Si _c	Si _d	Si _e
	-9.4	-38.8	-40.9	-42.3	-82.2
	-0.2	-27.1	-28.2	-29.4	-81.8

^a Reference 7; in CDCl₃. ^b In benzene-*d*₆ using Cr(acac)₃ as a paramagnetic relaxation agent. The intensities of the five lines were observed to be 1:2:2:1:1.

^c Also contains a [(CH₂)₄Si]₇, resonance at -29.85 ppm.

Isomers **3** and **4** could not be separated by either HPLC or GLC and were isolated as a mixture by HPLC.⁵ The identification of compound **4** was based primarily on its ²⁹Si NMR, which closely resembles the known spectrum of (trimethylsilyl)undecamethylcyclohexasilane,⁷ a permethyl compound with the same skeletal structure as **4** (Table II). A resonance for **3** is also found, and measurement of peak intensities establishes the ~12:1 ratio of **4**:**3** in the mixture.

Other spectral properties of **4** are in agreement with the assigned structure. The mass spectrum shows a base peak at *m/e* 588 corresponding to the parent molecular ion and fragments similar to those obtained from other cyclo-tetramethylenesilicon rotanes. The UV of the isomeric mixture [270 nm (sh, ε 4600), 245 (sh, 10500), 209 (sh, 44400)] closely matches **2** [275 nm (sh, ε 1200), 252 (5100), 208 (sh, 31300)], but not **3** [260 nm (sh, ε 5300), 236 (sh, 10000)]. The ¹³C NMR spectrum consists of 11 lines, falling into two groups from 10.4 to 17.7 ppm and from 27.1 to 29.5 ppm, assigned to carbons α and β to the silicon, respectively. The infrared spectrum shows only the C-H, C-C, and Si-C bands expected for **4**.

To see if the rearrangement leading to **4** would take place upon thermolysis, compound **2** was pyrolyzed neat, in an evacuated sealed tube, at 220 °C for 3 days. The only products were [(CH₂)₄Si]₅ (**5**, 15%), **2** (80%), and **3** (5%). Similar pyrolysis of **3** led to **5** (2%), **2** (3%), and recovered **3** (95%). The results show that **4** is not formed under these thermal conditions but that thermal redistribution of the cyclopolysilanes to give different ring sizes does take place. This is the first example of such thermal redistribution that has been reported.

The organosilicon rotanes are all colorless crystalline solids. Both [(CH₂)₅Si]₅ and [(CH₂)₅Si]₆ are inert to air, but the cyclo-tetramethylene compounds, especially **5**, tend to be mildly air sensitive. Although many of the chemical and physical properties of silicon rotanes resemble those of other peralkylcyclopolysilanes, some are rather different. A more complete account of our studies of these novel compounds will be published later.

Acknowledgment. This work was supported by the Air Force Office of Scientific Research, Air Force System Command, USAF, under Grant No. AFOSR 82-0067. The United States Government is authorized to reproduce and distribute reprints for governmental purposes notwithstanding any copyright notation thereon.

(7) Ishikawa, M.; Watanabe, M.; Iyoda, J.; Ikeda, H.; Kumada, M. *Organometallics* 1982, 1, 317.

Registry No. **2**, 84098-37-3; **3**, 84098-38-4; **4**, 84081-96-9; [(CH₂)₄Si]₅, 84081-92-5; [(CH₂)₄Si]₈, 84081-93-6; [(CH₂)₄Si]₉, 84098-39-5; [(CH₂)₄Si]₁₀, 84098-40-8; [(CH₂)₄Si]₁₁, 84098-41-9; [(CH₂)₄Si]₁₂, 84098-42-0; (CH₂)₄SiCl₂, 2406-33-9; (CH₂)₅SiCl₂, 2406-34-0; [(CH₂)₅Si]₅, 84081-94-7; [(CH₂)₅Si]₆, 84081-95-8; (tri-phenylsilyl)lithium, 791-30-0.

Silacrowns: Phase-Transfer Catalysts

Barry Arkles,* Kevin King, Roy Anderson, and William Peterson

Research Laboratories, Petrarch Systems Incorporated
Bristol, Pennsylvania 19007

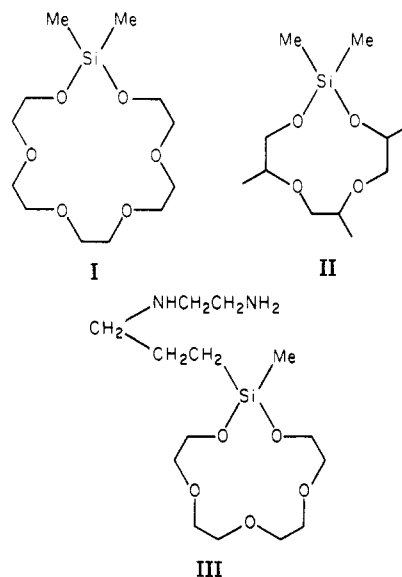
Received September 30, 1982

Summary: The synthesis, solubility enhancement, and phase-transfer catalysis properties of cyclic poly(alkyl-enoxy)silanes are described. The compounds have the

general structure R¹R²Si(OCH₂CH₂)_nO and are denoted silacrowns. Solubility enhancements of lithium, sodium, and potassium ions are a function of macrocycle and ion size. Phase-transfer catalysis of acetate, azide, cyanide, fluoride, and nitrite ions in displacement reactions are reported.

In the course of work on the immobilization of phase-transfer catalysts and in the transport of organic salts across liquid membranes, the ionophoric properties of silacrowns have been disclosed.^{1,2} Silacrowns have the

generalized structure R¹R²Si(OCH₂CH₂)_nO. Specific examples are dimethylsila-17-crown-6 (I), dimethylsila-3,6,9-trimethyl-11-crown-4 (II), and [3-(*N*-(2-aminoethyl)amino)propyl]methylsila-14-crown-5 (III). We now

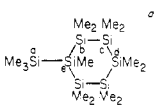
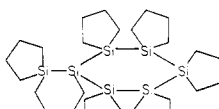


wish to report our preliminary findings on these materials. The silacrowns exhibit ionophoric properties that are

(1) Arkles, B.; King, K.; Peterson, W. In "Chemically Modified Surfaces in Catalysis and Electrocatalysis"; Miller, J. S., Ed.; American Chemical Society: Washington, D.C., 1982; ACS Symp. Ser. No. 192.

(2) Rico, E.; Pannell, K. H.; Arkles, B. "Transport of Na and K Picrates Across a Liquid Membrane Using New Silacrowns as Ionophores", presented 38th Southwest American Chemical Society, Meeting Dec 2, 1982.

Table II

	chem shifts, ppm				
	Si _a	Si _b	Si _c	Si _d	Si _e
	-9.4	-38.8	-40.9	-42.3	-82.2
	-0.2	-27.1	-28.2	-29.4	-81.8

^a Reference 7; in CDCl₃. ^b In benzene-*d*₆ using Cr(acac)₃ as a paramagnetic relaxation agent. The intensities of the five lines were observed to be 1:2:2:1:1.

^c Also contains a [(CH₂)₄Si]₇, resonance at -29.85 ppm.

Isomers 3 and 4 could not be separated by either HPLC or GLC and were isolated as a mixture by HPLC.⁵ The identification of compound 4 was based primarily on its ²⁹Si NMR, which closely resembles the known spectrum of (trimethylsilyl)undecamethylcyclohexasilane,⁷ a permethyl compound with the same skeletal structure as 4 (Table II). A resonance for 3 is also found, and measurement of peak intensities establishes the ~12:1 ratio of 4:3 in the mixture.

Other spectral properties of 4 are in agreement with the assigned structure. The mass spectrum shows a base peak at *m/e* 588 corresponding to the parent molecular ion and fragments similar to those obtained from other cyclo-tetramethylenesilicon rotanes. The UV of the isomeric mixture [270 nm (sh, ε 4600), 245 (sh, 10500), 209 (sh, 44400)] closely matches 2 [275 nm (sh, ε 1200), 252 (5100), 208 (sh, 31300)], but not 3 [260 nm (sh, ε 5300), 236 (sh, 10000)]. The ¹³C NMR spectrum consists of 11 lines, falling into two groups from 10.4 to 17.7 ppm and from 27.1 to 29.5 ppm, assigned to carbons α and β to the silicon, respectively. The infrared spectrum shows only the C-H, C-C, and Si-C bands expected for 4.

To see if the rearrangement leading to 4 would take place upon thermolysis, compound 2 was pyrolyzed neat, in an evacuated sealed tube, at 220 °C for 3 days. The only products were [(CH₂)₄Si]₅ (5, 15%), 2 (80%), and 3 (5%). Similar pyrolysis of 3 led to 5 (2%), 2 (3%), and recovered 3 (95%). The results show that 4 is not formed under these thermal conditions but that thermal redistribution of the cyclopolysilanes to give different ring sizes does take place. This is the first example of such thermal redistribution that has been reported.

The organosilicon rotanes are all colorless crystalline solids. Both [(CH₂)₅Si]₅ and [(CH₂)₅Si]₆ are inert to air, but the cyclo-tetramethylene compounds, especially 5, tend to be mildly air sensitive. Although many of the chemical and physical properties of silicon rotanes resemble those of other peralkylcyclopolysilanes, some are rather different. A more complete account of our studies of these novel compounds will be published later.

Acknowledgment. This work was supported by the Air Force Office of Scientific Research, Air Force System Command, USAF, under Grant No. AFOSR 82-0067. The United States Government is authorized to reproduce and distribute reprints for governmental purposes notwithstanding any copyright notation thereon.

(7) Ishikawa, M.; Watanabe, M.; Iyoda, J.; Ikeda, H.; Kumada, M. *Organometallics* 1982, 1, 317.

Registry No. 2, 84098-37-3; 3, 84098-38-4; 4, 84081-96-9; [(CH₂)₄Si]₅, 84081-92-5; [(CH₂)₄Si]₈, 84081-93-6; [(CH₂)₄Si]₉, 84098-39-5; [(CH₂)₄Si]₁₀, 84098-40-8; [(CH₂)₄Si]₁₁, 84098-41-9; [(CH₂)₄Si]₁₂, 84098-42-0; (CH₂)₄SiCl₂, 2406-33-9; (CH₂)₅SiCl₂, 2406-34-0; [(CH₂)₅Si]₅, 84081-94-7; [(CH₂)₅Si]₆, 84081-95-8; (tri-phenylsilyl)lithium, 791-30-0.

Silacrowns: Phase-Transfer Catalysts

Barry Arkles,* Kevin King, Roy Anderson, and William Peterson

Research Laboratories, Petrarch Systems Incorporated
Bristol, Pennsylvania 19007

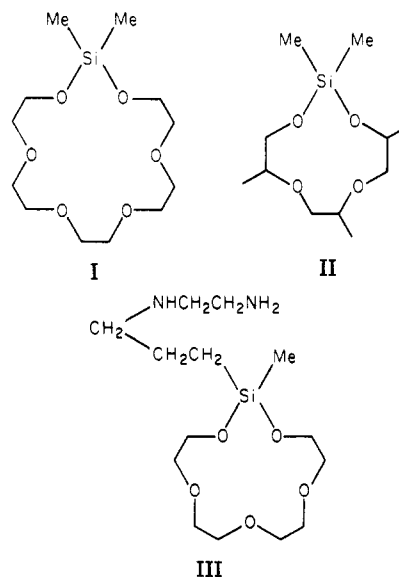
Received September 30, 1982

Summary: The synthesis, solubility enhancement, and phase-transfer catalysis properties of cyclic poly(alkyl-enoxy)silanes are described. The compounds have the

general structure R¹R²Si(OCH₂CH₂)_nO and are denoted silacrowns. Solubility enhancements of lithium, sodium, and potassium ions are a function of macrocycle and ion size. Phase-transfer catalysis of acetate, azide, cyanide, fluoride, and nitrite ions in displacement reactions are reported.

In the course of work on the immobilization of phase-transfer catalysts and in the transport of organic salts across liquid membranes, the ionophoric properties of silacrowns have been disclosed.^{1,2} Silacrowns have the

generalized structure R¹R²Si(OCH₂CH₂)_nO. Specific examples are dimethylsila-17-crown-6 (I), dimethylsila-3,6,9-trimethyl-11-crown-4 (II), and [3-(*N*-(2-aminoethyl)amino)propyl]methylsila-14-crown-5 (III). We now



wish to report our preliminary findings on these materials. The silacrowns exhibit ionophoric properties that are

(1) Arkles, B.; King, K.; Peterson, W. In "Chemically Modified Surfaces in Catalysis and Electrocatalysis"; Miller, J. S., Ed.; American Chemical Society: Washington, D.C., 1982; ACS Symp. Ser. No. 192.

(2) Rico, E.; Pannell, K. H.; Arkles, B. "Transport of Na and K Picrates Across a Liquid Membrane Using New Silacrowns as Ionophores", presented 38th Southwest American Chemical Society, Meeting Dec 2, 1982.

comparable to crown ethers in both cation specificity and enhancement of anionic reactivities. The synthesis of silacrowns is facile. The presence of the silicon atom provides an opportunity to introduce organic moieties without precedent in other crown ether systems. The compounds have low levels of acute oral toxicity and appear to have at least substantially lower pseudoestrogenic effects than the simple crown ether analogues.

The lower members of the cyclic poly(ethyleneoxy)silanes have been previously reported.³ They were produced in relatively poor yield by the interaction of chlorosilanes with lower ethylene glycols. Concomitant with our initial report silacrown structures with as many as 14 ring members were prepared by interaction of dimethylaminosilanes with lower ethylene glycols.⁴ Dimethylsiladibenzo-14-crown-5 was produced in 15% yield by reaction of dimethyldichlorosilane with the disodium bis(phenolate) precursor.⁵ In no cases were the ionophoric properties of these materials evaluated.

The silacrowns are readily prepared by transesterification of alkoxy silanes with polyethylene glycols. A typical reaction is $R^1R^2Si(OEt)_2 + HO(CH_2CH_2O)_nH \rightarrow R^1R^2Si(OCH_2CH_2)_nO + 2EtOH$. The conditions of transesterification must be selected to promote cyclization in preference to polymerization. The reaction may be catalyzed by a variety of materials, but alkoxy titanates are generally preferred. A wide range of organic groups (R^1R^2) can be readily substituted to alter solubility, phase partition, and reactivity of the silacrowns. The reactants are combined, and approximately 80–95% of the alcohol is slowly distilled from the reaction mixture. The product is removed from the reaction mixture by distillation at reduced pressure. Rearrangement in the presence of transesterification catalysts during the course of distillation results in the preferential removal of the more volatile silacrowns from the equilibrating mixture. The silacrowns are generally colorless, odorless liquids of moderate viscosity. As expected, the electron-impact mass spectra of the compounds do not exhibit molecular ions; the highest mass ions correspond to the loss of radicals from the silicon atoms. Sila-14-crown-5, sila-17-crown-6, and sila-20-crown-7 structures have been prepared. Substituents on the silicon include methyl, vinyl, phenyl, ethyl, and methoxy groups. The compounds and yields are given in Table I. As an example, the synthesis of vinylmethyl-14-crown-5 is provided.

Vinylmethylsila-14-crown-5. A 250-mL single-necked flask equipped with a magnetic stirrer and heating mantle was charged with 0.5 mol (93 mL) of vinylmethyldiethoxysilane, 0.5 mol (86 mL) of tetraethylene glycol and 0.5 mL of tetrabutyl titanate. The mixture was stirred at 50–60 °C for 16 h with a cold finger distillation head in place. The pot temperature was increased to 85–100 °C, and about 50 mL of ethanol was removed. The mixture was then distilled under vacuum. The fraction boiling at 129–131 °C at 0.5 mm was collected. Approximately 62 g of vinylmethylsila-14-crown-5 was isolated. The compound was identified by infrared and organic mass spectroscopy. The compound did not exhibit a molecular ion but exhibited $(M - CH_3)^+$ at 247 and $(M - CH=CH_2)^+$ at 235.

Solubility enhancement data for various inorganic salts in acetonitrile was determined under conditions similar

Table I. Silacrowns Prepared by Transesterification

compd	bp, °C (p, mmHg)	yield, %
dimethylsila-8-crown-3 ^a	90 (50)	
dimethylsila-11-crown-4 ^a	96 (9)	85
dimethylsila-14-crown-5	125–130 (0.5)	79
dimethylsila-17-crown-6	168–170 (0.3)	78
dimethylsila-20-crown-7	240–244 (0.2)	73
ethylmethylsila-14-crown-5	130–133 (0.5)	81
vinylmethylsila-14-crown-5	129–131 (0.5)	47
phenylmethylsila-14-crown-5	180–185 (0.1–0.15)	43
vinylmethylsila-17-crown-6	169–172 (0.3)	54
methoxymethylsila-17-crown-6	170–172 (0.3)	32
dimethylsila-3,6,9-trimethyl-11-crown-4	125–129 (0.2–0.3)	69
[3-(N-(2-aminoethyl)amino)propyl]methylsila-14-crown-5	221–228 (0.1)	35

^a Reported in ref 3.

to those reported by Liotta and Dabdoub.⁶ Data for the silacrowns are in Table II. On first approximation it is attractive to compare silacrowns to the simple crown ethers. Although there is one less member in the ring of the silacrown, the longer silicon–oxygen bonds result in an O–Si–O unit that is 75% of the length of an O–CH₂CH₂–O unit. Summation of bond lengths indicate an overall macrocycle circumference reduction of 4.5% when sila-14-crown-5 is compared to 15-crown-5. This simplistic comparison does not take into account the puckered multidentate structure that the crown ethers assume in cation complexes. Specificities and solubility enhancements appear to be similar for the silacrowns and crown ethers. One interesting result is that the greatest solubility enhancement for KBr is achieved with sila-20-crown-7 rather than sila-17-crown-6. The enhancement value of the sila-20-crown-7 is comparable to that of 18-crown-6. Potassium ions are often considered to have the “just right” diameter to enter the cavity of 18-crown-6. In fact, the complex, while nearly planar, does exhibit slight puckering.⁷ Since the potassium ion is slightly larger than the cavity of 18-crown-6, steric factors must account for a substantial part of the difference in solubility.

The silacrowns depart from ideal crown ether structure in that the oxygens are not uniformly distributed and that they are not uniformly basic. In the case of the cyclic siloxanes that contain alternating silicon and oxygen atoms, efforts to facilitate simple anionic reactions gave negative results. The use of cyclic siloxanes under more extreme conditions to promote anionic polymerization give both negative and positive results.^{8,9} This is consistent with the observation that cyclic siloxanes are weak ionophores with stability constants far lower than those of crown ethers.^{10,11} Nevertheless, the work suggests that the re-

(6) Liotta, C. L. In “Synthetic Multidentate Macrocyclic Compounds” Izatt, R. M., Christensen, J. J., Eds.; Academic Press: New York, 1978.

(7) Seiler, P.; Dobler, M.; Dunitz, J. D. *Acta Crystallogr., Sect. B* 1974, B30, 2744.

(8) Yuzhelevskii, Yu; Pchelintsev, V.; Fedoseeva, N. *Vysokomol. Soedin., Ser. B* 1975, 18 (11), 873; *Chem. Abstr.* 1975 86, 73181.

(9) Karger-Kocsis, J.; Szafner, A. *Makromol. Chem.* 1978, 179, 519.

(10) Olliff, C.; Pickering, G.; Rutt, K. *J. Inorg. Nucl. Chem.* 1980, 42, 288.

(3) Kriehle, R.; Burkhard, C. *J. Am. Chem. Soc.* 1947, 69, 2689.

(4) Phung, V. H. T.; Pham, B. C.; Kober, F. *Z. Anorg. Allg. Chem.* 1981, 472, 75.

(5) Liptuga, R. I.; Irodionova, L. F.; Lozinskii *Zh. Obshch. Khim.* 1978, 48, 1185.

Table II. Dimethylsilacrown Solubility Enhancements^a

crown	salt				
	LiCl	NaBr	KBr	KN ₃	KCN
11-4	2:1-4:1	2:1-3:1	4:1-5:1		
14-5	6:1-8:1	5:1-6:1	9:1-11:1		
17-6	3:1-4:1	4:1-5:1	11:1-14:1	18:1-20:1	10:1-11:1
20-7			45:1-50:1		

^a Solubility enhancements are expressed as ratios of the saturation solubility in 0.15 M silacrown in acetonitrile vs. acetonitrile.

Table III. Silacrown Solid/Liquid Phase-Transfer Catalysis of Cyanide Substitution^a

reactant	cation	catalyst	time, h	yield, %
benzyl chloride	K		48	29
benzyl chloride	K		75	25
benzyl chloride	K	18-6	1	99
benzyl chloride	K	17-6	16	100
benzyl bromide	K		4	1
benzyl bromide	K		48	54
benzyl bromide	K	18-6	6	100
benzyl bromide	K	D ₅	16	20
benzyl bromide	K	17-6	16	100
benzyl bromide	Na		4	1
benzyl bromide	Na	14-5	16	100
benzyl bromide	K	14-5	4	3
allyl bromide	K		16	1
allyl bromide	K	14-5	16	1
allyl bromide	K	17-6	16	74
hexyl bromide	K	18-6	40	100
octyl bromide	K	17-6	48	63
octyl chloride	K		48	19
octyl chloride	K	17-6	48	63
[(<i>p</i> (<i>m</i>)-(chloromethyl)phenyl)ethyl]-trimethoxysilane (mixed isomers)	K	17-6	48	100
trimethylsilyl chloride	K	17-6	72	85

^a All reactions run at room temperature with 0.05 M of reactant in 25 mL of acetonitrile and 0.13 M catalyst with a 100% molar excess of CN unless otherwise noted. Reaction times and conditions were not optimized; analysis by GC: (1) literature value from ref 6; (2) decamethylcyclopentasiloxane; (3) mixture of allyl cyanide and crotonitrile; (4) at reflux; (5) 20% excess only of KCN at reflux; (6) [(cyanomethyl)phenyl]ethyl]trimethoxysilane bp 122-125 °C (0.4 mmHg); 94% recovered.

placement of a single OCH₂CH₂O unit for an OSiO unit in a crown ether would not eliminate its ability to form cation complexes. The reduced basicity of oxygen atoms in alkoxy silanes compared to those in ethers is greater than would be expected by comparison of dipole moments. In general, the dipole moments of Si-O-C bonds are greater than those of Si-O-Si bonds and similar to those of C-O-C bonds.¹² Although it is difficult to draw analogy between the Si-O and C-O bond due to the more electropositive nature of silicon and the nonbonding orbital interaction of silicon and oxygen atoms, it is at least plausible to suggest that dipole interactions of silacrowns should be comparable to those of crown ethers.

The substitution reaction of cyanide with benzyl, allyl, alkyl, and silyl halides was evaluated with and without silacrown-promoted catalysis (Table III). Reaction conditions and times were not optimized. Despite the difference in solubility enhancement, dimethylsila-17-crown-6 appeared to be equivalent to 18-crown-6. The specificity of the dimethylsila-14-crown-5 for sodium ions and not potassium ions demonstrated in the solubility enhancement data is substantiated in the catalysis data.

(11) Olliff, C.; Pickering, G.; Rutt, K. *J. Inorg. Nucl. Chem.* 1980, 42, 1201.

(12) Dipole moments of compounds with C-O-C, Si-O-C, and Si-O-Si bonds, from compiled sources (Handbook of Chemistry and Physics, and Voronkov, The Siloxane Bond):

MeOMe	1.30	Me ₂ SiOMe	1.18	Me ₃ SiOSiMe ₃	0.78
EtOEt	1.15	Me ₂ Si(OMe) ₂	1.33	(Me ₂ SiO) ₅	1.35
		Me ₂ Si(OEt) ₂	1.15		

Table IV. Sila-17-crown-6-Catalyzed Reactions of Benzyl Bromide with KX^a

reactant	product	yield, %
KCN	benzyl cyanide	100
KOAc	benzyl acetate	100
KF	benzyl fluoride	5-10
KF at reflux 48 h	benzyl fluoride	35
KN ₃	benzyl azide	99
KNO ₂	benzyl nitrite	0
KNO ₂ at reflux 24 h	benzyl nitrite ^b	5-10

^a Reactions after 16 h at ambient temperature with 0.13 M dimethylsila-17-crown-6. ^b Includes isomers.

Substitution reactions of halogens, pseudohalogens, and organic anions were evaluated (Table IV). Displacements by acetate and azide proceeded similarly to cyanide. The weaker nucleophiles, fluoride and nitrite required more vigorous conditions. In the case of the fluoride it is possible the silacrown is destroyed in the course of the reaction.

The most conspicuous difference in reactivity of the silacrowns compared to the simple crown ethers is the susceptibility of the Si-OC bond to hydrolysis, particularly at pH extremes. In liquid/liquid phase-transfer reactions utilizing concentrated aqueous KCN, no substantial differences in displacement reactions were observed.

The difference in silacrown hydrolytic stability compared to the simple crown ethers may account for their reduced acute oral toxicity. Toxic effects of crown ethers are observed in doses as low as 100 mg/kg, initially affecting the central nervous system.¹³ They exhibit unusual

long-term pseudoestrogenic effects even at low levels resulting in testicular atrophy.¹⁴ The acute oral toxicity (LD50) of dimethylsila-14-crown-5 for rats is 9900 mg/kg, compared to 1020 mg/kg for 15-crown-5.¹⁵ During the course of the studies histologic examination indicated no significant changes in testicular function.¹⁶

Registry No. I, 83890-22-6; II, 84332-76-3; III, 84332-77-4; LiCl, 7447-41-8; NaBr, 7647-15-6; KBr, 7758-02-3; KN₃, 20762-60-1; KCN, 151-50-8; KOAc, 127-08-2; KF, 7789-23-3; KNO₂, 7758-09-0; dimethylsila-14-crown-5, 70851-49-9; dimethylsila-20-crown-7, 83890-23-7; ethylmethylsila-14-crown-5, 84332-75-2; vinylmethylsila-14-crown-5, 83890-24-8; phenylmethylsila-14-crown-5, 83890-27-1; vinylmethylsila-17-crown-6, 83890-25-9; methoxymethylsila-17-crown-6, 83890-26-0; vinylmethyl-diethoxysilane, 5507-44-8; tetraethylene glycol, 112-60-7; benzyl chloride, 100-44-7; benzyl bromide, 100-39-0; allyl bromide, 106-95-6; hexyl bromide, 111-25-1; octyl bromide, 111-83-1; octyl chloride, 111-85-3; [(*p*-(*m*)-(chloromethyl)phenyl)ethyl]trimethoxysilane, 68128-25-6; trimethylsilyl chloride, 75-77-4; benzyl cyanide, 140-29-4; allyl cyanide, 109-75-1; crotonitrile, 4786-20-3; hexyl cyanide, 629-08-3; octyl cyanide, 2243-27-8; [((cyanomethyl)phenyl)ethyl]trimethoxysilane, 84332-74-1; cyanotrimethylsilane, 7677-24-9; benzyl acetate, 140-11-4; benzyl fluoride, 350-50-5; benzyl azide, 622-79-7; benzyl nitrite, 935-05-7.

(13) Leong, B. K. *J. Chem. Eng. News* 1975, 53 (4), 5.

(14) Leong, B. K. J.; Ts'o, T. O. T.; Chenoweth, M. B. *Toxicol. Appl. Pharmacol.* 1974, 27, 342.

(15) Hendrixson, R. R.; Mack, M. P.; Palmer, R. A.; Ottolenghi, A.; Ghirardelli, R. G.; *Toxicol. Appl. Pharmacol.* 1978, 44 (2), 263.

(16) Toxicology performed by Springborn Institute for Bioresearch at Spencerville, OH, under direction of Richard Hiles. Two survivors of the highest dose level (12300 mg/kg) showed lowest teste weight, although at lower levels no correlation was observed. The significance of this result is uncertain, but testicular function was normal in the animals. The lowest lethal dose observed (LDLO) was 4300 mg/kg.

Structure of the Tebbe Reagent. An Intramolecular Complex?

Michelle M. Francl¹ and Warren J. Hehre²

Department of Chemistry, University of California
Irvine, California 92717

Received August 24, 1982

Summary: The geometry of the Tebbe reagent, Cp₂TiCH₂/ClAlMe₂, is explored theoretically via ab initio (STO-3G) calculations on a model complex, H₂TiCH₂/ClAlH₂. The calculated structure of the model shows the Lewis acid ClAlH₂ to be strongly bound to the titanium alkylidene, rather than, as often represented, only weakly associated.

Transition-metal carbene complexes are ubiquitous species in organometallic chemistry, exhibiting behavior ranging from methylene transfer² to catalysis of olefin metathesis³ and oligomerization.⁴ The Tebbe reagent,⁵ Cp₂TiCH₂/ClAlMe₂ (1), displays a strikingly similar pattern of reactivity; it is a highly selective catalyst for me-

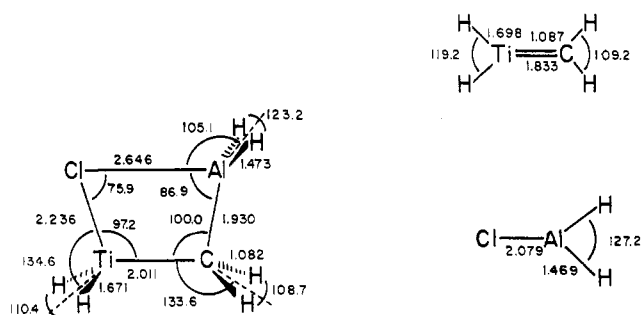
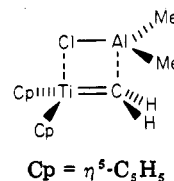
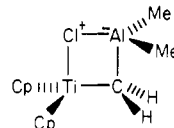


Figure 1. STO-3G optimized structure for H₂TiCH₂/ClAlH₂ (bond lengths in angstroms and angles in degrees).

tathesis of terminal olefins⁶ and an excellent methylenation agent.⁷ Hence 1 is often represented as a "protected" alkylidene complex, i.e., a weak complex between ClAlMe₂ and Cp₂Ti=CH₂.



Support for such a structure derives primarily from the parallels in observed chemistry. ¹H NMR results,⁵ however, are more suggestive of a cyclic structure, i.e.



Unfortunately, a lack of structural and thermochemical information about 1 makes it difficult to experimentally distinguish between these two limiting representations.

We report here the preliminary results of our theoretical investigations into the complexation of titanium alkylidenes with aluminum alkyl halides. Using the STO-3G^{8,9} basis set, we have obtained a structure for a model of the Tebbe reagent, H₂TiCH₂/ClAlH₂. This somewhat simplified model, in which hydrogen has been substituted for cyclopentadienyl ligands on titanium and for methyl groups on aluminum, was chosen to make the ab initio calculations more tractable. The titanium center on the model is extremely electron deficient, much more so than

(6) F. N. Tebbe, G. W. Parshall, and D. W. Ovenall, *J. Am. Chem. Soc.*, 101, 5074 (1979).

(7) S. H. Pine, R. Zahler, D. A. Evans, and R. H. Grubbs, *J. Am. Chem. Soc.*, 102, 3270 (1980).

(8) Although minimal basis sets have traditionally been thought to be inappropriate for use in ab initio calculations on transition metals, we have not found this to be so for all applications. While basis sets such as STO-3G do indeed perform poorly in some capacities, e.g., calculation of orbital energies, other tasks yield reasonable results. A brief comparison of available experimental and higher level theoretical data for group 4 metals with data from STO-3G calculations is presented in an earlier paper.¹² The results indicate a reasonable performance for STO-3G in the task of structure determinations, although it is clear that improved theoretical methods are necessary to accurately determine relative energetics. First row: (a) W. J. Hehre, R. F. Stewart, and J. A. Pople, *J. Chem. Phys.*, 51, 2657 (1969). Second row: W. J. Hehre, R. Ditchfield, R. F. Stewart, and J. A. Pople, *ibid.*, 52, 2769 (1970). First- and second-row transition metals: (c) W. J. Pietro and W. J. Hehre, *J. Comput. Chem.*, in press.

(9) All calculations have been performed by using the GAUSSIAN 83 program¹⁰ on Harris Corp. Slash 6, H100, and H800 digital computers.

(10) R. F. Hout, Jr., M. M. Francl, E. S. Blurock, W. J. Pietro, D. J. DeFrees, S. K. Pollack, B. A. Levi, R. Steckler, and W. J. Hehre, Quantum Chemistry Program Exchange, Indiana University, to be submitted for publication.

(1) Chevron Fellow.

(2) R. R. Schrock, *J. Am. Chem. Soc.*, 98, 5399 (1976).

(3) For a review see: T. J. Katz, *Adv. Organomet. Chem.* 16, 283 (1978).

(4) (a) R. R. Schrock, S. McLain, and J. Sancho, *Pure Appl. Chem.*, 52, 729 (1980); (b) J. D. Fellman, R. R. Schrock, and G. A. Rupprecht, *J. Am. Chem. Soc.*, 103, 5753 (1981).

(5) F. N. Tebbe, G. W. Parshall, and G. S. Reddy, *J. Am. Chem. Soc.*, 100, 3611 (1978).

long-term pseudoestrogenic effects even at low levels resulting in testicular atrophy.¹⁴ The acute oral toxicity (LD50) of dimethylsila-14-crown-5 for rats is 9900 mg/kg, compared to 1020 mg/kg for 15-crown-5.¹⁵ During the course of the studies histologic examination indicated no significant changes in testicular function.¹⁶

Registry No. I, 83890-22-6; II, 84332-76-3; III, 84332-77-4; LiCl, 7447-41-8; NaBr, 7647-15-6; KBr, 7758-02-3; KN₃, 20762-60-1; KCN, 151-50-8; KOAc, 127-08-2; KF, 7789-23-3; KNO₂, 7758-09-0; dimethylsila-14-crown-5, 70851-49-9; dimethylsila-20-crown-7, 83890-23-7; ethylmethylsila-14-crown-5, 84332-75-2; vinylmethylsila-14-crown-5, 83890-24-8; phenylmethylsila-14-crown-5, 83890-27-1; vinylmethylsila-17-crown-6, 83890-25-9; methoxymethylsila-17-crown-6, 83890-26-0; vinylmethyl-diethoxysilane, 5507-44-8; tetraethylene glycol, 112-60-7; benzyl chloride, 100-44-7; benzyl bromide, 100-39-0; allyl bromide, 106-95-6; hexyl bromide, 111-25-1; octyl bromide, 111-83-1; octyl chloride, 111-85-3; [(p-(m)-(chloromethyl)phenyl)ethyl]trimethoxysilane, 68128-25-6; trimethylsilyl chloride, 75-77-4; benzyl cyanide, 140-29-4; allyl cyanide, 109-75-1; crotonitrile, 4786-20-3; hexyl cyanide, 629-08-3; octyl cyanide, 2243-27-8; [((cyanomethyl)phenyl)ethyl]trimethoxysilane, 84332-74-1; cyanotrimethylsilane, 7677-24-9; benzyl acetate, 140-11-4; benzyl fluoride, 350-50-5; benzyl azide, 622-79-7; benzyl nitrite, 935-05-7.

(13) Leong, B. K. *J. Chem. Eng. News* 1975, 53 (4), 5.

(14) Leong, B. K. J.; Ts'o, T. O. T.; Chenoweth, M. B. *Toxicol. Appl. Pharmacol.* 1974, 27, 342.

(15) Hendrixson, R. R.; Mack, M. P.; Palmer, R. A.; Ottolenghi, A.; Ghirardelli, R. G.; *Toxicol. Appl. Pharmacol.* 1978, 44 (2), 263.

(16) Toxicology performed by Springborn Institute for Bioresearch at Spencerville, OH, under direction of Richard Hiles. Two survivors of the highest dose level (12300 mg/kg) showed lowest teste weight, although at lower levels no correlation was observed. The significance of this result is uncertain, but testicular function was normal in the animals. The lowest lethal dose observed (LDLO) was 4300 mg/kg.

Structure of the Tebbe Reagent. An Intramolecular Complex?

Michelle M. Francl¹ and Warren J. Hehre²

Department of Chemistry, University of California
Irvine, California 92717

Received August 24, 1982

Summary: The geometry of the Tebbe reagent, Cp₂TiCH₂/ClAlMe₂, is explored theoretically via ab initio (STO-3G) calculations on a model complex, H₂TiCH₂/ClAlH₂. The calculated structure of the model shows the Lewis acid ClAlH₂ to be strongly bound to the titanium alkylidene, rather than, as often represented, only weakly associated.

Transition-metal carbene complexes are ubiquitous species in organometallic chemistry, exhibiting behavior ranging from methylene transfer² to catalysis of olefin metathesis³ and oligomerization.⁴ The Tebbe reagent,⁵ Cp₂TiCH₂/ClAlMe₂ (1), displays a strikingly similar pattern of reactivity; it is a highly selective catalyst for me-

(1) Chevron Fellow.

(2) R. R. Schrock, *J. Am. Chem. Soc.*, 98, 5399 (1976).

(3) For a review see: T. J. Katz, *Adv. Organomet. Chem.* 16, 283 (1978).

(4) (a) R. R. Schrock, S. McLain, and J. Sancho, *Pure Appl. Chem.*, 52, 729 (1980); (b) J. D. Fellman, R. R. Schrock, and G. A. Rupprecht, *J. Am. Chem. Soc.*, 103, 5753 (1981).

(5) F. N. Tebbe, G. W. Parshall, and G. S. Reddy, *J. Am. Chem. Soc.*, 100, 3611 (1978).

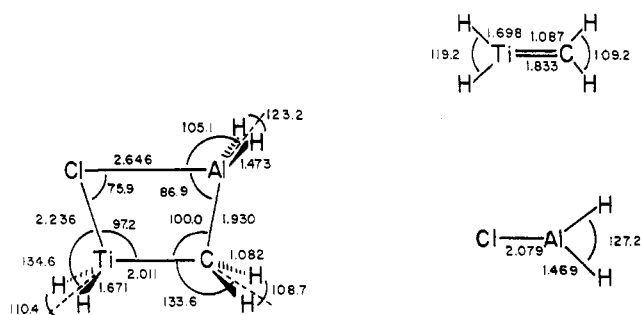
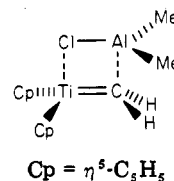
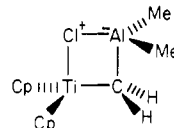


Figure 1. STO-3G optimized structure for H₂TiCH₂/ClAlH₂ (bond lengths in angstroms and angles in degrees).

tathesis of terminal olefins⁶ and an excellent methylenation agent.⁷ Hence 1 is often represented as a "protected" alkylidene complex, i.e., a weak complex between ClAlMe₂ and Cp₂Ti=CH₂.



Support for such a structure derives primarily from the parallels in observed chemistry. ¹H NMR results,⁵ however, are more suggestive of a cyclic structure, i.e.



Unfortunately, a lack of structural and thermochemical information about 1 makes it difficult to experimentally distinguish between these two limiting representations.

We report here the preliminary results of our theoretical investigations into the complexation of titanium alkylidenes with aluminum alkyl halides. Using the STO-3G^{8,9} basis set, we have obtained a structure for a model of the Tebbe reagent, H₂TiCH₂/ClAlH₂. This somewhat simplified model, in which hydrogen has been substituted for cyclopentadienyl ligands on titanium and for methyl groups on aluminum, was chosen to make the ab initio calculations more tractable. The titanium center on the model is extremely electron deficient, much more so than

(6) F. N. Tebbe, G. W. Parshall, and D. W. Ovenall, *J. Am. Chem. Soc.*, 101, 5074 (1979).

(7) S. H. Pine, R. Zahler, D. A. Evans, and R. H. Grubbs, *J. Am. Chem. Soc.*, 102, 3270 (1980).

(8) Although minimal basis sets have traditionally been thought to be inappropriate for use in ab initio calculations on transition metals, we have not found this to be so for all applications. While basis sets such as STO-3G do indeed perform poorly in some capacities, e.g., calculation of orbital energies, other tasks yield reasonable results. A brief comparison of available experimental and higher level theoretical data for group 4 metals with data from STO-3G calculations is presented in an earlier paper.¹² The results indicate a reasonable performance for STO-3G in the task of structure determinations, although it is clear that improved theoretical methods are necessary to accurately determine relative energetics. First row: (a) W. J. Hehre, R. F. Stewart, and J. A. Pople, *J. Chem. Phys.*, 51, 2657 (1969). Second row: W. J. Hehre, R. Ditchfield, R. F. Stewart, and J. A. Pople, *ibid.*, 52, 2769 (1970). First- and second-row transition metals: (c) W. J. Pietro and W. J. Hehre, *J. Comput. Chem.*, in press.

(9) All calculations have been performed by using the GAUSSIAN 83 program¹⁰ on Harris Corp. Slash 6, H100, and H800 digital computers.

(10) R. F. Hout, Jr., M. M. Francl, E. S. Blurock, W. J. Pietro, D. J. DeFrees, S. K. Pollack, B. A. Levi, R. Steckler, and W. J. Hehre, Quantum Chemistry Program Exchange, Indiana University, to be submitted for publication.

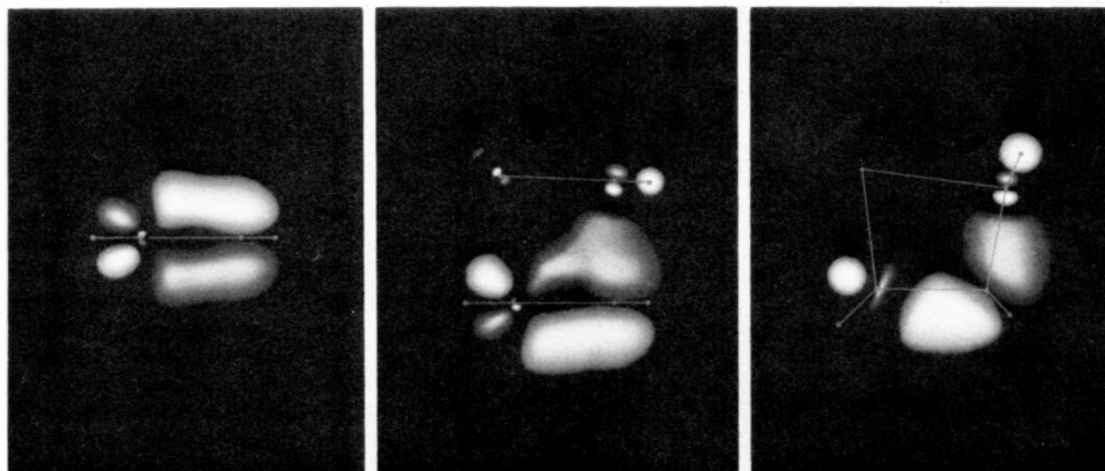
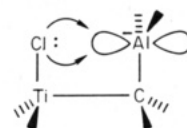


Figure 2. Left: π bond in $\text{H}_2\text{Ti}=\text{CH}_2$. Center: π bond in weak complex $\text{H}_2\text{Ti}=\text{CH}_2/\text{AlClH}_2$. Right: π bond in $\text{H}_2\text{TiCH}_2/\text{AlClH}_2$.

in the actual Tebbe reagent. Previous work has established that while geometrical changes accompanying saturation of the metal center are significant, they are uniform and easily anticipated. The TiC linkage in $\text{Cp}_2\text{Ti}(\text{CH}_3)\text{H}$, for example, is 2.14 Å at STO-3G, 0.05 Å longer than that in H_3TiCH_3 ; the multiple bond in $\text{Cp}_2\text{Ti}=\text{CH}_2$ is 1.876 Å compared to 1.833 Å in the 10-electron complex $\text{H}_2\text{Ti}=\text{CH}_2$.¹¹ Bond distances and angles calculated at STO-3G for $\text{Cp}_2\text{TiCH}_2\text{CHRCH}_2$ are in reasonable agreement with those determined experimentally for $\text{Cp}_2\text{TiCH}_2\text{CHRCH}_2$.¹² Thus, the model structure, while not the Tebbe reagent, would be expected to mimic the resultant changes in the alkylidene fragment upon complexation.

The calculated geometry of **2**, shown in Figure 1, differs greatly from those of separated metal carbene and Lewis acid fragments, which are also depicted. It does not support the notion that the two form a weakly bound complex. The TiC bond is nearly 0.2 Å longer than that in $\text{H}_2\text{Ti}=\text{CH}_2$ and approaches one appropriate for a normal single linkage, e.g., 2.096 Å in tetramethyltitanium,¹⁴ 2.053 Å in titanacyclobutane¹⁵ at the STO-3G level. Both the titanium-chloride and carbon-aluminum lengths, 2.236 Å and 1.930 Å, respectively, are only slightly longer than normal single bonds,¹⁶ e.g., 2.167 Å in TiCl_4 ¹⁷ and 1.899 Å in AlMe_3 ¹⁹ at the STO-3G level. On the other hand, the AlCl linkage in **2** is much longer than that in free Lewis acids, e.g., 2.050 Å in AlCl_3 at STO-3G.²⁰ All of these features, as well as the predicted orientation of the plane of the AlH_2

group (perpendicular rather than parallel to the TiC bond) suggest that the most appropriate representation of the model Tebbe reagent is in terms of a *intramolecular* complex, chlorine acting as the electron donor, aluminum as the acceptor, i.e.



The lengthening of TiC linkage in **2** strongly implies the destruction of the reactive π bond upon addition of the Lewis acid. Compare the highest occupied (π) molecular orbital of the uncomplexed alkylidene (Figure 2(left)) with that of a hypothetical weakly bound aluminum-alkylidene complex (Figure 2(center)).²¹ (We have simulated the weak complex by fixing the geometries of the alkylidene and Lewis acid at their respective STO-3G optimum values and optimizing only the intermolecular parameters.) The latter easily reveals its origin as the π bond of the uncomplexed structure and would be expected to react similarly. In contrast, the corresponding molecular orbital in the fully optimized complex **2**, also the highest occupied (Figure 2(right)), bears little resemblance to its antecedents. However, its reactivity should not be entirely different from that of the π bond in the weak complex. The symmetry of this orbital is the same, and it remains bonding between carbon and titanium (as well as between carbon and aluminum). As in the free carbene and in the weak complex, most of the density is localized on carbon, suggesting this as the likely site for electrophilic attack.

We do not expect these results to alter significantly on increased saturation of the titanium center. The principal structural changes expected, i.e., lengthening of the TiC and TiCl bonds, would, however, contribute to changes in the bonding of the complex. Reducing the Ti- CH_2 interaction should strengthen the Al-C bond, forcing the chlorine to continue in its role as donor to aluminum. On the other hand, the lessening of electron donation by chlorine to the transition-metal center will encourage donation to aluminum instead, probably at the expense of the Al-C bonding. The resultant effect of these opposing

(11) M. M. Francl, W. J. Pietro, R. F. Hout, Jr., and W. J. Hehre, *Organometallics*, **2**, 281-286 (1983).

(12) M. M. Francl and W. J. Hehre, unpublished results.

(13) J. B. Lee, G. J. Gajda, W. P. Schaefer, T. R. Howard, T. Ikariya, D. A. Strauss, and R. H. Grubbs, *J. Am. Chem. Soc.*, **103**, 7358 (1981).

(14) TiC bond lengths in low-temperature crystal structure for $\text{Ti}(\text{CH}_2\text{Ph})_4$ range from 2.04 to 2.21 Å. G. R. Davies, J. A. Jarvis, and B. T. Kilbourn, *J. Chem. Soc., Chem. Commun.* 1511 (1971).

(15) 2.127 and 2.113 Å in crystal structure for $\text{Cp}_2\text{TiCH}_2\text{CHPhCH}_2$.¹³

(16) In electron-deficient metal complexes, typical M-Cl bonds are much shorter than those in similar saturated systems, indicating significant donation by chlorine lone pairs to the metal. For example, the TiCl linkage in TiCl_4 is 2.170 Å,¹⁷ almost 0.2 Å shorter than in Cp_2TiCl_2 .¹⁸ We have observed this facility of donation by Cl theoretically as well.

(17) 2.170 Å from gas-phase electron diffraction. Y. Morino and U. Uehara, *J. Chem. Phys.*, **45**, 4543 (1966).

(18) A. Clearfield, D. Warner, A. Saldarriaga-Molena, R. Ropal, and I. Bernal, *Can. J. Chem.*, **53**, 1622 (1975).

(19) 1.957 Å from gas-phase electron diffraction. A. Almendinger, S. Halvorsen, and A. Haaland, *Acta Chem. Scand.*, **25**, 1937 (1971).

(20) 2.06 Å from gas-phase electron diffraction. I. Hargittai and M. Hargittai, *J. Chem. Phys.*, **60**, 2563 (1974).

(21) (a) R. F. Hout, Jr., W. J. Pietro, and W. J. Hehre, *J. Comput. Chem.*, in press; (b) R. F. Hout, Jr., W. J. Pietro, and W. J. Hehre, "Orbital Photography. A Pictorial Approach to Molecular Structure and Reactivity", Wiley, New York, in press. (c) R. F. Hout, Jr., W. J. Pietro, and W. J. Hehre, Quantum Chemistry Program Exchange, Indiana University, to be submitted for publication.

forces on the overall electronic structure of the complex should be minimal.

Despite the apparent dissimilarity between the free carbene and the protected system studied here, the Tebbe reagent effectively mimics the known chemistry of alkylidene complexes. Since the theoretical structure of 2 suggests that it is very strongly bound, it seems unlikely that the similarity arises from formation of a highly reactive free alkylidene complex via unaided equilibration with the Lewis acid. More likely, an incoming substrate or solvent molecule (or both) displaces the Lewis acid in a concerted fashion. Grubbs¹³ has noted that extremely bulky Lewis bases facilitate the formation of titanacyclobutanes from 1 and olefins, implying that the Lewis acid fragment is removed by the base. Exploration of these possibilities via further theoretical work is in progress.

Registry No. 1, 67719-69-1.

Reaction of HCl with Photoproduced Base-Substituted Manganese Carbonyl Radicals

Blaine H. Byers,* Timothy P. Curran,
Michael J. Thompson, and Linda J. Sauer

Department of Chemistry, College of the Holy Cross
Worcester, Massachusetts 01610

Received August 16, 1982

Summary: Near-UV irradiation of $Mn_2(CO)_8L_2$ ($L = PBu_3, P(OEt)_3$) in the presence of HCl and a variety of solvents yields both $HMn(CO)_4L$ and $Mn(CO)_4(L)Cl$. Evidence suggests the mechanism involves oxidative addition of HCl to 15- and 17-electron metal carbonyl radicals.

Evidence for the presence of metal carbonyl radicals (both neutral and ionic) in a variety of chemical reactions is growing rapidly.¹ By studying the chemistry of these radicals, a better understanding of probable chemical mechanisms is achieved. In addition to numerous CO substitution reactions,² neutral manganese carbonyl radicals have been observed to react, by a variety of proposed mechanisms, with small molecules, including CCl_4 ,³ O_2 ,⁴ I_2 ,⁴ Br_2 ,⁵ H_2 ,⁶ and HBr .⁷ In these reactions only single mononuclear products were detected. In comparison, while looking at the reaction of $Mn_2(CO)_8L_2$ ($L = PBu_3, P(OEt)_3$, and CO) with H_2O under acidic conditions, we observe that the reaction of HCl with photochemically generated $Mn(CO)_4L$ radicals is unique in that it produces two carbon-

yl-containing products, $cis-HMn(CO)_4L$ and $cis-Mn(CO)_4(L)Cl$. This report describes these HCl reactions under a variety of conditions and utilizes the appearance of two products for partial mechanism elucidation.

Most of the solvent combinations employed^{8a} reflect the attempt to study the reaction of these water-insoluble compounds with water. The substituted carbonyls show only small solvent effects. When $Mn_2(CO)_8L_2$ ($L = PBu_3$ and $P(OEt)_3$) is dissolved in any of the solvent systems used^{8a} and irradiated,^{8b} complete conversion of $cis-HMn(CO)_4L$ and $cis-Mn(CO)_4(L)Cl$ is observed within about 30 min.⁹ The rate of conversion shows some dependence on the HCl concentration. A small amount of hydrogen gas is also detected¹⁰ when the HCl concentration is high.

In contrast, $Mn_2(CO)_{10}$ exhibits very marked solvent effects. Irradiation of $Mn_2(CO)_{10}$ in the heterogeneous system (aqueous HCl/hexane) slowly produces $HMn(CO)_5$, $Mn(CO)_5Cl$, and some $[Mn(CO)_4Cl]_2$. After 24 h small amounts of hydrogen are also detected. However, irradiation of $Mn_2(CO)_{10}$ in the homogeneous system (aqueous HCl/ethanol/isopropyl ether) causes only slow decomposition. When $Mn_2(CO)_{10}$ is irradiated in the anhydrous HCl/hexane system, $Mn(CO)_5Cl$ begins forming after 5 min. The concentration of $Mn(CO)_5Cl$ increases for about 1 h and then gradually converts to $[Mn(CO)_4Cl]_2$. There is no IR spectroscopic evidence for $HMn(CO)_5$ under these conditions even when high concentrations of $Mn_2(CO)_{10}$ are employed.¹¹ This is consistent with the reported reaction between HBr and $Mn_2(CO)_{10}$ in cyclohexane where only $Mn(CO)_5Br$ was detected.⁷

When H_2SO_4 or $HC_2H_3O_2$ are employed in these photochemical reactions at concentrations comparable to those of HCl, $HMn(CO)_4L$ ($L = PBu_3, P(OEt)_3$) forms but much more slowly than when HCl is used. HNO_3 causes almost complete decomposition within 1 h.

Photochemically generated radicals have been shown to be substitutionally labile,² and there is significant evidence suggesting that facile dissociation of CO from these 17-electron radicals is involved in substitution reactions.¹² It follows that 15-electron radicals $Mn(CO)_3L$ are also involved in these presently reported reactions with HCl. If so, running reactions under an atmosphere of CO should significantly decrease the concentration of these 15-electron radicals and, thereby, alter the reaction. Indeed, when these HCl reactions are conducted under an atmosphere of CO, no hydride is formed and the rate of formation of chloride is reduced.¹³ In light of these findings we propose

(8) (a) Two sources of HCl were examined. Homogeneous conditions were obtained in the following manner: gaseous hydrogen chloride was bubbled through hexane, isopropyl ether, or a 4% (by volume) ethanol/isopropyl ether mixture; aqueous hydrochloric acid was mixed with a 4% (by volume) ethanol/isopropyl ether mixture. Heterogeneous conditions (two phases) resulted when aqueous hydrochloric acid was stirred with hexane. (b) Typically, reaction solutions are prepared under a nitrogen atmosphere by using pure solvents stored over molecular sieves or alumina. The solutions are then purged for 15 min by using oxygen-free nitrogen (Linde) and kept under a positive pressure of nitrogen during irradiation. A 250-W mercury high intensity discharge lamp (GE H250A37-5) is used in conjunction with Pyrex filtering ($\lambda > 300$ nm). When a band-pass filter (Corning CS7-60: λ_{max} 352 nm with a band width at half-height of 60 nm) is employed, the reaction is slower (presumably due to the decrease in intensity), but the same products are formed. Samples for IR and GC analysis are taken via a serum cap and syringe.

(9) Products are characterized by IR spectra: $HMn(CO)_4PBu_3$, ν_{CO} (cm^{-1} , isopropyl ether) 2057 (m), 1976 (m), 1960 (s), 1949 (s); $Mn(CO)_4(PBu_3)Cl$, ν_{CO} (cm^{-1} , isopropyl ether) 2087 (m), 2018 (m), 2006 (s), 1948 (s).

(10) Hydrogen is detected by GC using Porapak Q packing.

(11) Due to overlapping peaks, it is difficult to identify $HMn(CO)_5$ spectroscopically until it is in high enough concentration so that the weak vibration at 2116 cm^{-1} appears.

(12) Wegman, R. W.; Olsen, R. J.; Gard, D. R.; Faulkner, L. R.; Brown, T. L. *J. Am. Chem. Soc.* 1981, 103, 6089-6092 and references therein.

(1) (a) Nalesnik, T. E.; Orchin, M. *Organometallics* 1982, 1, 222-223. (b) Hershberger, J. W.; Klingler, R. J.; Kochi, J. K. *J. Am. Chem. Soc.* 1982, 104, 3034-3043. (c) Bruce, M. I.; Kehoe, D. C.; Matison, J. G.; Nicholson, B. K.; Rieger, P. H.; Williams, M. L. *J. Chem. Soc., Chem. Commun.* 1982, 442-444. (d) Krusic, P. J.; San Filippo, J., Jr.; Hutchinson, B.; Hance, R. L.; Daniels, L. M. *J. Am. Chem. Soc.* 1981, 103, 2129-2131.

(2) McCullen, S. B.; Brown, T. L. *Inorg. Chem.* 1981, 20, 3528-3533 and references therein.

(3) Wrighton, M. S.; Ginley, D. S. *J. Am. Chem. Soc.* 1975, 97, 2065-2072.

(4) (a) Haines, L. I. B.; Hoppgood, D.; Poë, A. J. *J. Chem. Soc. A* 1968, 421-428. (b) Jackson, R. A.; Poë, A. *Inorg. Chem.* 1978, 17, 997-1003. (c) Kramer, G.; Patterson, J.; Poë, A.; Ng, L. *Ibid.* 1980, 19, 1161-1169.

(5) (a) Hoppgood, D. J. Ph.D. Thesis, London University, 1966. (b) Kramer, G.; Patterson, J. R.; Poë, A. J. *J. Chem. Soc., Dalton Trans.* 1979, 1165.

(6) Byers, B. H.; Brown, T. L. *J. Am. Chem. Soc.* 1977, 99, 2527-2532.

(7) Bamford, C. H.; Burley, J. W.; Coldbeck, M. *J. Chem. Soc., Dalton Trans.* 1972, 1846-1852.

Reaction of hydrogen chloride with photoproduced base-substituted manganese carbonyl radicals

Blaine H. Byers, Timothy P. Curran, Michael J. Thompson, and Linda J. Sauer

Organometallics, **1983**, 2 (3), 459-460 • DOI: 10.1021/om00075a020 • Publication Date (Web): 01 May 2002

Downloaded from <http://pubs.acs.org> on April 24, 2009

More About This Article

The permalink <http://dx.doi.org/10.1021/om00075a020> provides access to:

- Links to articles and content related to this article
- Copyright permission to reproduce figures and/or text from this article



ACS Publications
High quality. High impact.

forces on the overall electronic structure of the complex should be minimal.

Despite the apparent dissimilarity between the free carbene and the protected system studied here, the Tebbe reagent effectively mimics the known chemistry of alkylidene complexes. Since the theoretical structure of **2** suggests that it is very strongly bound, it seems unlikely that the similarity arises from formation of a highly reactive free alkylidene complex via unaided equilibration with the Lewis acid. More likely, an incoming substrate or solvent molecule (or both) displaces the Lewis acid in a concerted fashion. Grubbs¹³ has noted that extremely bulky Lewis bases facilitate the formation of titanacyclobutanes from **1** and olefins, implying that the Lewis acid fragment is removed by the base. Exploration of these possibilities via further theoretical work is in progress.

Registry No. 1, 67719-69-1.

Reaction of HCl with Photoproduced Base-Substituted Manganese Carbonyl Radicals

Blaine H. Byers,* Timothy P. Curran,
Michael J. Thompson, and Linda J. Sauer

Department of Chemistry, College of the Holy Cross
Worcester, Massachusetts 01610

Received August 16, 1982

Summary: Near-UV irradiation of $\text{Mn}_2(\text{CO})_8\text{L}_2$ ($\text{L} = \text{PBu}_3$, $\text{P}(\text{OEt})_3$) in the presence of HCl and a variety of solvents yields both $\text{HMn}(\text{CO})_4\text{L}$ and $\text{Mn}(\text{CO})_4(\text{L})\text{Cl}$. Evidence suggests the mechanism involves oxidative addition of HCl to 15- and 17-electron metal carbonyl radicals.

Evidence for the presence of metal carbonyl radicals (both neutral and ionic) in a variety of chemical reactions is growing rapidly.¹ By studying the chemistry of these radicals, a better understanding of probable chemical mechanisms is achieved. In addition to numerous CO substitution reactions,² neutral manganese carbonyl radicals have been observed to react, by a variety of proposed mechanisms, with small molecules, including CCl_4 ,³ O_2 ,⁴ I_2 ,⁴ Br_2 ,⁵ H_2 ,⁶ and HBr .⁷ In these reactions only single mononuclear products were detected. In comparison, while looking at the reaction of $\text{Mn}_2(\text{CO})_8\text{L}_2$ ($\text{L} = \text{PBu}_3$, $\text{P}(\text{OEt})_3$, and CO) with H_2O under acidic conditions, we observe that the reaction of HCl with photochemically generated $\text{Mn}(\text{CO})_4\text{L}$ radicals is unique in that it produces two carbon-

yl-containing products, $\text{cis-HMn}(\text{CO})_4\text{L}$ and $\text{cis-Mn}(\text{CO})_4(\text{L})\text{Cl}$. This report describes these HCl reactions under a variety of conditions and utilizes the appearance of two products for partial mechanism elucidation.

Most of the solvent combinations employed^{8a} reflect the attempt to study the reaction of these water-insoluble compounds with water. The substituted carbonyls show only small solvent effects. When $\text{Mn}_2(\text{CO})_8\text{L}_2$ ($\text{L} = \text{PBu}_3$ and $\text{P}(\text{OEt})_3$) is dissolved in any of the solvent systems used^{8a} and irradiated,^{8b} complete conversion of $\text{cis-HMn}(\text{CO})_4\text{L}$ and $\text{cis-Mn}(\text{CO})_4(\text{L})\text{Cl}$ is observed within about 30 min.⁹ The rate of conversion shows some dependence on the HCl concentration. A small amount of hydrogen gas is also detected¹⁰ when the HCl concentration is high.

In contrast, $\text{Mn}_2(\text{CO})_{10}$ exhibits very marked solvent effects. Irradiation of $\text{Mn}_2(\text{CO})_{10}$ in the heterogeneous system (aqueous HCl/hexane) slowly produces $\text{HMn}(\text{CO})_5$, $\text{Mn}(\text{CO})_5\text{Cl}$, and some $[\text{Mn}(\text{CO})_4\text{Cl}]_2$. After 24 h small amounts of hydrogen are also detected. However, irradiation of $\text{Mn}_2(\text{CO})_{10}$ in the homogeneous system (aqueous HCl/ethanol/isopropyl ether) causes only slow decomposition. When $\text{Mn}_2(\text{CO})_{10}$ is irradiated in the anhydrous HCl/hexane system, $\text{Mn}(\text{CO})_5\text{Cl}$ begins forming after 5 min. The concentration of $\text{Mn}(\text{CO})_5\text{Cl}$ increases for about 1 h and then gradually converts to $[\text{Mn}(\text{CO})_4\text{Cl}]_2$. There is no IR spectroscopic evidence for $\text{HMn}(\text{CO})_5$ under these conditions even when high concentrations of $\text{Mn}_2(\text{CO})_{10}$ are employed.¹¹ This is consistent with the reported reaction between HBr and $\text{Mn}_2(\text{CO})_{10}$ in cyclohexane where only $\text{Mn}(\text{CO})_5\text{Br}$ was detected.⁷

When H_2SO_4 or $\text{HC}_2\text{H}_3\text{O}_2$ are employed in these photochemical reactions at concentrations comparable to those of HCl, $\text{HMn}(\text{CO})_4\text{L}$ ($\text{L} = \text{PBu}_3$, $\text{P}(\text{OEt})_3$) forms but much more slowly than when HCl is used. HNO_3 causes almost complete decomposition within 1 h.

Photochemically generated radicals have been shown to be substitutionally labile,² and there is significant evidence suggesting that facile dissociation of CO from these 17-electron radicals is involved in substitution reactions.¹² It follows that 15-electron radicals $\text{Mn}(\text{CO})_3\text{L}$ are also involved in these presently reported reactions with HCl. If so, running reactions under an atmosphere of CO should significantly decrease the concentration of these 15-electron radicals and, thereby, alter the reaction. Indeed, when these HCl reactions are conducted under an atmosphere of CO, no hydride is formed and the rate of formation of chloride is reduced.¹³ In light of these findings we propose

(8) (a) Two sources of HCl were examined. Homogeneous conditions were obtained in the following manner: gaseous hydrogen chloride was bubbled through hexane, isopropyl ether, or a 4% (by volume) ethanol/isopropyl ether mixture; aqueous hydrochloric acid was mixed with a 4% (by volume) ethanol/isopropyl ether mixture. Heterogeneous conditions (two phases) resulted when aqueous hydrochloric acid was stirred with hexane. (b) Typically, reaction solutions are prepared under a nitrogen atmosphere by using pure solvents stored over molecular sieves or alumina. The solutions are then purged for 15 min by using oxygen-free nitrogen (Linde) and kept under a positive pressure of nitrogen during irradiation. A 250-W mercury high intensity discharge lamp (GE H250A37-5) is used in conjunction with Pyrex filtering ($\lambda > 300$ nm). When a band-pass filter (Corning CS7-60: λ_{max} 352 nm with a band width at half-height of 60 nm) is employed, the reaction is slower (presumably due to the decrease in intensity), but the same products are formed. Samples for IR and GC analysis are taken via a serum cap and syringe.

(9) Products are characterized by IR spectra: $\text{HMn}(\text{CO})_4\text{PBu}_3$, ν_{CO} (cm^{-1} , isopropyl ether) 2057 (m), 1976 (m), 1960 (s), 1949 (s); $\text{Mn}(\text{CO})_4(\text{PBu}_3)\text{Cl}$, ν_{CO} (cm^{-1} , isopropyl ether) 2087 (m), 2018 (m), 2006 (s), 1948 (s).

(10) Hydrogen is detected by GC using Porapak Q packing. (11) Due to overlapping peaks, it is difficult to identify $\text{HMn}(\text{CO})_5$ spectroscopically until it is in high enough concentration so that the weak vibration at 2116 cm^{-1} appears.

(12) Wegman, R. W.; Olsen, R. J.; Gard, D. R.; Faulkner, L. R.; Brown, T. L. *J. Am. Chem. Soc.* 1981, 103, 6089-6092 and references therein.

(1) (a) Nalesnik, T. E.; Orchin, M. *Organometallics* 1982, 1, 222-223. (b) Hershberger, J. W.; Klingler, R. J.; Kochi, J. K. *J. Am. Chem. Soc.* 1982, 104, 3034-3043. (c) Bruce, M. I.; Kehoe, D. C.; Matison, J. G.; Nicholson, B. K.; Rieger, P. H.; Williams, M. L. *J. Chem. Soc., Chem. Commun.* 1982, 442-444. (d) Krusic, P. J.; San Filippo, J., Jr.; Hutchinson, B.; Hance, R. L.; Daniels, L. M. *J. Am. Chem. Soc.* 1981, 103, 2129-2131.

(2) McCullen, S. B.; Brown, T. L. *Inorg. Chem.* 1981, 20, 3528-3533 and references therein.

(3) Wrighton, M. S.; Ginley, D. S. *J. Am. Chem. Soc.* 1975, 97, 2065-2072.

(4) (a) Haines, L. I. B.; Hopgood, D.; Poë, A. J. *J. Chem. Soc. A* 1968, 421-428. (b) Jackson, R. A.; Poë, A. *Inorg. Chem.* 1978, 17, 997-1003. (c) Kramer, G.; Patterson, J.; Poë, A.; Ng, L. *Ibid.* 1980, 19, 1161-1169.

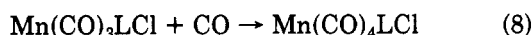
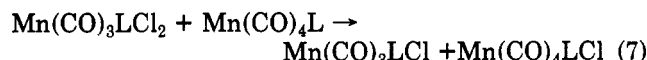
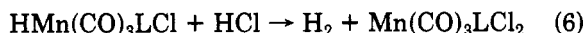
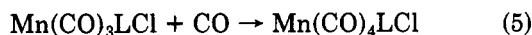
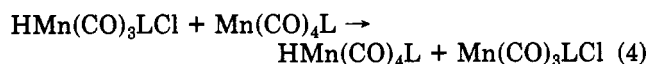
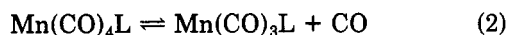
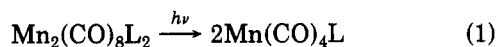
(5) (a) Hopgood, D. J. Ph.D. Thesis, London University, 1966. (b) Kramer, G.; Patterson, J. R.; Poë, A. J. *J. Chem. Soc., Dalton Trans.* 1979, 1165.

(6) Byers, B. H.; Brown, T. L. *J. Am. Chem. Soc.* 1977, 99, 2527-2532.

(7) Bamford, C. H.; Burley, J. W.; Coldbeck, M. *J. Chem. Soc., Dalton Trans.* 1972, 1846-1852.

the mechanism shown in Scheme I.

Scheme I



Photochemical bond homolysis (eq 1) is followed by facile CO dissociation (eq 2). In step 3 HCl undergoes a two-electron oxidative addition to a coordinatively unsaturated 15-electron radical. Such a process is common with HCl and 16-electron species.¹⁵ It has also been proposed that oxidative addition of H₂⁶ and HSn(*n*-Bu)₃¹⁶ to 15-electron metal carbonyl radicals occurs. The ligand effect, associated with the increase in reaction rate observed with the substituted compounds, further supports the oxidative addition pathway. The stronger Lewis bases PBu₃ and P(OEt)₃ (compared to the π acid CO) promote facile oxidation of the manganese. Hydrogen atom abstraction (eq 4) and CO addition (eq 5) complete the process. When larger amounts of HCl are present, a second HCl molecule interacts evolving H₂ gas (eq 6). Such a process has also been proposed for reactions of HI with Ir(I) species.¹⁷ Chlorine atom abstraction (eq 7) is then followed by CO addition (eq 8).

In step 9 one-electron oxidative addition (chloride abstraction) is indicated. However, given the H-Cl bond strength (420 kJ/mol), the solvent would likely play a role. Alternatively, an initial two-electron oxidative addition of HCl to Mn(CO)₄L occurs (producing a seven-coordinate, 19-electron radical) followed by loss of H. There is growing evidence¹⁸ that 19-electron radicals are formed via associative processes, especially in disubstituted radicals.^{18b} Step 9 predominates only when step 2 is suppressed by an atmosphere of CO.

An alternative pathway involves the interaction of an HCl molecule with a pair of solvent-caged radicals forming a four-centered intermediate. Such an interaction may be viewed either as a dinuclear, two-electron oxidative addition of HCl or as an HCl-promoted disproportionation.

A similar four-centered intermediate has been proposed for the oxidative addition of H₂ or H₂O to two Co(CN)₅³⁻, 17-electron radicals.^{15b} Also, disproportionation of metal carbonyl radicals in polar solvents is known.¹⁹

Evidence supportive of a four-centered concerted process was sought by studying the photochemical reaction of aqueous HCl with Mn₂(CO)₉PBu₃ dissolved in 4% ethanol/isopropyl ether. On the basis of electronic effects, a four-centered intermediate should favor formation of HMn(CO)₅ and Mn(CO)₄(PBu₃)Cl. If steric factors dominate, Mn(CO)₅Cl and HMn(CO)₄PBu₃ should form. Spectroscopic evidence indicates that only Mn₂(CO)₁₀, HMn(CO)₄PBu₃, and Mn(CO)₄(PBu₃)Cl form in significant amounts within 20 min. This evidence strongly argues against a four-centered intermediate. Furthermore, irradiation of Mn₂(CO)₉PBu₃ in the absence of HCl (4% ethanol/isopropyl ether) produces within 15 min a mixture of Mn₂(CO)₁₀ and Mn₂(CO)₈(PBu₃)₂ in equilibrium with Mn₂(CO)₉PBu₃. The appearance of these crossover products coupled with the lack of evidence for any anionic species, e.g., Mn(CO)₄L⁻, indicate simple metal-metal bond homolysis is occurring without rapid disproportionation.

Lastly, it is interesting to briefly compare the thermal and photochemical reactions of Mn₂(CO)₈L₂ (L = PBu₃, P(OEt)₃, and CO) with HCl. In the absence of light, thermal reactions (from 18 to 60 °C) of Mn₂(CO)₈L₂ with HCl show more pronounced ligand effects than the corresponding photochemical reactions. In all cases where reaction occurs, Mn(CO)₄(L)Cl always forms, whereas HMn(CO)₄L never is detected. The reactivity of L is in the order PBu₃ > P(OEt)₃ >> CO. Therefore, the ligand effect is somewhat similar to that in the photochemical process, but the lack of formation of HMn(CO)₄L strongly indicates a different mechanism is operable. Further studies including kinetic measurements on both the thermal and photochemical reactions are in progress.

Acknowledgment. We are grateful for the William and Flora Hewlett Foundation Grant of Research Corp. that provided financial support for this research.

Registry No. Mn₂(CO)₈(PBu₃)₂, 15609-33-3; Mn₂(CO)₈(P(OEt)₃)₂, 15488-14-9; HCl, 7647-01-0; HMn(CO)₄PBu₃, 56960-19-1; HMn(CO)₄P(OEt)₃, 84369-08-4; Mn(CO)₄(PBu₃)Cl, 84369-09-5; Mn(CO)₄(P(OEt)₃)Cl, 84369-10-8; H₂, 1333-74-0; CO, 630-08-0; Mn₂(CO)₁₀, 10170-69-1; Mn(CO)₅Cl, 14100-30-2; HMn(CO)₅, 16972-33-1; Mn₂(CO)₉PBu₃, 24476-71-9; hexane, 110-54-3; isopropyl ether, 108-20-3; ethanol, 64-17-5.

(19) Allen, D. M.; Cox, A.; Kemp, T. J.; Sultana, Q.; Pitts, R. B. *J. Chem. Soc., Dalton Trans.* 1976, 1189-1193.

(13) When a small amount of oxygen (air) is added to the reaction of Mn₂(CO)₈L₂ and HCl, the growth of HMn(CO)₄L is inhibited. The observed effect of added CO is somewhat similar and may reflect trace amounts of O₂ in the CO. However, the CO (Linde, CP grade) is passed through an activated manganese(II) oxide, oxygen-scavenging column¹⁴ prior to use. Further tests are being conducted.

(14) Brown, T. L.; Dickerhoof, D. W.; Bafus, D. A.; Morgan, G. L. *Rev. Sci. Instrum.* 1962, 33, 491-92.

(15) (a) Louw, W. J.; deWaal, D. J. A.; Gerber, T. I. A.; Demanet, C. M.; Copperthwaite, R. G. *Inorg. Chem.* 1982, 21, 1667-68. (b) Halpern, J. *Acc. Chem. Res.* 1970, 3, 386-392 and references therein.

(16) Wegman, R. W.; Brown, T. L. *Organometallics* 1982, 1, 47-52.

(17) Forster, D. *J. Chem. Soc., Dalton Trans.* 1979, 1639-1645.

(18) (a) Fox, A.; Malito, J.; Poë, A. *J. Chem. Soc., Chem. Commun.* 1981, 1052-1053. (b) McCullen, S. B.; Walker, H. W.; Brown, T. L. *J. Am. Chem. Soc.* 1982, 104, 4007-4008.

Redox-Catalyzed Carbonylation of an Iron Methyl Complex

Roy H. Magnuson,* Randy Melrowitz, Samu J. Zulu, and Warren P. Glering*

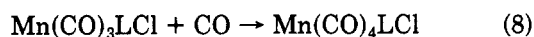
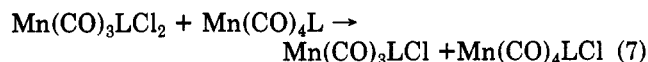
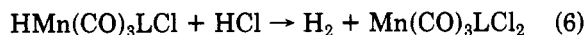
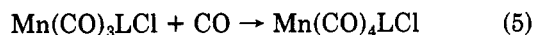
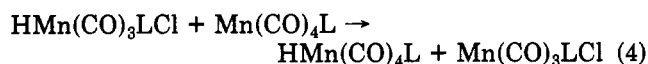
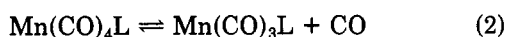
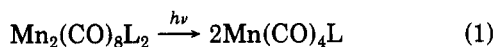
Department of Chemistry, Boston University
Boston, Massachusetts 02215

Received October 25, 1982

Summary: (η⁵-C₅H₅)(PPh₃)(CO)Fe(CH₃) undergoes a rapid redox-catalyzed migratory insertion that follows the rate law: rate = k [OX]₁[CO].

the mechanism shown in Scheme I.

Scheme I



Photochemical bond homolysis (eq 1) is followed by facile CO dissociation (eq 2). In step 3 HCl undergoes a two-electron oxidative addition to a coordinatively unsaturated 15-electron radical. Such a process is common with HCl and 16-electron species.¹⁵ It has also been proposed that oxidative addition of H₂⁶ and HS n (n -Bu)₃¹⁶ to 15-electron metal carbonyl radicals occurs. The ligand effect, associated with the increase in reaction rate observed with the substituted compounds, further supports the oxidative addition pathway. The stronger Lewis bases PBu₃ and P(OEt)₃ (compared to the π acid CO) promote facile oxidation of the manganese. Hydrogen atom abstraction (eq 4) and CO addition (eq 5) complete the process. When larger amounts of HCl are present, a second HCl molecule interacts evolving H₂ gas (eq 6). Such a process has also been proposed for reactions of HI with Ir(I) species.¹⁷ Chlorine atom abstraction (eq 7) is then followed by CO addition (eq 8).

In step 9 one-electron oxidative addition (chloride abstraction) is indicated. However, given the H-Cl bond strength (420 kJ/mol), the solvent would likely play a role. Alternatively, an initial two-electron oxidative addition of HCl to Mn(CO)₄L occurs (producing a seven-coordinate, 19-electron radical) followed by loss of H. There is growing evidence¹⁸ that 19-electron radicals are formed via associative processes, especially in disubstituted radicals.^{18b} Step 9 predominates only when step 2 is suppressed by an atmosphere of CO.

An alternative pathway involves the interaction of an HCl molecule with a pair of solvent-caged radicals forming a four-centered intermediate. Such an interaction may be viewed either as a dinuclear, two-electron oxidative addition of HCl or as an HCl-promoted disproportionation.

A similar four-centered intermediate has been proposed for the oxidative addition of H₂ or H₂O to two Co(CN)₅³⁻, 17-electron radicals.^{15b} Also, disproportionation of metal carbonyl radicals in polar solvents is known.¹⁹

Evidence supportive of a four-centered concerted process was sought by studying the photochemical reaction of aqueous HCl with Mn₂(CO)₉PBu₃ dissolved in 4% ethanol/isopropyl ether. On the basis of electronic effects, a four-centered intermediate should favor formation of HMn(CO)₅ and Mn(CO)₄(PBu₃)Cl. If steric factors dominate, Mn(CO)₅Cl and HMn(CO)₄PBu₃ should form. Spectroscopic evidence indicates that only Mn₂(CO)₁₀, HMn(CO)₄PBu₃, and Mn(CO)₄(PBu₃)Cl form in significant amounts within 20 min. This evidence strongly argues against a four-centered intermediate. Furthermore, irradiation of Mn₂(CO)₉PBu₃ in the absence of HCl (4% ethanol/isopropyl ether) produces within 15 min a mixture of Mn₂(CO)₁₀ and Mn₂(CO)₈(PBu₃)₂ in equilibrium with Mn₂(CO)₉PBu₃. The appearance of these crossover products coupled with the lack of evidence for any anionic species, e.g., Mn(CO)₄L⁻, indicate simple metal-metal bond homolysis is occurring without rapid disproportionation.

Lastly, it is interesting to briefly compare the thermal and photochemical reactions of Mn₂(CO)₈L₂ (L = PBu₃, P(OEt)₃, and CO) with HCl. In the absence of light, thermal reactions (from 18 to 60 °C) of Mn₂(CO)₈L₂ with HCl show more pronounced ligand effects than the corresponding photochemical reactions. In all cases where reaction occurs, Mn(CO)₄(L)Cl always forms, whereas HMn(CO)₄L never is detected. The reactivity of L is in the order PBu₃ > P(OEt)₃ >> CO. Therefore, the ligand effect is somewhat similar to that in the photochemical process, but the lack of formation of HMn(CO)₄L strongly indicates a different mechanism is operable. Further studies including kinetic measurements on both the thermal and photochemical reactions are in progress.

Acknowledgment. We are grateful for the William and Flora Hewlett Foundation Grant of Research Corp. that provided financial support for this research.

Registry No. Mn₂(CO)₈(PBu₃)₂, 15609-33-3; Mn₂(CO)₈(P(OEt)₃)₂, 15488-14-9; HCl, 7647-01-0; HMn(CO)₄PBu₃, 56960-19-1; HMn(CO)₄P(OEt)₃, 84369-08-4; Mn(CO)₄(PBu₃)Cl, 84369-09-5; Mn(CO)₄(P(OEt)₃)Cl, 84369-10-8; H₂, 1333-74-0; CO, 630-08-0; Mn₂(CO)₁₀, 10170-69-1; Mn(CO)₅Cl, 14100-30-2; HMn(CO)₅, 16972-33-1; Mn₂(CO)₉PBu₃, 24476-71-9; hexane, 110-54-3; isopropyl ether, 108-20-3; ethanol, 64-17-5.

(19) Allen, D. M.; Cox, A.; Kemp, T. J.; Sultana, Q.; Pitts, R. B. *J. Chem. Soc., Dalton Trans.* 1976, 1189-1193.

Redox-Catalyzed Carbonylation of an Iron Methyl Complex

Roy H. Magnuson,* Randy Melrowitz, Samu J. Zulu, and Warren P. Glering*

Department of Chemistry, Boston University
Boston, Massachusetts 02215

Received October 25, 1982

Summary: (η^5 -C₅H₅)(PPh₃)(CO)Fe(CH₃) undergoes a rapid redox-catalyzed migratory insertion that follows the rate law: rate = k [OX]₁[CO].

(13) When a small amount of oxygen (air) is added to the reaction of Mn₂(CO)₈L₂ and HCl, the growth of HMn(CO)₄L is inhibited. The observed effect of added CO is somewhat similar and may reflect trace amounts of O₂ in the CO. However, the CO (Linde, CP grade) is passed through an activated manganese(II) oxide, oxygen-scavenging column¹⁴ prior to use. Further tests are being conducted.

(14) Brown, T. L.; Dickerhoof, D. W.; Bafus, D. A.; Morgan, G. L. *Rev. Sci. Instrum.* 1962, 33, 491-92.

(15) (a) Louw, W. J.; deWaal, D. J. A.; Gerber, T. I. A.; Demanet, C. M.; Coppertwaite, R. G. *Inorg. Chem.* 1982, 21, 1667-68. (b) Halpern, J. *Acc. Chem. Res.* 1970, 3, 386-392 and references therein.

(16) Wegman, R. W.; Brown, T. L. *Organometallics* 1982, 1, 47-52.

(17) Forster, D. *J. Chem. Soc., Dalton Trans.* 1979, 1639-1645.

(18) (a) Fox, A.; Malito, J.; Poë, A. *J. Chem. Soc., Chem. Commun.* 1981, 1052-1053. (b) McCullen, S. B.; Walker, H. W.; Brown, T. L. *J. Am. Chem. Soc.* 1982, 104, 4007-4008.

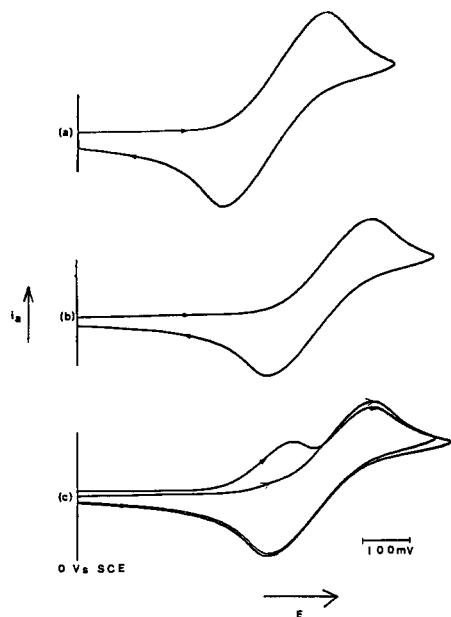
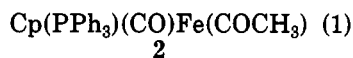


Figure 1. Cyclic voltammograms in CH_2Cl_2 containing 0.1 M TBAP at a scan of 200 mV s^{-1} and 0°C . Scan a is $(\eta^5\text{-C}_5\text{H}_5)\text{-}(\text{PPh}_3)\text{Fe}(\text{CO})(\text{CH}_3)$ under Ar atmosphere: $E_a = 480 \text{ mV}$; $E_c = 280$; $(E_a + E_c)/2 = 380 \text{ mV}$; $E_a - E_c = 200 \text{ mV}$. Scan b is $(\eta^5\text{-C}_5\text{H}_5)(\text{PPh}_3)\text{Fe}(\text{CO})(\text{COCH}_3)$ under CO atmosphere: $E_a = 570 \text{ mV}$; $E_c = 370 \text{ mV}$; $(E_a + E_c)/2 = 470 \text{ mV}$; $E_a - E_c = 200 \text{ mV}$. Scan c is $(\eta^5\text{-C}_5\text{H}_5)(\text{PPh}_3)\text{Fe}(\text{CO})(\text{CH}_3)$ under CO atmosphere: $E_{a1} = 415 \text{ mV}$; $E_{a2} = 570 \text{ mV}$; $E_c = 370 \text{ mV}$; $(E_{a2} + E_c)/2 = 470 \text{ mV}$; $E_{a2} - E_c = 200 \text{ mV}$.

Among metal-mediated ligand reactions, alkyl to acyl migratory insertion is of particular interest, as it is a key step in many important industrial processes.¹ Despite numerous kinetic and stereochemical studies, thermodynamic information is limited² and the role of the oxidation state of the metal in activation of the reaction has not been systematically addressed. Recently, we reported the thermodynamics of the rapid equilibration between alkyl and solvent-incorporated acyl complexes of formally Fe(III) cation radicals.^{3,4} Herein, we wish to present the first example of a redox-catalyzed carbonylation reaction and an assessment of the tremendous rate enhancement associated with a one-electron change in oxidation state of an iron complex.

The carbonylation reactions of the formally Fe(II) complex $(\text{Cp})(\text{PPh}_3)(\text{CO})\text{Fe}(\text{CH}_3)$ (eq 1) and closely related $(\text{Cp})(\text{PPh}_3)(\text{CO})\text{Fe}(\text{CH}_3) + \text{CO} \rightarrow$



derivatives are known to be thermodynamically favorable,⁵

(1) Alkyl to acyl migratory insertion reactions have been reviewed. (a) Collman, J. P.; Hegedus, L. S. "Principles and Applications of Organotransition Metal Chemistry"; University Science Books: Mill Valley, CA, 1980; pp 359-288. (b) Kuhlman, E. J.; Alexander, J. J. *Coord. Chem. Rev.* 1980, 33, 195-225. (c) Calderazzo, F. *Angew. Chem., Int. Ed. Engl.* 1977, 16, 299-311. (d) Wojcicki, A. *Adv. Organomet. Chem.* 1973, 11, 87-145. (e) Daub, G. W. *Prog. Inorg. Chem.* 1977, 22, 409.

(2) (a) Fachinetti, G.; Fochi, G.; Floriani, C. *J. Chem. Soc., Dalton Trans.* 1977, 1945-1950. (b) Calderazzo, F.; Cotton, F. A. *Proc. Int. Conf. Coord. Chem., 7th 1962*, Paper 6147. (c) Cotton, J. D.; Crisp, G. T.; Latif, L. *Inorg. Chim. Acta* 1981, 47, 171-176.

(3) Magnuson, R. H.; Meirowitz, R.; Zulu, S. J.; Giering, W. P. *J. Am. Chem. Soc.* 1982, 104, 5790-5791.

(4) Magnuson, R. H.; Zulu, S. J.; T'sai, W.-M.; Giering, W. P. *J. Am. Chem. Soc.* 1980, 102, 6887-6888.

(5) Flood, T. C.; Downs, H. "Abstracts of Papers", 176th National Meeting of the American Chemical Society, Miami, FL, Aug 1978, American Chemical Society: Washington, DC, 1978; INOR 27.

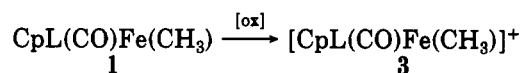
(6) Brunner, H.; Vogt, H., *J. Organomet. Chem.* 1981 210, 223-36.

but the rate is quite slow. For example, in 5 days no perceptible (<5%) conversion of 1 to the acetyl product 2 could be observed by either ^1H NMR or IR spectroscopy under mild conditions (1 atm of CO, 0°C , CH_2Cl_2 , 0.01 M 1). In striking contrast the addition of a few percent of an oxidant (ferricinium tetrafluoroborate or silver tetrafluoroborate) caused the conversion of 1 to 2 to be complete in 1-2 min, as evidenced by the appearance of a new acyl carbonyl absorbance at 1605 cm^{-1} and a shift in the terminal CO absorbance from 1900 to 1910 cm^{-1} in the IR spectrum of the mixture. The acetyl product 2 was isolated in 85-90% yield by column chromatography and was found to be identical (IR and ^1H NMR and melting point) with an authentic sample. No residual starting material was detected in the product mixture.

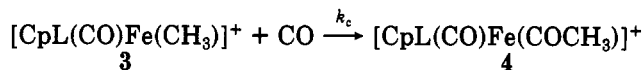
This redox catalysis can be rationalized in terms of the reaction sequence presented in Scheme I ($\text{L} = \text{PPh}_3$). The generation of a small amount of the methyl cation radical 3 permits the carbonylation, to form the acetyl cation radical 4, to proceed rapidly in the formally Fe(III) complex. In a subsequent electron-transfer step, 4 oxidizes the starting complex 1 to give the product 2 and regenerate the alkyliron(III) complex 3 for further propagation. This process will be catalytic provided the rates of migratory insertion on Fe(III) and the electron transfer are rapid compared to the parasitic decomposition of 3 or 4.

Scheme I

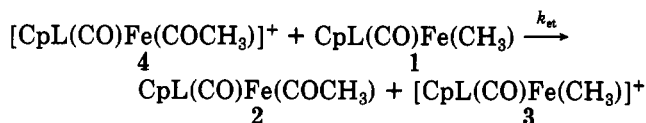
initiation



carbonylation



electron transfer



The existence of the formally Fe(III) complexes 3 and 4 is readily demonstrated by cyclic voltammetry (CV). Both 1 and 2 exhibit quasi-reversible oxidations (Figure 1) in CH_2Cl_2 at 200 mV s^{-1} under argon (1, $(E_a + E_c)/2 = 0.380 \text{ V}$ vs. SCE, $E_a - E_c = 200 \text{ mV}$; 2, $(E_a + E_c)/2 = 0.470 \text{ V}$, $E_a - E_c = 200 \text{ mV}$). From the potentials it can be seen that the electron-transfer reaction in Scheme I (in principle, an equilibrium) lies substantially to the right-hand side. Furthermore, IR evidence on solutions of the acetyl cation radical 4, obtained from bulk oxidation of 2 in CH_2Cl_2 ,⁴ shows that, even in the absence of external CO, decarbonylation does not occur rapidly, implying that the thermodynamic position of the carbonylation steps also lies well to the right on Fe(III).

Under 1 atm of CO the CV of 1 is dramatically altered and provides evidence for the redox catalysis (Figure 1c). As the potential for the alkyl oxidation wave was approached in an initial anodic scan, the anodic current rose but then peaked out suddenly and well before the E_a observed in the absence of CO. Continuation of the anodic scan resulted in a larger anodic wave at a potential appropriate for the oxidation of the acyl complex 2. The return cathodic scan and subsequent voltammograms

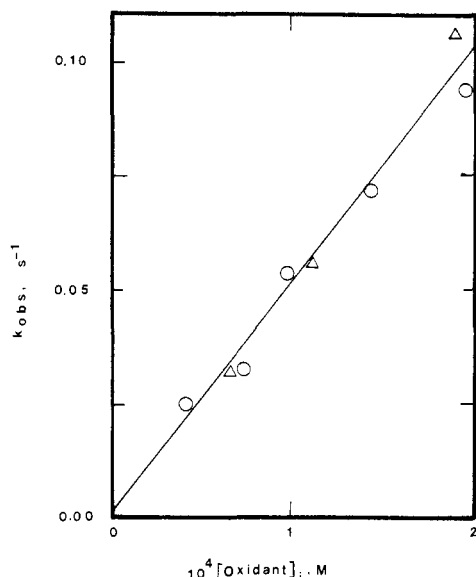


Figure 2. Dependence of the observed first-order rate constant on concentration of the initial oxidant (CH_2Cl_2 , 2°C , initially 1 atm of CO, and $\text{Cp}(\text{PPh}_3)\text{COFeCH}_3 = 0.10\text{--}0.15\text{ M}$): circles, ferricinium ion as oxidant; triangles, acetylferricinium ion as oxidant.

showed only the acyl couple ($4 + e^- \rightleftharpoons 2$). This behavior is consistent with partial electrogeneration of the alkyl cation radical **3** that then rapidly catalyzes the carbonylation of **1** to **2** in the region near the electrode.

The mechanism is Scheme I is strongly supported by kinetic studies in CH_2Cl_2 at 2°C . Runs were initiated by injection of a small volume of a solution of ferricinium or acetylferricinium tetrafluoroborate into solutions of **1** (10–15 mM), saturated with CO at 1 atm (ca. 6 mM), and the progress of the reaction was monitored by following the decrease in absorbance at 500 nm, associated with the conversion of **1** to **2**. Under these conditions of $[1] > [\text{CO}]$, first-order kinetics were observed, for which the rate constants were independent of the concentration of **1**, but linearly dependent on the initial concentration of the oxidizing agent, $[\text{OX}]_i$. Thus the experimental rate law is given by

$$\text{rate} = k[\text{CO}][\text{OX}]_i \quad k = 500 \pm 100 \text{ M}^{-1} \text{ s}^{-1} \quad (2)$$

in which there is zero-order dependence on **1**, and k has been evaluated from the slope of the plot in Figure 2. Under conditions where $[\text{CO}] \gg [1]$, a striking linear decrease in absorbance with time was observed. It continued until the absorbance corresponding to complete conversion to **2** was reached, when a sharp break occurred and the absorbance did not change further. This zero-order behavior is fully consistent with the rate law in eq 2.

With assumption of steady-state concentrations of **3** and **4**, the reaction sequence in Scheme I leads to the rate expression

$$\text{rate} = \frac{k_c k_{\text{et}} [1][\text{CO}][\text{OX}]}{k_{\text{et}} [1] + k_c [\text{CO}]} \quad (3)$$

Provided $k_{\text{et}} [1] \gg k_c [\text{CO}]$ (a reasonable condition, since the electron self-exchange reaction for related ferrocene derivatives is very rapid),⁷ the above expression simplifies to eq 2 in which the experimentally determined constant

k is to be equated with the Fe(III) carbonylation rate constant k_c . Thus, the rate of carbonylation of the formally iron(III) methyl complex **3** is conservatively estimated to be $10^7\text{--}10^8$ faster than the carbonylation rate of the formally Fe(II) species.

This difference between the rates of carbonylation in the Fe(II) and Fe(III) states is most likely attributable to a substantial reduction in the $d\pi$ donor ability of the metal center on oxidation, which allows a bent (or perhaps side-on) CO configuration in the activated complex to be energetically much more accessible.^{8,9} The crucial role of π back-bonding in the migratory insertion is also attested to by the ability of an external entering group, which is a strong π acid such as CO, to drive the reaction on Fe(II) thermodynamically much farther than a weaker π acid such as NCCH_3 ($K_{\text{CO}}/K_{\text{NCCH}_3} > 10^{15}$).¹⁰

It must be pointed out that parts per million concentration of an oxidant is, in principle, sufficient for the redox-catalyzed pathway to carry the entire reaction, so that interpretation of kinetic and stereochemical results must be done with caution. As this type of redox catalysis is most likely not restricted to iron, nor even to carbonylation reactions, the implications for organometallic reactivity may well be far-reaching.¹¹

Acknowledgment. We wish to thank the donors of the Petroleum Research Fund, administered by the American Chemical Society, and the Graduate School of Boston University for support of this research.

Registry No. 1, 12100-51-5; 2, 12101-02-9.

(8) Pladziejewicz, J. R.; Espenson, J. H. *J. Am. Chem. Soc.* **1973**, *95*, 56-63.

(9) Hoffman, R.; Berke, H. *J. Am. Chem. Soc.* **1978**, *100*, 7224-7236.

(10) $K_{\text{AN}} = 10^{-10} \text{ M}^{-1}$ and K_{CO} must be $> 10^5$ since no **1** is detectable after the catalyzed carbonylation of **1**.

(11) Enhanced reactivity toward ligand substitution has been reported in other 17-valence-electron organometallic species. (a) Hershberger, J. W.; Klingler, R. J.; Kochi, J. K. *J. Am. Chem. Soc.* **1982**, *104*, 3034-3043. (b) McCullen, S. B.; Walker, H. W.; Brown, T. C. *Ibid.* **1982**, *104*, 40089-4010. (c) Hepp, A. F.; Wrighton, M. S. *Ibid.* **1981**, *103*, 1258-1261. (d) Absi-Halabi, M.; Brown, T. L. *Ibid.* **1977**, *99*, 2982-2988.

$\text{Cp}_2\text{M}(s\text{-trans-}\eta^4\text{-butadiene})$ Complexes from Zirconocene and Hafnocene Dihalides and "Magnesium Butadiene"

Ulrich Dorf, Klaus Engel, and Gerhard Erker*

Abteilung für Chemie der Ruhr-Universität
D-4630 Bochum 1, Germany

Received September 28, 1982

Summary: Under the kinetic control reaction of "magnesium butadiene" (**2**) with Cp_2MCl_2 complexes **1a-c** ($\text{Cp} = \eta\text{-C}_5\text{H}_5$, $\eta\text{-C}_5\text{Me}_5$; $\text{M} = \text{Zr}, \text{Hf}$) gives (*s-trans*- η^4 -butadiene)metallocene complexes **4a-c**, the products expected from a stepwise reaction through Cp_2MCl -substituted crotylmagnesium halide intermediates **3**.

(2-Butene-1,4-diyl)magnesium (**2**; magnesium butadiene), conveniently obtained as an oligomer upon treatment of butadiene with magnesium metal in THF,¹ has been shown to be a versatile reagent for the preparation of

(1) Fujita, K.; Ohnuma, Y.; Yasuda, H.; Tani, H. *J. Organomet. Chem.* **1976**, *113*, 201.

(7) The observed first-order dependence on the concentration of carbon monoxide is consistent with either an associative process or with a two-step mechanism involving a 15-electron intermediate for which the concentration of CO is insufficient to detect rate saturation.

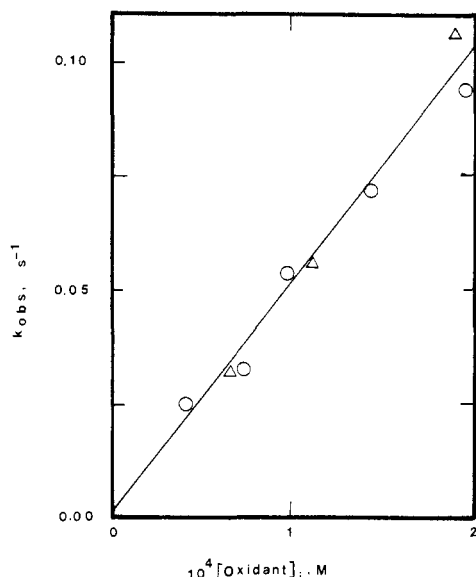


Figure 2. Dependence of the observed first-order rate constant on concentration of the initial oxidant (CH_2Cl_2 , 2°C , initially 1 atm of CO, and $\text{Cp}(\text{PPh}_3)\text{COFeCH}_3 = 0.10\text{--}0.15\text{ M}$): circles, ferricinium ion as oxidant; triangles, acetylferricinium ion as oxidant.

showed only the acyl couple ($4 + e^- \rightleftharpoons 2$). This behavior is consistent with partial electrogeneration of the alkyl cation radical **3** that then rapidly catalyzes the carbonylation of **1** to **2** in the region near the electrode.

The mechanism is Scheme I is strongly supported by kinetic studies in CH_2Cl_2 at 2°C . Runs were initiated by injection of a small volume of a solution of ferricinium or acetylferricinium tetrafluoroborate into solutions of **1** (10–15 mM), saturated with CO at 1 atm (ca. 6 mM), and the progress of the reaction was monitored by following the decrease in absorbance at 500 nm, associated with the conversion of **1** to **2**. Under these conditions of $[\text{1}] > [\text{CO}]$, first-order kinetics were observed, for which the rate constants were independent of the concentration of **1**, but linearly dependent on the initial concentration of the oxidizing agent, $[\text{OX}]_i$. Thus the experimental rate law is given by

$$\text{rate} = k[\text{CO}][\text{OX}]_i \quad k = 500 \pm 100 \text{ M}^{-1} \text{ s}^{-1} \quad (2)$$

in which there is zero-order dependence on **1**, and k has been evaluated from the slope of the plot in Figure 2. Under conditions where $[\text{CO}] \gg [\text{1}]$, a striking linear decrease in absorbance with time was observed. It continued until the absorbance corresponding to complete conversion to **2** was reached, when a sharp break occurred and the absorbance did not change further. This zero-order behavior is fully consistent with the rate law in eq 2.

With assumption of steady-state concentrations of **3** and **4**, the reaction sequence in Scheme I leads to the rate expression

$$\text{rate} = \frac{k_c k_{\text{et}} [\text{1}] [\text{CO}] [\text{OX}]}{k_{\text{et}} [\text{1}] + k_c [\text{CO}]} \quad (3)$$

Provided $k_{\text{et}} [\text{1}] \gg k_c [\text{CO}]$ (a reasonable condition, since the electron self-exchange reaction for related ferrocene derivatives is very rapid),⁷ the above expression simplifies to eq 2 in which the experimentally determined constant

k is to be equated with the Fe(III) carbonylation rate constant k_c . Thus, the rate of carbonylation of the formally iron(III) methyl complex **3** is conservatively estimated to be $10^7\text{--}10^8$ faster than the carbonylation rate of the formally Fe(II) species.

This difference between the rates of carbonylation in the Fe(II) and Fe(III) states is most likely attributable to a substantial reduction in the $d\pi$ donor ability of the metal center on oxidation, which allows a bent (or perhaps side-on) CO configuration in the activated complex to be energetically much more accessible.^{8,9} The crucial role of π back-bonding in the migratory insertion is also attested to by the ability of an external entering group, which is a strong π acid such as CO, to drive the reaction on Fe(II) thermodynamically much farther than a weaker π acid such as NCCH_3 ($K_{\text{CO}}/K_{\text{NCCH}_3} > 10^{15}$).¹⁰

It must be pointed out that parts per million concentration of an oxidant is, in principle, sufficient for the redox-catalyzed pathway to carry the entire reaction, so that interpretation of kinetic and stereochemical results must be done with caution. As this type of redox catalysis is most likely not restricted to iron, nor even to carbonylation reactions, the implications for organometallic reactivity may well be far-reaching.¹¹

Acknowledgment. We wish to thank the donors of the Petroleum Research Fund, administered by the American Chemical Society, and the Graduate School of Boston University for support of this research.

Registry No. 1, 12100-51-5; 2, 12101-02-9.

(8) Pladziejewicz, J. R.; Espenson, J. H. *J. Am. Chem. Soc.* **1973**, *95*, 56-63.

(9) Hoffman, R.; Berke, H. *J. Am. Chem. Soc.* **1978**, *100*, 7224-7236.

(10) $K_{\text{AN}} = 10^{-10} \text{ M}^{-1}$ and K_{CO} must be $> 10^5$ since no **1** is detectable after the catalyzed carbonylation of **1**.

(11) Enhanced reactivity toward ligand substitution has been reported in other 17-valence-electron organometallic species. (a) Hershberger, J. W.; Klingler, R. J.; Kochi, J. K. *J. Am. Chem. Soc.* **1982**, *104*, 3034-3043. (b) McCullen, S. B.; Walker, H. W.; Brown, T. C. *Ibid.* **1982**, *104*, 40089-4010. (c) Hepp, A. F.; Wrighton, M. S. *Ibid.* **1981**, *103*, 1258-1261. (d) Absi-Halabi, M.; Brown, T. L. *Ibid.* **1977**, *99*, 2982-2988.

$\text{Cp}_2\text{M}(s\text{-trans-}\eta^4\text{-butadiene)$ Complexes from Zirconocene and Hafnocene Dihalides and "Magnesium Butadiene"

Ulrich Dorf, Klaus Engel, and Gerhard Erker*

Abteilung für Chemie der Ruhr-Universität
D-4630 Bochum 1, Germany

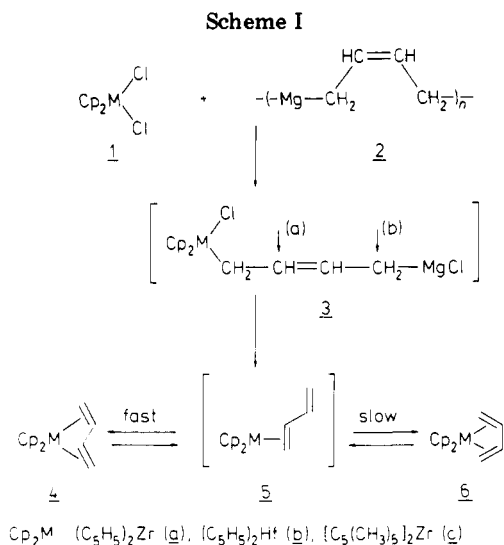
Received September 28, 1982

Summary: Under the kinetic control reaction of "magnesium butadiene" (**2**) with Cp_2MCl_2 complexes **1a-c** ($\text{Cp} = \eta\text{-C}_5\text{H}_5$, $\eta\text{-C}_5\text{Me}_5$; $\text{M} = \text{Zr}, \text{Hf}$) gives (*s-trans*- η^4 -butadiene)metallocene complexes **4a-c**, the products expected from a stepwise reaction through Cp_2MCl -substituted crotylmagnesium halide intermediates **3**.

(2-Butene-1,4-diyl)magnesium (**2**; magnesium butadiene), conveniently obtained as an oligomer upon treatment of butadiene with magnesium metal in THF,¹ has been shown to be a versatile reagent for the preparation of

(1) Fujita, K.; Ohnuma, Y.; Yasuda, H.; Tani, H. *J. Organomet. Chem.* **1976**, *113*, 201.

(7) The observed first-order dependence on the concentration of carbon monoxide is consistent with either an associative process or with a two-step mechanism involving a 15-electron intermediate for which the concentration of CO is insufficient to detect rate saturation.



(η^4 -diene)transition-metal complexes from metal halides.² Interestingly, the seemingly obvious reaction mechanism to account for this observation—formation of a metallacyclopentene intermediate via bond formation between the metal center and the most negatively charged terminal carbon atoms of the C_4 chain—clearly is incompatible with the reaction course established for electrophilic attack on “butadiene dianion” equivalents.³ The outcome of such stepwise reactions appears to be determined by the reactivity of the substituted allyl anion intermediate⁴ formed first. Consequently, under kinetic control the formation of three-membered not five-membered ring systems in the product-determining step is favored starting from “[$\text{C}_4\text{H}_6^{2-}$]” and gem dihalides.^{1,3} Using suitable reaction conditions, we now have obtained experimental evidence that this reaction pattern is also retained in the reaction of transition-metal dihalides 1a–c with “magnesium butadiene” 2.⁵

At ambient temperature the mutual rearrangement of the (η^4 -butadiene)zirconocene isomers is known to be fast ($4\text{a} \rightarrow 6\text{a}$: $\Delta G^\ddagger_{10.5^\circ\text{C}} = 22.7 \pm 0.3 \text{ kcal mol}^{-1}$).⁶ As expected, the well-known, independently accessible equilibrium mixture of (*s-cis*- and *s-trans*-butadiene)zirconocene complexes 6a and 4a (45:55) is obtained by treating an ethereal suspension of 2 with zirconocene dichloride at 25 °C. In contrast, performing this reaction as well as the subsequent workup below -10°C yields only (*s-trans*-butadiene)zirconocene (4a: ^{13}C NMR (toluene- d_6 , -10°C) δ 99 (Cp), 96 (d, $J = 152 \text{ Hz}$, CH), 59 (dd, $J = 149, 159 \text{ Hz}$, CH_2); 75% isolated yield). Within the accuracy of the low-temperature NMR (^1H , ^{13}C) analysis, under kinetic control exclusively isomer 4a is formed in the reaction of 1a with “magnesium butadiene” 2.

Analogous results have been obtained on reacting 2 with hafnocene dichloride (1b) and bis(η^5 -pentamethylcyclopentadienyl)zirconocene dichloride (1c). At 0 °C (*s-trans*-butadiene)hafnocene (4b:⁷ ^{13}C NMR (benzene- d_6)

δ 98.6 (Cp), 92.8 (d, $J = 147 \text{ Hz}$, CH), 57.8 (dd, $J = 142, 148 \text{ Hz}$, CH_2)) is formed. Clearly 4b is the thermodynamically less favored (butadiene)hafnocene isomer, since at 60 °C in benzene solution it completely rearranges to (*s-cis*-butadiene)hafnocene (6b: ^1H NMR (CH_2Cl_2 , -120°C) δ 5.17, 4.66 (s, 5 H each, Cp) 5.0 (m, 2 H, CH), 2.74, -0.73 (m, 2 H each, CH_2); ^{13}C NMR (benzene- d_6 , ambient temperature) δ 102.2 (Cp), 114.5 (d, $J = 156 \text{ Hz}$, CH), 45 (t, $J = 140 \text{ Hz}$, CH_2)). The thermally induced rearrangement $4\text{b} \rightarrow 6\text{b}$ can be described by a first-order rate law. A Gibbs activation energy of $\Delta G^\ddagger_{60^\circ\text{C}} = 24.7 \pm 0.3 \text{ kcal mol}^{-1}$ has been obtained for the isomerization process.

(*s-trans*-Butadiene)permethylzirconocene (4c: ^{13}C NMR (benzene- d_6) δ 11.7 (CH_3), 66.2 (dd, $J = 153, 142 \text{ Hz}$, CH_2), 102.0 (d, $J = 147 \text{ Hz}$, CH), 110.0 (Cp-C)) is formed exclusively upon treatment of 1c with 2 at 25 °C. Isomerization to the thermodynamically favored (*s-cis*-butadiene)isomer (6c: ^{13}C NMR (benzene- d_6 , ambient temperature) δ 11.8, 12.0 (CH_3), 56.5 (dd, $J = 150, 145 \text{ Hz}$, CH_2), (CH—hidden under solvent), 119.5, 119.4 (Cp-C)) has an even larger activation barrier: equilibration $4\text{c} \rightleftharpoons 6\text{c}$ slowly goes to completion (40:60) upon prolonged thermolysis at 140 °C ($\tau_{1/2} \approx 10 \text{ h}$).

From the observed formation of 4 under kinetic control in cases where (*s-trans*-butadiene)metallocenes are of about equal (4a,c) or even substantially lower thermodynamic stability (4b) than their *s-cis*-diene isomers 6a–c the reaction path followed can be deduced. Initial transition metal to carbon bond formation between 1 and the magnesium reagent 2 yields 3. This bimetallic intermediate shows the expected reactivity of a Cp_2MCl -substituted crotyl Grignard reagent.⁴ Preferred intramolecular nucleophilic attack by the internal allylic carbon center (a) leads to a formal analogue of a three-membered metallacyclic reaction product: the (η^2 -butadiene)metallocene intermediate 5, from independent trapping experiments^{6,8} known to equilibrate much more rapidly with 4 than with 6.

Acknowledgment. Financial aid from the Minister für Wissenschaft und Forschung des Landes Nordrhein-Westfalen is gratefully acknowledged.

Registry No. 1a, 1291-32-3; 1b, 12116-66-4; 1c, 54039-38-2; 2, 70809-00-6; 4a/6a, 75374-50-4; 4b/6b, 80185-89-3; 4c/6c, 84498-96-4.

(7) For ^1H NMR data see: Benn, R.; Schroth, G. *J. Organomet. Chem.* 1982, 228, 71.

(8) Erker, G.; Dorf, U.; Engel, K.; Atwood, J. L.; Hunter, W. E. *Angew. Chem.* 1982, 94, 915, 916.

Possible Formation of Ferrabenzene and Its Novel Conversion to 1,3-Diphenyl-2-methoxyferrocene

R. Ferede and Nell T. Allison*

Department of Chemistry, University of Arkansas
Fayetteville, Arkansas 72701

Received August 23, 1982

Summary: Introduction of (*E,E*)-1,4-dilithio-1,4-diphenylbutadiene (2) to $\eta^5\text{-C}_5\text{H}_5\text{Fe}(\text{CO})_2\text{I}$ followed by alkylation with $(\text{CH}_3)_3\text{OBF}_4$ gives 1,3-diphenyl-2-methoxyferrocene (4). Plausible intermediates in the formation of 4 include a ferrabenzene complex 3. After reductive elimination, loss of a carbonyl, and alkylation, 3 gives 4.

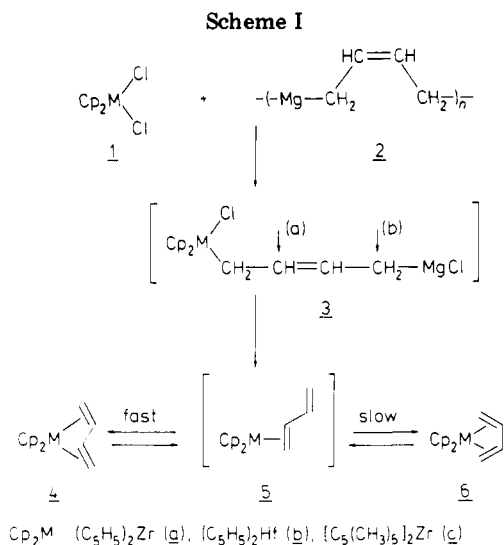
(2) Wreford, S. S.; Whitney, J. F. *Inorg. Chem.* 1981, 20, 3918, and references therein.

(3) Bahl, J. H.; Bates, R. B.; Beavers, W. A.; Mills, N. S. *J. Org. Chem.* 1976, 41, 1620. Richter, W. *J. Angew. Chem.* 1982, 94, 298.

(4) Benkeser, R. A. *Synthesis* 1971, 347.

(5) The reaction of 2 with 1a,b under thermodynamic control has been reported recently: Yasuda, H.; Kajihara, Y.; Mashima, K.; Nagasuna, K.; Lee, K.; Nakamura, A. *Organometallics* 1982, 1, 388.

(6) Erker, G.; Wicher, J.; Engel, K.; Rosenfeldt, F.; Dietrich, W.; Krüger, C. *J. Am. Chem. Soc.* 1980, 102, 6344. Erker, G.; Engel, K.; Krüger, C. 9th International Conference on Organometallic Chemistry, Toronto 1981, Abstr. 2 E 74.



(η^4 -diene)transition-metal complexes from metal halides.² Interestingly, the seemingly obvious reaction mechanism to account for this observation—formation of a metallacyclopentene intermediate via bond formation between the metal center and the most negatively charged terminal carbon atoms of the C₄ chain—clearly is incompatible with the reaction course established for electrophilic attack on “butadiene dianion” equivalents.³ The outcome of such stepwise reactions appears to be determined by the reactivity of the substituted allyl anion intermediate⁴ formed first. Consequently, under kinetic control the formation of three-membered not five-membered ring systems in the product-determining step is favored starting from “[C₄H₆²⁻]” and gem dihalides.^{1,3} Using suitable reaction conditions, we now have obtained experimental evidence that this reaction pattern is also retained in the reaction of transition-metal dihalides 1a–c with “magnesium butadiene” 2.⁵

At ambient temperature the mutual rearrangement of the (η^4 -butadiene)zirconocene isomers is known to be fast (4a \rightarrow 6a: $\Delta G^\ddagger_{10.5^\circ\text{C}} = 22.7 \pm 0.3$ kcal mol⁻¹).⁶ As expected, the well-known, independently accessible equilibrium mixture of (*s-cis*- and *s-trans*-butadiene)zirconocene complexes 6a and 4a (45:55) is obtained by treating an ethereal suspension of 2 with zirconocene dichloride at 25 °C. In contrast, performing this reaction as well as the subsequent workup below -10 °C yields only (*s-trans*-butadiene)zirconocene (4a: ¹³C NMR (toluene-*d*₈, -10 °C) δ 99 (Cp), 96 (d, *J* = 152 Hz, CH), 59 (dd, *J* = 149, 159 Hz, CH₂); 75% isolated yield). Within the accuracy of the low-temperature NMR (¹H, ¹³C) analysis, under kinetic control exclusively isomer 4a is formed in the reaction of 1a with “magnesium butadiene” 2.

Analogous results have been obtained on reacting 2 with hafnocene dichloride (1b) and bis(η^5 -pentamethylcyclopentadienyl)zirconocene dichloride (1c). At 0 °C (*s-trans*-butadiene)hafnocene (4b:⁷ ¹³C NMR (benzene-*d*₆)

δ 98.6 (Cp), 92.8 (d, *J* = 147 Hz, CH), 57.8 (dd, *J* = 142, 148 Hz, CH₂)) is formed. Clearly 4b is the thermodynamically less favored (butadiene)hafnocene isomer, since at 60 °C in benzene solution it completely rearranges to (*s-cis*-butadiene)hafnocene (6b: ¹H NMR (CHCl₃, -120 °C) δ 5.17, 4.66 (s, 5 H each, Cp), 5.0 (m, 2 H, CH), 2.74, -0.73 (m, 2 H each, CH₂); ¹³C NMR (benzene-*d*₆, ambient temperature) δ 102.2 (Cp), 114.5 (d, *J* = 156 Hz, CH), 45 (t, *J* = 140 Hz, CH₂)). The thermally induced rearrangement 4b \rightarrow 6b can be described by a first-order rate law. A Gibbs activation energy of $\Delta G^\ddagger_{60^\circ\text{C}} = 24.7 \pm 0.3$ kcal mol⁻¹ has been obtained for the isomerization process.

(*s-trans*-Butadiene)permethylzirconocene (4c: ¹³C NMR (benzene-*d*₆) δ 11.7 (CH₃), 66.2 (dd, *J* = 153, 142 Hz, CH₂), 102.0 (d, *J* = 147 Hz, CH), 110.0 (Cp-C)) is formed exclusively upon treatment of 1c with 2 at 25 °C. Isomerization to the thermodynamically favored (*s-cis*-butadiene)isomer (6c: ¹³C NMR (benzene-*d*₆, ambient temperature) δ 11.8, 12.0 (CH₃), 56.5 (dd, *J* = 150, 145 Hz, CH₂), (CH—hidden under solvent), 119.5, 119.4 (Cp-C)) has an even larger activation barrier: equilibration 4c \rightleftharpoons 6c slowly goes to completion (40:60) upon prolonged thermolysis at 140 °C ($\tau_{1/2} \approx 10$ h).

From the observed formation of 4 under kinetic control in cases where (*s-trans*-butadiene)metallocenes are of about equal (4a,c) or even substantially lower thermodynamic stability (4b) than their *s-cis*-diene isomers 6a–c the reaction path followed can be deduced. Initial transition metal to carbon bond formation between 1 and the magnesium reagent 2 yields 3. This bimetallic intermediate shows the expected reactivity of a Cp₂MCl-substituted crotyl Grignard reagent.⁴ Preferred intramolecular nucleophilic attack by the internal allylic carbon center (a) leads to a formal analogue of a three-membered metallacyclic reaction product: the (η^2 -butadiene)metallocene intermediate 5, from independent trapping experiments^{6,8} known to equilibrate much more rapidly with 4 than with 6.

Acknowledgment. Financial aid from the Minister für Wissenschaft und Forschung des Landes Nordrhein-Westfalen is gratefully acknowledged.

Registry No. 1a, 1291-32-3; 1b, 12116-66-4; 1c, 54039-38-2; 2, 70809-00-6; 4a/6a, 75374-50-4; 4b/6b, 80185-89-3; 4c/6c, 84498-96-4.

(7) For ¹H NMR data see: Benn, R.; Schroth, G. *J. Organomet. Chem.* 1982, 228, 71.

(8) Erker, G.; Dorf, U.; Engel, K.; Atwood, J. L.; Hunter, W. E. *Angew. Chem.* 1982, 94, 915, 916.

Possible Formation of Ferrabenzene and Its Novel Conversion to 1,3-Diphenyl-2-methoxyferrocene

R. Ferede and Nell T. Allison*

Department of Chemistry, University of Arkansas
Fayetteville, Arkansas 72701

Received August 23, 1982

Summary: Introduction of (*E,E*)-1,4-dilithio-1,4-diphenylbutadiene (2) to η^5 -C₅H₅Fe(CO)₂I followed by alkylation with (CH₃)₃OBF₄ gives 1,3-diphenyl-2-methoxyferrocene (4). Plausible intermediates in the formation of 4 include a ferrabenzene complex 3. After reductive elimination, loss of a carbonyl, and alkylation, 3 gives 4.

(2) Wreford, S. S.; Whitney, J. F. *Inorg. Chem.* 1981, 20, 3918, and references therein.

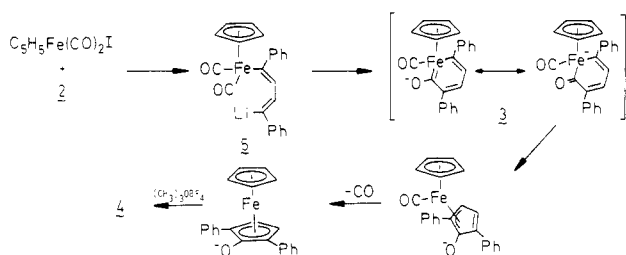
(3) Bahl, J. H.; Bates, R. B.; Beavers, W. A.; Mills, N. S. *J. Org. Chem.* 1976, 41, 1620. Richter, W. *J. Angew. Chem.* 1982, 94, 298.

(4) Benkeser, R. A. *Synthesis* 1971, 347.

(5) The reaction of 2 with 1a,b under thermodynamic control has been reported recently: Yasuda, H.; Kajihara, Y.; Mashima, K.; Nagasuna, K.; Lee, K.; Nakamura, A. *Organometallics* 1982, 1, 388.

(6) Erker, G.; Wicher, J.; Engel, K.; Rosenfeldt, F.; Dietrich, W.; Krüger, C. *J. Am. Chem. Soc.* 1980, 102, 6344. Erker, G.; Engel, K.; Krüger, C. 9th International Conference on Organometallic Chemistry, Toronto 1981, Abstr. 2 E 74.

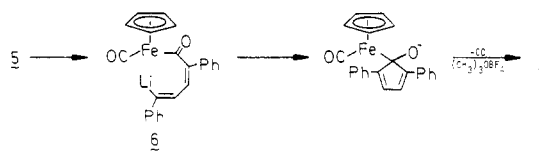
Scheme I



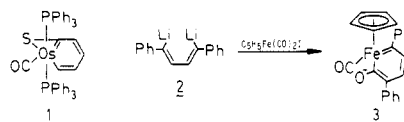
The importance of unsaturated transition metallacycles is apparent. Metallacyclopentadienes are novel and useful intermediates in reactions such as alkyne trimerizations.¹ Metallacyclobutenes are thought to be intermediates in the polymerization of alkynes² and precursors to metal carbenes that catalyze alkene metathesis.³ Metallacyclobutadienes, in turn, are being studied as potential alkyne metathesis catalysts.⁴ The osmacyclohexatriene or osmabenzene **1**, recently reported by Roper and co-workers, was generated by introducing $Os(CO)(CS)(PPh_3)_3$ to ethyne. This stable compound was found by X-ray analysis to contain a delocalized ring.⁵ We wish to report formation of 1,3-diphenyl-2-methoxyferrocene (**4**) via an apparent conversion from ferracyclohexatriene or ferrabenzene **3**.

As a rational approach toward the preparation of a metallacyclohexatriene moiety, we sought a method that would favor both a metal-carbon single bond (metal-alkyl bond) and a metal-carbon double bond (metal-carbene bond) formation. The reaction of alkyllithium reagents with transition-metal halides forming metal alkyls is well established.⁶ Furthermore, reaction of alkyllithium reagents with terminal carbonyls in metal carbonyl or metal acyl complexes generates metal carbenes (e.g., Fischer-type carbene complexes)⁷ or metal diacyl complexes (e.g., Lukehart's metallaacetylacetonate complexes)⁸ respectively. In order to prepare a transition metallabenzene, we combined these approaches by introducing

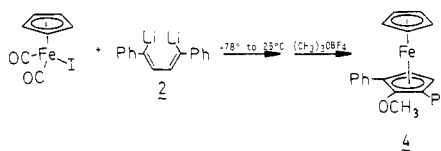
Scheme II



(*E,E*)-1,4-dilithio-1,4-diphenylbutadiene (**2**)⁹ to η^5 -cyclopentadienyliron dicarbonyl iodide ($C_5H_5Fe(CO)_2I$) with the assumption that concomitant formation of metal-alkyl and metal-carbene bonds would occur.



Addition of $C_5H_5Fe(CO)_2I$ in ethyl ether to a cold (Dry Ice/2-propanol bath) solution of **2** in ethyl ether was followed by warming to room temperature. Solid $(C-H_3)_3OBF_4$ was then added. Chromatography (alumina-pentane/benzene)¹⁰ yielded an air-sensitive red-orange oil identified as **4** (20%).¹¹



A credible mechanism for the formation of **1** is given in Scheme I. Reaction of **2** with $C_5H_5Fe(CO)_2I$ produces the σ complex **5**. Cyclization by attack on the carbonyl with the alkenyllithium moiety generates the ferrabenzene **3**. Under the reaction conditions, reductive elimination, loss of a terminal carbonyl, and alkylation give **4**. Alkylation may occur at any point during the conversion of **3** to **4**.¹⁰

The most likely alternative mechanism not involving ferrabenzene **3** is given in Scheme II. Alkyl migration to an adjacent carbonyl in **5** yields the acyl complex **6**. Intramolecular attack by the alkenyllithium moiety on this acyl carbonyl followed by loss of carbon monoxide and alkylation could give **4**.

The plausibility of a metallabenzene or metallacyclohexatriene intermediate as shown in Scheme I has recently found precedent. As mentioned earlier, Roper and co-workers have reported that the reaction of ethyne with $Os(CO)(CS)(PPh_3)_3$ yields a stable delocalized osmabenzene complex **1**.⁵ Schrock and co-workers, on the other hand, found that $(Me_3CO)_3WCEt$ reacts with 3-hexyne to give a pentaethylcyclopentadienyl ligand.¹³ In this case, a metallacyclohexatriene could be a likely intermediate. These results together with the possible generation of the ferracyclohexatriene **3** by our direct method and its conversion to **4** suggests that reductive elimination leading to cyclopentadienyl ligands may be a general decomposition pathway for complexes of this type.

Further study of Schemes I and II brings out a few crucial comparisons. In reactions of $(CO)_5ReCH_3$, alkyl-

(1) Vollhardt, K. P. C. *Acc. Chem. Res.* **1977**, *10*, 1. Hillard, R. L., III; Vollhardt, K. P. C. *J. Am. Chem. Soc.* **1977**, *99*, 4058. Naiman, A.; Vollhardt, K. P. C. *Angew. Chem., Int. Ed. Engl.* **1977**, *16*, 708. Funk, R. L.; Vollhardt, K. P. C. *J. Am. Chem. Soc.* **1979**, *101*, 215.

(2) Katz, T. J.; Savage, E. B.; Lee, S. J.; Nair, M. *J. Am. Chem. Soc.* **1980**, *102*, 7944.

(3) Katz, T. J.; Lee, S. J.; Nair, M.; Savage, E. B. *J. Am. Chem. Soc.* **1980**, *102*, 7942. Tebbe, F. N.; Harlow, R. L. *Ibid.* **1980**, *102*, 6149. McKinney, R. J.; Tulip, T. H.; Thorn, D. L.; Coolbaugh, T. S.; Tebbe, F. N. *Ibid.* **1981**, *103*, 5584.

(4) Wengrovius, J. H.; Sancho, J.; Schrock, R. R. *J. Am. Chem. Soc.* **1981**, *103*, 3932.

(5) Roper, W. R.; Elliott, G. P.; Waters, J. M. *J. Chem. Soc., Chem. Commun.* **1982**, 811.

(6) For examples of forming metal alkyl bonds with organolithium or Grignard reagents: cf. Green, M. L. H.; Mole, T. J. *Organomet. Chem.* **1968**, *12*, 404. Piper, T. S.; Wilkinson, G. J. *Inorg. Nucl. Chem.* **1956**, *3*, 104. Hullman, B. F.; Pauson, P. L. *Chem. Ind. (London)* **1955**, 653. Green, M. L. H.; Ishag, M.; Mole, T. Z. *Naturforsch., B: Anorg. Chem., Org. Chem., Biochem., Biol.* **1965**, *20B*, 598. Eisenstadt, A.; Scharf, G.; Fuchs, B. *Tetrahedron Lett.* **1971**, 679. For early transition metals see: Schrock, R. R.; Parshall, G. W. *Chem. Rev.* **1976**, *76*, 243.

(7) For carbene complex reviews see: Cardin, D. J.; Centinkaya, B.; Lappert, M. F. *Chem. Rev.* **1972**, *72*, 545. Cotton, F. A.; Lukehart, C. M. *Prog. Inorg. Chem.* **1972**, *16*, 487. Casey, C. P. In "Transition Metal Organometallics in Organic Synthesis"; Alper, H., Ed.; Academic Press: New York, **1976**; Vol. 1, Chapter 3.

(8) Lukehart, C. M.; Zeile, J. V. *J. Am. Chem. Soc.* **1977**, *99*, 4368. Lukehart, C. M.; Zeile, J. V. *Ibid.* **1976**, *98*, 2365. Lukehart, C. M.; Torrence, G. P.; Zeile, J. V. *Ibid.* **1975**, *97*, 6903. Darensbourg, M. J. *Organomet. Chem.* **1972**, *38*, 133. Casey, C. P.; Bunnell, C. A. *J. Chem. Soc., Chem. Commun.* **1974**, 733. Casey, C. P.; Bunnell, C. A. *J. Am. Chem. Soc.* **1976**, *98*, 436.

(9) Barton, T. J.; Nelson, A. J.; Clardy, J. *J. Org. Chem.* **1972**, *37*, 895. Atwell, W. H.; Weyenberg, D. R.; Gilman, H. *Ibid.* **1967**, *32*, 885.

(10) By extraction with pentane of the reaction mixture prior to chromatography **4** can be detected by ¹H NMR.

(11) ¹H NMR data for **4** (acetone-*d*₆): C_6H_5 , δ 3.9 (s, 5 H), $(C_6H_5)_2(C-H_3O)C_5H_2$, CH_3O , δ 3.2 (s, 3 H), C_5H_2 , 4.3 (s, 2 H), C_6H_5 , 7.4 (m, 10 H). ¹³C NMR (acetone-*d*₆): C_6H_5 , δ 72.7; $(C_6H_5)_2(C-H_3O)C_5H_2$, 138.6, 128.9, 128.2, 126.9, 123.3, 78.7, 62.5, 62.3. MS: 368 (M^+); IR (neat): 3020, 2920, 1590, 1500, 1455, 1435, 1370, 1095, 1000, 750, 680 cm^{-1} . Anal. Calcd for $C_{23}H_{20}OFe$: C, 75.02; H, 5.47. Found: C, 74.94; H, 5.44.

lithium reagents presumably attack a terminal carbonyl ligand without prior methyl migration.¹² Scheme I is consistent with this reactivity, whereas Scheme II allows an alkyl migration to precede nucleophilic attack by the alkenyllithium moiety. Another important difference between Schemes I and II is the nucleophilic attack of the alkenyllithium moiety on either the terminally bonded carbonyl of 5 or the acyl carbonyl of 6. Coordinated acyls in neutral transition-metal complexes, in general, are unreactive toward nucleophilic reagents.¹⁴ On the other hand, nucleophilic attack on terminal carbonyls by alkenyllithium reagents is well documented.^{8,12} In fact, Lukehart and co-workers found that introduction of methyl lithium to $C_5H_5Fe(CO)_2COCH_3$ (7) followed by protonation gave $C_5H_5Fe(CO)[C(CH_3)O\cdots H\cdots OC(CH_3)]$.⁸ Scheme I certainly parallels this reactivity in that the terminal carbonyl of 5, not the acyl carbonyl in 6 (Scheme II), reacts. Although Scheme II cannot be totally ruled out, we feel that the chemistry of 7 and isolation of 4 is compelling corroboration for Scheme I and the intermediacy of ferrabenzene 3. Further work on the isolation of or spectral evidence for ferrabenzene 3 and other transition metallabenzene and the reaction of other alkyl and alkenyldilithium reagents with transition-metal carbonyl halides is currently being pursued.

Acknowledgment. We are grateful to the Research Corp. for financial support. The FT NMR spectrometer employed was provided by a NSF departmental instrument grant. We thank Professor J. Hinton for his assistance in obtaining the ¹³C NMR spectrum.

Registry No. 2, 55373-67-6; 3, 84175-81-5; 4, 84175-80-4; $C_5H_5Fe(CO)_2I$, 12078-28-3; $(CH_3)_3OBF_4$, 420-37-1.

(12) Darst, K. P.; Lenhart, P. G.; Lukehart, C. M.; Warfield, L. T. *J. Organomet. Chem.* 1980, 195, 317. Recently (Lukehart, C. M.; Srinivasan, K. *Organometallics* 1982, 1, 1247, ref 11), Lukehart and Srinivasan led the reader to believe that they are presently looking at "metallabutadienes", which are generated by addition of alkenyllithiums to terminal carbonyls in $CpFe(CO)_2(vinyl)$. This certainly parallels Scheme I.

(13) Schrock, R. R.; Pederson, S. F.; Churchill, M. R.; Wasserman, H. *J. Am. Chem. Soc.* 1982, 104, 6808. We thank Professor Schrock for a preprint of this work.

(14) Collman, J. P.; Hegedus, L. S. "Principles and Applications of Organotransition Metal Chemistry"; University Science Books: Mill Valley, CA, 1980; p 303.

Oxidatively Induced Migration of Hydrogen from Metal to Carbon Monoxide

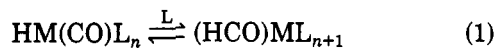
Alan Cameron, Vedene H. Smith,* and Michael C. Baird*

Department of Chemistry, Queen's University
Kingston, Ontario, Canada K7L 3N6

Received August 6, 1982

Summary: Copper(II) and cerium(IV) oxidations of the compounds $\eta^5-C_5H_5Fe(CO)_2H$ and $\eta^5-C_5H_5Mo(CO)_3H$ in alcohols produce the corresponding formic acid esters; by analogy with similar chemistry of the analogous iron and molybdenum alkyl compounds, the reactions must involve intermediate formyl compounds, possibly the first of the d block elements to be intentionally formed via 1,2 migration of hydrogen from metal to CO. Extended Hückel calculations demonstrate a likely relationship between these oxidatively induced migration reactions and the Lewis acid induced migration reactions of $MeMn(CO)_5$.

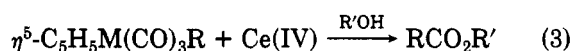
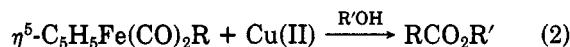
The formation of formyl complexes via migratory insertion of carbon monoxide into a transition metal-hydrogen bond (eq 1) has long been a goal in organometallic



chemistry, in large part because of the presumed importance of the reaction in the catalytic hydrogenation of carbon monoxide.¹⁻³ However, although formyl complexes can be prepared by treatment of carbonyl complexes with sources of hydride ion,⁴⁻⁸ they are often unstable with respect to "deinsertion", the reverse of (1). Thus where a route to deinsertion is kinetically accessible, the relatively high M-H bond strength generally drives (1) to the left.⁹

To date, while kinetic evidence for formyl intermediates exists¹⁰ and a formylrhodium compound has been prepared as in (1),¹¹ the only systematic approach to the inducement of (1) has been by Marks et al.¹² They showed that treatment of the thorium hydride $(\eta^5-C_5Me_5)_2ThH(OR)$ (R = bulky alkyl, aryl) with CO generates the η^2 -formyl species $(\eta^5-C_5Me_5)_2Th(\eta^2-CHO)OR$, in which the formyl structure is stabilized thermodynamically by coordination of the oxygen to the electrophilic metal atom. This approach may be of general utility, in view of the known proclivity of Lewis acids to coordinate and stabilize carbonyl groups in bridging and acyl positions.^{13,14}

We now wish to communicate a second, possibly general route to the formation of formyl compounds directly from carbonyl hydrides. The oxidative carbonylation reactions of eq 2 and 3 have known for several years.¹⁵⁻¹⁸



M = Mo, W; R, R' = alkyl

Although mechanisms are not generally understood in detail, there is good evidence¹⁸⁻²⁰ that the iron complexes,

- (1) Masters, C. *Adv. Organomet. Chem.* 1979, 17, 61.
- (2) Rofer-DePoorter, C. K. *Chem. Rev.* 1981, 81, 447.
- (3) Muetterties, E. L.; Stein, J. *Chem. Rev.* 1979, 79, 479.
- (4) Casey, C. P.; Andrews, M. A.; McAlister, D. R.; Rinz, J. E. *J. Am. Chem. Soc.* 1980, 102, 1927.
- (5) Tam, W.; Lin, G.-Y.; Gladysz, J. A. *Organometallics* 1982, 1, 525.
- (6) Thorn, D. L. *Organometallics* 1982, 1, 197.
- (7) Clark, G. R.; Headford, C. E. L.; Marsden, K.; Roper, W. R. *J. Organomet. Chem.* 1982, 231, 335.
- (8) Sweet, J. R.; Graham, W. A. G. *J. Am. Chem. Soc.* 1982, 104, 2811.
- (9) Gladysz, J. A. *Adv. Organomet. Chem.* 1982, 20, 1.
- (10) See, for instance, Pearson, R. G.; Walker, H. W.; Mauerman, H.; Ford, P. C. *Inorg. Chem.* 1981, 20, 2741.
- (11) Wayland, B. B.; Woods, B. A. *J. Chem. Soc., Chem. Commun.* 1981, 700. The authors, however, propose a radical rather than a migratory mode of formation.
- (12) Fagan, P. J.; Moloy, K. G.; Marks, T. J. *J. Am. Chem. Soc.* 1981, 103, 6959.
- (13) Shriver, D. F. *J. Organomet. Chem.* 1975, 94, 259.
- (14) Butts, S. B.; Strauss, S. H.; Holt, E. M.; Stimson, R. E.; Alcock, N. W.; Shriver, D. F. *J. Am. Chem. Soc.* 1980, 102, 5093.
- (15) Anderson, S. N.; Fong, C. W.; Johnson, M. D. *J. Chem. Soc., Chem. Commun.* 1973, 163.
- (16) Nicholas, K. M.; Rosenblum, M. *J. Am. Chem. Soc.* 1973, 95, 4449.
- (17) Bock, P. L.; Boschetto, D. J.; Rasmussen, J. R.; Demers, J. P.; Whitesides, G. M. *J. Am. Chem. Soc.* 1974, 96, 2814.
- (18) Rogers, W. N.; Page, J. A.; Baird, M. C. *Inorg. Chem.* 1981, 20, 3521.
- (19) Magnuson, R. H.; Zulu, S.; T'sai, W.-M.; Giering, W. P. *J. Am. Chem. Soc.* 1980, 102, 6887.

lithium reagents presumably attack a terminal carbonyl ligand without prior methyl migration.¹² Scheme I is consistent with this reactivity, whereas Scheme II allows an alkyl migration to precede nucleophilic attack by the alkenyllithium moiety. Another important difference between Schemes I and II is the nucleophilic attack of the alkenyllithium moiety on either the terminally bonded carbonyl of 5 or the acyl carbonyl of 6. Coordinated acyls in neutral transition-metal complexes, in general, are unreactive toward nucleophilic reagents.¹⁴ On the other hand, nucleophilic attack on terminal carbonyls by alkenyllithium reagents is well documented.^{8,12} In fact, Lukehart and co-workers found that introduction of methyl lithium to $C_5H_5Fe(CO)_2COCH_3$ (7) followed by protonation gave $C_5H_5Fe(CO)[C(CH_3)O\cdots H\cdots OC(CH_3)]$.⁸ Scheme I certainly parallels this reactivity in that the terminal carbonyl of 5, not the acyl carbonyl in 6 (Scheme II), reacts. Although Scheme II cannot be totally ruled out, we feel that the chemistry of 7 and isolation of 4 is compelling corroboration for Scheme I and the intermediacy of ferrabenzene 3. Further work on the isolation of or spectral evidence for ferrabenzene 3 and other transition metallabenzene and the reaction of other alkyl and alkenyldilithium reagents with transition-metal carbonyl halides is currently being pursued.

Acknowledgment. We are grateful to the Research Corp. for financial support. The FT NMR spectrometer employed was provided by a NSF departmental instrument grant. We thank Professor J. Hinton for his assistance in obtaining the ¹³C NMR spectrum.

Registry No. 2, 55373-67-6; 3, 84175-81-5; 4, 84175-80-4; $C_5H_5Fe(CO)_2I$, 12078-28-3; $(CH_3)_3OBF_4$, 420-37-1.

(12) Darst, K. P.; Lenhart, P. G.; Lukehart, C. M.; Warfield, L. T. *J. Organomet. Chem.* 1980, 195, 317. Recently (Lukehart, C. M.; Srinivasan, K. *Organometallics* 1982, 1, 1247, ref 11), Lukehart and Srinivasan led the reader to believe that they are presently looking at "metallabutadienes", which are generated by addition of alkenyllithiums to terminal carbonyls in $CpFe(CO)_2(vinyl)$. This certainly parallels Scheme I.

(13) Schrock, R. R.; Pederson, S. F.; Churchill, M. R.; Wasserman, H. *J. Am. Chem. Soc.* 1982, 104, 6808. We thank Professor Schrock for a preprint of this work.

(14) Collman, J. P.; Hegedus, L. S. "Principles and Applications of Organotransition Metal Chemistry"; University Science Books: Mill Valley, CA, 1980; p 303.

Oxidatively Induced Migration of Hydrogen from Metal to Carbon Monoxide

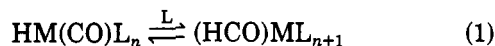
Alan Cameron, Vedene H. Smith,* and Michael C. Baird*

Department of Chemistry, Queen's University
Kingston, Ontario, Canada K7L 3N6

Received August 6, 1982

Summary: Copper(II) and cerium(IV) oxidations of the compounds $\eta^5-C_5H_5Fe(CO)_2H$ and $\eta^5-C_5H_5Mo(CO)_3H$ in alcohols produce the corresponding formic acid esters; by analogy with similar chemistry of the analogous iron and molybdenum alkyl compounds, the reactions must involve intermediate formyl compounds, possibly the first of the d block elements to be intentionally formed via 1,2 migration of hydrogen from metal to CO. Extended Hückel calculations demonstrate a likely relationship between these oxidatively induced migration reactions and the Lewis acid induced migration reactions of $MeMn(CO)_5$.

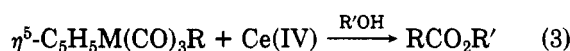
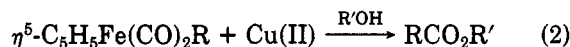
The formation of formyl complexes via migratory insertion of carbon monoxide into a transition metal-hydrogen bond (eq 1) has long been a goal in organometallic



chemistry, in large part because of the presumed importance of the reaction in the catalytic hydrogenation of carbon monoxide.¹⁻³ However, although formyl complexes can be prepared by treatment of carbonyl complexes with sources of hydride ion,⁴⁻⁸ they are often unstable with respect to "deinsertion", the reverse of (1). Thus where a route to deinsertion is kinetically accessible, the relatively high M-H bond strength generally drives (1) to the left.⁹

To date, while kinetic evidence for formyl intermediates exists¹⁰ and a formylrhodium compound has been prepared as in (1),¹¹ the only systematic approach to the inducement of (1) has been by Marks et al.¹² They showed that treatment of the thorium hydride $(\eta^5-C_5Me_5)_2ThH(OR)$ (R = bulky alkyl, aryl) with CO generates the η^2 -formyl species $(\eta^5-C_5Me_5)_2Th(\eta^2-CHO)OR$, in which the formyl structure is stabilized thermodynamically by coordination of the oxygen to the electrophilic metal atom. This approach may be of general utility, in view of the known proclivity of Lewis acids to coordinate and stabilize carbonyl groups in bridging and acyl positions.^{13,14}

We now wish to communicate a second, possibly general route to the formation of formyl compounds directly from carbonyl hydrides. The oxidative carbonylation reactions of eq 2 and 3 have known for several years.¹⁵⁻¹⁸



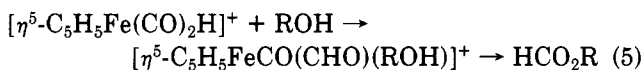
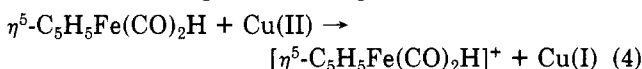
M = Mo, W; R, R' = alkyl

Although mechanisms are not generally understood in detail, there is good evidence¹⁸⁻²⁰ that the iron complexes,

- (1) Masters, C. *Adv. Organomet. Chem.* 1979, 17, 61.
- (2) Rofer-DePoorter, C. K. *Chem. Rev.* 1981, 81, 447.
- (3) Muetterties, E. L.; Stein, J. *Chem. Rev.* 1979, 79, 479.
- (4) Casey, C. P.; Andrews, M. A.; McAlister, D. R.; Rinz, J. E. *J. Am. Chem. Soc.* 1980, 102, 1927.
- (5) Tam, W.; Lin, G.-Y.; Gladysz, J. A. *Organometallics* 1982, 1, 525.
- (6) Thorn, D. L. *Organometallics* 1982, 1, 197.
- (7) Clark, G. R.; Headford, C. E. L.; Marsden, K.; Roper, W. R. *J. Organomet. Chem.* 1982, 231, 335.
- (8) Sweet, J. R.; Graham, W. A. G. *J. Am. Chem. Soc.* 1982, 104, 2811.
- (9) Gladysz, J. A. *Adv. Organomet. Chem.* 1982, 20, 1.
- (10) See, for instance, Pearson, R. G.; Walker, H. W.; Mauerman, H.; Ford, P. C. *Inorg. Chem.* 1981, 20, 2741.
- (11) Wayland, B. B.; Woods, B. A. *J. Chem. Soc., Chem. Commun.* 1981, 700. The authors, however, propose a radical rather than a migratory mode of formation.
- (12) Fagan, P. J.; Moloy, K. G.; Marks, T. J. *J. Am. Chem. Soc.* 1981, 103, 6959.
- (13) Shriver, D. F. *J. Organomet. Chem.* 1975, 94, 259.
- (14) Butts, S. B.; Strauss, S. H.; Holt, E. M.; Stimson, R. E.; Alcock, N. W.; Shriver, D. F. *J. Am. Chem. Soc.* 1980, 102, 5093.
- (15) Anderson, S. N.; Fong, C. W.; Johnson, M. D. *J. Chem. Soc., Chem. Commun.* 1973, 163.
- (16) Nicholas, K. M.; Rosenblum, M. *J. Am. Chem. Soc.* 1973, 95, 4449.
- (17) Bock, P. L.; Boschetto, D. J.; Rasmussen, J. R.; Demers, J. P.; Whitesides, G. M. *J. Am. Chem. Soc.* 1974, 96, 2814.
- (18) Rogers, W. N.; Page, J. A.; Baird, M. C. *Inorg. Chem.* 1981, 20, 3521.
- (19) Magnuson, R. H.; Zulu, S.; T'sai, W.-M.; Giering, W. P. *J. Am. Chem. Soc.* 1980, 102, 6887.

at least, react to form 17-electron cationic intermediates $[\eta^5\text{-C}_5\text{H}_5\text{Fe}(\text{CO})_2\text{R}]^+$. These apparently rearrange spontaneously in the alcohols R'OH to give solvated acyl intermediates $[\eta^5\text{-C}_5\text{H}_5\text{Fe}(\text{CO})(\text{COR})(\text{R}'\text{OH})]^+$ that in turn can undergo attack by alcohol²¹ or otherwise decompose to give esters.

Although the exact stoichiometries of the reactions and the reasons for acyl formation were not clear, it seemed possible that similar oxidative carboxylations of metal carbonyl hydrides might also occur, yielding formyl intermediates which could be trapped by their reactions with alcohols. We find accordingly that treatment of the yellow iron hydride $\eta^5\text{-C}_5\text{H}_5\text{Fe}(\text{CO})_2\text{H}$,²² with 3 molar equiv of $\text{CuCl}_2 \cdot 2\text{H}_2\text{O}$ in methanol, ethanol, and *n*-propanol leads to instantaneous formation of red solutions containing some $\eta^5\text{-C}_5\text{H}_5\text{Fe}(\text{CO})_2\text{Cl}$, identified by its IR spectrum.²³ Brief refluxing and distillation of the solvent mixtures from the copper- and iron-containing residues followed by GC analyses of the distillates showed that the major organic product from each alcohol was the corresponding formic acid ester. In the case of the reaction in ethanol, the yield of ethyl formate was about 60%, comparable with yields from reactions of the iron alkyls cited above and consistent with the following series of steps



A similar reaction of $\eta^5\text{-C}_5\text{H}_5\text{Mo}(\text{CO})_3\text{H}$ ²⁴ with ceric ammonium nitrate in methanol at 0 °C gave significant amounts of methyl formate (ultimately 25% yield) only on warming. The initial product appeared to be formic acid, and, as cerium(IV), like copper(II), is a one electron oxidant, it seems likely that the molybdenum hydride also reacted in a sequence as (4) and (5) but with adventitious water as well as with solvent.^{15,25} Thus in both metal systems, it seems that oxidation of the metal induces migration of hydrogen from the metal to a coordinated carbonyl group.²⁶

While the generality of this type of reaction is being investigated further, it seems reasonable to consider why oxidation induces migration. As has been pointed out elsewhere,²⁹ hydride transfer should be favoured if the

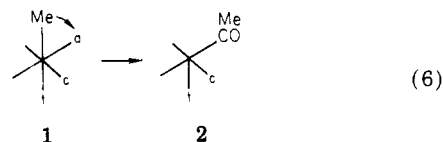
hydride ligand is electron rich and/or if the acceptor carbonyl group does not π bond strongly to the metal ion. In the latter instance the presumed receptor orbital, a vacant molecular orbital which is of predominantly CO π^* character, would lie at relatively low energy. In the case of the cationic 17-electron hydrides postulated here, the hydridic character of the metal-bonded hydrogens would be low, and their greater propensity toward migration than in the neutral parent compounds would presumably be a result of decreased back-donation to the carbonyl groups and hence a lowering of the π^* orbitals and an increase in their Lewis acid character.

This interpretation is possibly at odds, however, with work done elsewhere. Shriver et al.³⁰ have presented kinetic evidence that Lewis acids can induce the reaction of $\text{MeMn}(\text{CO})_5$ with CO to form $\text{MeCOMn}(\text{CO})_5$. It was suggested that the Lewis acids lower the activation energy for the methyl migration reaction by coordinating to the oxygen atom of the acceptor CO, although it was recognized that the so bifunctionally coordinated CO would become a much better π -electron acceptor^{13,14} (and therefore presumably deactivated to nucleophilic attack^{31,32}).

On this basis, it seems reasonable to consider the possibilities that the kinetically important Lewis acid interaction occurs directly either at the metal or at a CO other than the acceptor CO. In either case, metal-to-ligand π bonding with the acceptor CO should decrease, facilitating methyl migration to it.

Berke and Hoffmann have carried out extended Hückel molecular orbital calculations for the conversion of $\text{MeMn}(\text{CO})_5$ to acetyl derivatives via a five-coordinate intermediate $\text{MeCOMn}(\text{CO})_4$.³³ Although they found an indication that protonation of a CO cis to the methyl group may actually promote migration to that CO by decreasing the activation energy, the calculated effect (0.15 eV) was not large. Given the nature of the calculation, which considered essentially only the repulsive interactions of the Me^- and CO σ fragment orbital lone pairs in the absence of a metal atom, the suggested decrease in activation energy may not be significant.³⁴

We have accordingly carried out, using essentially the same geometries and parameters used by Berke and Hoffmann, extended Hückel calculations of the *total energies* involved on going from $\text{MeMn}(\text{CO})_5$ (1) to the square-pyramidal $\text{MeCOMn}(\text{CO})_4$ (2).



In close agreement with Berke and Hoffmann, we find an activation barrier for the unassisted reaction $1 \rightarrow 2$ of 0.81 eV. The Lewis acid catalysis of the reaction was modelled by placing a proton³⁵ on the acceptor carbonyl (position a), on a carbonyl cis to both the methyl and acceptor CO (position c), and on the carbonyl trans to the

(20) Klingler, R. J.; Kochi, J. K. *J. Organomet. Chem.* **1980**, *202*, 49.

(21) Johnson, R. W.; Pearson, R. G. *Inorg. Chem.* **1971**, *10*, 2091, and references therein.

(22) Green, M. L. H.; Nagy, P. L. *J. Organomet. Chem.* **1963**, *1*, 58.

(23) Dalton, J.; Paul, I.; Stone, F. G. A. *J. Chem. Soc. A* **1969**, 2744.

(24) Davison, A.; McCleverty, J. A.; Wilkinson, G. *J. Chem. Soc.* **1963**, 1133.

(25) Esterification of formic acid is facile at room temperature.

(26) While formation of a formyl species via an intermolecular process such as reaction of, for instance, $[\eta^5\text{-C}_5\text{H}_5\text{Fe}(\text{CO})_2\text{H}]^+$ with $[\eta^5\text{-C}_5\text{H}_5\text{Fe}(\text{CO})_2\text{H}]$ cannot at present be ruled out, such a reaction seems unlikely and cannot, of course, be a factor in the very similar reactions of alkyl compounds, (2) and (3).¹⁹⁻²⁰ Another alternative would involve solvent attack on a coordinated carbonyl group of $[\eta^5\text{-C}_5\text{H}_5\text{Fe}(\text{CO})_2\text{H}]^+$ or $[\eta^5\text{-C}_5\text{H}_5\text{Mo}(\text{CO})_3\text{H}]^+$ to give alkoxy carbonyl species. This pathway cannot be disproven but also seems unlikely as the structurally similar cation $[\eta^5\text{-C}_5\text{H}_5\text{Fe}(\text{CO})_3]^+$ is stable in aqueous solution.²⁷ We also calculate a stretching force constant of about 16.5 mdyn/Å for the carbonyl group of $[\eta^5\text{-C}_5\text{H}_5\text{FeCO}(\text{COMe})(\text{MeCN})]^+$ ¹⁹ and note that this value suggests that the CO group should be relatively unreactive even to amines.²⁸ For these reasons, it seems unlikely that $[\eta^5\text{-C}_5\text{H}_5\text{Fe}(\text{CO})_2\text{H}]^+$ would undergo nucleophilic attack by an alcohol on a carbonyl group.

(27) Green, M. L. H.; Ishaq, M.; Whitely, R. V. *J. Chem. Soc. A* **1967**, 1508. Many authors use water and methanol as solvents for reactions of this cation.

(28) Angelici, R. J. *Acc. Chem. Res.* **1972**, *5*, 335.

(29) Marsella, J. A.; Curtis, C. J.; Bercaw, J. E.; Caulton, K. G. *J. Am. Chem. Soc.* **1980**, *102*, 7244.

(30) Richmond, T. G.; Basolo, F.; Shriver, D. F. *Inorg. Chem.* **1982**, *21*, 1272.

(31) It seems intuitively reasonable, as is done in ref 29, to consider migratory insertion reactions to involve nucleophilic attack on the CO by the relatively negatively charged migrating ligands.

(32) Darensbourg, D. J.; Baldwin, B. J.; Froelich, J. A. *J. Am. Chem. Soc.* **1980**, *102*, 4088, discuss the factors affecting the ease of nucleophilic attack on coordinated CO.

(33) Berke, H.; Hoffmann, R. *J. Am. Chem. Soc.* **1978**, *100*, 7224.

(34) See caveat re reliability of extended Hückel calculations in introduction to ref 33.

(35) 1 Å from the oxygen atom, colinear with the CO bond.

methyl group (position t).³⁶ Protonation at a was found to lead to a slight increase in the activation energy (~ 0.05 eV), while protonation at c to t showed no change. If the metal-carbonyl and carbon-oxygen bond lengths were decreased (0.05 Å) and increased (0.1 Å), respectively,³⁸ the activation energies with protonation at a and t decreased to ~ 0.6 and ~ 0.7 , respectively. These results are disappointingly inconsistent with our presumption of the importance of the energy of a predominantly π^* orbital on the acceptor CO. They are much more in accord with the suggestion³³ that the principal contributor to the activation barrier is the repulsive interactions between the Me^- and the CO σ lone pairs and that the extent of destabilization decreases as the energy of the latter decreases.³³ These conclusions are easily extrapolated to the iron and molybdenum systems studied here, however, as oxidation of the metals would lower the metal CO σ bond orbitals even more than would protonation of the oxygen. Thus the Lewis acid-induced kinetic effect observed by Shriver et al.³⁰ and the oxidation-induced effect observed here and in eq 2 and 3 may be similar in origin.

Acknowledgment. We thank the Natural Sciences and Engineering Research Council for a scholarship to A.C. and for operating grants to V.H.S. and M.C.B.

Registry No. 1, 13601-24-6; 2, 71518-89-3; $\eta^5\text{-C}_5\text{H}_5\text{Fe}(\text{CO})_2\text{H}$, 35913-82-7; $\eta^5\text{-C}_5\text{H}_5\text{Mo}(\text{CO})_3\text{H}$, 12176-06-6; ethyl formate, 109-94-4; methyl formate, 107-31-3; propyl formate, 110-74-7.

(36) Force constant calculations³⁷ suggest that the extent of back-bonding, and hence the basicity,^{13,14} is greater for the CO trans to methyl than for the others.

(37) Kaesz, H. D.; Bau, R.; Hendrickson, D.; Smith, J. M. *J. Am. Chem. Soc.* 1967, 89, 2844.

(38) These are the directions anticipated from spectroscopic data.^{13,14} The 0.1 Å is the increase in CO bond length on going from $\text{Cr}(\text{CO})_5$ to $\text{Cr}(\text{CO})_6^+$.³⁹

(39) Hubbard, J. L.; Lichtenberger, D. L. *J. Am. Chem. Soc.* 1982, 104, 2132.

Nucleophilic Addition to (η^6 -Alkylbenzene) $\text{Cr}(\text{CO})_3$ Complexes. Dependence of Regioselectivity on the Size of the Alkyl Group and the Reactivity of the Nucleophile

M. F. Semmelhack,* J. L. Garcia, D. Cortes, R. Farina, R. Hong, and B. K. Carpenter†

Department of Chemistry, Princeton University
Princeton, New Jersey 08544

Department of Chemistry, Cornell University
Ithaca, New York 14853

Received October 27, 1982

Summary: The regioselectivity of addition of carbanions to (η^6 -alkylbenzene) $\text{Cr}(\text{CO})_3$ complexes correlates well with a frontier orbital picture using the lowest energy arene-centered molecular orbital in the (arene) $\text{Cr}(\text{CO})_3$ complex. However, the selectivity is sensitive to both the size of the alkyl substituent on the arene and the reactivity of the carbanion. Para substitution can become important with large alkyl groups and more stabilized

carbanions. Systematic variation of anion reactivity using 2-aryl-1,3-dithiane derivatives shows the effect clearly. A rationale based on a balance of charge control and orbital control is presented, employing extended Hückel theory calculations on the complexes.

Regioselectivity in the addition of carbon nucleophiles to substituted (η^6 -arene) $\text{Cr}(\text{CO})_3$ complexes has been studied experimentally,¹⁻⁵ correlations of substituent effects on selectivity have been put forward by using a frontier orbital picture based on LUMO for the free arene¹ and based on the conformation of the $\text{Cr}(\text{CO})_3$ group.^{6,7} A theoretical analysis of the influence of the $\text{Cr}(\text{CO})_3$ conformation on the pattern of charge densities⁸ is consistent with the powerful meta-directing effects of resonance donor substituents (OR, NR_2 , F)² and the enhanced para selectivity in the reaction of (*tert*-butylbenzene) $\text{Cr}(\text{CO})_3$ with $\text{LiC}(\text{OR})(\text{CH}_3)\text{CN}$, where $\text{R} = \text{C}(\text{CH}_3)\text{OC}_2\text{H}_5$ [35% meta/65% para compared to 95% meta in reaction of the same anion with (toluene) $\text{Cr}(\text{CO})_3$].¹ This one-parameter analysis—where the substituents influence the regioselectivity solely through their effect on the conformational preferences of the $\text{Cr}(\text{CO})_3$ group⁸—requires that ortho and para positions have similar reactivity and differ from the meta position. Unfortunately, it fails to account for preferred addition both ortho and meta (and not para) with toluene and chlorobenzene ligands^{1,2} and the special selectivity in additions to (*o*-dimethoxybenzene)-,¹ (naphthalene)-,¹ and (indole) $\text{Cr}(\text{CO})_3$ ³ complexes. It does not provide an explanation for the several reports of a change in regioselectivity with a change in the carbon nucleophile.¹⁻³ For example, 2-lithio-1,3-dithiane adds primarily at C-7 in the η^6 -*N*-methyl indole ligand, while $\text{LiC}(\text{CH}_3)_2\text{CN}$ adds primarily at C-4.³ In this paper, we report a series of experiments in which the size of the alkyl substituent and the reactivity of the carbon nucleophile are systematically varied in nucleophilic additions to (η^6 -alkylbenzene) $\text{Cr}(\text{CO})_3$ complexes. The data require a new picture, and we offer a rationalization based on a balance of orbital control and charge control features.

Complexes 1a-e were prepared by standard procedures⁹ and sublimed or recrystallized to high purity; anions A-E were prepared according to standard procedures. In a typical experiment, the solid complex 1a-e (1.0 mmol) was added at -78°C to a solution of the carbanion in THF (5 mL) containing HMPA (1.0 mmol), and the solution was allowed to stir at 0°C for 0.5 h. The solution was then cooled to -78°C and quenched by addition to a solution

(1) Semmelhack, M. F.; Clark, G. R.; Farina, R.; Saeman, M. *J. Am. Chem. Soc.* 1979, 101, 217.

(2) Semmelhack, M. F.; Clark, G. *J. Am. Chem. Soc.* 1977, 99, 1675.

(3) The regioselectivity in addition to the indole ligand is particularly interesting: (a) Kozikowski, A. P.; Isobe, K. *J. Chem. Soc., Chem. Commun.* 1978, 1076. (b) Semmelhack, M. F.; Clark, G. R.; Garcia, J. L.; Harrison, J. J.; Thebtaranonth, Y.; Wulff, W.; Yamashita, A. *Tetrahedron* 1981, 37, 3957-3966. (c) Semmelhack, M. F.; Wulff, W.; Garcia, J. L. *J. Organomet. Chem.* 1982, in press.

(4) Jackson, W. R.; Rae, I. D.; Wong, M. G.; Semmelhack, M. F.; Garcia, J. L. *J. Chem. Soc., Chem. Commun.* 1982, in press.

(5) Rose, E. *J. Organomet. Chem.* 1981, 221, 147.

(6) Solladie-Cavallo, A.; Wipff, G. *Tetrahedron Lett.* 1980, 3047-3051.

(7) Direct evidence for the proposed conformational preferences in solution is obtained for NMR correlations. For relevant data and leading references, see: Solladie-Cavallo, A.; Suffert, J. *Org. Magn. Reson.* 1980, 14, 426-430.

(8) Albright, T. A.; Carpenter, B. K. *Inorg. Chem.* 1980, 19, 3092.

(9) For 1a, see: Jackson, W. R.; Nicholls, B.; Whiting, M. C. *J. Chem. Soc.* 1960, 469. For 1b and 1c, see: Jackson, W. R.; Jennings, W. B.; Rennison, S. C.; Spratt, R. *J. Chem. Soc. B* 1969, 1214. For 1d, see: Nicholls, B.; Whiting, M. C. *J. Chem. Soc.* 1959, 551. For 1e, see: van Muers, F.; van der Toorn, J. M.; van Bekkum, H. *J. Organomet. Chem.* 1976, 113, 341-351.

* To whom correspondence should be addressed at Princeton University.

† Cornell University.

methyl group (position t).³⁶ Protonation at a was found to lead to a slight increase in the activation energy (~ 0.05 eV), while protonation at c to t showed no change. If the metal-carbonyl and carbon-oxygen bond lengths were decreased (0.05 Å) and increased (0.1 Å), respectively,³⁸ the activation energies with protonation at a and t decreased to ~ 0.6 and ~ 0.7 , respectively. These results are disappointingly inconsistent with our presumption of the importance of the energy of a predominantly π^* orbital on the acceptor CO. They are much more in accord with the suggestion³³ that the principal contributor to the activation barrier is the repulsive interactions between the Me^- and the CO σ lone pairs and that the extent of destabilization decreases as the energy of the latter decreases.³³ These conclusions are easily extrapolated to the iron and molybdenum systems studied here, however, as oxidation of the metals would lower the metal CO σ bond orbitals even more than would protonation of the oxygen. Thus the Lewis acid-induced kinetic effect observed by Shriver et al.³⁰ and the oxidation-induced effect observed here and in eq 2 and 3 may be similar in origin.

Acknowledgment. We thank the Natural Sciences and Engineering Research Council for a scholarship to A.C. and for operating grants to V.H.S. and M.C.B.

Registry No. 1, 13601-24-6; 2, 71518-89-3; $\eta^5\text{-C}_5\text{H}_5\text{Fe}(\text{CO})_2\text{H}$, 35913-82-7; $\eta^5\text{-C}_5\text{H}_5\text{Mo}(\text{CO})_3\text{H}$, 12176-06-6; ethyl formate, 109-94-4; methyl formate, 107-31-3; propyl formate, 110-74-7.

(36) Force constant calculations³⁷ suggest that the extent of back-bonding, and hence the basicity,^{13,14} is greater for the CO trans to methyl than for the others.

(37) Kaesz, H. D.; Bau, R.; Hendrickson, D.; Smith, J. M. *J. Am. Chem. Soc.* 1967, 89, 2844.

(38) These are the directions anticipated from spectroscopic data.^{13,14} The 0.1 Å is the increase in CO bond length on going from $\text{Cr}(\text{CO})_5$ to $\text{Cr}(\text{CO})_6^+$.³⁹

(39) Hubbard, J. L.; Lichtenberger, D. L. *J. Am. Chem. Soc.* 1982, 104, 2132.

Nucleophilic Addition to (η^6 -Alkylbenzene) $\text{Cr}(\text{CO})_3$ Complexes. Dependence of Regioselectivity on the Size of the Alkyl Group and the Reactivity of the Nucleophile

M. F. Semmelhack,* J. L. Garcia, D. Cortes, R. Farina, R. Hong, and B. K. Carpenter†

Department of Chemistry, Princeton University
Princeton, New Jersey 08544

Department of Chemistry, Cornell University
Ithaca, New York 14853

Received October 27, 1982

Summary: The regioselectivity of addition of carbanions to (η^6 -alkylbenzene) $\text{Cr}(\text{CO})_3$ complexes correlates well with a frontier orbital picture using the lowest energy arene-centered molecular orbital in the (arene) $\text{Cr}(\text{CO})_3$ complex. However, the selectivity is sensitive to both the size of the alkyl substituent on the arene and the reactivity of the carbanion. Para substitution can become important with large alkyl groups and more stabilized

carbanions. Systematic variation of anion reactivity using 2-aryl-1,3-dithiane derivatives shows the effect clearly. A rationale based on a balance of charge control and orbital control is presented, employing extended Hückel theory calculations on the complexes.

Regioselectivity in the addition of carbon nucleophiles to substituted (η^6 -arene) $\text{Cr}(\text{CO})_3$ complexes has been studied experimentally,¹⁻⁵ correlations of substituent effects on selectivity have been put forward by using a frontier orbital picture based on LUMO for the free arene¹ and based on the conformation of the $\text{Cr}(\text{CO})_3$ group.^{6,7} A theoretical analysis of the influence of the $\text{Cr}(\text{CO})_3$ conformation on the pattern of charge densities⁸ is consistent with the powerful meta-directing effects of resonance donor substituents (OR, NR_2 , F)² and the enhanced para selectivity in the reaction of (*tert*-butylbenzene) $\text{Cr}(\text{CO})_3$ with $\text{LiC}(\text{OR})(\text{CH}_3)\text{CN}$, where $\text{R} = \text{C}(\text{CH}_3)\text{OC}_2\text{H}_5$ [35% meta/65% para compared to 95% meta in reaction of the same anion with (toluene) $\text{Cr}(\text{CO})_3$].¹ This one-parameter analysis—where the substituents influence the regioselectivity solely through their effect on the conformational preferences of the $\text{Cr}(\text{CO})_3$ group⁸—requires that ortho and para positions have similar reactivity and differ from the meta position. Unfortunately, it fails to account for preferred addition both ortho and meta (and not para) with toluene and chlorobenzene ligands^{1,2} and the special selectivity in additions to (*o*-dimethoxybenzene)-,¹ (naphthalene)-,¹ and (indole) $\text{Cr}(\text{CO})_3$ ³ complexes. It does not provide an explanation for the several reports of a change in regioselectivity with a change in the carbon nucleophile.¹⁻³ For example, 2-lithio-1,3-dithiane adds primarily at C-7 in the η^6 -*N*-methyl indole ligand, while $\text{LiC}(\text{CH}_3)_2\text{CN}$ adds primarily at C-4.³ In this paper, we report a series of experiments in which the size of the alkyl substituent and the reactivity of the carbon nucleophile are systematically varied in nucleophilic additions to (η^6 -alkylbenzene) $\text{Cr}(\text{CO})_3$ complexes. The data require a new picture, and we offer a rationalization based on a balance of orbital control and charge control features.

Complexes 1a-e were prepared by standard procedures⁹ and sublimed or recrystallized to high purity; anions A-E were prepared according to standard procedures. In a typical experiment, the solid complex 1a-e (1.0 mmol) was added at -78°C to a solution of the carbanion in THF (5 mL) containing HMPA (1.0 mmol), and the solution was allowed to stir at 0°C for 0.5 h. The solution was then cooled to -78°C and quenched by addition to a solution

(1) Semmelhack, M. F.; Clark, G. R.; Farina, R.; Saeman, M. *J. Am. Chem. Soc.* 1979, 101, 217.

(2) Semmelhack, M. F.; Clark, G. *J. Am. Chem. Soc.* 1977, 99, 1675.

(3) The regioselectivity in addition to the indole ligand is particularly interesting: (a) Kozikowski, A. P.; Isobe, K. *J. Chem. Soc., Chem. Commun.* 1978, 1076. (b) Semmelhack, M. F.; Clark, G. R.; Garcia, J. L.; Harrison, J. J.; Thebtaranonth, Y.; Wulff, W.; Yamashita, A. *Tetrahedron* 1981, 37, 3957-3966. (c) Semmelhack, M. F.; Wulff, W.; Garcia, J. L. *J. Organomet. Chem.* 1982, in press.

(4) Jackson, W. R.; Rae, I. D.; Wong, M. G.; Semmelhack, M. F.; Garcia, J. L. *J. Chem. Soc., Chem. Commun.* 1982, in press.

(5) Rose, E. *J. Organomet. Chem.* 1981, 221, 147.

(6) Solladie-Cavallo, A.; Wipff, G. *Tetrahedron Lett.* 1980, 3047-3051.

(7) Direct evidence for the proposed conformational preferences in solution is obtained for NMR correlations. For relevant data and leading references, see: Solladie-Cavallo, A.; Suffert, J. *Org. Magn. Reson.* 1980, 14, 426-430.

(8) Albright, T. A.; Carpenter, B. K. *Inorg. Chem.* 1980, 19, 3092.

(9) For 1a, see: Jackson, W. R.; Nicholls, B.; Whiting, M. C. *J. Chem. Soc.* 1960, 469. For 1b and 1c, see: Jackson, W. R.; Jennings, W. B.; Rennison, S. C.; Spratt, R. *J. Chem. Soc. B* 1969, 1214. For 1d, see: Nicholls, B.; Whiting, M. C. *J. Chem. Soc.* 1959, 551. For 1e, see: van Muers, F.; van der Toorn, J. M.; van Bekkum, H. *J. Organomet. Chem.* 1976, 113, 341-351.

* To whom correspondence should be addressed at Princeton University.

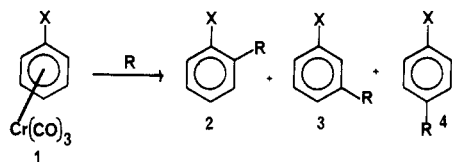
† Cornell University.

Table I. Variation in the Size of the Alkyl Substituent

entry	complex	anion	product ratio o:m:p ^b	combined yield, ^a %
1	a, X = Me	C	0:96:4 ^f	75
2	b, X = Et	C	0:94:6	89
3	c, X = <i>i</i> -Pr	C	0:80:20	88
4	d, X = <i>t</i> -Bu	C	0:35:65	86
5	e, X = CH(<i>t</i> -Bu) ₂	C	0:0:100	(17) ^{c,e}
6	a, X = Me	B	1:97:2	95
7 ^d	d, X = <i>t</i> -Bu	B	0:55:45	78
8	e, X = CH(<i>t</i> -Bu) ₂	B	0:0:100	63
9 ^d	a, X = Me	D	52:46:2	94
10	a, X = Me	E	52:46:2	96
11	c, X = <i>i</i> -Pr	E	47:46:7	86
12	d, X = <i>t</i> -Bu	E	45:32:23	88
13 ^d	a, X = Me	A	35:63:2	88
14	d, X = <i>t</i> -Bu	A	28:48:24	51

^a Yields are based on weight of isolated material after distillation and/or chromatography. ^b The ratios are from GLPC. ^c This reaction could not be driven to more than 40–50% conversion. ^d From ref 2. ^e The yield is based on products 2, 3, and 4 with R = COCH₃ as described in the text. ^f This yield was determined by quantitative GLPC.

Table II. Variation in Reactivity of the Nucleophile



substituent series: a, X = Me; b, X = Et; c, X = *i*-Pr; d, X = *t*-Bu; e, X = CH(*t*-Bu)₂

anion series: A, R = CH₂CN; B, R = C(CH₃)₂CN; C, R = C(OR)₁(CH₃)CN, R₁ = C(CH₃)OC₂H₅; D, R = 1,3-dithian-2-yl; E, R = CH₂SPh; F, R =

entry	complex	anion F	ratio m:p	combined yield, ^c %	σ_p for X
1	1d	X = O ⁻	73:27 ^a	84	
2	1d	X = NMe ₂	63:37 ^a	80	-0.83
3	1d	X = NMe ₂	57:43 ^b	78	-0.83
4	1d	X = OMe	54:46 ^a	71	-0.27
5	1d	X = Me	43:57 ^a	75	-0.17
6	1d	X = H	28:72 ^a	75	0
7	1d	X = H	23:77 ^b	85	0
8	1d	X = Cl	21:79 ^a	80	+0.23

^a The medium is THF. ^b A mixture of THF/HMPA (4:1) was used. ^c The yields are the average of at least two runs, based on distilled and/or chromatographed material.

of iodine (10 mmol) in 5 mL of THF. After 3 h at 25 °C, the mixture was partitioned between ether and water, the excess iodine was removed with sodium bisulfite and from the ether was isolated a mixture of disubstituted arenes 2, 3, and 4 that was analyzed by GLPC to generate the data in Table I. For anion C, substitution in the ortho position is never significant; the relative amounts of meta and para substitution are strongly dependent on the steric bulk of the alkyl group, with a range of 96% meta (1a) to 100% para (1e) (entries 1 and 5, for example). The anion of 2-lithio-2-methylpropionitrile (B) gave a similar pattern

under identical conditions (entries 6–8). The sulfur-stabilized anions such as 2-lithio-1,3-dithiane (D, entry 9) and LiCH₂SPh (E, entries 10–12) give powerful selectivity for ortho and meta substitution, with para becoming significant (23%) only with the *tert*-butylbenzene ligand and at the expense of meta. Similarly, LiCH₂CN (A, entries 13 and 14) reacted with the toluene ligand primarily at the ortho and meta positions; again the *tert*-butyl substituent gave enhanced para selectivity and relatively less meta.

While it is reasonable to assume that anions such as B and E differ in reactivity, they are likely also to differ in other properties that might influence regioselectivity. To get a less complicated picture of the relation between regioselectivity and anion reactivity, we carried out the set of experiments summarized in Table II. A series of 2-(para-substituted phenyl)-2-lithio-1,3-dithianes were prepared¹⁰ in THF and allowed to add to 1d. Oxidation with excess iodine as before gave mixtures of 2,2-diaryl-1,3-dithianes (3F, 4F) that were identified after hydrolysis to benzophenone derivatives.¹¹ In all cases, the product (2F) from ortho attack was present in a yield of less than 3%. It was assumed that the reactivity of the anions would parallel the σ_p constants determined¹² for substituents X, increasing down the columns of Table II. The selectivity ratio of meta:para also changed in a regular way, from 73:27 for the most reactive anion (entry 1) to 23:77 for the least reactive anion (entry 7). A plot of ln (para_X/para_H) vs. σ_p gives a straight line of slope 0.97 with correlation coefficient 0.96. While systematic kinetic studies have not been completed, we have shown by competition experiments that the relative reactivities toward 1d of anions F (X = H) and F (X = Me₂N) are in the ratio 1:10, suggesting a direct relation between σ_p constant and reactivity toward 1d. We suggest these data demonstrate a strong dependence of selectivity on anion reactivity.



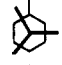
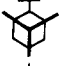
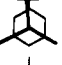
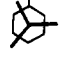
Taken together, the results presented in Tables I and II allow several general conclusions. (1) Steric effects are important when comparing primary, secondary, and tertiary carbanions; ortho substitution is nearly completely inhibited with tertiary anions, no matter what the substituent on the arene ligand, but steric effects of substituents on the arene are less severe. (2) When steric effects are less dominant, ortho substitution can be comparable

(10) The 2-aryl-1,3-dithianes were prepared from the corresponding *p*-substituted benzaldehydes, 1,3-propanedithiol, and boron trifluoride etherate. The anions F were generated *n*-butyllithium under standard conditions: Seebach, D.; Corey, E. J. *J. Org. Chem.* 1975, 40, 231.

(11) The product 2,2-diaryl-1,3-dithianes, 3F and 4F, were treated with red mercuric oxide, aqueous THF, and boron trifluoride etherate according to a general procedure: Vedejs, E.; Fuchs, P. L. *J. Org. Chem.* 1971, 36, 366. The resulting benzophenones were analyzed and separated by GLPC and fully characterized by ¹H NMR spectral data. The regioselectivity in the reaction is assumed to be directly reflected in the ratio of benzophenone isomers detected. We have shown that a typical mixture of the dithiane products can be hydrolyzed without selective loss of one of the isomers. There is still the question as to whether the oxidative quenching of the reaction perturbs the regioselectivity. We have no direct way of calibrating this process, but we have shown in related work that other modes of quenching (such as addition of strong acid and protonation of the cyclohexadienyl ligand) instead of oxidation give the same mixture of regioisomers.

(12) The substituent constants were obtained from the compilation appearing in: Gordon, A. J.; Ford, R. A. "The Chemist's Companion"; Wiley: New York, 1972; p 152. No comprehensive correlation of the reactivity of anions F in addition to 1d and σ_p has been reported. We are unaware of pK_a data related to anions F that could reveal a correlation of σ_p with anion stability. However, a para phenyl substituent (anion F, X = phenyl) lowers the pK_a by 2 units (Streitwieser, A.; Ewing, S. P. *J. Am. Chem. Soc.* 1975, 97, 190). The parent anion (F, X = H) has been shown to exist as a monomer in THF/TMEDA and as a contact ion pair in the solid state (see: Amstutz, R.; Dunitz, J. D.; Seebach, D. *Angew. Chem., Int. Ed. Engl.* 1981, 20, 405). Our analysis is based on the assumption that the para substituents will have a strong effect on the reactivity of anions F.

Table III. EHT Coefficients for the Lowest Unoccupied Arene-Centered¹⁶ Molecular Orbital in Mono-Substituted (Arene)Cr(CO)₃ Complexes

complex (conformatn)	LUMO coefficients						total energy, eV
	1	2	3	4	5	6	
	0.00	-0.55	0.41	0.00	-0.41	0.55	-1311.885
	0.00	-0.41	0.55	0.00	-0.55	-0.41	-1311.865
	-0.03	-0.54	0.52	0.08	-0.49	0.46	-1311.899
	0.00	-0.55	0.41	0.00	-0.41	0.56	-1628.845
	0.00	-0.41	0.55	0.00	-0.55	0.41	-1628.347
	0.01	-0.55	0.51	0.10	-0.50	0.45	-1628.198

to meta, reaching up to 1:1 ratios of ortho:meta with reactive anions. (3) Para substitution becomes important only with large alkyl substituents on the arene ligand and primarily at the expense of meta substitution. (4) The extent of para substitution is very sensitive to the stability of the nucleophile, with higher para selectivity correlating with a more stabilized carbanion.

Table III displays the results of EHT calculations on selected monosubstituted (arene)Cr(CO)₃ complexes.¹³ From these data, we conclude the *pattern* of coefficients in the relevant LUMO¹⁶ is relatively insensitive to the conformation of the Cr(CO)₃ unit,¹⁷ is closely parallel in distribution of coefficients with the pattern for LUMO of the uncomplexed arene,¹⁸ and is consistent with orbital-controlled substitution at the ortho and meta positions.

We favor an explanation of the experimental results

(13) All calculations were performed by using the extended Hückel method.¹⁴ A modified Wolfsberg-Helmholz formula was used.¹⁵ The parameters used were described before,⁹ except that the elements H_{ij} were unweighted.

(14) (a) Hoffmann, R. *J. Phys. Chem.* 1963, 39, 1397. (b) Hoffmann, R.; Lipscomb, W. N. *Ibid.* 1962, 36, 3179, 3489. (c) Hoffmann, R.; Lipscomb, W. N. *Ibid.* 1962, 37, 2872.

(15) Ammeter, J. H.; Bürg, H. B.; Thibeault, J. C.; Hoffmann, R. *J. Am. Chem. Soc.* 1978, 100, 3686.

(16) There are several unoccupied molecular orbitals calculated to be within 1.0 eV of the calculated LUMO. Only one of these is substantially localized on the arene ligand (arene π^* -like), typically located in the calculation at about 0.5–0.75 eV above LUMO. The first prediction from these data is that nucleophile addition would be most favorable at the carbonyl ligand or at the chromium atom, where the calculated LUMO is primarily localized. Since it is clear that the first detectable intermediate in nucleophile addition is from exo addition to the arene ligand, several possible explanations can be put forward. (1) The relative energy ordering of the lower unoccupied orbitals in the complexes from the EHT calculations is not proper, and the arene-centered orbital is, in fact, the LUMO. (2) The initial addition is at the CO or Cr atom, but it is reversible and the product-determining step is anti addition to the arene ligand (controlled by the arene-centered UMO). (3) While frontier orbital control would predict addition at the Cr or CO, other factors such as steric effects may disfavor this mode of addition. In any case, the work described here is not intended to address the question of why addition occurs at the arene ligand but seeks to develop a correlation through frontier MO theory that gives useful predictions of regioselectivity. Therefore, we focus on the lower UMO that is arene centered. The full results of the calculations will be presented in the article describing this work.

(17) In ref 8, it was established that according to EHT calculations, charge densities on the arene ligand are sensitive to conformation; charge-controlled ortho/para selectivity was proposed.

(18) (a) Heilbronner, E.; Straub, P. A. "HMO"; Springer-Verlag: New York, 1966. (b) Bowers, K. W. In "Radical Ions"; Kaiser, E. T., Keven, L., Eds.; Interscience, New York, 1968, p 211. (c) Bowers, K. W. *Adv. Magn. Reson.* 1965, 1, 317.

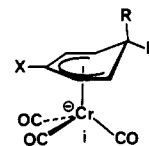
based on the perturbation theory analysis of Klopman¹⁹ and Salem.²⁰ We assume the important orbital interaction is between the lowest energy arene-centered unoccupied MO (UMO)¹⁶ (Table III) and HOMO for the carbanion, and that HOMO for the anion lies at lower energy than the relevant UMO for the complex. The picture is clearest with the substituted 2-aryl-1,3-dithianyl anions, F (Table II). With the relatively high-energy HOMO for anion F (X = O⁻), frontier orbital overlap dominates the expression¹⁹ for interaction of the reactants; ortho/meta (only meta is observed) addition is favored relative to para. As the energy of the HOMO of F is lowered (descending Table II) frontier orbital interaction is weakened and charge-control begins to dominate; the polarization of the arene ligand induced by conformational effects in the complex leads to ortho/para selectivity (only para is observed) consistent with the earlier analysis.^{8,17} We feel the orbital control vs. charge-control also applies to the unusual selectivity features in addition to (η^6 -indole)Cr(CO)₃³ and may have general application.²¹

Acknowledgment. We wish to acknowledge support from the National Science Foundation (Grant CHE 79-05561) and useful discussions with Professors Albright (Houston) and Hoffmann (Cornell).

(19) (a) Klopman, G. *J. Am. Chem. Soc.* 1968, 90, 223. (b) Klopman, G. "Chemical Reactivity and Reaction Paths"; Wiley, New York, 1974.

(20) Salem, L. *J. Am. Chem. Soc.* 1968, 90, 543 and 553.

(21) Other explanations for the dependence of regioselectivity on anion reactivity can be presented. For example, the nature of the transition state leading to the intermediate **i** might be more reactant-like as the reactivity of the anion increases. Conformational barriers in the intermediates (**i**) are not known but are expected to be large,²² and therefore the particular geometry of the product shown in **i** would be strongly preferred. If substituents (X in **i**) exert steric or electronic effects on the stability of **i**, then these factors might be important for reactions with a late, product-like transition state (addition of a more stabilized anion). This picture can account for the experimental facts available now but needs to be solidified with more information about the effect of substituents on the stability of **i**, the conformational barriers in **i**, and the nature of the transition state leading to **i**.



(22) Albright, T. A.; Hofmann, P.; Hoffmann, R. *J. Am. Chem. Soc.* 1977, 99, 7546.

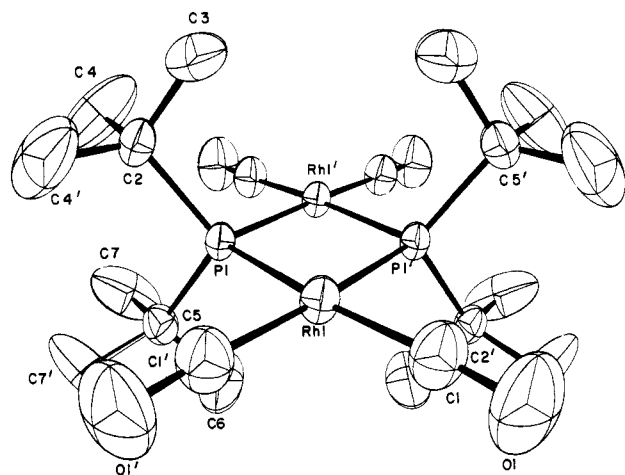


Figure 2. View of isomer 2 viewed along the Rh-Rh bond. Key parameters are in ref 10.

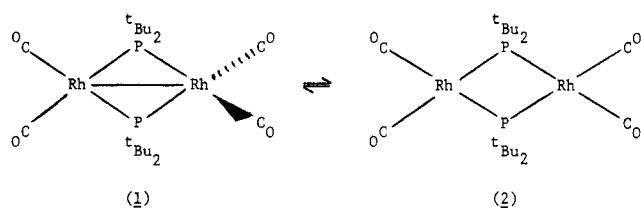


Figure 3.

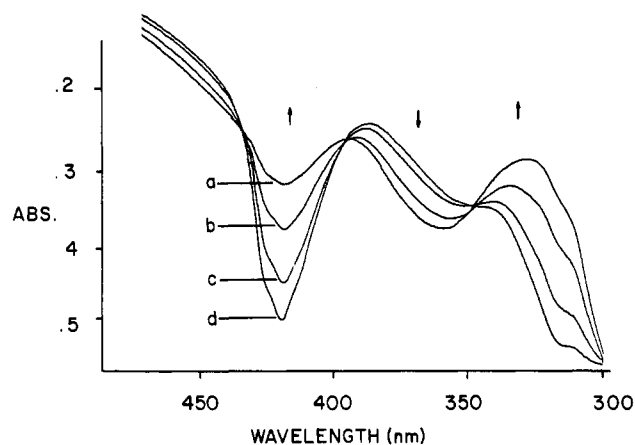


Figure 4. Visible absorption spectra of $[\text{Rh}(\mu\text{-}t\text{-Bu}_2\text{P})(\text{CO})_2]_2$ in 7.5×10^{-5} M toluene solution: a, 53 °C; b, 48 °C; c, 38 °C; d, 25 °C.

formed by the Rh_2P_2 core and thus has an unusual tetrahedral environment. The Rh-Rh distance is 2.7609 (9) Å, well within the limits expected for a single rhodium-rhodium bond.¹¹ The di-*tert*-butylphosphido bridges are notably asymmetric with the Rh-P distances to the "tetrahedral" (Rh1) end of the molecule being significantly shorter than those to the "planar end" by an average of ca. 0.21 Å. The bonding parameters for the central Rh_2P_2 core are therefore similar to those found for $(\text{COD})\text{Rh}(\mu\text{-Ph}_2\text{P})_2\text{Rh}(\text{PEt}_3)_2$ (Rh-Rh)¹² (see below).

In the orange-yellow isomer 2 (Figure 2) all the terminal carbonyls as well as the rhodium and phosphorus atoms lie in the same plane giving both rhodium atoms planar

environments. The molecule resides on a $2/m$ symmetry site resulting in equal Rh-P bond distances. A major structural difference between 1 and 2 is that the Rh-Rh separation in 2 is now 3.717 (1) Å, no longer a reasonable distance for a bonding interaction. The planar dimer 2 thus resembles the planar $\text{Pt}_2(\text{PPh}_2)_2(\text{diphos})_2^{2+}$ cation that has a similar nonbonding Pt-Pt distance of 3.699 (1) Å.¹³

The interesting feature of this system is that a metal-metal bond appears to be reversibly formed and cleaved accompanied merely by a geometrical isomerism: distortion in the bridging phosphido groups and a twist through 90° by two CO groups (Figure 3). The two isomers must be very close in energy for them to interconvert so easily. It is unusual that either one can be so easily and selectively isolated by altering the rate of cooling of solutions. The apparent planar/tetrahedral equilibrium for one end of the dinuclear rhodium system is similar to that found for a number of mononuclear nickel(I) systems.¹⁴ Although in the latter case metal-metal bond cleavage and formation are not involved.

In hydrocarbon solutions 1 and 2 give identical ^1H , $^{31}\text{P}\{^1\text{H}\}$, and $^{13}\text{C}\{^1\text{H}\}$ NMR and IR spectra. The IR (hexane) shows terminal CO vibrations.⁸ The $^{31}\text{P}\{^1\text{H}\}$ NMR in toluene- d_8 shows a triplet at room temperature (δ 402.8 relative to H_3PO_4 ; $^1J_{\text{Rh-P}} = 102$ Hz) that is split into a doublet of doublets at -80 °C ($^1J_{\text{Rh-P}} = 128.2, 67.1$ Hz). Surprisingly both signals have identical chemical shifts. The carbonyl region of the $^{13}\text{C}\{^1\text{H}\}$ NMR (^{13}CO enriched, 50.3 MHz) consists of two signals at -80 °C; a doublet at δ 202.5 ($^1J_{\text{Rh-C}} = 83.8$ Hz) and a doublet of doublets of doublets at δ 194.73 ($^1J_{\text{Rh-C}} = 71.6$ $^2J_{\text{P-C}} = 47.5, 13.4$ Hz). On warming, at -20 °C the resonances collapse into two broad humps that merge into a single broad resonance at 0 °C. Further warming to +50 °C yields a sharp doublet of triplets δ 199.8 ($^1J_{\text{Rh-C}} = 75.1$ Hz, $^2J_{\text{P-C}} = 10.7$ Hz).

Hydrocarbon solutions of the isomeric mixture are thermochromic. At -80 °C they are deep red and become increasingly lighter on warming until at +50 °C they are pale orange-yellow.

The UV-visible spectra (300-500 nm in toluene) from +25 to +53 °C clearly show three isosbestic points (Figure 3), indicating that the species responsible for the absorptions in this region are in equilibrium with each other.¹⁵

The spectroscopic data are consistent with a temperature-dependent equilibrium between an unsymmetrical species that is the major component in solution at -80 °C and a symmetrical isomer that predominates at ambient temperatures and above. Although $^{13}\text{C}\{^1\text{H}\}$ data are consistent with these species being similar to 1 and 2, the $^{31}\text{P}\{^1\text{H}\}$ data appear to contradict this straightforward explanation since in the solid state 1 and 2 have notably different M_2P_2 framework geometries. Thus the species in solution may not necessarily be identical with those found in the solid state. Previous studies on some Ph_2P -bridged systems have shown correlations between low-field ^{31}P chemical shifts and the presence of metal-metal bonding and acute M-P-M angles.¹⁶ Larger M-P-M angles and no metal bonds were found with ^{31}P shifts to much higher fields. However, Garrou has noted that not

(13) Carty, A. J.; Hartstock, F.; Taylor, N. J. *Inorg. Chem.* 1982, 21, 1349.

(14) See: Cotton, F. A.; Wilkinson, G. "Advanced Inorganic Chemistry"; Wiley: New York, 1980; p 793.

(15) Recorded on a Cary 17 instrument: at 25 °C, λ_{max} 421 nm (ϵ 6800), 363 (ϵ 3360); at 53 °C, λ_{max} 421 nm (ϵ 4560), 363 (ϵ 4200). Unfortunately at present our equipment cannot be used below ca. 15 °C.

(16) Carty, A. J. *Adv. Chem. Ser.* 1982, No. 196, 163.

(11) The Rh-Rh bond falls near the center of the normal range for Rh-Rh single bonds; Cowie, M.; Dwight, S. K. *Inorg. Chem.* 1980, 19, 209.

(12) Meek, D. W.; Kreter, P. E.; Christoph, G. G. *J. Organomet. Chem.* 1982, 231, C53.

enough data have been accumulated to allow unequivocal structural assignments to be made solely on this basis.¹⁷ The data that we have accumulated so far for a considerable number of μ -*t*-Bu₂P complexes also permit no simple correlations to be made.¹⁸ In any case one would expect considerably different ³¹P chemical shifts for species with different M₂P₂ framework geometries such as 1 and 2. One explanation for the ³¹P data is that all of the species observed by NMR in solution have very similar M₂P₂ frameworks. The observed spectral changes would then be only due to changes in carbonyl geometry that should not greatly affect the ³¹P chemical shifts. If this is so then the formation or cleavage of the Rh-Rh bond in 1 and 2, respectively, could be taking place only on crystallization from solution. Further speculation on the species in solution is unwarranted at this stage.

Although few other dinuclear rhodium bis(phosphido) complexes have been reported,¹⁹ there is some similarity between the structure of isomer 1 and that of the complex (COD)Rh(μ -Ph₂P)₂Rh(PEt₃)₂ recently reported by Meek.¹² Like 1, this complex contains both "tetrahedral" and "planar" rhodium atoms, a rhodium-rhodium bond, and two notably asymmetric phosphido bridges. The bonding has been described as arising from a [Rh(μ -Ph₂P)₂(PEt₃)₂]⁻ anion chelating to a [(COD)Rh]⁺ cation with a donor bond between the rhodium atoms. It is possible that the bonding in 1 could be described in similar terms. However, the structure 1 is most unusual since all four terminal ligands (CO) are identical. We are currently investigating the structures of 1 and 2 and related complexes using theoretical calculations.²⁰

In solution [Rh(μ -*t*-Bu₂P)(CO)₂]₂ readily undergoes ¹³CO/¹²CO exchange²¹ indicating that the CO ligands are quite labile. The presence of labile CO ligands suggests the possibility of catalytic activity. [Rh(μ -*t*-Bu₂P)(CO)₂]₂ does not catalyze hydrogenation under mild conditions; however, it does form a catalytically active system for hydroformylation of hex-1-ene.²² There appears to be no apparent decomposition. It has been noted that some catalytic systems involving triphenylphosphine complexes are deactivated by the formation of μ -Ph₂P compounds.²³ However, some Ph₂P-bridged rhodium complexes are active hydrogenation catalysts,¹⁹ and other examples of catalysis by phosphido-bridged complexes are known.^{16,24} The rhodium μ -*t*-Bu₂P system remains catalytically active at elevated temperatures even for prolonged periods.²³ Under these conditions new phosphido-bridged species are formed and they are currently under investigation.

(17) Garrou, P. E. *Chem. Rev.* 1981, 81, 229 and references therein.

(18) For example, in [Rh(μ -*t*-BuCH₂)₂P(CO)₂]₂, which has a planar structure similar to 2 and a nonbonding Rh-Rh distance of 3.741 Å, δ (³¹P) equals 260 ppm while in [Ir(μ -*t*-Bu₂P)(CO)₂]₂ with two "tetrahedral" cobalt atoms and a short Ir-Ir separation of 2.544 Å δ (³¹P) equals 262 ppm.

(19) Kreter, P. E.; Meek, D. W. *Inorg. Chem.* in press.

(20) In collaboration with Professor T. A. Albright, University of Houston.

(21) On treatment of either 1 or 2 with ¹³CO (2 tm, 30 min) at room temperature in hexane new IR bands are observed for 1 at 2000 (w), 1939 (s), 1928 (s), and 1895 (m) cm⁻¹. The change is reversed on treatment with ¹²CO.

(22) Typical conditions: 1 or 2 (0.034 mmol) and hex-1-ene (5.0 mL, 40.0 mmol) stirred in a glass pressure vessel under CO/H₂ (1:1), 2 atm, and ambient temperature. After 10 h, 1-heptanal (48%) and 2-methylhexanal (45%) are formed (GLC, mass spectroscopy) in approximately 95% conversion. We have so far not optimized the conditions for yield or product ratio.

(23) For example, RhH(CO)(PPh₃)₃ decomposes in solution on heating, giving μ -Ph₂P complexes; see ref 9 above and also ref 9 in: Kurtev, K.; Ribola, D.; Jones, R. A.; Cole-Hamilton, D. J. Wilkinson, G. *J. Chem. Soc. Dalton Trans.* 1980, 55.

Acknowledgment. We thank the Dow Chemical Co., Midland, MI (R.A.J.) and the National Science Foundation (J.L.A. and R.A.J.) for financial support. We thank Johnson-Matthey Ltd. for a loan of RhCl₃·xH₂O. We also thank Professor D. W. Meek, The Ohio State University, for a copy of his paper on diphenylphosphido-bridged rhodium complexes prior to publication.

Supplementary Material Available: Tables of final fractional coordinates, anisotropic thermal parameters, and bond distances and angles for compounds 1 and 2 and listings of structure factor amplitudes for 1 and 2 (23 pages). Ordering information is given on any current masthead page.

(24) See: Ryan, R. C.; Pittman, C. U.; Connor, J. P. *J. Am. Chem. Soc.* 1977, 99, 1986 for hydroformylation using Co₄(CO)₁₀(μ -PPh)₂. See also the following references for recent examples of stoichiometric reactions related to homogeneous catalysis: Carty, A. J.; Taylor, N. J.; Smith, W. F. *J. Chem. Soc., Chem. Commun.* 1979, 750. Carty, A. J.; MacLaughlin, S. A.; Taylor, N. J. *J. Am. Chem. Soc.* 1981, 103, 2456. Breen, M. J.; Duttera, M. R.; Geoffroy, G. L.; Novotnak, G. C.; Roberts, D. A.; Shulman, P. M.; Steinmetz, G. R. *Organometallics* 1982, 1, 1008. MacLaughlin, S. A.; Carty, A. J.; Taylor, N. J. *Can. J. Chem.* 1982, 60, 87. Carty, A. J. *Pure Appl. Chem.* 1982, 54, 113.

A Novel Palladium Complex with Iron-Palladium Dative Bonding Derived from 1,2,3-Trithia[3]ferrocenophane, (Ph₃P)PdFe(SC₅H₄)₂·0.5C₆H₅CH₃

Dietmar Seyferth,* Barry W. Hames,¹ and Thomas G. Rucker²

Department of Chemistry
Massachusetts Institute of Technology
Cambridge, Massachusetts 02139

Martin Cowle* and Raymond S. Dickson

Department of Chemistry, The University of Alberta
Edmonton, Alberta, Canada T6G 2G2

Received November 3, 1982

Summary: The reaction of Pd(PPh₃)₄ with 1,2,3-trithia[3]ferrocenophane affords the unusual heterobinuclear species (Ph₃P)PdFe(SC₅H₄)₂. An X-ray structure determination of this complex as the hemitoluene solvate reveals a dative Fe→Pd bond (2.878 (1) Å).

The insertion of low-valent, coordinatively unsaturated species of type L₂M (M = Ni, Pd, Pt; L = tertiary phosphine) into the S-S bond of (μ -S₂)Fe₂(CO)₆ was reported recently.^{3,4} Such insertion into S-S bonds of organic disulfides is a characteristic reaction of such transition-

(1) Natural Sciences and Engineering Research Council (Canada) Postdoctoral Fellow, 1981-1982.

(2) Undergraduate (UROP) research participant.

(3) Seyferth, D.; Henderson, R. S.; Gallagher, M. G. *J. Organomet. Chem.* 1980, 193, C75.

(4) Day, V. W.; Lesch, D. A.; Rauchfuss, T. B. *J. Am. Chem. Soc.* 1982, 104, 1290.

A novel palladium complex with iron-palladium dative bonding derived from 1,2,3-trithia[3]ferrocenophane, $(\text{Ph}_3\text{P})\text{PdFe}(\text{SC}_5\text{H}_4)_2 \cdot 0.5\text{C}_6\text{H}_5\text{CH}_3$

Dietmar Seyferth, Barry W. Hames, Thomas G. Rucker, Martin Cowie, and Raymond S. Dickson

Organometallics, **1983**, 2 (3), 472-474 • DOI: 10.1021/om00075a027 • Publication Date (Web): 01 May 2002

Downloaded from <http://pubs.acs.org> on April 24, 2009

More About This Article

The permalink <http://dx.doi.org/10.1021/om00075a027> provides access to:

- Links to articles and content related to this article
- Copyright permission to reproduce figures and/or text from this article



ACS Publications
High quality. High impact.

enough data have been accumulated to allow unequivocal structural assignments to be made solely on this basis.¹⁷ The data that we have accumulated so far for a considerable number of μ -*t*-Bu₂P complexes also permit no simple correlations to be made.¹⁸ In any case one would expect considerably different ³¹P chemical shifts for species with different M₂P₂ framework geometries such as 1 and 2. One explanation for the ³¹P data is that all of the species observed by NMR in solution have very similar M₂P₂ frameworks. The observed spectral changes would then be only due to changes in carbonyl geometry that should not greatly affect the ³¹P chemical shifts. If this is so then the formation or cleavage of the Rh-Rh bond in 1 and 2, respectively, could be taking place only on crystallization from solution. Further speculation on the species in solution is unwarranted at this stage.

Although few other dinuclear rhodium bis(phosphido) complexes have been reported,¹⁹ there is some similarity between the structure of isomer 1 and that of the complex (COD)Rh(μ -Ph₂P)₂Rh(PEt₃)₂ recently reported by Meek.¹² Like 1, this complex contains both "tetrahedral" and "planar" rhodium atoms, a rhodium-rhodium bond, and two notably asymmetric phosphido bridges. The bonding has been described as arising from a [Rh(μ -Ph₂P)₂(PEt₃)₂]⁻ anion chelating to a [(COD)Rh]⁺ cation with a donor bond between the rhodium atoms. It is possible that the bonding in 1 could be described in similar terms. However, the structure 1 is most unusual since all four terminal ligands (CO) are identical. We are currently investigating the structures of 1 and 2 and related complexes using theoretical calculations.²⁰

In solution [Rh(μ -*t*-Bu₂P)(CO)₂]₂ readily undergoes ¹³CO/¹²CO exchange²¹ indicating that the CO ligands are quite labile. The presence of labile CO ligands suggests the possibility of catalytic activity. [Rh(μ -*t*-Bu₂P)(CO)₂]₂ does not catalyze hydrogenation under mild conditions; however, it does form a catalytically active system for hydroformylation of hex-1-ene.²² There appears to be no apparent decomposition. It has been noted that some catalytic systems involving triphenylphosphine complexes are deactivated by the formation of μ -Ph₂P compounds.²³ However, some Ph₂P-bridged rhodium complexes are active hydrogenation catalysts,¹⁹ and other examples of catalysis by phosphido-bridged complexes are known.^{16,24} The rhodium μ -*t*-Bu₂P system remains catalytically active at elevated temperatures even for prolonged periods.²³ Under these conditions new phosphido-bridged species are formed and they are currently under investigation.

(17) Garrou, P. E. *Chem. Rev.* 1981, 81, 229 and references therein.

(18) For example, in [Rh(μ -(*t*-BuCH₂)₂P)(CO)₂]₂, which has a planar structure similar to 2 and a nonbonding Rh-Rh distance of 3.741 Å, δ (³¹P) equals 260 ppm while in [Ir(μ -*t*-Bu₂P)(CO)₂]₂ with two "tetrahedral" cobalt atoms and a short Ir-Ir separation of 2.544 Å δ (³¹P) equals 262 ppm.

(19) Kreter, P. E.; Meek, D. W. *Inorg. Chem.* in press.

(20) In collaboration with Professor T. A. Albright, University of Houston.

(21) On treatment of either 1 or 2 with ¹³CO (2 tm, 30 min) at room temperature in hexane new IR bands are observed for 1 at 2000 (w), 1939 (s), 1928 (s), and 1895 (m) cm⁻¹. The change is reversed on treatment with ¹²CO.

(22) Typical conditions: 1 or 2 (0.034 mmol) and hex-1-ene (5.0 mL, 40.0 mmol) stirred in a glass pressure vessel under CO/H₂ (1:1), 2 atm, and ambient temperature. After 10 h, 1-heptanal (48%) and 2-methylhexanal (45%) are formed (GLC, mass spectroscopy) in approximately 95% conversion. We have so far not optimized the conditions for yield or product ratio.

(23) For example, RhH(CO)(PPh₃)₃ decomposes in solution on heating, giving μ -Ph₂P complexes; see ref 9 above and also ref 9 in: Kurtev, K.; Ribola, D.; Jones, R. A.; Cole-Hamilton, D. J. Wilkinson, G. *J. Chem. Soc. Dalton Trans.* 1980, 55.

Acknowledgment. We thank the Dow Chemical Co., Midland, MI (R.A.J.) and the National Science Foundation (J.L.A. and R.A.J.) for financial support. We thank Johnson-Matthey Ltd. for a loan of RhCl₃·xH₂O. We also thank Professor D. W. Meek, The Ohio State University, for a copy of his paper on diphenylphosphido-bridged rhodium complexes prior to publication.

Supplementary Material Available: Tables of final fractional coordinates, anisotropic thermal parameters, and bond distances and angles for compounds 1 and 2 and listings of structure factor amplitudes for 1 and 2 (23 pages). Ordering information is given on any current masthead page.

(24) See: Ryan, R. C.; Pittman, C. U.; Connor, J. P. *J. Am. Chem. Soc.* 1977, 99, 1986 for hydroformylation using Co₂(CO)₈(μ -PPh)₂. See also the following references for recent examples of stoichiometric reactions related to homogeneous catalysis: Carty, A. J.; Taylor, N. J.; Smith, W. F. *J. Chem. Soc., Chem. Commun.* 1979, 750. Carty, A. J.; MacLaughlin, S. A.; Taylor, N. J. *J. Am. Chem. Soc.* 1981, 103, 2456. Breen, M. J.; Duttera, M. R.; Geoffroy, G. L.; Novotnak, G. C.; Roberts, D. A.; Shulman, P. M.; Steinmetz, G. R. *Organometallics* 1982, 1, 1008. MacLaughlin, S. A.; Carty, A. J.; Taylor, N. J. *Can. J. Chem.* 1982, 60, 87. Carty, A. J. *Pure Appl. Chem.* 1982, 54, 113.

A Novel Palladium Complex with Iron-Palladium Dative Bonding Derived from 1,2,3-Trithia[3]ferrocenophane, (Ph₃P)PdFe(SC₅H₄)₂·0.5C₆H₅CH₃

Dietmar Seyferth,* Barry W. Hames,¹ and Thomas G. Rucker²

Department of Chemistry
Massachusetts Institute of Technology
Cambridge, Massachusetts 02139

Marlin Cowle* and Raymond S. Dickson

Department of Chemistry, The University of Alberta
Edmonton, Alberta, Canada T6G 2G2

Received November 3, 1982

Summary: The reaction of Pd(PPh₃)₄ with 1,2,3-trithia[3]ferrocenophane affords the unusual heterobinuclear species (Ph₃P)PdFe(SC₅H₄)₂. An X-ray structure determination of this complex as the hemitoluene solvate reveals a dative Fe→Pd bond (2.878 (1) Å).

The insertion of low-valent, coordinatively unsaturated species of type L₂M (M = Ni, Pd, Pt; L = tertiary phosphine) into the S-S bond of (μ -S₂)Fe₂(CO)₆ was reported recently.^{3,4} Such insertion into S-S bonds of organic disulfides is a characteristic reaction of such transition-

(1) Natural Sciences and Engineering Research Council (Canada) Postdoctoral Fellow, 1981-1982.

(2) Undergraduate (UROP) research participant.

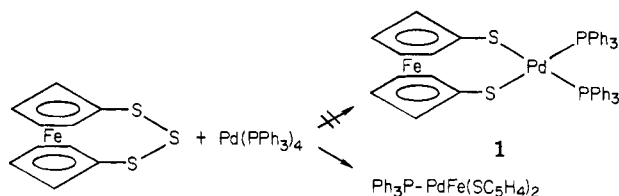
(3) Seyferth, D.; Henderson, R. S.; Gallagher, M. G. *J. Organomet. Chem.* 1980, 193, C75.

(4) Day, V. W.; Lesch, D. A.; Rauchfuss, T. B. *J. Am. Chem. Soc.* 1982, 104, 1290.

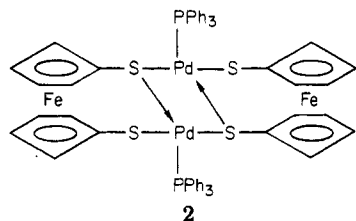
metal species.⁵ Recent interest at MIT in heteroatom-bridged ferrocenophanes⁶ led us to consider the known⁷ 1,2,3-trithia[3]ferrocenophane as an interesting substrate for such insertion reactions.⁸ Our studies in this area are not yet completed, but in view of the interesting and unexpected product obtained, we wish to communicate the results obtained in our study of the reaction of tetrakis(triphenylphosphine)palladium(0) with 1,2,3-trithia[3]ferrocenophane.

The reaction is quite simply carried out. A solution of 7.8 mmol of $\text{Pd}(\text{PPh}_3)_4$ ⁹ and 8.2 mmol of 1,2,3-trithia[3]ferrocenophane⁷ was prepared in 200 mL of THF under nitrogen. This red solution was stirred for 2 h at room temperature, and then the solvent was removed at reduced pressure. The red-brown residue was extracted with 2:3 CH_2Cl_2 /pentane. Column chromatography (silicic acid; first the same solvent mixture and then pure CH_2Cl_2) eluted triphenylphosphine (4.3 g, contaminated by a trace amount of ferrocene) and then a red solid. The latter was recrystallized from CH_2Cl_2 /hexane to give 3.68 g of a red powder, mp $\sim 170^\circ\text{C}$ dec. Another (slow) recrystallization from CH_2Cl_2 /toluene/hexane gave analytically pure product as a microcrystalline toluene solvate, $(\text{PPh}_3)_2\text{PdFe}(\text{SC}_5\text{H}_4)_2 \cdot 0.5\text{C}_6\text{H}_5\text{CH}_3$, mp $108\text{--}110^\circ\text{C}$.¹⁰ Field desorption mass spectrometry established the monomeric constitution indicated.¹¹ The ^1H , ^{13}C , and ^{31}P NMR spectra were in agreement with this formulation.

The formation of apparently ligand-deficient $(\text{PPh}_3)_2\text{PdFe}(\text{SC}_5\text{H}_4)_2$ was surprising. The expected, straightforward product was 1. On the basis of the microanalysis,



which showed that only *one* PPh_3 ligand per Pd was present, a dimeric formulation, 2, in which there was $\text{S} \rightarrow \text{Pd}$ bonding, seemed reasonable. The field desorption



mass spectrometry result that the product was a monomer left two alternatives: (1) the Pd atom in the complex was coordinatively unsaturated or (2) there was $\text{Fe} \rightarrow \text{Pd}$ coordination. The product seemed much too unreactive for a coordinatively unsaturated Pd complex (no reactions, at room temperature, with PPh_3 , CO, or NO).

In order to resolve this interesting structural question, a structure determination by X-ray diffraction was un-

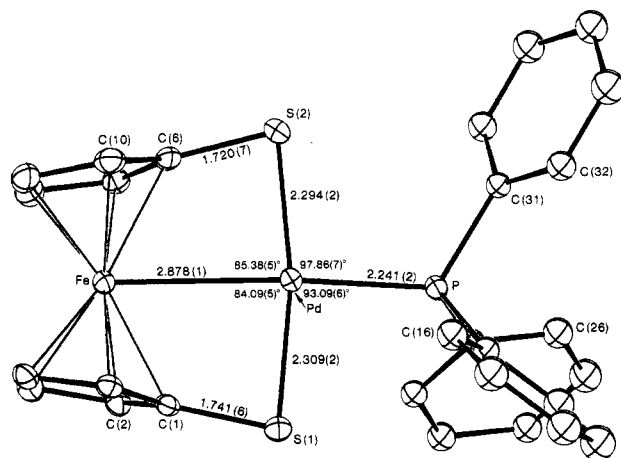


Figure 1. Perspective view of $(\text{PPh}_3)_2\text{PdFe}(\text{SC}_5\text{H}_4)_2$ showing the numbering scheme and some relevant bond lengths and angles (other relevant parameters are given in the text). Thermal ellipsoids are shown at the 20% level.

dertaken. Fortunately, the microcrystalline sample obtained by recrystallization from CH_2Cl_2 /toluene/hexane had contained a small number of larger crystals.

The compound crystallizes in the monoclinic space group $C2/c$ with eight complex molecules and four toluene molecules per unit cell.¹² Crystal data are as follows: $a = 39.258(5) \text{ \AA}$, $b = 10.548(2) \text{ \AA}$, $c = 13.612(4) \text{ \AA}$, $\beta = 101.69(2)^\circ$; $V = 5519.7 \text{ \AA}^3$, $\rho_{\text{calcd}} = 1.595 \text{ g cm}^{-3}$, $\rho_{\text{obsd}} = 1.594 \text{ g cm}^{-3}$; $\mu(\text{Mo K}\alpha) = 13.9 \text{ cm}^{-1}$; $R_F = 0.040$, $R_{wF} = 0.046$ for 3255 unique reflections with $F^2 \geq 3\sigma(F^2)$ and 205 parameters varied. Data were collected up to $2\theta = 52.0^\circ$ using graphite-monochromated Mo $K\alpha$ radiation on an Enraf-Nonius CAD-4 diffractometer. The structure was solved by standard Patterson and Fourier methods and was refined by full-matrix least-squares techniques.¹³

The complex molecule, shown in Figure 1, is a rather unusual heterobinuclear Fe-Pd complex in which the metal centers are held together by the cyclopentadienethiolato groups (SC_5H_4) and what appears to be a dative $\text{Fe} \rightarrow \text{Pd}$ bond (vide infra). Both SC_5H_4 ligands are η^5 bound in a pseudo-trans configuration to iron (much as in ferrocene and its derivatives) and are σ bound to Pd through the sulfur atoms. The coordination about Pd is a slightly distorted square plane in which the sulfur atoms are mutually trans as are the PPh_3 group and the Fe atom of the ferrocenyl moiety. Both Pd-S distances (average 2.302 \AA) appear normal although they are at the short end of the range observed ($2.284(4)\text{--}2.431(3) \text{ \AA}$) in some mono- and bis(thiolato)palladium(II) complexes.¹⁴⁻¹⁸ Similarly the Pd-P distance ($2.241(2) \text{ \AA}$) is one of the shortest observed in typical Pd- PPh_3 complexes (range 2.230

(12) The other possible space group Cc has been ruled out owing to the successful refinement of the structure in $C2/c$ and by the location of all hydrogen atoms except those of the toluene methyl group. In $C2/c$ the toluene molecules occupy the four-electron crystallographic diads resulting in at least a two-fold disorder of the methyl hydrogens.

(13) Phenyl carbon atoms of the PPh_3 groups were refined as rigid groups (D_{6h} symmetry, C-C distances = 1.392 \AA) with individual isotropic thermal parameters; all hydrogens except those of the methyl group were included as fixed contributions in their idealized positions; all other nonhydrogen atoms were refined anisotropically.

(14) Bailey, P. M.; Taylor, S. H.; Maitlis, P. M. *J. Am. Chem. Soc.* 1978, 100, 4711.

(15) Piovesana, O.; Sestili, L.; Bellitto, C.; Flamini, A.; Tomassini, M.; Zanazzi, P. F.; Zanzari, A. R. *J. Am. Chem. Soc.* 1977, 99, 5190.

(16) Ahmed, J.; Itoh, K.; Matsuda, I.; Ueda, F.; Ishii, Y.; Ibers, J. A. *Inorg. Chem.* 1977, 16, 620.

(17) Chen, H. W.; Fackler, J. P. *Inorg. Chem.* 1978, 17, 22.

(18) Roundhill, D. M.; Roundhill, S. G. N.; Beaulieu, W. B.; Bagchi, U. *Inorg. Chem.* 1980, 19, 3365.

(5) See the 11 references given in ref 3.

(6) Seyferth, D.; Withers, H. P., Jr. *J. Organomet. Chem.* 1980, 185, C1.

(7) Bishop, J. J.; Davison, A.; Katcher, M. L.; Lichtenberg, D. W.; Merrill, R. E.; Smart, J. C. *J. Organomet. Chem.* 1971, 27, 241.

(8) This compound was used since the 1,2-dithia[2]ferrocenophane apparently is unknown.

(9) Coulson, D. R. *Inorg. Synth.* 1972, 13, 121.

(10) Anal. Calcd. for $\text{C}_{31.5}\text{H}_{27}\text{S}_2\text{PFePd}$: C, 57.07; H, 4.11. Found: C, 56.83; H, 4.11.

(11) Calcd for $^{12}\text{C}_{28}\text{H}_{23}\text{S}_2\text{P}^{32}\text{S}_2\text{Fe}^{106}\text{Pd}$: m/z 616. Found: m/z 617 (the expected $M + 1$ peak).

(4)-2.349 (2) Å).¹⁹⁻²⁴ These short Pd-S and Pd-P distances are possibly a consequence of the coordinative unsaturation at Pd which results in these electron donating ligands being tightly bound to the electron-deficient metal center.

The Fe-Pd distance (2.878 (1) Å) is rather long for a single bond but corresponds, we suggest, to a weak dative Fe→Pd bond. This bond is necessary to give Pd a favorable 16-electron configuration; without it a very unsaturated and reactive 14-electron configuration would result. Although the Fe-Pd distance is long, being significantly longer than those observed in clusters containing Fe-Pd single bonds (2.599 (1)-2.698 (1) Å),²⁵ it is not unreasonably long for such a bond; Pd-Pd single bond distances up to 2.790 (2) Å²⁶ and Fe-Fe distances up to 2.890 (6) Å²⁷ have been reported.

The geometry about Fe is surprisingly close to that of ferrocene even though Pd seems to be coordinated to the iron center; the two eclipsed SC₅H₄ groups are only 19.6° from parallel resulting in a rather large Cp1-Fe-Cp2²⁸ angle of 165.2°. In other dicyclopentadienylmetal complexes, Cp₂ML_n, in which one or more groups, L_n, are bound to the metal, the Cp-M-Cp angles are within the range 126-147°. The relatively small tilt of the SC₅H₄ groups in the present species may suggest that the Fe-Pd bond is weak. It is also possible that the small tilt represents a compromise between the electronic requirements of the Fe, Pd, and S atoms. A significantly greater tilt of the SC₅H₄ groups would result in longer (and presumably less favorable) Pd-S contacts and C-S-Pd angles that are even more acute than those presently observed; these values (81.6 (2) and 82.6 (2)°) are already much smaller than the idealized value that would be near the tetrahedral limit.

(19) Kai, Y.; Yasuoka, N.; Kasai, N. *Bull. Chem. Soc. Jpn.* 1979, 52, 737.

(20) Zenitani, Y.; Inoue, K.; Kai, Y.; Yasuoka, N.; Kasai, N. *Bull. Chem. Soc. Jpn.* 1976, 49, 1531.

(21) Zenitani, Y.; Tokunan, H.; Kai, Y.; Yasuoka, N.; Kasai, N. *Bull. Chem. Soc. Jpn.* 1978, 51, 1730.

(22) Horike, M.; Kai, Y.; Yasuoka, N.; Kasai, N. *J. Organomet. Chem.* 1974, 72, 441.

(23) Del Piero, G.; Cesari, M. *Acta Crystallogr., Sect. B* 1979, B35, 2411.

(24) Milki, K.; Kai, Y.; Yasuoka, N.; Kasai, N. *J. Organomet. Chem.* 1979, 165, 79.

(25) Longoni, G.; Manassero, M.; Sansoni, M. *J. Am. Chem. Soc.* 1980, 102, 3242.

(26) Browall, K. W.; Bursh, T.; Interrante, L. V.; Kasper, J. S. *Inorg. Chem.* 1972, 11, 1800.

(27) Einstein, F. W. B.; Trotter, J. *J. Chem. Soc. A* 1967, 824.

(28) Cp1 and Cp2 refer to the centroids of the cyclopentadiene groups.

(29) Cowie, M.; Gauthier, M. D. *Inorg. Chem.* 1980, 19, 3142.

(30) Jones, T.; Hanlan, A. J. L.; Einstein, F. W. B.; Sutton, D. *J. Chem. Soc., Chem. Commun.* 1980, 1078.

(31) Schultz, A. J.; Stearley, K. L.; Williams, J. M.; Mink, R.; Stucky, G. D. *Inorg. Chem.* 1977, 16, 3303.

(32) Kirillova, N. I.; Gusev, A. I.; Struchkov, Yu. T. *Zh. Strukt. Khim.* 1972, 13, 473.

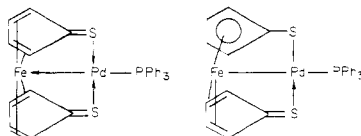
(33) Van Bolhuis, F.; de Boer, E. J. M.; Teuben, J. H. *J. Organomet. Chem.* 1979, 170, 299.

(34) Prout, K.; Cameron, T. S.; Forder, R. A.; Critchley, S. R.; Denton, B.; Rees, G. V. *Acta Crystallogr., Sect. B* 1974, B30, 2290 and references therein.

(35) Prout, K.; Critchley, S. R.; Rees, G. V. *Acta Crystallogr., Sect. B* 1974, B30, 2305.

(36) Fachinetti, G.; Floriani, C.; Marchetti, F.; Mellini, M. *J. Chem. Soc., Dalton Trans.* 1978, 1398.

(37) A reviewer has suggested the alternative resonance forms shown. We shall consider this possibility in our full paper on our work in this area.



Other parameters within the complex are essentially as expected; the average C-C distance of the SC₅H₄ groups (1.42 Å) compares well with the predicted value of 1.43 Å and the C-C-C angles (average 108.0°) are typical; the S-C distances appear normal for such distances in thiolato groups;¹⁴⁻¹⁸ and the range in Fe-C distances (2.039 (7)-2.154 (7) Å) also appears normal.

Acknowledgment. We thank the University of Alberta, the Natural Sciences and Engineering Research Council of Canada, and the National Science Foundation of the United States for financial support and Dr. R. G. Ball for X-ray data collection. The FD-MS data were obtained at the MIT Mass Spectrometry Facility (supported by NIH Division of Research Resources, Grant No. RR00317; K. Biemann, principal investigator) through the kind offices of Dr. Catherine E. Costello.

Registry No. Pd(PPh₃)₄, 14221-01-3; (Ph₃P)PdFe(SC₅H₄)₂, 0.5C₆H₅CH₃, 84393-86-2; 1,2,3-trithia[3]ferrocenophane, 32677-78-4.

Supplementary Material Available: Tables summarizing the crystal data and intensity collection details, positional and thermal parameters for atoms and groups, and bond lengths and angles, a stereoview of title compound, and a listing of the observed and calculated structure amplitudes (18 pages). Ordering information is given on any current masthead page.

Synthesis and Structure of a Coordinately Unsaturated Trinuclear Rhodium Cluster

R. R. Burch and E. L. Muetterties*

Department of Chemistry, University of California Berkeley, California 94720

M. R. Thompson and V. W. Day*

Department of Chemistry, University of Nebraska Lincoln, Nebraska 68588
The Crystallitics Company
Lincoln, Nebraska 68501

Received October 6, 1982

Summary: A new coordinately unsaturated metal cluster $\{(\mu_3\text{-H})(\mu\text{-H})_2\text{Rh}_3(\mu\text{-Cl})[\mu\text{-OP}(\text{O-}i\text{-C}_3\text{H}_7)_2]_2[\text{P}(\text{O-}i\text{-C}_3\text{H}_7)_3]_3\}^-$ was prepared by the reaction of $[\text{ClRh}(\text{ethylene})_2]_2$ first with triisopropyl phosphite to form $[\text{ClRh}[\text{P}(\text{O-}i\text{-C}_3\text{H}_7)_3]_2]_2$ that was then allowed to react with $[\text{BH}(\text{O-}i\text{-C}_3\text{H}_7)_3]^-$ in the presence of hydrogen. The anionic cluster was isolated in single crystal form as the potassium complex. This potassium complex has the remarkable property of dissolving in saturated hydrocarbons. An X-ray crystallographic study and NMR study established the essential structural and stereochemical features of the rhodium cluster: the rhodium atoms describe a near isosceles triangle with the two short edges bridged by phosphonate ligands and the third edge by chlorine. One of the hydride hydrogen atoms is proposed to lie at a face bridging site. The other two may be bridging the two short edges or terminally bonded to rhodium atoms. The single crystals of the potassium complex were monoclinic of space group $P2_1/n$ with $a = 14.122(5)$ Å, $b = 28.529(9)$ Å, $c = 16.417(4)$ Å, and $\beta = 103.74(2)^\circ$.

Most molecular metal clusters are characterized by a bonding configuration in which all low-lying molecular

(4)–2.349 (2) Å).^{19–24} These short Pd–S and Pd–P distances are possibly a consequence of the coordinative unsaturation at Pd which results in these electron donating ligands being tightly bound to the electron-deficient metal center.

The Fe–Pd distance (2.878 (1) Å) is rather long for a single bond but corresponds, we suggest, to a weak dative Fe→Pd bond. This bond is necessary to give Pd a favorable 16-electron configuration; without it a very unsaturated and reactive 14-electron configuration would result. Although the Fe–Pd distance is long, being significantly longer than those observed in clusters containing Fe–Pd single bonds (2.599 (1)–2.698 (1) Å),²⁵ it is not unreasonable long for such a bond; Pd–Pd single bond distances up to 2.790 (2) Å²⁶ and Fe–Fe distances up to 2.890 (6) Å²⁷ have been reported.

The geometry about Fe is surprisingly close to that of ferrocene even though Pd seems to be coordinated to the iron center; the two eclipsed SC₅H₄ groups are only 19.6° from parallel resulting in a rather large Cp1–Fe–Cp2²⁸ angle of 165.2°. In other dicyclopentadienylmetal complexes, Cp₂ML_n, in which one or more groups, L_n, are bound to the metal, the Cp–M–Cp angles are within the range 126–147°.^{29–36} The relatively small tilt of the SC₅H₄ groups in the present species may suggest that the Fe–Pd bond is weak. It is also possible that the small tilt represents a compromise between the electronic requirements of the Fe, Pd, and S atoms. A significantly greater tilt of the SC₅H₄ groups would result in longer (and presumably less favorable) Pd–S contacts and C–S–Pd angles that are even more acute than those presently observed; these values (81.6 (2) and 82.6 (2)°) are already much smaller than the idealized value that would be near the tetrahedral limit.

(19) Kai, Y.; Yasuoka, N.; Kasai, N. *Bull. Chem. Soc. Jpn.* 1979, 52, 737.

(20) Zenitani, Y.; Inoue, K.; Kai, Y.; Yasuoka, N.; Kasai, N. *Bull. Chem. Soc. Jpn.* 1976, 49, 1531.

(21) Zenitani, Y.; Tokunan, H.; Kai, Y.; Yasuoka, N.; Kasai, N. *Bull. Chem. Soc. Jpn.* 1978, 51, 1730.

(22) Horike, M.; Kai, Y.; Yasuoka, N.; Kasai, N. *J. Organomet. Chem.* 1974, 72, 441.

(23) Del Piero, G.; Cesari, M. *Acta Crystallogr., Sect. B* 1979, B35, 2411.

(24) Miki, K.; Kai, Y.; Yasuoka, N.; Kasai, N. *J. Organomet. Chem.* 1979, 165, 79.

(25) Longoni, G.; Manassero, M.; Sansoni, M. *J. Am. Chem. Soc.* 1980, 102, 3242.

(26) Broll, K. W.; Bursh, T.; Interrante, L. V.; Kasper, J. S. *Inorg. Chem.* 1972, 11, 1800.

(27) Einstein, F. W. B.; Trotter, J. *J. Chem. Soc. A* 1967, 824.

(28) Cp1 and Cp2 refer to the centroids of the cyclopentadiene groups.

(29) Cowie, M.; Gauthier, M. D. *Inorg. Chem.* 1980, 19, 3142.

(30) Jones, T.; Hanlan, A. J. L.; Einstein, F. W. B.; Sutton, D. *J. Chem. Soc., Chem. Commun.* 1980, 1078.

(31) Schultz, A. J.; Stearley, K. L.; Williams, J. M.; Mink, R.; Stucky, G. D. *Inorg. Chem.* 1977, 16, 3303.

(32) Kirillova, N. I.; Gusev, A. I.; Struchkov, Yu. T. *Zh. Strukt. Khim.* 1972, 13, 473.

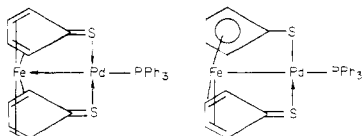
(33) Van Bolhuis, F.; de Boer, E. J. M.; Teuben, J. H. *J. Organomet. Chem.* 1979, 170, 299.

(34) Prout, K.; Cameron, T. S.; Forder, R. A.; Critchley, S. R.; Denton, B.; Rees, G. V. *Acta Crystallogr., Sect. B* 1974, B30, 2290 and references therein.

(35) Prout, K.; Critchley, S. R.; Rees, G. V. *Acta Crystallogr., Sect. B* 1974, B30, 2305.

(36) Fachinetti, G.; Floriani, C.; Marchetti, F.; Mellini, M. *J. Chem. Soc., Dalton Trans.* 1978, 1398.

(37) A reviewer has suggested the alternative resonance forms shown. We shall consider this possibility in our full paper on our work in this area.



Other parameters within the complex are essentially as expected; the average C–C distance of the SC₅H₄ groups (1.42 Å) compares well with the predicted value of 1.43 Å and the C–C–C angles (average 108.0°) are typical; the S–C distances appear normal for such distances in thiolato groups;^{14–18} and the range in Fe–C distances (2.039 (7)–2.154 (7) Å) also appears normal.

Acknowledgment. We thank the University of Alberta, the Natural Sciences and Engineering Research Council of Canada, and the National Science Foundation of the United States for financial support and Dr. R. G. Ball for X-ray data collection. The FD-MS data were obtained at the MIT Mass Spectrometry Facility (supported by NIH Division of Research Resources, Grant No. RR00317; K. Biemann, principal investigator) through the kind offices of Dr. Catherine E. Costello.

Registry No. Pd(PPh₃)₄, 14221-01-3; (Ph₃P)PdFe(SC₅H₄)₂·0.5C₅H₅CH₃, 84393-86-2; 1,2,3-trithia[3]ferrocenophane, 32677-78-4.

Supplementary Material Available: Tables summarizing the crystal data and intensity collection details, positional and thermal parameters for atoms and groups, and bond lengths and angles, a stereoview of title compound, and a listing of the observed and calculated structure amplitudes (18 pages). Ordering information is given on any current masthead page.

Synthesis and Structure of a Coordinately Unsaturated Trinuclear Rhodium Cluster

R. R. Burch and E. L. Muetterties*

Department of Chemistry, University of California Berkeley, California 94720

M. R. Thompson and V. W. Day*

Department of Chemistry, University of Nebraska Lincoln, Nebraska 68588
The Crystallitics Company
Lincoln, Nebraska 68501

Received October 6, 1982

Summary: A new coordinately unsaturated metal cluster $\{(\mu_3\text{-H})(\mu\text{-H})_2\text{Rh}_3(\mu\text{-Cl})[\mu\text{-OP}(\text{O}-i\text{-C}_3\text{H}_7)_2]_2[\text{P}(\text{O}-i\text{-C}_3\text{H}_7)_3]_3\}^-$ was prepared by the reaction of $[\text{ClRh}(\text{ethylene})_2]_2$ first with triisopropyl phosphite to form $\{\text{ClRh}[\text{P}(\text{O}-i\text{-C}_3\text{H}_7)_3]_2\}_2$ that was then allowed to react with $[\text{BH}(\text{O}-i\text{-C}_3\text{H}_7)_3]^-$ in the presence of hydrogen. The anionic cluster was isolated in single crystal form as the potassium complex. This potassium complex has the remarkable property of dissolving in saturated hydrocarbons. An X-ray crystallographic study and NMR study established the essential structural and stereochemical features of the rhodium cluster: the rhodium atoms describe a near isosceles triangle with the two short edges bridged by phosphonate ligands and the third edge by chlorine. One of the hydride hydrogen atoms is proposed to lie at a face bridging site. The other two may be bridging the two short edges or terminally bonded to rhodium atoms. The single crystals of the potassium complex were monoclinic of space group $P2_1/n$ with $a = 14.122$ (5) Å, $b = 28.529$ (9) Å, $c = 16.417$ (4) Å, and $\beta = 103.74$ (2)°.

Most molecular metal clusters are characterized by a bonding configuration in which all low-lying molecular

orbitals are filled.^{1,2} Consequently, the clusters are *relatively* nonreactive. To enhance cluster reactivity and potential catalytic activity, we have sought synthetic pathways to coordinately unsaturated clusters, especially clusters in which each metal atom site is coordinately unsaturated.² One such family of clusters that we have developed is comprised of two closely related classes $\{(\mu\text{-H})\text{Rh}[\text{PY}_3]_2\}_x$ and $\{(\mu\text{-H})\text{Rh}[\eta^4\text{-diene}]\}_4$, in which the electron count per rhodium atom is 14 and the rhodium primary coordination sphere is four-coordinate and square planar. Most of these are structurally defined through crystallographic studies and are partially characterized in terms of stoichiometric and catalytic chemistry.³⁻¹³ In seeking improved syntheses of these clusters, we succeeded for the specific class of phosphite clusters and, in the process, found as a byproduct a new unsaturated (by electron count) trinuclear rhodium cluster that has individual rhodium atoms of formal oxidation states of +1 and +3. Described herein is the synthesis, the crystallographic study and structural analysis of the new anionic cluster $[\text{H}_3\text{Rh}_3(\mu\text{-Cl})[\mu\text{-OP}(\text{O-}i\text{-C}_3\text{H}_7)_2]_2[\text{P}(\text{O-}i\text{-C}_3\text{H}_7)_3]_3]^-$ in the form of a tight potassium ion complex.

Reaction of $\{(\mu\text{-Cl})\text{Rh}(\text{C}_2\text{H}_4)_2\}_2$ ¹⁵ first with 4 equiv of triisopropyl phosphite and then with $\text{KBH}(\text{O-}i\text{-C}_3\text{H}_7)_3$ in an H_2 atmosphere gave primarily the known dimer $\{(\mu\text{-H})\text{Rh}[\text{P}(\text{O-}i\text{-C}_3\text{H}_7)_3]_2\}_2$ and up to 15% yields of $\text{K}[\text{H}_3\text{Rh}_3\text{Cl}[\mu\text{-OP}(\text{O-}i\text{-C}_3\text{H}_7)_2]_2[\text{P}(\text{O-}i\text{-C}_3\text{H}_7)_3]_3]$, 1, which has both bridging hydride and bridging $\text{OP}(\text{O-}i\text{-C}_3\text{H}_7)_2$ ligands.¹⁴ Although scission of phosphite carbon-oxygen bonds is a relatively common¹⁵⁻²⁴ observation for metal phosphite reactions, the formation of bridging $\mu\text{-OP}(\text{OR})_2$

and closely related²³ ligands in polynuclear metal complexes typically requires elevated reaction temperatures.

The potassium complex of this new anionic cluster has the remarkable property of alkane solubility; in fact, single crystals of the complex were obtained by recrystallization from pentane. The single crystals at $20 \pm 1^\circ\text{C}$ were monoclinic of space group $P2_1/n$ [a special setting of $P2_1/c-C_{2h}$ (No. 14)]²⁵ with $a = 14.122(5) \text{ \AA}$, $b = 28.529(9) \text{ \AA}$, $c = 16.417(4) \text{ \AA}$, $\beta = 103.74(2)^\circ$, $V = 6451.4 \text{ \AA}^3$, and $Z = 4$ ($\mu_r(\text{Mo K}\alpha) = 1.02 \text{ mm}^{-1}$, $d_{\text{calcd}} = 1.380 \text{ g cm}^{-3}$). Three-dimensional X-ray diffraction data were collected on a parallelepiped-shaped crystal for 11828 independent reflections, with $2\theta_{\text{MoK}\alpha} < 50.70^\circ$ on a Nicolet P1 auto-diffractometer using graphite-monochromated $\text{Mo K}\alpha$ radiation and full (1° wide) ω scans. The three rhodium atoms were located by using direct methods (MULTAN), and the remaining non-hydrogen atoms were located from difference Fourier syntheses. The resulting structural parameters were refined to convergence [$R(\text{unweighted, based on } F) = 0.058$ for 3943 independent reflections having $I > 3\sigma(I)$] in cycles of empirically weighted full-matrix least-squares refinement using anisotropic thermal parameters for all non-hydrogen atoms.^{28,31} The crystallographic study precisely established the position of all non-hydrogen atoms in $\text{K}[\text{H}_3\text{Rh}_3(\mu\text{-Cl})[\mu\text{-OP}(\text{O-}i\text{-C}_3\text{H}_7)_2]_2[\text{P}(\text{O-}i\text{-C}_3\text{H}_7)_3]_3]$. A near isosceles triangle was formed by the rhodium atoms with Rh-Rh separations of 2.778(2), 2.792(2), and 3.066(2) \AA . Each rhodium atom had one terminal (two-center, two-electron) triisopropyl phosphite ligand. The two short edges were bridged by the bifunctional phosphonate ligand 2, and the long edge

(1) Muetterties, E. L.; Rhodin, T. N.; Band, E.; Brucker, C. F.; Pretzer, W. R. *Chem. Rev.*, 1979, 91-140.

(2) (a) Muetterties, E. L. *Catal. Rev.—Sci. Eng.* 1981, 23, 69-87. (b) *Inorg. Chim. Acta* 1981, 50, 1-9.

(3) Day, V. W.; Fredrich, M. F.; Reddy, G. S.; Sivak, A. J.; Pretzer, W. R. Muetterties, E. L. *J. Am. Chem. Soc.* 1977, 99, 8091-8093.

(4) Sivak, A. J.; Muetterties, E. L. *J. Am. Chem. Soc.* 1979, 101, 4878-4887.

(5) Brown, R. K.; Williams, J. M.; Fredrich, M. F.; Day, V. W.; Sivak, A. J.; Muetterties, E. L. *Proc. Natl. Acad. Sci. U.S.A.* 1979, 76, 2099-2102.

(6) Brown, R. K.; Williams, J. M.; Sivak, A. J.; Muetterties, E. L. *Inorg. Chem.* 1980, 19, 370-374.

(7) Teller, R. G.; Williams, J. M.; Koetzle, T. F.; Burch, R. R.; Gavin, R. M.; Muetterties, E. L. *Inorg. Chem.* 1981, 20, 1806-1811.

(8) Muetterties, E. L.; Sivak, A. J.; Brown, R. K.; Williams, J. M.; Fredrich, M. F.; Day, V. W. *Fundam. Res. Homogeneous Catal.*, [Proc. Int. Workshop] 1979, 3, 487-497.

(9) Burch, R. R.; Muetterties, E. L.; Schultz, A. J.; Gebert, E. G.; Williams, J. M. *J. Am. Chem. Soc.* 1981, 103, 5517-5522.

(10) Burch, R. R.; Muetterties, E. L.; Day, V. W. *Organometallics* 1982, 1, 188-197.

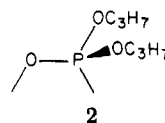
(11) Burch, R. R.; Muetterties, E. L.; Teller, R. G.; Williams, J. M. *J. Am. Chem. Soc.* 1982, 104, 4257-4258.

(12) Kulzick, M.; Price, R. T.; Muetterties, E. L.; Day, V. W. *Organometallics* 1982, 1, 1256-1258.

(13) Meier, E.-B.; Burch, R. R.; Muetterties, E. L.; Day, V. W. *J. Am. Chem. Soc.* 1982, 104, 2661-2663.

(14) To a solution of 0.40 g (1.03 mmol) of $[\text{ClRh}(\text{C}_2\text{H}_4)_2]$ in approximately 50 mL of tetrahydrofuran was added a solution of 0.94 g (4.52 mmol) of $\text{P}(\text{O-}i\text{-C}_3\text{H}_7)_3$ in 5 mL of tetrahydrofuran dropwise over the course of approximately 45 min. The resulting solution was stirred at room temperature for an additional 2 h. The solution was then cooled to -78°C , and a steady flow of H_2 gas was passed through the reaction vessel (approximately 5 mL/min). Excess pressure was relieved through a mineral oil bubbler. A solution of 2.30 mL of 1 M $\text{KBH}(\text{O-}i\text{-C}_3\text{H}_7)_3$ in tetrahydrofuran (2.30 mmol) was added dropwise over the course of 3 h. The solution was allowed to warm to room temperature and was stirred for an additional 5 h. The tetrahydrofuran was removed by vacuum distillation; and the residue was extracted with pentane and filtered through a fine porosity frit. The filtrate was then cooled to -78°C . A small crop of orange-red crystals formed which were isolated by filtration: yield 20 mg (15%). The yield of this compound was highly variable, and this yield represents the highest yield yet obtained. In all these preparations, further cooling of the solution led to the crystallization of $\{(\mu\text{-H})\text{Rh}[\text{P}(\text{O-}i\text{-C}_3\text{H}_7)_3]_2\}_2$ in approximately 60% yield. Anal. Calcd for $\text{C}_{39}\text{H}_{34}\text{ClK}_2\text{O}_{15}\text{P}_3\text{Rh}_3$: C, 34.91; H, 7.01; P, 11.56; Cl, 2.65; K, 2.92. Found: C, 35.57; H, 7.06; P, 11.62; Cl, 3.2; K, 2.8.

(15) Haines, R. J.; Nolte, C. R. *J. Organomet. Chem.* 1970, 24, 725-736.



was bridged by the chlorine atom. Unfortunately, none of the hydride hydrogen atoms could be directly located with the X-ray diffraction data. However, the combination of the NMR data and the structural inferences allow a

(16) Goh, L.-Y.; D'Aniello, M. J., Jr.; Slater, S.; Muetterties, E. L.; Tavanaiepour, I.; Chang, M. I.; Fredrich, M. F.; Day, V. W. *Inorg. Chem.* 1979, 18, 192-197.

(17) Werner, H.; Feser, R. Z. *Anorg. Allg. Chem.* 1979, 458, 301-308.

(18) Muetterties, E. L.; Kirner, J. F.; Evans, W. J.; Watson, P. L.; Abdel-Meguid, S. S.; Tavanaiepour, I.; Day, V. W. *Proc. Natl. Acad. Sci. U.S.A.* 1978, 75, 1056-1059.

(19) Choi, H. W.; Gavin, R. M.; Muetterties, E. L. *J. Chem. Soc., Chem. Commun.* 1979, 1085.

(20) Day, V. W.; Tavanaiepour, I.; Abdel-Meguid, S. S.; Kirner, J. F.; Goh, L.-Y.; Muetterties, E. L. *Inorg. Chem.* 1982, 21, 657-663.

(21) Choi, H. W.; Muetterties, E. L. *J. Am. Chem. Soc.* 1982, 104, 153-161.

(22) Schunn, R. A.; Demitras, G. C.; Choi, H. W.; Muetterties, E. L. *Inorg. Chem.* 1981, 20, 4023-4025.

(23) Orpen, A. G.; Sheldrich, G. M. *Acta Crystallogr., Sect. B* 1978, B34, 1992-1994.

(24) Pomeroy, R. K.; Alex, R. F. *J. Chem. Soc., Chem. Commun.* 1980, 1114-1115.

(25) "International Tables for X-Ray Crystallography", Kynoch Press: Birmingham, England, 1969; Vol. I, p 99.

(26) "International Tables for X-Ray Crystallography", Kynoch Press: Birmingham, England, 1974; Vol. IV, pp 55-66.

(27) Crystal dimensions of $0.20 \times 0.30 \times 0.35 \text{ mm}$.

(28) A recent tabulation²⁹ of atomic scattering factors was used for all non-hydrogen atoms and those for Rh, K, Cl, and P were corrected³⁰ for anomalous dispersion effects.

(29) Reference 26; pp 149-150.

(30) Reference 26; pp 99-101.

(31) In the following presentation and discussion of structural parameters the first number in parentheses following an averaged value for a bond length or angle is the root-mean-square estimated standard deviation of an individual datum. The second and third numbers, when given, are the average and maximum deviations from the averaged value, respectively; the fourth number is the number of individual values included in the average.

Table I. Selected Bond Lengths (Å) and Angles (deg) in Crystalline $K\{H_3Rh_3(\mu-Cl)[\mu-OP(O-i-C_3H_7)_2]_2[P(O-i-C_3H_7)_3]_3\}^a$

Bond Lengths ^b			
Rh ₁ -Rh ₂	2.778 (2)	Rh ₁ -H ₁₂ ^c	1.75 (-)
Rh ₁ -Rh ₃	2.792 (2)	Rh ₁ -H ₁₃ ^c	1.75 (-)
Rh ₂ ···Rh ₃	3.066 (2)	Rh ₁ -H ₁₂₃ ^c	2.00 (-)
Rh-P(phosphite)	2.194 (5, 2, 3, 3)	Rh ₂ -H ₁₂₃ ^c	2.12 (-)
Rh-P(phosphonate)	2.185 (5, 1, 1, 2)	Rh ₃ -H ₁₂₃ ^c	2.00 (-)
Rh ₁ -O(phosphonate)	2.273 (10, 12, 12, 2)	Rh ₂ -H ₁₂ ^c	2.38 (-)
Rh ₂ -Cl	2.439 (5, 3, 3, 2)	Rh ₃ -H ₁₃ ^c	2.40 (-)
P ₄ -O _{4b} (phosphonate)	1.53 (1, 1, 1, 2)	C-O	1.47 (2, 2, 4, 13)
P-O(isopropoxy)	1.61 (1, 2, 3, 13)	C-C	1.51 (4, 5, 15, 26)
		K-O	2.86 (1, 13, 21, 7)
Bond Angles ^b			
P ₁ -Rh ₁ -O _{4b}	105.8 (3, 14, 14, 2)	P ₄ -Rh ₂ -H ₁₂₃ ^c	72 (-, 3, 3, 2)
O _{4b} -Rh ₁ -O _{5b}	92.5 (3)	Cl-Rh ₂ -H ₁₂₃ ^c	93 (-, 2, 2, 2)
P ₁ -Rh ₁ -H ₁₂₃ ^c	180.0 (-)	Rh ₂ -Cl-Rh ₃	77.9 (1)
O _{4b} -Rh ₁ -H ₁₃ ^c	180.0 (-)	Rh ₂ -P ₄ -O _{4b}	111.1 (4, 8, 8, 2)
O _{5b} -Rh ₁ -H ₁₂ ^c	180.0 (-)	Rh ₁ -O _{4b} -P ₄	101.6 (5, 4, 4, 2)
P ₄ -Rh ₂ -Cl	163.3 (2, 9, 9, 2)	Rh ₂ -Rh ₁ -Rh ₃	66.8 (1)
P ₂ -Rh ₂ -H ₁₂₃ ^c	148 (-, 4, 4, 2)	Rh ₁ -Rh ₂ -Rh ₃	56.6 (1, 2, 2, 2)
P ₂ -Rh ₂ -P ₄	98.3 (2, 16, 16, 2)		
P ₃ -Rh ₂ -Cl	98.4 (2, 25, 25, 2)		

^a Bond lengths and angles have been averaged for chemically distinct groups of atoms wherever appropriate, according to idealized C_s - m symmetry. The first number in parentheses following an averaged value for a bond length or angle is the root-mean-square estimated standard deviation of an individual datum. The second and third numbers, when given, are the average and maximum deviations from the averaged value, respectively; the fourth number is the number of individual values included in the average. ^b Atoms are labeled in agreement with Figures 1 and 2 and Tables II and III. ^c Idealized atomic coordinates were calculated for the three hydride hydrogens assuming the Rh₁ is an octahedral Rh(III) center with a *fac* disposition of three hydride ligands. H₁₂₃ is the face-bridging hydride.

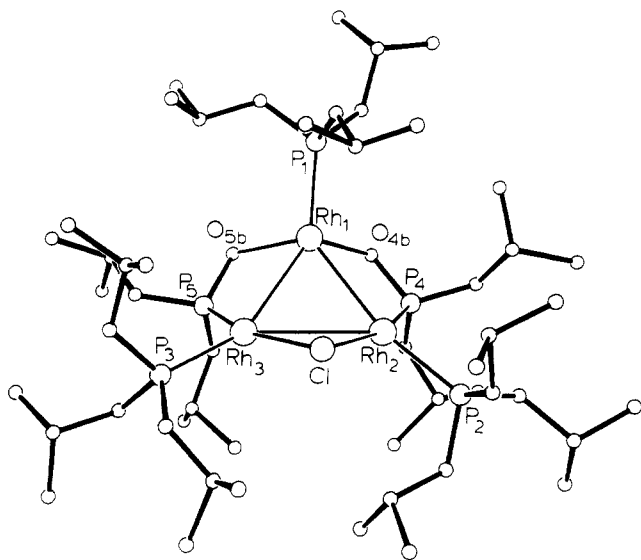


Figure 1. Perspective ORTEP drawing of the solid-state structure for the non-hydrogen atoms of the $[H_3Rh_3(\mu-Cl)[\mu-OP(O-i-C_3H_7)_2]_2[P(O-i-C_3H_7)_3]_3]^-$ anion. Rhodium atoms are represented by large open circles while phosphorus and chlorine atoms are represented by medium-sized open circles; oxygen and carbon atoms are represented by small open circles.

plausible placement of hydride hydrogen atoms as discussed below.

The magnitude of the two short Rh-Rh distances of 2.778 and 2.792 Å in the cluster is comparable to three-center, two-electron Rh(I)-H-Rh(I) distances in related clusters: for example, the Rh-Rh separation in the hydride edge-bridged cluster $\{(\mu-H)Rh[P(OCH_3)_3]_2\}_3$ is 2.824 (2) Å.⁶ However, the more appropriate comparison is with three-center, two-electron Rh(I)-H-Rh(III) distances. In this comparison, the model structure is $\{H_2-$

$[(CH_3)_2N)_3P]_2Rh^{III}(\mu-H)_2Rh^I[P(N(CH_3)_2)_3]_2\}$, where the Rh-Rh separation is 2.734 (1) Å.¹³ Hence the two short Rh-Rh edges *may be* bridge bonded by a single hydrogen (hydride) atom. As established by the X-ray study, the short edges are also bridged by the bifunctional phosphonate ligands but the intrinsic effect of these bridging ligands on the Rh-Rh separations cannot be objectively assessed. For the long edge bridged by the chlorine atom, the Rh-Rh separation of 3.066 (2) Å is comparable to those established for analogous complexes with Rh(I)-Cl-Rh(I) three-center, four-electron bonding interactions. Illustrated in Figure 1 is the basic coordination skeleton for the rhodium cluster exclusive of hydrogen and potassium atoms, and presented in Table I are relevant bond distances and bond angles.

The suggested edge-bridging hydrogen atoms for the two short edges would occupy two of the three relatively open areas in the heavy-atom framework structure. These hydride hydrogen atoms are proposed to lie on, or near, the $O_{4b} \rightarrow Rh_1$ and $O_{5b} \rightarrow Rh_1$ vector extensions above the $Rh_1 \rightarrow Rh_2$ and $Rh_1 \rightarrow Rh_3$ vectors, respectively, and may be symmetrically or unsymmetrically bridging. If the latter obtains, then the limiting case would be two cis terminal hydride ligands on the unique Rh_1 atom. The remaining "open" area close to the three rhodium atoms is the face of the Rh_3 triangle opposite the face from which the chlorine atom and the two proposed edge bridging hydrogen atoms project. NMR data, discussed below, indicate that all three phosphite phosphorus atoms are trans to a hydride hydrogen atom. Thus, the vector extension of $P_1 \rightarrow Rh_1$ for the unique triisopropyl phosphite ligand should nearly pass through a hydride hydrogen atom—a face-bridging hydride would be close to this vector extension. Furthermore, such a face-bridging hydride hydrogen atom would be close to trans positions to the remaining two phosphite phosphorus atoms. There is no crystallographically established example of a triply

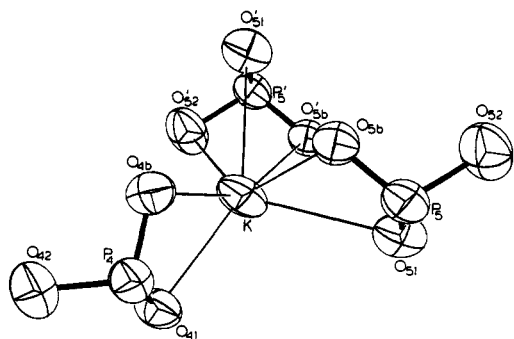


Figure 2. Perspective ORTEP drawing of the K^+ coordination sphere in crystals of $K\{H_3Rh_3(\mu-Cl)[\mu-OP(O-i-C_3H_7)_2]_2[P(O-i-C_3H_7)_3]_3\}$. All atoms are represented by thermal vibration ellipsoids drawn to encompass 50% of the electron density. Atoms labeled without a prime (') belong to the molecule shown in Figure 1; atoms labeled with a prime are related to those in Figure 1 by the crystallographic inversion center at $(\frac{1}{2}, 0, \frac{1}{2})$ in the unit cell.

bridging hydride ligand in a trinuclear metal cluster, but such a ligand has been proposed for three specific trinuclear metal clusters; all established examples of triply bridging hydride ligands involve tetranuclear, or larger, metal clusters.³²

Although $\{(\mu_3-H)(\mu-H)Rh_3(\mu-Cl)[\mu-OP(O-i-C_3H_7)_2]_2[P(O-i-C_3H_7)_3]_3\}^{33}$ is not required to possess any rigorous crystallographic symmetry in crystals of 1, it does approximate closely its maximum possible symmetry of C_s-m with Rh_1 , P_1 , and Cl lying in the pseudomirror plane that makes a dihedral angle of 87.6° with the plane of the rhodium triangle. Phosphonate atoms P_4 , P_5 , O_{4b} , and O_{5b} are coplanar to within 0.03 \AA and lie $1.44\text{--}1.55 \text{ \AA}$ below the rhodium triangle.

Each potassium cation is coordinated in the lattice to seven phosphonate oxygen atoms of two symmetry-related cluster anions ($K-O$ distances range from 2.704 (11) to 3.071 (11) \AA). This KO_7 coordination framework is shown in Figure 2. Inversion-center related pairs of cluster anions are held together in the lattice by the interaction of two such potassium cations, the $K\cdots K'$ separation is 3.655 (5) \AA . Encapsulation of the two potassium ions in this dimeric ion complex renders the periphery of this molecular dimer hydrocarbon in character and fully accounts for the pentane solubility of the potassium salt. Actually, the compound is not a salt in the conventional sense of the word but is a very tight multiple ion complex.

The crystalline and solution state structures of the rhodium cluster appear to be fully analogous as judged by 1H and ^{31}P NMR data.³⁴ Also, these NMR data support the hydride ligand placements implicated from the X-ray diffraction data and crystallographic analysis. Three types of phosphorus atom environments of relative populations 1:2:2, analogous to the solid state structure were established

by the ^{31}P and $^{31}P\{^1H\}$ experiments. Each phosphorus atom is directly bonded to a single rhodium atom as judged by the large $P-Rh$ doublet splittings. Also, the ^{31}P NMR resonances for all three phosphite ligands showed fairly large $P-H$ (hydride) doublet splittings. The magnitudes of the J_{PH} values suggest that the hydride ligand that is strongly spin coupled to a phosphite phosphorus atom should form an angle close to 180° with the $Rh-P$ vector. In the $ClRh_3P_3P'_2H_3$ framework structure as proposed for the crystalline state, there is only one hydride ligand trans to phosphite phosphorus atoms, namely, the proposed face-bridging hydride ligand. Basically, the unique $H-Rh_1-P_1$ angle should be closer to 180° (Table I) than the two essentially equivalent $H-Rh_2-P_2$ and $H-Rh_3-P_3$ angles, and in fact, the J_{PH} value for P_1 and $H(\mu_3-H)$ coupling is larger than that for P_2 and H and for P_3 and $H(\mu_3-H)$: 120 Hz vs. 57 Hz . Thus the placement of a hydride ligand in a face-bridging position as proposed from the crystallographic study is fully consistent with the ^{31}P NMR data, but the other two hydride placements cannot be assessed by these data. Analogously, the 1H NMR data support the definition of the $ClRh_3P_3P'_2(\mu_3-H)$ framework but provide no definitive information concerning the placement of the remaining two hydride ligands. In the hydride region of the 1H NMR spectrum, there were two resonances of unequal intensity.³⁵ The larger of the two was somewhat broad and exhibited no fine structure at temperatures ranging from $+20$ to -65°C . The smaller intensity resonance was very broad and structureless at 20°C , but at -65°C , there were three maxima discernible with a separation between the first and third of $\sim 125 \text{ Hz}$. This fine structure is due to a $H-P$ coupling and probably is a poorly resolved, overlapping doublet of triplets, as expected from the ^{31}P spectral parameters, representing the unique triply bridging hydride ligand. The spectra broadened with further temperature decrease. At these low temperatures, there is an adverse viscosity effect upon the hydrogen atom relaxation times; note that the molecular weight of the dimeric ion complex is ~ 2675 .

Electronically, this new rhodium cluster is analogous to the hydrogen adducts of $\{(\mu-H)Rh(PY_3)_2\}_x$ clusters: $\{H[(H_7C_3-i-O)_3P]_2Rh(\mu-H)_3Rh[P(O-i-C_3H_7)_3]_2\}$, 3, $\{H_2-[(CH_3)_2N]_3P]_2Rh^{III}(\mu-H)_2Rh^I[P(N(CH_3)_2)_3]_2\}$, 4, and most notably $H_3Rh_3[P(OCH_3)_3]_6$, 5. In the new cluster 1, the unique rhodium atom is formally $Rh(III)$ and may be considered to be octahedrally coordinated (Table I).³⁶ The other two rhodium atoms in 1 are formally $Rh(I)$ atoms and have nearly square-planar, four-coordinate geometry (Table I), ignoring the interaction of the two, possible edge-bridging hydride ligands.³⁶ A precise structural comparison of 1 with the trinuclear analogue 5 is not possible because 5 has not been obtained yet in a single crystal form adequate for a crystallographic analysis but the similarity of 1 to 4, in the context of bond distances and angles for the $Rh(I)$ and $Rh(III)$ coordination spheres is close.

We are seeking the synthesis of other salts of this rhodium cluster that may permit an unambiguous placement of the hydride hydrogen atoms through either crystallographic or NMR data.

(32) Teller, R. G.; Bau, R. *Struct. Bonding (Berlin)* 1981, 44, 1-82.

(33) If the two equivalent hydride ligand atoms are in the alternatively limiting positions of terminal ligands on Rh_1 , then the formula representation is $\{(\mu_3-H)(H)_2Rh_3(\mu-Cl)[\mu-OP(O-i-C_3H_7)_2]_2[P(O-i-C_3H_7)_3]_3\}$.

(34) NMR data are as follows: 1H NMR (toluene- d_6 , $+20^\circ\text{C}$, $(CH_3)_4Si$ reference; 250 MHz) 5.25 (br), 4.95 (br) (this resonance overlapped with the one at $+5.25$ ppm), $+1.38$ (complex envelope of resonances for the $POCHCH_3$ 1H nuclei), -10.4 (br, $w_{1/2} \approx 90 \text{ Hz}$), -20.4 ppm (br); 1H NMR (toluene- d_6 , -65°C ; 250 MHz) $+5.40$ (br), $+5.10$ (br), $+4.60$ (br), $+1.38$ (complex envelope of resonances for the $POCHCH_3$ 1H nuclei), -10.1 (br m), -20.0 ppm (br); ^{31}P NMR (toluene- d_6 , $+20^\circ\text{C}$, 85% H_3PO_4 reference; 72.9 MHz) $+144.7$ (ddm, (1), $J_{PRh} = 270 \text{ Hz}$, $J_{PH} = 120 \text{ Hz}$), $+130.2$ (ddm, (2), $J_{PRh} = 338 \text{ Hz}$, $J_{PH} = 57 \text{ Hz}$), $+118.2$ ppm (d, (2), $J_{PRh} = 209 \text{ Hz}$); $^{31}P\{^1H\}$ NMR (toluene- d_6 , $+20^\circ\text{C}$; at 72.9 MHz) $+144.7$ (dm, (1), $J_{PRh} = 270 \text{ Hz}$), $+130.2$ (dm, (2), $J_{PRh} = 338 \text{ Hz}$), $+118.2$ ppm (d, (2), $J_{PRh} = 209 \text{ Hz}$).

(35) The relative intensities of these two hydride resonances could not accurately be assessed because of the significantly different relaxation times. The ratio could be either 1:2 or 2:3 but not 1:4.

(36) In a strict sense, the characterization of Rh_1 as a six-coordinate $Rh(III)$ center and of Rh_2 and Rh_3 as four-coordinate, planar $Rh(I)$ requires the limiting stereochemistry in which the two equivalent hydride ligands are terminal ligands on Rh_1 .

Acknowledgment. This research was supported by the National Science Foundation. The rhodium chloride was supplied on a loan grant from Johnson Matthey, Inc. Additional support of the research was in the form of a Camille and Henry Dreyfus Teacher-Scholar Award (V.W.D.), a Miller Professorship (E.L.M.) from the Miller Institute for Basic Research in Science, and a National

Science Predoctoral Fellowship (R.R.B.).

Registry No. 1, 84499-56-9; Rh, 7440-16-6; $[\text{ClRh}(\text{C}_2\text{H}_4)_2]_2$, 12081-16-2; $\text{KBH}(\text{O}-i\text{-C}_3\text{H}_7)_3$, 42278-67-1.

Supplementary Material Available: Tables of atomic coordinates (Table II), anisotropic thermal parameters (Table III), and structure factors (23 pages). Ordering information is given on any current masthead page.

Additions and Corrections

L. D. Hutchins, E. N. Duesler, and R. T. Paine: Structure and Bonding in a Phosphenium Ion-Iron Complex, $\text{Fe}[\eta^5\text{-(CH}_3)_5\text{C}_5\text{]}(\text{CO})_2[\text{PN}(\text{CH}_3)\text{CH}_2\text{CH}_2\text{NCH}_3]$. A Demonstration of Phosphenium Ion Acceptor Properties. 1982, 1, 1254.

On page 1256, the formula given in the last paragraph, $\text{FeCp}(\text{CO})_2\text{SO}_2$, had a minus charge inadvertently missing. The formula should read $\text{FeCp}(\text{CO})_2\text{SO}_2^-$.

Miguel Parra-Hake, Michael F. Rettig, Richard M. Wing, and John C. Woolcock: Chloropalladation of *exo*-9-Methylbicyclo[6.1.0]non-4-ene. Inversion of Configuration at Carbon Bound to Palladium and at Carbon Bound to Chlorine 1982, 1, 1478-1480.

The Pd-Cl bond distances were incompletely reported.

The Pd-Cl distance with Cl trans to C(1) is 2.516 (3) Å, and the Pd-Cl distance with Cl trans to C(4)C(5) is 2.396 (3) Å. As expected the alkyl function exerts a greater trans influence than the olefin function.

H. Yasuda, Y. Kajihara, K. Mashima, K. Nagasuna, K. Lee, and A. Nakamura: 1,3-Diene Complexes of Zirconium and Hafnium Prepared by the Reaction of Enediylmagnesium with MCl_2Cp_2 . A Remarkable Difference between the Zirconium and Hafnium Analogues As Revealed by ^1H NMR and Electronic Spectra 1982, 1, 388.

An important ^1H NMR parameter to evaluate the trans geometry of the diene complexes was left out of Table V. Add the following coupling constants (Hz) to Table V: 1 (trans isomer), $J_{56} = 15.5$; 7, $J_{56} = 15.0$; 8 (trans isomer), $J_{56} = 14.8$; $\text{Os}_3(\text{CO})_{10}(\text{C}_4\text{H}_6)$, $J_{56} = 11.4$; C_4H_6 , $J_{56} = 10.3$.

Book Reviews

Organic Reactions. Volume 28. Edited by W. G. Dauben (Editor-in-chief). Wiley, New York. 1982. VII + 347 pp. \$39.50.

The publication of a new volume in this widely acclaimed and firmly established series is an occasion of keen anticipation for every chemist engaged in organic synthesis. Each volume has offered chapters treating important synthetic methods in a comprehensive manner. Authoritative coverage of a reaction's scope and limitations, mechanism, related synthetic processes, and experimental variables is supplemented by specific experimental procedures and a tabular survey of the reaction's use from literature citations. For many versatile and frequently used reactions, classic name reactions and their modern counterparts, such surveys have been a godsend for the chemist seeking to apply a known method to an unknown synthesis.

The present volume extends such coverage to the Reimer-Tiemann reaction (36 pp., by H. Wynberg and E. W. Meijer), the Friedländer synthesis of quinolines (163 pp., by C.-C. Cheng and S.-J. Yan), and the directed aldol reaction (130 pp., by T. Mukaiyama). These chapters, however, meet one's high expectations for the series in varying degrees. Although each method addresses ways of making carbon-carbon bonds, undoubtedly the most versatile and useful reaction is that of the directed aldol reactions with metal enolates. Mukaiyama has composed an excellent and

comprehensive discussion of this relatively new and exciting area. This chapter is necessary reading for any aspirant in organic synthesis. The high yields, the loco- and stereoselectivity, and the great potential of this method will command increasing attention.

The Reimer-Tiemann and Friedländer reactions, on the other hand, may be classic name reactions, but they are more circumscribed in their utility. The action of chloroform and alkali on phenols or heterocycles, more often than not, gives low yields of formyl or ring expansion derivatives; in fact, good yields are attained only in exceptional cases. One might have expected phase-transfer conditions to have rejuvenated the Reimer-Tiemann reaction but, as the authors admit, little impact has thus far been felt. Although it gives high yields, the Friedländer reaction, in all of its manifestations (140 pp. of tables), is still restricted to the synthesis of quinolines. One could ask whether such a lengthy chapter is necessary to convey the scope of such a limited method.

All the chapters are carefully organized and composed, making it easy for the reader to evaluate the method and to find pertinent mechanistic or experimental detail. As to the narrow applicability of some of the methods covered, perhaps "Organic Reactions" must now offer coverage of more limited methods. The diligence of the editors of the previous 27 volumes may have preempted most

of the truly broad synthetic methods.

John J. Eisch, State University of New York at Binghamton

Advances in Organometallic and Inorganic Polymer Science. Edited by C. E. Carraher (Wright State), J. E. Sheats (Rider College), and C. U. Pittman (University of Alabama). Marcel Dekker, New York. 1982. xii + 449 pages. \$67.50.

This volume is the first in a series of monographs that will give an overview of the research being conducted in the field of organometallic polymers. It was, however, somewhat disconcerting to notice that these papers originally appeared in the *Journal of Macromolecular Science—Chemistry*.

The chapter on polymetallocenylenes by Neuse is an excellent review on the synthesis and characterization of poly-1,1'-ferrocenylenes and their potential application and expected future developments. "Polymers for the Controlled Release of Organotin Toxin" by Subramanian and Somosekharen describe efforts to produce controlled release antifouling toxins from copolymers of tributyltin acrylate and acrylates, epoxies, urethanes, aziridines, and polyesters.

An interesting chapter by Carraher et al. describes their studies on the identification of thermal degradation products of titanium polyethers using combined thermogravimetric analysis—mass spectrometry. Three chapters are devoted to the presentation of data on organometallic conducting polymers that have metal-like properties.

Carlini and Sbrana review "Catalysis by Transition Metal Derivatives Bound to Structurally Ordered Polymers" with emphasis on examples where the characteristics of the polymer exert an influence on the heterogenized homogeneous catalysts.

The chapter by Allcock et al. on poly(difluorophosphazene) describes what appears to be a novel reagent for the preparation of a new class of poly(organophosphazenes) that possess substituents linked to the skeleton through direct phosphorus-carbon bonds.

The chapter on "Metal Vapor Synthesis of Organometal Polymers and Polymer-Supported Metal Clusters" by Francis and Ozin describes the generation of polymer-stabilized small metal clusters by the deposition of metal vapor into a fluid polymer and the interaction of vapor-generated, small metal clusters with polymers.

Overall the book serves the purpose of providing reviews in the areas of Organometallic and Inorganic Polymers. The index appears to be fairly useful in accessing the data contained in this monograph. This volume should be of general interest to organometallic chemists.

P. E. Garrou, Dow Chemical-New England Laboratory

Advances in Organometallic Chemistry. Volume 20. Edited by F. G. A. Stone and R. West. Academic Press, New York. 1980. ix + 369 pages. \$56.00.

This series is consistently excellent in the quality of the scientific reviews that it contains and the manner in which they are presented to the reader. Volume 20 continues in this tradition with a collection of six extensive and topical articles covering organometallic chemistry of main-group and transition elements. Each review is authored by chemists who are active researchers in the areas whereof they write.

The first chapter (38 pages), by John A. Gladysz, deals with *Transition Metal Formyl Complexes*. The syntheses and reactions of these compounds are discussed in detail, and their relevance to catalytic reactions, particularly CO reduction, is emphasized. Key literature is covered through part of 1981, and an addendum provides a listing of notable additions that appeared after the body of the chapter had been completed.

The second review (74 pages), by Gordon K. Anderson, covers the *Organic Chemistry of Gold*. This article covers the literature up to mid-1980 and is the first major review of this topic to appear since 1970. Extensive coverage of synthesis and reactivity of Au(I) and Au(III) compounds containing σ and π ligands is presented, together with comparisons of the reactivities of both oxidation states. The chapter concludes with a brief comparison of organogold compounds with those of other metals, particularly Pt and Hg.

Chapter 3 (42 pages) is entitled *Arsonium Ylides* and represents a useful contribution from Huang Yaozeng and Shen Yanchang of the People's Republic of China. While this general topic has been reviewed recently elsewhere, this article focuses to some extent on studies emanating from Shanghai. This is indeed a timely review of these results, since the authors point out that "our work was interrupted, and some of our findings were delayed in publication for about 15 years". Methods of preparation, structure and physical properties, chemical reactivity, and synthetic applications are covered.

The fourth contribution (104 pages), by Wolfgang A. Herrmann, covers the rapidly growing number of compounds containing a *Methylene Bridge*. Comprehensive coverage of synthesis, structure and bonding, spectroscopic characterization, and chemical reactivity of μ -methylene compounds is provided, together with discussion of the catalytic relevance of these species to CO reduction on metal surfaces. Concluding sections on group 4A congeners of μ -methylene compounds and μ -(ω , ω')-alkanediyl complexes add perspective and provide a view of some synthetic challenges for the future. An extensive addendum is provided, covering numerous developments in this burgeoning area that were published after the main text was submitted.

Nucleophilic Displacement at Silicon: Recent Developments and Mechanistic Implications (47 pages), by R. J. P. Corriu and C. Guerin, reviews recent progress in this area, with special focus on factors controlling the stereochemistry of substitution and on a frontier orbital approach to understanding the mechanisms of these reactions. In view of the authors' prominent contributions to this field, it is not surprising that many of the literature citations are drawn from their own work.

The final article, *The Biological Methylation of Metals and Metalloids* (43 pages), by John S. Thayer and F. E. Brinckman, concentrates on rate studies of transmethylation reactions, both in vitro and in vivo, with additional discussion of the mechanisms of these reactions. Once again, an addendum of up to date literature citations is provided.

While the price, and the diversity of topics, make this volume an unlikely acquisition for the individual chemist, it will surely join the ranks of its 19 predecessors on the shelves of every chemistry library.

Russell P. Hughes, Dartmouth College

Gmelin Handbook of Inorganic Chemistry, 8th Edition, Sn, Organotin Compounds, Part 9, Triorganotin-Sulfur Compounds. H. Schumann and I. Schumann, volume authors, H. Bitterer, volume editor. Gmelin Institut für Anorganische Chemie der Max-Planck-Gesellschaft zur Förderung der Wissenschaften and Springer-Verlag, Berlin/Heidelberg/New York. 1982. iv + 276 pages. DM 727, \$322.80 (in English).

As the authors of this volume state, "Organotin-sulfur compounds are among the most important industrial organometallic compounds". For this reason, many organotin compounds containing a tin-sulfur bond have been prepared in industrial, as well as in academic laboratories. Of these, many have been either inadequately reported (in patents) or inadequately characterized, having been isolated only as "pot-bottoms" from their reaction mixtures. Nevertheless, many organotin-sulfur compounds have been characterized, either adequately or to some extent, and, of these, those in which the organotin moiety is a triorganotin group provide grist for the Schumann's tin mill in the present volume.

Only compounds of type R_3SnSR' are covered in this book. The substituent R' can vary widely. It can be an alkyl or aryl group, but it may also be part of a sulfur-functional group such as thiocarbamate, thiocarbonate, isothiocyanate, isothioureia, mono- or dithiocarboxylate, iminodithiocarbonate, thiophosphate, etc. Also covered are compounds of type R_3SnSH , R_3SnSO_2 , $R_3SnSSiR_3$, $R_3SnSGeR_3$, R_3SnSBR_2 , R_3SnSNa , $R_3SnSMn(CO)_5$, and $(R_3SnSR')Cr(CO)_5$ and other metal carbonyls in which trialkyltin mercaptides are present as ligands.

As usual, syntheses and all physical, spectroscopic, and chemical properties are provided in great detail, as is information on applications and biological properties. The comprehensive literature coverage (through the end of 1980) includes journal articles, reviews, patents, theses, and conference reports. The patent coverage is important and is based on those patents abstracted by "Chemical Abstracts".

of the truly broad synthetic methods.

John J. Eisch, *State University of New York at Binghamton*

Advances in Organometallic and Inorganic Polymer Science. Edited by C. E. Carraher (Wright State), J. E. Sheats (Rider College), and C. U. Pittman (University of Alabama). Marcel Dekker, New York. 1982. xii + 449 pages. \$67.50.

This volume is the first in a series of monographs that will give an overview of the research being conducted in the field of organometallic polymers. It was, however, somewhat disconcerting to notice that these papers originally appeared in the *Journal of Macromolecular Science—Chemistry*.

The chapter on polymetallocenylenes by Neuse is an excellent review on the synthesis and characterization of poly-1,1'-ferrocenylenes and their potential application and expected future developments. "Polymers for the Controlled Release of Organotin Toxin" by Subramanian and Somosekharen describe efforts to produce controlled release antifouling toxins from copolymers of tributyltin acrylate and acrylates, epoxies, urethanes, aziridines, and polyesters.

An interesting chapter by Carraher et al. describes their studies on the identification of thermal degradation products of titanium polyethers using combined thermogravimetric analysis—mass spectrometry. Three chapters are devoted to the presentation of data on organometallic conducting polymers that have metal-like properties.

Carlini and Sbrana review "Catalysis by Transition Metal Derivatives Bound to Structurally Ordered Polymers" with emphasis on examples where the characteristics of the polymer exert an influence on the heterogenized homogeneous catalysts.

The chapter by Allcock et al. on poly(difluorophosphazene) describes what appears to be a novel reagent for the preparation of a new class of poly(organophosphazenes) that possess substituents linked to the skeleton through direct phosphorus-carbon bonds.

The chapter on "Metal Vapor Synthesis of Organometal Polymers and Polymer-Supported Metal Clusters" by Francis and Ozin describes the generation of polymer-stabilized small metal clusters by the deposition of metal vapor into a fluid polymer and the interaction of vapor-generated, small metal clusters with polymers.

Overall the book serves the purpose of providing reviews in the areas of Organometallic and Inorganic Polymers. The index appears to be fairly useful in accessing the data contained in this monograph. This volume should be of general interest to organometallic chemists.

P. E. Garrou, *Dow Chemical-New England Laboratory*

Advances in Organometallic Chemistry. Volume 20. Edited by F. G. A. Stone and R. West. Academic Press, New York. 1980. ix + 369 pages. \$56.00.

This series is consistently excellent in the quality of the scientific reviews that it contains and the manner in which they are presented to the reader. Volume 20 continues in this tradition with a collection of six extensive and topical articles covering organometallic chemistry of main-group and transition elements. Each review is authored by chemists who are active researchers in the areas whereof they write.

The first chapter (38 pages), by John A. Gladysz, deals with *Transition Metal Formyl Complexes*. The syntheses and reactions of these compounds are discussed in detail, and their relevance to catalytic reactions, particularly CO reduction, is emphasized. Key literature is covered through part of 1981, and an addendum provides a listing of notable additions that appeared after the body of the chapter had been completed.

The second review (74 pages), by Gordon K. Anderson, covers the *Organic Chemistry of Gold*. This article covers the literature up to mid-1980 and is the first major review of this topic to appear since 1970. Extensive coverage of synthesis and reactivity of Au(I) and Au(III) compounds containing σ and π ligands is presented, together with comparisons of the reactivities of both oxidation states. The chapter concludes with a brief comparison of organogold compounds with those of other metals, particularly Pt and Hg.

Chapter 3 (42 pages) is entitled *Arsonium Ylides* and represents a useful contribution from Huang Yaozeng and Shen Yanchang of the People's Republic of China. While this general topic has been reviewed recently elsewhere, this article focuses to some extent on studies emanating from Shanghai. This is indeed a timely review of these results, since the authors point out that "our work was interrupted, and some of our findings were delayed in publication for about 15 years". Methods of preparation, structure and physical properties, chemical reactivity, and synthetic applications are covered.

The fourth contribution (104 pages), by Wolfgang A. Herrmann, covers the rapidly growing number of compounds containing a *Methylene Bridge*. Comprehensive coverage of synthesis, structure and bonding, spectroscopic characterization, and chemical reactivity of μ -methylene compounds is provided, together with discussion of the catalytic relevance of these species to CO reduction on metal surfaces. Concluding sections on group 4A congeners of μ -methylene compounds and μ -(ω , ω')-alkanediyl complexes add perspective and provide a view of some synthetic challenges for the future. An extensive addendum is provided, covering numerous developments in this burgeoning area that were published after the main text was submitted.

Nucleophilic Displacement at Silicon: Recent Developments and Mechanistic Implications (47 pages), by R. J. P. Corriu and C. Guerin, reviews recent progress in this area, with special focus on factors controlling the stereochemistry of substitution and on a frontier orbital approach to understanding the mechanisms of these reactions. In view of the authors' prominent contributions to this field, it is not surprising that many of the literature citations are drawn from their own work.

The final article, *The Biological Methylation of Metals and Metalloids* (43 pages), by John S. Thayer and F. E. Brinckman, concentrates on rate studies of transmethylation reactions, both in vitro and in vivo, with additional discussion of the mechanisms of these reactions. Once again, an addendum of up to date literature citations is provided.

While the price, and the diversity of topics, make this volume an unlikely acquisition for the individual chemist, it will surely join the ranks of its 19 predecessors on the shelves of every chemistry library.

Russell P. Hughes, *Dartmouth College*

Gmelin Handbook of Inorganic Chemistry, 8th Edition, Sn, Organotin Compounds, Part 9, Triorganotin-Sulfur Compounds. H. Schumann and I. Schumann, volume authors, H. Bitterer, volume editor. Gmelin Institut für Anorganische Chemie der Max-Planck-Gesellschaft zur Förderung der Wissenschaften and Springer-Verlag, Berlin/Heidelberg/New York. 1982. iv + 276 pages. DM 727, \$322.80 (in English).

As the authors of this volume state, "Organotin-sulfur compounds are among the most important industrial organometallic compounds". For this reason, many organotin compounds containing a tin-sulfur bond have been prepared in industrial, as well as in academic laboratories. Of these, many have been either inadequately reported (in patents) or inadequately characterized, having been isolated only as "pot-bottoms" from their reaction mixtures. Nevertheless, many organotin-sulfur compounds have been characterized, either adequately or to some extent, and, of these, those in which the organotin moiety is a triorganotin group provide grist for the Schumann's tin mill in the present volume.

Only compounds of type R_3SnSR' are covered in this book. The substituent R' can vary widely. It can be an alkyl or aryl group, but it may also be part of a sulfur-functional group such as thiocarbamate, thiocarbonate, isothiocyanate, isothioureia, mono- or dithiocarboxylate, iminodithiocarbonate, thiophosphate, etc. Also covered are compounds of type R_3SnSH , R_3SnSO_2 , $R_3SnSSiR_3$, $R_3SnSGeR_3$, $R_3SnSBR'_2$, R_3SnSNa , $R_3SnSMn(CO)_5$, and $(R_3SnSR')Cr(CO)_5$ and other metal carbonyls in which trialkyltin mercaptides are present as ligands.

As usual, syntheses and all physical, spectroscopic, and chemical properties are provided in great detail, as is information on applications and biological properties. The comprehensive literature coverage (through the end of 1980) includes journal articles, reviews, patents, theses, and conference reports. The patent coverage is important and is based on those patents abstracted by "Chemical Abstracts".

The detailed accounts of the currently available review literature which might be useful to the reader are a valuable feature of the organotin series. The general review literature (with "organometallic compounds", "organometallic compounds of the main-group 4 elements", "organotin compounds" as categories) is up-dated and further collections of reviews and patents on organotin chalcogenides and organotin-sulfur compounds are pertinent to the subject matter of this volume.

A useful empirical and substituent group formula index concludes the book. Together with the fairly detailed table of contents, this makes it rather easy to find the compounds one is looking for. The Gmelin Handbook volumes are not really suitable for browsing, but as comprehensive reference works, they are invaluable. No chemical library should be without them.

Further volumes of the Gmelin organotin series will deal with the remaining organotin-sulfur compounds, including the industrially important $R_2Sn(SR')_2$ derivatives.

Dietmar Seyferth, *Massachusetts Institute of Technology*

Gmelin Handbook of Inorganic Chemistry, 8th Edition, Uranium. Supplement Volume A5. Spectra. W. T. Carnall, Hannah M. Crosswhite, Henry M. Crosswhite, D. J. Lam, B. W. Veal, and B. Kanellakopulos, volume authors. C. Keller and K.-C. Buschbeck, volume editors. Gmelin Institut für Anorganische Chemie der Max-Planck-Gesellschaft zur Förderung der Wissenschaften and Springer-Verlag, Berlin/Heidelberg/New York. 1982. v + 269 pages. DM 717, \$318.40.

The Gmelin Institute is presently involved in a major effort to update the 1936 "Uran" volume of the "Handbuch der Anorganische Chemie" series. Part A covers the element uranium, part B, the metal and its alloys, part C, certain of the compounds, part D, the solution chemistry, and part E, the coordination compounds. This volume (A5) deals with the spectroscopy of uranium and its compounds (including organometallic compounds). It covers the scientific literature through 1979.

In chapter 1, Henry M. Crosswhite (Argonne National Laboratory) provides a comprehensive discussion of the atomic spectra of gaseous uranium atoms and ions (not of great interest to most organometallic chemists). In chapter 2, William T. Carnall (Argonne National Laboratory) presents a succinct and up-to-date

picture of current results and theory concerning the absorption and luminescence spectra of uranium compounds. The comprehensive coverage is by oxidation state, and adequate critical coverage is given to organouranium compounds. Chapter 3, by Hannah M. Crosswhite and William T. Carnall (Argonne National Laboratory), discusses the X-ray emission spectroscopy of uranium and will not be useful to most organometallic researchers. Photoemission spectroscopy is the topic of chapter 4 by Boyd W. Veal and Daniel J. Lam (Argonne National Laboratory). Although this chapter presents an excellent discussion of XPS and UPS results for purely inorganic uranium compounds (e.g., oxides, halides, nitrides), there is no discussion of uranium organometallic compounds nor even a reference to direct the reader. This is disappointing since a considerable and important literature of gas-phase UPS studies now exists for organouranium compounds. Fortunately, some discussion of these results is provided in a Supplement Volume E2 chapter by B. Kanellakopulos. Chapter 5 of the present volume by Henry R. Hoekstra (Argonne National Laboratory) summarizes the vibrational spectra of uranium compounds. Unfortunately, the coverage largely focuses upon uranyl compounds, and even important inorganic topics such as UF_6 and $U(BH_4)_4$ are not given full coverage. There is no mention of the numerous studies involving organometallic compounds nor is the reader referred to the aforementioned chapter by Kanellakopulos that fortunately does touch upon some aspects of the vibrational spectra. Chapters 6, 7, and 8 by Basil Kanellakopulos (Kernforschungszentrum Karlsruhe) discuss EPR, NMR, and Mössbauer spectroscopy, respectively. All give excellent expositions of the subject matter, and the former two, although not dealing specifically with organouranium compounds, will be useful to organometallic chemists interested in f elements. Kanellakopulos directs the reader to his chapter in volume E2 as well as to other literature for discussion of the NMR spectra of uranium organometallic compounds. Post-1979 EPR data on organouranium complexes could not be included.

As in all Gmelin volumes, volume A5 provides an explanation of the Gmelin classification scheme and a table of conversion factors. This monograph clearly provides a wealth of spectroscopic information on uranium compounds and will be of general interest to actinide researchers. The coverage of uranium organometallic compounds, however, is rather light, and in view of the high price, this volume seems most appropriate for institutional library purchases.

Tobin J. Marks, *Northwestern University*